

Determining the Role of FKBPL Signalling in Cardiac Fibrosis and Heart Disease

by **Michael Chhor**

Thesis submitted in fulfilment of the requirements for
the degree of

Doctor of Philosophy

under the supervision of A/Prof Lana McClements and Dr
Kristine McGrath

University of Technology Sydney
Faculty of Science
August 2023

Certificate of Original Authorship

I, **Michael Chhor** declare that this thesis, is submitted in fulfilment of the requirements for the award of **Doctor of Philosophy**, in the **Faculty of Science** at the University of Technology Sydney. This thesis is wholly my own work unless otherwise referenced or acknowledged. In addition, I certify that all information sources and literature used are indicated in the thesis. This document has not been submitted for qualifications at any other academic institution. This research is supported by the Australian Government Research Training Program.

Production Note:

Signature: Signature removed prior to publication.

Date: 1st August 2023

Acknowledgements

I am not very good at writing things like this, but I would like to dedicate this section to all of those who have helped me through my PhD candidature. This has been arguably the most turbulent and difficult time of my life thus far. That being said, I have grown the most as a person and scientist during this time and learned many invaluable skills and lessons. I am grateful for the opportunity to pursue this candidature. I pray that the work displayed in this thesis can contribute to a greater cause.

My biggest acknowledgement goes to my supervisors Lana and Kristine, whom I am eternally grateful for. They have granted me a wild amount of support through this candidature despite my shortcomings and have been ever-present in any situation I've needed assistance. I've learnt a lot from them both and hope to be better in the future. I don't think I would have been able to complete this PhD if I had any other supervisors. Thank you for carrying me to the finish line. In saying that, I think I've also been really lucky with the colleagues I've been able to interact and work with on a day-to-day basis from both the McClements and McGrath group that have unknowingly been giving me free therapy. They have made the best of the worst time and have also helped me on so many levels.

Finally, a big, big, thank you to my friends, family, and my dog Bloo, who have supported me emotionally, financially, and through making sure I don't starve. They didn't really understand what I do but supported me regardless.

COVID-19 Impact

The COVID-19 pandemic was a tough time globally, and during this period the scope of this project was shifted to accommodate for the inability to perform experiments.

- Prior to the COVID-19 lockdown, the 2019 bushfires with my area of residence negatively impacted my respiratory health and I was unable to travel to campus to perform experiments.
- The COVID-19 lockdowns proved to be tough on experiments that were planned or abruptly halted. Originally, key pathways for cardiovascular disease were to be examined *in vivo* from a type I diabetes mellitus and type II diabetes mellitus mouse model in *fkbp1*^{+/-} or wild type mice. *Ex vivo* experiments on the heart and aorta samples were to be processed and extracted for protein and RNA to identify marker expression. Due to the inability to perform experimental work during this lockdown, the chapter predominantly focusing on the role of FKBPL in diabetes mellitus was instead replaced with a scoping review (Chapter 5) detailing the current biomarkers for cardiac remodelling in patients with diabetes mellitus.
- Similarly, an *in vivo* hypertensive angiotensin-II mouse model in *fkbp1*^{+/-} or wild type mice was planned. *In vivo* baseline measurements and *ex vivo* assessments on inflammatory and fibrotic markers through RT-qPCR, western blotting, and immunohistochemistry were to be performed. Due to the time constraints of my candidature, we instead performed an *in vitro* study to create a 2D and 3D model of fibrosis with human fetal fibroblast cells (HFF08) with and without FKBPL siRNA knockdown and treated with profibrotic and/or hypoxic factors.

List of Publications

- **Chhor, M.**; Tulpar, E.; Nguyen, T.; Cranfield, C.G.; Gorrie, C.A.; Chan, Y.L.; Chen, H.; Oliver, B.G.; McClements, L.; McGrath, K.C. E-Cigarette Aerosol Condensate Leads to Impaired Coronary Endothelial Cell Health and Restricted Angiogenesis. *Int. J. Mol. Sci.* **2023**, *24*, 6378. <https://doi.org/10.3390/ijms24076378>
Published 28th March 2023 (IF: 5.6) (Chapter 2)
- Chen, H.; **Chhor, M.**; Rayner, B.; McGrath, K.; McClements, L. Evaluation of the diagnostic accuracy of current biomarkers in heart failure with preserved ejection fraction: A systematic review and meta-analysis. *Archives of Cardiovascular Health* **2021**, *12*, 793-804. <https://doi.org/10.1016/j.acvd.2021.10.007>
Published 19th November 2021 (IF: 3.0) (Chapter 4)
- **Chhor, M.**; Chen, H.; Jerotić, D.; Tešić, M.; Nikolić, V.N.; Pavlović, M.; Vučić, R.M.; Rayner, B.; Watson, C.J.; Ledwidge, M.; McDonald, K.; Robson, T.; McGrath, K.C.; McClements, L. FK506-Binding Protein like (FKBPL) Has an Important Role in Heart Failure with Preserved Ejection Fraction Pathogenesis with Potential Diagnostic Utility. *Biomolecules* **2023**, *13*, 395. <https://doi.org/10.3390/biom13020395>
Published 18th February 2023 (IF: 5.5) (Chapter 4)
- **Chhor, M.**; Law, W.; Pavlovic, M.; Aksentijevic, D.; McGrath, K.; McClements, L. Diagnostic and prognostic biomarkers reflective of cardiac remodelling in diabetes mellitus: A scoping review. *Diabet Med.* **2023**, *40*:e15064. [doi:10.1111/dme.15064](https://doi.org/10.1111/dme.15064)
Published 7th February 2023 (IF: 3.5) (Chapter 5)

Conferences & Presentations

- Australian Society for Medical Research 2020 - Presentation
- Institute for Biomedical Materials and Devices 2020 - Presentation
- Taylor's University Graduate Research Symposium 2021 – Poster & Presentation. 'Best Oral Presenter' for Life Sciences

Statement of Author Contribution

- Chhor, M.; Tulpar, E.; Nguyen, T.; Cranfield, C.G.; Gorrie, C.A.; Chan, Y.L.; Chen, H.; Oliver, B.G.; McClements, L.; McGrath, K.C. E-Cigarette Aerosol Condensate Leads to Impaired Coronary Endothelial Cell Health and Restricted Angiogenesis. *Int. J. Mol. Sci.* **2023**, *24*, 6378. <https://doi.org/10.3390/ijms24076378>

Author	Signature	Contribution
Michael Chhor	Production Note: Signature removed prior to publication.	Completed all the experiments, analysis, and discussion of the results except for the in vivo study, and also wrote the manuscript.
Esra Tulpar	Production Note: Signature removed prior to publication.	Contributed to data acquisition, analysis and interpretation.
Tara Nguyen	Production Note: Signature removed prior to publication.	Contributed to data acquisition, analysis and interpretation.
Charles G. Cranfield	Production Note: Signature removed prior to publication.	Contributed to data acquisition, analysis and interpretation, and manuscript editing.
Catherine A. Gorrie	Production Note: Signature removed prior to publication.	Contributed to data acquisition, analysis and interpretation, and manuscript editing.
Yik Lung Chan	Production Note: Signature removed prior to publication.	Contributed to data acquisition, analysis and interpretation.
Hui Chen	Production Note: Signature removed prior to publication.	Contributed to data acquisition, analysis and interpretation, and manuscript editing.

Brian G. Oliver	Production Note: Signature removed prior to publication.	Contributed to data acquisition, analysis and interpretation, and manuscript editing.
Kristine C. McGrath	Production Note: Signature removed prior to publication.	Supervised Michael Chhor, conceptualised the study and contributed to data acquisition, analysis and interpretation and manuscript editing.
Lana McClements	Production Note: Signature removed prior to publication.	Supervised Michael Chhor, conceptualised the study and contributed to data acquisition, analysis and interpretation and manuscript editing.

- Chhor, M.; Barman, S.; Heidari, F.; Alqudah, A.; Grieve, D.; Robson, T.; McGrath, K.; McClements, L. Emerging Role of FK506-binding protein like (FKBPL) in Cardiac Fibrosis. (Manuscript; Chapter 3)

Author	Signature	Contribution
Michael Chhor	Production Note: Signature removed prior to publication.	Michael Chhor completed all the experiments, data analysis and interpretation. Michael also wrote the whole manuscript.
Shreya Barman	Production Note: Signature removed prior to publication.	Shreya Barman contributed to some experiments, and data analysis and interpretation, manuscript writing.
Fatemeh Heidari	Production Note: Signature removed prior to publication.	Fatemeh Heidari contributed to some experiments, data analysis and manuscript writing.
Abdelrahim Alqudah	Production Note: Signature removed prior to publication.	Abdelrahim Alqudah performed in vivo experiments and contributed to data analysis and manuscript writing.
Amy Bottomley	Production Note: Signature removed prior to publication.	Amy Bottomley contributed significant to microscopy, image acquisition and analysis.
Tracy Robson	Production Note: Signature removed prior to publication.	Tracy Robson provided FKBPL transgenic mice and contributed to data interpretation and manuscript writing.
David Greave	Production Note: Signature removed prior to publication.	David Grieve contributed significantly to in vivo experiments, data analysis and interpretation.
Kristine C. McGrath	Production Note: Signature removed prior to publication.	Kristine C. McGrath supervised Michael Chhor and contributed to data analysis and interpretation and manuscript writing.
Lana McClements	Production Note: Signature removed prior to publication.	Lana McClements supervised Michael Chhor, conceptualised the study and contributed to data analysis and interpretation and manuscript editing.

- Chhor, M.; Chen, H.; Jerotić, D.; Tešić, M.; Nikolić, V.N.; Pavlović, M.; Vučić, R.M.; Rayner, B.; Watson, C.J.; Ledwidge, M.; McDonald, K.; Robson, T.; McGrath, K.C.; McClements, L. FK506-Binding Protein like (FKBPL) Has an Important Role in Heart Failure with Preserved Ejection Fraction Pathogenesis with Potential Diagnostic Utility. *Biomolecules* **2023**, *13*, 395. <https://doi.org/10.3390/biom13020395>

Author	Signature	Contribution
Michael Chhor	Production Note: Signature removed prior to publication.	Completed all the experiments, analysis, and discussion of the results except for conducting the <i>in vitro</i> experiments, and also wrote the manuscript.
Hao Chen	Production Note: Signature removed prior to publication.	Contributed to the experimental design, data acquisition, analysis and interpretation.
Djordja Jerotic	Production Note: Signature removed prior to publication.	Contributed to data acquisition, analysis and interpretation.
Milorad Tešić	Production Note: Signature removed prior to publication.	Conceived the study; recruited the patients; performed echocardiography; retrieved the samples; recorded the clinical characteristics; stratified the patient cohorts; and edited the manuscript.
Valentina N. Nikolić	Production Note: Signature removed prior to publication.	Conceived the study; recruited the patients; performed echocardiography; retrieved the samples; recorded the clinical characteristics; stratified the patient cohorts; and edited the manuscript.
Milan Pavlović	Production Note: Signature removed prior to publication.	Conceived the study; recruited the patients; performed echocardiography; retrieved the samples; recorded the clinical characteristics; stratified the patient cohorts; and edited the manuscript.

Rada M. Vučić	Production Note: Signature removed prior to publication.	Conceived the study; recruited the patients; performed echocardiography; retrieved the samples; recorded the clinical characteristics; stratified the patient cohorts; and edited the manuscript.
Benjamin Rayner	Production Note: Signature removed prior to publication.	Contributed to the experimental design, data acquisition, analysis and interpretation.
Chris J. Watson	Production Note: Signature removed prior to publication.	Contributed to the conception, experimental design or data interpretation.
Mark Ledwidge	Production Note: Signature removed prior to publication.	Contributed to the conception, experimental design or data interpretation.
Kenneth McDonald	Production Note: Signature removed prior to publication.	Contributed to the conception, experimental design or data interpretation.
Tracy Robson	Production Note: Signature removed prior to publication.	Contributed to the conception, experimental design or data interpretation.
Kristine C. McGrath	Production Note: Signature removed prior to publication.	Supervised Michael Chhor, conceptualised the study and contributed to data analysis and interpretation.
Lana McClements	Production Note: Signature removed prior to publication.	Supervised Michael Chhor, conceptualised the study and contributed to data acquisition, analysis and interpretation and manuscript editing.

- Chen, H.; Chhor, M.; Rayner, B.; McGrath, K.; McClements, L. Evaluation of the diagnostic accuracy of current biomarkers in heart failure with preserved ejection fraction: A systematic review and meta-analysis. *Archives of Cardiovascular Diseases* **2021**, 12, 793-804. <https://doi.org/10.1016/j.acvd.2021.10.007>

Author	Signature	Contribution
Hao Chen	Production Note: Signature removed prior to publication.	First author on the paper and conducted the search, identified the studies, performed the statistical analyses and wrote the first draft of this manuscript.
Michael Chhor	Production Note: Signature removed prior to publication.	Second author conducted the literature search, screened, assessed, and identified the studies, extracted the data, and contributed to the writing.
Benjamin S. Rayner	Production Note: Signature removed prior to publication.	Supervised Hao Chen and Michael Chhor and reviewed the quality of the studies.
Kristine C. McGrath	Production Note: Signature removed prior to publication.	Supervised Hao Chen and Michael Chhor and reviewed the quality of the studies.
Lana McClements	Production Note: Signature removed prior to publication.	Supervised Hao Chen and Michael Chhor and reviewed the quality of the studies. Conceptualized the study and edited the manuscript.

- Chhor, M.; Law, W.; Pavlovic, M.; Aksentijevic, D.; McGrath, K.; McClements, L. Diagnostic and prognostic biomarkers reflective of cardiac remodelling in diabetes mellitus: A scoping review. *Diabet Med.* **2023**, 40:e15064. <https://doi.org/10.1111/dme.15064>

Author	Signature	Contribution
Michael Chhor	Production Note: Signature removed prior to publication.	Michael Chhor developed methodology, performed data extraction, analysis, interpretation, created figures and graphical abstract, and wrote the manuscript.
William Law	Production Note: Signature removed prior to publication.	Contributed to data extraction, interpretation, and manuscript content.
Milan Pavlović	Production Note: Signature removed prior to publication.	Contributed to the analysis and interpretation of the clinical data.
Dunja Aksentijevic	Production Note: Signature removed prior to publication.	Contributed to the analysis and interpretation of the clinical data and manuscript writing.
Kristine C. McGrath	Production Note: Signature removed prior to publication.	Supervised Michael Chhor and William Law, conceptualised the study and contributed to data acquisition, analysis and interpretation and manuscript editing.
Lana McClements	Production Note: Signature removed prior to publication.	Supervised Michael Chhor and William Law, conceptualised the study and contributed to data acquisition, analysis and interpretation and manuscript editing.

Table of Contents

Chapter 1 Introduction.....	5
1.1 Cardiovascular Disease	6
1.1.1 Endothelial Dysfunction in CVD	9
1.1.2 E-Cigarettes as an emerging risk factor for CVD.	13
1.1.3 Diabetes mellitus as a risk factor for CVD.....	15
1.2 Cardiac Fibrosis	19
1.2.1 Cardiac Remodelling leading to cardiac fibrosis	19
1.2.2 Key inflammatory mechanisms in the development of cardiac fibrosis ...	20
1.3 Heart Failure	22
1.3.1 Different phenotypes of heart failure	23
1.3.2 Current biomarkers used for the diagnosis and progression of heart failure	24
1.3.3 Treatment of heart failure.....	26
1.4 The biological and pathological functions of FKBPL	27
1.4.1 FKBPL is a key anti-angiogenic protein	28
1.4.2 FKBPL has an emerging role in inflammation	30
1.4.3 FKBPL as a potential novel target or biomarker of CVD	33
1.5 Hypothesis and Aims	36
Chapter 2 E-cigarette Aerosol Condensate leads to Impaired Coronary Endothelial Cell Health and Restricted Angiogenesis	39
2.1 Abstract.....	42
2.2 Introduction	43
2.3 Methods	45
2.3.1 Generation of EAC.....	45
2.3.2 Cell Culture and Treatment Models	47

2.3.3 Cytotoxicity Assay	47
2.3.4 Intracellular Reactive oxygen Species (ROS) Assay	48
2.3.5 Enzyme-Linked Immunosorbent Assay (ELISA)	48
2.3.6 Animal Exposure	49
2.3.7 Immunohistochemistry of the Heart Tissue	50
2.3.8 Reverse Transcription-Polymerase Chain Reaction (RT-qPCR)	51
2.3.9 Tethered Bilayer Lipid Membrane (tBLMs) Assay	52
2.3.10 Statistical Analysis	53
2.4 Results	53
2.4.1 Exposure of HCAEC to EAC-Treated Lung Cell Conditioned Media Results in Cytotoxicity	53
2.4.2 Direct Exposure to EAC or Indirectly to EAC-Lung Cell Conditioned Media Induces ROS Levels	55
2.4.3 Adhesion Molecule Expression Increases in HCAEC after EAC Exposure for ICAM-1, but not VCAM-1	57
2.4.4 EAC from Nicotine Containing e-Liquid Alters Membrane Permeability ..	59
2.4.5 E-Cigarette Aerosol Increases ICAM-1 mRNA Expression in Murine Hearts	61
2.4.6 Cardiac Angiogenesis Markers Are Dysregulated by E-Cig Aerosol Exposure	62
2.5 Discussion	63
2.6 Conclusion	71
2.7 Declarations	71
2.8 References	72
2.9 Supplementary Info	80
Chapter 3 Elucidating the role of FKBPL in in vitro Cardiac Fibrosis Models	82
3.1 Abstract	85
3.2 Introduction	86

3.3 Methods	88
3.3.1 FKBPL Transgenic Mice	88
3.3.2 Collagen Staining Assessment	89
3.3.3 3D Bioprinted Model of Cardiac Fibrosis.....	89
3.3.4 Cell Proliferation Assay.....	90
3.3.5 Live/Dead Viability Assay.....	90
3.3.6 Immunofluorescence Staining.....	91
3.3.7 Network Formation.....	92
3.3.8 Cell Culture and Treatments	92
3.3.9 Transfection	92
3.3.10 Reverse Transcription-polymerase chain reaction (RT-qPCR)	93
3.3.11 Western Blotting.....	94
3.3.12 Monocyte Adhesion Assay.....	95
3.3.13 Statistical Analysis	95
3.4 Results	96
3.4.1 FKBPL transgenic mice (<i>fbkpl</i> ^{+/-}) seem to be protected against cardiac fibrosis	96
3.4.2 FKBPL regulation in the new 3D bioprinted model of cardiac fibrosis.....	98
3.4.3 Regulation of pro-fibrotic mechanisms by FKBPL in 2D cell culture	107
3.5 Discussion.....	114
3.6 Conclusion	120
3.7 Declarations	121
3.8 References.....	123
3.9 Supplementary Info.....	129
Chapter 4 Evaluating the Biomarker Potential of FKBPL in Risk Stratification and Diagnosis of Heart Failure with Preserved Ejection Fraction.....	133
4.1 Abstract.....	136
4.2 Introduction	137

4.3 Methods	138
4.3.1 Search strategy and selection criteria	138
4.3.2 Data Extraction	139
4.3.3 Quality Assessment	140
4.3.4 Statistical Analysis	140
4.4 Results	141
4.4.1 Search Results.....	141
4.4.2 N-terminal pro-B-type natriuretic peptide	143
4.4.3 B-type natriuretic peptide	145
4.4.4 Galectin-3	146
4.4.5 Suppression of tumorigenesis-2	147
4.5 Discussion.....	149
4.6 Conclusion	153
4.7 Declarations	154
4.8 References.....	155
4.9 Supplementary Info	159
4.10 Abstract.....	164
4.11 Introduction	165
4.12 Methods	167
4.12.1 Cell culture and Treatments.....	167
4.12.2 Cell Size Analysis	167
4.12.3 Western Blot	167
4.12.4 Reverse Transcription-Polymerase Chain Reaction (RT-qPCR)	168
4.12.5 Participants and Samples	169
4.12.6 Plasma Marker Measurement.....	171
4.12.7 Statistical Analysis	171
4.13 Results	172

4.13.1 FKBPL Peptide Mimetic, AD-01, and Angiotensin-II (Ang-II) Increase Cardiomyoblast Cell and Nucleus Size; However, AD-01 in the Presence of Ang-II Abrogates Ang-II-Induced Cardiac Hypertrophy	172
4.13.2 AD-01 Abrogates Ang-II-Induced Increases in FKBPL Protein Expression.....	174
4.13.3 FKBPL Plasma Concentration Is Increased in Patients with HFpEF but Does Not Differ between Subgroups	177
4.13.4 FKBPL Is Positively Correlated with IVST, Indicative of Microvascular Dysfunction.....	179
4.14 Discussion.....	180
4.15 Conclusion	184
4.16 Declarations	185
4.17 References.....	186
4.18 Supplementary Info	189
Chapter 5 Evaluating the current biomarkers reflective of early cardiac remodelling in diabetes mellitus	192
5.1 Abstract.....	195
5.2 Introduction	196
5.3 Methods	199
5.3.1 Research Question	199
5.3.2 Identification of Studies.....	199
5.3.3 Study Selection.....	199
5.3.4 Data Extraction	200
5.4 Results.....	201
5.4.1 Study Selection.....	201
5.4.2 Study Characteristics	207
5.4.3 Level of evidence and biomarker classification.....	210
5.5 Discussion.....	210

5.5.1 NT-proBNP and BNP as a measure of cardiac remodelling	211
5.5.2 Inflammatory biomarkers of cardiac remodelling	213
5.5.3 Cardiac-specific biomarkers.....	216
5.5.4 Metabol(om)ic markers of T2D and CVD: Future perspectives.....	219
5.6 Conclusion	222
5.7 Declarations	223
5.8 References.....	224
Chapter 6 Discussion	235
6.1 General Discussion.....	236
6.1.1 E-cigarettes as an emerging threat for CVDs	241
6.1.2 FKBPL-mediated mechanism in the development of cardiac hypertrophy and fibrosis	243
6.1.3 FKBPL's biomarker potential in CVD and HF	246
6.2 General conclusion	249
6.3 Future Perspectives	251
References.....	253
Appendix	264

List of Figures

Figure 1.1 Mechanisms of different risk factors leading to endothelial cell dysfunction in CVD. Modifiable cardiovascular risk factors including diabetes mellitus, cigarette/e-cigarette smoking, and hypertension or obesity increase levels of oxidative stress and inflammatory mediators within endothelial cells. This can lead to endothelial cell activation, increasing inflammatory markers and adhesion molecule expression, decreasing vasodilation and angiogenesis before subsequent development of endothelial dysfunction. Created with BioRender.com. **12**

Figure 1.2 Mechanisms of DM leading to CVD. Hyperglycaemia and insulin resistance related mitochondrial dysfunction increases the production of AGEs and its receptors. An increase in profibrotic, oxidative, and inflammatory signalling causes endothelial dysfunction, hypertrophy, and inflammation that leads to CVD. Created with BioRender.com **18**

Figure 1.3 Pathological remodelling of the myocardium. Myocardial injury such as MI illicit an inflammatory response that recruits inflammatory markers and immune cells through the RAAS and TGF- β pathway. Resident fibroblasts begin differentiation into myofibroblasts that signal the beginning of ECM remodelling through increased signalling of fibrotic markers. Prolonged ECM remodelling and scar formation reduces contractility and function of the myocardium resulting in cardiac fibrosis and eventual HF. Created with BioRender.com. **21**

Figure 1.4 FKBPL mimetic AD-01/ALM201. AD-01 (preclinical) and ALM201 (clinical) are both peptide derivatives of FKBPL based on its 23/24 amino acid sequence within the anti-angiogenic domain, thus retaining the same anti-cancer and anti-angiogenic functions..... **29**

Figure 1.5 Inflammatory pathway of FKBPL. FKBPL is bound to cell surface receptor CD44 before it can exert its anti-angiogenic and cancer stem cell inhibitory function. Decreased FKBPL levels have shown to increase the modulation of CD44, NF κ B, and STAT3 pathways. Resultant effects are in increased angiogenesis, inflammation, and endothelial dysfunction, which are all parameters associated with the development of CVD. **32**

Figure 1.6 Biological and Pathological functions of FKBPL. FKBPL binds to CD44 before it can exert its anti-angiogenic and cancer stem cell inhibitory function. Following FKBPL-CD44 complex formation, there is an inhibition on the inflammatory STAT3-N κ FB signalling. Recent work by Janusewski et al. (2020) showed implicated FKBPL, for the first time, as a determinant of cardiovascular disease. Previous work has also shown that FKBPL as a chaperone protein forms a complex with HSP90 and oestrogen receptor (ER) regulating ER signalling, which is independent of CD44. **35**

Figure 2.1 Experimental Setup for e-cigarette aerosol condensate collection. **46**

Figure 2.2 Cell viability in HCAEC exposed to (A) Direct effects of EAC. MTT Assay was performed on HCAEC after exposure to various concentration of EAC

generated from: (i) a PG/VG solution (non-flavoured), (ii) 0 mg nicotine (tobacco flavoured), and (iii) 18 mg nicotine (tobacco flavoured) for 24 h. (B) Indirect effects of EAC. A549 epithelial lung cells were exposed to EAC under the same conditions. Media from the treated A549 cells were then used to treat HCAEC on a separate plate for 24 h before cell viability was assessed via MTT assay. Results are expressed as mean \pm SEM (n = 4 biological replicates). One-way ANOVA with Bonferroni post-tests was used for statistical analysis; * p < 0.05, ** p < 0.01, *** p < 0.001 versus Ctrl. 55

Figure 2.3 Reactive oxygen species levels in HCAEC after (A) Direct EAC exposure. ROS levels were measured in HCAEC after exposure to various concentration of EAC generated from: (i) a PG/VG standard (non-flavoured), (ii) 0 mg nicotine (tobacco flavoured), and (iii) 18 mg nicotine (tobacco flavoured) at for 24 h Data shown is expressed as a mean \pm SEM (n = 3 biological replicates). (B) Indirect effects of EAC. A549 epithelial lung cells were exposed to EAC under the same conditions. Media from the treated A549 cells were then used to treat HCAEC on a separate plate for 24 h before a DCF assay was performed. Data shown is expressed as a mean \pm SEM (n = 5 biological replicates). One-way ANOVA with Bonferroni post-tests was used for statistical analysis, ** p < 0.01; **** p < 0.0001 versus Ctrl. 56

Figure 2.4 Expression of cellular adhesion molecules after exposure to EAC treatment. HCAEC were exposed to various concentrations of EAC generated from: (i) 0 mg nicotine (tobacco flavoured) and (ii) 18 mg nicotine (tobacco flavoured) for 24 h. (A) VCAM-1 protein expression. (B) ICAM-1 protein expression. (C) Indirect effects of EAC on ICAM-1 protein exposure. A549 epithelial lung cells were exposed to EAC under the same conditions. Media from the treated A549 cells were then used to treat HCAEC on a separate plate for 24 h before measuring ICAM-1 protein levels. Results are expressed as mean \pm SEM (n = 3 biological replicates). One-way ANOVA with Bonferroni post-tests was used for statistical analysis, ** p < 0.01 versus Ctrl. 58

Figure 2.5 (A) Changes in membrane conduction of tethered bilayer lipid membranes (tBLM) in response to EAC (1% and 10%) in 100 mM NaCl 10 mM tris pH 7 buffer (n = 3). EAC solutions containing nicotine increase membrane conduction (membrane permeability). The effect of the nicotine-containing EAC rapidly falls away following a buffer wash. **(B)** In contrast, only minor changes of the membrane capacitances are observed in the same tBLMs, suggesting permeability changes aren't related to large membrane structural changes..... 60

Figure 2.6 Cardiac VCAM1, ICAM1, and CD31 mRNA expression following treatment of mice with e-cigarettes with or without nicotine. RT-qPCR was performed on the left ventricle of mice exposed to ambient air (SHAM) or e-Cig aerosol (0 mg, 18 mg nicotine). **(A)** FKBPL. **(B)** CD31. **(C)** VCAM-1. **(D)** ICAM-1. All data expressed as mean fold change \pm SEM (n = 5–9). One-way ANOVA with Bonferroni post-test was used for statistical analysis, * p < 0.05 versus Sham. 62

Figure 2.7 (A) Immunohistochemical on seven-week-old Balb/c female mice left ventricle sections (Scale bar = 20 μ m). Mice were treated in 3 groups: SHAM

(ambient air), 0 mg (no nicotine), and 18 mg (nicotine) treatment groups. Sections were stained for FKBPL (green), CD31 (red), and DAPI (blue) and images were taken at 20×. **(B)** FKBPL staining intensity was quantified as the mean greyscale value in three images per sample, ** p < 0.005 (SHAM vs. 18 mg). **(C)** CD31 staining intensity was quantified as the mean greyscale value in three images per sample, * p < 0.05 (SHAM vs. 18 mg). Results are expressed as mean ± SEM (n = 5–9) compared to SHAM. One-way ANOVA with Kruksal-Wallis post-tests was used for statistical analysis..... 63

Figure 3.1 . Cardiac fibrosis measured by collagen deposition and collagen 1A1 gene expression is reduced in low FKBPL settings. (A) Percentage of collagen deposition within the left ventricle from wild type (*Fkbp1^{+/+}*) or FKBPL transgenic (*Fkbp1^{+/-}*) mice, was assessed following picosirius staining. Five sections per heart were imaged at 40x magnification and area of cardiac fibrosis represented by collagen ratio determined (n≥8, unpaired t-test, ***<0.001). RNA was extracted from murine wild type (*Fkbp1^{+/+}*) or FKBPL transgenic (*Fkbp1^{+/-}*) left ventricle and quantitative polymerase chain reaction (qPCR) performed to determine the mRNA expression of six pro-fibrotic genes: **(B)** type I collagen alpha chain (Col1A1) **(C)** type III collagen alpha chain 1 (Col 3A1), **(D)** fibroblast specific protein (FSP-1), **(E)** periostin (POSTN), **(F)** connective tissue growth factor (CTGF), **(G)** fibronectin (FN-1). The mRNA expression was normalised to the house-keeping gene, β-actin. All data was expressed as mean fold change ± SEM; n≥8, unpaired t-test or Mann-Whitney test, *p<0.05. 97

Figure 3.2 Optimising 3D bioprinted cardiac fibrosis model through extracellular matrix selection. Fetal fibroblast cells (HFF08) were bioprinted using RASTRUM platform within hydrogels of varying stiffnesses (Matrix 1; Px01.31P,~0.7kPa, Matrix 2; Px01.29P,~0.7kPa, Matrix 3; Px03.29P,~3kPa) and containing different cardiac peptide composition to mimic fibronectin, β-laminin, collagen I, into a 96-well plate. Treatments were added on day 4 and 7 to include DMOG (1mM) and/or TGF-β (1ng/ml) and/or AD-01 (100nM). After 14 days in culture a live/dead viability assay was performed. Calcein AM dye (green) was used to stain live cells whereas ethidium homodimer-III (red) to stain dead cells. **(A)** Representative images of 3D fibroblast networks after 14 days in culture in the presence of various treatment combinations and within three different matrix types. The networks were captured on IncuCyte at 10x magnification. Total area of live cells **(B)**, total area of dead cells **(C)** and the live-to-dead cell ratio, between matrix 1 and 2 were determined using IncuCyte analysis software **(D)**. Data is presented presented as mean ± SEM; n=4-5, quadruplicates; unpaired t-test; **p=0.006..... 99

Figure 3.3 Optimising 3D bioprinted cardiac fibrosis model through extracellular matrix selection. Fetal fibroblast cells (HFF08) were bioprinted using RASTRUM platform within hydrogels of varying stiffnesses (Matrix 1; Px01.31P, ~0.7kPa, Matrix 2; Px01.29P,~0.7kPa, Matrix 3; Px03.29P,~3kPa) and containing different cardiac peptide composition to mimic fibronectin, β-laminin, collagen I, into a 96-well plate. Treatments were added on day 4 and 7 to include DMOG (1mM) and/or TGF-β (1ng/ml) and/or AD-01 (100nM). After 14 days in culture a live/dead

viability assay was performed. Calcein AM dye (green) was used to stain live cells whereas ethidium homodimer-III (red) to stain dead cells. **(A)** Representative images of 3D fibroblast networks after 14 days in culture in the presence of various treatment combinations and within three different matrix types. The networks were captured on IncuCyte at 10x magnification. Total area of live cells **(B)**, total area of dead cells **(C)** and the live-to-dead cell ratio, between matrix 1 and 2 were determined using IncuCyte analysis software **(D)**. Data is presented as mean \pm SEM; n=3, quadruplicates; unpaired t-test; **p=0.006..... 101

Figure 3.4 Fibroblast cell proliferation in 3D culture over time and in the presence of various treatments. HFF08 cells were 3D bioprinted within Matrix 2 (Px01.29P, ~0.7kPa) in a 96-well plate and allowed to form networks. Treatments were added on day 4 and 7 to include DMOG (1mM) and/or TGF- β (1ng/ml). AD-01 (100nM) treatment was added on day 7 and the cells were left in 3D culture for the total of 14 days. On Day 3, 7, 11 and 14, cells were washed with PBS before adding alamarBlue-containing foetal fibroblast media and incubated for 16 hours at 37°C before fluorescence was read on the plate reader at 530 nm excitation and 590 nm emission. The absorbance for treatments was normalised to control. n=4-6, quadruplicates; one-way ANOVA (repeated measures); *p<0.05, **p<0.01, ***p<0.001 102

Figure 3.5 3D network formation within cardiac fibroblast model following various pro-fibrotic treatments. Following 14 days in 3D culture, fibroblast networks were phase contrast imaged using the Incucyte Live-Cell Analysis System (Sartorius AG, Germany) at 10x magnification for network formation analysis. Images were analysed and quantified in Image J, using the Angiogenesis Analyzer to detect and map the nodes, branch length and number of networks. **(A)** Representative images showing phase contrast and tracing of the networks. **(B)** The number of junctions and **(C)** the total branch length were quantified normalised to control. n \geq 8; one-way ANOVA with Sidak's multiple comparison test; *p<0.05; **p<0.01, ***p<0.001; ****p<0.0001..... 104

Figure 3.6 Immunofluorescence staining of FKBPL, vimentin and α -SMA in 3D bioprinted cardiac fibrosis model. Following 14 days in 3D cell culture, fibroblast networks were fixed in 4% paraformaldehyde, blocked and incubated with primary antibodies: FKBPL, vimentin and α -SMA, overnight. The following day cells in 3D culture were washed and incubated with secondary antibody overnight before images were taken. Imaging was performed on the Nikon Ti Live inverted wide-field microscope (Nikon, Japan) at 20x magnification with three random images per well taken. Z stacks (0.2 μ m optical slices) were acquired using a 0.5 AU pinhole. Fluorescence intensity per antibody, vimentin **(B)**, FKBPL **(C)** indicating protein expression per treatment was quantified relative to the control group and normalised to DAPI using Image J. n \geq 7; one-way ANOVA with Tukey multiple comparison test; *p<0.05; **p<0.01, ***p<0.001; ****p<0.0001. 106

Figure 3.7 FKBPL and cardiac fibrosis genes expression following exposure of HFF08 fibroblast cells to pro-fibrotic and hypoxia stimuli, and FKBPL peptide mimetic, AD-01. HFF08 cells were seeded at 0.2×10^5 cells/well overnight before

treatments were added for 24 h. These included pro-fibrotic stimuli, TGF- β (10ng/ml) and/or hypoxia stimuli, DMOG (1mM) with or without FKBPL peptide mimetic, AD-01 (100nM). Following 24-hour treatment, RNA was extracted and *Fkbpl* (**A**), postin (*Postn*; **B**), fibroblast specific protein (*Fsp-1*; **C**), connective tissue growth factor (*Ctgf*; **D**), type I collagen alpha chain 1 (*Col1a1*; **E**) and matrix metalloproteinase-2 (*Mmp-2*; **F**), gene expression quantified by RT-qPCR. Expression of target mRNA was normalised to housekeeping gene β -actin or 18S. N=3; one-way ANOVA with post-hoc multiple comparisons test, *p<0.05; **p<0.01, ***p<0.001; ****p<0.0001. **108**

Figure 3.8 Cardiac fibrosis genes expression following FKBPL knockdown and treatment with pro-fibrotic stimuli, TGF- β , and FKBPL-peptide mimetic, AD-01.

HFF08 cells were seeded at 0.2×10^5 cells/well overnight before FKBPL or non-targeting (NT) siRNA was used for transfection of HFF08 cells for 24 h followed by 24 h of treatment with TGF- β (10ng/ml) alone or in combination with AD-01 (100nM). Subsequently, RNA was extracted and *Fkbpl* (**A**), postin (*Postn*; **B**), fibroblast specific protein (*Fsp-1*; **C**), connective tissue growth factor (*Ctgf*; **D**), type I collagen alpha chain 1 (*Col1a1*; **E**) and matrix metalloproteinase-2 (*Mmp-2*; **F**), gene expression quantified by RT-qPCR. Expression of target mRNA was normalised to housekeeping gene β -actin or 18S. N=3; two-way ANOVA with post-hoc multiple comparisons test, *p<0.05; **p<0.01, ***p<0.001; ****p<0.0001. **110**

Figure 3.9 FKBPL and α -SMA protein expression in both normal and low FKBPL settings following exposure of HFF08 fibroblast cells to pro-fibrotic and hypoxia stimuli, with or without FKBPL peptide mimetic, AD-01.

HFF08 cells were seeded at 0.2×10^5 cells/well overnight before treatments were added or FKBPL/NT siRNA transfection performed, for 24 h. The treatments included pro-fibrotic stimuli, TGF- β (10ng/ml) and/or hypoxia stimuli, DMOG (1mM) with or without FKBPL peptide mimetic, AD-01 (100nM). Following 24-h treatment in both untransfected (**A&B**) and transfected cells (**C&D**), protein was extracted for Western blotting and membrane was probed with FKBPL (**A&C**) and α -SMA (**B&D**) antibodies. The protein band intensity was determined using Image J. Protein expression was normalised to GAPDH and control. N \geq 3; one-way ANOVA (**A&B**) or two-way ANOVA (**C&D**) with post-hoc multiple comparisons test, *p<0.05..... **112**

Figure 3.10 The effect of FKBPL knockdown or mimic and profibrotic/hypoxic treatment on monocyte adhesion to fibroblast cells.

(**A**) HFF08 fibroblast cells were seeded (0.2×10^5 cells/well) and either treated the following day with TGF- β (10ng/ml), and/or DMOG (1mM) \pm AD-01 (100nM) for 24 h or (**B**) transfected with FKBPL/NT siRNA for 24 h before TGF- β (10ng/ml) alone or with AD-01 (100nM) added for a further 24 h. For both conditions, after treatments, HFF08 cells were co-incubated with calcein green AM labelled THP-1 (human monocytic cells) and allowed to attach for 30 mins at 37°C. Fluorescent cells were captured using Incucyte and quantified in ImageJ before being normalised to control. Data presented as mean \pm SEM, (A-B); n=5; one-way ANOVA with post-hoc multiple comparison test..... **113**

Figure 4.1 Summary of the study workflow and the number of included studies.

A. Workflow of the systematic search according to PRISMA guidelines. **B.** Summary

quality assessment of included studies independently evaluated using the QUADAS-2 tool. **C.** Outcomes of quality assessment of each included study. HFpEF: heart failure with preserved ejection fraction; LVEF: left ventricular ejection fraction; PRISMA: Preferred Reporting Items for Systematic reviews and Meta-Analyses; QUADAS-2: Quality Assessment for Diagnostic Accuracy Studies-2..... **142**

Figure 4.2 Diagnostic assessment of NT-proBNP in HFpEF using a bivariate, random-effects model. A. Forest plot of 12 studies that investigated the diagnostic performance of NT-proBNP in HFpEF, with sensitivity and specificity reported. **B.** Forest plot of $\ln(\text{DOR})$ related to the diagnostic accuracy of NT-proBNP in HFpEF. **C.** Plot of the HSROC curve showing the estimated pooled diagnostic accuracy. **D.** Plot of the HSROC curve showing the 95% CI of each study that evaluated the diagnostic accuracy of NT-proBNP in HFpEF. AUC: area under the curve; CI: confidence interval; FN: false negative; FP: false positive; HFpEF: heart failure with preserved ejection fraction; HSROC: hierarchical summary of receiver operating characteristic; $\ln(\text{DOR})$: natural logarithm-transformed diagnostic odds ratio; NT-proBNP: N-terminal pro-B-type natriuretic peptide; TN: true negative; TP: true positive. **144**

Figure 4.3 Diagnostic assessment of BNP in HFpEF using a bivariate, random-effects model. A. Forest plot of seven studies that investigated the diagnostic performance of BNP in HFpEF, with sensitivity and specificity reported. **B.** Forest plot of $\ln(\text{DOR})$ related to the diagnostic accuracy of BNP in HFpEF. **C.** Plot of the HSROC curve showing the estimated pooled diagnostic accuracy. **D.** Plot of the HSROC curve showing the 95% CI of each study that evaluated the diagnostic accuracy of BNP in HFpEF. AUC: area under the curve; BNP: B-type natriuretic peptide; CI: confidence interval; FN: false negative; FP: false positive; HFpEF: heart failure with preserved ejection fraction; HSROC: hierarchical summary of receiver operating characteristic; $\ln(\text{DOR})$: natural logarithm-transformed diagnostic odds ratio; TN: true negative; TP: true positive. **146**

Figure 4.4 Diagnostic assessment of Gal-3 in HFpEF using a bivariate, random-effects model. A. Forest plot of three studies that investigated the diagnostic performance of Gal-3 in HFpEF, with sensitivity and specificity reported. **B.** Forest plot of $\ln(\text{DOR})$ regarding the diagnostic accuracy of Gal-3 in HFpEF. **C.** Plot of the HSROC curve showing the estimated pooled diagnostic accuracy. **D.** Plot of the HSROC curve showing the 95% CI of each study that evaluated the diagnostic accuracy of Gal-3 in HFpEF. AUC: area under the curve; CI: confidence interval; FN: false negative; FP: false positive; Gal-3: galectin-3; HFpEF: heart failure with preserved ejection fraction; HSROC: hierarchical summary of receiver operating characteristic; $\ln(\text{DOR})$: natural logarithm-transformed diagnostic odds ratio; TN: true negative; TP: true positive. **147**

Figure 4.5 Diagnostic assessment of ST2 in HFpEF using a bivariate, random-effects model. A. Forest plot of three studies that investigated the diagnostic performance of ST2 in HFpEF, with sensitivity and specificity reported. **B.** Forest plot of $\ln(\text{DOR})$ regarding the diagnostic accuracy of ST2 in HFpEF. **C.** Plot of the HSROC curve showing the estimated pooled diagnostic accuracy. **D.** Plot of the

HSROC curve showing the 95% CI of each study that evaluated the diagnostic accuracy of ST2 in HFpEF. AUC: area under the curve; CI: confidence interval; FN: false negative; FP: false positive; HFpEF: heart failure with preserved ejection fraction; HSROC: hierarchical summary of receiver operating characteristic; ln(DOR): natural logarithm-transformed diagnostic odds ratio; ST2: suppression of tumorigenesis-2; TN: true negative; TP: true positive..... 148

Figure 4.6 H9C2 cardiomyocyte cell size measurements following treatment with (i) Ang-II (100 nM), (ii) AD-01 (100 nM) and (iii) Ang-II (100 nM) + AD-01 (100 nM). (A) Relative nucleus size 24 h after treatments. (B) Relative nucleus size 48 h after treatments. (C) Relative cell size 24 h after treatments. (D) Relative cell size 48 h after treatments. Results expressed as Mean ± SEM (n = 6); One-way ANOVA with Tukey's post-hoc; ** p < 0.01, **** p < 0.0001 against control; Ang-II—angiotensin II; AD-01—FKBPL-based therapeutic peptide..... 173

Figure 4.7 H9C2 cardiomyocyte mRNA expression of FKBPL, BNP and ANP following Ang-II and/or AD-01 treatment. H9C2 cells were exposed to treatment groups (i) Ang-II (100 nM), (ii) AD-01 (100 nM) and (iii) Ang-II (100 nM) + AD-01 (100 nM) for 24 or 48 h before RNA lysates were collected and qPCR performed. (A) FKBPL mRNA expression at 24 h; (B) BNP mRNA expression at 24 h; (C) ANP mRNA expression at 24 h; (D) FKBPL mRNA expression at 48 h; (E) BNP mRNA expression at 48 h; (F) ANP mRNA expression at 48 h. Results expressed as Mean ± SEM (n ≥ 4), One-way ANOVA with Tukey's post-hoc. * p < 0.05. Ang-II—angiotensin II; AD-01—FKBPL-based therapeutic peptide..... 175

Figure 4.8 FKBPL protein expression in H9C2 cardiomyocytes following Ang-II and/or AD-01 treatment. H9C2 cells were exposed to treatment groups (i) Ang-II (100 nM), (ii) AD-01 (100 nM) and (iii) Ang-II (100 nM) + AD-01(100 nM) for 48 h. Relative FKBPL expression was measured. Results expressed as Mean ± SEM (n = 3); One-way ANOVA with Tukey's post-hoc; * p < 0.05 against control; # p < 0.05 against Ang-II group. Ang-II—angiotensin II; AD-01—FKBPL-based therapeutic peptide. 176

Figure 4.9 FKBPL plasma protein concentrations in patients with HFpEF. Patients were divided into subgroups based on HFpEF symptoms: HCM (n = 15), chronic HFpEF (n = 9) and acute decompensated HFpEF (n = 9). (A) FKBPL plasma concentration of combined HFpEF subgroups compared to controls (n = 40). (B) FKBPL plasma concentration within HFpEF subgroups, compared to controls. Results expressed as Mean ± SD; One-way ANOVA with Tukey's post-hoc; * p < 0.05, ** p < 0.005. HCM—hypertrophic cardiomyopathy; HFpEF—chronic heart failure with preserved ejection fraction; AD-HFpEF—acute decompensated HFpEF. 177

Figure 4.10 Biomarker plasma protein concentrations in subgroups of HFpEF. Patients were divided into subgroups based on HFpEF symptoms, HCM (n = 15), chronic HFpEF (n = 9) or acute decompensated HFpEF (n = 9). (A) NT-proBNP plasma concentration of HFpEF subgroups measured by ELISA. (B) FKBPL plasma concentration of HFpEF subgroups measured by ELISA. (C) Gal-3 plasma concentration of HFpEF subgroups measured by ELISA. Results expressed as Mean

± SEM, One-way ANOVA with Tukey’s post-hoc. HCM—hypertrophic cardiomyopathy; HFpEF—chronic heart failure with preserved ejection fraction; AD-HFpEF—acute decompensated HFpEF..... 178

Figure 5.1 PRISMA flow diagram of search methodology 201

Figure 5.2 Distribution of adult participants according to country of study.
 United States of America (*n* = 9), Denmark (*n* = 3), International (*n* = 3), Italy (*n* = 3), China (*n* = 2), Europe (*n* = 2), France (*n* = 2), Spain (*n* = 2), Taiwan (*n* = 2). The following countries were not represented in the figure (*n* = 1): Australia, Egypt, England, Germany, Greece, Iran, Ireland, Japan, Netherlands, Norway, Romania, Russia, Sweden, Turkey, and Ukraine. 208

Figure 6.1 Schematic representation of the effect of E-cigarette aerosol directly on endothelial cell function or after first-pass metabolism by epithelial lung cells. Aerosolised toxic compounds from e-Cigs can incite endothelial cell activation. Resultant effects of decreased cell viability, increased ROS, increased CAM expression, and impaired angiogenesis follow. After first pass metabolism of epithelial cells, an enhanced effect may be pronounced. 238

List of Tables

Table 2.1 qPCR primers and nucleotide sequence	51
Table 3.1 Human primers forward and reverse sequencing.....	93
Table 3.2 Human primers forward and reverse sequencing.....	94
Table 4.1 Characteristics of included studies	143
Table 4.2 Patient group and clinical characteristics	170
Table 4.3 Correlations between FKBPL and echocardiography parameters. .	179
Table 4.4 Pearson’s correlations between FKBPL, NT-proBNP and Gal-3.....	180
Table 5.1 Descriptive characteristics of included cardiac remodelling studies.	202
Table 5.2 Potential Biomarkers Identified in adults.....	209

Abbreviations

ACE	Angiotensin converting enzyme
ACE-Is	Angiotensin-converting enzyme inhibitors
AGE	Advanced glycation end product
AHA	American Heart Association
Akt	Protein kinase B
Ang-II	Angiotensin II
BH4	(6R)-5,6,7,8-tetrahydrobiopterin
BNP	Brain natriuretic peptide
CAM	Cellular adhesion molecules
CF	Cardiac fibroblasts
cGMP	Guanosine 3',5'-cyclic monophosphate
CHD	Congestive heart disease
CTGF	Connective tissue growth factor
CVD	Cardiovascular disease
dbCM	Diabetic cardiomyopathy
DM	Diabetes mellitus
e-Cig	Electronic cigarette
ECM	Extracellular matrix
eNOS	Nitric oxide synthase
ESC	European Society of Cardiology
FKBPL	FK506-binding protein-like
FKBPs	FK506-binding proteins
Gal-3	Galectin-3
GLUT4	Glucose transporter type 4
H₂O₂	Hydrogen peroxide
HF	Heart failure
HFmrEF	Heart failure with mid-range ejection fraction
HFpEF	Heart failure with preserved ejection fraction

HFrEF	Heart failure with reduced ejection fraction
HIF	Hypoxia inducible factor
HSP90	Heat shock protein 90
Hs-TnT	High sensitivity troponin
ICAM-1	Intracellular adhesion molecule1
IHD	Ischemic heart disease
IL-1	Interleukin-1
IL-6	Interleukin-6
LDL	Low-density lipoproteins
LOX-1	Oxidized LDL receptor
LV	Left ventricular
LVEF	Left ventricular ejection fraction
MAPK	Mitogen-activated protein kinases
MCF	Myofibroblasts
MI	Myocardial infarction
MMPs	Matrixmetalloproteinases
MRAs	Mineralocorticoid receptor antagonists
mTOR	Mammalian target of rapamycin
nAChR	nicotinic acetylcholine receptor
NADPH	Nicotinamide adenine dinucleotide phosphate
NF-κB	Nuclear factor kappa light chain enhancer of activated B cells
NO	Nitric oxide
NOX	Nicotinamide adenine dinucleotide phosphate oxidase
NT-proBNP	N-terminal-pro-B-Type natriuretic peptide
NYHA	New York Heart Association
O₂⁻	Superoxide anion
ONOO⁻	Peroxynitrite
PDGF	Platelet derived growth factor
PG	Propylene glycol
PGFs	Platelet growth factors
PI3K	Phosphatidylinositol 3-kinase

RAAS	Renin-angiotensin-aldosterone system
RAGE	Receptor for advanced glycation end products
ROS	Reactive oxygen species
SGLT2	Sodium–glucose cotransporters 2
SOD	Superoxide dimutase
ST2	Suppression of tumorigenicity 2
STAT3	Signal transducers and activators of transcription 3
T1D	Type I Diabetes mellitus
T2D	Type 2 Diabetes mellitus
TGF-β	Transforming growth factor beta
Th	T helper
TLR	Toll-like receptor
TNF-α	Tumour necrosis factor alpha
TPR	Tetra trico peptide repeat
VCAM-1	Vascular cell adhesion molecule 1
VEGF	Vacular endothelial growth factor
VG	Vegetable glycerin
vSMC	Vascular smooth muscle cells
α-SMA	alpha smooth muscle actin

Abstract

Cardiovascular Diseases (CVDs) are the leading cause of mortality worldwide and hold a huge socioeconomic burden. Clinical manifestations of CVD are often heterogeneous and caused by various risk factors and co-morbidities that can lead to patient mortality and heart failure (HF). This multifactorial nature of CVD creates difficulty in determining the exact mechanisms of CVD pathophysiology and results in poor patient prognosis. Thus, in this thesis, we aim to elucidate key mechanisms in CVD pathophysiology including the emerging role of an immunophilin protein, FK506-binding protein like (FKBPL).

E-cigarettes (e-Cigs) have quickly gained popularity amongst all age groups and have a public perception that they are less harmful than tobacco cigarettes due to the lack of research on their health effects. In this study (Chapter 2), we examined the effect of tobacco flavoured e-Cig condensate (EAC)(±nicotine) on human coronary artery endothelial cells (HCAEC) before and after first pass metabolism by epithelial lung cells, and the impact of e-Cig aerosol on the heart in a mouse model. It was determined that, *in vitro*, EAC significantly decreased cell viability ($p < 0.05 - 0.001$), increased ROS production ($p < 0.01 - 0.0001$), and increased cellular adhesion molecule expression (ICAM1, $p < 0.01$). *Ex vivo* experiments showed an increase in FKBPL and ICAM-1 mRNA expression ($p < 0.05$) and increased FKBPL ($p < 0.005$) and CD31 protein expression ($p < 0.05$) in conditions containing nicotine. Thus, it was shown that e-Cigs have negative effects upon endothelial cell health that can contribute to endothelial dysfunction and aberrant angiogenesis potentially leading to CVD.

Cardiac fibrosis is a condition characterised by increased collagen deposition into the extracellular matrix (ECM) and pathological remodelling of the myocardium, often

preceding HF. In Chapter 3, the role of FKBPL within cardiac fibrosis was elucidated for the first time, using human fetal fibroblasts, which were treated with hypoxic (DMOG, 1mM) and fibrotic stimuli (TGF- β , 10ng/ml) in 2D and 3D cell culture. FKBPL-based peptide mimetic, AD-01 (100nM), was used to determine its therapeutic potential in conjunction with FKBPL-mediated mechanism in cardiac fibrosis. Picosirius staining (for collagen fibres) and qPCR were performed *ex vivo* using left ventricles (LV) from 26-week-old *fkbp1*^{+/-} transgenic or wild type mice (n \geq 8 per group). Staining revealed significantly decreased deposition of collagen within the LV tissues of the *fkbp1*^{+/-} transgenic mice, and decreased expression of collagen 1a1 (*col1a1*) mRNA. The 2D model similarly exhibited an increased expression of *col1a1* (p<0.05), following TGF- β exposure, that was potentiated in the presence of AD-01 (p<0.0001) and also increased *mmp2* mRNA (p<0.05) expression. Following the knockdown of FKBPL, α -SMA was reduced, suggesting, together with the results obtained with AD-01, that low FKBPL expression may have cardioprotective effects in cardiac fibrosis. Innovative 3D bioprinted model of cardiac fibrosis led to formation of stable networks, which increased in the presence of profibrotic stimuli (p<0.05-0.0001) in conjunction with FKBPL downregulation, which was significant in hypoxic conditions + AD-01 (p<0.05).

Heart failure with preserved ejection fraction (HFpEF) is complex in its multifactorial pathophysiology and the mechanisms involved are less understood than other HF subtypes, and thus has no effective treatments. Firstly, in Chapter 4, we performed systematic review and meta-analysis of the current biomarkers used in the diagnosis of HFpEF. Through the assessment of their sensitivity and specificity, the natriuretic peptides, NT-proBNP and BNP, revealed to be the most reliable markers of HFpEF. Secondly, as part of the same Chapter 4, we examined the role of FKBPL in HFpEF

pathogenesis and its potential as a biomarker. *In vitro*, rat cardiomyoblasts were treated with hypertensive stimulus, Angiotensin-II, Ang-II, to induce a model of cardiac hypertrophy, and additionally, plasma samples from HFpEF patients were used to measure the concentration of NT-proBNP, Gal-3, and FKBPL. Individually, AD-01 and Ang-II both induced cardiac hypertrophy, however, when combined, this effect was mitigated. Plasma sample measurements revealed increased FKBPL in HFpEF patients, however FKBPL was unable to stratify between the subtypes of HFpEF. Thus, in this study we propose the possibility of a negative feedback mechanism of AD-01 within cardiac hypertrophy mediated by FKBPL, and its potential as a biomarker and therapeutic target in HFpEF.

In the final Chapter 5, we performed a scoping review on current diagnostic and prognostic biomarkers for cardiac remodelling in patients with diabetes mellitus (DM). Cardiac remodelling precedes the development of cardiac fibrosis, where identification of the initial symptoms could help construct preventative measures and improve patient outcomes. Furthermore, in this population of patients, DM is a common comorbidity of CVD that represents an amplified risk factor for the development of HF and cardiovascular mortality. In this scoping review we systematically screened databases for this group of patients and recorded the biomarkers that were currently measured. We identified NT-proBNP as the most clinically used biomarker although not specific to cardiac remodelling. The biomarkers showing potential in identifying early sign of cardiac remodelling in DM included inflammatory and fibrotic markers such as galectin-3, cardiac troponin, and C-reactive protein. Further research into the mechanisms of cardiac remodelling and fibrosis is required to identify a potential specific biomarker and therapeutic target towards personalised medicine.

Overall, in this thesis, adverse impact of E-Cigs on cardiovascular health that increases the expression of anti-angiogenic FKBPL and inflammatory markers, was demonstrated. FKBPL shows promising therapeutic target potential in cardiac hypertrophy and fibrosis and could be used in the diagnosis of HFpEF in conjunction with other well-established biomarkers including NT-pro-BNP and Gal-3. Further research is needed to specifically elucidate the role of cardiac remodelling biomarkers including FKBPL in DM population.

Chapter 1

Introduction

Introduction

1.1 Cardiovascular Disease

Cardiovascular disease (CVD) including heart disease are uniform terms describing conditions of the heart and blood vessel¹⁻³. In CVDs, the presence of one condition is commonly accompanied by another due to overlapping mechanisms between risk factors and co-morbidities⁴. The most common causes of mortality in CVD are ischemic heart disease (IHD), stroke, and congestive heart disease (CHD)⁵. Genetic and non-modifiable risk factors such as age, gender, and family history have been implicated in the pathogenesis of CVD's and its related conditions, however, more relevant are the modifiable risk factors that are within our control⁶. The development of CVD is largely associated with modifiable behavioural lifestyle risk factors including tobacco smoking, obesity, high cholesterol, and high blood pressure, and physical inactivity^{1,5,7}. Recently, E-cigarettes have exponentially increased in use both recreationally, and as an alternative to tobacco smoking, with recent research describing their adverse health effects, they are emerging as a new modifiable risk factor for CVD³. The incidence of CVDs have sharply risen in the last few decades due to the societal transition to a technology driven lifestyle associated with unhealthy and sedentary habits^{3,6,8}. Resultant of this lifestyle, people are generally more susceptible to developing CVD often due to co-morbidities including diabetes mellitus (DM), hypertension, and atherosclerosis⁶.

Symptoms of CVDs are often silent, highly variable and are not indicative of underlying disease until the point of a heart attack or stroke, that can, then, uncover or lead to heart failure (HF)^{9,10}. The symptoms of a myocardial infarction (MI) or heart attack include chest pains, nausea, dyspnea, and fainting, whereas common stroke

symptoms include dizziness, numbness of one side of the body, speech slurring, confusion, and unconsciousness^{9,10}. Treatment options for CVDs remain difficult due to the multifactorial nature of the disease, but the main strategy is centered on the reduction of impact from independent and modifiable risk factors (e.g. hypertension, hypercholesterolemia, obesity, smoking), or comorbidities (e.g. diabetes mellitus, chronic kidney disease, chronic heart failure, peripheral artery disease) and acute care (e.g. MI, stroke, acute heart failure) if necessary^{9,11,12}.

Prevention and treatment of CVD involve direct lifestyle changes of the individual. Increased physical activity, improved diet, and cessation of smoking reduce the risk of cardiovascular events and improve outcomes³. Hypertension is an established independent risk factor of CVD that is also indicative of additional comorbidities. Together, these risk factors have compounding effects compared to their individual counterparts, hence pharmacotherapy of CVD involves several classes of drugs that commonly ameliorate the stress on the heart and effectively reduce blood pressure and these associated risk factors¹³. These medication classes include: angiotensin-converting enzyme (ACE) inhibitors, beta-blockers, calcium channel blockers, diuretics, and statins. ACE inhibitors are prescribed for patients with high blood pressure and heart failure, they inhibit angiotensin II (Ang-II) levels inducing vasodilation, reduction in blood pressure and hypertrophogenic action on the heart, hence alleviating strain on the heart¹⁴. Beta-blockers are commonly prescribed in patients who have experienced cardiac arrhythmias or MI. Beta-blockers are not as effective at reducing blood pressure as ACE inhibitors however can reduce blood pressure through decreasing the heart rate and force of contraction that can prevent future cerebral and myocardial infarctions¹⁴. Calcium channel blockers are used to relax blood vessels through vasodilation and lower the force of contraction through

inhibiting the influx of cellular calcium, effectively lowering blood pressure, peripheral resistance, and/or cardiac output, preserving the heart function¹⁴. Diuretics regulate electrolyte and water homeostasis by inducing diuresis hence removing accumulated fluids (i.e. pulmonary or ankle oedema) through urine, which can also lead to a fall in blood pressure (i.e. thiazide diuretics), and cardiac workload¹⁴. Statins are one type of lipid lowering agents that inhibit the production of low-density lipoproteins (LDL) and total cholesterol within the liver by inhibiting HMG CoA reductase enzyme; extensive clinical trials have shown that statins can reduce the incidence of fatal and non-fatal cardiovascular events¹³. Also, the combination of statins and anti-hypertensives demonstrated an increased protection from cardiovascular events¹³.

Despite the fact that CVD is the leading cause of death, it is becoming even more common and widespread globally¹⁵. While only accounting for 10% of all worldwide deaths in the 20th century, CVDs are currently accounting for 31% of all deaths^{1,3}. In Australia alone, CVD-related hospitalisations and deaths accounted for 11% and 27% of all patients, respectively, in 2019¹⁶. From an economic viewpoint, the financial burden on the Australian health system was 8.7% or \$11.8 billion dollars¹⁷. Thus, with the epidemiological rise in CVDs and their socioeconomic burden across the world, they present a pending global issue. Nevertheless, the pathogenic mechanisms leading to various CVDs are still not fully understood, impeding the development and utilization of effective therapies. Whilst the close management of modifiable risk factors is important, elucidation of disease and therapeutic mechanisms will inform the development of future and improved monitoring strategies and therapies that could reduce the burden of CVD and prevent premature death¹⁸.

1.1.1 Endothelial Dysfunction in CVD

The endothelium is a single cell layer lining the inner surface of blood vessels, acting as a semipermeable barrier between the blood and vessel wall^{19–22}. The endothelial cells localised on the innermost surface of the vasculature allow for unique physical and neurohormonal responses, such as modulating vascular tone, cellular adhesion, inflammation, platelet aggregation, fibrinolysis, and hormone trafficking^{23,24}. Systemic and persistent inflammation induced by upregulation of inflammatory mediators that causes increased endothelial cell activation and subsequent endothelial dysfunction, can attribute to the pathogenesis of CVD. This is observed in atherosclerosis, a common underlying condition that can lead to HF, arterial complications and aneurysms^{22,25}. Exacerbated by CVD risk factors including DM, hypertension, smoking and hyperlipidaemia, endothelial dysfunction is defined as a disruption to normal endothelial cell homeostasis that can lead to impaired permeability of the endothelium^{22,26}. Subsequent effects of endothelial dysfunction result in impaired vascular function, pro-inflammatory, and prothrombic activity. Consequently, this leads to arterial remodelling, hypertension^{21,23}, and disrupted angiogenesis, all of which are signs of early atherogenesis and conditionally associated with CVD^{20,27,28}.

The maintenance of adequate endothelial function relies extensively on the balance between endothelial nitric oxide (NO) and free radicals or reactive oxygen species (ROS), where cardiovascular risk factors are known to disrupt this balance^{22,23,29}. NO synthesised from L-arginine via nitric oxide synthase (eNOS), plays an important role in endothelial homeostasis and CVD pathophysiology, exhibiting anti-inflammatory, anti-oxidative, anti-platelet aggregation effects, and vasodilation^{30,31}. An imbalance of these chemicals where there is elevated ROS production and depleted NO, results in

oxidative stress, and interferes with endothelial cell signalling and function leading to atherosclerosis^{22,31}. Nicotinamide adenine dinucleotide phosphate (NADPH) oxidase activity plays a key role in NO production where increased NADPH activity produces increased levels of superoxide anions (O_2^-) that exert oxidative stress on the endothelial cells^{30,31}. This process is noted as eNOS uncoupling in which eNOS monomers are unable to dimerise due to insufficient cofactors (6R)-5,6,7,8-tetrahydrobiopterin (BH4) and insufficient endothelial NO, hence leading to the production of O_2^- rather than NO³⁰. Excess O_2^- free radicals outweigh antioxidant molecules such as superoxide dismutase (SOD) and freely react with other molecules including hydrogen peroxide (H_2O_2) or peroxynitrite ($ONOO^-$) which also contribute to eNOS uncoupling³⁰. This process becomes cyclical, where the oxidative stress further increases the production of more free radicals, perpetuating the state of endothelial dysfunction.

Inflammation and oxidative stress are inextricably intertwined, with inflammation decreasing levels of biological NO, and oxidative stress increasing levels of pro-inflammatory mediators^{26,30}. In a pro-oxidative and pro-inflammatory state, inflammatory mediators (e.g. interleukin-1 (IL-1), interleukin-6 (IL-6), tumour necrosis factor alpha (TNF- α)), chemoattractant molecules (vascular cell adhesion molecule 1 (VCAM-1) and intracellular adhesion molecule 1 (ICAM-1)), and immune cells (neutrophils, macrophages, and T cells) are all upregulated through signalling of the critical nuclear factor kappa light chain enhancer of activated B cells (NF- κ B) pathway³². Cellular adhesion molecules, ICAM-1 and VCAM-1, are crucial in the initial inflammatory response in atherogenesis, promoting the invasion of monocytes and T lymphocytes in the subendothelial space, then transforming into macrophages that engulf lipoproteins to form lipid-loaded foam cells, beginning the formation of the

atherosclerotic plaque^{26,33}. Endothelin-1 and Ang-II are both potent vasoconstrictive and pro-oxidant molecules secreted by the endothelium and regulated by NO, which stimulate the oxidised LDL receptor (LOX-1) contributing to reduced eNOS expression and expression of CAMs^{26,31,34}. Following the formation of the atherosclerotic plaque, macrophages secrete growth factors including platelet derived growth factor (PDGF) and cytokines (IL-1) that increase vascular smooth muscle cell (vSMC) and interstitial collagen signalling and synthesis^{26,33}. SMCs migrate from the tunica media to the tunica intima, producing collagen and elastin that constitute the fibrous cap of the plaque, eventually leading to the protrusion of the plaque into the blood vessel lumen³³. Matrix metalloproteinases (MMPs), namely MMP-2 and MMP-9, are also activated in response to decreased NO bioavailability and can cause the break down of the fibrous cap, leading to rupturing, thrombus formation, and MI²⁶. Hence, inflammation and oxidative stress exacerbated by CVD risk factors are pivotal to the development of endothelial dysfunction and CVDs (Figure 1.1).

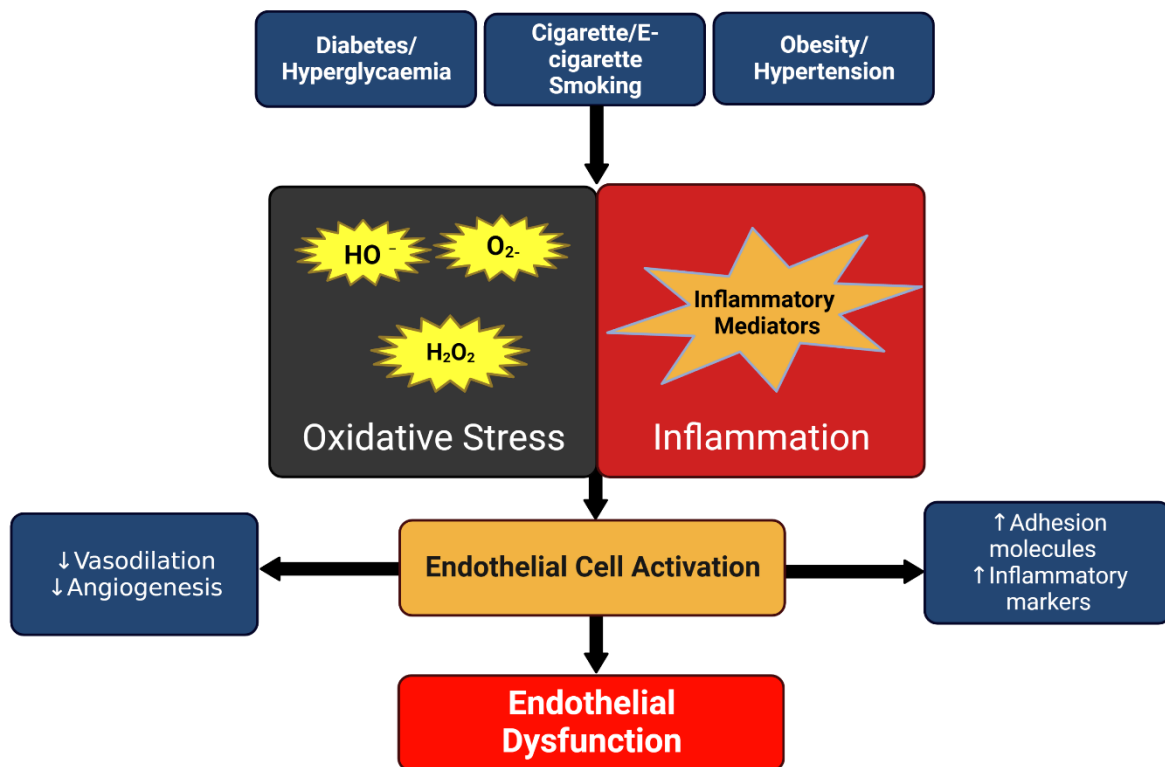


Figure 1.1 Mechanisms of different risk factors leading to endothelial cell dysfunction in CVD. Modifiable cardiovascular risk factors including diabetes mellitus, cigarette/e-cigarette smoking, and hypertension or obesity increase levels of oxidative stress and inflammatory mediators within endothelial cells. This can lead to endothelial cell activation, increasing inflammatory markers and adhesion molecule expression, decreasing vasodilation and angiogenesis before subsequent development of endothelial dysfunction. Created with BioRender.com.

1.1.2 E-Cigarettes as an emerging risk factor for CVD.

The electronic cigarette (e-Cig) is a smoking cessation device that has emerged as a form of nicotine replacement therapy in the recent decade; however, its effects on cardiac health are not well known³⁵. E-Cig design varies within the market, but all models contain a battery, e-liquid tank and an atomizer. When fired, the battery heats the metal atomizer to vaporize the liquid and deliver it as an aerosol. These devices typically use a flavoured liquid-based substance containing nicotine, known as e-liquid or e-juice. E-liquid can come in a plethora of flavours, but include the same bases; a mixture of propylene glycol (PG), vegetable glycerine (VG), and optionally, nicotine³⁶. Although initially targeted towards current smokers who aim to quit and advertised as safer alternative to tobacco cigarettes³⁷, a large amount of the user base are non-smokers and young adolescents, who are currently the largest demographic of e-Cig use³⁸. While e-Cigs do fulfil their purpose of smoking cessation, there is a debate whether these e-Cig devices are any better than traditional cigarette use³⁹.

E-Cig use has been associated with a perceived harmlessness due to the lack of combustible products and lack of harmful constituents that has been proven otherwise in recent studies⁴⁰. Research on the long term effects of smoking cigarettes and its cytotoxic effects are well documented, whereas e-Cig research is in its infancy³⁷. As a relatively new device, the long term effects have yet to be examined, however, acute studies have shown similar damaging effects between tobacco smoking and e-Cigs with potential implications in CVD. The pathophysiology of e-Cig and tobacco smoking-induced cardiovascular damage occurs through increased oxidative stress, inflammation, and cardiac sympathetic activity^{41,42}. E-Cig use results in an acute change in heart rate and blood pressure⁴¹ that may have an adverse effect on

endothelial function. As inflammation and oxidative stress are driving mechanisms in inducing endothelial dysfunction, previous studies have found e-Cig aerosol to have both proinflammatory and oxidative stress effects on endothelial cells *in vitro*, *in vivo*, and in patients⁴²⁻⁴⁴. Increased oxidative stress in e-Cig users has been attributed to increased levels of LDL oxidation, commonly presenting in people with diabetes mellitus and tobacco smokers⁴². In comparison to tobacco cigarettes, the components of e-Cig aerosol have shown comparable effects in terms of cytotoxicity and oxidative stress, possibly attributed to the constituents of e-liquid⁴⁵.

Notable concerns have arisen from the heated constituents of e-liquid (PG/VG, flavouring, nicotine) as a means of inducing systemic inflammation and oxidative stress, though advertised otherwise⁴². A closer inspection of the heated components of e-liquid through liquid and gas chromatography revealed trace amounts of carcinogenic compounds similarly present within tobacco smoke, fine particulate matter, and even metals^{40,46,47}. Namely, formaldehyde, acetaldehyde, and acrolein were found within the e-Cig aerosol, all three of which are known to be found in tobacco smoke and contribute to CVD pathogenesis⁴⁰.

Despite these findings, there remains large variabilities in the current studies surrounding e-Cig use with factors ranging from the device and e-liquid type, to personal behavioural habits^{42,48}. Studies have also been shown that between the comparison of e-Cigs and traditional cigarette use, although both with cardiotoxic effects, e-Cigs exhibited this to a lesser extent⁴⁹. Hence, with the discrepancy in e-Cig research findings and increasing adolescent market, there is an alarming need to elucidate the effects and mechanisms of e-Cig use on cardiovascular health.

1.1.3 Diabetes mellitus as a risk factor for CVD

Diabetes mellitus (DM) is a chronic metabolic disease characterised by hyperglycaemia where the body produces an insufficient amount of insulin (type 1 DM, T1D), or the cells do not appropriately respond to insulin (Type 2 DM, T2D)⁵⁰. DM is an epidemic disease of global proportions that currently affects 422 million people globally, where T2D comprises 85-95% of this population, and this number only continues to rise^{51,52}. Many risk factors for DM overlap with CVD, including a sedentary lifestyle, obesity, and hereditary factors⁵². As a chronic disease, DM symptoms are often overlooked and silent until the consequences of hyperglycaemia are apparent. At a later stage of the disease, these symptoms include thirst, hunger, weight loss, fatigue, frequent urination, repeated infections, and irritability^{51,52}. The effect of hyperglycaemia on the endothelium and blood vessels plays a significant role in the dysfunction of these organs where there are both abnormal macrovascular and microvascular features^{28,53}. Hyperglycaemia within the bloodstream from abnormal insulin utilization can lead to neovascular complications within the eye, heart, kidney, and nerves^{50,54}.

Hyperglycaemic control in the blood stream is involved in a myriad of mechanisms that are pathophysiologically similar to hypertension in increasing oxidative stress, proinflammatory mediators and an immune response⁵⁵. The key mechanism of hyperglycaemia-induced vascular damage is associated with the build-up of advanced glycation end-products (AGEs)⁵⁵. AGEs accumulate within the extracellular matrix (ECM) of blood vessels, stimulate the production of ROS and are antigenic eliciting an immune response⁵⁵. The main cell surface receptors of AGEs are scavenger receptors and receptors for AGEs (RAGE), with action mediated by the transforming growth

factor beta (TGF- β), NF- κ B, NADPH oxidase (NOX), and mitogen-activated protein kinases (MAPK) pathways. Downstream signalling of these pathways increases the expression of adhesion molecules including VCAM-1, E-selectin, vascular endothelial growth factor (VEGF), and proinflammatory cytokines (IL-1, IL-6, TNF- α)^{32,55,56}. In DM, there is increased circulating concentrations of AGEs and RAGEs, which lead to the increased activation of all these signalling pathways in vSMC resulting in increased inflammation, fibrosis, prothrombotic effects and overall vascular damage including endothelial dysfunction (Figure 1.2)^{55,57}. Patients with T2D and other cardiovascular risk factors like coronary artery disease and hypertension have reportedly 2- to 4- fold increased risk of mortality due to CVD compared to people with only one of these conditions or those without DM alone^{54,57}. The amplified risk carried by people with DM is likely attributed to the synergistic effects of hyperglycaemia and its comorbidities on the microvasculature of the body⁵⁷.

Diabetic cardiomyopathy (dbCM) is noted as the abnormality of cardiac structure and function in people with DM without other cardiovascular risk factors^{58,59}. Often, dbCM in its initial stages asymptotically manifests subclinical cardiac features including left ventricular (LV) hypertrophy, fibrosis, and abnormal cell signalling before pathophysiological changes towards diastolic and systolic dysfunction, and eventual HF develop^{58,59}. Hyperglycaemia and insulin resistance play an important role in the pathophysiology of diabetic and cardiac remodelling, affecting the metabolic regulation of glucose transporter type 4 (GLUT4). GLUT4 action is mediated by the phosphatidylinositol 3-kinase (PI3K) and protein kinase B (Akt) pathways in cardiac tissue, and in dbCM is decreased, lowering its recruitment to the plasma membrane and effective glucose uptake, leading to cardiac hypertrophy⁵⁸. Similarly, these conditions of the diabetic heart, signal the renin-angiotensin-aldosterone system

(RAAS) and the products of AGEs, can affect the homeostasis of cardiomyocytes and endothelial cells through increased oxidative stress, intracellular lipid accumulation and lipotoxicity⁵⁹. Effectively, these cellular changes cause cardiac hypertrophy, cardiomyocyte death and differentiation into myofibroblasts, inflammation, ECM remodelling, and fibrosis⁵⁹. Furthermore, inflammatory cytokines (TNF- α , Ang-II, IL-6) and TGF- β are upregulated following these changes, which contribute to the cardiac stiffness and hypertrophy, and ECM remodelling^{58,59}. Thus, in DM, glucose dysregulation and lipid metabolism play a pivotal role in the activation of the inflammatory, pro-fibrotic, and oxidative pathways that results in adverse cardiac remodelling, and leads to cardiac dysfunction and eventual HF⁵⁹. Due to the combination of these factors, DM is an established risk factors for CVD and increased importance on its management and care is imperative to reduce the burden of CVDs⁶⁰.

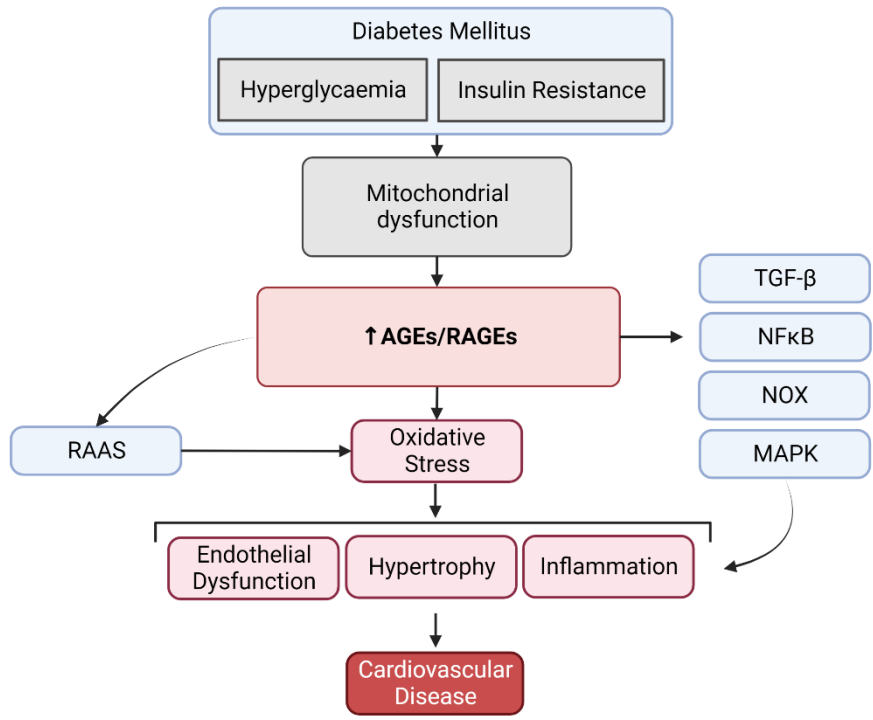


Figure 1.2 Mechanisms of DM leading to CVD. Hyperglycaemia and insulin resistance related mitochondrial dysfunction increases the production of AGEs and its receptors. An increase in profibrotic, oxidative, and inflammatory signalling causes endothelial dysfunction, hypertrophy, and inflammation that leads to CVD. Created with BioRender.com

1.2 Cardiac Fibrosis

1.2.1 Cardiac Remodelling leading to cardiac fibrosis

Cardiac remodelling is defined as both physiological (positive) or pathological (adverse) remodelling of the myocardium^{61,62}. Cardiac remodelling often occurs due to pathogenic risk factors, metabolic and inflammatory stimuli, and/or cardiovascular damage, commonly associated with changes in the left ventricle structure^{61,62}. It is initially a reparative process in compensation to cardiac injury (e.g. following MI) but when these structural changes are sustained for a period of time, they become harmful and pathological modelling ensues resulting in ventricular stiffness, hypertrophy, and HF^{61,63}. Cardiac fibrosis develops following adverse cardiac remodelling and denotes an excess in the deposition of extracellular matrix (ECM) proteins, similarly as a reparative process in replacing dead cardiomyocytes, forming collagen-based scars⁶⁴.

ECM homeostasis plays a central role in modulating cardiac fibrosis, where cardiac fibroblasts (CF) serve the function of maintaining structural integrity⁶⁴. In response to acute myocardial injury such as myocardial infarction, CFs transform into activated myofibroblasts (MCF) which conversely elevate secreted ECM proteins to promote fibrotic repair mechanisms⁶⁵. Furthermore, excess collagen is production at a faster rate of its degradation, accumulating within the ECM and reducing overall contractility⁶⁵. These pathological changes manifest as cardiomyocyte hypertrophy and apoptosis, chamber dilation, and result in HF⁶⁵.

1.2.2 Key inflammatory mechanisms in the development of cardiac fibrosis

Inflammation is a common condition present in different forms of CVDs and has inextricably been tied to endothelial dysfunction as a fundamental mechanism in their pathogenesis⁶⁶. Inflammation plays a key role in the development of cardiac fibrosis through the release of cytokines, chemokines, and growth factors that stimulate the fibrotic response in cardiac fibroblasts and cardiomyocytes⁶⁴. In response to pathological stress, inflammatory cells including monocytes, neutrophils, and macrophages are recruited and invade the site of injury, releasing pro-inflammatory cytokines TNF- α , IL-1, and IL-6^{64,65}.

Conversely, chronic systemic inflammation can also contribute to cardiomyocyte death and trigger the fibrotic response⁶⁴. Clinical research has associated the upregulation of these inflammatory markers to directly regulate the fibrotic mediators associated with remodelling such as, Ang-II, fibronectin, and MMPs, that increase collagen-I deposition and connective tissue growth factor (CTGF)^{64,67,68}. The NF- κ B pathway is a critical regulator of inflammation, upstream of these inflammatory mediators, which contribute to the removal of necrotic tissue and differentiation of fibroblasts to myofibroblasts via the TGF- β pathway^{58,59,64,65}. Myofibroblasts then trigger the release of ECM proteins such as MMPs to degrade the ECM and deposit collagen, thus beginning the scar formation within the myocardium⁶⁵. In the late stages of scar formation, collagen tensile strength increases and further reduces contractility of the myocardium, and myofibroblasts undergo phenotypic changes that release the contractile protein, alpha smooth muscle actin (α SMA), that contributes to this process^{64,65}. Hence, though an initial response to maintain cardiac function and

structural integrity, the inflammatory response and persistent fibrotic state can contribute to ventricular stiffness and hypertrophy, leading to HF (Figure 1.3)⁶⁵.

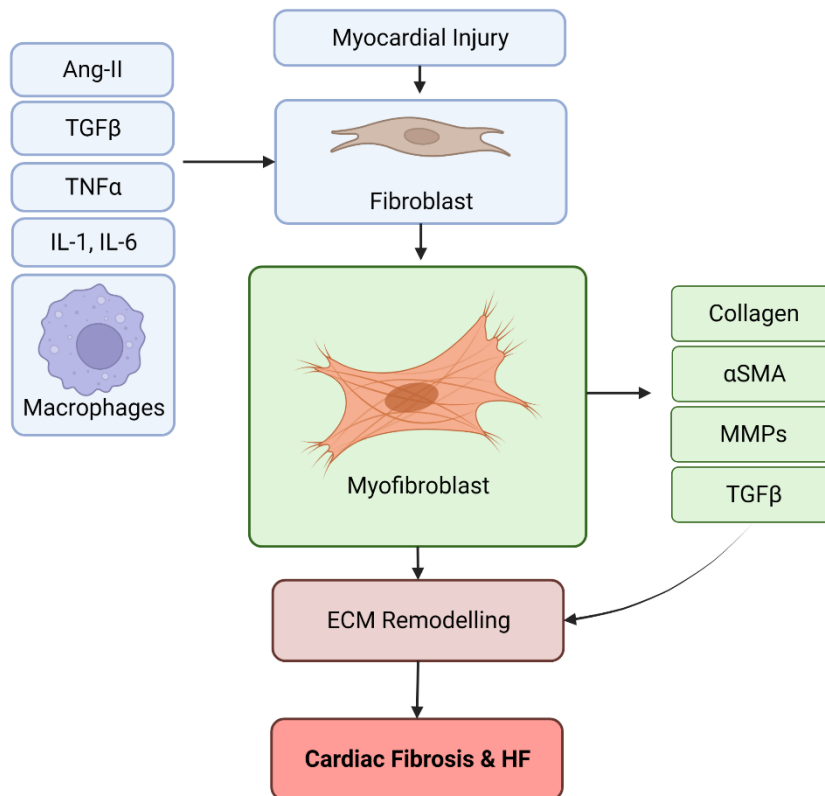


Figure 1.3 Pathological remodelling of the myocardium. Myocardial injury such as MI illicit an inflammatory response that recruits inflammatory markers and immune cells through the RAAS and TGF-β pathway. Resident fibroblasts begin differentiation into myofibroblasts that signal the beginning of ECM remodelling through increased signalling of fibrotic markers. Prolonged ECM remodelling and scar formation reduces contractility and function of the myocardium resulting in cardiac fibrosis and eventual HF. Created with BioRender.com.

1.3 Heart Failure

HF is an increasingly prominent clinical condition in our ageing population, which is hard to define as a specific disease^{69,70}. Traditionally, HF is defined as a condition where the heart is unable to fulfil the metabolic needs of the body organs due to abnormal function and/or structure^{70,71}. HF is often associated with modifiable risk factors akin with those of CVD such as old age, sedentary lifestyle, obesity, tobacco smoking, and high blood pressure and cholesterol⁷². In Australia alone, there is an estimated 480,000 patients affected with HF and an additional 60,000 newly diagnosed each year. This number is only expected to increase and place further economic burden on the Australian healthcare system due to frequent hospitalisation of HF patients⁷³.

Cardiac remodelling, systematic hypertension and inflammation are key mechanisms implicated in HF that induce the death of cardiomyocytes and cause structural changes that lead to myocardial stiffness and diastolic dysfunction, and eventual HF⁶⁴. These adaptive mechanisms are mediated through the RAAS and sympathoadrenergic pathways influence inter- and intracellular actions towards chamber dilation and hypertrophy^{74,72}. Patients with HF will exhibit both diastolic and systolic dysfunction where the heart has difficulty contracting and relaxing, respectively⁷². Symptomatically, this will manifest in patients through signs of dyspnoea, ankle swelling, and general fatigue⁷⁴.

1.3.1 Different phenotypes of heart failure

HF is classified into three subtypes dependent on the left ventricular ejection fraction (LVEF); HF with preserved ejection fraction (HFpEF, LVEF $\geq 50\%$), HF with mid-range ejection fraction (HFmrEF, LVEF 41-49%), and HF with reduced ejection fraction (HFrEF, LVEF $\leq 40\%$)^{69,75}. HFmrEF was only recently defined, and it places people between HFpEF and HFrEF, although the management for this type of HF is still unclear. The pathophysiology between subtypes lies within their respective underlying mechanisms. HFrEF can be attributed to an acute or chronic loss of cardiomyocytes due to MI, myocarditis, or valvular diseases, leading to systolic dysfunction and the inability of the left ventricle to contract⁷⁴. Conversely, HFpEF characteristically exhibits cardiomyocyte hypertrophy, intracellular fibrosis, and inflammation, which results in the inability of the left ventricle to relax⁷⁴. Notably, HFpEF is pathophysiologically heterogeneous and associated with chronic comorbidities (T2D, hypertension, obesity) that cause inflammation, and can lead to endothelial dysfunction cascades into its own adaptive mechanisms (NO availability, oxidative stress, vasoconstriction)⁷⁴. All types of HF are associated with poor mortality rates of 50% within 5-years of diagnosis; however, the pathophysiology of HFrEF is better understood, and is managed well pharmacologically⁷⁶.

In accordance with these phenotypes, another classification method based on the New York Heart Association (NYHA) system categorises patients into four classes based on the severity of symptoms^{75,77}. Class I includes patients diagnosed with CVD without any noticeable symptoms and hindrance to daily activity; Class II includes patients with slight limitations in physical activity; Class III patients have noticeable physical limitations, and Class IV patients are symptomatic even at rest and are unable to

perform any physical activity without discomfort^{71,75}. In accordance with the worsening symptoms with increasing NYHA classification, mortality of these patients similarly rises. The 1-year mortality rate for patients with NYHA class I and II range between 10-15%, 15-20% for NYHA class III, and 20-50% for NYHA class IV⁷⁸.

1.3.2 Current biomarkers used for the diagnosis and progression of heart failure

As a complex clinical condition stemming from various aetiologies including coronary artery disease, hypertension, DM, both the definition and diagnosis of HF are challenging and include several parameters^{70,71,75}. The current diagnostic algorithm begins with the identification of the clinical symptoms related to breathing and performing daily activities, decreased energy, weight gain, and abdominal or leg swelling⁷¹. Next is screening patients for history of HF risk factors and performing echocardiographic measurements before biomarkers levels are included^{71,75}.

The current clinical guidelines from the American Heart Association (AHA) and the European Society of Cardiology (ESC) designate N-terminal-pro-B-Type natriuretic peptide (NT-proBNP) and brain natriuretic peptide (BNP) as the biomarkers of choice in the diagnosis of HF⁷⁹. Natriuretic peptides are importantly mediated by the MAPK and RAAS signalling pathways⁸⁰. In the context of HF, they play a key role in cardiac homeostasis, are secreted by cardiomyocytes upon myocardial stretch in the form of BNP or NT-proBNP and regulate the proliferation and permeability of SMCs and endothelial cells, respectively, to inhibit cardiac hypertrophy and fibrosis⁸⁰. Hence both natriuretic peptides are widely researched and clinically utilized as a biomarker for HF^{81,83}.

Once NT-proBNP and BNP biomarkers concentration exceeds the threshold of ≥ 125 pg/mL and 35 pg/mL, respectively, echocardiography is performed to determine LV function and classification into HF phenotype determined⁷⁵. In either case, both natriuretic peptides have been thoroughly researched in patient cohorts with high sensitivity and are currently the most reliable diagnostic biomarkers for HF diagnosis and prognosis⁸¹. However, studies have found both specificity and sensitivity issues with these diagnostic methods, where natriuretic peptides can also be increased due to other factors including old age, anaemia, and renal failure or have even found to be decreased in patients with obesity⁸¹. Additionally, between the subtypes of HF, levels of both BNP and NT-proBNP have been reportedly higher in HF_{rEF} compared to HF_{pEF}, and although lower cut-off values for these biomarkers are advised, this can lead to a higher incidence of false positives and unnecessary testing⁸². Clinically, the role of natriuretic peptides has also been studied in the prognosis of HF, showing that a higher BNP is associated with a worse prognosis of the patient and have a five-fold greater mortality⁸¹. However, research has shown that when assessing natriuretic peptides with another biomarker implicated in the pathophysiology of HF, the predicted prognosis of the patient is much better⁸¹. An example of this synergistic effect has been demonstrated in studies combining NT-proBNP with inflammatory markers including high sensitivity troponin (hs-TnT) and suppression of tumorigenicity 2 (ST2) which showed better prognostic utility than their individual counterparts⁸¹.

Natriuretic peptides may be the most thoroughly studied biomarkers that have progressed to the clinic, however, there are many other markers that have been investigated, showing potential to be used as clinical biomarkers for HF diagnosis and prognosis. The biomarkers are categorised by their mechanisms relating to the pathogenesis of HF, namely myocardial stretch biomarkers, inflammatory biomarkers,

oxidative stress biomarkers, and ECM biomarkers⁸³. Troponin, C-reactive protein, MMP's, and galectin-3 (Gal-3) have been implicated in the fibrotic and inflammatory mechanisms leading to HF and show great biomarker potential however are not specific to HF and can be indicative of myocardial injury or other underlying conditions^{81,83}. Furthermore, the gap in the knowledge lies in the differentiation between the HF subtypes, where there are currently no biomarkers used for this purpose⁸⁴. Current clinically utilized biomarkers, NT-proBNP or BNP, are not as reliable in HFmEF/HFpEF diagnosis and prognosis, and more specific biomarkers are needed. The lack of progress in this field could be due to poorly understood pathogenesis of HFpEF which is often multifactorial, often associated with chronic comorbidities⁷⁴. Hence, this is an important area to further research or discover other potential biomarkers for both diagnosis and prognosis in HF, particularly HFpEF, to improve patient management and outcomes.

1.3.3 Treatment of heart failure

Treatment and management of chronic HF can begin immediately following diagnosis through individual effort. Through lifestyle changes, mainly in the form of improving cardiac health through physical activity, the patient quality of life can be improved, and hospitalisations reduced by mitigating the effects of modifiable risk factors⁷⁵. In the scope of phenotype specific HF treatments, pharmacotherapy has been well-studied and implemented in the effective treatment of HFrEF, reducing hospitalisation, and patient mortality, but not in patients with HFpEF⁷⁵. HFrEF pharmacotherapy targets the RAAS pathway and sympathetic nervous systems with a combination of drug classes including angiotensin-converting enzyme inhibitors (ACE-Is), beta-blockers,

and mineralocorticoid receptor antagonists (MRAs)⁷⁵. The management and outcomes of HFrEF have been thoroughly studied in comparison to HFpEF. Currently, HFpEF management lacks effective treatments that have shown to reduce patient mortality and morbidity. Nevertheless, like HFrEF patients, studies on HFpEF patients show similar pharmacotherapy approach with many patients being prescribed ACE-Is, beta-blockers and MRAs. Neprilysin inhibitors are emerging as new treatments for HF, which work by increasing guanosine 3',5'-cyclic monophosphate (cGMP) resulting in vasodilation, natriuresis, diuresis, increased glomerular filtration rate and have also anti-hypertrophic and anti-fibrotic effects⁸⁵. Sodium–glucose cotransporters 2 (SGLT2) inhibitors are used to treat DM, however they have also shown beneficial effects in HF, including HFpEF and HFmrEF, by improving homeostatic balance, reducing blood pressure, decreasing arterial stiffness, and activating sympathetic nervous system⁸⁵. These agents have demonstrated 25% reduction in HF worsening or cardiovascular death⁸⁵. Thus, treatment for HFpEF patients is targeted at improving individual symptoms and aetiologies including co-morbidities and may include additional treatments such as loop diuretics to improve exercise capacity and hypertension⁷⁵. Hence, there remains a large gap in the knowledge of HF treatment specifically for the HFpEF phenotype that calls for further investigation into the mechanisms of the underlying pathophysiology of HF to improve patient outcomes.

1.4 The biological and pathological functions of FKBP

Immunophilins are a superfamily of proteins that play a role in protein to protein interactions essential for cell function and cell cycle control. The FK506-binding proteins (FKBPs) family of immunophilins similarly have a wide range of functional

roles, notably, as co-chaperones within steroid hormone receptor complexes formed with heat shock protein 90 (HSP90) through their tetra trico peptide repeat (TPR) domain^{86–88}. The FKBP's roles have been well documented in cancer treatments and diagnosis due to their immunosuppressive properties^{86,89}.

FK506-binding protein-like (FKBPL) is a divergent member belonging to the FKBP family and naturally secreted by endothelial, epithelial and fibroblast cells^{87,90}. However, FKBPL appears to have different or opposite functions to other family members, whilst it also has a critical role in steroid receptor complex regulation, spanning glucocorticoid, estrogen, and androgen receptors⁸⁸.

1.4.1 FKBPL is a key anti-angiogenic protein

Over the last decade, FKBPL's role as an important antiangiogenic protein has been well documented by demonstrating its ability to inhibit endothelial cell migration and tubule formation and as such has been developed into a novel treatment for solid cancers targetting tumour angiogenesis and cancer stem cells^{86,90}. Novel anticancer therapeutic based on FKBPL's anti-angiogenic domain was developed by Almac Discovery as 24-amino acid peptide, AD-01(preclinical candidate), and 23-amino acid peptide, ALM201 (clinical candidate)(Figure 1.4). Both of these agents have been evaluated *in vitro* and *in vivo* showing inhibition of tumour angiogenesis and cancer stem cell signalling^{91–93}. ALM201 has recently completed a Phase Ia clinical trials for the treatment of ovarian cancer showing a very good safety profile⁹⁴ and as a result it received Orphan Drug Approval by Food and Drug Administration in the USA. Published data have associated FKBPL overexpression with increased survival in

breast cancer patients, showing potential as a prognostic biomarker in breast cancer⁸⁶. Valentine et al. (2011)⁸⁷ was the first report, which demonstrated that FKBPL and its therapeutic peptide derivative, AD-01, signal through the CD44 pathway and are potent anti-angiogenic agents. Its mechanism through CD44 has also demonstrated FKBPL's ability to inhibit cancer stem cell signalling in breast and ovarian cancer^{86,87,90}. A recent study⁹² in ovarian cancer reported that FKBPL is an inhibitor of CD44-STAT3 signalling. CD44 is a cell surface adhesion molecule that regulates metastasis in cancers⁹⁵, but it is also involved in inflammation, angiogenesis and endothelial cell function implicated in the development of CVDs⁹⁶. Thus FKBPL exhibits potential not only as an anti-cancer protein, but given it is a critical regulator of angiogenesis and recently, inflammation, it is possibly interlinked in the signalling mechanisms of CVD.

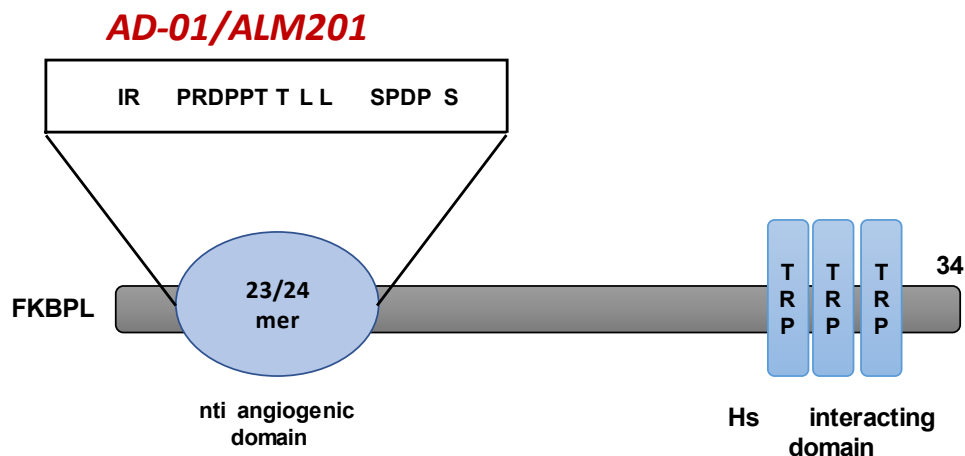


Figure 1.4 FKBPL mimetic AD-01/ALM201. AD-01 (preclinical) and ALM201 (clinical) are both peptide derivatives of FKBPL based on its 23/24 amino acid sequence within the anti-angiogenic domain, thus retaining the same anti-cancer and anti-angiogenic functions.

1.4.2 FKBPL has an emerging role in inflammation

Angiogenesis describes the formation of new blood vessels from existing vasculature that has a key role in developmental and wound healing pathways, where irregularities in this process can incite the development of pathological conditions, such as ischemic CVDs, chronic kidney diseases, cancer, and diabetic retinopathy^{90,97}. As described above, FKBPL's role in cancer has been well established, with notably functions as an anti-angiogenic protein that inhibits endothelial cell migration and tubule formation⁸⁶. Current anti-angiogenic treatments targeting tumour growth in clinical settings operate via the VEGF pathway, that are often associated with severe adverse effects, resistance, and tumour metastasis⁸⁸. Interestingly, the anti-angiogenic domain of FKBPL that AD-01 therapeutic peptide design is based on, is different from the region of FKBPL responsible for binding to HSP90, and its mechanism of action is via the CD44 pathway^{87,98}. Both endogenous FKBPL and AD-01 bind to the cell surface receptor, CD44, triggering a cascade of downstream signalling to inhibit CD44 signalling whilst upregulating CD44 protein expression, via negative feedback mechanism that results in decreased cell migration. On the other hand, the knockdown of FKBPL shows opposite, pro-angiogenic phenotype, measured by accelerated endothelial cell wound closure⁸⁸. In the same paper, it was shown that CD44 is essential for FKBPL- and AD-01-mediated anti-angiogenic mechanism of action and that the downstream effects on cell migration and tubulin-actin dynamics occur via the focal adhesion pathway and RHoA effector proteins⁸⁸.

In the physiological settings, the role of FKBPL was not very well known until Yakkundi et al. developed a heterozygous knockdown FKBPL transgenic mice (*Fkbp1*^{+/−}) where homozygous knockout of FKBPL was not embryonically viable, demonstrating a

critical role for FKBPL in both developmental and physiological angiogenesis^{88,98}. Although viable, heterozygous *Fkbp1*^{+/-} mice and zebrafish displayed signs of aberrant blood vessel development, where this effect seems to be absent in CD44 deficient zebrafish, again demonstrating a critical role for CD44 in FKBPL-mediated effect on vasculature^{98,99}. Thus at the physiological level, low levels of FKBPL have been associated with a pro-angiogenic response, albeit causing impaired vascular integrity and early signs of endothelial dysfunction⁹⁹ (Figure 1.5.)

Given that aberrant angiogenesis and endothelial dysfunction are underlying causes of a number of CVDs including HFpEF⁷⁴ and in the context of DM, the evidence for FKBPL's role in these settings are also emerging. In a preliminary report as part of a conference proceedings, the importance of FKBPL in metabolic and cardiac function was investigated in *fkbpl*^{+/-} mice with superimposed DM, confirming that in the low FKBPL settings, glucose and fat metabolisms were impaired, both in diabetic and non-diabetic mice whereas cardiac function shows signs of diastolic dysfunction only in non-diabetic *fkbpl*^{+/-} mice¹⁰⁰. Interestingly, the latter mice also showed cardiac pro-inflammatory response¹⁰⁰. Another recent preliminary report demonstrated that FKBPL could be involved in the mechanisms of cardiac fibrosis, where increased FKBPL expression was observed in cardiac fibroblasts treated with pro-fibrotic stimuli, TGF- β ¹⁰¹.

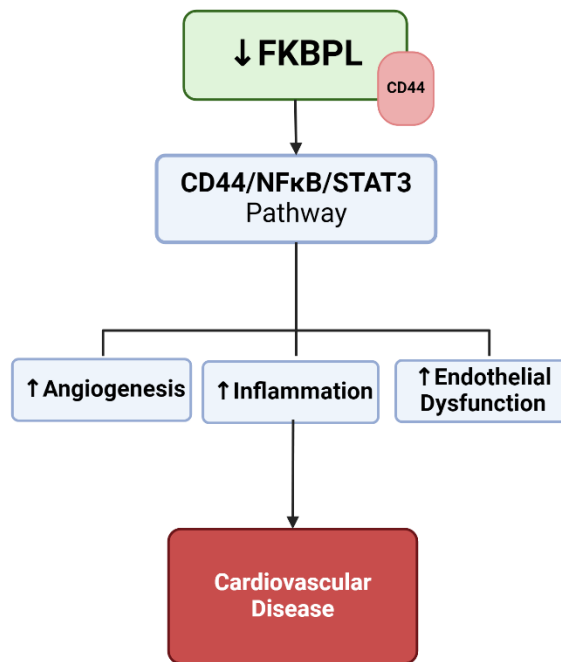


Figure 1.5 Inflammatory pathway of FKBPL. FKBPL is bound to cell surface receptor CD44 before it can exert its anti-angiogenic and cancer stem cell inhibitory function. Decreased FKBPL levels have shown to increase the modulation of CD44, NFκB, and STAT3 pathways. Resultant effects are in increased angiogenesis, inflammation, and endothelial dysfunction, which are all parameters associated with the development of CVD.

1.4.3 FKBPL as a potential novel target or biomarker of CVD

Inflammatory mechanisms play a pivotal role in response to infections, and commonly underly critical mechanisms in the pathophysiology of many chronic diseases such as DM and atherosclerosis¹⁰². Within the heart, the inflammatory response orchestrates a plethora of cell-to-cell interactions and mechanisms contributing to ECM remodelling, oxidative stress, angiogenesis, and fibrosis in response to tissue and cell damage^{102,103}. In these settings, macrophages play a key role in the receptor response, expressing Toll-like receptors (TLR) that activate key inflammatory pathways including the NF-κB and signal transducers and activators of transcription 3 (STAT3) pathway^{98,102}. The induction of the general inflammatory response initiates T helper (Th) cells that cascade cytokines signalling and the proinflammatory immune response that can amplify these signalling effects¹⁰².

FKBPL's role in inflammation lies in its natural secretion by endothelial and fibroblast cells, both subject to the modulation of inflammatory pathways that alter their function upon extracellular stimuli^{86,102}. FKBPL's anti-angiogenic function should be also considered in the scope of the inflammatory response, where aberrant angiogenesis is a hallmark feature of many chronic diseases underpinned by inflammation including ischemic CVDs, chronic kidney diseases, cancer, and diabetic retinopathy⁹⁷. Studies have shown that angiogenesis and inflammation share close links and show potentiating and synergistic effects in the scope of CVD where these pathological conditions can increase the signalling of their respective markers in a vicious cycle^{97,103,104}. Macrophage activation and cytokine recruitment in inflammation often occur in hypoxic conditions via hypoxia-inducible factor (HIF), a key factor in eliciting

a pro-angiogenic response⁹⁷. Additionally, studies have found the protein RBCK1¹⁰⁵, a regulator of the NF-κB pathway, is a novel upstream regulator of FKBPL¹⁰⁶. Similarly, FKBPL has demonstrated the ability to target the STAT3 inflammatory signalling pathway in ovarian cancer⁹². Furthermore, as explained above, FKBPL regulates glucose and fat metabolism and in addition to its function in glucocorticoid receptor signalling⁹⁸, it could be important in both metabolic and vascular dysfunction observed in DM that can lead to CVD. Through the PI3K/Akt/mammalian target of rapamycin (mTOR) signalling pathways, the formation of AGEs in DM is linked to endothelial dysfunction and inflammation, underlying causes of irregular angiogenesis⁵⁶. In a recent report using human plasma samples, FKBPL concentration was shown to be increased in DM or CVD individually but not in people with both DM and CVD, which suggests the presence of compensatory mechanisms that needs to be explored further⁹⁸. In the same study, FKBPL was positively correlated with parameters of diastolic dysfunction in the absence of DM and negatively correlated with fasting glucose and glycated haemoglobin⁹²; the latter observation was aligned to *in vivo* study in FKBPL transgenic mice with superimposed DM, described above⁹⁸. A summary of FKBPL's biological and pathological functions in CVD is described in Figure 1.6.

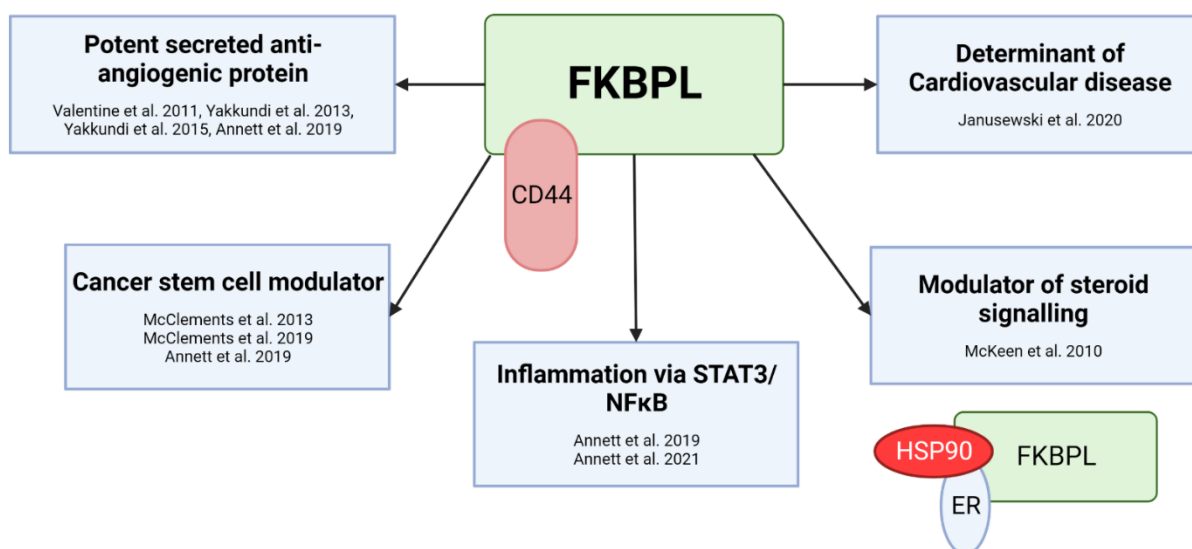


Figure 1.6 Biological and Pathological functions of FKBPL. FKBPL binds to CD44 before it can exert its anti-angiogenic and cancer stem cell inhibitory function. Following FKBPL-CD44 complex formation, there is an inhibition on the inflammatory STAT3-NkFB signalling. Recent work by Janusewski et al. (2020) showed implicated FKBPL, for the first time, as a determinant of cardiovascular disease. Previous work has also shown that FKBPL as a chaperone protein forms a complex with HSP90 and oestrogen receptor (ER) regulating ER signalling, which is independent of CD44.

1.5 Hypothesis and Aims

FKBPL's distinct role as an anti-angiogenic protein has been established by its binding to CD44. Recent findings have exhibited further implications of the FKBPL-CD44 complex that span inflammatory signalling, implicating its role in the pathophysiology of CVD through means of angiogenesis, inflammation, vascular integrity, and endothelial dysfunction. Thus, in this thesis, we propose the inherent role of FKBPL in the inflammatory mechanisms leading to cardiac fibrosis and heart disease. We hypothesised that FKBPL plays an important role in angiogenic, inflammatory, and fibrotic signalling in the early stages of cardiac remodelling leading to HF, and that it can be harnessed as a diagnostic and therapeutic target.

Aim 1: *Investigating the Effect of E-cigarette Vapour on Endothelial cells and the Role of FKBPL.*

- *In vitro:* Human coronary artery endothelial cells were treated with e-cigarette aerosol condensate (PG/VG, 0mg, 18mg; 1%, 2%, 4%, 8%). Endothelial cell health parameters were examined through MTT assay, DCF assay, and ELISA for VCAM-1 and ICAM-1 expression. Experiments were also performed in a co-culture model after first pass metabolism by A549 human epithelial lung cells.
- *In vivo:* Female BalB/c mice were treated with ambient air or e-cigarette aerosol (0mg, 18mg) for 12 weeks (2x/day) before the left ventricle was harvested. RT-qPCR and immunofluorescent staining were performed to determine the expression of VCAM-1/ICAM-1 and/or FKBPL/CD31, respectively.

Aim 2: *Elucidating the role of FKBPL in in vitro Cardiac Fibrosis Models*

- *In vitro*: Human fetal fibroblast (HFF08) with and without FKBPL siRNA knockdown were treated with profibrotic and hypoxic factors (TGF- β , 10ng/ml, DMOG, 1mM) and FKBPL therapeutic peptide mimetic (AD-01, 100mM). Cells protein and RNA were collected, and the expression of fibrotic markers at the mRNA level as well as monocyte adhesion, determined. An innovative 3D bioprinted model of cardiac fibrosis was also developed and characterised in the context of pro-fibrotic and hypoxic conditions and AD-01 treatment.
- *In vivo*: Left ventricles from *fkbp1^{+/-}* transgenic and wild type mice were harvested, stained for collagen deposition using picosirius red staining, and RT-qPCR performed to determine the expression of several key fibrotic markers.

Aim 3: Evaluating the Biomarker Potential of FKBPL in Risk Stratification and Diagnosis of Heart Failure with Preserved Ejection Fraction.

- *Systematic review*: A systematic review and meta-analysis were performed to verify the accuracy of clinically used biomarkers in the diagnosis of chronic HFpEF. Included studies were analysed through random-effect models based on sensitivity and specificity of biomarkers to estimate the pooled diagnostic accuracy. The literature search included studies from 1900-2021 from the databases: PubMed, Web of Science, MEDLINE and SCOPUS. The meta-analysis was performed following the PRISMA guidelines for systematic reviews and meta-analyses.
- *In vitro*: Models of cardiac hypertrophy were cultured with H9C2 rat cardiomyoblasts treated with a combination of hypertensive treatment, angiotensin-II (100nM), and/or AD-01 (100nM), for 24- and 48-hours. Cell hypertrophy was determined using cell and nucleus measurements of

cardiomyoblasts. RNA and protein lysates were extracted from treated cardiomyoblasts to measure mRNA and/or protein expression of FKBPL, BNP, and/or ANP to exemplify the role of FKBPL in cardiac hypertrophy.

- *Clinical sample studies:* Human plasma concentrations of FKBPL, NT-proBNP, and Gal-3 were measured in patients with HFpEF (acute HFpEF, chronic HFpEF, and hypertrophic cardiomyopathy) and a control group. Correlations between the respective markers and echocardiographic parameters were performed.

Aim 4: Evaluating the current biomarkers reflective of early cardiac remodelling in diabetes mellitus.

- A scoping review was performed on the topic of diagnostic and prognostic biomarkers reflective of cardiac remodelling in DM. In order to determine the most suitable biomarkers for this population of patients, biomarkers were recorded from included studies and critically appraised describing the most prominent clinically used biomarkers and noting the presence of potential and emerging biomarkers. The literature search included studies from 2003-2021 from the reputable databases: MEDLINE, Scopus, Web of Science, PubMed, and Cochrane library. The scoping review was performed following the PRISMA guidelines for scoping reviews.

Chapter 2

E-cigarette Aerosol Condensate leads to Impaired Coronary Endothelial Cell Health and Restricted Angiogenesis

Cigarette smoking has long been one of the leading modifiable risk factors and cause of heart failure and cardiovascular disease. Research detailing the carcinogenic and cytotoxic compounds found within tobacco cigarettes have been extensively studied, bringing awareness to consumers about its detrimental health effects, and shifting its social perception. E-cigarettes have surged in popularity in the last decade as a smoking cessation tool amongst cigarette smokers and non-smokers. The public opinion currently views E-cigarettes as a less harmful alternative to tobacco smoking with a plethora of playful chemical flavourings. However, preliminary research reveals the possible cytotoxic effects of E-cigarette use on the heart that may be akin to that of tobacco smoking. Here in this chapter, we examine the effects of E-cigarette aerosol condensate on human coronary artery endothelial cells to determine its effects on endothelial health *in vitro* and heart health *ex vivo*. The involvement of FKBPL mechanism in this effect was also studied here. Our study findings show, for the first time, that E-cigarette aerosol condensate (EAC) can have detrimental effects on cell viability, increased reactive oxygen species production, increased inflammatory markers, and impaired cardiac angiogenesis *in vivo* through upregulation of FKBPL.

Cigarette Aerosol Condensate Leads to Impaired Coronary Endothelial Cell Health and Restricted Angiogenesis

Michael Chhor¹, Esra Tulpar¹, Tara Nguyen¹, Charles G. Cranfield¹, Catherine A. Gorrie¹, Yik Lung Chan¹, Hui Chen¹, Brian G. Oliver¹, Lana McClements^{1,2, *} and Kristine C. McGrath^{1 *}

1 School of Life Sciences, Faculty of Science, University of Technology Sydney, Sydney, NSW 2007, Australia; michael.chhor@student.uts.edu.au (M.C.); esra.s.tulpar@student.uts.edu.au (E.T.); tara.nguyen@uts.edu.au (T.N.); charles.cranfield@uts.edu.au (C.G.C.); catherine.gorrie@uts.edu.au (C.A.G.); yik.chan@uts.edu.au (Y.L.C.); hui.chen-1@uts.edu.au (H.C.); brian.oliver@uts.edu.au (B.G.O.)

2 Institute for Biomedical Materials and Devices, Faculty of Science, University of Technology Sydney, Sydney, NSW 2007, Australia

* Correspondence: lana.mcclements@uts.edu.au (L.M.); kristine.mcgrath@uts.edu.au (K.C.M.)

Keywords: e-vaping; cardiovascular disease; smoking; nicotine; atherosclerosis

2.1 Abstract

Cardiovascular disease (CVD) is a leading cause of mortality worldwide, with cigarette smoking being a major preventable risk factor. Smoking cessation can be difficult due to the addictive nature of nicotine and the withdrawal symptoms following cessation. Electronic cigarettes (e-Cigs) have emerged as an alternative smoking cessation device, which has been increasingly used by non-smokers; however, the cardiovascular effects surrounding the use of e-Cigs remains unclear. This study aimed to investigate the effects of e-Cig aerosol condensate (EAC) (0 mg and 18 mg nicotine) in vitro on human coronary artery endothelial cells (HCAEC) and in vivo on the cardiovascular system using a mouse model of 'e-vaping'. In vitro results show a decrease in cell viability of HCAEC when exposed to EAC either directly or after exposure to conditioned lung cell media ($p < 0.05$ vs. control). Reactive oxygen species were increased in HCAEC when exposed to EAC directly or after exposure to conditioned lung cell media ($p < 0.0001$ vs. control). ICAM-1 protein expression levels were increased after exposure to conditioned lung cell media (18 mg vs. control, $p < 0.01$). Ex vivo results show an increase in the mRNA levels of anti-angiogenic marker, *FKBPL* ($p < 0.05$ vs. sham), and endothelial cell adhesion molecule involved in barrier function, *ICAM-1* ($p < 0.05$ vs. sham) in murine hearts following exposure to electronic cigarette aerosol treatment containing a higher amount of nicotine. Immunohistochemistry also revealed an upregulation of FKBPL and ICAM-1 protein expression levels. This study showed that despite e-Cigs being widely used for tobacco smoking cessation, these can negatively impact endothelial cell health with a potential to lead to the development of cardiovascular disease.

2.2 Introduction

Cardiovascular diseases (CVD) and the resultant vascular complications are a major cause of mortality, accounting for 31% of all deaths worldwide [1,2]. The development of CVD is multifactorial and has been associated with risk factors including tobacco cigarette smoking, obesity, high cholesterol, and high blood pressure [2,3]. Notably, 10% of all CVD cases are attributable to smoking tobacco cigarettes [4]. Depending on an individual's frequency and habit, smoking can increase the risk by at least two-fold for developing conditions including heart failure and acute myocardial infarction (AMI) compared to the other risk factors [5]. Additionally, it is reported that smoking can act synergistically with other risk factors such as hypertension and diabetes mellitus in multiplying the level of risk for CVD development [6].

Electronic cigarettes (E-Cigs) have recently emerged as a supposedly less toxic and less carcinogenic alternative to traditional cigarettes without any combustion [7]. E-Cigs are electronic devices that can differ in design between brands; however, they are generally composed of a rechargeable battery, an e-liquid tank (with thousands of potential flavouring) and an atomiser element that heats and aerosolises the e-liquid to create a vapour for smoking. The e-liquid is comprised of propylene glycol (PG), vegetable glycerin (VG), and, optionally, nicotine. There is also a large market for different flavouring [8–10]. E-Cigs use has been traditionally perceived as harmless, with recent trends showing an increase in usage amongst current smokers, but additionally, non-smokers and young adolescents [7,11]. Studies have reported the presence of carbonyl compounds in e-Cig aerosols, notably: formaldehyde, acetaldehyde, and acrolein, as well as long-chain and cyclic alkanes and alkenes [12]. Additionally, trace amounts of metals have been reported, such as aluminum, barium,

chromium, and cadmium within the e-Cig aerosol [10,13]. These chemicals are known to be harmful and cytotoxic, causing pulmonary and cardiovascular stress [14]. Whilst these chemicals have been reported to be lower in concentration from their traditional tobacco cigarette counterparts, there remain many other residual chemicals generated during the heating process in addition to the role of nicotine that could contribute to early atherogenesis [15].

Endothelial cells play an important role in cardiovascular homeostasis, regulating the permeability of the arterial vessels, and are the first responders to inflammatory stimuli [16]. Endothelial dysfunction (ED) is an early critical event that leads to atherosclerosis and heart failure, affecting vascular integrity through reduced vasodilation, increased inflammation, and prothrombic activity [17,18]. Experimental studies have demonstrated that exposure to the harmful chemicals generated from tobacco smoke not only results in vascular dysfunction, but also leads to the activation of the vascular endothelium as a result of a shift to a pro-oxidative state and increased expression of adhesion molecules on the surface of endothelial cells—an early event in atherosclerosis [19,20].

FK506 binding protein-like (FKBPL), an anti-angiogenic protein and key determinant of CVD, was shown to be increased in human plasma as a result of smoking [21]. FKBPL is secreted by endothelium, and when knocked down in mice, it leads to endothelial dysfunction and impaired vascular integrity [22], suggesting that angiogenic balance is the key to maintaining healthy endothelium. CD31/PECAM1 is an endothelial cell adhesion and signalling molecule that mediates both homophilic and heterophilic adhesion in angiogenesis [23,24]. Increased levels of CD31 have also previously been associated with early COPD and cardiovascular complications as a result of smoking [25,26].

While e-Cigs have been considered a safe alternative to conventional cigarettes, their potential as a smoking cessation device remains controversial. Moreover, of concern is the rising usage of e-Cigs by adolescents and young adults who were never exposed to tobacco cigarettes. This is concerning given that the safety profile of e-Cigs is still unknown, including its impact on the cardiovascular system. Therefore, in this study, we aimed to determine the impact of e-Cigs aerosol condensate (EAC) on endothelial cell homeostasis through the assessment of its effects on the viability of human coronary artery endothelial cells (HCAECs). We further investigate EAC's contributions to endothelium inflammation, oxidative stress, and angiogenesis as part of the mechanisms implicated in this effect. Finally, the immediate impact of nicotine on cell membrane ion permeability was demonstrated using a tethered bilayer lipid membrane (tBLM) assay. The expression of key inflammatory endothelial cell (ICAM-1 and VCAM-1) and angiogenesis markers (FKBPL and CD31) were also assessed *ex vivo* in hearts from mice exposed to e-Cigs aerosol *in vivo*. It is hypothesized that EAC and e-cigarette aerosols will affect endothelial cell health, increasing the expression of inflammatory and anti-angiogenic markers related to endothelial dysfunction and the pathogenesis of cardiovascular disease.

2.3 Methods

2.3.1 Generation of EAC

E-Cigs utilise e-liquids that are heated to generate e-Cig vapour inhaled by users. To simulate a more physiological method of exposure, in preference of using e-liquid directly, we opted to heat the e-liquid as this will result in altered chemical composition to generate an aerosol [12]. For this study, EAC was generated using a KangerTech

SUBOX mini e-cigarette device (KangerTech, Shenzhen, China) and tobacco flavoured e-liquid (Vape Empire, Sydney, NSW, Australia), both with (18 mg/mL), and without (0 mg/mL) nicotine. As a vehicle control, EAC was also generated from a stock solution composed of 80% propylene glycol and 20% vegetable glycerine (PG/VG) without tobacco flavour—the base composition of the e-liquid used for this study. The e-cigarette device was set at 30 W, and the air pump was simultaneously switched on for 5 s bursts, with 20 s to rest in between bursts. This setup created a vacuum trap that drew e-cigarette smoke into a 25 cm² flask where the vaporised condensate was collected (Figure 2.1). The freshly generated condensate was rested upon dry ice for a minimum of 30 min before diluting to the final working concentrations and used immediately.

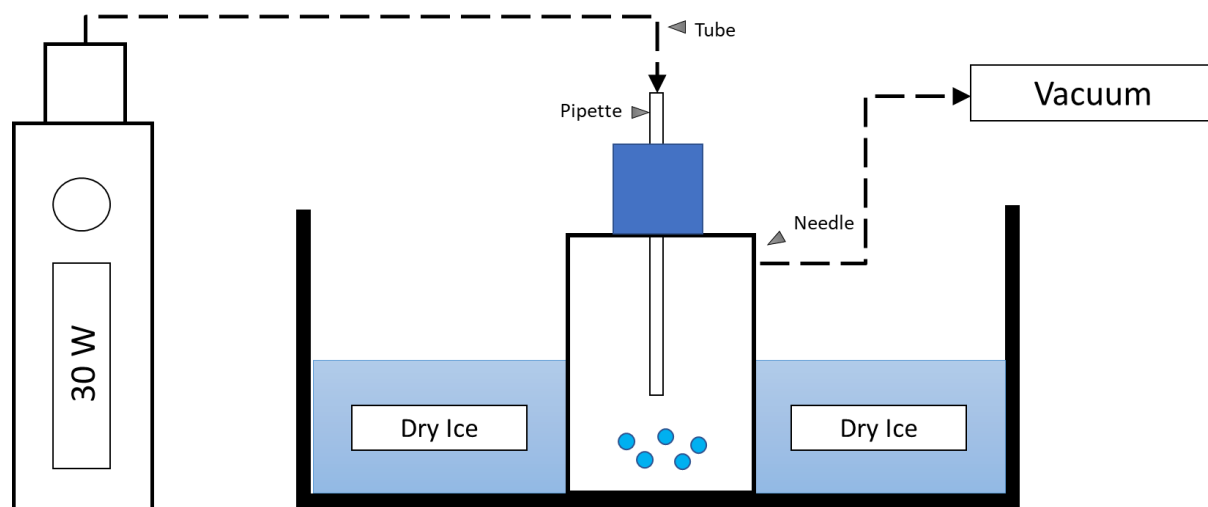


Figure 2.1 Experimental Setup for e-cigarette aerosol condensate collection

2.3.2 Cell Culture and Treatment Models

HCAECs (Cell Applications, San Diego, CA, USA) were cultured in Endothelial Cell Growth Medium (Cell Applications, San Diego, CA, USA) and used from passages 1–10 in this current study. To study the metabolic process of lung tissue, we used A549 cells to model alveolar Type II pulmonary epithelium. A549 cells, human alveolar basal epithelial cell line from adenocarcinoma (A549; ATCC, Manassas, Virginia, USA), were cultured in DMEM (Thermo Fisher Scientific, Gibco, Waltham, MA, USA) supplemented with 10% foetal bovine serum (FBS) at 37 °C in a humidified atmosphere containing 5% CO₂. A549 cells were used from passages 3–11 in this study.

A monoculture and indirect co-culture model using undiluted conditioned media (reviewed in Vis et al., 2020 [65]) treatment were utilized for this study. The monoculture involved direct treatment of the HCAECs with the EAC for 24 h. For the co-culture model, the A549 cells were seeded at 1×10^5 cells per well in a 12-well plate and exposed to the EAC for 24 h. HCAEC were then exposed to the conditioned media (100%) obtained from the EAC-exposed A549 cells for an additional 24 h.

2.3.3 Cytotoxicity Assay

HCAEC were seeded at a concentration of 1×10^4 cells per well in a 96-well plate and treated with EAC or conditioned media for 24 h. HCAEC not exposed to EAC or EAC containing A549 conditioned media was used as the negative control. Following treatment, MTT reagent (10 µL of 5 mg/mL MTT; Sigma Aldrich, Castle Hill, NSW, Australia) was added to the media and cells were incubated for 3 h. Following

incubation, the MTT/media mix was removed, cells were then washed with PBS before the addition of dimethyl sulfoxide (DMSO; 100 μ L) to each well and absorbance at 565 nm was measured. Results were expressed as a percentage of negative control indicative of cell viability.

2.3.4 Intracellular Reactive oxygen Species (ROS) Assay

HCAEC were seeded in a 96-well plate and treated with EAC or conditioned media for 24 h as described above. HCAEC not treated with EAC was used as the negative control, and cells treated with hydrogen peroxide (H_2O_2) were used as a positive control. Following treatment, the cells were incubated with 20,70-dichlorodihydrofluorescein diacetate (H_2DCFDA) stain, and ROS level was determined as previously described [66]. Results were expressed as a percentage of negative control ROS activity.

2.3.5 Enzyme-Linked Immunosorbent Assay (ELISA)

HCAEC were seeded in a 96-well plate and treated for 24 h with EAC. HCAEC not treated with EAC was used as the negative control. After treatment, ELISA was performed on the cells as previously described to determine the expression of the markers, VCAM-1 and ICAM-1 [66]. Cotinine concentration was measured in plasma using an ELISA kit (Abnova, Taipei, Taiwan) as per the manufacturer's instructions.

2.3.6 *Animal Exposure*

Seven-week-old Balb/c female mice (n = 28) purchased from Animal Resource Centre (Perth, Western Australia, Australia) were housed in a 12 h light:12 h dark cycle with food and water available ad libitum. Following one week of acclimatisation, the mice in the same home cages were randomly assigned into three treatment groups (n = 9–10 per group) and exposed to ambient air (Sham): e-Cig aerosol generated from tobacco flavoured eliquid with nicotine (18 mg/mL) or without nicotine (0 mg/mL). Each group was subjected to their respective treatment in a 9 L chamber filled with e-Cig aerosol in two fifteen minute intervals with a five-minute aerosol free period in between, twice daily. Treatment conditions were based on previous maternal studies equating this exposure period to the smoke from two tobacco cigarettes. Tissue analysis on a subset of samples was performed in a double-blind manner, with group code only revealed during data analysis [67]. After 12 weeks of exposure, the mice were sacrificed, the left ventricle carefully excised, and snap-frozen in liquid nitrogen.

The human relevance of exposure to nicotine-containing e-Cig aerosol in this model has been characterised by the serum cotinine levels, a stable nicotine metabolite, measured 16 to 20 h post last exposure to sham/E-Cig aerosol [40]. Serum cotinine level were as follows sham: 3.31 ± 0.386 ng/mL; 18 mg: 17.41 ± 5.138 ng/mL; 0 mg: 5.97 ± 2.94 ng/mL. Additionally, previous studies have reported similar nicotine delivery volumes between e-Cigs and tobacco cigarettes (mean 1.3 mg e-Cig; 0.5–1.5 mg tobacco cigarette) [68]. These comparisons justify the comparison of cotinine levels between e-Cigs and cigarette users, in addition to the human relevance of mouse model illuminating the effects of e-Cig use. All animal experimental procedures were conducted in accordance with the guidelines described by the Australian National

Health and Medical Research council code of conduct for animals with approval from the University of Technology Sydney Animal Care and Ethics Committee (ETH15-0025).

2.3.7 Immunohistochemistry of the Heart Tissue

The frozen left ventricles (LV) were halved, embedded in OCT, and sectioned (10 µm) using a Cryostat NX70 (Thermo Fisher Scientific, Gibco, Waltham, MA, USA). Slides were adhered onto gelatin-coated slides by air drying for 20 min before they were fixed in 10% formalin at -20 °C in the freezer for 20 min. Slides were washed in PBST (phosphate buffer saline + 0.1 Tween-20), incubated in blocking buffer (3% Goat serum diluted in 1% BSA in PBST-PBS with 0.1% Triton-X) for 1 h at room temperature before incubation with rabbit anti-FKBPL polyclonal antibody (1:100, Proteintech, Manchester, UK) and mouse anti-CD31 monoclonal antibody (1:100, Proteintech, Manchester, UK) in a humidity chamber. The sections were then washed with PBST (3 times over 15 min), incubated with donkey antirabbit AlexaFlour 488 and goat anti-mouse Alexfluor 594 (Abcam, Cambridge, UK) at 1:500 dilution, and counterstained with DAPI (Thermo Fisher Scientific, Gibco, Waltham, MA, USA; 1:20,000) at room temperature for 1 hr. Three images per section were captured at 20× magnification using an Olympus BX51 fluorescence microscope with an Olympus DP73 camera at varying exposure times (DAPI: 50 ms; FKBPL: 100 ms; CD31: 100 ms). ImageJ 1.53a was used to calculate the mean greyscale value of the fluorescent intensity of FKBPL and CD31 where values were normalised to the SHAM group as previously described [69,70]. To assess the validity of the immunohistochemistry

staining, a negative control containing no primary antibody was used for each staining group.

2.3.8 Reverse Transcription-Polymerase Chain Reaction (RT-qPCR)

Total RNA was extracted from the other half of the LV by homogenisation in TRISURE (Bioline, Australia) using 1.4 mm zirconium oxide beads (Precellys, Bertin Technologies, Montigny-le-Bretonneux, France). Total RNA was then reverse transcribed using a Tetro cDNA synthesis kit (Bioline, Eveleigh, NSW, Australia) before qPCR was performed using SensiFAST SYBR No-ROX Kit (Bioline, Eveleigh, NSW, Australia) using the primers listed in Table 2.1. Total mRNA expression levels were calculated using the $2^{-\Delta\Delta CT}$ method using β -actin as the reference gene [69].

Table 2.1 qPCR primers and nucleotide sequence

Primer Name	Primer Sequence (5' 3')
<i>β-actin</i> (sense)	GATGTATGAAGGCTTTGGTC
<i>β-actin</i> (anti-sense)	TGTGCACTTTTATTGGTCTC
<i>ICAM-1</i> (sense)	CAGTCTACAACCTTTTCAGCTC
<i>ICAM-1</i> (anti-sense)	CACACTTCACAGTTACTTGG
<i>VCAM-1</i> (sense)	ACTGATTATCCAAGTCTCTCC
<i>VCAM-1</i> (anti-sense)	CCATCCACAGACTTTAATACC
<i>CD31</i> (sense)	CATCGCCACCTTAATAGTTG
<i>CD31</i> (anti-sense)	CCAGAAACATCATCATAACCG
<i>FKBPL</i> (sense)	TCTCTCAGGGATCAGGAG
<i>FKBPL</i> (anti-sense)	TATTTAAGATTTGCTGGGCG

2.3.9 *Tethered Bilayer Lipid Membrane (tBLMs) Assay*

Gold-coated microscope slides with a monolayer coating of 10% benzyl disulphide eleven-oxygen-ethylene-glycol reservoir linkers with a C20 phytanyl group as 'tethers' and 90% four-oxygen-ethylene-glycol reservoir linkers with a terminal OH group as 'spacers' were purchased from SDx Tethered Membranes Pty Ltd., Sydney, Australia. A lipid bilayer was then anchored to the slides using a solvent-exchange technique that employed 3 mM ethanolic solutions of 1,2-Dioleoyl-sn-glycero-3-phosphocholine (DOPC) (Avanti Polar Lipids Inc., Alabaster, AL, USA) [70]. The solvent used for the exchange was 100 mM NaCl 10 mM Tris buffer at pH 7. Dilutions of the EAC used this same buffer. Measurements of membrane conductance were done using swept frequency electrical impedance spectroscopy using an applied potential of 25 mV peak-to-peak, ranging from 0.1 Hz to 2000 Hz, delivered using a Tethapod™ electrical impedance spectrometer (SDx Tethered Membranes Pty Ltd., Sydney, Australia). The data from the impedance and phase profiles were fitted to an equivalent circuit consisting of a constant phase element, representing the imperfect capacitance of the tethering gold electrode and reservoir region, in series with a resistor/capacitor representing the lipid bilayer and a resistor, to represent the impedance of the surrounding electrolyte solution, as described previously [71]. A proprietary adaptation of a Levenberg–Marquardt fitting routine incorporated into the TethaQuick™ software v2.0.56 (SDx Tethered Membranes Pty Ltd., Sydney, Australia) was used to fit the data.

2.3.10 Statistical Analysis

All results are expressed as a mean \pm SEM. The data was checked for normal distribution before parametric (one-way ANOVA) or non-parametric tests (Kruskal-Wallis) with post-hoc multiple comparison tests were used. GraphPad Prism v8.00 (IBM, Boston, MA, USA) was used to analyse the results. Results with $p < 0.05$ were considered significant.

2.4 Results

2.4.1 Exposure of HCAEC to EAC-Treated Lung Cell Conditioned Media Results in Cytotoxicity

HCAEC directly exposed to 4% and 8% EAC generated from PG/VG without flavouring or nicotine showed a significant reduction in cell viability to $34 \pm 8.9\%$ ($p < 0.001$)/ $47 \pm 10.9\%$ ($p < 0.05$) and $29 \pm 4.9\%$ ($p < 0.01$)/ $38 \pm 2.2\%$ ($p < 0.01$) compared to the control cells, respectively (Figure 2.2A). A decrease in cell viability to $46 \pm 6.2\%$ ($p < 0.05$ versus control cells) was shown for HCAEC exposed to tobacco flavour EAC generated from e-liquid without (0 mg/mL) nicotine at the more concentrated EAC of 8%.

Using e-Cigs, the aerosol first comes into contact with the lung epithelial cells before influencing endothelial cells. Thus, to determine whether the response to the EAC from lung epithelial cells would affect the viability of HCAEC, A549 epithelial lung cells were exposed to EAC for 24 h before the conditioned media was used to treat HCAEC for another 24 h. Similar to the response of HCAEC directly exposure of EAC, exposure of conditioned lung epithelial cell media exposed to 4 and 8% EAC generated from

PG/VG without flavouring or nicotine resulted in significantly reduced HCAEC viability (Figure 2.2B). Exposure of conditioned lung epithelial cell media exposed to EAC generated from tobacco flavoured e-liquid without nicotine (0 mg/mL) also resulted in a decrease in cell viability to $32 \pm 4.9\%$ ($p < 0.001$) compared to the control cells (Figure 2.2B).

Whilst the MTT assay is a widely used assay for detecting cellular toxicity, there are confounding variables that should be considered when performing the assay [27]. To assess if our EAC could reduce MTT, we performed an MTT assay to determine if there were any interference of the MTT dye with the EAC. The results show no difference in absorbance for the lower concentrations of EAC, except PG/VG at 2% where a significant increase in absorbance from 1.0 (ctrl) to 1.09 (** $p < 0.01$; Figure S1) was observed. A significant increase was also observed for 8% EAC 0 mg and 18 mg with absorbance of 1.2 and 1.1, respectively (** $p < 0.0001$ vs. Ctrl). This suggests a minor catalytic effect of EAC on MTT reduction that is mediated by EAC.

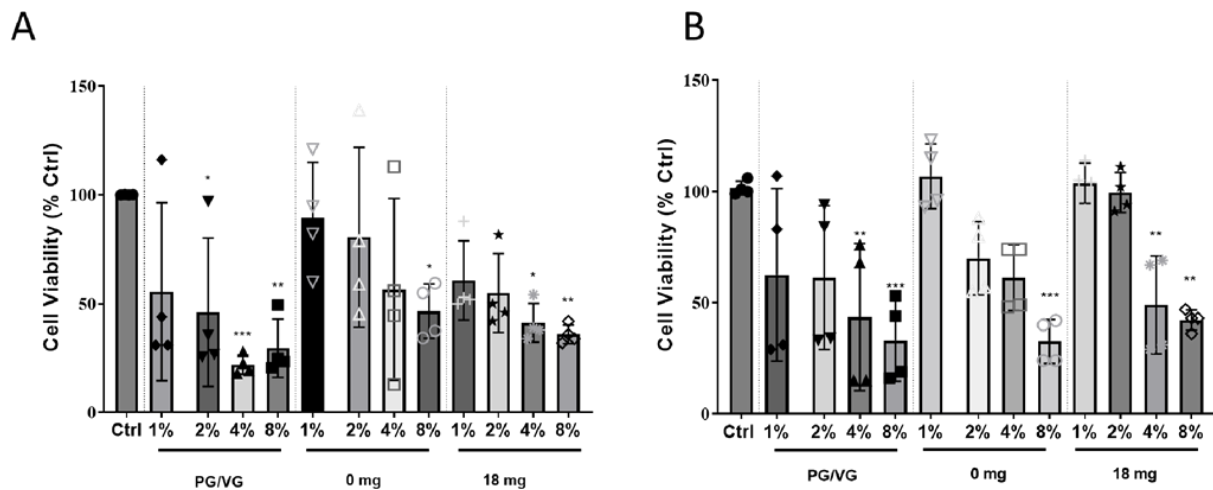


Figure 2.2 Cell viability in HCAEC exposed to (A) Direct effects of EAC. MTT Assay was performed on HCAEC after exposure to various concentration of EAC generated from: (i) a PG/VG solution (non-flavoured), (ii) 0 mg nicotine (tobacco flavoured), and (iii) 18 mg nicotine (tobacco flavoured) for 24 h. (B) Indirect effects of EAC. A549 epithelial lung cells were exposed to EAC under the same conditions. Media from the treated A549 cells were then used to treat HCAEC on a separate plate for 24 h before cell viability was assessed via MTT assay. Results are expressed as mean \pm SEM (n = 4 biological replicates). One-way ANOVA with Bonferroni post-tests was used for statistical analysis; * p < 0.05, ** p < 0.01, *** p < 0.001 versus Ctrl.

2.4.2 Direct Exposure to EAC or Indirectly to EAC-Lung Cell Conditioned Media Induces ROS Levels

ROS have been shown to play a crucial role in inducing endothelial dysfunction and oxidative stress in cells, a key mechanism behind atherogenesis and heart failure [28,29]. HCAEC exposed directly to 8% EAC generated from PG/VG or tobacco flavour e-liquid with (18 mg/mL) nicotine solution showed an increase in ROS levels by ~7.5-fold (p < 0.01) compared to control (Figure 2.3A).

Given the results of the cell viability experiments (Figure 2.2A), we had selected 2% EAC, as this did not result in a significant reduction of cell viability following direct exposure for PG/VG and 4% EAC to assess for effects on the ROS levels produced

by HCAEC in coculture conditions. Similar to the results observed in monoculture, an increase in ROS levels were shown in the co-culture model for HCAEC exposed to lung epithelial cell conditioned media for 4% PG/VG EAC, 4% tobacco flavoured EAC with (18 mg), or without nicotine (0 mg) by 6.7-fold, 3.2-fold, and 3.5-fold compared to the control, respectively ($p < 0.0001$; Figure 2.3B). HCAEC exposed to lung cell conditioned media showed a significant increase in ROS levels for 2% PG/VG EAC and 2% tobacco flavoured EAC without nicotine (0 mg) by 2.7-fold and 2.6-fold compared to the control, respectively ($p < 0.0001$; Figure 2.3B). No significance was shown for 2% tobacco flavoured EAC with (18 mg).

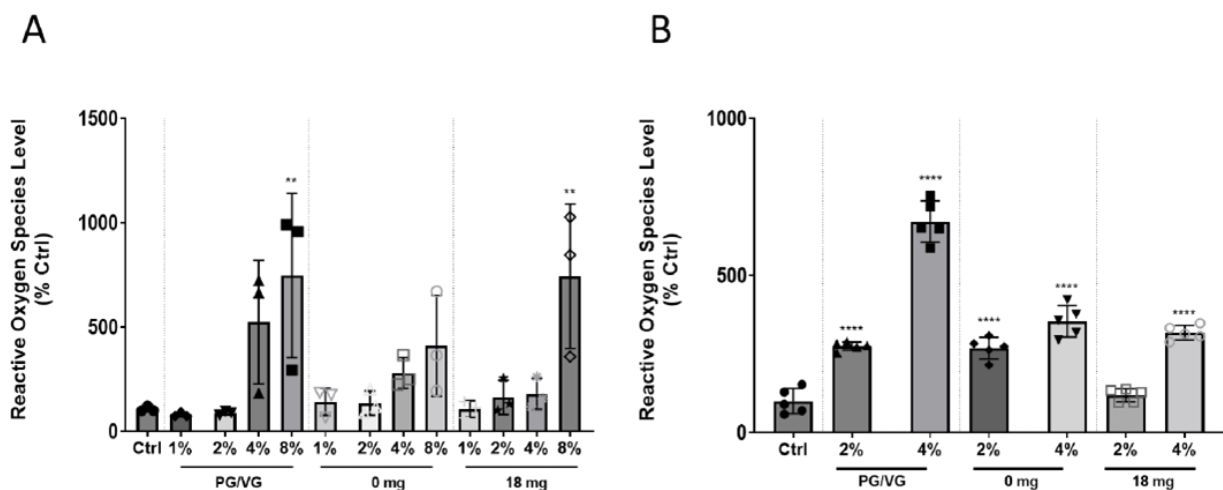


Figure 2.3 Reactive oxygen species levels in HCAEC after (A) Direct EAC exposure. ROS levels were measured in HCAEC after exposure to various concentration of EAC generated from: (i) a PG/VG standard (non-flavoured), (ii) 0 mg nicotine (tobacco flavoured), and (iii) 18 mg nicotine (tobacco flavoured) at for 24 h. Data shown is expressed as a mean \pm SEM ($n = 3$ biological replicates). (B) Indirect effects of EAC. A549 epithelial lung cells were exposed to EAC under the same conditions. Media from the treated A549 cells were then used to treat HCAEC on a separate plate for 24 h before a DCF assay was performed. Data shown is expressed as a mean \pm SEM ($n = 5$ biological replicates). One-way ANOVA with Bonferroni post-tests was used for statistical analysis, ** $p < 0.01$; **** $p < 0.0001$ versus Ctrl.

2.4.3 Adhesion Molecule Expression Increases in HCAEC after EAC Exposure for ICAM-1, but not VCAM-1

A critical early event in atherogenesis is the adhesion of monocytes to the endothelium. The adhesion of monocytes occurs when the endothelial cells become activated in response to several factors, including oxidative stress, which leads to the upregulation of cell adhesion molecules (CAMs), such as VCAM-1 and ICAM-1 [17]. VCAM-1 or ICAM-1 protein levels were not significantly changed in HCAEC monoculture regardless of EAC used (Figure 2.4A, B). Although no significance was shown, an increase in ICAM-1 protein expression level to $60 \pm 21.1\%$ ($p = 0.068$ compared to control) could also be observed for HCAEC directly exposed to 2% EAC generated from e-liquid containing 18 mg/mL (Figure 2.4B). Given the monoculture showed a strong trend to changes for ICAM-1 protein levels with nicotine at 2% EAC, next, we only assessed the ICAM-1 levels in the co-culture model using 2% EAC. In contrast to the results of HCAEC directly exposed to EAC, exposure of HCAECs to conditioned media from lung epithelial cells treated with 2% EAC generated from e-liquid containing 18 mg/mL, an $83 \pm 8.9\%$ ($p < 0.01$ compared to control) increase in ICAM-1 protein levels was observed (Figure 2.4C).

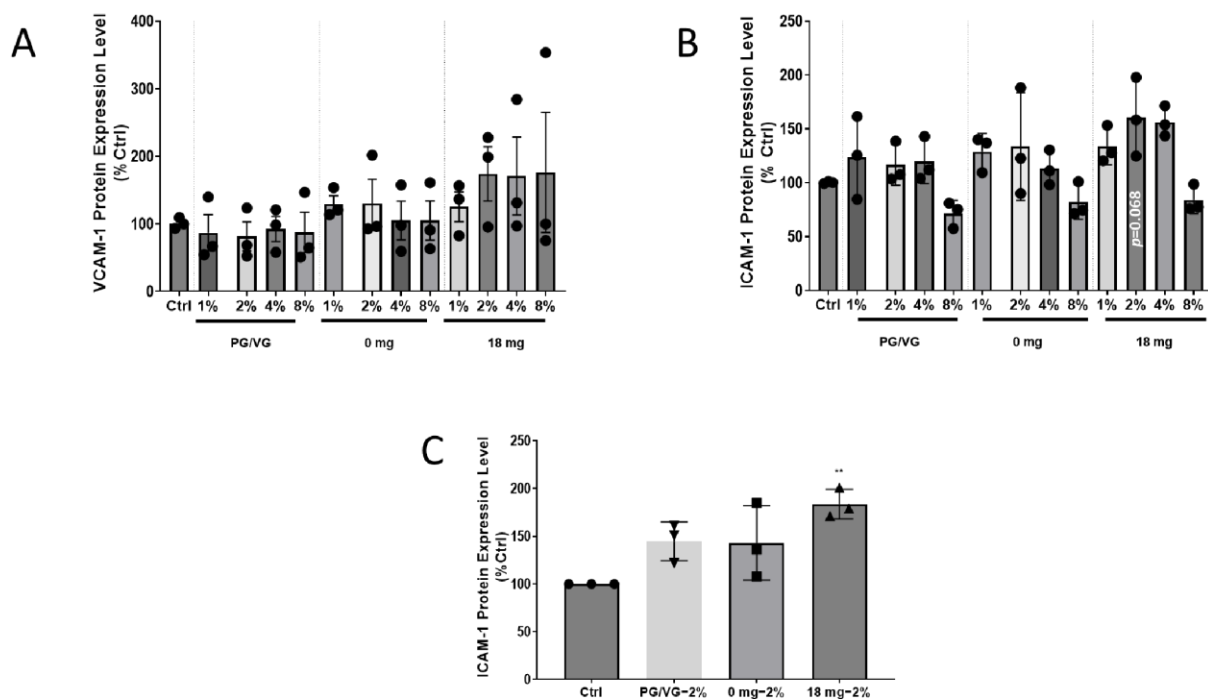


Figure 2.4 Expression of cellular adhesion molecules after exposure to EAC treatment. HCAEC were exposed to various concentrations of EAC generated from: (i) 0 mg nicotine (tobacco flavoured) and (ii) 18 mg nicotine (tobacco flavoured) for 24 h. (A) VCAM-1 protein expression. (B) ICAM-1 protein expression. (C) Indirect effects of EAC on ICAM-1 protein exposure. A549 epithelial lung cells were exposed to EAC under the same conditions. Media from the treated A549 cells were then used to treat HCAEC on a separate plate for 24 h before measuring ICAM-1 protein levels. Results are expressed as mean \pm SEM (n = 3 biological replicates). One-way ANOVA with Bonferroni post-tests was used for statistical analysis, ** p < 0.01 versus Ctrl.

2.4.4 EAC from Nicotine Containing e-Liquid Alters Membrane Permeability

Given nicotine is known to be membrane-permeable, we next assessed if EAC has an effect on membrane permeability using a tethered bilayer lipid membranes (tBLMs) assay [30]. These tBLMs are a model cell membrane anchored to a gold electrode that, when used in conjunction with electrical impedance spectroscopy techniques, enable a measure of how compounds and solutions can alter membrane structure and permeability to ions [31]. We tested 1% and 10% EAC generated from e-liquid with and without nicotine on tBLMs and measured the effects on membrane ion permeabilization using electrical impedance spectroscopy (Figure 2.5A). When the EAC is sourced from a fluid containing 18 mg/mL nicotine and applied to the tBLM, there is a marked increase in membrane conduction as measured using electrical impedance spectroscopy.

In contrast to the change in membrane conduction, the membrane capacitance does not show similar changes (Figure 2.5B). Membrane capacitance is a measure of membrane thickness and/or water content [31]. This data suggest that the EACs are not causing any significant membrane structural changes.

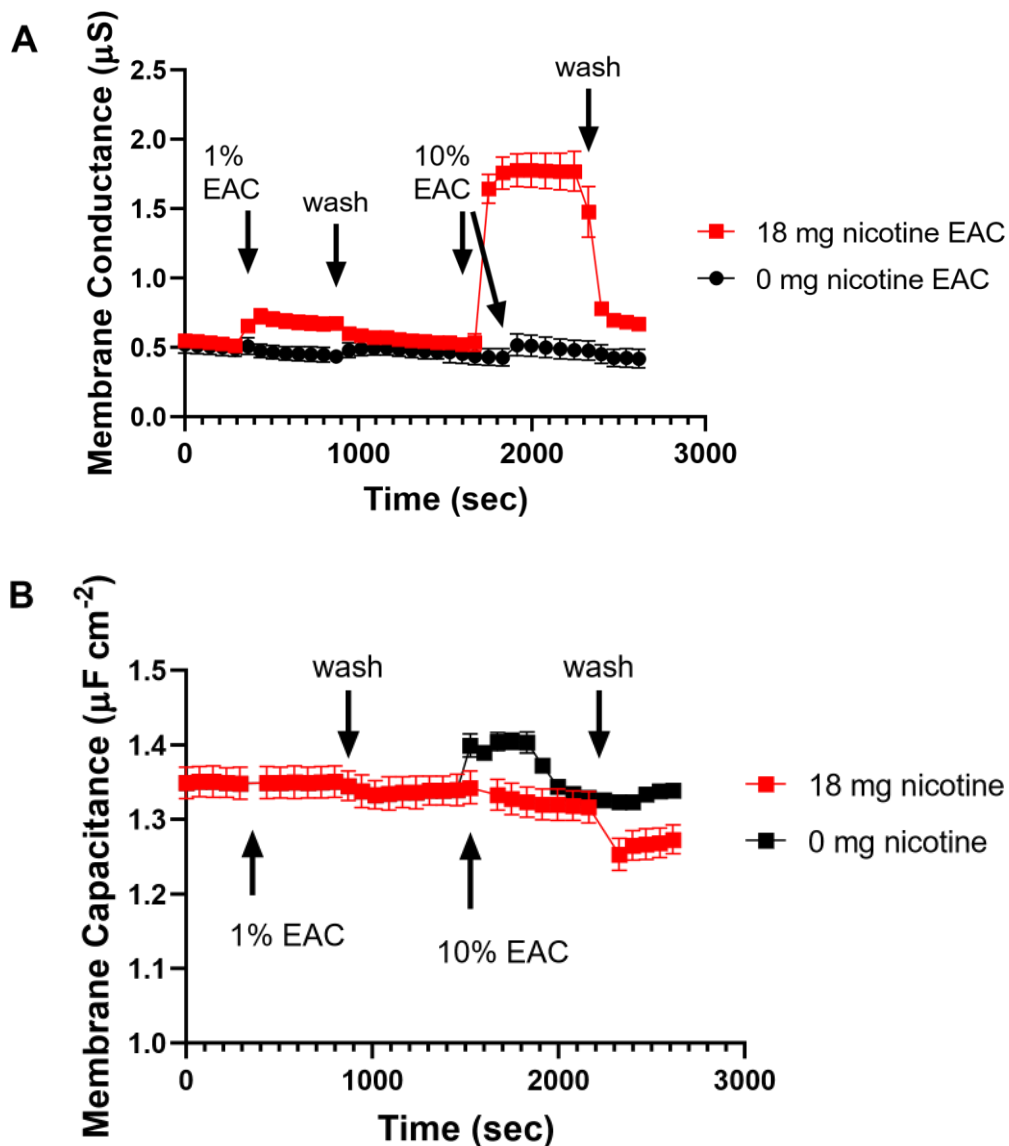


Figure 2.5 (A) Changes in membrane conduction of tethered bilayer lipid membranes (tBLM) in response to EAC (1% and 10%) in 100 mM NaCl 10 mM tris pH 7 buffer ($n = 3$). EAC solutions containing nicotine increase membrane conduction (membrane permeability). The effect of the nicotine-containing EAC rapidly falls away following a buffer wash. **(B)** In contrast, only minor changes of the membrane capacitances are observed in the same tBLMs, suggesting permeability changes aren't related to large membrane structural changes.

2.4.5 E-Cigarette Aerosol Increases ICAM-1 mRNA Expression in Murine Hearts

Adhesion molecules play a critical role in the pathogenesis of atherosclerosis, embedded with the inflammatory and immune response [32]. Systemic inflammation is a pivotal process of atherosclerosis and similarly contributes to the implication of endothelial cell activation in the pathogenesis of developing heart failure [33]. We therefore assessed the expression of adhesion molecules in animals exposed to e-Cig aerosol with or without nicotine. A significant difference in the mRNA expression of ICAM-1 and FKBPL levels were shown between the SHAM and 18 mg nicotine groups and SHAM and 0 mg nicotine groups, respectively (Figure 2.6B, C, $p < 0.05$). Contrastingly, the mRNA expression of VCAM-1 and CD31 exhibited no significant difference between groups (Figure 2.6A, D).

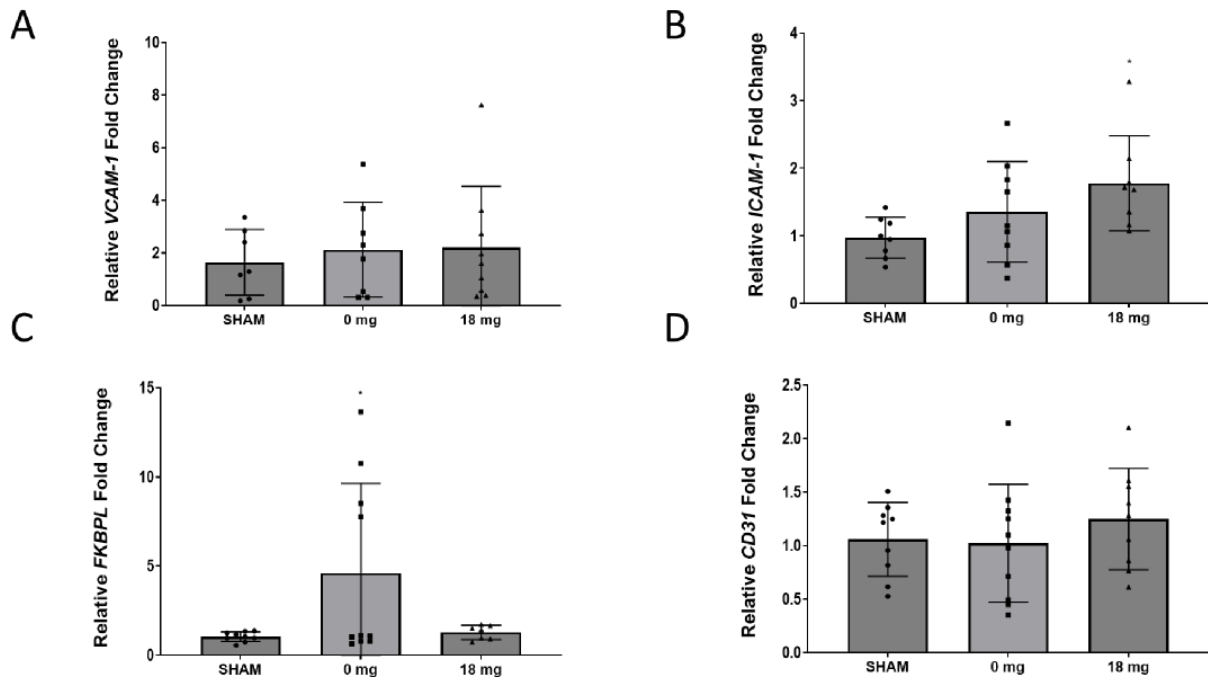


Figure 2.6 Cardiac VCAM1, ICAM1, and CD31 mRNA expression following treatment of mice with e-cigarettes with or without nicotine. RT-qPCR was performed on the left ventricle of mice exposed to ambient air (SHAM) or e-Cig aerosol (0 mg, 18 mg nicotine). **(A)** FKBPL. **(B)** CD31. **(C)** VCAM-1. **(D)** ICAM-1. All data expressed as mean fold change \pm SEM (n = 5–9). One-way ANOVA with Bonferroni post-test was used for statistical analysis, * p < 0.05 versus Sham.

2.4.6 Cardiac Angiogenesis Markers Are Dysregulated by E-Cig Aerosol Exposure

Angiogenic impaired regulation is an integral process in the development of cardiovascular diseases and therapeutic interventions. We therefore assessed FKBPL and CD31 protein expression in the LV of mice exposed to e-Cig aerosol with or without nicotine. Whilst no significant change in FKBPL or CD31 mRNA expression was observed, immunohistochemistry showed a significant 10-fold increase in FKBPL protein in 18 mg nicotine treatment group (p < 0.01) (Figure 2.7B) compared to the SHAM group. CD31 level paralleled the trend of FKBPL protein expression, where a significant 1.7-fold increase was seen in the 18 mg nicotine treatment group (p < 0.05) (Figure 2.7C).

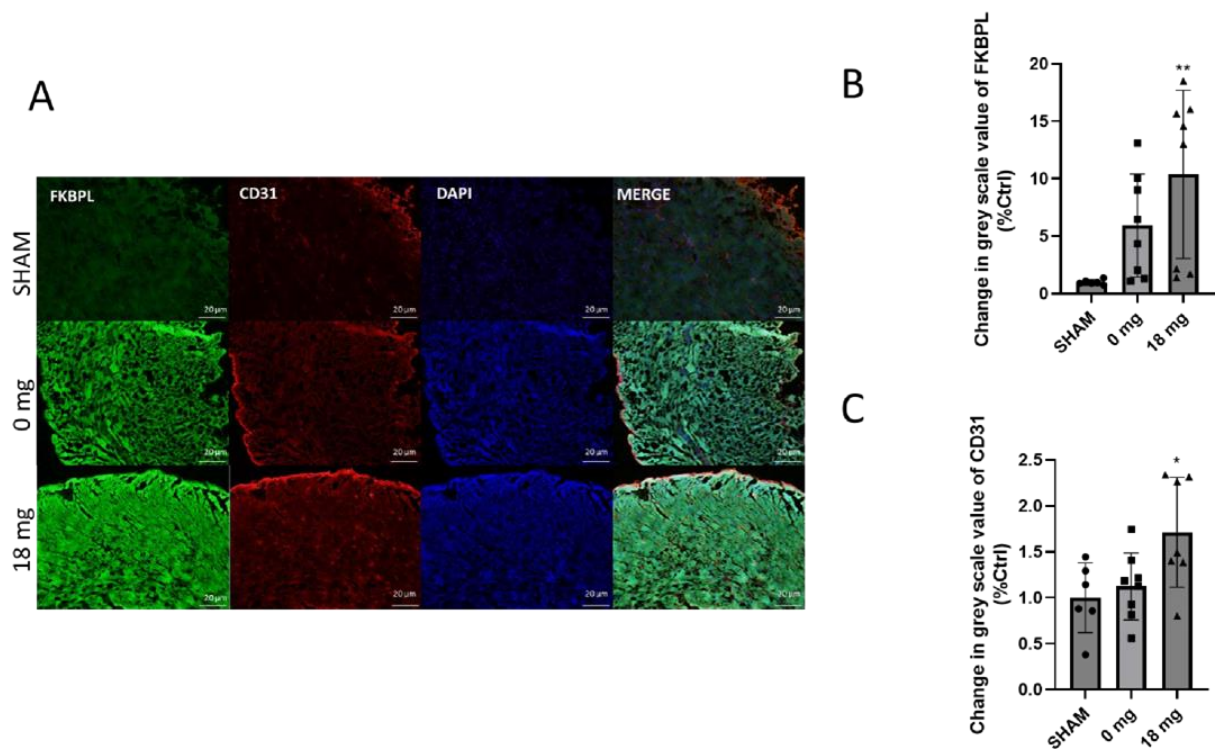


Figure 2.7 (A) Immunohistochemical on seven-week-old Balb/c female mice left ventricle sections (Scale bar = 20 μ m). Mice were treated in 3 groups: SHAM (ambient air), 0 mg (no nicotine), and 18 mg (nicotine) treatment groups. Sections were stained for FKBP1 (green), CD31 (red), and DAPI (blue) and images were taken at 20 \times . **(B)** FKBP1 staining intensity was quantified as the mean greyscale value in three images per sample, ** $p < 0.005$ (SHAM vs. 18 mg). **(C)** CD31 staining intensity was quantified as the mean greyscale value in three images per sample, * $p < 0.05$ (SHAM vs. 18 mg). Results are expressed as mean \pm SEM ($n = 5-9$) compared to SHAM. One-way ANOVA with Kruskal-Wallis post-tests was used for statistical analysis.

2.5 Discussion

The goal of the present study was to assess the effects of the use of e-Cigs on the health of endothelial cells. Our in vitro studies show endothelial cells exposed directly to EAC generated from the base e-liquid solution (PG/VG), e-liquid solution with or without nicotine induced a decrease cell viability, and an increase in ROS levels. Importantly, our study is the first to show that these adverse effects were exacerbated or remained even after exposure to lung cells using our indirect co-culture-like

treatment model. In vivo, cardiac changes indicative of angiogenesis was observed in animals, albeit only in animals exposed to e-Cig aerosol containing nicotine. These findings suggest e-Cigs can modulate and induce adverse changes to endothelial cells and the heart.

We wanted to evaluate the effects of e-Cig vaping where the e-liquid is heated through a device to generate aerosol that is subsequently inhaled by the user. Current studies vary in the methodologies used to collect and use e-Cig aerosol [14]. In this study, we chose to collect the condensate from the e-Cig aerosol to evaluate their effects on the health of endothelial cells at varying concentrations. Many studies exhibit the effect of e-Cig aerosol in individual cultures of a single cell type in which they can examine, for example, the respiratory tract or the endothelial effect [34]. In this study, we used both A549 epithelial lung cells and HCAECs to emulate the process of contacting the epithelial layer of the lung first before the e-Cigs metabolites reach the endothelial cells in the blood vessel. The exposure conditions used are based on previous studies within the same institute (UTS [35]). Tobacco flavouring was chosen due to its popularity amongst cigarette smokers [35] and relatively low ROS [36] content compared to its flavoured alternatives, and it is also the only flavour approved by the FDA [37]. Commercially available e-liquids can range from nicotine concentration of 0 mg/mL up to a concentration of 24 mg/mL, where 10 mg/mL appears to be the median amount for most users [38,39]. The chosen nicotine dose of 18 mg/mL is reflective of light smokers based on previously measured plasma cotinine levels [40,41]. Together, these treatment groups provide a reflective model of human e-Cig use, and importantly, our study shows that endothelial cells and markers of cardiac health are affected by e-Cig aerosol both in vitro and in vivo.

In this study, we demonstrated a significant reduction in cell viability of HCAECs following direct exposure to EAC generated from the e-liquid base constituents, PG and VG, alone. Noticeably, cell viability is shown to be decreased in all treatment groups, regardless of nicotine or flavouring, particularly using 8% EAC. This is consistent with the observations in the *in vivo* studies, where the effects on the lung, kidney, and liver seem to be nicotine-independent, suggesting the toxicity of heated base constituents and other mechanical factors, such as device settings, in the aerosolisation product [40–42]. The cytotoxic effect of PG/VG may be attributed to the thermal decomposition of the components, which produce toxic carbonyl compounds that are similarly present in cigarette smoke [43–45]. It was found that even the PG/VG treatment, absent of both flavouring and nicotine, is cytotoxic towards endothelial cells and possibly more so than the other treatment groups. Our results are in alignment with Anderson et al. (2016) [7] and Putzhammer et al. (2016) [46], who similarly showed significantly reduced cell viability in human umbilical vein endothelial cells (HUVEC) exposed to tobacco flavour and a variety of e-liquids. Of interest in our study, however, is that we showed significant cytotoxic effects in HCAECs exposed to conditioned media from lung cells exposed to EAC generated from the base/tobacco e-liquid (with or without nicotine), indicating the EAC likely initiate pro-inflammatory conditions in lung epithelial cells that subsequently induced a detrimental effect on the HCAECs.

Oxidative damage as a result of an imbalance in antioxidants and ROS levels has been shown to play an important role in atherogenesis and endothelial dysfunction during cigarette smoking [47–49]. In this study, we showed that HCAEC exposed directly to EAC at high concentrations with or without nicotine resulted in increased ROS levels in endothelial cells compared to the controls. Our results corroborate with

previous studies, which showed e-Cig vapour extracts increased levels of ROS expression in varying types of endothelial cells and that the pre-treatment of antioxidants on cells abrogated this effect [7,46,50,51]. Nitric oxide (NO) generated by endothelial nitric oxide synthase (eNOS) plays a crucial role in maintaining vascular physiology. In an oxidative stress state, eNOS uncoupling occurs, which results in ROS rather than NO being produced, cascading into the production of peroxynitrite (ONOO-) that has oxidative and cytotoxic effects, exacerbating endothelial dysfunction [52]. Whilst we did not assess if EAC induced eNOS uncoupling in HCAECs, El-Mahdy et al. recently demonstrated in situ induction of Nox-dependent ROS production and uncoupling of endothelial NO synthase by e-Cig exposure [53]. Decreased cell viability was similarly observed with HCAECs exposed to conditioned media from lung cells, even at small doses of 2% EAC, demonstrating significantly increased ROS levels. Whether lung cells exposed to EAC result in an increase in the secretion of pro-inflammatory cytokines and therefore induce further adverse effects on the HCAECs requires further investigation.

The oxidative stress response is linked to the inflammatory pathway, both of which lead to a disruption in the endothelial equilibrium and subsequently endothelial dysfunction, pivotal in the early stages of atherosclerosis. The first step in endothelial dysfunction is the expression of molecules that aid in the adhesion of monocytes to the endothelium and subsequent migration into the subendothelial space [54]. Whilst no change in VCAM1/ICAM-1 protein expression was observed following direct EAC treatment, indirect EAC treatment induced an increase in ICAM-1 in the HCAEC. In line with results from our study, a study by Makwana et al. (2021) [55] showed a significant increase in ICAM-1 expression in human aortic endothelial cells (HAECs) within a cardiovascular microfluidic model was reported following treatment with

traditional cigarette conditioned media, but not e-Cig conditioned media. Makwana et al., (2021) [55] also determined a significant e-Cig aerosol-induced (at the highest dose) increase in THP-1 monocyte adhesion to HAECs albeit only within 10 min of the adhesion period that diminished over time; the effect of tradition cigarette condition media was more pronounced at longer time points. Similarly, Muthumalage et al. (2017) [56] found significant dose-dependent increases in the proinflammatory cytokine, IL-8, following in vitro treatment of monocytic cells with flavoured e-liquid. IL-8 and ICAM-1 are, respectively, chemoattractant and adhesion molecules that are involved in monocyte adhesion [52]. However, it is noted that expression of these molecules can be dependent on the specific cell and stimuli type. It is noted that ROS generation reportedly increases ICAM-1 transcription in endothelial cells, but not always in epithelial cells [57]. This presents a possible ICAM-1 specific role in adhesion regulation after exposure to e-Cig condensate in endothelial cells. However, further investigation is required such as a monocyte adhesion assay that was performed by Makwana et al. (2021) [55] to determine the direct and indirect effect of EAC on THP-1 adhesion to HCAEC. Nevertheless, the assessment of murine hearts obtained from an in vivo model where mice were exposed to e-Cig aerosol with or without nicotine for 12 weeks showed an increase in cardiac ICAM-1 protein levels in mice exposed to e-Cig aerosol containing nicotine, suggesting that in vivo ICAM-1 could be initiating these early atherosclerosis changes. Nicotine has been demonstrated to have anti-inflammatory properties, suggesting that other factors, such as flavouring or the combination of both, are responsible for the increased inflammatory response [58].

In relation to angiogenesis, although changes were observed at the mRNA level only with 0 mg nicotine, FKBPL at the protein level was significantly increased following

exposure to nicotine e-Cig aerosol (18 mg). Similarly, CD31 [21,59] was also increased following exposure to e-Cig aerosol with nicotine, perhaps as part of the compensatory mechanism. The changes at the mRNA and protein levels are not always aligned, and it is well-known that FKBPL undergoes post translational modification due to its co-chaperone role [22,23]. Both FKBPL and CD31 related phenotypical changes are due to the changes at the protein level rather than the mRNA level. Hence, these results are more relevant to the downstream effects than the mRNA levels. The determinant factor for these results appears to involve the presence of nicotine, which has been shown to have pro-angiogenic properties [13]. Nicotine exhibits dose-dependent impacts on endothelial cell homeostasis and exhibits angiogenic effects that may be responsible for the pathogenesis of diseases like atherosclerosis [5,15,43]. Nicotinic acetylcholine receptors (nAChRs) are ligand-gated cation channels abundant in endothelial cells and mediate functions, such as proliferation, migration, and angiogenesis in vivo [60]. The effects of nicotine binding to these receptors include endothelium vasodilation, reduced NO availability and eNOS uncoupling, and directly acting on the elements involved in plaque formation [52,61]. Increases in FKBPL as a key anti-angiogenic regulator [62,63] and CD31 in the presence of nicotine are indicative of restrictive angiogenesis and perhaps a compensatory increase in the number of endothelial cells [22], suggesting that the combination of e-Cigs with nicotine are damaging to the cardiac vasculature causing early endothelial cell damage. This was also demonstrated in vitro. Furthermore, using our tethered membrane conductance platform, it was determined that nicotine is capable of altering the permeability of lipid bilayers to ions, such as Na⁺, which would have implications for a cell's ability to maintain membrane potential homeostasis. The nicotine was also readily washed from the membrane, suggesting it has a rapid off-

rate, as predicted by its membrane–water partition coefficient [64]. This is consistent with the rapid “hit” that smokers might feel upon initial nicotine exposure, which then rapidly falls away. Ultimately, nicotine plays a critical role in cell migration and vascular permeability, all of which can stimulate the development of atherosclerotic CVD [61].

Whilst we did not determine the exact mechanistic pathway of e-Cig aerosol that led to the adverse effects on endothelial health, we show that tobacco flavouring and nicotine can affect the extent of these adverse effects. However, this is the first study that implicates a critical anti-angiogenic protein, FKBPL, in the EAC-induced endothelial/heart damage. Unlike our *in vivo* results, our *in vitro* findings suggest that e-Cig aerosols affect endothelial homeostasis independent of nicotine. It has been shown that endothelial cell sensitivity of particulates, independent of nicotine, can elicit pro-inflammatory responses that disrupt endothelial cell homeostasis and progress CVD pathogenesis [16].

To the best of our knowledge, this is the first study to demonstrate the disruption of endothelial homeostasis following exposure to conditioned media from lung epithelial cells exposed to EAC, which seems to be more pronounced than direct EAC-exposure. This result is significant as it demonstrates that e-Cig use can potentially lead to the activation of endothelial cells, even after the EAC undergoes first-pass metabolism by lung epithelial cells. We are also reporting, for the first time, changes in a key anti-angiogenic mechanism mediated through FKBPL in murine hearts following exposure to E-cig aerosol with nicotine, suggesting that this combination can lead to cardiac damage and diastolic dysfunction, which we have previously shown in human studies where FKBPL was increased in the presence of diastolic dysfunction [21].

The limitations of this research article may be attributed to the wide and unregulated nature of the e-Cig market. We only used one flavour, one dose, and one e-Cig device in the animal model. There are thousands of e-Cig liquid flavours available in the market, and the by-products and constituents of the e-liquid differ between flavours. We only chose a relatively low dose exposure seen in light smokers, which cannot represent the situation of heavy smokers. Similarly, the e-Cig device market has grown exponentially in recent years, where different generations and styles of devices will contain varying atomiser strengths that can affect the aerosolisation process and chemical products of the e-liquids. We also used a different source of PG/VG mixture from that used in the commercial e-liquid and did not determine the exact amount of nicotine in our in vitro experiments. We used the conditioned media from A549 cells following exposure to EAC to assess if there are any metabolites from the A549 that could subsequently affect the HCAEC, the results may be an effect of unsuitable culture medium. Nevertheless, the control cells in the indirect co-culture like model were exposed similarly to conditioned media therefore any further effect from the EAC could still be observed. Future studies should examine the use of transwell membrane to confirm the results. We also note that the absorbance reading with incubation of the EAC with MTT reagent alone indicated interference of the EAC with the MTT assay. Therefore, future studies should ensure EAC-only controls are included when performing the MTT assay in addition to using complementary assays, such as the lactate dehydrogenase assay or live/dead staining to confirm the results. A further limitation of the study is that it remains largely descriptive of the effects of e-Cig extract, and more in-depth future studies addressing FKBPL-related molecular mechanism should be performed. We believe that these limitations must be taken into consideration in future studies. Additionally, there is no direct comparison of EAC to

the effects of tobacco cigarettes, which needs to be compared in future studies. There was some variation in cardiac FKBPL and CD31 expression within the groups from our in vivo study, which could be due to a small number of murine hearts per group that were processed for analyses. Increasing the number of mice per group or performing Western blot on homogenized tissue adjusted to a housekeeping protein may reduce variability.

2.6 Conclusion

Whilst the long-term adverse effects of e-Cig use on cardiovascular health are yet unknown, this study demonstrated that e-Cig condensates are associated with an increase in endothelial cell oxidative stress, inflammation, and cytotoxicity. This can impair endothelial cell integrity, lead to the restricted angiogenesis in the heart, and result in atherosclerosis and subsequently CVD.

2.7 Declarations

Author Contributions: All the experiments, analysis, and discussion of the results obtained in this study were completed by student M.C. except for the in vivo study. Conceptualisation: K.C.M. and L.M. Data acquisition, analysis and interpretation: E.T., T.N., Y.L.C., C.G.C., H.C., C.A.G., B.G.O., L.M. and K.C.M. Manuscript writing: M.C. Manuscript editing: K.C.M., L.M., C.G.C., H.C. and B.G.O. All authors have read and agreed to the published version of the manuscript.

Funding: This project funded was funded by the Australian Government RTP Fees Offset Scholarship as part of author Michael Chhor's doctoral degree. The animal study was supported by a project grant awarded to Hui Chen and Brian G Oliver by

Australian National Health & Medical Research Council (APP1158186). Yik Lung Chan is supported by the Peter Doherty Fellowship, National Health & Medical Research Council of Australia.

Institutional Review Board Statement: The animal study protocol was approved by the Animal Care and Ethics Committee at the University of Technology Sydney (ETH15-0025).

Informed Consent Statement: Not applicable.

Data Availability Statement: All relevant data are contained within the article.

Conflicts of Interest: The authors have no relevant financial or non-financial interest to disclose.

2.8 References

1. Stewart, J.; Manmathan, G.; Wilkinson, P. Primary prevention of cardiovascular disease: A review of contemporary guidance and literature. *JRSM Cardiovasc. Dis.* **2017**, *6*, 204800401668721.
2. Cardiovascular Diseases. Available online: https://www.who.int/health-topics/cardiovascular-diseases/#tab=tab_1 (accessed on 22 April 2020).
3. ABS. Heart, Stroke and Vascular Disease. Available online: <https://www.abs.gov.au/statistics/health/health-conditions-andrisks/heart-stroke-and-vascular-disease/latest-release>. (accessed on 22 April 2020).
4. WHO. *WHO Global Report: Mortality Attributable to Tobacco*; WHO: Geneva, Switzerland, 2014.
5. Banks, E.; Joshy, G.; Korda, R.; Stavreski, B.; Soga, K.; Egger, S.; Day, C.; Clarke, N.; Lewington, S.; Lopez, A. Tobacco smoking and risk of 36

cardiovascular disease subtypes: Fatal and non-fatal outcomes in a large prospective Australian study. *BMC Med.* **2019**, *17*, 128.

6. Abbot, N.C.; Stead, L.F.; White, A.R.; Barnes, J. Hypnotherapy for smoking cessation. *Cochrane Database Syst. Rev.* **1998**, CD001008.

7. Anderson, C.; Majeste, A.; Hanus, J.; Wang, S. E-Cigarette Aerosol Exposure Induces Reactive Oxygen Species, DNA Damage, and Cell Death in Vascular Endothelial Cells. *Toxicol. Sci.* **2016**, *154*, 332–340. Tayyarah, R.; Long, G.A. Comparison of select analytes in aerosol from e-cigarettes with smoke from conventional cigarettes and with ambient air. *Regul. Toxicol. Pharmacol.* **2014**, *70*, 704–710.

8. Cobb, N.K.; Byron, M.J.; Abrams, D.B.; Shields, P.G. Novel nicotine delivery systems and public health: The rise of the 'E-Cigarette'. *Am. J. Public Health* **2010**, *100*, 2340–2342. Skotsimara, G.; Antonopoulos, A.; Oikonomou, E.; Siasos, G.; Ioakeimidis, N.; Tsalamandris, S.; Charalambous, G.; Galiatsatos, N.; Vlachopoulos, C.; Tousoulis, D. Cardiovascular effects of electronic cigarettes: A systematic review and meta-analysis. *Eur. J. Prev. Cardiol.* **2019**, *26*, 1219–1228. Tan, A.S.L.; Bigman, C.A. E-Cigarette Awareness and Perceived Harmfulness Prevalence and Associations with Smoking Cessation Outcomes. *Am. J. Prev. Med.* **2014**, *47*, 141–149.

9. Patel, D.; Taudte, R.; Nizio, K.; Herok, G.; Cranfield, C.; Shimmon, R. Headspace analysis of E-cigarette fluids using comprehensive two dimensional GC×GC-TOF-MS reveals the presence of volatile and toxic compounds. *J. Pharm. Biomed. Anal.* **2021**, *196*, 113930.

10. Whitehead, A.K.; Erwin, A.P.; Yue, X. Nicotine and vascular dysfunction. *Acta Physiol.* **2021**, *231*, e13631.

11. Cheng, T. Chemical evaluation of electronic cigarettes. *Tob. Control* **2014**, *23*, ii11.

12. George, J.; Hussain, M.; Vadiveloo, T.; Ireland, S.; Hopkinson, P.; Struthers, A.; Donnan, P.; Khan, F.; Lang, C. Cardiovascular Effects of Switching from Tobacco Cigarettes to Electronic Cigarettes. *J. Am. Coll. Cardiol.* **2019**, *74*, 3112.

13. Barber, K.E.; Ghebrehiwet, B.; Yin, W.; Rubenstein, D.A. Endothelial Cell Inflammatory Reactions Are Altered in the Presence of E-Cigarette Extracts of Variable Nicotine. *Cell. Mol. Bioeng.* **2017**, *10*, 124.
14. Rajendran, P.; Rengarajan, T.; Thangavel, J.; Nishigaki, Y.; Sakthisekaran, D.; Sethi, G.; Nishigaki, I. The Vascular Endothelium and Human Diseases. *Int. J. Biol. Sci.* **2013**, *9*, 1057.
15. Förstermann, U.; Xia, N.; Li, H. Roles of vascular oxidative stress and nitric oxide in the pathogenesis of atherosclerosis. *Circ. Res.* **2017**, *120*, 713–735.
16. Celermajer, D.S.; Sorensen, K.; Gooch, V.; Miller, O.; Sullivan, I.; Lloyd, J.; Deanfield, J.; Spiegelhalter, D. Non-invasive detection of endothelial dysfunction in children and adults at risk of atherosclerosis. *Lancet* **1992**, *340*, 1111–1115.
17. Bernhard, D.; Csordas, A.; Henderson, B.; Rossmann, A.; Kind, M.; Wick, G. Cigarette smoke metal-catalyzed protein oxidation leads to vascular endothelial cell contraction by depolymerization of microtubules. *FASEB J.* **2005**, *19*, 1096–1107.
18. Januszewski, A.S.; Watson, C.; O’Niell, V.; McDonald, L.; Ledwidge, M.; Robson, T.; Jenkins, A.; Keech, A.; McClements, L. FKBPL is associated with metabolic parameters and is a novel determinant of cardiovascular disease. *Sci. Rep.* **2020**, *10*, 21655.
19. Yakkundi, A.; Bennett, R.; Herenandez-Negrete, I.; Delalande, J.; Hanna, M.; Lyubomska, O.; Arthur, K.; Short, A.; McKeen, H.; Nelson, L.; et al. FKBPL is a critical antiangiogenic regulator of developmental and pathological angiogenesis. *Arterioscler. Thromb. Vasc. Biol.* **2015**, *35*, 845–854.
20. DeLisser, H.M.; Christofidou-Solomidou, M.; Strieter, R.; Burdick, M.; Robinson, C.; Wexler, R.; Kerr, J.; Garlanda, C.; Merwin, J.; Madri, J.; et al. Involvement of endothelial PECAM-1/CD31 in angiogenesis. *Am. J. Pathol.* **1997**, *151*, 671.
21. Lertkiatmongkol, P.; Liao, D.; Mei, H.; Hu, Y.; Newman, P.J. Endothelial functions of PECAM-1 (CD31). *Curr. Opin. Hematol.* **2016**, *23*, 253.

22. Gordon, C.; Gudi, K.; Krause, A.; Sackrowitz, R.; Harvey, B.; Strulovici-Barel, Y.; Mezey, J.; Crystal, R. Circulating Endothelial Microparticles as a Measure of Early Lung Destruction in Cigarette Smokers. *Am. J. Respir. Crit. Care Med.* **2012**, *184*, 224–232.
23. Kato, R.; Mizuno, S.; Kadowaki, M.; Shiozaki, K.; Akai, M.; Nakagawa, K.; Oikawa, T.; Iguchi, M.; Osanai, K.; Ishizaki, T.; et al. Sirt1 expression is associated with CD31 expression in blood cells from patients with chronic obstructive pulmonary disease. *Respir. Res.* **2016**, *17*, 139.
24. Ghasemi, M.; Turnbull, T.; Sebastian, S.; Kempson, I. The mtt assay: Utility, limitations, pitfalls, and interpretation in bulk and single-cell analysis. *Int. J. Mol. Sci.* **2021**, *22*, 12827.
25. Van der Pol, A.; van Gilst, W.H.; Voors, A.A.; van der Meer, P. Treating oxidative stress in heart failure: Past, present and future. *Eur. J. Heart Fail.* **2019**, *21*, 425–435.
26. Incalza, M.A.; D’Oria, R.; Natalicchio, A.; Perrini, S.; Laviola, L.; Giorgino, F. Oxidative stress and reactive oxygen species in endothelial dysfunction associated with cardiovascular and metabolic diseases. *Vascul. Pharmacol.* **2018**, *100*, 1–19.
27. Squier, C.A. Penetration of nicotine and nitrosornicotine across porcine oral mucosa. *J. Appl. Toxicol.* **1986**, *6*, 123–128.
28. Alghalayini, A.; Garcia, A.; Berry, T.; Cranfield, C.G. The Use of Tethered Bilayer Lipid Membranes to Identify the Mechanisms of Antimicrobial Peptide Interactions with Lipid Bilayers. *Antibiotics* **2019**, *8*, 12.
29. Galkina, E.; Ley, K. Vascular adhesion molecules in atherosclerosis. *Arterioscler. Thromb. Vasc. Biol.* **2007**, *27*, 2292–2301.
30. Patel, R.B.; Colangelo, L.; Bielinski, S.; Larson, N.; Ding, J.; Allen, N.; Michos, E.; Shah, S.; Lloyd-Jones, D. Circulating vascular cell adhesion molecule-1 and incident heart failure: The multi-ethnic study of atherosclerosis (MESA). *J. Am. Heart Assoc.* **2020**, *9*, e019390.

31. Qasim, H.; Karim, Z.A.; Rivera, J.O.; Khasawneh, F.T.; Alshbool, F.Z. Impact of Electronic Cigarettes on the Cardiovascular System. *J. Am. Heart Assoc.* **2017**, *6*, e006353.
32. Romijnders, K.A.G.J.; Krusemann, E.; Boesveldt, S.; de Graaf, K.; de Vries, H.; Talhout, R. E-Liquid Flavor Preferences and Individual Factors Related to Vaping: A Survey among Dutch Never-Users, Smokers, Dual Users, and Exclusive Vapers. *Int. J. Environ. Res. Public Health* **2019**, *16*, 4661.
33. Cao, Y.; Wu, D.; Ma, Y.; Ma, X.; Wang, S.; Li, F.; Li, M.; Zhang, T. Toxicity of electronic cigarettes: A general review of the origins, health hazards, and toxicity mechanisms. *Sci. Total Environ.* **2021**, *772*, 145475.
34. FDA. Premarket Tobacco Product Marketing Granted Orders. Available online: <https://www.fda.gov/tobacco-products/premarket-tobacco-product-applications/premarket-tobacco-product-marketing-granted-orders> (accessed on 22 April 2020).
35. Fischman, J.S.; Sista, S.; Lee, D.K.; Cuadra, G.A.; Palazzolo, D.L. Flavorless vs. Flavored Electronic Cigarette-Generated Aerosol and E-Liquid on the Growth of Common Oral Commensal Streptococci. *Front. Physiol.* **2020**, *11*, 1513.
36. Smets, J.; Baeyens, F.; Chaumont, M.; Adriaens, K.; van Gucht, D. When Less is More: Vaping Low-Nicotine vs. High-Nicotine E-Liquid is Compensated by Increased Wattage and Higher Liquid Consumption. *Int. J. Environ. Res. Public Health* **2019**, *16*, 723.
37. Chen, H.; Li, G.; Chan, Y.; Chapman, D.; Sukjamnong, S.; Nguyen, T.; Annissa, T.; McGrath, K.; Sharma, P.; Oliver, B. Maternal E-cigarette exposure in mice alters DNA methylation and lung cytokine expression in offspring. *Am. J. Respir. Cell Mol. Biol.* **2018**, *58*, 366–377.
38. Li, G.; Chan, Y.; Wang, B.; Saad, S.; George, J.; Oliver, B.; Chen, H. E-cigarettes damage the liver and alter nutrient metabolism in pregnant mice and their offspring. *Ann. N. Y. Acad. Sci.* **2020**, *1475*, 64–77.

39. Li, G.; Chan, Y.; Nguyen, L.; Mak, C.; Zaky, A.; Answer, A.; Shi, Y.; Nguyen, T.; Pollock, C.; Oliver, B.; et al. Impact of maternal e-cigarette vapor exposure on renal health in the offspring. *Ann. N. Y. Acad. Sci.* **2019**, *1452*, 65–77.
40. Behar, R.Z.; Wang, Y.; Talbot, P. Comparing the cytotoxicity of electronic cigarette fluids, aerosols and solvents. *Tob. Control* **2018**, *27*, 325.
41. Kosmider, L.; Sobczak, A.; Fik, M.; Knysak, J.; Zaciera, M.; Kurek, J.; Goniewicz, M. Carbonyl Compounds in Electronic Cigarette Vapors: Effects of Nicotine Solvent and Battery Output Voltage. *Nicotine Tob. Res.* **2014**, *16*, 1319.
42. Farsalinos, K.E.; Voudris, V.; Poulas, K. E-cigarettes generate high levels of aldehydes only in 'dry puff' conditions. *Addiction* **2015**, *110*, 1352–1356.
43. Putzhammer, R.; Doppler, C.; Jakschitz, T.; Heinz, K.; Förste, J.; Danzl, K.; Messner, B.; Bernhard, D. Vapours of US and EU Market Leader Electronic Cigarette Brands and Liquids Are Cytotoxic for Human Vascular Endothelial Cells. *PLoS ONE* **2016**, *11*, e0157337.
44. Carnevale, R.; Sciarretta, S.; Violi, F.; Nocella, C.; Loffredo, L.; Perri, L.; Peruzzi, M.; Marullo, A.; De Falco, E.; Chimenti, I.; et al. Acute Impact of Tobacco vs. Electronic Cigarette Smoking on Oxidative Stress and Vascular Function. *Chest* **2016**, *150*, 606–612.
45. Cai, H.; Harrison, D.G. Endothelial dysfunction in cardiovascular diseases: The role of oxidant stress. *Circ. Res.* **2000**, *87*, 840–844.
46. Stocker, R.; Keaney, J.F. Role of Oxidative Modifications in Atherosclerosis. *Physiol. Rev.* **2004**, *84*, 1381–1478.
47. Rao, P.S.S.; Ande, A.; Sinha, N.; Kumar, A.; Kumar, S. Effects of Cigarette Smoke Condensate on Oxidative Stress, Apoptotic Cell Death, and HIV Replication in Human Monocytic Cells. *PLoS ONE* **2016**, *11*, e0155791.
48. Zhao, J.; Zhang, Y.; Sisler, J.D.; Shaffer, J.; Leonard, S.S.; Morris, A.M.; Qian, Y.; Bello, D.; Demokritou, P. Assessment of reactive oxygen species generated by electronic cigarettes using acellular and cellular approaches. *J. Hazard. Mater.* **2018**, *344*, 549–557.

49. Münzel, T.; Hahad, O.; Kuntic, M.; Keaney, J.; Deanfield, J.; Daiber, A. Effects of tobacco cigarettes, e-cigarettes, and waterpipe smoking on endothelial function and clinical outcomes. *Eur. Heart J.* **2020**, *41*, 4057–4070.
50. El-Mahdy, M.A.; Ewees, M.; Eid, M.; Mahgoup, E.; Khaleel, S.; Zweier, J. Electronic cigarette exposure causes vascular endothelial dysfunction due to NADPH oxidase activation and eNOS uncoupling. *Am. J. Physiol.-Heart Circ. Physiol.* **2022**, *322*, H549–H567.
51. Steyers, C.M.; Miller, F.J. Endothelial Dysfunction in Chronic Inflammatory Diseases. *Int. J. Mol. Sci.* **2014**, *15*, 11324–11349.
52. Makwana, O.; Smith, G.; Flockton, H.; Watters, G.; Lowe, F.; Breheny, D. Impact of cigarette versus electronic cigarette aerosol conditioned media on aortic endothelial cells in a microfluidic cardiovascular model. *Sci. Rep.* **2021**, *11*, 4747.
53. Muthumalage, T.; Prinz, M.; Ansah, K.; Gerloff, J.; Sundar, I.; Rahman, I. Inflammatory and Oxidative Responses Induced by Exposure to Commonly Used e-Cigarette Flavoring Chemicals and Flavored e-Liquids without Nicotine. *Front. Physiol.* **2018**, *8*, 1130.
54. Roebuck, K.A. Oxidant stress regulation of IL-8 and ICAM-1 gene expression: Differential activation and binding of the transcription factors AP-1 and NF-kappaB (Review). *Int. J. Mol. Med.* **1999**, *4*, 223–230.
55. Gerloff, J.; Sundar, I.; Freter, R.; Sekera, E.; Friedman, A.; Robinson, R.; Pagano, T.; Rahman, I. Inflammatory Response and Barrier Dysfunction by Different e-Cigarette Flavoring Chemicals Identified by Gas Chromatography–Mass Spectrometry in e-Liquids and e-Vapors on Human Lung Epithelial Cells and Fibroblasts. *Appl. Vitro. Toxicol.* **2017**, *3*, 28–40.
56. Richards, C.; Sesperez, K.; Chhor, M.; Ghorpandour, S.; Rennie, C.; Chung Ming, C.; Evenhuis, C.; Nikolic, V.; Orlic, N.K.; Mikovic, Z.; et al. Characterisation of Cardiac Health in the Reduced Uterine Perfusion Pressure Model and a 3D Cardiac Spheroid Model, of Preeclampsia. *Biol. Sex Differ.* **2021**, *12*, 31.

57. Cooke, J.P. Angiogenesis and the role of the endothelial nicotinic acetylcholine receptor. *Life Sci.* **2007**, *80*, 2347.
58. Lee, J.; Cooke, J.P. Nicotine and Pathological Angiogenesis. *Life Sci.* **2012**, *91*, 1058.
59. Alqudah, A.; Eastwood, K.; Jerotic, D.; Todd, N.; Hoch, D.; McNally, R.; Obradovic, D.; Dugalic, S.; Hunter, A.; Holmes, V.; et al. FKBPL and SIRT-1 Are Downregulated by Diabetes in Pregnancy Impacting on Angiogenesis and Endothelial Function. *Front. Endocrinol.* **2021**, *12*, 459.
60. Todd, N.; McNally, R.; Alqudah, A.; Jerotic, D.; Suvakov, S.; Obradovic, D.; Hoch, D.; Hombrebueno, J.; Campos, G.; Watson, C.; et al. Role of A Novel Angiogenesis FKBPL-CD44 Pathway in Preeclampsia Risk Stratification and Mesenchymal Stem Cell Treatment. *J. Clin Endocrinol. Metab.* **2021**, *106*, 26.
61. Santi, P. Partition and transport of verapamil and nicotine through artificial membranes. *Int. J. Pharm.* **1991**, *68*, 43–49.
66. 65. Vis, M.A.M.; Ito, K.; Hofmann, S. Impact of Culture Medium on Cellular Interactions in in vitro Co-culture Systems. *Front. Bioeng. Biotechnol.* **2020**, *8*, 911.
67. McGrath, K.C.Y.; Li, X.H.; McRobb, L.S.; Heather, A.K. Inhibitory Effect of a French Maritime Pine Bark Extract-Based Nutritional Supplement on TNF- α -Induced Inflammation and Oxidative Stress in Human Coronary Artery Endothelial Cells. *Evid.-Based Complement. Altern. Med.* **2015**, *2015*, 260530.
68. Nguyen, T.; Li, G.E.; Chen, E.; Cranfield, C.G.; McGrath, K.C.; Gorrie, C.A. Maternal E-Cigarette Exposure Results in Cognitive and Epigenetic Alterations in Offspring in a Mouse Model. *Chem. Res. Toxicol.* **2018**, *31*, 601–611.
69. StHelen, G.; Havel, C.; Dempsey, D.A.; Jacob, P.; Benowitz, N.L. Nicotine delivery, retention and pharmacokinetics from various electronic cigarettes. *Addiction* **2016**, *111*, 535–544.

70. Bustin, S.A. Absolute quantification of mRNA using real-time reverse transcription polymerase chain reaction assays. *J. Mol. Endocrinol.* **2000**, *25*, 169–193.
71. Cranfield, C.; Carne, S.; Martinac, B.; Cornell, B. The assembly and use of tethered bilayer lipid membranes (tBLMs). *Methods Mol. Biol.* **2015**, *1232*, 45–53.
72. Berry, T.; Dutta, D.; Chen, R.; Leong, A.; Wang, H.; Donald, W.; Parviz, M.; Cornell, B.; Willcox, M.; Kumar, N.; et al. Lipid Membrane Interactions of the Cationic Antimicrobial Peptide Chimeras Melimine and Cys-Melimine. *Langmuir* **2018**, *34*, 11586–11592.

2.9 Supplementary Info

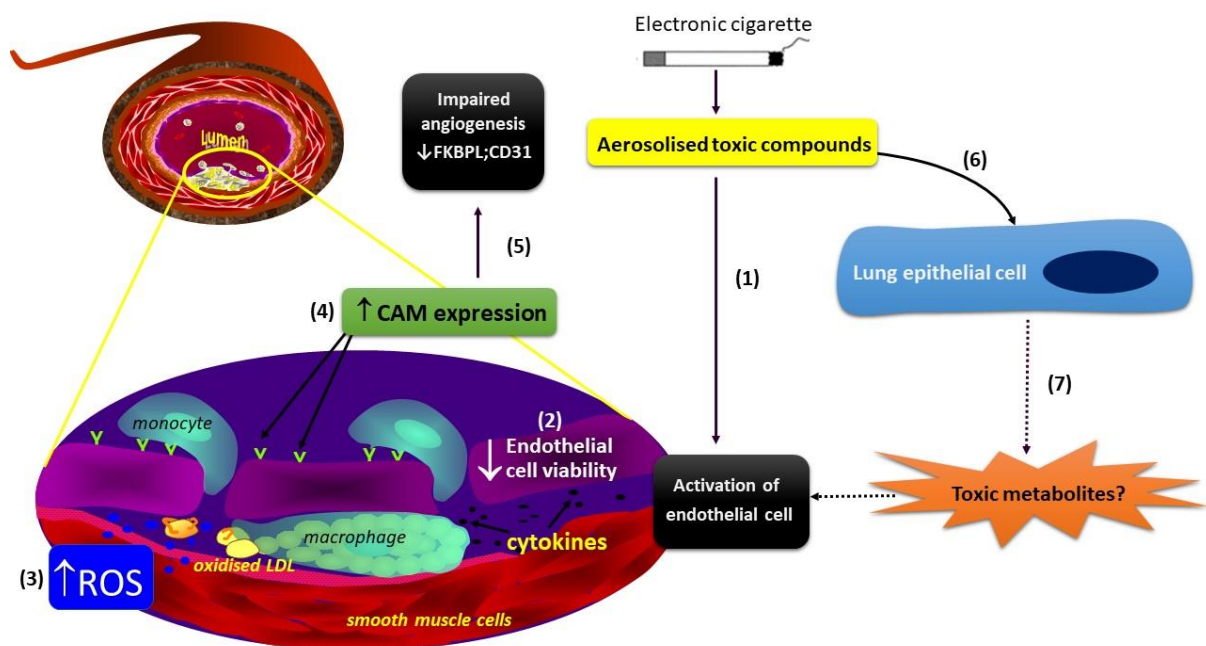


Figure S-2.1 Graphical Abstract. Graphical Abstract. Schematic representation of the effect of E-cigarette aerosol directly on endothelial cell function or after first-pass metabolism by epithelial lung cells. Aerosolised toxic compounds from e-Cigs can incite endothelial cell activation. Resultant effects of decreased cell viability, increased ROS, increased CAM expression, and impaired angiogenesis follow. After first pass metabolism of epithelial cells, an enhanced effect may be pronounced.

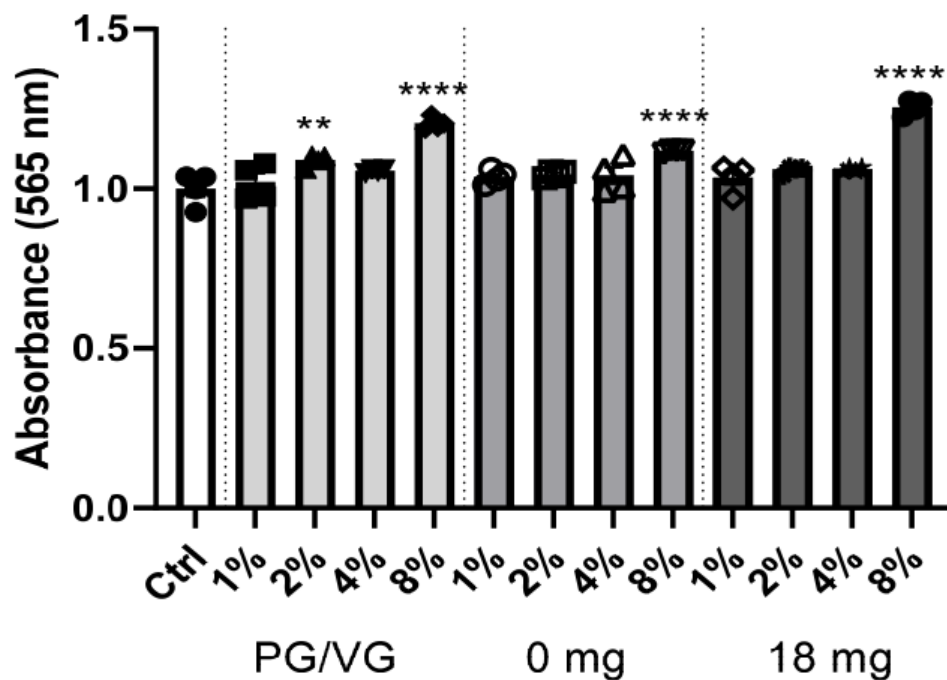


Figure S-2.2 Absorbance of cell-free Endothelial Cell Growth Medium containing different concentrations of EAC after 3 hours of incubation with MTT reagent (10 μ L of 5 mg/mL MTT). Results are expressed as mean \pm SEM (n=4). One-way ANOVA with Bonferroni post-tests was used for statistical analysis; **p<0.01, ****p<0.0001 versus Ctrl.

Chapter 3

Elucidating the role of FKBPL in *in vitro* Cardiac Fibrosis Models

Cardiac fibrosis is a complex physiological process that is present in several cardiovascular diseases, ultimately resulting in heart failure. As a multifactorial process, understanding of its current mechanisms requires further research, as well as effective treatment methods. FKBPL's emerging role in inflammation and secretion by fibroblast cells implicates the possibility of its involvement in the fibrotic process. In this chapter, we elucidated the role of FKBPL as a potential pathogenic mechanism of cardiac fibrosis by using representative human fetal fibroblast cells under the stimulation of fibrotic and hypoxic treatments, and AD-01, as an FKBPL-based therapeutic peptide mimetic. FKBPL was also knocked down in fibroblasts to determine its effect of cardiac fibrosis markers and monocyte adhesion. Comparably, we expand on this scope with two different *in vitro* models (2D & 3D) to better understand and represent the complex cell-cell and cell-extracellular matrix (ECM) interactions within a 3D environment using the new technology and specialised hydrogel containing cardiac peptides representative of cardiac physiological environment within a 3D Bioprinter. The findings of this study reveal FKBPL's potential cardioprotective role at reduced levels through decreased collagen and α -SMA expression, or TGF- β /HIF-1 α -mediated effects that should be explored further.

merging Role of FK5 6 binding rotein like (FKBPL) in cardiac fibrosis

Michael Chhor¹, Shreya Barman¹, Fatemeh Heidari¹, Amy L. Bottomley², Abdelrahim Alqudah^{3,4}, David Grieve³, Tracy Robson⁵, Kristine McGrath¹, Lana McClements^{1,3*}

¹ *School of Life Sciences, Faculty of Science, University of Technology Sydney, NSW, Australia*

² *Australian Institute of Microbiology and Infection, Faculty of Science, University of Technology Sydney, Sydney, NSW, Australia.*

³ *The Wellcome-Wolfson Institute for Experimental Medicine, School of Medicine, Dentistry and Biomedical Sciences, Queen's University Belfast, Northern Ireland, UK*

⁴ *Department of Clinical Pharmacy and Pharmacy Practice, Faculty of Pharmaceutical Sciences, The Hashemite University, Zarqa, Jordan*

⁵ *School of Pharmacy and Biomolecular Sciences, Royal College of Surgeons in Ireland, University of Medicine and Health Sciences, Dublin, Ireland.*

*Corresponding author

Lana McClements

E-mail: lane.mcclements@uts.edu.au

- **This research article is currently under preparation for submission**

Keywords: FKBPL, fibrosis, heart failure, 3D bioprinting

3.1 Abstract

Background: Cardiac fibrosis characterised by increased collagen deposition and extracellular matrix (ECM) remodelling is one of the main causes of heart failure. Inflammation and hypoxia are key processes in cardiac fibrosis although the mechanisms are poorly understood. In this study, we elucidated, for the first time, the role of FKBPL in cardiac fibrosis models.

Methods: Left ventricle tissue was collected from 26-week-old *fkbp1*^{+/-} transgenic or wild type mice (n≥8 per group) and collagen deposition and gene expression assessed using picrosirius staining or qPCR, respectively. Innovative 3D bioprinted model of cardiac fibrosis was developed using fetal fibroblast cells (HFF08) and customised ECM cardiac components and pro-fibrotic/hypoxic factors (TGF- β , 10ng/ml, DMOG, 1mM) \pm FKBPL mimetic (AD-01, 100mM). In parallel, 2D *in vitro* models were also employed.

Results: In the left ventricles from *fkbp1*^{+/-} mice, collagen deposition (p<0.001) and *col1a1* mRNA expression (p<0.05), were reduced, compared to controls. In 3D bioprinted model, fibroblasts formed networks spontaneously and stimulated by all treatments (p<0.05-0.0001). This was in conjunction with reduced FKBPL expression that was significant in the presence of DMOG/AD-01 treatment (p<0.05). In 2D cell culture, AD-01 potentiated TGF- β -induced *col1a1* (p<0.001) and *mmp2* mRNA (p<0.05) expression whereas DMOG or reduced FKBPL expression abrogated this (p<0.05-0.001). Following siRNA FKBPL transfection, α -SMA was reduced (p<0.05). No differences were observed in monocyte adhesion assay.

Conclusion: Low FKBPL expression could be protective in cardiac fibrosis through the reduction in collagen production and α -SMA expression, or TGF- β /HIF-1 α -

mediated effects. Therapeutic strategies that inhibit FKBPL should be explored to abrogate cardiac fibrosis.

3.2 Introduction

Heart disease is the leading cause of death worldwide and cardiac fibrosis is one of the key underlying pathologies. Cardiac fibrosis is characterised by the accumulation of extracellular matrix (ECM) proteins, particularly collagen I and III, by cardiac fibroblasts within the cardiac muscle [1]. However, currently there is no cure for cardiac fibrosis. The main physiological function of cardiac fibroblasts is to maintain the homeostasis of the ECM providing structural support for the cardiomyocytes hence enabling mechanical and electrophysiological functions of the heart [2]. Cardiac fibroblasts comprise less than 20% of the heart with the vast majority originating from embryonic epicardium [3]–[5] and are more hypoxic with increased glycolytic metabolism compared to other interstitial cells within the heart [6]. Following myocardial infarction (MI), where there is a substantial cardiomyocyte death, inflammation and subsequently fibrosis are activated in order to repair cardiac damage. Due to the limited regenerative capacity of the heart, tissue repair as a result of MI involves removal of necrotic cardiomyocytes by the collagen-rich fibrotic scar tissue [7]. This leads to pathological cardiac remodelling, which adversely impacts the function of the heart in the long-term. However, it maintains structural integrity and prevents devastating complications including cardiac rupture [8]. This process is initiated by infiltrating inflammatory cells including monocytes, that once at the site of injury, they differentiate into macrophages, and together with neutrophils and lymphocytes, remove the necrotic tissue [7], [9]. As a result of this process, a number

of critical pro-inflammatory and profibrotic factors are secreted including transforming growth factor beta (TGF- β), fibroblast growth factors (FGFs), platelet-derived growth factor (PDGF), interleukin (IL)-6 and IL-1 β , which stimulate cardiac fibroblasts proliferation and differentiation into myofibroblasts [1], [9], [10]. Other circulating progenitors or surrounding precursor cells could also be the source of myofibroblasts [11]. During this process, myofibroblasts acquire new phenotype characterised by increased expression of α -smooth muscle actin (α -SMA) that become more contractile and are able to secrete larger amounts of ECM including collagen. They also release matrix metalloproteinases (MMPs), which degrade the ECM and remove matrix debris from the wound [12], [13]. Excess ECM and collagen deposition together with MMP matrix degradation leads to adverse remodelling stage that can persist for months and ultimately results in fibrotic scar formation. Nevertheless, the mechanisms of cardiac fibrosis are not very well understood, which has impeded the development of effective treatments.

An emerging immunophilin protein, FK506-binding protein like (FKBPL), is a divergent member of this group, expressed ubiquitously with the strongest expression in fibroblasts and endothelial cells [14]–[16]. Full knockout of FKBPL in mice was embryonically lethal demonstrating its critical role in developmental and physiological angiogenesis [16]. FKBPL has also been shown to regulate STAT3-NF κ B inflammatory mechanisms in ovarian cancer [17], however its role in cardiac fibrosis is still emerging [18]. Inhibition of other immunophilins such as FKBP12 and cyclophilin A, led to reduction in cardiac fibrosis in various in vitro and in vivo models [19]. In the context of cardiovascular disease, previous studies have shown that FKBPL is one of the key determinants of cardiovascular disease in people without

diabetes mellitus [20] and it has a role in cardiac hypertrophy with potential diagnostic utility of heart failure with preserved ejection fraction [21]. A therapeutic peptide based on the active anti-angiogenic domain of FKBPL was developed and preclinical 24-amino acid candidate peptide, AD-01, has been shown to bind CD44 and inhibit migration of both endothelial and cancer cells [14]. We have also shown that AD-01 is able to inhibit angiotensin-II (Ang-II)-induced cardiac hypertrophy by downregulating FKBPL [21]. A clinical candidate 23-amino acid peptide, ALM20, completed Phase Ia clinical trials for the treatment of solid tumours and was granted an orphan drug status by the Food and Drug Administration for treatment of ovarian cancer [22]. The aims of this study are to further explore the role of FKBPL in cardiac fibrosis using FKBPL transgenic mouse model and in vitro models of cardiac fibrosis that include treatments with profibrotic stimuli, TGF- β and/or hypoxic stimuli, dimethylxalylglycine (DMOG), in the presence or absence of FKBPL-therapeutic peptide, AD-01. We also report on a novel 3D bioprinted model of cardiac fibrosis.

3.3 Methods

3.3.1 FKBPL Transgenic Mice

All in vivo experiments were conducted according to the UK Animals (Scientific Procedures) Act 1986 and approved by the Queen's University Belfast Animal Welfare and Ethical Review Committee. Male wild type (C57BL/6J) and FKBPL transgenic mice (Fkbpl^{+/-}) mice were housed in groups of up to 5, under standard conditions of a 12 h light-dark cycle at a constant temperature of 21°C. All mice were bred from an established colony at Queen's University Belfast [16] and were aged between 8-12

weeks and >20 g body weight. Genotyping of the mice was performed as described before [16]. Mice were fed a regular chow diet for 13 weeks before mice were sacrificed by being terminally anaesthetised by i.p. injection of a mixture of ketamine (100 mg/kg) and xylazine (10 mg/kg) and the tissues including the heart collected for downstream ex vivo analysis.

3.3.2 Collagen Staining Assessment

Paraffin-embedded left ventricular heart sections were processed and stained with picrosirius red stain (Fluka Analytical, UK). Images were taken at 40x magnification using a Nikon Eclipse 80i microscope. Collagen fibres were then quantified in five random sections per heart, analysing two separate fields of view per section and excluding coronary vessels and perivascular regions. The images were analysed using Image J software by subjecting them to grey scale transformation to adjust the threshold.

3.3.3 3D Bioprinted Model of Cardiac Fibrosis

HFF08 cells were bioprinted using the RASTRUM 3D cell culture platform (Inventia Life Sciences, Australia), following a specifically generated protocol via the RASTRUM cloud software (Inventia Life Sciences, Australia). Sterile filtered water, 70% ethanol, and proprietary bioinks and activators were added to a RASTRUM cartridge following software prompts to create the base layer matrix in a black 96-well plate (PerkinElmer, USA). Cells were printed at 4×10^5 cells/ml as an imaging plug; a conformation that centralises the matrix and cells in a circular area in the middle of the well. Following

bioprinting, 150 μ L of foetal fibroblast growth media was added to each well. Cells were monitored daily using the Incucyte to follow 3D network formation for a span of 10-14 days. Treatments were added on day 4 and 7 once fibroblast networks were formed. As part of the optimisation, matrix selection was also performed using three different types of matrices of varying stiffnesses (0.7kPa or 3kPa) and containing different activators/peptides mimicking cardiac microenvironment to determine the most suitable ECM.

3.3.4 Cell Proliferation Assay

Cell proliferation was measured in the 3D bioprinted plate using alamarBlue (Thermo-fisher Scientific, USA). At days 1, 3, 7 and 10, cells were washed with PBS before adding 90 μ L of foetal fibroblast media and 10 μ L of alamarBlue reagent to each well. Cells are incubated for 16 hours at 37°C before fluorescence was read on the plate reader at 530 nm excitation and 590 nm emission. Cells are aspirated before washing with PBS and replenished with 100 μ L of foetal fibroblast media and treatment.

3.3.5 Live/Dead Viability Assay

Fibroblasts (HFF08) cell viability within the 3D culture was determined using a Viability/Cytotoxicity Assay Kit for Live & Dead Cells (Biotium, USA). Working solutions of 1 μ M Calcein AM, 2 μ M Ethidium homodimer-III and 10 μ g/mL Hoechst 33342 (Thermo Fisher Scientific, USA) were added to each well, and incubated at 37°C for 30 minutes. Subsequently, cells were washed and imaged using the live cell imaging

system, IncuCyte, at 10x magnification. Cell viability was quantified using the area of live and dead cells before a live-to-dead cell ratio was calculated.

3.3.6 *Immunofluorescence Staining*

The 3D bioprinted were firstly fixed in 4% PFA (Sigma-Aldrich, USA) for 20 minutes at room temperature, washed three times with 150 μ L of PBS before 100 μ L of blocking solution (1% BSA, 3% goat serum in PBST) was added to each well and incubated overnight at 4°C. Cells were washed three times with 150 μ L of PBS for 30 minutes before incubating with the primary antibody diluted in blocking solution, overnight at 4°C. FKBPL rabbit polyclonal (1:500; Abcam, UK), Vimentin mouse monoclonal (1:500; Abcam, UK), and α -SMA rabbit monoclonal antibody (1: 500; Abcam, UK) were used as the primary antibodies. The following day, cells were washed three times with 150 μ L of PBS before incubating with the secondary antibodies. Goat Anti-Mouse IgG H&L (AlexaFlour 488; 1:400; Abcam, UK) and Goat Anti-Rabbit IgG H&L (Alexa Fluor 594; 1:400; Abcam, UK) along with 4',6-diamindion-2- phenylindole (DAPI: Thermo Fisher Scientific, USA) diluted in blocking solution were added to each well to incubate overnight at 4°C. Cells were washed three times with 150 μ L of PBS for 30 minutes before adding 150 μ L of PBS to prepare for immunofluorescent imaging. Imaging was performed on the Nikon Ti Live inverted wide-field microscope (Nikon, Japan) at 20x magnification with three random images per well taken. Z stacks (0.2 μ m optical slices) were acquired using a 0.5 AU pinhole as previously described [23]. Fluorescence intensity per antibody indicating protein expression per treatment was quantified relative to the control group and normalised to DAPI using Image J.

3.3.7 Network Formation

Prior to and following treatment of the 3D bioprinted cells, whole well phase contrast images of each well were captured using the Incucyte Live-Cell Analysis System (Sartorius AG, Germany) at 10x magnification for network formation analysis. Images were analysed and quantified in Image J, using the Angiogenesis Analyzer as previously described [24] to detect and map the nodes, branch length and number of networks. The data was normalised to the control group with no treatments added.

3.3.8 Cell Culture and Treatments

Human foetal fibroblasts (HFF08) were kindly donated by Prof Bernard E Tuch. HFF08 cells were cultured in foetal fibroblast culture medium (Sigma-Aldrich, United Kingdom). Cells were grown and used up to passage 20 for both 2D and 3D culture experiments. Cells were treated with a combination of TGF- β (10ng/mL) (Sigma-Aldrich, United Kingdom), dimethyloxalylglycine (DMOG) (1mM) (Sigma-Aldrich, United Kingdom), and AD-01 (100nM) (Sigma-Aldrich, United Kingdom). Treatment groups were as follows: i)TGF- β , ii)TGF- β + AD-01, iii)DMOG, iv)DMOG + AD01, v)DMOG + TGF- β , vi)TGF- β + DMOG + AD01 used in both 2D and 3D culture models.

3.3.9 Transfection

HFF08 cells were seeded at 0.2×10^5 cells/ml in a 48-well plate (Corning, USA) with 300 μ L of growth medium per well. The following day, complete medium was replaced with Opti-MEM reduced serum medium (Thermo Fisher Scientific, USA) and siRNA

transfection solutions added to the required wells. FKBPL siRNA knockdown was performed in the 2D culture model using Lipofectamine RNAiMAX (ThermoFisher Scientific, USA), ON-target plus NTsiRNA (10 μ M) (Dharmacon, United Kingdom) and ON-target plus FKBPL siRNA (10 μ M) using concentrations accordant to the manufacturer's instructions. The cells were incubated with the transfection solutions for 48 hours before cells were detached and used for downstream experiments.

3.3.10 Reverse Transcription-polymerase chain reaction (RT-qPCR)

Total RNA was extracted from HFF08 cells cultured in a 6-well plate (Company, Location) in the 2D culture model in the presence of treatments for 24h as described above. For ex vivo analysis, total RNA was extracted from frozen heart sections of the left ventricle. Reverse transcription was performed using a Tetro cDNA Synthesis Kit (Bioline, Australia) before performing RT-qPCR using a SensiFAST SYBR No-ROX Kit (Bioline, Australia). The sequence of the primers used are listed in Table 3.1 & 3.2. Total mRNA expression were calculated using the $2^{-\Delta\Delta CT}$ method using β -actin and 18S as the reference genes.

Table 3.1 Human primers forward and reverse sequencing

Gene	Forward	Reverse
β ctin	GACGACATGGAGAAAATCTC	ATGATCTGGGTCATCTTCTC
8S	CGGCTACCACATCCAAGGAA	GCTGGAATTACCGCGGCT
FKBPL	CATTTAGCTTTGGAAGGAGAG	TCCAATTGTATTGACTGGTG
S 4a	AAGTTCAAGCTCAACAAGTC	CAGCTTCATCTGTCTTTTC
COL	GCTATGATGAGAAATCAACCG	TCATCTCCATTCTTTCCAGG
POSTN	ATACTCTCCAGTGTTCTGAG	TTGGCAGAATCAGGAATTAG
CTGF	TTAAGAAGGGCAAAAAGTGC	CATACTCCACAGAATTTAGCTC
MMP2	GTGATCTTGACCAGAATACC	GCCAATGATCCTGTATGTG
MMP	AAGGATGGGAAGTACTGG	GCCCAGAGAAGAAGAAAAG

Table 3.2 Human primers forward and reverse sequencing

Gene	Forward	Reverse
β-Actin	GATGTATGAAGGCTTTGGTC	TGTGCACTTTTATTGGTCTC
Col3A1	ACTCAAGAGTGGAGAATACTG	AACATGTTTCTTCTCTGCAC
Col1A1	CGTATCACCAAACCTCAGAAG	GAAGCAAAGTTTCCTCCAAG
FN1	CCTATAGGATTGGAGACACG	GTTGGTAAATAGCTGTTCCG
FSP-1	TATTCAGCACTTCCTCTCTC	CCTCTTTGCCTGAGTATTTG
POSTN	CCATTAACGGAATCAAGAATGG	AACTTGTTTGGCAGAATCAG
CTGF	GAGGAAAACATTAAGAAGGGC	AGAAAGCTCAAACCTTGACAG

3.3.11 Western Blotting

Total protein was extracted from 5x10⁵ HFF08 cells cultured in a 6-well plate (Corning, USA) and treated for 24 h hours as described above in the 2D culture model. Proteins were separated by molecular weights using sodium dodecyl sulfate polyacrylamide gel electrophoresis (SDS-PAGE). The loading buffer for SDS-PAGE was Laemmli sample buffer containing the reducing agent dithiothreitol (DTT). The standard ladder used to estimate the molecular weight of protein was Kaleidoscope protein ladders (Bio-Rad Laboratories, USA). FKBPL rabbit monoclonal antibody (1: 1,000; Abcam, UK) and α-SMA rabbit monoclonal antibody (1: 1,000; Abcam, UK) were used as the primary antibodies for probing alongside with GADPH (1: 8,000; Abcam, UK) to normalise the relative protein expression. The membrane was scanned by ChemiDoc imaging system (Bio-Rad Laboratories, USA). The scanned pictures with peptide bands were processed through ImageJ for quantification normalised to the reference gene.

3.3.12 *Monocyte Adhesion Assay*

HFF08 cells were seeded in a 96-well plate (Corning, USA) at 1×10^5 cells per well for 24 hours. Following 24 hours, treatments were added as described above. Human monocytic cells (THP-1; ATCC, USA) were resuspended at 7×10^5 cells/mL in serum free RPMI media (Thermo-fisher Scientific, USA), and spiked with 20 μ L of calcein green (Thermo-fisher Scientific, USA) before being incubated for 30 minutes at 37°C. Next, cells were washed with 100 μ L of PBS, and 100 μ L of spiked cell suspension was added to each well and incubated for a further 30 minutes. Non-adherent THP-1 cells were removed with a PBS wash, and subsequently 100 μ L of PBS was added to each well. Whole well images were captured using the Incucyte Live-Cell Analysis System (Sartorius AG, Germany) at 10x magnification for green fluorescence of the adhered cells. Quantification of the adhered cells were performed on these images using Image J (NIHS, USA), where fluorescent adhered cells were identified by size using the cell counter function.

3.3.13 *Statistical Analysis*

All results are expressed as a mean \pm SEM. The data was assessed for normal distribution to determine whether parametric or non-parametric tests should be used for data analysis. For ex vivo data analysis, unpaired t-test or Mann-Whitney were used. In vitro data was analysed using either parametric one-way ANOVA with Sidak's post-hoc multiple comparison tests or non-parametric test (Kruskal-Wallis) in GraphPad Prism 9.5 (IBM, USA). The in vitro data with FKBPL or NT siRNA transfection was analysed using two-way ANOVA. Data from the 3D cell viability assay

was analysed using one-way ANOVA (repeated measures). Results with $p < 0.05$ were considered significant.

3.4 Results

3.4.1 FKBPL transgenic mice (*fkbp1^{+/-}*) seem to be protected against cardiac fibrosis

Cardiac fibrosis is characterised by increased collagen deposition that can lead to stiffening of the left ventricle and subsequently reduced heart function. To assess the role of FKBPL in interstitial fibrosis, we performed picosirius red staining on the left ventricle from both *Fkbp1* knockdown (*Fkbp1^{+/-}*) and wild type (*Fkbp1^{+/+}*), mice, at 26 weeks of age. Measured as the percentage of collagen fibres within the left ventricle tissue, collagen deposition was significantly reduced in *Fkbp1^{+/-}* mice compared to wild type controls (Figure 3.1A, $n \geq 8$, $p < 0.001$). Similarly, left ventricle type I collagen alpha chain (*Col1a1*) mRNA expression was reduced in *Fkbp1* knockdown mice (Figure 3.1B, $n \geq 8$, $p < 0.05$) whereas no difference was observed in other fibrotic genes including *Col3a1* (Figure 3.1C), *Fsp-1* (Figure 3.1D), *Postn* (Figure 3.1E), *Ctgf* (Figure 3.1F) and *Fn-1* (Figure 3.1G).

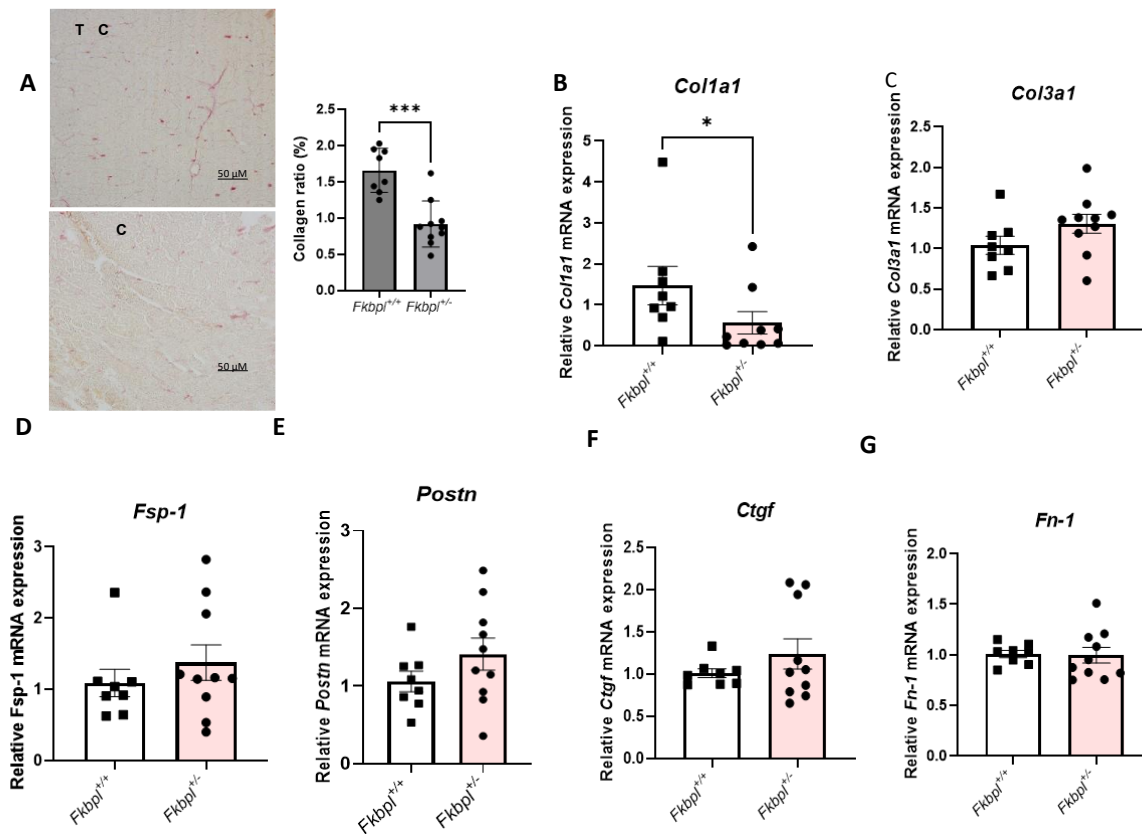


Figure 3.1 . Cardiac fibrosis measured by collagen deposition and collagen 1A1 gene expression is reduced in low FKBPL settings. (A) Percentage of collagen deposition within the left ventricle from wild type (*Fkbpl*^{+/+}) or FKBPL transgenic (*Fkbpl*^{+/-}) mice, was assessed following picrosirius staining. Five sections per heart were imaged at 40x magnification and area of cardiac fibrosis represented by collagen ratio determined (n≥8, unpaired t-test, ***<0.001). RNA was extracted from murine wild type (*Fkbpl*^{+/+}) or FKBPL transgenic (*Fkbpl*^{+/-}) left ventricle and quantitative polymerase chain reaction (qPCR) performed to determine the mRNA expression of six pro-fibrotic genes: **(B)** type I collagen alpha chain (Col1A1) **(C)** type III collagen alpha chain 1 (Col 3A1), **(D)** fibroblast specific protein (FSP-1), **(E)** periostin (POSTN), **(F)** connective tissue growth factor (CTGF), **(G)** fibronectin (FN-1). The mRNA expression was normalised to the house-keeping gene, β-actin. All data was expressed as mean fold change ± SEM; n≥8, unpaired t-test or Mann-Whitney test, *p<0.05.

3.4.2 FKBPL regulation in the new 3D bioprinted model of cardiac fibrosis

Given that collagen synthesis and deposition was reduced in low FKBPL settings, next, we wanted to explore the role of FKBPL signalling in cardiac fibrosis models. For this purpose, we developed an innovative in-house 3D bioprinted model of cardiac fibrosis using the RASTRUM cell culture platform. This 3D model bioprinted fetal fibroblast cells (HFF08) within various matrices that specifically mimic cardiac ECM. Therefore, three different matrices in the presence of various pro-fibrotic treatments (TGF- β , DMOG, AD-01) were evaluated in terms of their role in supporting fibroblast cell survival and network formation. Matrix 1 contained cardiac ECM peptides that mimic fibronectin and had ~ 0.7 kPa stiffness, Matrix 2 was of the same stiffness but contained additional peptides that mimic β -laminin, collagen 1 and hyaluronic acid whereas Matrix 3 was the stiffest (~ 3 kPa) and contained the same peptides as Matrix 2. Based on the cell morphology, survival and ability to form networks, Matrix 1 and 2 were selected as the most appropriate matrices for our model of cardiac fibrosis (Figure 3.2A). Matrix 3 did not support the development of any fibroblast networks (Figure 3.2A). Matrix 1 and 2 were further compared in terms of cell viability where the total area occupied by live versus dead cells was quantified (Figure 3.2B-D). In general, the presence of Matrix 2 appeared to support fibroblasts better, measured by an increased trend in the percentage of live cells (Figure 3.2B), and live to dead cell ratio (Figure 3.2D; $p=0.006$). Hence, Matrix 2 was employed for subsequent experiments.

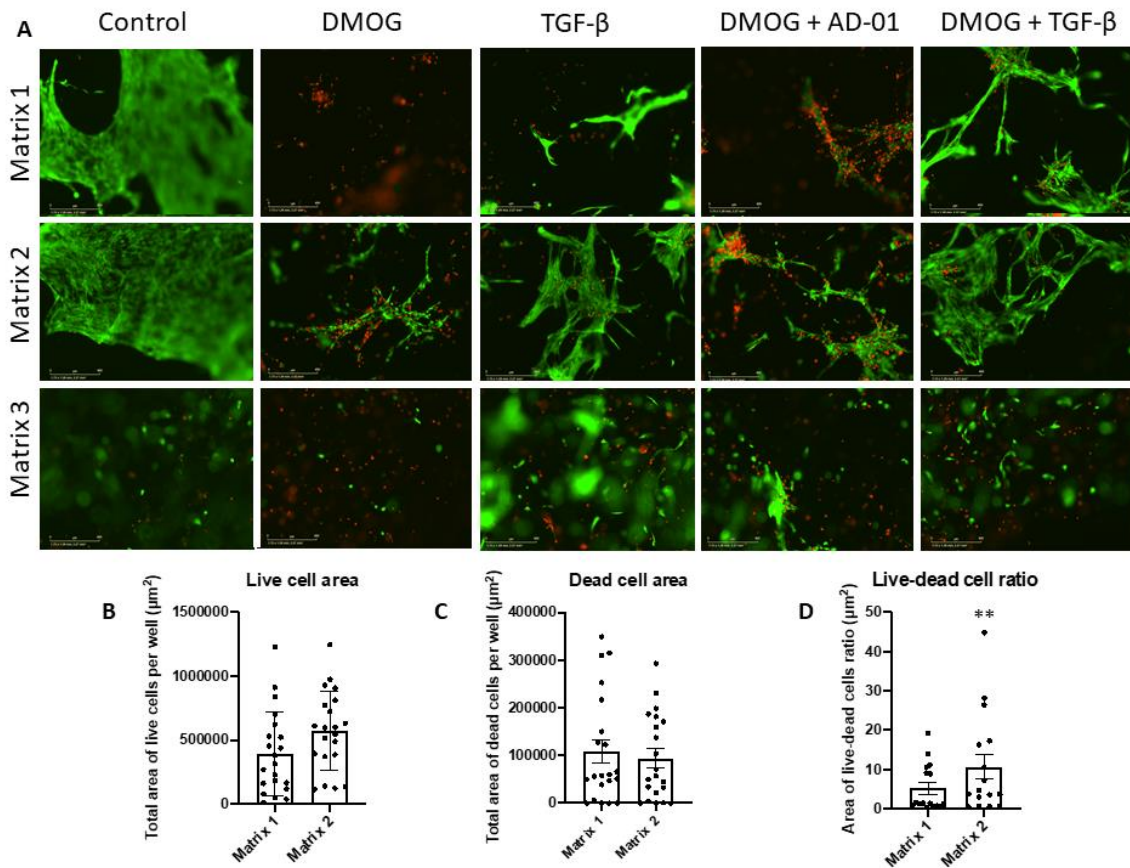


Figure 3.2 Optimising 3D bioprinted cardiac fibrosis model through extracellular matrix selection. Fetal fibroblast cells (HFF08) were bioprinted using RASTRUM platform within hydrogels of varying stiffnesses (Matrix 1; Px01.31P, ~0.7kPa, Matrix 2; Px01.29P, ~0.7kPa, Matrix 3; Px03.29P, ~3kPa) and containing different cardiac peptide composition to mimic fibronectin, β -laminin, collagen I, into a 96-well plate. Treatments were added on day 4 and 7 to include DMOG (1mM) and/or TGF- β (1ng/ml) and/or AD-01 (100nM). After 14 days in culture a live/dead viability assay was performed. Calcein AM dye (green) was used to stain live cells whereas ethidium homodimer-III (red) to stain dead cells. **(A)** Representative images of 3D fibroblast networks after 14 days in culture in the presence of various treatment combinations and within three different matrix types. The networks were captured on IncuCyte at 10x magnification. Total area of live cells **(B)**, total area of dead cells **(C)** and the live-to-dead cell ratio, between matrix 1 and 2 were determined using IncuCyte analysis software **(D)**. Data is presented as mean \pm SEM; n=4-5, quadruplicates; unpaired t-test; **p=0.006.

Using Matrix 2, following 14 days in 3D bioprinted cell culture, the effects of various pro-fibrotic treatments were evaluated in 3D cell culture (Figure 3A). Whilst there was no statistically significant difference between various treatment combinations, there was a clear trend towards reduced live to dead cell ratio in the presence of TGF- β treatment (Figure 3.3B). The presence of hypoxic and pro-angiogenic treatment, DMOG [25], or anti-angiogenic FKBPL-based peptide mimetic, AD-01 [14], did not seem to rescue this trend towards a decrease in fibroblast cell survival (Figure 3.3B). Furthermore, the proliferation of fibroblast cells in the 3D cell culture were assessed using alamarBlue assay. Whilst no difference was observed between different treatment combinations (TGF- β , TGF- β +AD-01, DMOG, DMOG+AD-01, DMOG+TGF- β , DMOG+ TGF- β +AD-01), there was a clear increase in fibroblast proliferation over time in every group (Figure 3.4, $p < 0.05$).

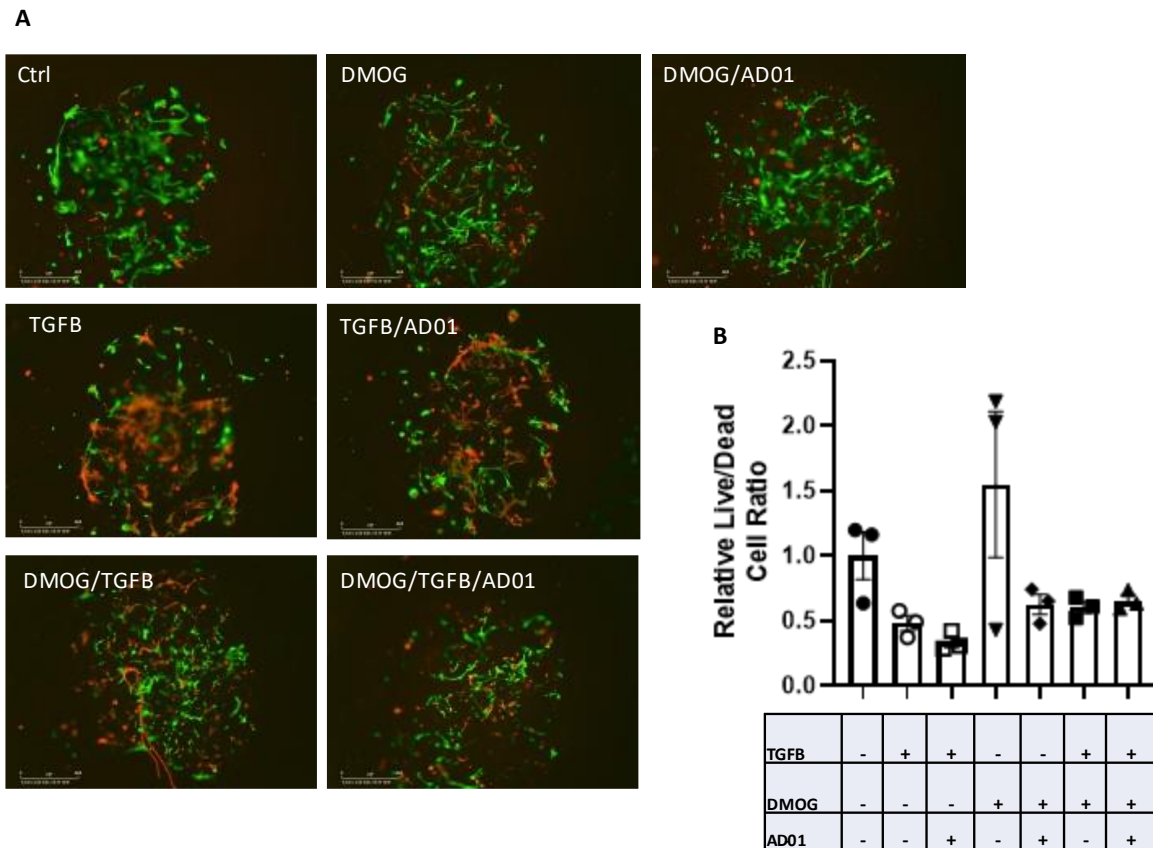


Figure 3.3 Optimising 3D bioprinted cardiac fibrosis model through extracellular matrix selection. Fetal fibroblast cells (HFF08) were bioprinted using RASTRUM platform within hydrogels of varying stiffnesses (Matrix 1; Px01.31P, ~0.7kPa, Matrix 2; Px01.29P, ~0.7kPa, Matrix 3; Px03.29P, ~3kPa) and containing different cardiac peptide composition to mimic fibronectin, β -laminin, collagen I, into a 96-well plate. Treatments were added on day 4 and 7 to include DMOG (1mM) and/or TGF- β (1ng/ml) and/or AD-01 (100nM). After 14 days in culture a live/dead viability assay was performed. Calcein AM dye (green) was used to stain live cells whereas ethidium homodimer-III (red) to stain dead cells. **(A)** Representative images of 3D fibroblast networks after 14 days in culture in the presence of various treatment combinations and within three different matrix types. The networks were captured on IncuCyte at 10x magnification. Total area of live cells **(B)**, total area of dead cells **(C)** and the live-to-dead cell ratio, between matrix 1 and 2 were determined using IncuCyte analysis software **(D)**. Data is presented as mean \pm SEM; n=3, quadruplicates; unpaired t-test; **p=0.006.

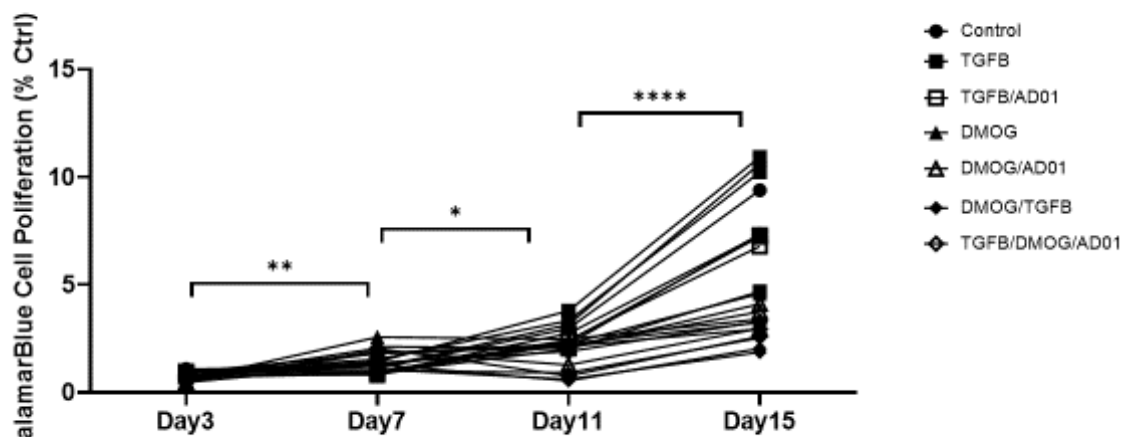


Figure 3.4 Fibroblast cell proliferation in 3D culture over time and in the presence of various treatments. HFF08 cells were 3D bioprinted within Matrix 2 (Px01.29P, ~0.7kPa) in a 96-well plate and allowed to form networks. Treatments were added on day 4 and 7 to include DMOG (1mM) and/or TGF- β (1ng/ml). AD-01 (100nM) treatment was added on day 7 and the cells were left in 3D culture for the total of 14 days. On Day 3, 7, 11 and 14, cells were washed with PBS before adding alamarBlue-containing foetal fibroblast media and incubated for 16 hours at 37°C before fluorescence was read on the plate reader at 530 nm excitation and 590 nm emission. The absorbance for treatments was normalised to control. n=4-6, quadruplicates; one-way ANOVA (repeated measures); *p<0.05, **p<0.01, ***p<0.001

In light of fibroblasts' mesenchymal nature [4], network formation was assessed in optimal 3D bioprinted conditions and in the presence of various treatments (Figure 3.5A). This was quantified by the number of junctions (Figure 3.5B) and the total branch length (Figure 3.5C), following 14 days in 3D cell culture. Interestingly, even though TGF- β led to a trend towards a decrease in fibroblast viability, there was an increase in network formation compared to control (Figure 3.5B, $p < 0.01$; Figure 3.5C, $p < 0.0001$). The addition of AD-01 or DMOG did not have any influence on this process and maintained a statistically significant increase in both the number of junctions (Figure 3.5B, $p < 0.0001$) and the total branch length (Figure 3.5C, $p < 0.0001$). Similarly, DMOG alone also increased the fibroblast network formation (Figure 3.5B&C, junctions: $p < 0.001$; branches: $p < 0.0001$), which did not change in the presence of AD-01. Finally, the combination of TGF- β , DMOG and AD-01 did not show statistically significant difference in the number of junctions (Figure 3.5B), whereas the total branch length was increased, compared to control (Figure 3.5C, $p < 0.05$).

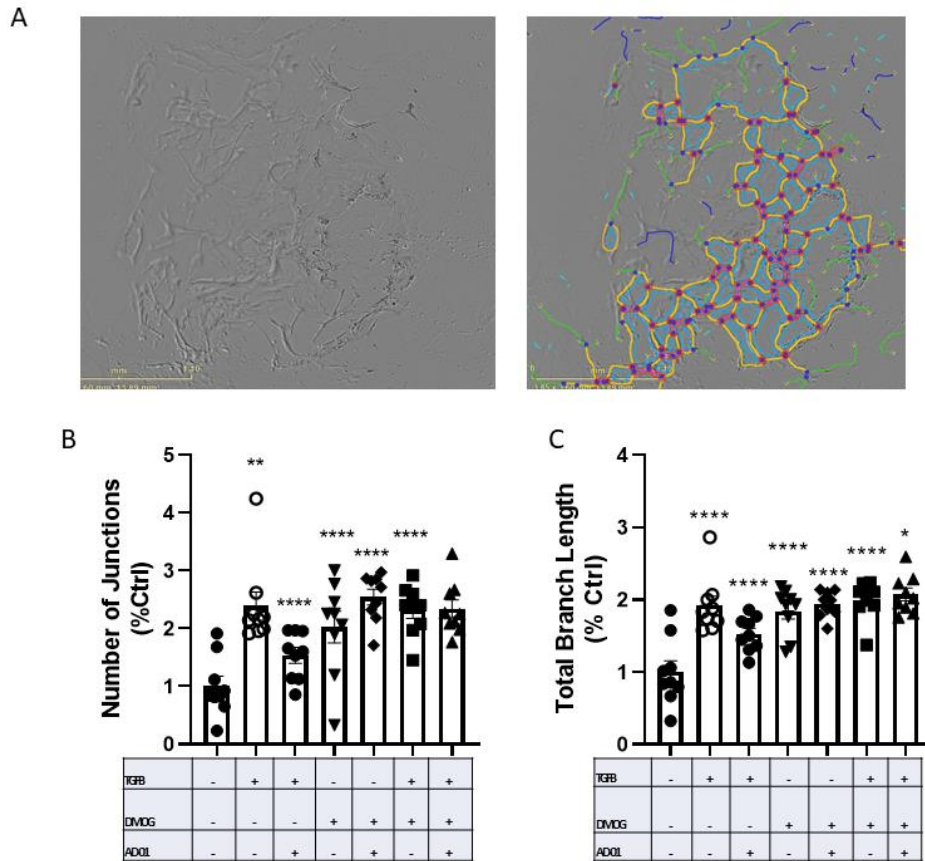


Figure 3.5 3D network formation within cardiac fibroblast model following various pro-fibrotic treatments. Following 14 days in 3D culture, fibroblast networks were phase contrast imaged using the Incucyte Live-Cell Analysis System (Sartorius AG, Germany) at 10x magnification for network formation analysis. Images were analysed and quantified in Image J, using the Angiogenesis Analyzer to detect and map the nodes, branch length and number of networks. **(A)** Representative images showing phase contrast and tracing of the networks. **(B)** The number of junctions and **(C)** the total branch length were quantified normalised to control. $n \geq 8$; one-way ANOVA with Sidak's multiple comparison test; * $p < 0.05$; ** $p < 0.01$, *** $p < 0.001$; **** $p < 0.0001$.

Once the 3D cardiac fibrosis model was established and the effect of different pro-fibrotic treatments on cell survival and network formation determined, next step was to investigate the regulation of pro-fibrotic markers, vimentin and α -SMA, as well as FKBPL as a novel mechanism of fibrosis, within the 3D bioprinted cardiac fibrosis model (Figure 3.6A). Vimentin has been used widely to label cardiac fibroblasts [26] whereas α -SMA positive cells are activated fibroblasts or myofibroblasts, the cell phenotype that develops once resident fibroblasts undergo differentiation as part of the fibrosis process [7]. In conjunction with reduced network formation induced by all treatment combinations including TGF- β , DMOG \pm AD-01, overall, vimentin and FKBPL expression was downregulated, however this was only statistically significant in the presence of DMOG alone (Figure 3.6B, $p < 0.001$), DMOG + AD-01 ($p < 0.05$) and DMOG+TGF- β +AD-01 ($p < 0.01$).

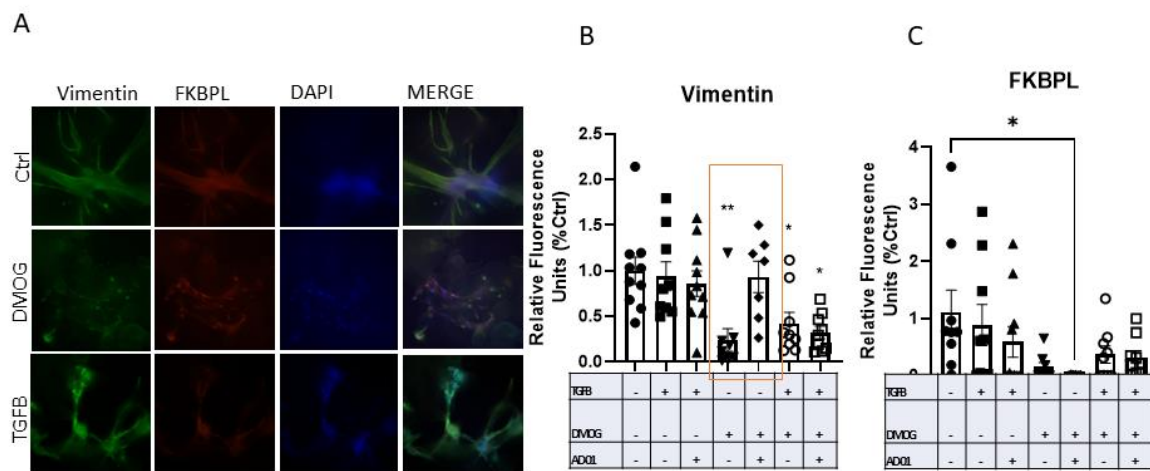


Figure 3.6 Immunofluorescence staining of FKBPL, vimentin and α -SMA in 3D bioprinted cardiac fibrosis model. Following 14 days in 3D cell culture, fibroblast networks were fixed in 4% paraformaldehyde, blocked and incubated with primary antibodies: FKBPL, vimentin and α -SMA, overnight. The following day cells in 3D culture were washed and incubated with secondary antibody overnight before images were taken. Imaging was performed on the Nikon Ti Live inverted wide-field microscope (Nikon, Japan) at 20x magnification with three random images per well taken. Z stacks (0.2 μ m optical slices) were acquired using a 0.5 AU pinhole. Fluorescence intensity per antibody, vimentin (**B**), FKBPL (**C**) indicating protein expression per treatment was quantified relative to the control group and normalised to DAPI using Image J. $n \geq 7$; one-way ANOVA with Tukey multiple comparison test; * $p < 0.05$; ** $p < 0.01$, *** $p < 0.001$; **** $p < 0.0001$.

3.4.3 Regulation of pro-fibrotic mechanisms by FKBPL in 2D cell culture

Using 2D cell culture, the role of FKBPL in cardiac fibrosis process was further explored by exposing fibroblasts to TGF- β and/or DMOG treatments and downregulating FKBPL expression via siRNA or overexpressing FKBPL using AD-01 peptide mimetic [14]. First, the effect on a number of pro-fibrotic genes was determined, following various treatment combinations, TGF- β /DMOG/AD-01, for 24h. This was reflective of early changes in the cardiac fibrosis process, and whilst Fkbpl, Postn, Fsp-1 and Ctgf mRNA expression did not show any significant changes in any treatment conditions (Figure 3.7A-D), Col1a1 mRNA expression was increased following TGF- β \pm AD-01 treatment compared to control (Figure 3.7E; TGF- β , $p < 0.01$; TGF- β +AD-01, $p < 0.0001$). Although AD-01 appears to exacerbate Col1a1 mRNA expression, this was not significant compared to TGF- β alone. Interestingly, the presence of DMOG appears to abrogate TGF- β -induced increased expression in Col1a1 mRNA ($p < 0.05$; Figure 3.7E). Furthermore, Mmp-2 mRNA expression showed statistically significant expression only when TGF- β and AD-01 treatment were used together (Figure 3.7F, $p < 0.05$) suggesting that FKBPL might play a role in early cardiac remodelling and fibrosis process where high expression of FKBPL could be detrimental.

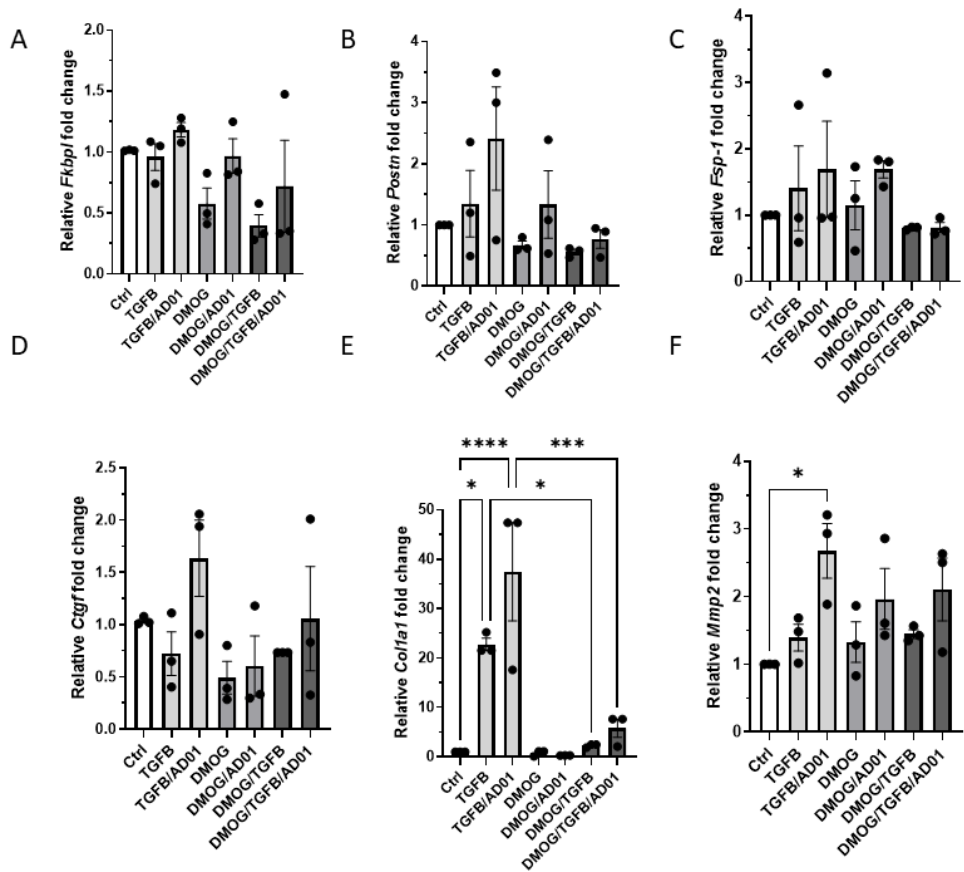


Figure 3.7 FKBPL and cardiac fibrosis genes expression following exposure of HFF08 fibroblast cells to pro-fibrotic and hypoxia stimuli, and FKBPL peptide mimetic, AD-01. HFF08 cells were seeded at 0.2×10^5 cells/well overnight before treatments were added for 24 h. These included pro-fibrotic stimuli, TGF- β (10ng/ml) and/or hypoxia stimuli, DMOG (1mM) with or without FKBPL peptide mimetic, AD-01 (100nM). Following 24-hour treatment, RNA was extracted and *Fkbp1* (A), postin (*Postn*; B), fibroblast specific protein (*Fsp-1*; C), connective tissue growth factor (*Ctgf*; D), type I collagen alpha chain 1 (*Col1a1*; E) and matrix metalloproteinase-2 (*Mmp-2*; F), gene expression quantified by RT-qPCR. Expression of target mRNA was normalised to housekeeping gene β -actin or 18S. N=3; one-way ANOVA with post-hoc multiple comparisons test, * $p < 0.05$; ** $p < 0.01$, *** $p < 0.001$; **** $p < 0.0001$.

When FKBPL was knocked down and TGF- β \pm AD-01 added, no changes in Fkbpl, Postn and Fsp-1, mRNA, were observed. Interestingly, there were a number of differences in Col1a1 mRNA expression. Within the control, TGF- β or TGF- β +AD-01, conditions, there was no difference between NT and FKBPL knockdown groups (Figure 3.8A-F), however, the presence of AD-01 in low FKBPL settings (FKBPL siRNA) was able to abrogate increased Col1a1 mRNA expression induced by TGF- β (TGF- β vs TGF- β +AD-01, $p < 0.01$), which was not the case for NT siRNA (Figure 3.8D). Nevertheless, Col1a1 mRNA expression was still higher than the control following TGF- β +AD-01 treatment in both NT ($p < 0.01$) and FKBPL ($p < 0.05$) siRNA settings. FKBPL knockdown did not influence TGF- β -induced expression in Col1a1 mRNA ($p < 0.0001$). Similarly, Mmp2 mRNA expression was reduced when TGF- β and AD-01 were used together, compared to control, in lower FKBPL settings (Figure 3.8F, $p < 0.05$), and AD-01 was able to abrogate TGF- β -induced increase in Mmp2 mRNA, only following FKBPL siRNA transfection (Figure 3.8F, $p < 0.001$).

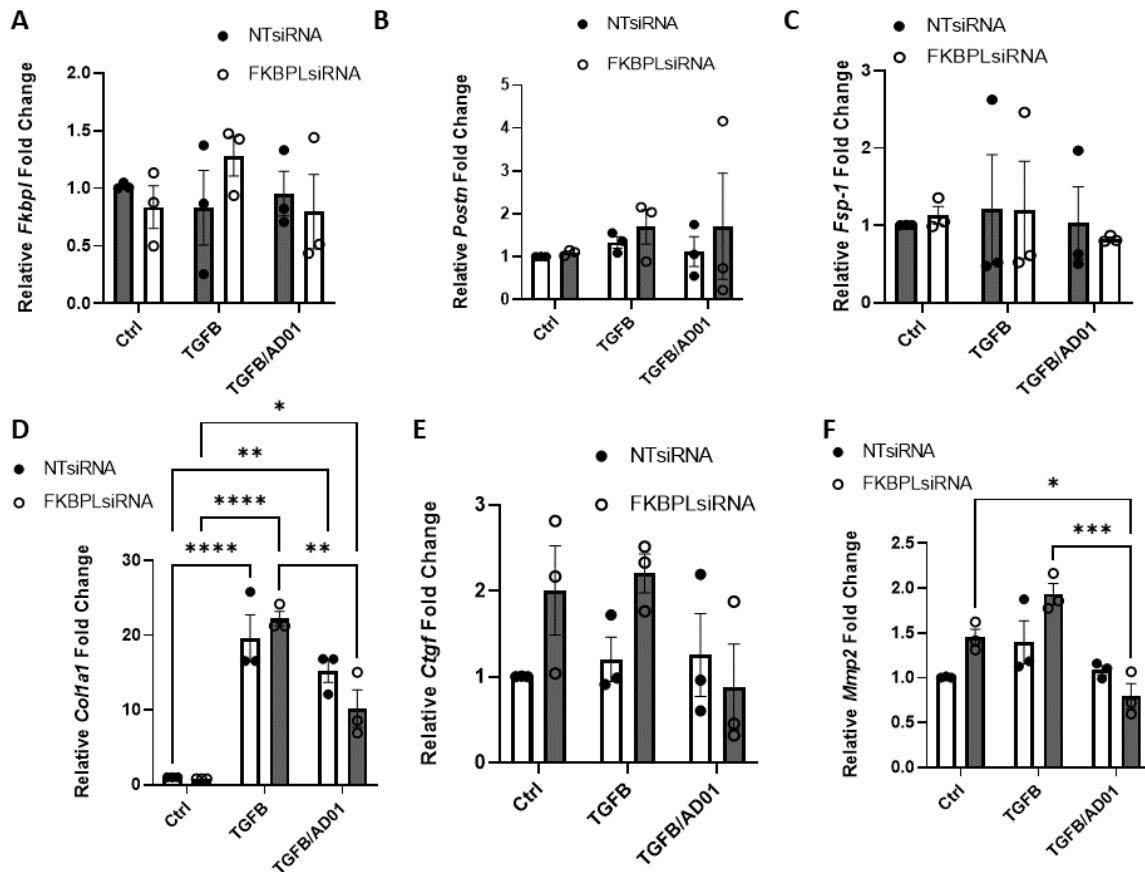


Figure 3.8 Cardiac fibrosis genes expression following FKBPL knockdown and treatment with pro-fibrotic stimuli, TGF- β , and FKBPL-peptide mimetic, AD-01. HFF08 cells were seeded at 0.2×10^5 cells/well overnight before FKBPL or non-targeting (NT) siRNA was used for transfection of HFF08 cells for 24 h followed by 24 h of treatment with TGF- β (10ng/ml) alone or in combination with AD-01 (100nM). Subsequently, RNA was extracted and *Fkbp1* (**A**), postin (*Postn*; **B**), fibroblast specific protein (*Fsp-1*; **C**), connective tissue growth factor (*Ctgf*; **D**), type I collagen alpha chain 1 (*Col1a1*; **E**) and matrix metalloproteinase-2 (*Mmp-2*; **F**), gene expression quantified by RT-qPCR. Expression of target mRNA was normalised to housekeeping gene β -actin or 18S. N=3; two-way ANOVA with post-hoc multiple comparisons test, * $p < 0.05$; ** $p < 0.01$, *** $p < 0.001$; **** $p < 0.0001$.

Next, we determined the effect of pro-fibrotic treatments both in normal and FKBPL knockdown settings on the expression of α -SMA in fibroblasts, indicative of myofibroblast presence and cardiac fibrosis. We have shown previously that HFF08 fetal fibroblast cells can differentiate into myofibroblasts under the influence of TGF- β that led to an increase in α -SMA expression [27]. Here, we aimed to emulate early cardiac fibrosis process and treat the cell with pro-fibrotic treatments for 24h only. Whilst, neither TGF- β or DMOG \pm AD-01 induced any changes in FKBPL (Figure 3.9A) or α -SMA protein expression (Figure 9B), FKBPL siRNA knockdown (Figure 3.9C) led to a reduction in α -SMA protein expression only in the absence of TGF- β \pm AD-01 treatment (Figure 3.9D, $p < 0.05$).

Finally, given that inflammation is one of the key early processes in cardiac fibrosis involving monocyte infiltration at the site of injury, for example following MI [9], we investigated the effect of the same treatments in the context of normal and lower FKBPL expression on monocyte adhesion to fibroblasts. Surprisingly, no difference was observed with any treatment combinations or as a result of lower FKBPL expression (Figure 3.10). This could be due to the fact that treatments were only administered for 24 h. However, in our previous study, even with 72 h TGF- β treatment, we did not observe a significant increase in monocyte adhesion [27].

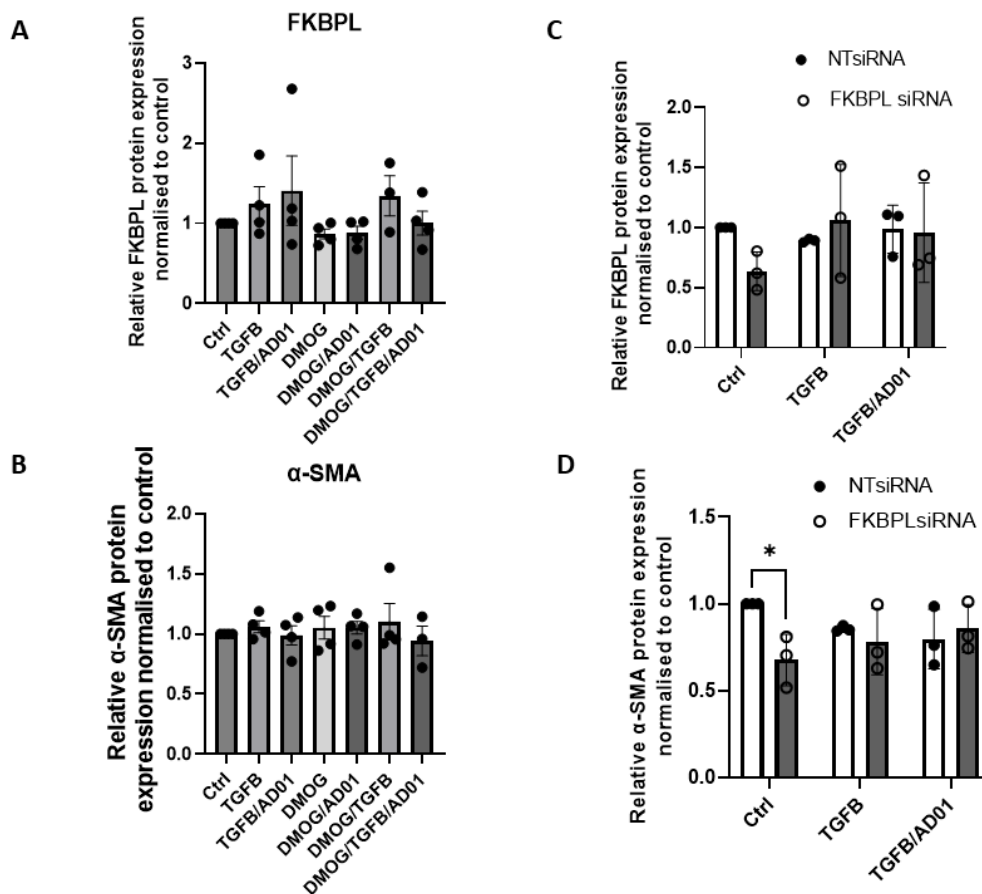


Figure 3.9 FKBPL and α -SMA protein expression in both normal and low FKBPL settings following exposure of HFF08 fibroblast cells to pro-fibrotic and hypoxia stimuli, with or without FKBPL peptide mimetic, AD-01. HFF08 cells were seeded at 0.2×10^5 cells/well overnight before treatments were added or FKBPL/NT siRNA transfection performed, for 24 h. The treatments included pro-fibrotic stimuli, TGF- β (10ng/ml) and/or hypoxia stimuli, DMOG (1mM) with or without FKBPL peptide mimetic, AD-01 (100nM). Following 24-h treatment in both untransfected (**A&B**) and transfected cells (**C&D**), protein was extracted for Western blotting and membrane was probed with FKBPL (**A&C**) and α -SMA (**B&D**) antibodies. The protein band intensity was determined using Image J. Protein expression was normalised to GAPDH and control. $N \geq 3$; one-way ANOVA (**A&B**) or two-way ANOVA (**C&D**) with post-hoc multiple comparisons test, $*p < 0.05$.

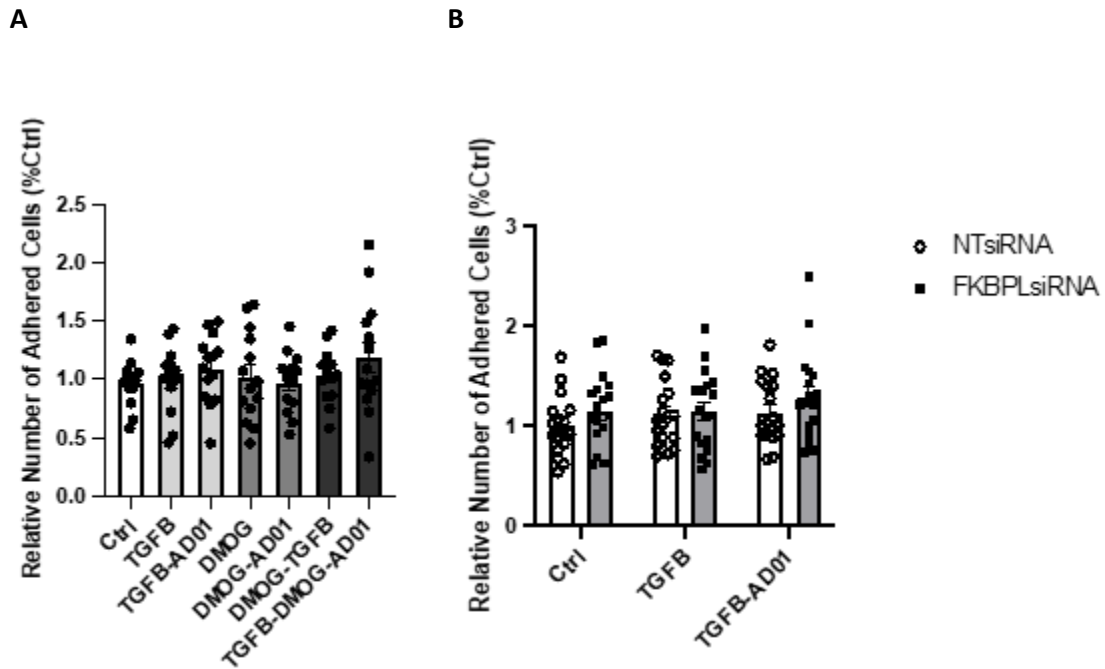


Figure 3.10 The effect of FKBPL knockdown or mimic and profibrotic/hypoxic treatment on monocyte adhesion to fibroblast cells. (A) HFF08 fibroblast cells were seeded (0.2×10^5 cells/well) and either treated the following day with TGF- β (10ng/ml), and/or DMOG (1mM) \pm AD-01 (100nM) for 24 h or **(B)** transfected with FKBPL/NT siRNA for 24 h before TGF- β (10ng/ml) alone or with AD-01 (100nM) added for a further 24 h. For both conditions, after treatments, HFF08 cells were co-incubated with calcein green AM labelled THP-1 (human monocytic cells) and allowed to attach for 30 mins at 37°C. Fluorescent cells were captured using Incucyte and quantified in ImageJ before being normalised to control. Data presented as mean \pm SEM, (A-B); n=5; one-way ANOVA with post-hoc multiple comparison test.

3.5 Discussion

In this study, we report, for the first time, an emerging role for FKBPL in cardiac fibrosis using i) *ex vivo* left ventricular tissues from mice with low background FKBPL expression compared to wild-type controls, ii) an innovative 3D cardiac fibrosis model with specific ECM constituents that reflect cardiac microenvironment and iii) 2D cell culture models following FKBPL knockdown and/or pro-fibrotic treatments. In our *fbpl*^{+/-} transgenic mice at ~24 weeks of age, collagen deposition and synthesis were decreased within the left ventricular tissue. However, no changes were seen in other cardiac pro-fibrotic genes including *postn1*, *col3a1*, *fsp-1*, *ctgf* and *fn-1*. As part of the physiological process, collagen plays an important role in cardiac ECM homeostasis where a fine balance is maintained between its production and degradation [28]. In cardiac fibrosis the balance is dysregulated leading to a higher rate of collagen production compared to collagen degradation [29]. The ECM remodelling through the excess collagen deposition can lead to stiff and fibrotic tissue within the heart, and a loss of contractile cardiomyocytes that impair critical cardiac functions, as a precursor to heart failure [1], [7]. *Col1a1* gene contributes to the majority of the collagen production within the ECM. On the other hand, *col3a1* is responsible for ~11% of collagen synthesis [29]. Thus, given that in low FKBPL settings, both *col1a1* mRNA expression and collagen deposition are significantly reduced, this suggests that FKBPL plays an important role in cardiac collagen production. Although there were no changes in other pro-fibrotic genes, this could be related to timing and shorter or longer duration of *in vivo* experiment (young or older *fbpl*^{+/-} mice) or induction of more pronounced cardiac fibrosis that utilise MI [1] or diabetes mellitus [30] models, might be required to establish the influence on different pro-fibrotic markers. For

example, *fsp-1* is one of the main contributors to fibroblast cell proliferation and collagen production through p53 [31]. *Postn* is upregulated in response to mechanical stress, inflammation, and ECM modulation [32], all of which are implicated in cardiac fibrosis. Previous research has shown that TGF- β also regulates *postn* through Smad-mediated mechanism [33]. Interestingly, periostin was difficult to detect at the mRNA level and not present at all at the protein level in healthy hearts whereas its expression significantly increased in the failing heart tissue [32]. Although the *ctgf* gene regulates the synthesis of CTGF, a matricellular protein, its pro-fibrotic function is cell-specific and comes from its secretion by activated fibroblasts rather than cardiomyocytes [34]. Finally, *fn-1* promotes proliferation of activated myofibroblasts and is involved in ECM polymerization contributing to collagen deposition, hence also playing an important role in cardiac fibrosis [35].

In light of the fact that remodelling of cardiac ECM by fibroblasts plays a key role in cardiac fibrosis, which is a complex and multifactorial process, it is challenging to recapitulate this in a 2D in vitro model [36]. The lack of reliable and representative models of cardiac fibrosis has impeded the development of effective treatments hence better understanding of the mechanisms of the disease is necessary. 3D in vitro models are more representative of the physiological environment recapitulating complex cell-cell and cell-microenvironment interactions allowing for investigations into pathogenic mechanisms and drug testing more reliably than in 2D. Various 3D in vitro approaches have been used to mimic cardiac fibrosis including microfluidic chip devices, bioengineered cardiac tissues, cardiac spheroids and organoids, and manual encapsulation of cardiac fibroblasts within hydrogels [37]– [39]. 3D bioprinting is an emerging technique that although harsh on cells, can be customised to produce

precise, biologically relevant models incorporating specific ECM components tailored for a specific cell type. Here, we employed RASTRUM 3D cell culture platform that uses synthetic hydrogels for bioprinting, to generate robust cardiac fibrosis models. Even though fetal fibroblasts were utilized, we adjusted the ECM components to reflect cardiac microenvironment given that remodelling of the ECM by collagen deposition, is one of the key mechanisms in cardiac fibrosis [28]. Fibronectin, β -laminin, collagen I and hyaluronic acid are common cardiac ECM proteins synthesised by fibroblasts that act as scaffolds providing supporting structures to cardiac cells and regulate fibroblast proliferation, migration and ECM and cardiac remodelling[40]–[42]. In our 3D bioprinted model of cardiac fibrosis, we demonstrated that fetal fibroblasts can naturally organise into large 3D networks within the ECM, which is representative of cardiac fibroblast cell morphology within the heart tissue [43]. Cardiac fibrosis was induced by adding a well-established pro-fibrotic stimulus, TGF- β , and/or hypoxic stimulus or HIF-1 α activator, DMOG, while FKBPL's role was investigated using its therapeutic peptide mimetic, AD-01. Previous work has shown that cardiac fibroblasts are more hypoxic than other cardiac interstitial subpopulations and express highly HIF-1 α [6]. Also, HIF-1 α plays an important role in cardiac fibrosis post-MI by regulating excessive fibroblasts proliferation and activation [6]. Hypoxia appears to be involved in driving inflammation via increased secretion of IL-6 and TGF- β by cardiac fibroblasts that leads to the development of cardiac fibrosis [44]. Furthermore, we have shown before that FKBPL expression increased under the influence of TGF- β in cardiac fibroblasts and that it is regulated by hypoxia hence we used its peptide mimetic to induce FKBPL-specific changes in our 3D cardiac fibrosis model [18]. Whilst TGF- β -containing treatments showed a trend towards reduced fibroblast survival in our 3D model, proliferation was stimulated from day 3 to day 15. On the other hand, DMOG

did not seem to affect fibroblast cell survival however proliferation was not as pronounced in DMOG containing conditions compared to TGF- β . Interestingly, all treatment combinations, TGF- β \pm DMOG \pm AD-01, showed increased fibroblast network formation in conjunction with an overall trend towards decreased FKBPL expression. This was surprising for AD-01, although we have shown before that AD-01 in the presence of stress stimuli such as angiotensin-II appears, shows a restorative effect on cardiac hypertrophy whilst reducing the expression of FKBPL, through likely negative feedback mechanism [21] that needs to be explored further, particularly in terms of miRNA regulation.

Nevertheless, in the 2D models of cardiac fibrosis where fibroblasts were treated with the same stimuli combinations as in the 3D cell culture, AD-01 in combination with TGF- β appears to potentiate collagen-production gene, col1a1, and ECM remodelling enzyme, mmp-2. Interestingly, when FKBPL was modestly knocked down in 2D in fibroblast, the expression of Col1a1 or Mmp-2 was reduced when AD-01 was added to TGF- β treatment. This is in support of our findings from fkbpl \pm transgenic mice, providing further evidence that low FKBPL serum might be protective against cardiac fibrosis [16]. Similar to ex vivo results, no other pro-fibrotic genes were affected including postn, fsp-1 and ctgf. In lower FKBPL settings in 2D cell culture, with 40-50% FKBPL reduction, α -SMA was also reduced, in the absence of TGF- β \pm AD-01 treatment. As α -SMA is a well-established marker of myofibroblasts, the cell type generated through differentiation of fibroblasts that drive cardiac fibrosis as described above. This effect could be attributed to lower expression of FKBPL leading to pro-angiogenic phenotype [16] and in light of previous research suggesting that angiogenesis can enhance cardiac function following a MI-induced cardiac fibrosis [45]

however, this mechanism must be further explored. Aligned to this, our previous work in the reduced uterine perfusion pressure rat model of preeclampsia, shows increased FKBPL expression within the heart in conjunction with cardiac fibrosis [46].

Interestingly, we did not see any effects on monocyte adhesion to fibroblast cells in any treatment conditions (TGF- β \pm DMOG \pm AD-01) or when FKBPL was knocked down. This could be due to the short treatment duration of 24 h and hence it might need to be extended to 72-96h in the future or by increasing the incubation of THP-1 monocyte cells on treated HFF08 cells to 1 hour as previously done [47]. Nevertheless, in the previously published work from our laboratory, time course optimisation experiments showed 30 min to be the optimal time for monocyte adhesion [27]. Furthermore, in the same paper using the same experimental design with THP-1 monocytes and HFF08 fetal fibroblasts following 48-72h treatment with TGF- β , we did not see any significant changes in monocyte adhesion [27], suggesting perhaps longer exposure time to 96h or increasing the concentration of TGF- β to 25ng/ml as used in previous research [48], might be required. Other studies have shown pro-fibrotic effects in vitro after exposure to 10 ng/mL TGF- β for 72 hours that induced fibroblast to myofibroblast differentiation [49] and induced cardiac fibrosis in cardiac spheroids [37], [50]. DMOG treatment has been shown to produce hypoxic effects within 24 hours through overexpression of hypoxia-inducible factor α [51],

Hypoxia and TGF- β have well established roles in regulating inflammatory response [44], [52]. As described above, following MI, affected area of the heart becomes hypoxic, which stimulates the recruitment of inflammatory cells including monocytes to the site of injury [9]. Monocytes infiltrate the tissue, differentiate into macrophages,

and attempt to clear damaged tissue from the wound [12]. There is a positive correlation between the number of macrophages and the extent of hypoxia or the concentration of pro-inflammatory growth factors and cytokines [9], [53]. Therefore, monocytes adhesion is one of the early pathological processes leading to cardiac fibrosis.

The limitations of this study are that fetal fibroblasts were used as opposed to primary cardiac fibroblasts, however 3D bioprinting technique utilises high pressure to eject cells from nozzles in conjunction with shear stress that can damage cells and is harsh on primary cells. To counteract this limitation, we used specific cardiac ECM peptides that play an important role in cardiac fibrosis, and a well-known pro-fibrotic treatment, TGF- β , in conjunction with hypoxic environment that is representative of cardiac fibroblasts or MI-induced cell damage that can lead to cardiac fibrosis. We did not knockdown FKBPL in the 3D bioprinted model due to transient nature of siRNA transfection so further studies should aim to knockout FKBPL using CRISPR-Cas9 platform before bioprinting fibroblast cells. Picrosirius or collagen staining should also be employed to assess the extent of fibrosis in the 3D bioprinted model. The knockdown of FKBPL in 2D was also modest therefore using CRISPR-Cas9 knockout approach could be optimal in the future. Furthermore, male mice were used due to their predictable nature due to their lack of oestrogen and progesterone. Future studies should implement both sexes to observe differences in FKBPL plasma levels between genders. Nevertheless, given the critical role of FKBPL in various cell functions, small changes in FKBPL expression (40-50%) have previously shown substantial phenotypic differences [16], [54], [55]. Future studies should also explore different durations of treatment for 2D experiments and perhaps induce diabetes mellitus or MI

in *fbpl*^{+/-} transgenic mice to investigate further the role of FKBPL in cardiac fibrosis. Therapeutic strategies that reduce FKBPL expression such as mesenchymal stem cell secretome [56] could be employed in normal FKBPL settings to prevent or reduce the extent of cardiac fibrosis.

3.6 Conclusion

In summary, this is the first full report on the emerging role of FKBPL in cardiac fibrosis suggesting that the decreased FKBPL may be beneficial through inhibition of collagen production and reduction in α -SMA expression, highly expressed by activated myofibroblasts. Opposite to lower FKBPL expression, FKBPL peptide mimetic, AD-01, appears to exacerbate the expression of pro-fibrotic and ECM remodelling genes in the presence of TGF- β . Nevertheless, when AD-01 is added in the lower FKBPL settings, the effects appear to be opposite compared to conditions with normal FKBPL expression, leading to reduction in collagen producing genes. Furthermore, we developed an innovative 3D bioprinted model of cardiac fibrosis that incorporates ECM components representative of human heart and key factors driving cardiac fibrosis. This 3D model could be utilised in the future to test potential therapeutics for treatment of cardiac fibrosis, which is currently limited, and accelerate the development of effective therapies for this difficult to treat condition. The model could also be used to study various aspects of cardiac fibrosis that would aid our understanding of the important pathogenic mechanisms thus identifying therapeutic targets. Developing novel strategies or through repurposing that can inhibit FKBPL in cardiac fibrosis settings, could be beneficial perhaps due to its anti-angiogenic function or its

involvement in inflammation, towards abrogating cardiac fibrosis and decreasing the burden of future heart failure.

3.7 Declarations

Ethics approval and consent to participate

Not applicable

Consent for publication

Not applicable

Availability of data and materials

Data will be made available upon a reasonable request.

Competing interests

The authors declare that they have no competing interests.

Funding

Project funded by the Australian Government RTP Fees Offset Scholarship as part of author Michael Chhor's doctoral degree.

Acknowledgements

The authors gratefully acknowledge the use of the Nikon Ti widefield microscope in the Microbial Imaging Facility (MIF) at the Australian Institute of Microbiology and Infection in the Faculty of Science, the University of Technology Sydney.

3.8 References

- [1] N. G. Frangogiannis, "Cardiac fibrosis," *Cardiovascular Research*, vol. 117, no. 6, pp. 1450–1488, May 2021, doi: 10.1093/cvr/cvaa324.
- [2] C. A. Souders, S. L. K. Bowers, and T. A. Baudino, "Cardiac Fibroblast," *Circulation Research*, vol. 105, no. 12, pp. 1164–1176, Dec. 2009, doi: 10.1161/CIRCRESAHA.109.209809.
- [3] A. C. Gittenberger-de Groot, M.-P. F. M. Vrancken Peeters, M. M. T. Mentink, R. G. Gourdie, and R. E. Poelmann, "Epicardium-Derived Cells Contribute a Novel Population to the Myocardial Wall and the Atrioventricular Cushions," *Circulation Research*, vol. 82, no. 10, pp. 1043–1052, Jun. 1998, doi: 10.1161/01.RES.82.10.1043.
- [4] R. Muñoz-Chápuli, J. M. Pérez-Pomares, D. Macías, L. García-Garrido, R. Carmona, and M. González-Iriarte, "The epicardium as a source of mesenchyme for the developing heart.," *Italian journal of anatomy and embryology = Archivio italiano di anatomia ed embriologia*, vol. 106, no. 2 Suppl 1, pp. 187–96, 2001.
- [5] A. R. Pinto et al., "Revisiting Cardiac Cellular Composition," *Circulation Research*, vol. 118, no. 3, pp. 400–409, Feb. 2016, doi: 10.1161/CIRCRESAHA.115.307778.
- [6] V. Janbandhu et al., "Hif-1a suppresses ROS-induced proliferation of cardiac fibroblasts following myocardial infarction," *Cell Stem Cell*, vol. 29, no. 2, pp. 281-297.e12, 2022, doi: 10.1016/j.stem.2021.10.009.
- [7] J. G. Travers, F. A. Kamal, J. Robbins, K. E. Yutzey, and B. C. Blaxall, "Cardiac Fibrosis," *Circulation Research*, vol. 118, no. 6, pp. 1021–1040, Mar. 2016, doi: 10.1161/CIRCRESAHA.115.306565.
- [8] X.-M. Gao, D. A. White, A. M. Dart, and X.-J. Du, "Post-infarct cardiac rupture: Recent insights on pathogenesis and therapeutic interventions," *Pharmacology & Therapeutics*, vol. 134, no. 2, pp. 156–179, May 2012, doi: 10.1016/j.pharmthera.2011.12.010.

- [9] M. P. Czubryt, "Common threads in cardiac fibrosis, infarct scar formation, and wound healing," *Fibrogenesis & Tissue Repair*, vol. 5, no. 1, p. 19, Dec. 2012, doi: 10.1186/1755-1536-5-19.
- [10] T. Methatham, R. Nagai, and K. Aizawa, "A New Hypothetical Concept in Metabolic Understanding of Cardiac Fibrosis: Glycolysis Combined with TGF- β and KLF5 Signaling," *International Journal of Molecular Sciences*, vol. 23, no. 8, p. 4302, Apr. 2022, doi: 10.3390/ijms23084302.
- [11] J. R. Crawford, S. B. Haudek, K. A. Cieslik, J. Trial, and M. L. Entman, "Origin of Developmental Precursors Dictates the Pathophysiologic Role of Cardiac Fibroblasts," *Journal of Cardiovascular Translational Research*, vol. 5, no. 6, pp. 749–759, Dec. 2012, doi: 10.1007/s12265-012-9402-7.
- [12] J. G. Travers, F. A. Kamal, J. Robbins, K. E. Yutzey, and B. C. Blaxall, "Cardiac fibrosis: The fibroblast awakens," *Circ Res*, vol. 118, no. 6, pp. 1021–1040, Mar. 2016, doi: 10.1161/CIRCRESAHA.115.306565.
- [13] A. V. Shinde, C. Humeres, and N. G. Frangogiannis, "The role of α -smooth muscle actin in fibroblast-mediated matrix contraction and remodeling," *Biochim Biophys Acta Mol Basis Dis*, vol. 1863, no. 1, pp. 298–309, Jan. 2017, doi: 10.1016/J.BBADIS.2016.11.006.
- [14] A. Yakkundi et al., "The Anti-Migratory Effects of FKBPL and Its Peptide Derivative, AD-01: Regulation of CD44 and the Cytoskeletal Pathway," *PLoS ONE*, vol. 8, no. 2, 2013, doi: 10.1371/journal.pone.0055075.
- [15] L. McClements, S. Annett, A. Yakkundi, and T. Robson, "The role of Peptidyl prolyl isomerases in ageing and vascular diseases," *Current Molecular Pharmacology*, vol. 9, no. 2, 2015, doi: 10.2174/1874467208666150519115729.
- [16] A. Yakkundi et al., "FKBPL is a critical antiangiogenic regulator of developmental and pathological angiogenesis," *Arteriosclerosis, Thrombosis, and Vascular Biology*, vol. 35, no. 4, 2015, doi: 10.1161/ATVBAHA.114.304539.
- [17] S. Annett et al., "FKBPL-based peptide, ALM201, targets angiogenesis and cancer stem cells in ovarian cancer," *British Journal of Cancer*, Nov. 2019, doi: 10.1038/s41416-019-0649-5.

- [18] L. McClements, B. Rayner, A. Alqudah, D. Grieve, and T. Robson, "FKBPL, a novel player in cardiac ischaemia and fibrosis," *Journal of Molecular and Cellular Cardiology*, vol. 140, p. 5, Mar. 2020, doi: 10.1016/j.yjmcc.2019.11.008.
- [19] A. Alqudah, R. AbuDalo, E. Qnais, M. Wedyan, M. Oqal, and L. McClements, "The emerging importance of immunophilins in fibrosis development," *Molecular and Cellular Biochemistry*, vol. 478, no. 6, pp. 1281–1291, Jun. 2023, doi: 10.1007/s11010-022-04591-1.
- [20] A. S. Januszewski et al., "FKBPL is associated with metabolic parameters and is a novel determinant of cardiovascular disease," *Scientific Reports*, vol. 10, no. 1, p. 21655, Dec. 2020, doi: 10.1038/s41598-020-78676-6.
- [21] M. Chhor et al., "FK506-Binding Protein like (FKBPL) Has an Important Role in Heart Failure with Preserved Ejection Fraction Pathogenesis with Potential Diagnostic Utility," *Biomolecules*, vol. 13, no. 2, p. 395, Feb. 2023, doi: 10.3390/biom13020395.
- [22] A. El Helali et al., "A first-in-human Phase I dose-escalation trial of the novel therapeutic peptide, ALM201, demonstrates a favourable safety profile in unselected patients with ovarian cancer and other advanced solid tumours," *British Journal of Cancer*, vol. 127, no. 1, pp. 92–101, Jul. 2022, doi: 10.1038/s41416-022-01780-z.
- [23] S. M. Ghorbanpour et al., "A placenta-on-a-chip model to determine the regulation of FKBPL and galectin-3 in preeclampsia," *Cellular and Molecular Life Sciences*, vol. 80, no. 2, p. 44, Feb. 2023, doi: 10.1007/s00018-022-04648-w.
- [24] G. Carpentier et al., "Angiogenesis Analyzer for ImageJ — A comparative morphometric analysis of 'Endothelial Tube Formation Assay' and 'Fibrin Bead Assay,'" *Scientific Reports*, vol. 10, no. 1, p. 11568, Jul. 2020, doi: 10.1038/s41598-020-67289-8.
- [25] S.-M. KIM et al., "Enhanced angiogenic activity of dimethyloxalylglycine-treated canine adipose tissue-derived mesenchymal stem cells," *Journal of Veterinary Medical Science*, vol. 81, no. 11, pp. 1663–1670, 2019, doi: 10.1292/jvms.19-0337.
- [26] E. M. Zeisberg and R. Kalluri, "Origins of Cardiac Fibroblasts," *Circulation Research*, vol. 107, no. 11, pp. 1304–1312, Nov. 2010, doi: 10.1161/CIRCRESAHA.110.231910.

- [27] C. Rennie et al., "In vitro evaluation of a hybrid drug-delivery nanosystem for fibrosis prevention in cell therapy for Type 1 diabetes," *Nanomedicine*, vol. 18, no. 1, pp. 53–66, Jan. 2023, doi: 10.2217/nnm-2022-0231.
- [28] D. Fan, A. Takawale, J. Lee, and Z. Kassiri, "Cardiac fibroblasts, fibrosis and extracellular matrix remodeling in heart disease," *Fibrogenesis & Tissue Repair*, vol. 5, no. 1, p. 15, Dec. 2012, doi: 10.1186/1755-1536-5-15.
- [29] J.-Y. Exposito, U. Valcourt, C. Cluzel, and C. Lethias, "The Fibrillar Collagen Family," *International Journal of Molecular Sciences*, vol. 11, no. 2, pp. 407–426, Jan. 2010, doi: 10.3390/ijms11020407.
- [30] M. Chhor, W. Law, M. Pavlovic, D. Aksentijevic, K. McGrath, and L. McClements, "Diagnostic and prognostic biomarkers reflective of cardiac remodelling in diabetes mellitus: A scoping review," *Diabetic Medicine*, vol. 40, no. 5, May 2023, doi: 10.1111/dme.15064.
- [31] Y. Tamaki et al., "Metastasis-associated protein, S100A4 mediates cardiac fibrosis potentially through the modulation of p53 in cardiac fibroblasts," *Journal of Molecular and Cellular Cardiology*, vol. 57, pp. 72–81, Apr. 2013, doi: 10.1016/j.yjmcc.2013.01.007.
- [32] S. Zhao et al., "Periostin expression is upregulated and associated with myocardial fibrosis in human failing hearts," *Journal of Cardiology*, vol. 63, no. 5, pp. 373–378, May 2014, doi: 10.1016/j.jjcc.2013.09.013.
- [33] P. Snider, K. N. Standley, J. Wang, M. Azhar, T. Doetschman, and S. J. Conway, "Origin of Cardiac Fibroblasts and the Role of Periostin," *Circulation Research*, vol. 105, no. 10, pp. 934–947, Nov. 2009, doi: 10.1161/CIRCRESAHA.109.201400.
- [34] L. E. Dorn, J. M. Petrosino, P. Wright, and F. Accornero, "CTGF/CCN2 is an autocrine regulator of cardiac fibrosis," *Journal of Molecular and Cellular Cardiology*, vol. 121, pp. 205–211, Aug. 2018, doi: 10.1016/j.yjmcc.2018.07.130.
- [35] I. Valiente-Alandi et al., "Inhibiting Fibronectin Attenuates Fibrosis and Improves Cardiac Function in a Model of Heart Failure," *Circulation*, vol. 138, no. 12, pp. 1236–1252, Sep. 2018, doi: 10.1161/CIRCULATIONAHA.118.034609.

- [36] G. Palano, A. Foinquinos, and E. Müllers, "In vitro Assays and Imaging Methods for Drug Discovery for Cardiac Fibrosis," *Frontiers in Physiology*, vol. 12, Jul. 2021, doi: 10.3389/fphys.2021.697270.
- [37] G. A. Figtree, K. J. Bubb, O. Tang, E. Kizana, and C. Gentile, "Vascularized Cardiac Spheroids as Novel 3D in vitro Models to Study Cardiac Fibrosis," *Cells Tissues Organs*, vol. 204, no. 3–4, pp. 191–198, 2017, doi: 10.1159/000477436.
- [38] O. Mastikhina et al., "Human cardiac fibrosis-on-a-chip model recapitulates disease hallmarks and can serve as a platform for drug testing," *Biomaterials*, vol. 233, p. 119741, Mar. 2020, doi: 10.1016/j.biomaterials.2019.119741.
- [39] V. Picchio et al., "Multicellular 3D Models for the Study of Cardiac Fibrosis," *International Journal of Molecular Sciences*, vol. 23, no. 19, p. 11642, Oct. 2022, doi: 10.3390/ijms231911642.
- [40] M. Suleiman, N. Abdulrahman, H. Yalcin, and F. Mraiche, "The role of CD44, hyaluronan and NHE1 in cardiac remodeling," *Life Sciences*, vol. 209, pp. 197–201, Sep. 2018, doi: 10.1016/j.lfs.2018.08.009.
- [41] H.-Y. Chiang, V. A. Korshunov, A. Serour, F. Shi, and J. Sottile, "Fibronectin Is an Important Regulator of Flow-Induced Vascular Remodeling," *Arteriosclerosis, Thrombosis, and Vascular Biology*, vol. 29, no. 7, pp. 1074–1079, Jul. 2009, doi: 10.1161/ATVBAHA.108.181081.
- [42] K. J. Hamill, K. Kligys, S. B. Hopkinson, and J. C. R. Jones, "Laminin deposition in the extracellular matrix: a complex picture emerges," *Journal of Cell Science*, vol. 122, no. 24, pp. 4409–4417, Dec. 2009, doi: 10.1242/jcs.041095.
- [43] L. Nelson et al., "FKBPL: A marker of good prognosis in breast cancer," *Oncotarget*, vol. 6, no. 14, 2015, doi: 10.18632/oncotarget.3528.
- [44] J.-H. Wang et al., "Hypoxia-stimulated cardiac fibroblast production of IL-6 promotes myocardial fibrosis via the TGF- β 1 signaling pathway," *Laboratory Investigation*, vol. 96, no. 8, pp. 839–852, Aug. 2016, doi: 10.1038/labinvest.2016.65.
- [45] H. Hara, N. Takeda, and I. Komuro, "Pathophysiology and therapeutic potential of cardiac fibrosis," *Inflammation and Regeneration*, vol. 37, no. 1, p. 13, Dec. 2017, doi: 10.1186/s41232-017-0046-5.

- [46] C. Richards et al., “Characterisation of cardiac health in the reduced uterine perfusion pressure model and a 3D cardiac spheroid model, of preeclampsia,” *Biology of Sex Differences*, vol. 12, no. 1, p. 31, Dec. 2021, doi: 10.1186/s13293-021-00376-1.
- [47] M. R. Adams, W. Jessup, D. Hailstones, and D. S. Celermajer, “L-Arginine Reduces Human Monocyte Adhesion to Vascular Endothelium and Endothelial Expression of Cell Adhesion Molecules,” *Circulation*, vol. 95, no. 3, pp. 662–668, Feb. 1997, doi: 10.1161/01.CIR.95.3.662.
- [48] M. Dobaczewski et al., “Smad3 Signaling Critically Regulates Fibroblast Phenotype and Function in Healing Myocardial Infarction,” *Circulation Research*, vol. 107, no. 3, pp. 418–428, Aug. 2010, doi: 10.1161/CIRCRESAHA.109.216101.
- [49] A. C. Midgley et al., “Transforming Growth Factor- β 1 (TGF- β 1)-stimulated Fibroblast to Myofibroblast Differentiation Is Mediated by Hyaluronan (HA)-facilitated Epidermal Growth Factor Receptor (EGFR) and CD44 Co-localization in Lipid Rafts,” *Journal of Biological Chemistry*, vol. 288, no. 21, pp. 14824–14838, May 2013, doi: 10.1074/jbc.M113.451336.
- [50] T. C. L. Bracco Gartner et al., “Anti-fibrotic Effects of Cardiac Progenitor Cells in a 3D-Model of Human Cardiac Fibrosis,” *Frontiers in Cardiovascular Medicine*, vol. 6, 2019, doi: 10.3389/fcvm.2019.00052.
- [51] A. Singh, J. W. Wilson, C. J. Schofield, and R. Chen, “Hypoxia-inducible factor (HIF) prolyl hydroxylase inhibitors induce autophagy and have a protective effect in an in-vitro ischaemia model,” *Scientific Reports*, vol. 10, no. 1, p. 1597, Jan. 2020, doi: 10.1038/s41598-020-58482-w.
- [52] A. Yoshimura, Y. Wakabayashi, and T. Mori, “Cellular and molecular basis for the regulation of inflammation by TGF- β ,” *Journal of Biochemistry*, vol. 147, no. 6, pp. 781–792, Jun. 2010, doi: 10.1093/jb/mvq043.
- [53] C. Murdoch, S. Tazzyman, J. Harrison, J. Yeomans, and M. Muthana, “Macrophage-mediated response to hypoxia in disease,” *Hypoxia*, p. 185, Nov. 2014, doi: 10.2147/HP.S49717.

[54] R. Bennett et al., "RALA-mediated delivery of FKBPL nucleic acid therapeutics," *Nanomedicine*, vol. 10, no. 19, 2015, doi: 10.2217/nnm.15.115.

[55] L. McClements et al., "Targeting treatment-resistant breast cancer stem cells with FKBPL and its peptide derivative, AD-01, via the CD44 pathway," *Clinical Cancer Research*, vol. 19, no. 14, 2013, doi: 10.1158/1078-0432.CCR-13-0595.

[56] N. Todd et al., "Role of A Novel Angiogenesis FKBPL-CD44 Pathway in Preeclampsia Risk Stratification and Mesenchymal Stem Cell Treatment," *The Journal of Clinical Endocrinology & Metabolism*, vol. 106, no. 1, pp. 26–41, Jan. 2021, doi: 10.1210/clinem/dgaa403.

3.9 Supplementary Info

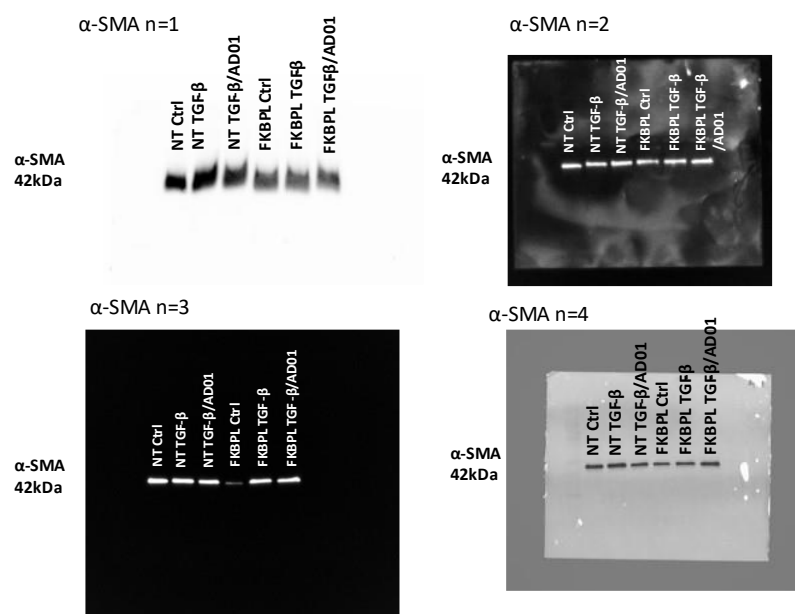


Figure S 3.1 α -SMA protein expression in both normal and low FKBPL settings following exposure of HFF08 fibroblast cells to pro-fibrotic and hypoxia stimuli, with or without FKBPL peptide mimetic, AD-01. Full sized Western blot (Figure 3.9)

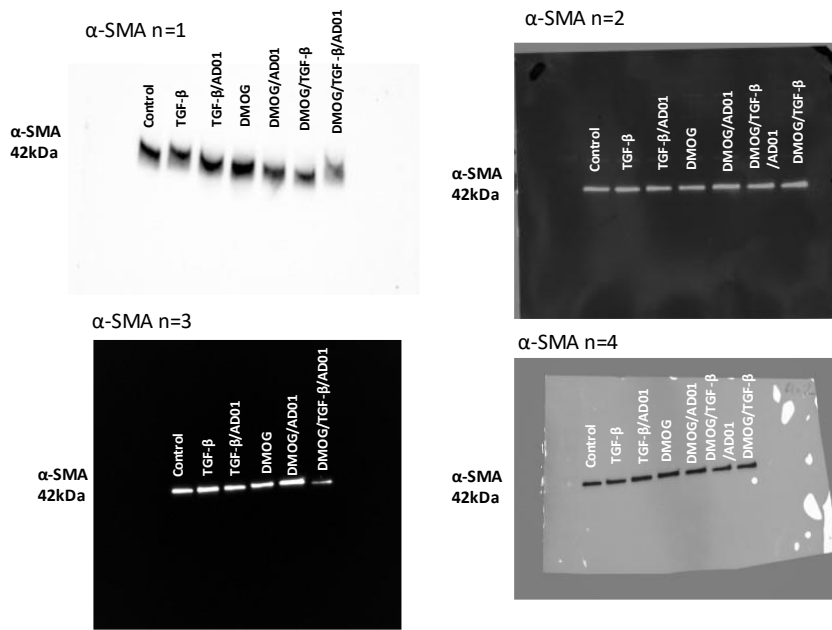


Figure S 3.2 α -SMA protein expression in HFF08 fibroblast cells exposed to pro-fibrotic and hypoxia stimuli, with or without FKBPL peptide mimetic, AD-01. Full sized Western blot (Figure 3.9)

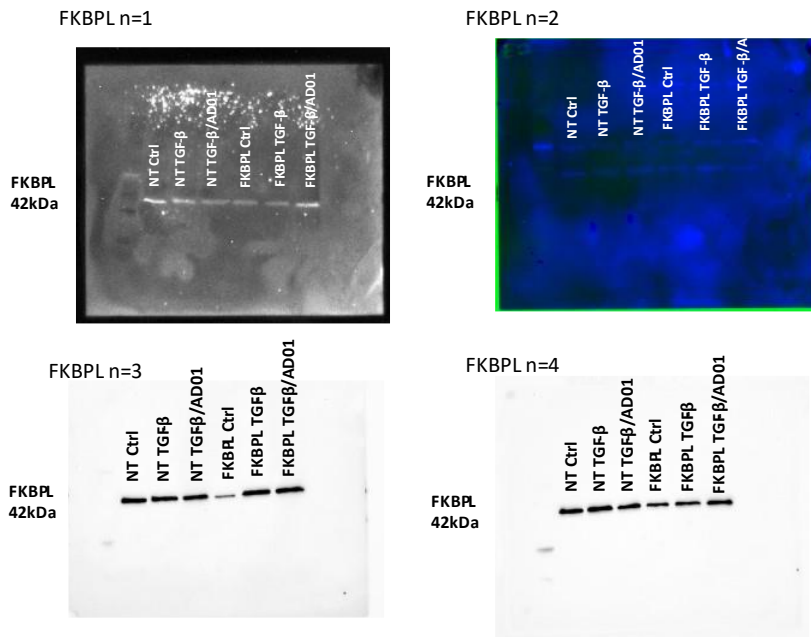


Figure S 3.3 FKBPL protein expression in both normal and low FKBPL settings following exposure of HFF08 fibroblast cells to pro-fibrotic and hypoxia stimuli, with or without FKBPL peptide mimetic, AD-01. Full sized Western blot (Figure 3.9)

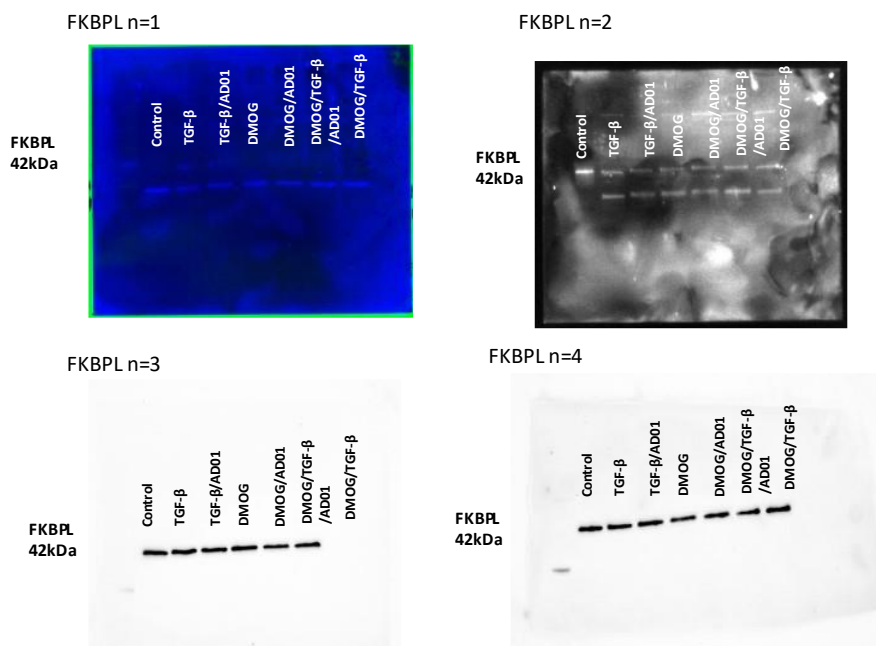


Figure S 3.4 FKBPL protein expression in HFF08 fibroblast cells exposed to pro-fibrotic and hypoxia stimuli, with or without FKBPL peptide mimetic, AD-01. Full sized Western blot (Figure 3.9)

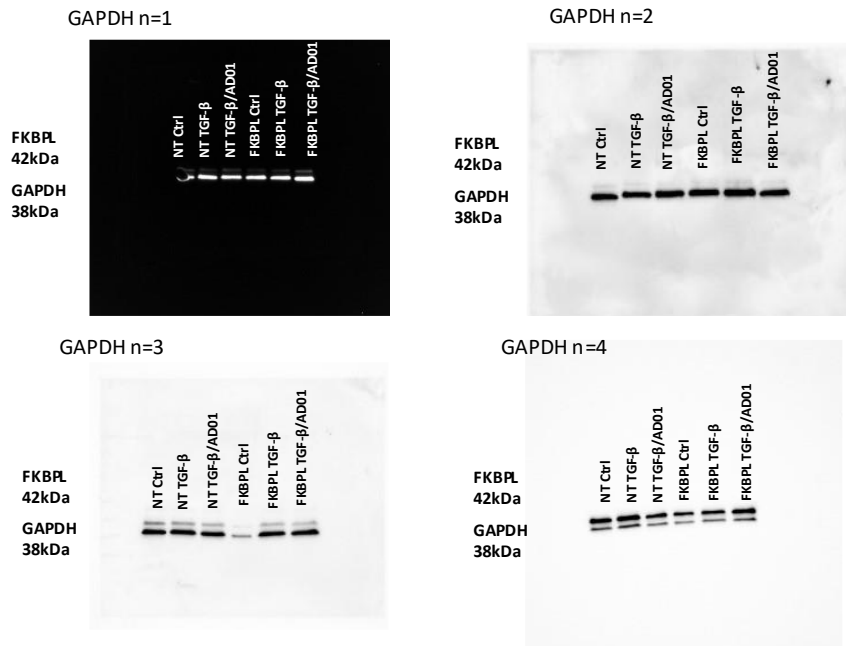


Figure S 3.5 GAPDH protein expression in both normal and low FKBP settings following exposure of HFF08 fibroblast cells to pro-fibrotic and hypoxia stimuli, with or without FKBP peptide mimetic, AD-01. Full sized Western blot (Figure 3.9)

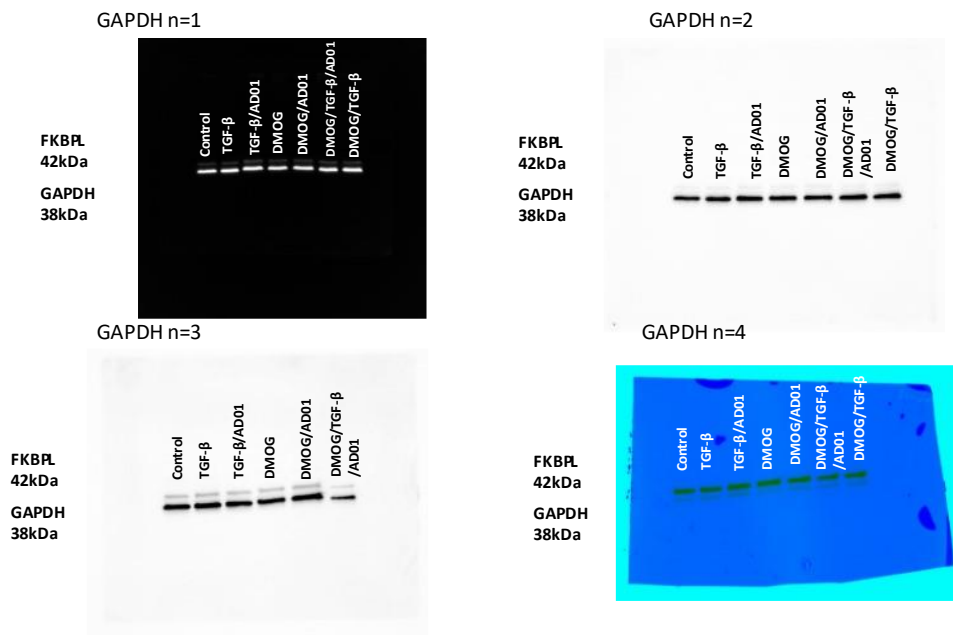


Figure S 3.6 GAPDH protein expression in HFF08 fibroblast cells exposed to pro-fibrotic and hypoxia stimuli, with or without FKBP peptide mimetic, AD-01. Full sized Western blot (Figure 3.9)

Chapter 4

Evaluating the Biomarker Potential of FKBPL in Risk Stratification and Diagnosis of Heart Failure with Preserved Ejection Fraction

Heart failure (HF) is the most common end point of various cardiovascular diseases that requires appropriate pharmacological and lifestyle management in order to improve patient prognosis and survival. There are three main subtypes of heart failure: HF with reduced ejection fraction (HFrEF), HF with mid-range ejection fraction (HFmrEF) and HF with preserved ejection fraction (HFpEF), the latter of which is the hardest one to treat as a heterogenous condition with poorly understood pathological mechanisms. In this Chapter, we first performed a systematic review and meta-analysis evaluating current biomarkers for HFpEF, which identified four promising biomarkers (NT-proBNP, BNP, Gal-3 and ST2) from 19 studies eligible for meta-analysis. In the next study as part of this Chapter, we investigated the role of a novel protein, FK506-binding protein like (FKBPL) and its therapeutic peptide mimetic, AD-01, in HFpEF, as critical mediators of angiogenesis and inflammation which are key mechanisms in the pathogenesis of heart failure. We investigated FKBPL's role in the pathogenesis of HFpEF and as a biomarker using *in vitro* models of cardiomyoblasts treated with angiotensin II (Ang-II) and/or AD-01, and plasma samples from patients with different types of HFpEF, respectively. Cardiomyoblasts treated with Ang-II or AD-01 exhibited increased cell and nucleus size, however AD-01 was found to abrogate the hypertrophic effects from Ang-II treatment, implicating FKBPL signalling in cardiomyoblast hypertrophy. FKBPL in plasma samples from HFpEF patients was increased compared to controls and negatively correlated with echocardiographic parameters indicative microvascular dysfunction.

valuation of the diagnostic accuracy of current biomarkers in heart failure with reserved ejection fraction: systematic review and meta analysis

Hao Chen^{1,2}, Michael Chhor¹, Benjamin S. Rayner¹, Kristine McGrath¹, Lana McClements^{1*}

¹ *School of Life Sciences, Faculty of Science, University of Technology Sydney, NSW, Australia*

² *Inflammation Group, Heart Research Institute, University of Sydney, 2006 NSW, Australia.*

*Corresponding author

Lana McClements

E-mail: lane.mcclements@uts.edu.au

Keywords: Heart failure with preserved ejection fraction; HFpEF; Biomarkers; Diagnosis; Meta-analysis

4.1 Abstract

Background: A number of circulating biomarkers are currently utilized for the diagnosis of chronic heart failure with preserved ejection fraction (HFpEF). However, due to HFpEF heterogeneity, the accuracy of these biomarkers remains unclear.

Aims: This study aimed to systematically determine the diagnostic accuracy of currently available biomarkers for chronic HFpEF.

Methods: PubMed, Web of Science, MEDLINE and SCOPUS databases were searched systematically to identify studies assessing the diagnostic accuracy of biomarkers of chronic HFpEF with left ventricular ejection fraction (LVEF) $\geq 50\%$. All included studies were independently assessed for quality and relevant information was extracted. Random-effects models were used to estimate the pooled diagnostic accuracy of HFpEF biomarkers.

Results: The search identified 6145 studies, of which 19 were included. Four biomarkers were available for meta-analysis. The pooled sensitivity of B-type natriuretic peptide (BNP) (0.787, 95% confidence interval [CI] 0.719–0.842) was higher than that of N-terminal pro-BNP (NT-proBNP) (0.696, 95% CI 0.599–0.779) in chronic HFpEF diagnosis. However, NT-proBNP showed improved specificity (0.882, 95% CI 0.778–0.941) compared to BNP (0.796, 95% CI 0.672–0.882). Galectin-3 (Gal-3) exhibited a reliable diagnostic adequacy for HFpEF (sensitivity 0.760, 95% CI 0.631–0.855; specificity 0.803, 95% CI 0.667–0.893). However, suppression of tumorigenesis-2 (ST2) displayed limited diagnostic performance for chronic HFpEF diagnosis (sensitivity 0.636, 95% CI 0.465–0.779; specificity 0.595, 95% CI 0.427–0.743).

Conclusion: NT-proBNP and BNP appear to be the most reliable biomarkers in chronic HFpEF with NT-proBNP showing higher specificity and BNP showing higher sensitivity. Although Gal-3 appears more reliable than ST2 in HFpEF diagnosis, the conclusions are limited as only three studies were included in this meta-analysis.

4.2 Introduction

Heart failure (HF) is an increasingly prominent disease in developed countries, placing a significant burden on patients and healthcare systems. It currently affects ~64 million people worldwide, with a rising prevalence [1]. HF is a complex syndrome characterized by abnormal cardiac structure and function of the heart, with impaired ability to fill and/or eject blood at normal pressure. In line with this definition, the latest clinical guidelines commonly classify HF into two subtypes based on the left ventricular ejection fraction (LVEF) [2], [3]. An LVEF < 50 % is typically considered as HF with reduced LVEF (HFrEF), and LVEF \geq 50 % is defined as HF with preserved LVEF (HFpEF). However, HF patients with LVEF ranging from 40 % to 50 % have recently been classified as HF with mid-range EF [2] or HFpEF borderline [3], an emerging grey area between HFrEF and HFpEF. HFpEF has increased in prevalence in recent years and is now associated with similar mortality rates as HFrEF [4]. However, this is controversial and HFrEF is still considered the more severe type of HF with the higher mortality rate [5], [6]. Although HFpEF is often associated with less severe manifestations, currently available treatments remain limited for symptomatic control and ineffective for HFpEF management [7].

Circulating biomarkers are employed regularly in the diagnosis and prognosis of HFpEF. They have additional potential to provide a better understanding of the underlying pathogenesis, which could lead to the development of effective therapies. Natriuretic peptides, including B-type natriuretic peptide (BNP) and N-terminal pro-BNP (NT-proBNP), are recommended for the diagnosis of HFpEF [2], [3]. In addition, galectin-3 (Gal-3) and suppression of tumorigenesis-2 (ST2) are emerging as clinical markers for risk stratification of HFpEF [3]. Nevertheless, their diagnostic reliability remains controversial due to the heterogeneity of data reported. Meta-analyses have been performed on the diagnostic accuracy of NT-proBNP and BNP for HFpEF with substantial heterogeneity observed [8], which may affect the application of the findings. Another relevant meta-analysis reported biomarkers in female patients with HFpEF and pre-eclampsia, whereas there were insufficient included studies for meta-analyses solely in HFpEF [9]. In this study, we systematically performed meta-analyses to comprehensively assess the diagnostic potential of all current biomarkers in the context of HFpEF only (defined as LVEF \geq 50 %).

4.3 Methods

4.3.1 Search strategy and selection criteria

A systematic search was conducted to assess the diagnostic accuracy of biomarkers in HFpEF using the following databases: PubMed, Web of Science, MEDLINE and SCOPUS (1900 to February 2021). The literature search was performed using 'HFpEF AND biomarker' as well as other synonymous terms outlined in Text A.1. We included studies that defined HFpEF as per the latest clinical guidelines published by the American Heart Association (AHA) or European Society of Cardiology (ESC), including the presence of symptoms and signs of HF, and LVEF \geq 50 % as confirmed

by echocardiography [2], [3]. The history of congestive HF and the aetiology of HFpEF were not restricted in the definition of HFpEF.

To determine the biomarkers' suitability for HFpEF diagnosis, published data from observational studies that assessed the diagnostic accuracy of individual biomarkers to discriminate between cohorts or groups with and without chronic HFpEF were included. Studies were selected if diagnostic performance measures of individual biomarkers were reported. Studies were excluded if they were: non-English language publications, letters, editorials, conference abstracts, meta-analyses and reviews. Secondary or post-hoc studies in the excluded meta-analysis or review publications were only considered if the inclusion criteria were met.

4.3.2 Data Extraction

Two independent investigators (H. C., M. C.) extracted data from included studies. Disagreements were resolved by consensus with a third investigator (L. M.). The recommendations of the Preferred Reporting Items for Systematic reviews and Meta-Analyses (PRISMA) guidelines [10] and a relevant guideline specialized for biomarker meta-analysis [11] were followed for data extraction. A conventional 2 × 2 table consisting of true positive (TP), true negative (TN), false positive (FP) and false negative (FN) was extracted from each included study. Only published data were extracted.

4.3.3 *Quality Assessment*

The included studies were assessed for quality independently by three co-authors (M. C., B. S. R., K. M.) using the Quality Assessment for Diagnostic Accuracy Studies-2 (QUADAS-2) tool [12], which was composed of four domains:

- patient selection;
- index test;
- reference standard;
- patient flow and timing (for sub-questions, see Text A.2).

Low risk of bias in a domain referred to positive answers in all sub-questions. High risk of bias in a domain was defined as negative answers in 2/2 or 3/3 sub-questions. Unclear risk of bias was defined as 1/2, 1/3 or 2/3 negative answers. Results were compared between assessors, and in case of disagreement, individual studies were discussed to achieve a consensus.

4.3.4 *Statistical Analysis*

The analyses of diagnostic accuracy test were performed in R (4.0.3) using ‘mada’ package, where a bivariate, random-effects meta-analysis model was applied. The analyses of diagnostic biomarkers were based on sensitivity and specificity discriminating between groups with and without HFpEF. The estimated sensitivity and specificity were calculated using the 2 × 2 tables extracted from the included studies. The sensitivity and specificity were pooled and analysed to generate random-effects model forest plots and random-effects model hierarchical summary of receiver

operating characteristic (HSROC) curves. Natural logarithm-transformed diagnostic odds ratio (ln-DOR) was reported along with heterogeneity of Higgins' I^2 and Cochran's Q. Publication bias was assessed through visual inspection of funnel plots of ln(DOR). Meta-analyses were only generated for diagnostic markers that were evaluated in three or more independent studies.

4.4 Results

4.4.1 Search Results

The results for diagnostic markers of HFpEF yielded 6145 articles, of which 19 [13], [14], [15], [16], [17], [18], [19], [20], [21], [22], [23], [24], [25], [26], [27], [28], [29], [30], [31] met the inclusion criteria with sufficient evidence to conduct meta-analyses on individual biomarkers (Table 4.1; Fig. 4.1A). The overall quality of these studies was high (Fig. 4.1B and 4.1C). Approximately equal numbers of studies were prospective and retrospective ($n = 10$ and $n = 9$, respectively; Table 4.1). In total, 1452 patients with HFpEF and 1429 without HFpEF were included from all 19 studies. All patients were at the chronic stage of HFpEF and free from valvular diseases. Patients with HFpEF were generally older adults (mean age > 50 years old), with a control group appropriately matched for age and sex. Overall, selected studies yielded a total of four different diagnostic markers: NT-proBNP, BNP, Gal-3 and ST2. Natriuretic peptides were the most commonly reported diagnostic markers (17 studies), which is in line with their well-established role in current HFpEF management [2], [3]. We were unable to complete meta-analyses on emerging biomarkers such as matrix metalloproteinases and growth differentiation factor 15 due to a small number of

studies identified in relation to their diagnostic potential in HFpEF (< 3). However, these biomarkers, along with their supporting citations, are reported in Table S4.1).

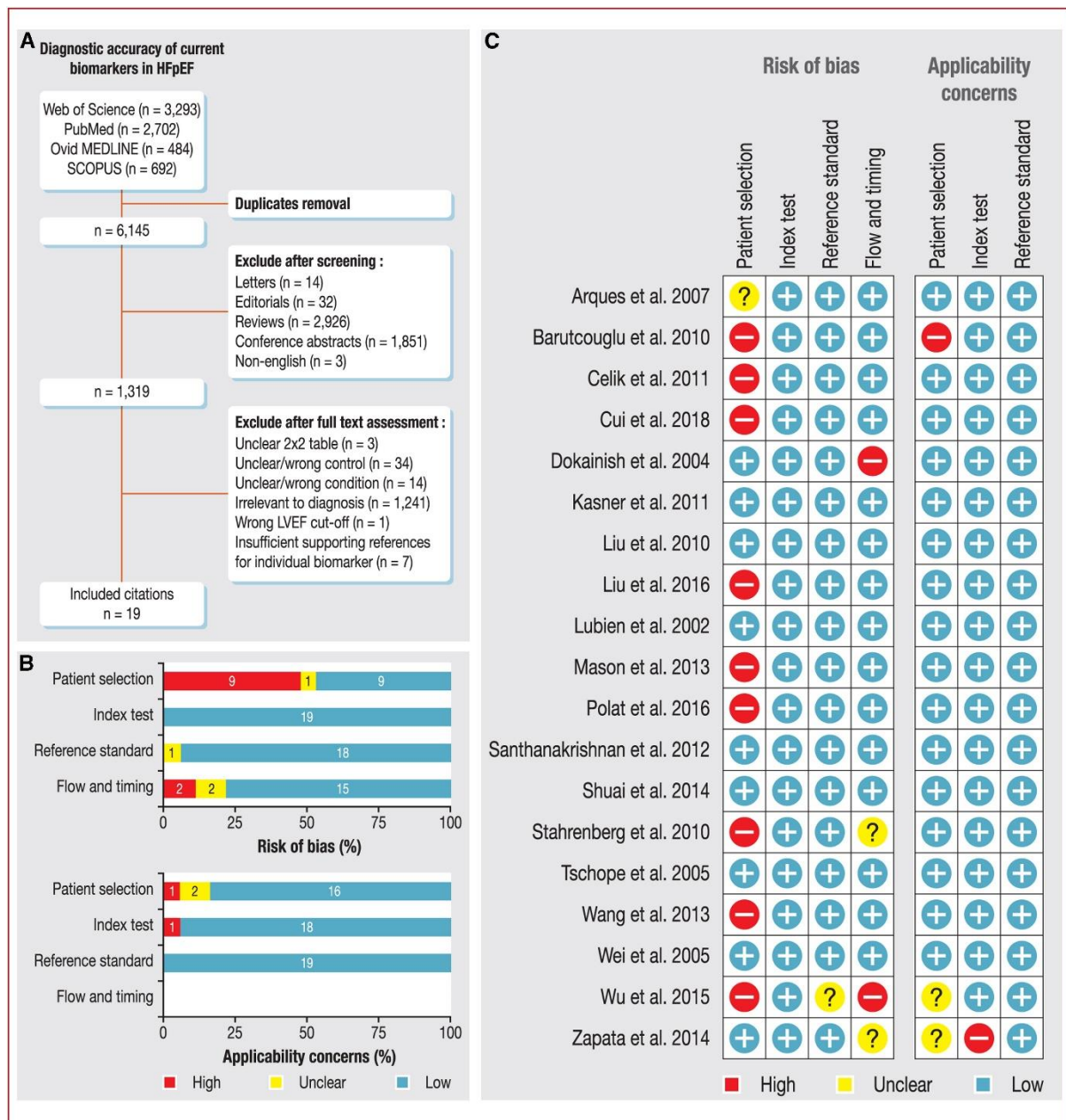


Figure 4.1 Summary of the study workflow and the number of included studies.

A. Workflow of the systematic search according to PRISMA guidelines. **B.** Summary quality assessment of included studies independently evaluated using the QUADAS-2 tool. **C.** Outcomes of quality assessment of each included study. HFpEF: heart failure with preserved ejection fraction; LVEF: left ventricular ejection fraction; PRISMA: Preferred Reporting Items for Systematic reviews and Meta-Analyses; QUADAS-2: Quality Assessment for Diagnostic Accuracy Studies-2.

Table 4.1 Characteristics of included studies

Study	Study design	Location	HFpEF				Control ^a			
			Mean LVEF (%)	n	Women (%)	Mean age (years)	Mean LVEF (%)	n	Women (%)	Mean age (years)
Liu et al., 2016 [17]	Retrospective	China	NA	50	46	64	NA	50	54	64
Cui et al., 2018 [15]	Retrospective	China	60	172	56	73	59	30	40	67
Tschope et al., 2005 [23]	Prospective	Germany	68	68	46	51	65	50	44	49
Santhanakrishnan et al., 2012 [20]	Prospective	Singapore	60	50	42	69	66	50	54	63
Stahrenberg et al., 2010 [22]	Retrospective	Germany	60	142	64	73	62	188	66	56
Kasner et al., 2011 [16]	Prospective	Germany	NA	107	40	53	NA	73	43	51
Dokainish et al., 2004 [26]	Prospective	USA	NA	19	NA	NA	NA	27	NA	NA
Liu et al., 2010 [27]	Prospective	China	65	39	50	52	67	20	46	46
Wei et al., 2005 [29]	Prospective	China	65	61	32	70	67	74	35	66
Lubien et al., 2002 [28]	Prospective	USA	NA	119	11	71	NA	175	9	60
Wang et al., 2013 [31]	Retrospective	China	68	68	54	68	68	39	33	60
Arques et al., 2007 [25]	Prospective	France	60	22	27	58	62	19	55	57
Mason et al., 2013 [18]	Retrospective	UK	NA	57	NA	NA	NA	308	NA	NA
Shuai et al., 2011 [21]	Prospective	China	66	45	52	67	67	53	50	62
Polat et al., 2016 [19]	Retrospective	Turkey	59	44	45	60	61	38	47	57
Celik et al., 2012 [14]	Retrospective	Turkey	72	71	63	57	68	50	38	56
Zapata et al., 2014 [24]	Prospective	Spain	60	50	51	68	59	36	19	57
Barutcuoglu et al., 2010 [13]	Retrospective	Turkey	NA	122	51	55	NA	119	55	53
Wu et al., 2015 [30]	Retrospective	China	68	146	62	70	NA	30	63	63

HF: heart failure; HFpEF: heart failure with preserved ejection fraction; LVEF: left ventricular ejection fraction; NA: not available.
^a Control is defined as participants without evidence of HF.

4.4.2 N-terminal pro-B-type natriuretic peptide

Studies that used NT-proBNP as a diagnostic marker of chronic HFpEF (12 studies [13], [14], [15], [16], [17], [18], [19], [20], [21], [22], [23], [24]; 978 patients) reported optimal sensitivity and specificity at NT-proBNP cut-off concentrations ranging from 65 to 477 pg/mL, with the median of 227 pg/mL (Fig. 4.2A). Interestingly, the four studies that used an NT-proBNP cut-off around 227 pg/mL [19], [20], [21], [22] had different values of sensitivity but consistent specificity. The pooled ln(DOR) was 2.97 (95 % confidence interval [CI] 2.19–3.76), and relatively low heterogeneity was observed (Higgins' I² = 26.362 %, Cochran's Q = 14.938, P = 0.185) (Fig. 4.2B). The random-effects HSROC curve revealed moderate sensitivity (0.696, 95 % CI 0.599–0.779) and reliable specificity (0.882, 95 % CI 0.778–0.941) in terms of the diagnostic performance of NT-proBNP in HFpEF, with an estimated area under the curve (AUC) of 0.836 (Fig. 4.2C). Fig. 2D shows the 95 % CI region for each study that used NT-proBNP as a diagnostic marker. Generally, the 95 % CI region of false positive rate

appeared larger than that of sensitivity for most relevant studies. According to the funnel plot (Fig. S4.1), there was some evidence of publication bias with NT-proBNP. However, the high statistical significance ($P < 0.01$) of all 12 relevant studies suggests that the publication bias is not the underlying cause of this funnel asymmetry.

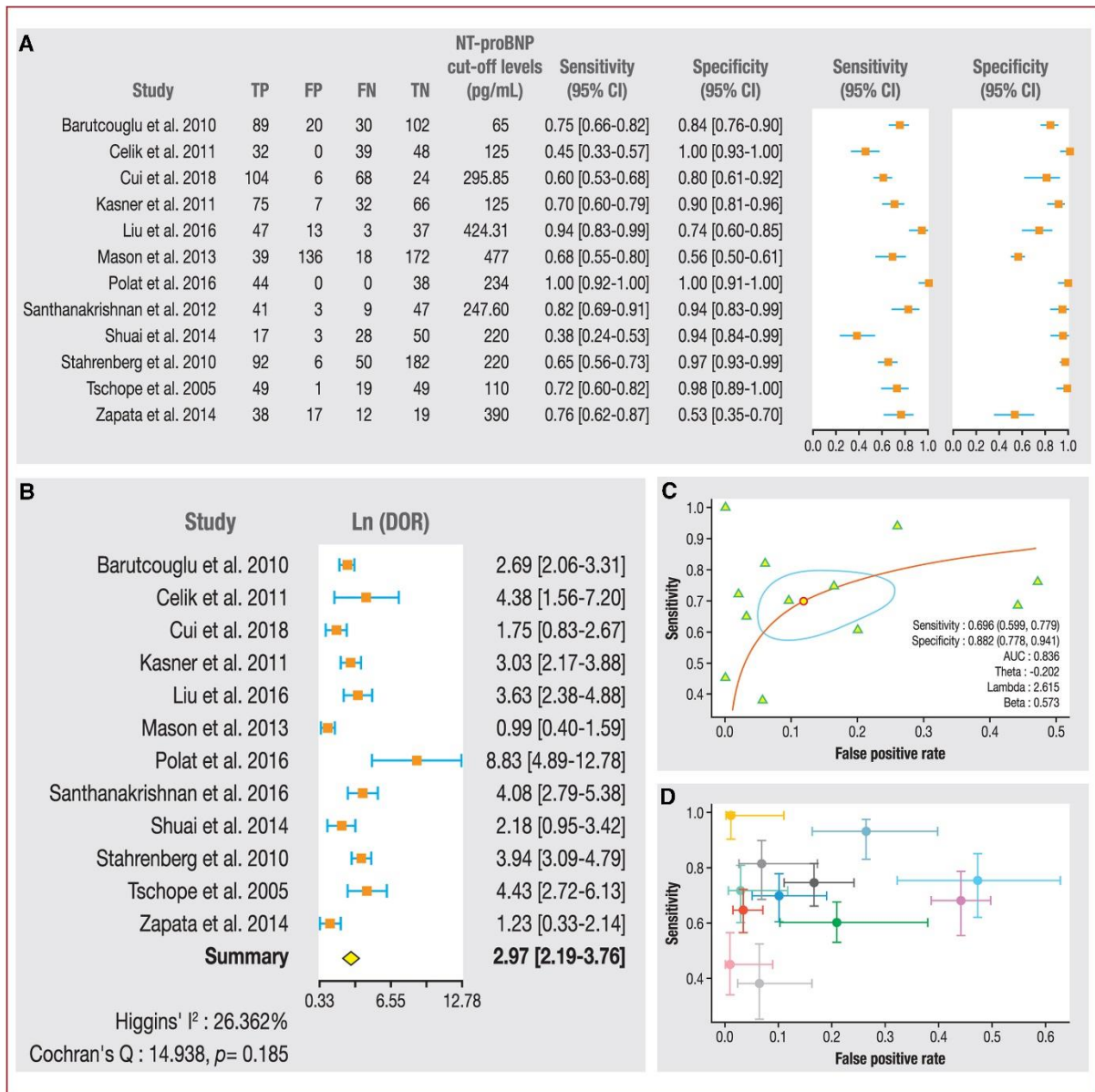


Figure 4.2 Diagnostic assessment of NT-proBNP in HFpEF using a bivariate, random-effects model. A. Forest plot of 12 studies that investigated the diagnostic performance of NT-proBNP in HFpEF, with sensitivity and specificity reported. **B.** Forest plot of $\ln(\text{DOR})$ related to the diagnostic accuracy of NT-proBNP in HFpEF. **C.** Plot of the HSROC curve showing the estimated pooled diagnostic accuracy.

D. Plot of the HSROC curve showing the 95% CI of each study that evaluated the diagnostic accuracy of NT-proBNP in HFpEF. AUC: area under the curve; CI: confidence interval; FN: false negative; FP: false positive; HFpEF: heart failure with preserved ejection fraction; HSROC: hierarchical summary of receiver operating characteristic; $\ln(\text{DOR})$: natural logarithm-transformed diagnostic odds ratio; NT-proBNP: N-terminal pro-B-type natriuretic peptide; TN: true negative; TP: true positive.

4.4.3 *B-type natriuretic peptide*

Seven studies [18], [24], [25], [26], [27], [28], [29] that investigated the diagnostic performance of BNP in HFpEF were analysed, with data extracted from 367 patients with HFpEF. The cut-off levels of BNP varied from 40 to 354 pg/mL (median 125 pg/mL) (Fig. 4.3A). In the random-effects forest plot (Fig. 4.3B), the pooled $\ln(\text{DOR})$ was 2.70 (95 % CI 1.68–3.72), with no heterogeneity observed (Higgins' $I^2 = 0\%$, Cochran's $Q = 4.422$, $P = 0.620$). The pooled estimated sensitivity (0.787, 95 % CI 0.719–0.842) and specificity (0.796, 95 % CI 0.672–0.882) were well balanced when using BNP to diagnose HFpEF (Fig. 4.3C). The pooled AUC was 0.842. The number of participants was relatively small in three of the studies [25], [26], [27], resulting in the largest variance shown in Fig. 4.3D. Similarly, to NT-proBNP, the funnel plot of BNP is asymmetrical (Fig S4.2). However, the high statistical significance ($P < 0.01$) of all relevant studies suggests that publication bias is not the underlying cause of this funnel asymmetry.

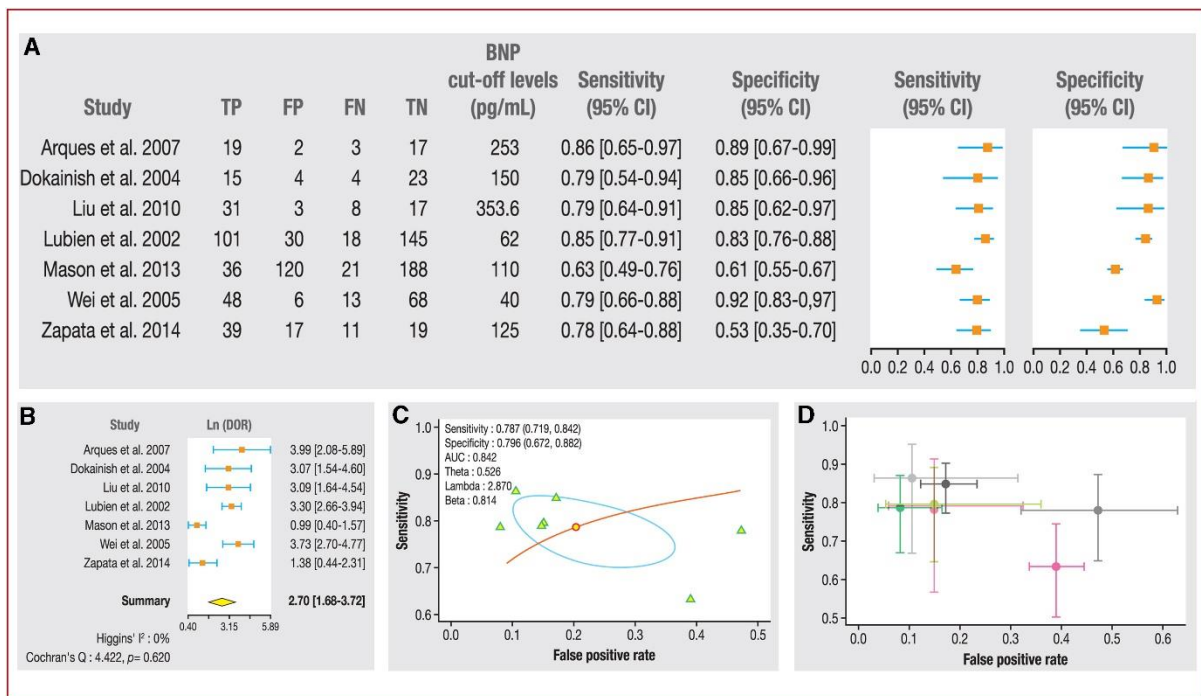


Figure 4.3 Diagnostic assessment of BNP in HFpEF using a bivariate, random-effects model. A. Forest plot of seven studies that investigated the diagnostic performance of BNP in HFpEF, with sensitivity and specificity reported. **B.** Forest plot of $\ln(\text{DOR})$ related to the diagnostic accuracy of BNP in HFpEF. **C.** Plot of the HSROC curve showing the estimated pooled diagnostic accuracy. **D.** Plot of the HSROC curve showing the 95% CI of each study that evaluated the diagnostic accuracy of BNP in HFpEF. AUC: area under the curve; BNP: B-type natriuretic peptide; CI: confidence interval; FN: false negative; FP: false positive; HFpEF: heart failure with preserved ejection fraction; HSROC: hierarchical summary of receiver operating characteristic; $\ln(\text{DOR})$: natural logarithm-transformed diagnostic odds ratio; TN: true negative; TP: true positive.

4.4.4 Galectin-3

Analyses were performed on the diagnostic accuracy of Gal-3 using three studies [15], [19], [30]. The data were evaluated based on a total of 362 patients with HFpEF. Gal-3 cut-offs of 1.8 to 10.7 ng/mL (median 9.6 ng/mL) were reported (Fig. 4.4A). The pooled $\ln(\text{DOR})$ was 2.94 (95 % CI 1.61–4.28), whereas substantial heterogeneity was

observed (Higgins' I² = 48.598 %, Cochran's Q = 3.891, P = 0.143) (Fig. 4.4B). Sensitivity was relatively high (0.760, 95 % CI 0.631–0.855), as was specificity (0.803, 95 % CI 0.667–0.893) (Fig. 4.4C). The AUC was 0.851 for the diagnostic performance of Gal-3. Fig. 4.4D shows larger variance on false positive rate compared to sensitivity.

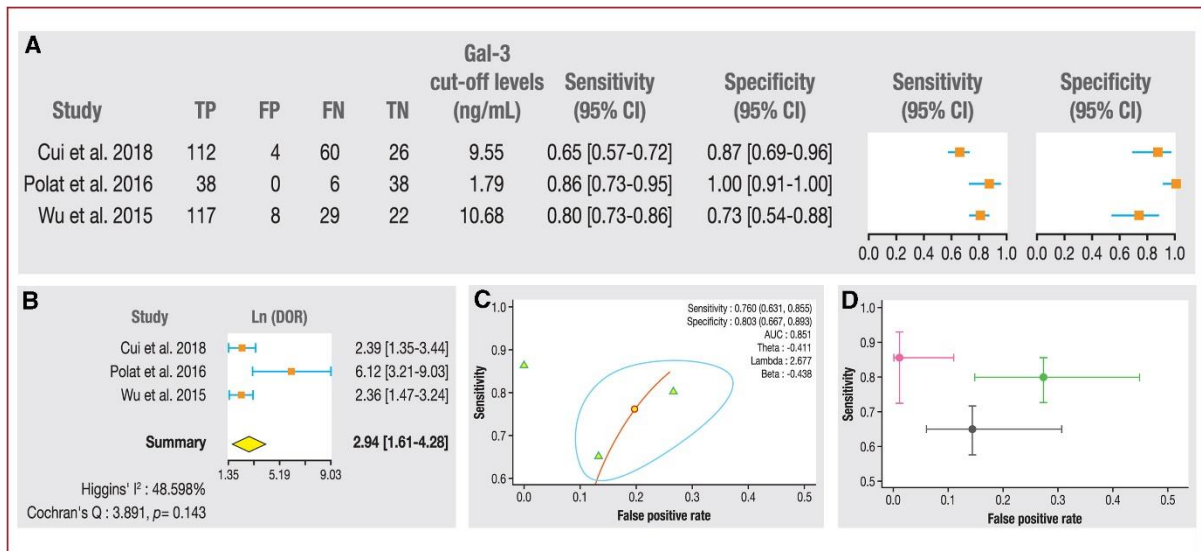


Figure 4.4 Diagnostic assessment of Gal-3 in HFpEF using a bivariate, random-effects model. A. Forest plot of three studies that investigated the diagnostic performance of Gal-3 in HFpEF, with sensitivity and specificity reported. **B.** Forest plot of ln(DOR) regarding the diagnostic accuracy of Gal-3 in HFpEF. **C.** Plot of the HSROC curve showing the estimated pooled diagnostic accuracy. **D.** Plot of the HSROC curve showing the 95% CI of each study that evaluated the diagnostic accuracy of Gal-3 in HFpEF. AUC: area under the curve; CI: confidence interval; FN: false negative; FP: false positive; Gal-3: galectin-3; HFpEF: heart failure with preserved ejection fraction; HSROC: hierarchical summary of receiver operating characteristic; ln(DOR): natural logarithm-transformed diagnostic odds ratio; TN: true negative; TP: true positive.

4.4.5 Suppression of tumorigenesis-2

Three studies [15], [20], [31] reported the diagnostic accuracy of ST2 in chronic HFpEF, with an adequate pooled number of patients with HFpEF (n = 290), and the distribution of participants was well balanced across the studies. The cut-off levels of

ST2 varied substantially across the three studies, ranging from 69 to 26470 pg/mL (Fig. 4.5A). The pooled $\ln(\text{DOR})$ of ST2 as an individual diagnostic marker in HFpEF was 1.00 (95 % CI -0.07–2.07), with minimal heterogeneity (Higgins' $I^2 = 3.959\%$, Cochran's $Q = 2.082$, $P = 0.353$) (Fig. 4.5B). In line with the poor $\ln(\text{DOR})$, sensitivity (0.636, 95 % CI 0.465–0.779) and specificity (0.595, 95 % CI 0.427–0.743) as well as AUC (0.647) were all unreliable (Fig. 4.5C). Although the number of participants was satisfactory in each study, the reported diagnostic accuracy varied highly, particularly in terms of false positive rate (Fig. 4.5D).

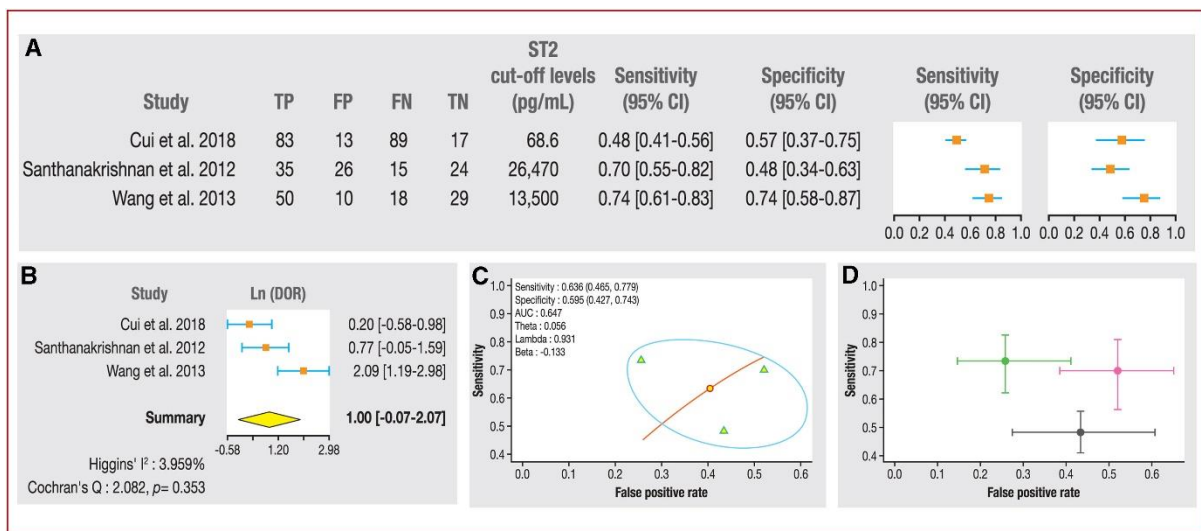


Figure 4.5 Diagnostic assessment of ST2 in HFpEF using a bivariate, random-effects model. A. Forest plot of three studies that investigated the diagnostic performance of ST2 in HFpEF, with sensitivity and specificity reported. **B.** Forest plot of $\ln(\text{DOR})$ regarding the diagnostic accuracy of ST2 in HFpEF. **C.** Plot of the HSROC curve showing the estimated pooled diagnostic accuracy. **D.** Plot of the HSROC curve showing the 95% CI of each study that evaluated the diagnostic accuracy of ST2 in HFpEF. AUC: area under the curve; CI: confidence interval; FN: false negative; FP: false positive; HFpEF: heart failure with preserved ejection fraction; HSROC: hierarchical summary of receiver operating characteristic; $\ln(\text{DOR})$: natural logarithm-transformed diagnostic odds ratio; ST2: suppression of tumorigenesis-2; TN: true negative; TP: true positive.

4.5 Discussion

HF can be categorized as acute or chronic, and it is possible and common for HF patients to experience acute episodes (e.g. acute exacerbation or decompensation) of HF with underlying chronic symptoms. Chronic underlying HFpEF accounts for a large proportion of its population and it must be noted that the biomarkers assessed in this study were performed in the context of patients with chronic HFpEF [32].

The diagnosis of chronic HFpEF is challenging as it is a multifactorial syndrome; it does not only include preserved LVEF, but additional symptoms of chronic HF are also considered in diagnosis [33]. However, the reliability of currently available biomarkers in the diagnosis of HFpEF remains partially unclear. Our study is the first to systematically and comprehensively review the currently available circulating biomarkers (defined as proteins detected in blood-derived samples) in the diagnosis of chronic HFpEF. The main findings of this study are:

- NT-proBNP ($\ln(\text{DOR}) = 2.97$) and BNP ($\ln(\text{DOR}) = 2.70$) are the two most reliable individual diagnostic markers for HFpEF, albeit the diagnostic adequacy of both natriuretic peptides in chronic HFpEF remains moderate;
- NT-proBNP shows higher specificity (0.882) than BNP (0.796) in the diagnosis of chronic HFpEF, whereas the sensitivity and specificity of BNP (0.787 and 0.796, respectively) are more balanced than for NT-proBNP (0.696 and 0.882, respectively);
- Gal-3, an emerging biomarker for HFpEF management, displays promising diagnostic performance ($\ln(\text{DOR}) = 2.94$) for HFpEF;

- ST2 shows no diagnostic potential ($\ln(\text{DOR}) = 1.00$) as an individual biomarker for the diagnosis of chronic HFpEF.

Compared to a previous HFpEF biomarker meta-analysis [8], a lower degree of heterogeneity was detected in our study, as the heterogeneity statistics were only utilized for the estimation of $\ln(\text{DOR})$ rather than sensitivity and specificity. However, substantial heterogeneity was present related to the diagnostic accuracy of Gal-3, which could be due to the retrospective design of all relevant selected studies [15], [19], [30]. In addition, specificity of 1.00 was introduced by one of the studies [19], which could be due to random chance. Another explanation for the heterogeneity could be caused by the wide difference of cut-off levels of Gal-3 (1.8, 9.6 and 10.7 ng/mL). The heterogeneous nature of HFpEF may also play a role in these differences between the studies included for Gal-3. All these underlying causes of heterogeneity could limit the applicability of the results of Gal-3. Therefore, it is important to note that the reliable diagnostic discriminative power of Gal-3 remains questionable.

A limited number of studies were included for the evaluation of the diagnostic accuracy of Gal-3 and ST2 in HFpEF, with only 362 and 290 patients with HFpEF, respectively. Trends of rising HF prevalence are shared amongst all countries, yet it is interesting that the studies included in the Gal-3 meta-analysis were largely conducted in Asia. With factors such as an ageing population and younger age range for HF patients, the generalizability of the findings in this study to patients of different ethnicities may be limited [32].

Natriuretic peptides are currently the most widely utilized biomarkers that support HFpEF diagnosis. Frequently, laboratories and clinical guidelines recommend the use of NT-proBNP over BNP in HFpEF diagnosis as the first-line option. This is likely due to the stability of NT-proBNP in blood samples for over 72 hours at room temperature without the need for additives. On the other hand, BNP is only stable in blood samples for 24 hours at room temperature, and the blood collection tubes are required to be coated with ethylenediaminetetraacetic acid [34].

NT-proBNP and BNP are strongly recommended for HFpEF diagnosis by current clinical guidelines [2], [3], which is why there are a good number of high-quality observational studies evaluating these biomarkers. As such, the diagnostic reliability of NT-proBNP and BNP is well-validated in our study. In this diagnostic accuracy meta-analysis, the pooled specificity of NT-proBNP for diagnosing HFpEF was higher than that of BNP, however the pooled sensitivity of BNP was better than NT-proBNP, consistent with another HFpEF biomarker meta-analysis [8]. Interestingly, both sensitivity and specificity of BNP were well balanced and reasonable. The AUC and $\ln(\text{DOR})$ of NT-proBNP and BNP were satisfactory for diagnostic purposes. Therefore, the reliability of NT-proBNP and BNP are equal as diagnostic markers for chronic HFpEF, given that both natriuretic peptides are in the same biological pathway [35]. However, differential sensitivity and specificity were reported for NT-proBNP and BNP in HFpEF diagnosis, suggesting different utility in clinical settings. Due to the high specificity of NT-proBNP for HFpEF diagnosis, it is likely that NT-proBNP is more suitable for ruling out HFpEF. Higher sensitivity could be more applicable to secondary or tertiary care, whereas reliable specificity could be more important in primary care settings.

Overall, fairly consistent cut-off levels of NT-proBNP have been reported by relevant studies, with the best specificity being observed above 100-125 pg/mL [14], [16], [23], which is consistent with the cut-off (> 125 pg/mL) recommended by the 2016 ESC clinical guidelines for HF [2] and the new Heart Failure Association that include Pretest assessment, Echocardiographic and natriuretic peptide score, Functional testing in case of uncertainty, Final aetiology (HFA-PEFF) diagnostic algorithm [36]. Three studies utilized higher cut-off values of NT-proBNP (424 pg/mL [17] and 477 pg/mL [18], 390 pg/mL [24]), which led to the lowest specificity. This could further support utilizing the recommended cut-off values for NT-proBNP of approximately 100 pg/mL for the diagnosis of HFpEF. Despite the recommended cut-off level of BNP being 35 pg/mL [2], [36], the cut-off values for BNP reported by the studies we included varied widely. In addition, one study reported that the cut-off value of ~35 pg/mL provided an unreliable diagnostic accuracy (sensitivity: 0.67; specificity: 0.73) for chronic HFpEF [37]. However, considerably higher cut-off levels for BNP were reported in other relevant studies. Further population-based comparable investigations of the diagnostic performance of BNP at different cut-off concentrations for HFpEF diagnosis are therefore necessary.

ST2 is emerging as a new diagnostic marker for HFpEF and is recommended by the latest AHA guidelines [3]. Nevertheless, we observed a limited diagnostic accuracy of ST2 in chronic HFpEF diagnosis, supported by three studies reporting differential findings [15], [20], [31]. The limited diagnostic value of ST2 in HFpEF is likely caused by the lack of association of ST2 with left ventricular function and structure [38]. Despite the limited performance of ST2 in chronic HFpEF, ST2 is beneficial in the acute settings [39]. Although ST2 has been shown to be associated with HF diagnosis

above the cut-off concentration of 35 ng/mL, as recommended by the Food and Drug Administration [40], the diagnostic adequacy in HF subtypes, including HFpEF and HFrEF, were modest in an older adult population [41]. Therefore, the optimal cut-off value of ST2 in HF subtypes should be re-evaluated in future observational studies that include specific HF phenotype.

Collectively, the specificity of NT-proBNP, BNP and Gal-3 are generally higher than their sensitivity, suggesting a more advanced ability of ruling out HFpEF, consistent with the proposals in current guidelines [2], [42]. Generally, these biomarkers play a critical role in discriminating acute HF from non-cardiac dyspnoea in acute settings, as their concentrations are significantly elevated [39], [43]. However, the opposite is true in chronic settings where the levels of biomarkers could be closer to normal ranges. Therefore, diagnosis of chronic HFpEF is still challenging, especially given the common comorbidities that further complicate the diagnosis. Overall, in line with the recommendations of the HFA-PEFF diagnostic algorithm [36], biomarkers should be used in addition to echocardiography for the early diagnosis of HFpEF. Future studies should therefore investigate the clinical utility of current biomarkers in combination with echocardiographic measurements.

4.6 Conclusion

HFpEF accounts for approximately half of all patients with HF, and it is associated with similar mortality to HFrEF, yet it is ineffectively managed with pharmacotherapies. Due to the poorly understood pathogenesis of HFpEF, there are often delays in its

diagnosis and treatment, leading to worse outcomes for HFpEF patients. Accurate biomarkers are critical for the early diagnosis of HFpEF, emphasizing the urgent need for biomarker discovery and validation. Nevertheless, in this meta-analysis, it was demonstrated that NT-proBNP and BNP remain the most reliable biomarkers for HFpEF diagnosis. NT-proBNP is possibly more reliable for chronic HFpEF diagnosis given its more consistent and less varied cut-off diagnostic values and higher specificity than BNP. Gal-3 also displays a reliable diagnostic discriminative power, however the high heterogeneity between the studies limits the applicability of Gal-3's for HFpEF diagnosis based on published studies included here. ST2 appears to have limited diagnostic potential for chronic HFpEF. Therefore, more robust and larger studies are warranted to evaluate these biomarkers and discover new biomarkers for HFpEF diagnosis and prognosis.

4.7 Declarations

Funding: Hao Chen and Michael Chhor are supported by an Australian Government Research Training Program (RTP) Stipend and RTP Fee-Offset Scholarship through University of Technology Sydney.

Authors' contributions: H. C. (supervised by B. S. R., K. M. and L. M.) conducted the search, identified the studies, performed the statistical analyses and wrote the first draft of this manuscript. M. C. conducted the search, screened, assessed and identified the studies, extracted the data and contributed to the writing. B. S. R., M. C. and K. M. reviewed the quality of the studies. L. M. conceptualized the study and edited the manuscript. All authors reviewed and approved the manuscript.

Disclosure of interest: The authors declare that they have no competing interest.

4.8 References

[1] Groenewegen A, Rutten FH, Mosterd A, Hoes AW. Epidemiology of heart failure. *Eur J Heart Fail* 2020;22:1342—56.

[2] Ponikowski P, Voors AA, Anker SD, et al. 2016 ESC Guidelines for the diagnosis and treatment of acute and chronic heart failure: The Task Force for the diagnosis and treatment of acute and chronic heart failure of the European Society of Cardiology (ESC). Developed with the special contribution of the Heart Failure Association (HFA) of the ESC. *Eur Heart J* 2016;37:2129—200.

[3] Yancy CW, Jessup M, Bozkurt B, et al. 2017 ACC/AHA/HFSA Focused Update of the 2013 ACCF/AHA Guideline for the Management of Heart Failure: A Report of the American College of Cardiology/American Heart Association Task Force on Clinical Practice Guidelines and the Heart Failure Society of America. *Circulation* 2017;136:e137—61.

[4] Owan TE, Hodge DO, Herges RM, Jacobsen SJ, Roger VL, Redfield MM. Trends in prevalence and outcome of heart failure with preserved ejection fraction. *N Engl J Med* 2006;355:251—9.

[5] Lam CSP, Gamble GD, Ling LH, et al. Mortality associated with heart failure with preserved vs. reduced ejection fraction in a prospective international multi-ethnic cohort study. *Eur Heart J* 2018;39:1770—80.

[6] Meta-analysis Global Group in Chronic Heart Failure (MAGGIC). The survival of patients with heart failure with preserved or reduced left ventricular ejection fraction: An individual patient data meta-analysis. *Eur Heart J* 2012;33:1750—7.

[7] Zheng SL, Chan FT, Nabeebaccus AA, et al. Drug treatment effects on outcomes in heart failure with preserved ejection fraction: A systematic review and meta-analysis. *Heart* 2018;104:407—15.

- [8] Remmelzwaal S, van Ballegooijen AJ, Schoonmade LJ, et al. Natriuretic peptides for the detection of diastolic dysfunction and heart failure with preserved ejection fraction—a systematic review and meta-analysis. *BMC Med* 2020;18:290.
- [9] Alma LJ, Bokslag A, Maas A, Franx A, Paulus WJ, de Groot CJM. Shared biomarkers between female diastolic heart failure and pre-eclampsia: A systematic review and meta-analysis. *ESC Heart Fail* 2017;4:88—98.
- [10] Moher D, Liberati A, Tetzlaff J, Altman DG, Group PRISMA. Preferred reporting items for systematic reviews and metaanalyses: The PRISMA statement. *BMJ* 2009;339:b2535.
- [11] Liu Z, Yao Z, Li C, Liu X, Chen H, Gao C. A step-by-step guide to the systematic review and meta-analysis of diagnostic and prognostic test accuracy evaluations. *Br J Cancer* 2013;108:2299—303.
- [12] Whiting PF, Rutjes AW, Westwood ME, et al. QUADAS-2: A revised tool for the quality assessment of diagnostic accuracy studies. *Ann Intern Med* 2011;155:529—36.
- [13] Barutcuoglu B, Parildar Z, Basol G, Gurgun C, Tekin Y, Bayindir O. The detection of left ventricular diastolic dysfunction in hypertensive patients: Performance of N-terminal probrain natriuretic peptide. *Blood Press* 2010;19:212—7.
- [14] Celik A, Koc F, Kadi H, et al. Relationship between red cell distribution width and echocardiographic parameters in patients with diastolic heart failure. *Kaohsiung J Med Sci* 2012;28:165—72.
- [15] Cui Y, Qi X, Huang A, Li J, Hou W, Liu K. Differential and predictive value of galectin-3 and soluble suppression of tumorigenicity-2 (sST2) in heart failure with preserved ejection fraction. *Med Sci Monit* 2018;24:5139—46.
- [16] Kasner M, Gaub R, Westermann D, et al. Simultaneous estimation of NT-proBNP on top to mitral flow Doppler echocardiography as an accurate strategy to diagnose diastolic dysfunction in HFNEF. *Int J Cardiol* 2011;149:23—9.
- [17] Liu S, Iskandar R, Chen W, et al. Soluble glycoprotein 130 and heat shock protein 27 as novel candidate biomarkers of chronic heart failure with preserved ejection fraction. *Heart Lung Circ* 2016;25:1000—6.

- [18] Mason JM, Hancock HC, Close H, et al. Utility of biomarkers in the differential diagnosis of heart failure in older people: Findings from the heart failure in care homes (HFinCH) diagnostic accuracy study. *PLoS One* 2013;8:e53560.
- [19] Polat V, Bozcali E, Uygun T, Opan S, Karakaya O. Diagnostic significance of serum galectin-3 levels in heart failure with preserved ejection fraction. *Acta Cardiol* 2016;71:191—7.
- [20] Santhanakrishnan R, Chong JP, Ng TP, et al. Growth differentiation factor 15, ST2, high-sensitivity troponin T, and N-terminal pro brain natriuretic peptide in heart failure with preserved vs. reduced ejection fraction. *Eur J Heart Fail* 2012;14:1338—47.
- [21] Shuai XX, Chen YY, Lu YX, et al. Diagnosis of heart failure with preserved ejection fraction: Which parameters and diagnostic strategies are more valuable? *Eur J Heart Fail* 2011;13: 737—45.
- [22] Stahrenberg R, Edelmann F, Mende M, et al. The novel biomarker growth differentiation factor 15 in heart failure with normal ejection fraction. *Eur J Heart Fail* 2010;12: 1309—16.
- [23] Tschope C, Kasner M, Westermann D, Gaub R, Poller WC, Schultheiss HP. The role of NT-proBNP in the diagnostics of isolated diastolic dysfunction: Correlation with echocardiographic and invasive measurements. *Eur Heart J* 2005;26:2277—84.
- [24] Zapata L, Betbese AJ, Roglan A, Ordonez-Llanos J. Use of Btype natriuretic peptides to detect the existence and severity of diastolic dysfunction in non-cardiac critically ill patients: A pilot study. *Minerva Anestesiol* 2014;80:194—203.
- [25] Arques S, Roux E, Sbragia P, et al. Usefulness of bedside tissue Doppler echocardiography and B-type natriuretic peptide (BNP) in differentiating congestive heart failure from noncardiac cause of acute dyspnea in elderly patients with a normal left ventricular ejection fraction and permanent, nonvalvular atrial fibrillation: Insights from a prospective, monocenter study. *Echocardiography* 2007;24:499—507.
- [26] Dokainish H, Zoghbi WA, Lakkis NM, Quinones MA, Nagueh SF. Comparative accuracy of B-type natriuretic peptide and tissue Doppler echocardiography in the diagnosis of congestive heart failure. *Am J Cardiol* 2004;93:1130—5.

- [27] Liu H, Zhang YZ, Gao M, Liu BC. Elevation of B-type natriuretic peptide is a sensitive marker of left ventricular diastolic dysfunction in patients with maintenance haemodialysis. *Biomarkers* 2010;15:533—7.
- [28] Lubien E, DeMaria A, Krishnaswamy P, et al. Utility of B-natriuretic peptide in detecting diastolic dysfunction: Comparison with Doppler velocity recordings. *Circulation* 2002;105:595—601.
- [29] Wei T, Zeng C, Chen L, et al. Bedside tests of B-type natriuretic peptide in the diagnosis of left ventricular diastolic dysfunction in hypertensive patients. *Eur J Heart Fail* 2005;7:75—9.
- [30] Wu CK, Su MY, Lee JK, et al. Galectin-3 level and the severity of cardiac diastolic dysfunction using cellular and animal models and clinical indices. *Sci Rep* 2015;5:17007.
- [31] Wang YC, Yu CC, Chiu FC, et al. Soluble ST2 as a biomarker for detecting stable heart failure with a normal ejection fraction in hypertensive patients. *J Card Fail* 2013;19:163—8.
- [32] Chen YT, Wong LL, Liew OW, Richards AM. Heart failure with reduced ejection fraction (HFrEF) and preserved ejection fraction (HFpEF): The diagnostic value of circulating microRNAs. *Cells* 2019;8:1651.
- [33] Gazewood JD, Turner PL. Heart failure with preserved ejection fraction: Diagnosis and management. *Am Fam Physician* 2017;96:582—8.
- [34] Weber M, Hamm C. Role of B-type natriuretic peptide (BNP) and NT-proBNP in clinical routine. *Heart* 2006;92:843—9.
- [35] de Lemos JA, McGuire DK, Drazner MH. B-type natriuretic peptide in cardiovascular disease. *Lancet* 2003;362:316—22.
- [36] Pieske B, Tschope C, de Boer RA, et al. How to diagnose heart failure with preserved ejection fraction: the HFA-PEFF diagnostic algorithm: A consensus recommendation from the Heart Failure Association (HFA) of the European Society of Cardiology (ESC). *Eur Heart J* 2019;40:3297—317.

[37] Arques S, Jaubert MP, Bonello L, et al. Usefulness of basal B-type natriuretic peptide levels for the diagnosis of diastolic heart failure in young patients: An echocardiographic catheterization study. *Int J Cardiol* 2010;145:51—2.

[38] AbouEzzeddine OF, McKie PM, Dunlay SM, et al. Suppression of tumorigenicity 2 in heart failure with preserved ejection fraction. *J Am Heart Assoc* 2017;6:e004382.

[39] Mueller T, Gegenhuber A, Leitner I, Poelz W, Haltmayer M, Dieplinger B. Diagnostic and prognostic accuracy of galectin3 and soluble ST2 for acute heart failure. *Clin Chim Acta* 2016;463:158—64.

[40] US Food and Drug Administration. Substantial equivalence determination decision summary assay only template. https://www.accessdata.fda.gov/cdrh_docs/reviews/k111452.pdf. [accessed 25 October 2021].

[41] Parikh RH, Seliger SL, Christenson R, Gottdiener JS, Psaty BM, deFilippi CR. Soluble ST2 for prediction of heart failure and cardiovascular death in an elderly, community-dwelling population. *J Am Heart Assoc* 2016;5:e003188.

[42] Paulus WJ, Tschope C, Sanderson JE, et al. How to diagnose diastolic heart failure: A consensus statement on the diagnosis of heart failure with normal left ventricular ejection fraction by the Heart Failure and Echocardiography Associations of the European Society of Cardiology. *Eur Heart J* 2007;28:2539—50.

[43] Maisel AS, McCord J, Nowak RM, et al. Bedside B-Type natriuretic peptide in the emergency diagnosis of heart failure with reduced or preserved ejection fraction. Results from the Breathing Not Properly Multinational Study. *J Am Coll Cardiol* 2003;41:2010—7.

4.9 Supplementary Info

Table S4.1 Data extraction for diagnostic biomarkers of HFpEF with < 3 studies.

	TP	FP	FN	TN
TIMP1				
Ahmed et al. 2006 [1]	24	3	2	20
Angiogenin				

Jiang et al. 2014 [2]	6	1	3	15
sgp130				
Liu et al. 2016 [3]	44	10	6	40
hsp27				
Liu et al. 2016 [3]	44	8	6	42
cBIN1				
Nikolova et al. 2018 [4]	29	1	23	51
GDF15				
Santhanakrishnan et al. 2012 [5]	46	8	4	42
Stahrenberg et al. 2010 [6]	116	27	26	161
hs-TnT				
Santhanakrishnan et al. 2012 [5]	41	6	9	44
Adiponectin				
Bazaeva et al. 2017 [7]	33	2	2	33
Copeptin				
Mason et al. 2013 [8]	30	142	24	166
MR-proADM				
Mason et al. 2013 [8]	36	120	21	188
MR-proANP				
Mason et al. 2013 [8]	40	126	17	182

cBIN1: cardiac bridging integrator 1; FN: false negative; FP: false positive; GDF15: growth differentiation factor 15; HFpEF: heart failure with preserved ejection fraction; hsp27: heat shock protein 27; hs-TnT: high-sensitivity troponin T; MR-proADM: mid-regional pro-adrenomedullin; MR-proANP: mid-regional pro-atrial natriuretic peptide; sgp130: soluble glycoprotein 130; TIMP1: tissue inhibitor of metalloproteinases 1; TN: true negative; TP: true positive.

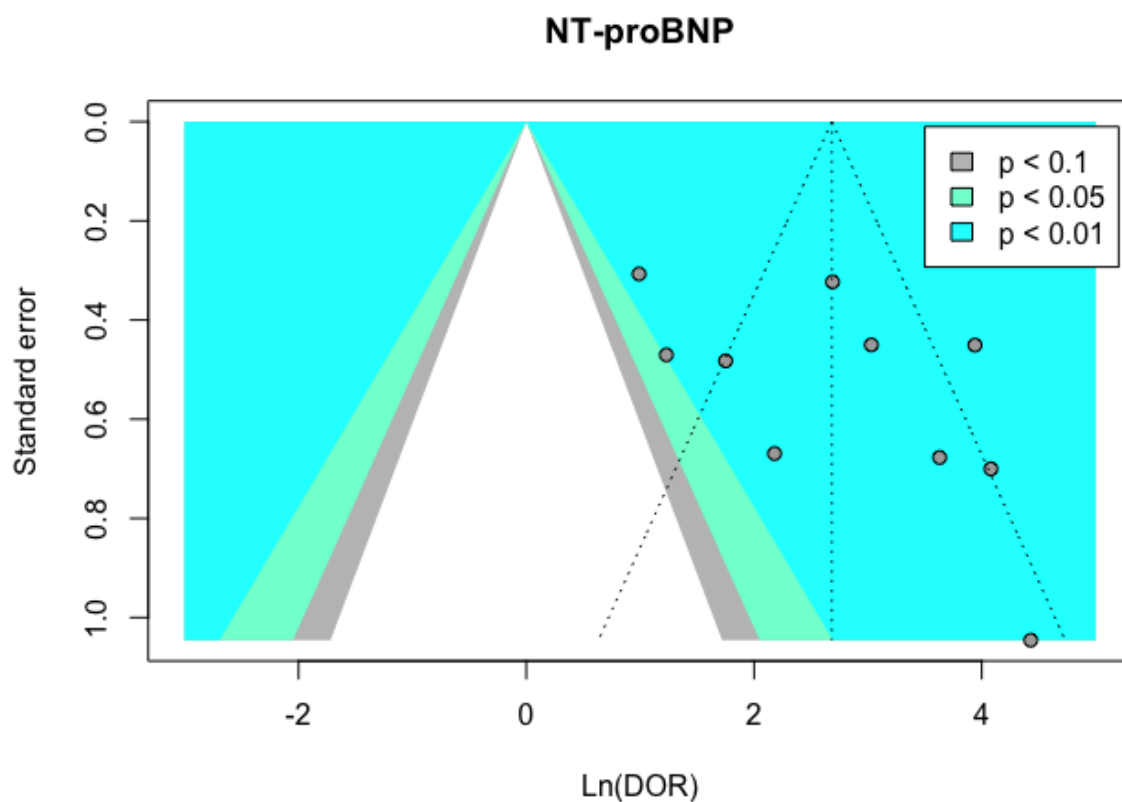


Figure S4.1 BNP: B-type natriuretic peptide; HFpEF: heart failure with preserved ejection fraction; ln(DOR): logarithm-transformed diagnostic odds ratio. HFpEF: heart failure with preserved ejection fraction; ln(DOR): logarithm-transformed diagnostic odds ratio; NT-proBNP: N-terminal pro-B-type natriuretic peptide.

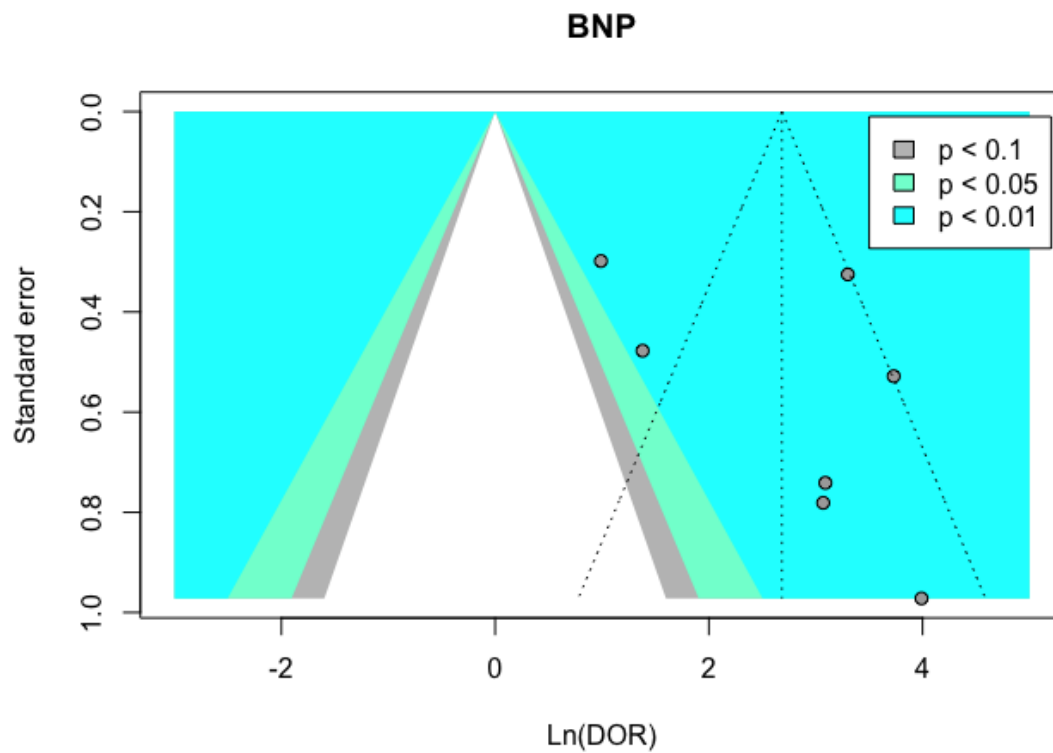


Figure S4.2 Funnel plot of $\ln(\text{DOR})$ of the diagnostic accuracy of BNP in HFpEF. BNP: B-type natriuretic peptide; HFpEF: heart failure with preserved ejection fraction; $\ln(\text{DOR})$: logarithm-transformed diagnostic odds ratio.

FK5 6 Binding Protein like (FKBPL) Has an Important Role in Heart Failure with Preserved Ejection Fraction Pathogenesis with Potential Diagnostic Utility

Michael Chhor ¹, Hao Chen ¹, Djurdja Jeroti'c ², Milorad Teši'c ^{2,3}, Valentina N. Nikoli'c ⁴, Milan Pavlovi'c ⁵, Rada M. Vu'ci'c ^{6,7}, Benjamin Rayner ⁸, Chris J. Watson ⁹, Mark Ledwidge ^{10,11}, Kenneth McDonald ^{10,11}, Tracy Robson ¹², Kristine C. McGrath ¹ and Lana McClements ^{1,9, *}

1 Faculty of Science, School of Life Sciences, University of Technology Sydney, Broadway, NSW 2007, Australia

2 Faculty of Medicine, University of Belgrade, 11000 Belgrade, Serbia

3 Clinic for Cardiology, University Clinical Center of Serbia, 11000 Belgrade, Serbia

4 Department of Pharmacology and Toxicology, Faculty of Medicine, University of Nis, 18000 Nis, Serbia

5 Department of Internal Medicine—Cardiology, Faculty of Medicine, University of Nis, 18000 Nis, Serbia

6 Department of Internal Medicine, Faculty of Medical Sciences, University of Kragujevac, 34000 Kragujevac, Serbia

7 Department of Cardiology, Clinical Centre of Kragujevac, 34000 Kragujevac, Serbia

8 Inflammation Group, Heart Research Institute, University of Sydney, Sydney, NSW 2006, Australia

9 Wellcome-Wolfson Institute for Experimental Medicine, Queen's University Belfast, Belfast BT9 7BL, UK

10 STOP-HF Unit, St. Vincent's University Hospital, D04 T6F4 Dublin, Ireland

11 School of Medicine, University College Dublin, D04 V1W8 Dublin, Ireland

12 School of Pharmacy and Biomolecular Sciences, Royal College of Surgeons in Ireland, D02 YN77 Dublin, Ireland

*Corresponding author: Lana McClements

E-mail: lane.mcclements@uts.edu.au

Keywords: heart failure; biomarkers; heart failure with preserved ejection fraction; HFpEF; HCM; hypertrophic cardiomyopathy; FKBPL; plasma; angiotensin; AD-01

4.10 Abstract

Heart failure (HF) is the leading cause of hospitalisations worldwide, with only 35% of patients surviving the first 5 years after diagnosis. The pathogenesis of HF with preserved ejection fraction (HFpEF) is still unclear, impeding the implementation of effective treatments. FK506-binding protein like (FKBPL) and its therapeutic peptide mimetic, AD-01, are critical mediators of angiogenesis and inflammation. Thus, in this study, we investigated—for the first time—FKBPL's role in the pathogenesis and as a biomarker of HFpEF. In vitro models of cardiac hypertrophy following exposure to a hypertensive stimulus, angiotensin-II (Ang-II, 100 nM), and/or AD-01 (100 nM), for 24 and 48 h were employed as well as human plasma samples from people with different forms of HFpEF and controls. Whilst the FKBPL peptide mimetic, AD-01, induced cardiomyocyte hypertrophy in a similar manner to Ang-II ($p < 0.0001$), when AD-01 and Ang-II were combined together, this process was abrogated ($p < 0.01$ – 0.0001). This mechanism appears to involve a negative feedback loop related to FKBPL ($p < 0.05$). In human plasma samples, FKBPL concentration was increased in HFpEF compared to controls ($p < 0.01$); however, similar to NT-proBNP and Gal-3, it was unable to stratify between different forms of HFpEF: acute HFpEF, chronic HFpEF and hypertrophic cardiomyopathy (HCM). FKBPL may be explored for its biomarker and therapeutic target potential in HFpEF.

4.11 Introduction

Heart failure (HF) is a complex cardiovascular disease (CVD) that is characterised by a failure to meet circulatory demands [1]. Apart from genetic causes, common modifiable risk factors include obesity, diabetes mellitus, high blood pressure and smoking. Clinical symptoms include fatigue, weight gain, shortness of breath, and difficulty performing daily tasks [2]. Worldwide, HF is estimated to affect 40 million people annually [2]. In Australia, CVD is responsible for 25% of all mortalities, reaching an economic cost of 11.8 billion dollars per year [3]. HF diagnosis includes clinical symptoms, patient history and echocardiographic measurements [2]. Classification of HF into its phenotypes is based on the symptoms present and the left ventricular ejection fraction (EF). The European Society of Cardiology guidelines outline that an $EF \leq 40\%$ is defined as heart failure with a reduced ejection fraction (HFrEF), an $EF \geq 50\%$ as heart failure with a preserved ejection fraction (HFpEF) and an EF between 41–49% as heart failure with a mildly reduced ejection fraction (HFmrEF) [1,4]. Despite accounting for almost half the cases of HF, those with HFpEF have poorer management and prognosis compared to patients with HFrEF [5].

In conjunction with HF diagnosis, biomarker measurements provide crucial information surrounding the pathophysiology, severity and progression of HF [1]. Natriuretic peptides are the choice biomarkers to aid in such diagnosis—namely, brain natriuretic peptide (BNP) and N-terminal (NT)-pro hormone BNP (NT-proBNP), which are both reflective of myocardial stretch. Clinically, both BNP and NT-proBNP are reliable diagnostic and prognostic markers of HF. However, BNP levels have been shown to be elevated in cases of pulmonary and renal diseases but are decreased in overweight patients [6]. NT-proBNP, in addition to having a longer half-life than BNP, has been

shown to be less affected by parameters such as obesity—perhaps increasing its clinical utility [6]. Additionally, Galectin-3 is emerging as a promising biomarker of HFpEF [7]—the expression of which is positively correlated with adverse cardiac remodelling [8].

FK506-binding protein like (FKBPL) is a divergent member of the immunophilin family known for its role as a secreted anti-angiogenic protein that exhibits its action via CD44, establishing its critical role in angiogenesis [9,10]. Additionally, FKBPL has been shown to regulate steroid receptor and inflammatory signalling via CD44, HSP90 and STAT3, with an important regulatory function in vascular health [10–12]. AD-01 and ALM201 are FKBPL-based therapeutic peptides developed based on its anti-angiogenic domain, demonstrating effective anti-inflammatory and anti-angiogenic effects [13]. Even though full FKBPL knockout has been shown to be embryonically lethal, heterozygous knockdown of FKBPL in mice does not lead to any clinically detectable adverse phenotype; however, at the proteomic level, it shows early signs of endothelial dysfunction and impaired vascular integrity [10]. Recently, it was shown that FKBPL plasma concentrations are increased in the presence of CVD and the absence of diabetes mellitus compared to healthy controls, and FKBPL is positively correlated with the echocardiographic parameters of diastolic dysfunction [12]. However, its diagnostic or pathogenic role has not previously been demonstrated in HF. In light of these important functions associated with FKBPL, it is likely that it may have a role in the development of HF—particularly HFpEF—since inflammation and microvascular dysfunction are hallmark features of HFpEF [14]. Thus, this study evaluated the role of FKBPL in the development of cardiac hypertrophy and HFpEF using *in vitro* models of cardiomyoblasts exposed to a hypertensive stimulus,

angiotensin-II (Ang-II), and/or the FKBPL mimetic AD-01, as well as human plasma samples from people with different forms of HFpEF and controls.

4.12 Methods

4.12.1 Cell culture and Treatments

H9C2 rat cardiomyoblasts (Sigma Aldrich, Castle Hill, Australia) were cultured in Dulbecco's Modified Eagle's Medium (DMEM) (Thermofisher, Waltham, MA, USA), supplemented with 10% foetal bovine serum (FBS) (Thermofisher, Waltham, MA, USA). Cells were treated with Ang-II (100 nM)(Sigma Aldrich, Castle Hill, Australia), AD-01 (100 nM) (Sigma Aldrich, Castle Hill, Australia) or a combination of Ang-II and AD-01 for 48 h before measuring the cell/nucleus size and extracting RNA and protein.

4.12.2 Cell Size Analysis

The cell and nucleus size were determined using an Axio Imager A2 microscope (Carl Zeiss AG, Oberochen, Germany) and ZEISS Zen 2 imaging software (Carl Zeiss AG, Oberochen, German, v.1.0) at 20× magnification. ImageJ (National Institutes of Health, Bethesda, MD, USA) was used to measure and quantify cell/nucleus size.

4.12.3 Western Blot

Proteins were separated by molecular weight using sodium dodecyl sulfate polyacrylamide gel electrophoresis (SDS-PAGE). The loading buffer for the SDS-

PAGE was Laemmli sample buffer (Bio-Rad Laboratories, Hercules, CA, USA) containing the reducing agent dithiothreitol (DTT), according to Laemmli (1970) [15]. The standard ladder used to estimate the molecular weight of the proteins was a Kaleidoscope protein ladder (Bio-Rad Laboratories, Hercules, CA, USA). FKBPL primary antibody (1:1000; in PBS; Proteintech, Rosemont, IL, USA) was used, alongside a β -actin primary antibody (1:10,000; in PBS; Abcam, Cambridge, UK) to normalise the relative FKBPL concentration. The membrane was scanned using the ChemiDoc imaging system (Bio-Rad Laboratories, Hercules, CA, USA). The scanned pictures with peptide bands were processed through ImageJ for relative quantification.

4.12.4 Reverse Transcription-Polymerase Chain Reaction (RT-qPCR)

Total RNA was extracted from the treated cells using the ISOLATE II RNA Mini Kit (Bioline, Eveleigh, Australia), following the manufacturer's guidelines. Reverse transcription was then performed using RT kit iScript Reverse transcription Supermix (Bio-Rad Laboratories, Hercules, CA, USA), before qPCR was performed using a SensiFAST SYBR No-ROX Kit (Bioline, Everleigh, Australia) and the primers listed for β -actin (FW:5'-CGCGAGTACAACCTTCTTGC-3' and RW:5'-CGTCATCCATGGCGAACTGG-3'), FKBPL (FW:5'-TGGCCTCTCAGGTCTGAACTA-3' and RW:5'-TGGGGACTGCTGCTTAATCG-3'), BNP (FW:5'-TCCTTAATCTGTCGCCGCTG-3' and RW:5'-TCCAGCAGCTTCTGCATCG-3'), and ANP (FW:5'-CTGGGACCCCTCCGATAGAT-3' and RW:5'-TTCGGTACCGGAAGCTGTTG-3'). Total mRNA expression levels were calculated using the $2^{-\Delta\Delta CT}$ method, using β -actin as the reference gene.

4.12.5 *Participants and Samples*

A total of 33 patients diagnosed with HFpEF were enrolled in this study, according to the latest guidelines for HF [16]. Transthoracic echocardiography was performed and blood samples were collected from each participant at the time of the outpatient visit or hospital admission. Patients were excluded if there was a presence of significant valvular disease. Patients were divided into three sub-groups of HFpEF depending on their clinical symptoms: HCM (n = 15), acute HFpEF (n = 9) and chronic HFpEF (n = 9). A control group (n = 40) of participants who were high-risk for CVD, but without left ventricular diastolic dysfunction, were also included in this study (Table 4.2). All participants provided written consent prior to inclusion and blood collection. This study was conducted in accordance with the Declaration of Helsinki and ethical approval was obtained from individual hospitals and institutions.

Table 4.2 Patient group and clinical characteristics

Characteristics	Controls (n = 40)	Acute HFpEF (n = 9)	Chronic HFpEF (n = 9)	HCM (n = 15)
Age (years)	72.43 ± 6.4	73.4 ± 13.3	64.6 ± 10.6	50.7 ± 13.6
Female (no. [%])	13 (37.1)	4 (44.4)	3 (33.3)	3 (20)
BMI (kg/m ²)	27.6 ± 5.3	32 ± 4.4	28 ± 2.5	25.9 ± 4.1
EF (%)	n/a	57.6 ± 10.9	57.4 ± 8.0	64.5 ± 3.8
NYHA Class	n/a	I/II/III	I/II	I/II
Diabetes n (%)	20 (54)	5 (56)	2 (22)	0 (0)
NT-proBNP (ng/mL)	n/a	13.8 ± 20.9	2.3 ± 3.0	3.2 ± 3.0
FKBPL (ng/mL)	1.26 ± 0.3	1.8 ± 0.6	1.5 ± 0.9	1.6 ± 0.8
Gal-3 (ng/mL)	n/a	10.9 ± 6.6	8.5 ± 4.5	7.5 ± 4.6
Echocardiography measurement				
EDD (mm)	n/a	55.0 ± 11.6	52.8 ± 6.9	47.5 ± 5.5
ESD (mm)	n/a	37 ± 9.6	35.3 ± 8.2	28.9 ± 4.2
IVST (mm)	n/a	12.3 ± 2.9	12.4 ± 2.4	17.9 ± 2.3
PWT (mm)	n/a	11.7 ± 2.1	12.1 ± 1.5	9.3 ± 1.7
Medications				
Aspirin (no. [%])	n/a	7 (78)	4 (44)	1 (7)
Purinergic receptor antagonists (no. [%])	n/a	5 (56)	3 (33)	0
Statins (no. [%])	n/a	6 (67)	3 (33)	2 (13)
Isosorbide mononitrate (no. [%])	n/a	3 (33)	1 (11)	0
Beta-blockers (no. [%])	n/a	9 (100)	6 (67)	14 (93)
ACE-inhibitors (no. [%])	n/a	7 (78)	5 (56)	4 (27)
Diuretics (no. [%])	n/a	4 (44)	4 (44)	4 (27)
Calcium channel blockers (no. [%])	n/a	3 (33)	2 (22)	1 (7)
Warfarin (no. [%])	n/a	1 (11)	1 (11)	0
Amiodarone (no. [%])	n/a	0	0	1 (7)
PPIs (no. [%])	n/a	4 (44)	3 (33)	0
Trimetazidine (no. [%])	n/a	1 (11)	1 (11)	0
Molsidomine (no. [%])	n/a	1 (11)	1 (11)	0
Spirolactone (no. [%])	n/a	0	3 (33)	0
Allopurinol (no. [%])	n/a	0	1 (11)	0
Aminophylline (no. [%])	n/a	0	2 (22)	0

n/a—not applicable; BMI, body mass index; HF, heart failure; HFpEF, heart failure with preserved ejection fraction; EDD, end-diastolic dimension; EF, ejection fraction; ESD, end-systolic dimension; IVST, intraventricular septal thickness; PWT, posterior wall thickness; NT-proBNP, N-terminal pro-B-type natriuretic peptide; and NYHA, New York Heart Association Functional Classification; PPIs, proton pump inhibitors.

4.12.6 *Plasma Marker Measurement*

Blood samples collected from participants were centrifuged at 3000× g for 10 min to collect plasma. Plasma FKBPL concentrations were measured using an FKBPL ELISA assay (Cloud-Clone, Wuhan, China), following the manufacturer's guidelines. Plasma NTproBNP and Gal-3 concentrations were also measured using an ELISA (NT-proBNP, Abcam, Cambridge, UK; Gal-3, Elabscience, Wuhan, China). Gal-3 and NT-proBNP concentrations were not measured within the control group—comparisons were only performed between different HFpEF groups.

4.12.7 *Statistical Analysis*

All results are expressed as a mean ± SEM or SD. The data were checked for normal distribution before performing parametric tests (one-way ANOVA) with post-hoc multiple comparison testing. Correlations between two continuous variables were assessed based on the Pearson's correlation coefficient. Statistical significance was defined as $p < 0.05$ (two-sided). Statistical analyses were performed using SPSS software, version 24 (IBM Corp, Armonk, NY, USA) and GraphPad Prism v8.00 (Graphpad Software, Boston, MA, USA). Results with $p < 0.05$ were considered significant.

4.13 Results

4.13.1 FKBPL Peptide Mimetic, AD-01, and Angiotensin-II (Ang-II) Increase Cardiomyoblast Cell and Nucleus Size; However, AD-01 in the Presence of Ang-II Abrogates Ang-II-Induced Cardiac Hypertrophy

Given that cardiac hypertrophy often leads to HFpEF, we determined the effect of a hypertensive stimuli, Ang-II, on the nucleus and cell size of cultured H9C2 cardiomyoblasts [17,18]. Cardiomyoblast nucleus and cell size were significantly increased following both 24 h and 48 h treatment with Ang-II compared to the control (Figure 4.6A–D, $p < 0.0001$). The effect on the nucleus size was more pronounced after the 48 h treatment with Ang-II (~70% increase) compared to the 24 h treatment (~13% increase). In the presence of AD-01 alone, nucleus size was also increased with both the 24 h (~60% increase) and 48 h treatment (~40% increase; Figure 4.6A, B, $p < 0.0001$). Interestingly, following the 24 h treatment with AD-01, cell size was modestly decreased (~7% decrease; Figure 4.6C, $p < 0.0001$), whereas the 48 h treatment with AD-01 led to an increase in cell size similar to that in the nucleus size (Figure 4.6D, $p < 0.0001$). When the AD-01 treatment was added to the Ang-II exposure, the increase in the nucleus size was abrogated both at 24 and 48 h ($p < 0.01$ and $p < 0.0001$, respectively; Figure 4.6A, B). The cardiomyoblast cell size was also abrogated when AD-01 was added to Ang-II both at 24 and 48 h ($p < 0.0001$); at both time points, AD-01 in the presence of Ang-II led to a ~30–40% reduction in cell size compared to Ang-II exposure alone (Figure 4.6C, D).

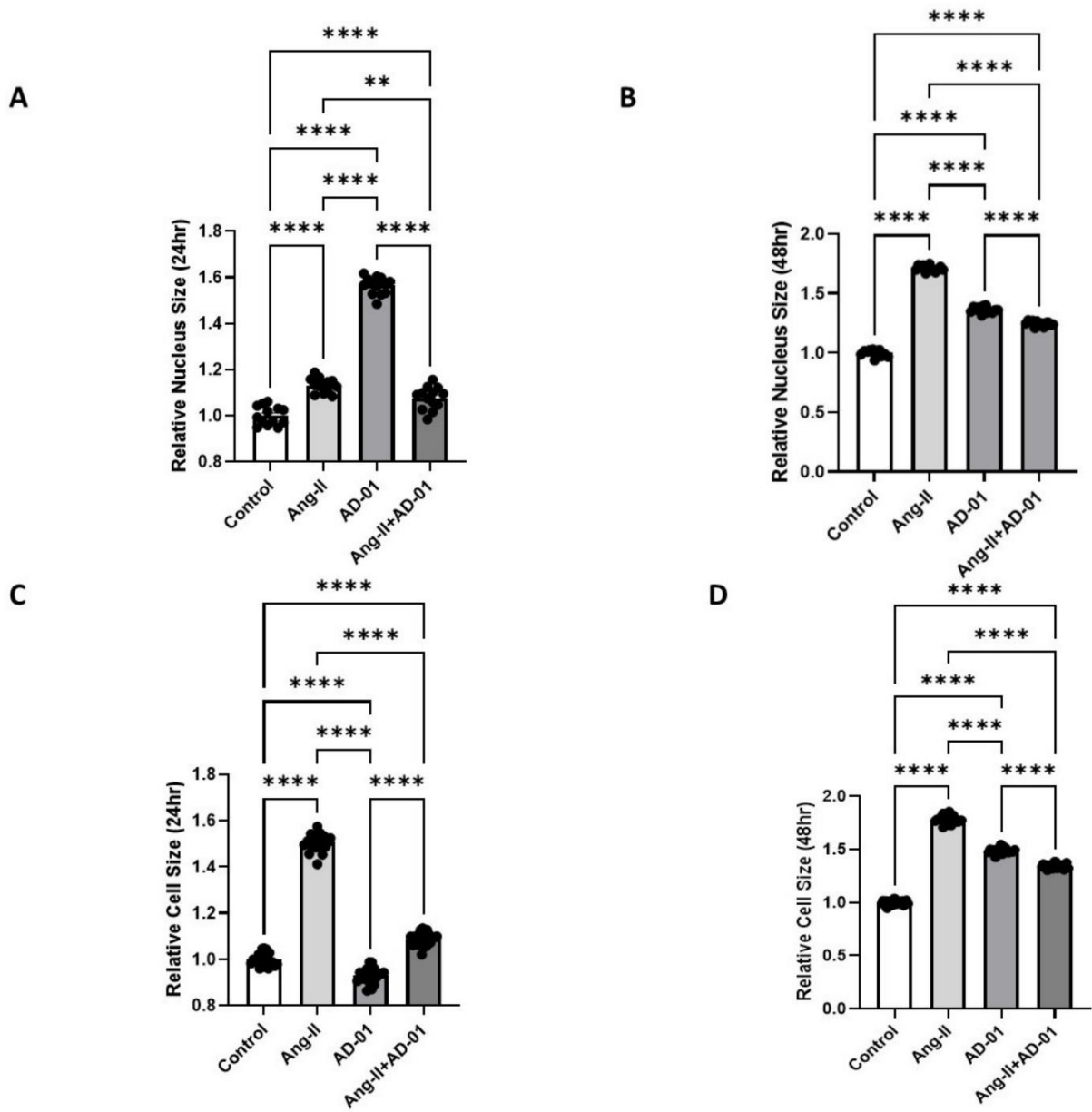


Figure 4.6 H9C2 cardiomyocyte cell size measurements following treatment with (i) Ang-II (100 nM), (ii) AD-01 (100 nM) and (iii) Ang-II (100 nM) + AD-01 (100 nM). (A) Relative nucleus size 24 h after treatments. (B) Relative nucleus size 48 h after treatments. (C) Relative cell size 24 h after treatments. (D) Relative cell size 48 h after treatments. Results expressed as Mean \pm SEM (n = 6); One-way ANOVA with Tukey's post-hoc; ** p < 0.01, ** p < 0.0001 against control; Ang-II—angiotensin II; AD-01—FKBPL-based therapeutic peptide.**

4.13.2 AD-01 Abrogates Ang-II-Induced Increases in FKBPL Protein Expression

Next, we determined FKBPL, BNP and ANP mRNA expression following 24 h treatment with Ang-II and/or AD-01. Apart from with ANP following Ang-II exposure, no significant change was obtained in the mRNA expression of any of the three genes (Figure 4.7A–C). Following 48 h exposure of H9C2 cells to Ang-II, AD-01 or Ang-II + AD-01, the only statistically significant change was observed in FKBPL mRNA expression after AD-01 treatment ($p < 0.05$), and although BNP and ANP mRNA expression showed a trend towards an increase, this was not statistically significant at 48 h (Figure 4.7D–F). The increase in all three genes (FKBPL, BNP and ANP) was the largest following 48 h treatment with AD-01, compared to Ang-II or Ang-II plus AD-01. AD-01 in the presence of Ang-II showed a much lower induction in gene expression than AD-01 alone although this was not statistically significant (Figure 4.7D–F).

Interestingly, at the protein level, cardiomyoblasts exposed to Ang-II for 48 h showed a significant increase in FKBPL expression compared to the control (Figure 4.8, $p < 0.05$), and although not significant, a trend towards increased FKBPL protein expressed was observed following AD-01 treatment ($p = 0.07$). In combination with Ang-II, AD-01 was able to abrogate Ang-II-induced FKBPL overexpression (Figure 4.8, $p < 0.05$).

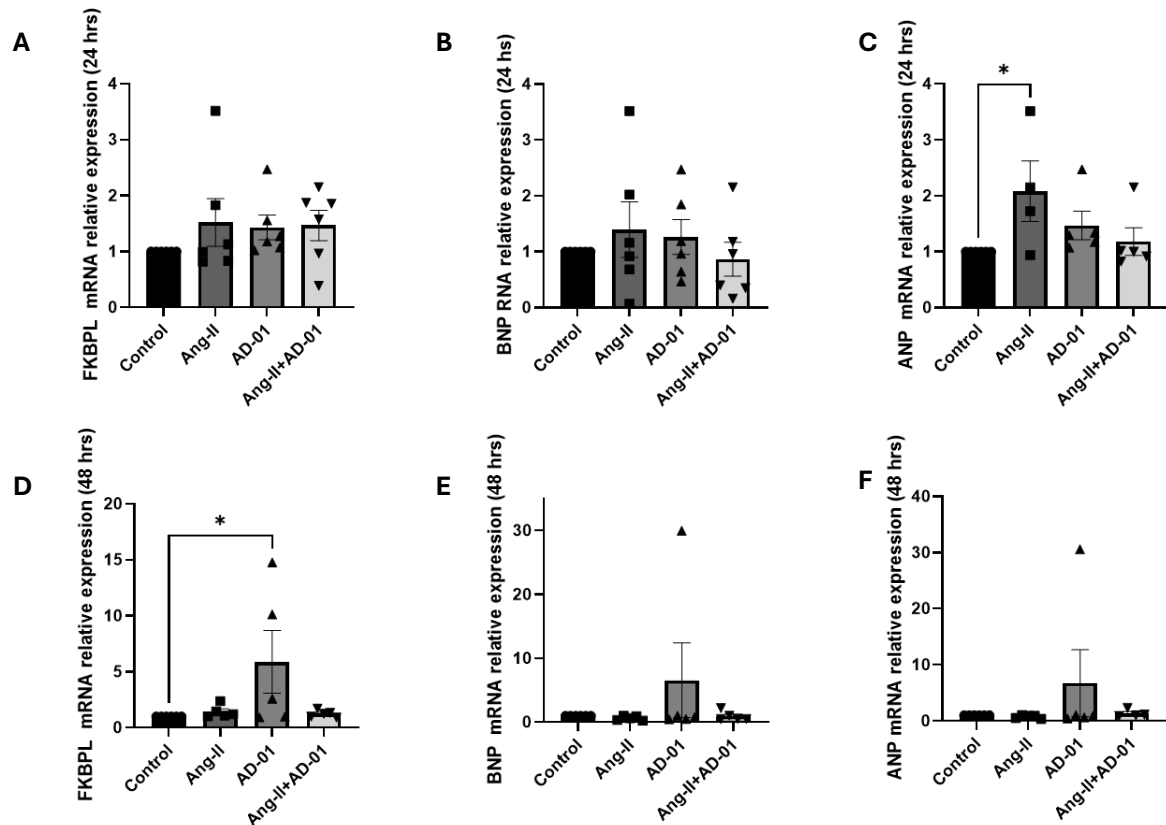


Figure 4.7 H9C2 cardiomyocyte mRNA expression of FKBPL, BNP and ANP following Ang-II and/or AD-01 treatment. H9C2 cells were exposed to treatment groups (i) Ang-II (100 nM), (ii) AD-01 (100 nM) and (iii) Ang-II (100 nM) + AD-01 (100 nM) for 24 or 48 h before RNA lysates were collected and qPCR performed. **(A)** FKBPL mRNA expression at 24 h; **(B)** BNP mRNA expression at 24 h; **(C)** ANP mRNA expression at 24 h; **(D)** FKBPL mRNA expression at 48 h; **(E)** BNP mRNA expression at 48 h; **(F)** ANP mRNA expression at 48 h. Results expressed as Mean \pm SEM ($n \geq 4$), One-way ANOVA with Tukey's post-hoc. * $p < 0.05$. Ang-II—angiotensin II; AD-01—FKBPL-based therapeutic peptide.

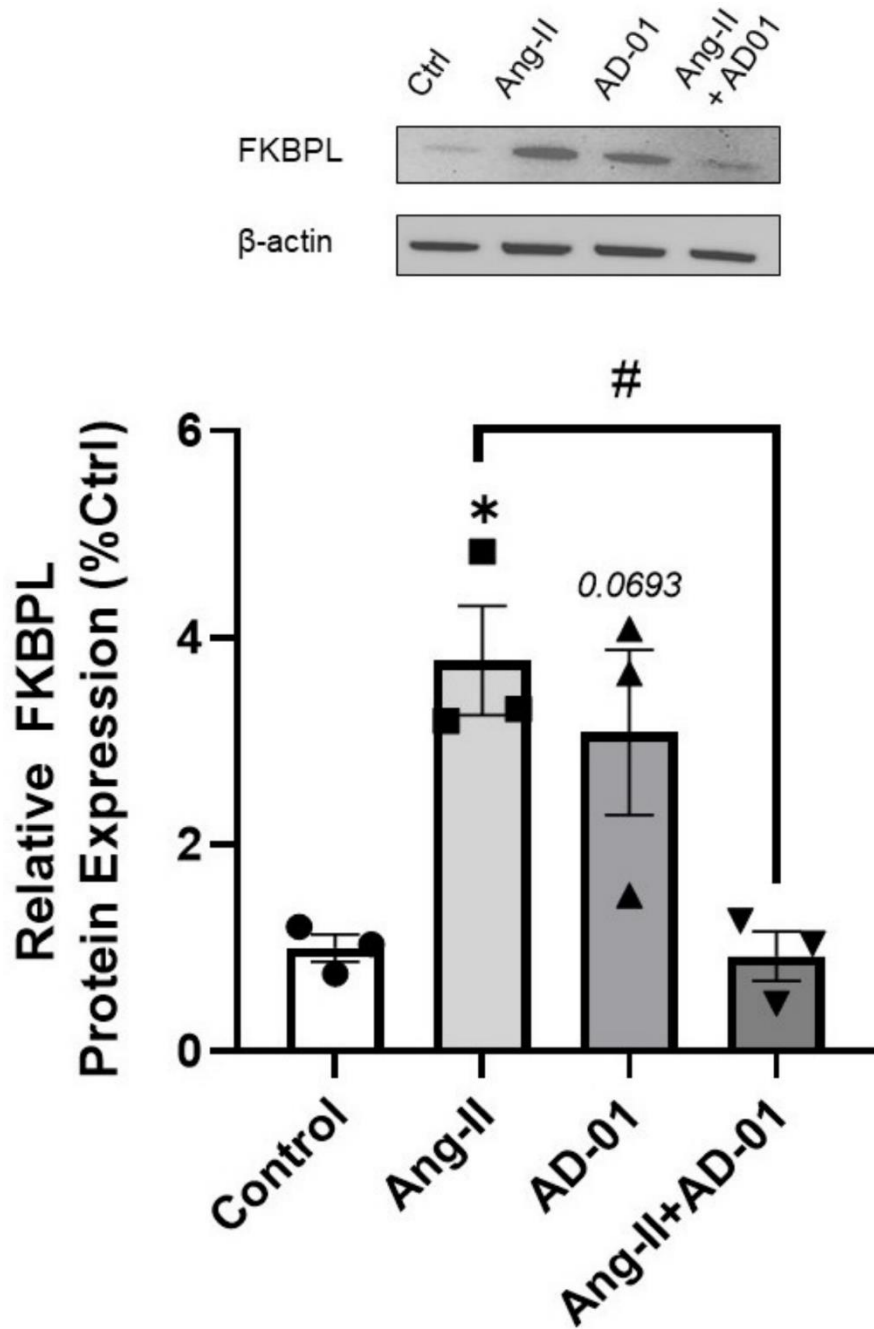


Figure 4.8 FKBPL protein expression in H9C2 cardiomyocytes following Ang-II and/or AD-01 treatment. H9C2 cells were exposed to treatment groups (i) Ang-II (100 nM), (ii) AD-01 (100 nM) and (iii) Ang-II (100 nM) + AD-01(100 nM) for 48 h. Relative FKBPL expression was measured. Results expressed as Mean \pm SEM ($n = 3$); One-way ANOVA with Tukey's post-hoc; * $p < 0.05$ against control; # $p < 0.05$ against Ang-II group. Ang-II—angiotensin II; AD-01—FKBPL-based therapeutic peptide.

4.13.3 FKBPL Plasma Concentration Is Increased in Patients with HFpEF but Does Not Differ between Subgroups

The FKBPL plasma concentration was increased when all the HFpEF subgroups were combined together ($1.645 \text{ ng/mL} \pm 0.75 \text{ SD}$) and compared to the controls ($1.26 \text{ ng/mL} \pm 0.3 \text{ SD}$); Figure 4.9A, $p < 0.01$. However, when different HFpEF forms were separated into subgroups (acute, chronic and HCM), FKBPL plasma concentrations were only significantly increased in the acute HFpEF subgroup compared to the control (Figure 4.9B, $p < 0.05$), although there was a trend of increased FKBPL concentrations in HCM compared to controls ($p = 0.07$).

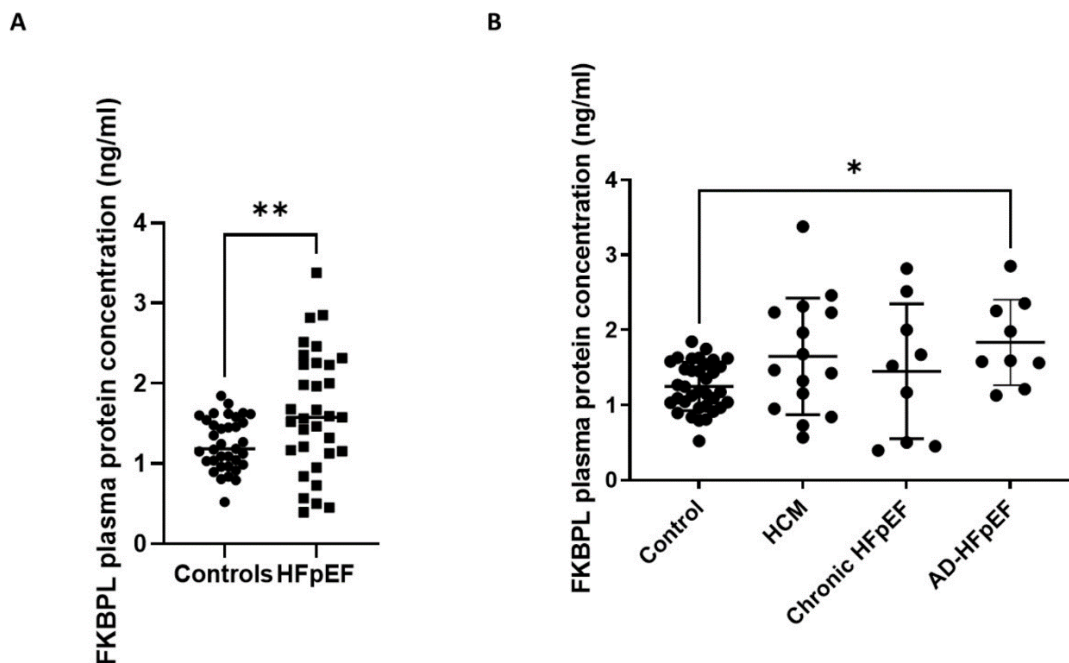


Figure 4.9 FKBPL plasma protein concentrations in patients with HFpEF. Patients were divided into subgroups based on HFpEF symptoms: HCM ($n = 15$), chronic HFpEF ($n = 9$) and acute decompensated HFpEF ($n = 9$). **(A)** FKBPL plasma concentration of combined HFpEF subgroups compared to controls ($n = 40$). **(B)** FKBPL plasma concentration within HFpEF subgroups, compared to controls. Results expressed as Mean \pm SD; One-way ANOVA with Tukey's post-hoc; * $p < 0.05$, ** $p < 0.005$. HCM—hypertrophic cardiomyopathy; HFpEF—chronic heart failure with preserved ejection fraction; AD-HFpEF—acute decompensated HFpEF.

When FKBPL plasma concentrations were compared between different HFpEF forms, no significant differences were observed between HCM, acute and chronic HFpEF (Figure 4.10A). Interestingly, a well-established biomarker, NT-proBNP, and an emerging biomarker, Gal-3, also did not show significant differences between the three forms of HFpEF. Nevertheless, NT-proBNP showed a trend towards an increase in acute HFpEF compared to HCM ($p = 0.08$) or chronic HFpEF ($p = 0.1$).

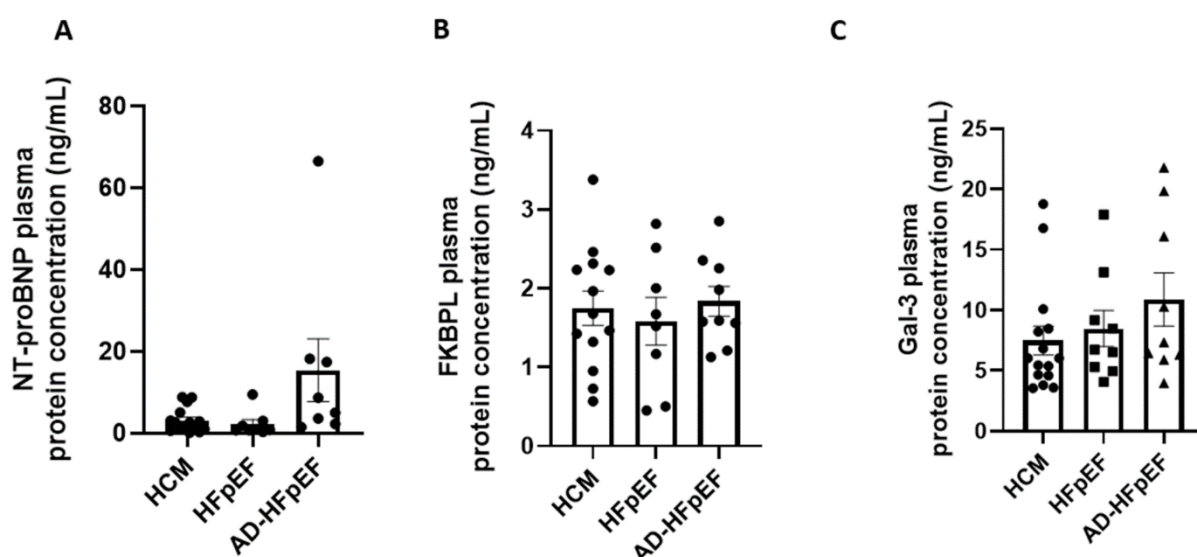


Figure 4.10 Biomarker plasma protein concentrations in subgroups of HFpEF. Patients were divided into subgroups based on HFpEF symptoms, HCM ($n = 15$), chronic HFpEF ($n = 9$) or acute decompensated HFpEF ($n = 9$). **(A)** NT-proBNP plasma concentration of HFpEF subgroups measured by ELISA. **(B)** FKBPL plasma concentration of HFpEF subgroups measured by ELISA. **(C)** Gal-3 plasma concentration of HFpEF subgroups measured by ELISA. Results expressed as Mean \pm SEM, One-way ANOVA with Tukey's post-hoc. HCM—hypertrophic cardiomyopathy; HFpEF—chronic heart failure with preserved ejection fraction; AD-HFpEF—acute decompensated HFpEF.

4.13.4 FKBPL Is Positively Correlated with IVST, Indicative of Microvascular Dysfunction

Echocardiographic measurements are clinically used alongside symptomatic assessments of HF patients and biomarkers, providing key information on cardiac structure and function [4]. In this study we measured limited echocardiographic parameters including end-diastolic diameter (EDD), end-systolic diameter (ESD), posterior wall thickness (PWT) and intraventricular septal thickness (IVST); this is because we have previously shown correlations between FKBPL and echocardiographic parameters [12], whereas the aim of the study was to investigate FKBPL mechanisms in HFpEF patients specifically, in light of its significant role in vasculature function. Correlation analyses (Table 4.3) showed that FKBPL was positively correlated with IVST ($r_s = 0.621$, $p < 0.000$) and negatively correlated with ESD and PWT ($r_s = -0.361$, $p = 0.042$; $r_s = -0.401$, $p = 0.021$). There was no significant correlation between FKBPL and NT-proBNP or Gal-3 (Table 4.4). NT-proBNP and Gal-3 showed a positive correlation between each other ($r_s = 0.464$, $p < 0.007$).

Table 4.3 Correlations between FKBPL and echocardiography parameters.

	FKBPL	EDD	ESD	IVST	PWT
Pearson Correlation	1	-0.281	-0.361 *	0.621 ***	-0.401 *
FKBPL Sig. (2-tailed)		0.119	0.042	0.000	0.021
N	33	32	32	33	33

Two-tailed test, * $p < 0.05$, *** $p < 0.001$.

Table 4.4 Pearson's correlations between FKBPL, NT-proBNP and Gal-3.

		FKBPL	NT-proBNP	Gal-3
FKBPL	Pearson Correlation	1	0.063	-0.042
	Sig. (2-tailed)		0.731	0.815
	N	33	32	33
NT-proBNP	Pearson Correlation	0.063	1	0.464 **
	Sig. (2-tailed)	0.731		0.007
	N	32	32	32
Gal-3	Pearson Correlation	-0.042	0.464 **	1
	Sig. (2-tailed)	0.815	0.007	
	N	33	32	33

Two-tailed test, ** $p < 0.01$.

4.14 Discussion

HF pathophysiology is complex and involves various mechanistic pathways as part of its development and progression. Changes in cardiomyocyte cell morphology and function play a key role in the progression of the key mechanisms and processes involved in HF pathogenesis [19]. The renin-angiotensin-aldosterone system (RAAS) is activated by hypovolemia and the sympathetic nervous system. The main product of the RAAS is Ang-II, which has compensatory systemic effects that, if they persist, can exacerbate HF. This is because, in HF, Ang-II is stimulated to maintain cardiac output through increased vasoconstriction, salt retention, contractility, and the activation of inflammatory mediators [1,20,21]. The neuroendocrine pathological mechanisms of HF are regulated by the sympathetic nervous system and are linked to the RAAS [21]. Ang-II has been implicated in adverse cardiac remodelling and leads to an increase in interstitial fibrosis, contributing to HF [1]. Adverse cardiac remodelling

through hypertrophy, besides physical alterations, modulates gene expression and the viability of cardiomyocytes, which may contribute to cardiac dysfunction and HF [19]. Interestingly, a recent report demonstrated that the presence of adverse cardiac remodelling in HFpEF patients is associated with worse outcomes compared to those without adverse remodelling [22].

Our findings in this study reveal an interesting mechanism involving Ang-II and FKBPL-based peptide therapeutic, AD-01, when examining their effects on cell and nucleus size. Ang-II or AD-01 treatment led to a significant increase in both cell and nucleus size at 24 and 48 h, with Ang-II and AD-01 displaying similar trends—except in terms of cell size following 24 h treatment. Interestingly, when these two treatments were combined, Ang-II and AD-01 exhibited a significant decrease in cell and nucleus size compared to individual treatments, akin to the size of the control group. Consistent with these findings, 48 h treatment with Ang-II or AD-01 increased the protein expression of FKBPL, which was again abolished when combining these two treatments together. FKBPL plays a critical role in developmental and pathological angiogenesis and vascular function, which has been demonstrated in previous studies in which a murine homozygous knockout of FKBPL was embryonically lethal, whereas heterozygous knockdown resulted in impaired vascular integrity [10,11,23]. Furthermore, FKBPL has been shown to operate via the STAT3 [13], CD44 [24] and nuclear factor kappa B (NF- κ B) [9] inflammatory pathways that commonly underly HF pathophysiology [25]. Thus, vascular dysfunction due to aberrant endothelial cell homeostasis, pro-inflammatory signalling and restricted angiogenesis potentially implicate FKBPL in the development of HF. Our findings suggest that AD-01 may exacerbate hypertrophy within cardiomyocytes—likely via FKBPL. However, there

exists a compensatory mechanism when Ang-II is present; AD-01 abrogates this effect via a negative feedback mechanism to reverse the hypertrophic effect. As an FKBPL mimetic, AD-01 has been shown previously and, in this study, to increase FKBPL mRNA and protein expression when used alone [24]; this mechanism is altered in the presence of Ang-II, whereby FKBPL expression is normalised. These findings present a complex and compensatory mechanism of AD-01 as a FKBPL mimetic, in producing an anti-hypertrophic effect in Ang-II-induced myopathy that needs to be further studied.

In evaluating the biomarker potential of FKBPL in HFpEF, NT-proBNP and Gal-3 plasma concentrations were also measured in this study. NT-proBNP has been well-established in the clinical diagnosis of HF [4], whereas Gal-3—although not clinically used—has been presented in recent literature as a promising biomarker candidate for the diagnosis of HFpEF [7,26]. Gal-3's diverse functionality in inflammation contributes to myocardial remodelling and fibrosis [8], where the inhibition of Gal-3 has been reported to ameliorate these conditions [27]. Previous reports have shown that FKBPL plasma concentrations are increased in the presence of CVD [12] and in the absence of diabetes mellitus, compared to healthy controls. FKBPL is also positively correlated with parameters of diastolic dysfunction including left atrium volume and size, IVST at the end of diastole and deceleration time [12]. In the same study, FKBPL was positively correlated with a clinically used marker of HFpEF, BNP, and it was one of the determinants of CVD in conjunction with age, gender, total-cholesterol, and systolic blood pressure (SBP) [12]. Here, we showed that the FKBPL plasma concentration was significantly increased between the control group and patients with HFpEF, implicating FKBPL's possible role as a biomarker for HFpEF. In further evaluating the

biomarker potential of FKBPL in HFpEF, FKBPL plasma concentrations were found to be significantly increased when comparing the control group to acute HFpEF and only showed an increasing trend in HCM—suggesting a mechanistic role for FKBPL in the pathophysiology and progression of HFpEF. Previous studies have shown that in a murine model of HFpEF, deletion of STAT3 in cardiomyocytes resulted in the manifestation of the clinical characteristics of HFpEF [28]. Given that FKBPL is increased in HFpEF patients, and that it inhibits the inflammatory STAT3 pathway [13], this mechanism may contribute towards HFpEF pathophysiology.

When comparing different forms of HFpEF, our study found no significant differences in the plasma concentrations of FKBPL, NT-proBNP or Gal-3. Therefore, none of the examined biomarkers have shown to be able to stratify between specific forms of HFpEF in this study. FKBPL has previously been reported to be positively correlated with BNP [11]; however, we found no correlation with either NT-proBNP or Gal-3, whereas the latter two were positively correlated with each other. This is likely due to the diverse role of FKBPL in HFpEF, which is independent of NT-proBNP and Gal-3, and it might contribute to different pathogenic processes and mechanisms involved in microvascular dysfunction, inflammation and restricted angiogenesis. This could also be specific to our patient samples.

In patients with HCM, the presence of microvascular dysfunction has been recognized as a strong predictor of clinical deterioration and mortality [29,30]. In fact, myocardial wall thickness is the strongest predictor of reduced global hyperaemic myocardial blood flow in HCM [31]. Subsequently, there is a higher probability of the development of myocardial fibrosis in segments with reduced hyperaemic myocardial blood flow

[32]. Our study demonstrated a clinically relevant positive correlation between FKBPL and IVST, likely implicating FKBPL in the microvascular dysfunction of the LV hypertrophy, which is related to the pathogenesis of HFpEF [33,34]. This was also confirmed in the in vitro part of the study where the FKBPL peptide mimetic, AD-01, induced cardiomyoblast hypertrophy whilst also increasing FKBPL expression.

The limitations of this study include the cross-sectional nature of the study in terms of the recruited controls and modest patient numbers. Nevertheless, we included well-known biomarkers of HFpEF—NT-proBNP and Gal-3—as a comparison and supported the findings with in vitro models of HFpEF that aligned with the clinical sample findings, showing that FKBPL is positively correlated with HFpEF and, potentially, its progression.

4.15 Conclusion

In this study, we demonstrated for the first time that FKBPL may be implicated in HFpEF. An FKBPL-based peptide therapeutic, AD-01, was able to abrogate Ang-II-induced FKBPL upregulation and cardiomyoblasts hypertrophy. Aligned to this, FKBPL human plasma levels were increased in HFpEF compared to controls; however, FKBPL was unable to distinguish between different forms of HFpEF, similar to NT-proBNP and Gal-3. Finally FKBPL was positively correlated with an echocardiography parameter reflective of cardiac microvascular dysfunction and hypertrophy, further strengthening the evidence for its role in the pathogenesis of HFpEF.

4.16 Declarations

Author Contributions: M.C. performed the experiments, data analysis and interpretation and wrote the manuscript. H.C. performed and analysed experiments. D.J. analysed and interpreted data. M.T., V.N.N., M.P. and R.M.V., conceived the study; recruited the patients; performed echocardiography; retrieved the samples; recorded the clinical characteristics; stratified the patient cohorts; and edited the manuscript. B.R. supervised H.C. and contributed to the experimental design, data acquisition, analysis and interpretation. C.J.W., T.R., K.M. and M.L. contributed to the conception, experimental design or data interpretation. L.M. and K.C.M. supervised M.C. and K.C.M. contributed to data analysis and interpretation. L.M. conceived the study, the study design, performed experiments, data analysis and interpretation; and edited the manuscript. All authors have read and agreed to the published version of the manuscript.

Funding: The current study was funded by the Research and Development Fund, Faculty of Science, University of Technology Sydney (Lana McClements). Michael Chhor was supported by an Australian Government Research Training Program (RTP) Stipend and RTP Fee-Offset Scholarship through the University of Technology Sydney.

Institutional Review Board Statement: The study was conducted in accordance with the Declaration of Helsinki and approved by the Human Ethics Committee of the University of Technology Sydney (ETH19-3461) on 13 August 2019. The use of the control samples and data was obtained from the STOP-HF study and was approved by the research ethics committee of St. Vincent's University Hospital, Dublin, which

conformed to the principles of the Helsinki Declaration [35–37]. Informed Consent Statement: All participants provided written informed consent. The study was approved by all participating institutional human ethics boards.

Data Availability Statement: The data presented in this study are available on request from the corresponding author.

Acknowledgments: We thank the participants for taking part in this study and any healthcare staff for helping with the recruitment.

Conflicts of Interest: The authors declare no conflict of interest.

4.17 References

1. Malik, A.; Brito, D.; Vaqar, S.; Chhabra, L. *Congestive Heart Failure*; StatPearls: Tampa, FL, USA, 2022.
2. Baman, J.R.; Ahmad, F.S. Heart Failure. *JAMA* **2020**, *324*, 1015
3. Australian Institute of Health and Welfare. *Heart, Stroke and Vascular Disease: Australian Facts*; AIHW, Australian Government: Darlinghurst, Australia. Available online: <https://www.aihw.gov.au/reports/heart-stroke-vascular-diseases/hsvd-facts/contents/about> (accessed on 13 February 2023).
4. McDonagh, T.A.; Metra, M.; Adamo, M.; Gardner, R.S.; Baumhach, A.; Böhm, M.; Burri, H.; Butler, J.; Čelutkienė, J.; Chioncel, O.; et al. 2021 ESC Guidelines for the diagnosis and treatment of acute and chronic heart failure. Developed by the Task Force for the diagnosis and treatment of acute and chronic heart failure of the European Society of Cardiology (ESC) With the special contribution of the Heart Failure Association (HFA) of the ESC. *Eur. Heart J.* **2021**, *42*, 4901.
5. Inamdar, A.A.; Inamdar, A.C. Heart Failure: Diagnosis, Management and Utilization. *J. Clin. Med.* **2016**, *5*, 62.
6. Lewis, R.A.; Durrington, C.; Condliffe, R.; Kiely, D.G. BNP/NT-proBNP in pulmonary arterial hypertension: Time for point-of-care testing? *Eur. Respir. Rev.* **2020**, *29*, 200009.
7. Chen, H.; Chhor, M.; Rayner, B.S.; McGrath, K.; McClements, L. Evaluation of the diagnostic accuracy of current biomarkers in heart failure with preserved ejection fraction: A systematic review and meta-analysis. *Arch. Cardiovasc. Dis.* **2021**, *114*, 793–804.
8. Andrejic, O.M.; Vucic, R.M.; Pavlovic, M.; McClements, L.; Stokanovic, D.; Jevtovic–Stoimenov, T.; Nikolic, V.N. Association between Galectin-3 levels within central and peripheral venous blood, and adverse left ventricular remodelling after first acute myocardial infarction. *Sci. Rep.* **2019**, *9*, 13145.

9. Annett, S.; Spence, S.; Garcarena, C.; Campbell, C.; Dennehy, M.; Drakeford, C.; Lai, J.; Dowling, J.; Moore, G.; Yakkundi, A.; et al. The immunophilin protein FKBPL and its peptide derivatives are novel regulators of vascular integrity and inflammation via NF- κ B signaling. *bioRxiv* **2021**.
10. Yakkundi, A.; Bennett, R.; Hernández-Negrete, I.; Delalande, J.-M.; Hanna, M.; Lyubomska, O.; Arthur, K.; Short, A.; McKeen, H.; Nelson, L.; et al. FKBPL Is a Critical Antiangiogenic Regulator of Developmental and Pathological Angiogenesis. *Arter. Thromb. Vasc. Biol.* **2015**, *35*, 845–854.
11. Alqudah, A.; Eastwood, K.-A.; Jerotic, D.; Todd, N.; Hoch, D.; McNally, R.; Obradovic, D.; Dugalic, S.; Hunter, A.J.; Holmes, V.A.; et al. FKBPL and SIRT-1 Are Downregulated by Diabetes in Pregnancy Impacting on Angiogenesis and Endothelial Function. *Front. Endocrinol.* **2021**, *12*, 459.
12. Januszewski, A.S.; Watson, C.J.; O'Neill, V.; McDonald, K.; Ledwidge, M.; Robson, T.; Jenkins, A.J.; Keech, A.C.; McClements, L. FKBPL is associated with metabolic parameters and is a novel determinant of cardiovascular disease. *Sci. Rep.* **2020**, *10*, 1–7.
13. Annett, S.; Moore, G.; Short, A.; Marshall, A.; McCrudden, C.; Yakkundi, A.; Das, S.; McCluggage, W.G.; Nelson, L.; Harley, I.; et al. FKBPL-based peptide, ALM201, targets angiogenesis and cancer stem cells in ovarian cancer. *Br. J. Cancer* **2019**, *122*, 361–371.
14. Chen, H.; Tesic, M.; Nikolic, V.N.; Pavlovic, M.; Vucic, R.M.; Spasic, A.; Jovanovic, H.; Jovanovic, I.; Town, S.E.L.; Padula, M.P.; et al. Systemic Biomarkers and Unique Pathways in Different Phenotypes of Heart Failure with Preserved Ejection Fraction. *Biomolecules* **2022**, *12*, 1419.
15. Laemmli, U.K. Cleavage of Structural Proteins during the Assembly of the Head of Bacteriophage T4. *Nature* **1970**, *227*, 680–685.
16. Ponikowski, P.; Voors, A.; Anker, S.; Bueno, H.; Cleland, J.; Coats, A.; Falk, V.; González-Juanatey, J.R.; Harjola, V.-P.; Jankowska, E.; et al. 2016 ESC Guidelines for the diagnosis and treatment of acute and chronic heart failure: The Task Force for the diagnosis and treatment of acute and chronic heart failure of the European Society of Cardiology (ESC) Developed with the special contribution of the Heart Failure Association (HFA) of the ESC. *Eur. Heart J.* **2016**, *37*, 2129–2200.
17. Van Heerebeek, L.; Hamdani, N.; Handoko, M.L.; Falcao-Pires, I.; Musters, R.J.; Kupreishvili, K.; Ijsselmuiden, A.J.; Schalkwijk, C.G.; Bronzwaer, J.G.; Diamant, M.; et al. Diastolic stiffness of the failing diabetic heart: Importance of fibrosis, advanced glycation end products, and myocyte resting tension. *Circulation* **2008**, *117*, 43–51.
18. Watkins, S.J.; Borthwick, G.M.; Arthur, H.M. The H9C2 cell line and primary neonatal cardiomyocyte cells show similar hypertrophic responses in vitro. *Vitr. Cell. Dev. Biol. Anim.* **2011**, *47*, 125–131.
19. Peter, A.K.; Bjerke, M.A.; Leinwand, L.A. Biology of the cardiac myocyte in heart disease. *Mol. Biol. Cell* **2016**, *27*, 2149–2160.
20. Nakano, S.; Muramatsu, T.; Nishimura, S.; Senbonmatsu, T. Cardiomyocyte and Heart Failure. In *Current Basic and Pathological Approaches to the Function of Muscle Cells and Tissues—From Molecules to Humans*; IntechOpen: London, UK, 2012.
21. Orsborne, C.; Chaggar, P.S.; Shaw, S.M.; Williams, S.G. The renin-angiotensin-aldosterone system in heart failure for the non-specialist: The past, the present and the future. *Postgrad. Med. J.* **2016**, *93*, 29–37.

22. Xu, L.; Pagano, J.; Chow, K.; Oudit, G.Y.; Haykowsky, M.J.; Mikami, Y.; Howarth, A.G.; White, J.A.; Howlett, J.G.; Dyck, J.R.; et al. Cardiac remodelling predicts outcome in patients with chronic heart failure. *ESC Heart Fail.* **2021**, *8*, 5352–5362.
23. Todd, N.; McNally, R.; Qudhah, A.; Jerotic, D.; Suvakov, S.; Obradovic, D.; Hoch, D.; Hombrebueno, J.R.; Campos, G.L.; Watson, C.J.; et al. Role of A Novel Angiogenesis FKBPL-CD44 Pathway in Preeclampsia Risk Stratification and Mesenchymal Stem Cell Treatment. *J. Clin. Endocrinol. Metab.* **2020**, *106*, 26–41.
24. Yakkundi, A.; McCallum, L.; O’Kane, A.; Dyer, H.; Worthington, J.; McKeen, H.D.; McClements, L.; Elliott, C.; McCarthy, H.; Hirst, D.G.; et al. The Anti-Migratory Effects of FKBPL and Its Peptide Derivative, AD-01: Regulation of CD44 and the Cytoskeletal Pathway. *PLoS ONE* **2013**, *8*, e55075.
25. Zeng, H.; Chen, J.-X. Microvascular Rarefaction and Heart Failure With Preserved Ejection Fraction. *Front. Cardiovasc. Med.* **2019**, *6*, 15.
26. De Boer, R.A.; Edelmann, F.; Cohen-Solal, A.; Mamas, M.A.; Maisel, A.; Pieske, B. Galectin-3 in heart failure with preserved ejection fraction. *Eur. J. Heart Fail.* **2013**, *15*, 1095–1101.
27. Zhong, X.; Qian, X.; Chen, G.; Song, X. The role of galectin-3 in heart failure and cardiovascular disease. *Clin. Exp. Pharmacol. Physiol.* **2018**, *46*, 197–203.
28. Zhao, W.; Chen, Y.; Yang, W.; Han, Y.; Wang, Z.; Huang, F.; Qiu, Z.; Yang, K.; Jin, W. Effects of Cardiomyocyte-Specific Deletion of STAT3—A Murine Model of Heart Failure With Preserved Ejection Fraction. *Front. Cardiovasc. Med.* **2020**, *7*, 613123.
29. Cecchi, F.; Olivotto, I.; Gistri, R.; Lorenzoni, R.; Chiriatti, G.; Camici, P.G. Coronary Microvascular Dysfunction and Prognosis in Hypertrophic Cardiomyopathy. *N. Engl. J. Med.* **2003**, *349*, 1027–1035.
30. Tesic, M.; Beleslin, B.; Giga, V.; Jovanovic, I.; Marinkovic, J.; Trifunovic, D.; Petrovic, O.; Dobric, M.; Aleksandric, S.; Juricic, S.; et al. Prognostic Value of Transthoracic Doppler Echocardiography Coronary Flow Velocity Reserve in Patients With Asymmetric Hypertrophic Cardiomyopathy. *J. Am. Heart Assoc.* **2021**, *10*, e021936.
31. Bravo, P.E.; Pinheiro, A.; Higuchi, T.; Rischpler, C.; Merrill, J.; Santaularia-Tomas, M.; Abraham, M.R.; Wahl, R.L.; Abraham, T.P.; Bengel, F.M. PET/CT Assessment of Symptomatic Individuals with Obstructive and Nonobstructive Hypertrophic Cardiomyopathy. *J. Nucl. Med.* **2012**, *53*, 407–414.
32. Ismail, T.F.; Hsu, L.-Y.; Greve, A.M.; Gonçalves, C.; Jabbour, A.; Gulati, A.; Hewins, B.; Mistry, N.; Wage, R.; Roughton, M.; et al. Coronary microvascular ischemia in hypertrophic cardiomyopathy—A pixel-wise quantitative cardiovascular magnetic resonance perfusion study. *J. Cardiovasc. Magn. Reson.* **2014**, *16*, 49.
33. Yang, Y.; Li, Z.; Guo, X.; Zhou, Y.; Chang, Y.; Yang, H.; Yu, S.; Ouyang, N.; Chen, S.; Sun, G.; et al. Interventricular Septum Thickness for the Prediction of Coronary Heart Disease and Myocardial Infarction in Hypertension Population: A Prospective Study. *J. Clin. Med.* **2022**, *11*, 7152.
34. Kansal, S.; Roitman, D.; Sheffield, L.T. Interventricular septal thickness and left ventricular hypertrophy. An echocardiographic study. *Circulation* **1979**, *60*, 1058–1065.
35. Ledwidge, M.; Gallagher, J.; Conlon, C.; Tallon, E.; O’Connell, E.; Dawkins, I.; Watson, C.; O’Hanlon, R.; Bermingham, M.; Patle, A.; et al. Natriuretic peptide-

based screening and collaborative care for heart failure: The STOP-HF randomized trial. *JAMA* **2013**, *310*, 66–74.

36. Tonry, C.; McDonald, K.; Ledwidge, M.; Hernandez, B.; Glezeva, N.; Rooney, C.; Morrissey, B.; Pennington, S.R.; Baugh, J.A.; Watson, C.J. Multiplexed measurement of candidate blood protein biomarkers of heart failure. *ESC Heart Fail.* **2021**, *8*, 2248–2258.
37. Watson, C.J.; Gallagher, J.; Wilkinson, M.; Russell-Hallinan, A.; Tea, I.; James, S.; O'Reilly, J.; O'Connell, E.; Zhou, S.; Ledwidge, M.; et al. Biomarker profiling for risk of future heart failure (HFpEF) development. *J. Transl. Med.* **2021**, *19*, 61.

4.18 Supplementary Info

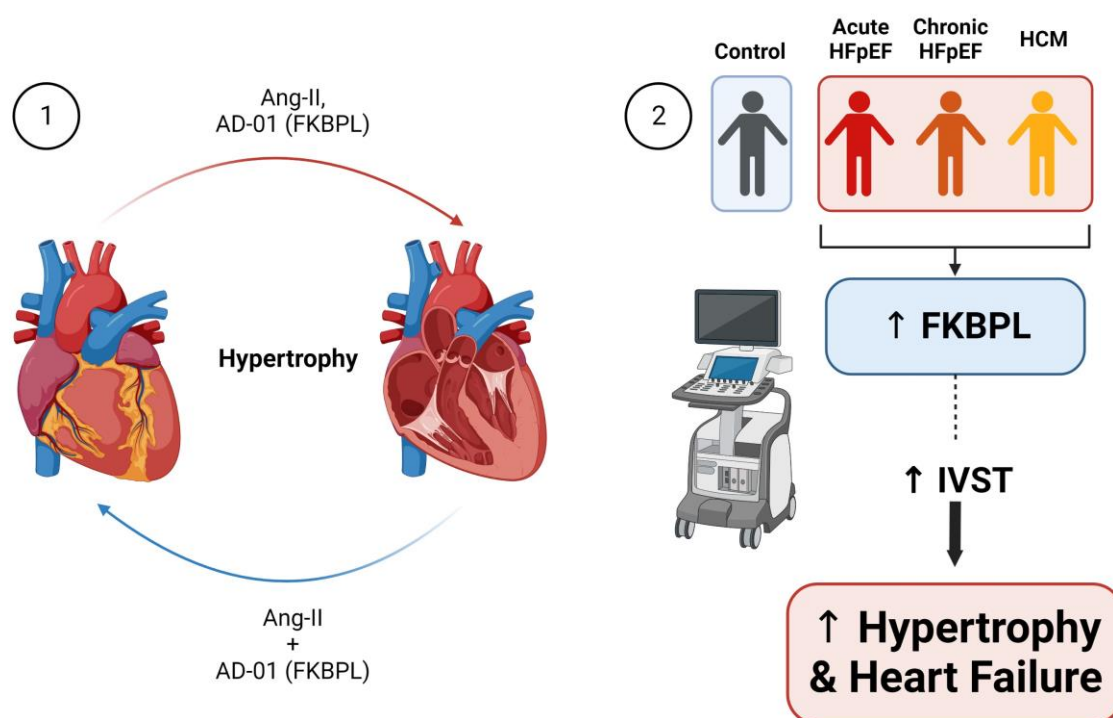


Figure S4.3 Graphical Abstract. (1) FKBPL mimetic AD-01 and hypertensive stimulus Ang-II similarly induce the hypertrophy of cardiomyoblasts. This effect is abrogated when both treatments are combined, possibly through an FKBPL mediated mechanism. (2) Patients with HFpEF exhibited higher levels of plasma FKBPL overall, though FKBPL was unable to stratify between the different types of HFpEF compared to other biomarkers. Increased plasma FKBPL was correlated with increased IVST, reflective of microvascular dysfunction and hypertrophy, likely resulting in heart failure.

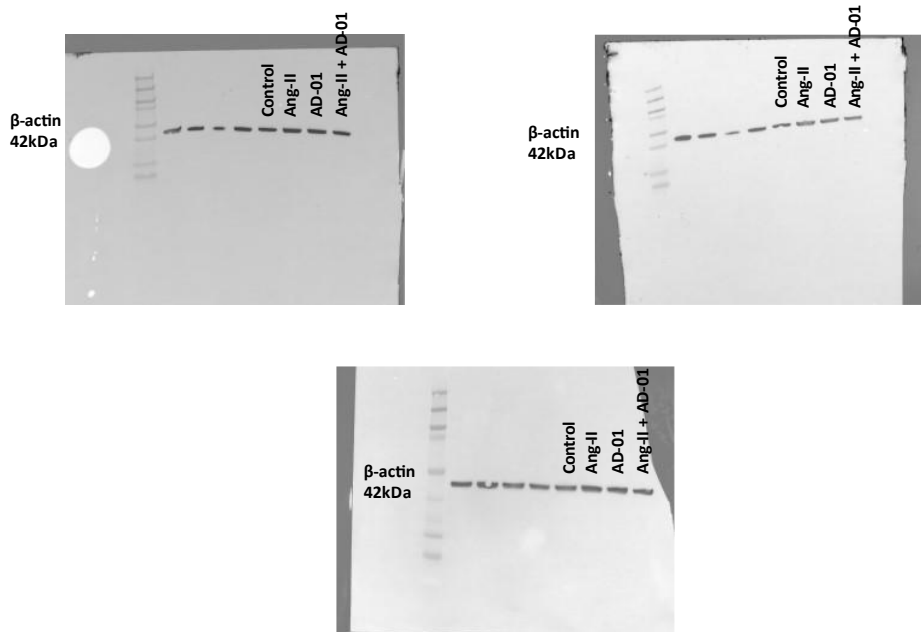


Figure S4.4 β -actin protein expression in H9C2 cardiomyocytes following Ang-II and/or AD-01 treatment. H9C2 cells were exposed to treatment groups (i) Ang-II (100 nM), (ii) AD-01 (100 nM) and (iii) Ang-II (100 nM) + AD-01(100 nM) for 48h. Full size Western blot (Figure 4.8).

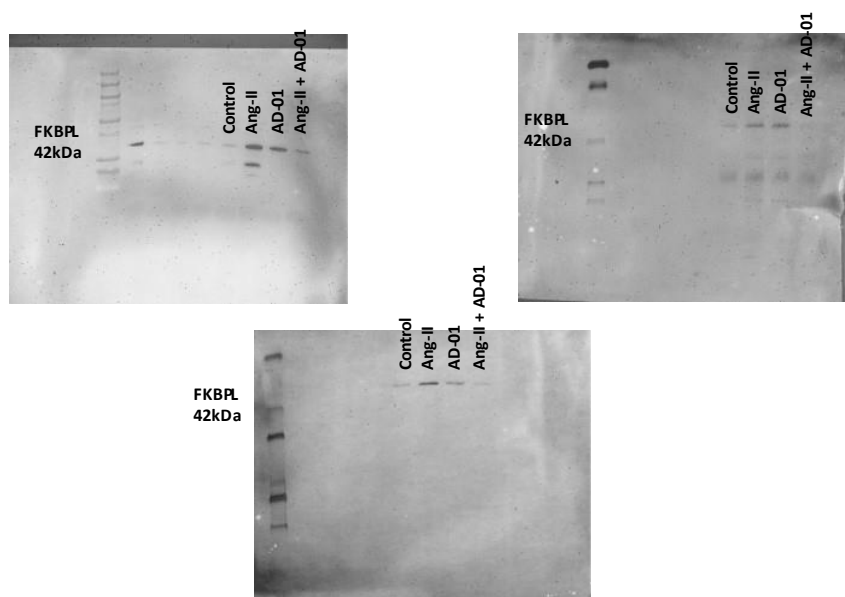


Figure S4.5 FKBPL protein expression in H9C2 cardiomyocytes following Ang-II and/or AD-01 treatment. H9C2 cells were exposed to treatment groups (i) Ang-II (100 nM), (ii) AD-01 (100 nM) and (iii) Ang-II (100 nM) + AD-01(100 nM) for 48h. Full size Western blot (Figure 4.8).

Chapter 5

Evaluating the current biomarkers reflective of early cardiac remodelling in diabetes mellitus

Cardiac remodelling is a predominant pathophysiological precursor to cardiac fibrosis, a key process implicated in cardiovascular diseases. As a multifactorial condition, it remains difficult to identify the early symptoms and signs associated with cardiac remodelling, hence requiring the need for biomarkers used in its early detection. Diabetes mellitus (DM) is a similarly predominant condition related to cardiovascular disease that heterogeneously affects various organs within the body, including the heart. In DM, impaired metabolic homeostasis drives neurohormonal, inflammatory, and fibrinogenic responses that contribute to cardiac remodelling and accelerate the progression of HF. Patients with DM carry two-three times higher risk of morbidity from cardiovascular diseases than patients without DM. Comparably lower amounts of research exist for this population of patients, hence, in this study we systematically evaluated the current biomarkers that have been used in research spanning patients with both signs of cardiac remodelling and DM. Whilst it has been shown before that FKBPL is increased in DM, in the presence of CVD there is a compensatory mechanism that needs to be explored further but it is beyond the scope of this PhD project.

Diagnostic and prognostic biomarkers reflective of cardiac remodelling in diabetes mellitus: scoping review

Michael Chhor¹, William Law¹, Milan Pavlovic², Dunja Aksentijevic³, Kristine McGrath¹,
Lana McClements^{1*}

¹ School of Life Sciences, Faculty of Science, University of Technology Sydney, New South Wales, Sydney, Australia

² Department of Internal Medicine - Cardiology, Faculty of Medicine, University of Nis, Nis, Serbia

³ Centre for Biochemical Pharmacology, William Harvey Research Institute, Barts and the London School of Medicine and Dentistry, Queen Mary University of London, London, UK

*Corresponding author

Lana

McClements

E-mail: lane.mcclements@uts.edu.au

Keywords: biomarker, cardiac fibrosis, cardiovascular disease, heart failure, metabolomics, scoping review

5.1 Abstract

Aims: The aim of this scoping review is to evaluate the current biomarkers used in the assessment of adverse cardiac remodelling in people with diabetes mellitus (DM) and in the diagnosis and prognosis of subsequent cardiovascular disease. We aim to discuss the biomarkers' pathophysiological roles as a reflection of the cardiac remodelling mechanisms in the presence of DM.

Methods: We performed the literature search to include studies from 2003 to 2021 using the following databases: MEDLINE, Scopus, Web of Science, PubMed, and Cochrane library. Articles that met our inclusion criteria were screened and appraised before being included in this review. The PRISMA guidelines for Scoping Reviews were followed.

Results: Our literature search identified a total of 43 eligible articles, which were included in this scoping review. We identified 15 different biomarkers, each described by at least two studies, that were used to determine signs of cardiac remodelling in cardiovascular disease (CVD) and people with DM. NT-proBNP was identified as the most frequently employed biomarker in this context; however, we also identified emerging biomarkers including hs-CRP, hs-cTnT, and Galectin-3.

Conclusion: There is a complex relationship between DM and cardiovascular health, where more research is needed. Current biomarkers reflective of adverse cardiac remodelling in DM are often used to diagnose other CVDs, such as NT-proBNP for heart failure. Hence there is a need for identification of specific biomarkers that can detect early signs of cardiac remodelling in the presence of DM. Further research into these biomarkers and mechanisms can deepen our understanding of their role in DM-associated CVD and lead to better preventative therapies.

5.2 Introduction

Cardiovascular disease (CVD) is an umbrella term encompassing any disorder affiliated with the heart and blood vessels, such as coronary artery disease (CAD) and heart failure (HF).¹ CVD is currently the highest cause of mortality worldwide, representing 32% of all deaths globally.² For perspective, prevalent cases of CVD have reportedly doubled between 1990 and 2019 from 271 million to 523 million people. CVD resultant deaths have similarly followed this trend and increased from 12.1 million to 18.6 million people between 1990 and 2019.³ Consequently, it is fast becoming a serious financial and medical burden to the entire population.

Meanwhile, diabetes mellitus (DM) is also a pervasive and deleterious disease. Worldwide, DM affects 422 million people and accounts for 1.6 million deaths a year.⁴ There are two key pathological processes that cause the development of DM: inadequate insulin production by beta islet cells of pancreas, and insulin resistance (IR), which results from impaired insulin response in peripheral tissues. DM is a heterogenous disease with multiple organs involved in the aetiology: liver, skeletal muscles, pancreas, kidneys, brain, small intestine, and adipose tissue.⁵ Hyperglycaemia associated with DM consequently triggers a surfeit of macro- and microvascular complications.⁶

The risk of CVD morbidity in DM is approximately two-three times more likely compared to those without DM.⁷ The Framingham Heart Study concluded that type-2 diabetes mellitus (T2D) independently increases the HF risk up to two-fold in men and

five-fold in women compared to matched controls.^{8,9} Thus, accelerated HF is a common clinical manifestation of CVD in T2D.⁵ DM progression leads to specific changes to myocardial structure, function, and metabolism, collectively defined as diabetic cardiomyopathy (dbCM).^{5,10} Hyperglycaemia, insulin resistance as well as lipotoxicity drive numerous fibrogenic pathways, triggering generation of reactive oxygen species (ROS), enhancing neurohumoral responses, stimulating growth factor cascades (i.e., TGF- β /Smad3 and PDGFs), inducing pro-inflammatory cytokines and chemokines, generating advanced glycation end-products (AGEs), stimulating the AGE-receptor for AGE (RAGE) axis, and up-regulating fibrogenic extracellular matrix proteins.¹¹ Despite DM-triggered fibrogenic signalling sharing common characteristics in multiple tissues, diabetic myocardium develops more pronounced and clinically significant fibrosis.¹¹

Myocardial fibrosis plays an essential role in cardiac remodelling and is linked to DM and many CVDs.¹² Its primary culprit is cardiac fibroblast (CF) to myofibroblast (MF) differentiation. CFs are one of the largest cardiac cell populations, responsible for extracellular matrix (ECM) homeostasis, however, once harmed they transform into MFs.¹³ This considerably elevates ECM protein levels, which adversely augment ECM heart structure and promote formation of scar tissue.¹⁴ In DM, myocardial fibrosis and cardiac remodelling have become structural hallmarks of a diabetic heart. In fact, in absence of traditional cardiovascular risk factors, including hypertension, valvular disease and overt CAD, dbCM develops.¹⁵ Interestingly, myocardial fibrosis and adverse remodelling are the first signs of dbCM.^{15,16}

People with DM show signs of impaired left ventricular (LV) function, thickness, and remodelling, often resulting in LV diastolic dysfunction. Cardiac remodelling is a compensatory process exacerbated when the heart is under duress; however, exact mechanisms have yet to be elucidated. Insulin resistance and AGEs are key mechanisms in this compensation that may explain the development of hypertrophy of the heart in the presence of DM.¹⁷ Conversely, it should be noted that insulin sensitivity and signalling pathways play a significant role in dbCM both exacerbating its progression, but also having cardioprotective mechanisms. Particularly through the activation of the PI3Ka/Akt pathway, the suppression of cardiac ROS, and inflammation in dbCM, insulin signalling exhibit a mechanistic role in the diabetic heart. It should be noted that this evidence stems from animal studies and may not correspond to a human scenario.¹⁸ Thus, the effects of DM on cardiac remodelling evidently contain many complex mechanisms that need to be further studied.

Hence, this scoping review aims to provide an assessment of current biomarkers available that can be utilised in the detection of myocardial fibrosis/remodelling and, diagnosis and prognosis of subsequent CVD or cardiovascular complications. Through assessing the viability of these biomarkers, efficient diagnostic, prognostic and therapeutic interventions could be developed to detect or stop the progression of myocardial fibrosis/remodelling in its early stages. This could aid early detection of myocardial fibrosis/cardiac remodelling to stop its permanent damage, and most importantly attenuate the development of lethal CVDs, such as HF, particularly in people with DM.

5.3 Methods

5.3.1 Research Question

The purpose of this scoping review is to appraise the current biomarkers used in the diagnosis of cardiac remodelling and prognosis of CVD, linking their pathophysiological roles as a reflection of the underlying mechanisms.

5.3.2 Identification of Studies

This scoping review was conducted following the PRISMA guideline for Scoping Reviews.¹⁹ The following search term sets were used:

Set (A): biomarker OR marker OR markers.

Set (B): cardiac remodelling OR remodelling OR cardiac remodeling OR remodeling.

Set (C): diabetes or diabetes mellitus.

The following databases: MEDLINE, Scopus, Web of Science, PubMed, and Cochrane library. All searches were conducted from June to September 2021 by investigators MC and WL.

5.3.3 Study Selection

Inclusion criteria

Studies that were included had the main aim of assessing cardiac remodelling using a biomarker in people with DM. This includes studies that did not focus solely on DM

but had a subpopulation of people with DM within the study. Studies that did not have a control group of people without DM were also selected. Only studies written in the English language were included.

Exclusion criteria

Studies that were excluded did not examine people with DM or have a biomarker measure indicative of cardiac remodelling. Further studies that were excluded were review articles, articles not in English, and case reports.

5.3.4 Data Extraction

Following full-text screening, papers that met the selection criteria were scanned for extraction. The following details were extracted: Year, Author, Country, Patient Characteristics, Patient numbers with DM or in the control group, Mean Age, Biomarker, Biomarker Classification, and Level of Evidence. No review protocol was available specific to the purposes of this scoping review, hence biomarker classification and the level of evidence were appropriated as per a scoping review conducted by De Luca Canto et al. 2015²⁰. The biomarker clinical application was classified as: (1) potential biomarker(s) of cardiac remodelling; (2) inconclusive biomarker of cardiac remodelling, and (3) evidence not supportive as potential biomarker of cardiac remodelling. The level of evidence was classified as A (well-designed prognostic or diagnostic studies on relevant population), B (prognostic or diagnostic studies with minor limitations, overwhelmingly consistent evidence from observational studies) or C (observational studies [case-control and cohort design]).

5.4 Results

5.4.1 Study Selection

Two independent investigators, MC and WL, identified 4400 papers using the search terms set in the five databases outlined in the methodology. After removing any duplicate papers, a total of 1774 papers remained for Title and Abstract screening. Following the initial screening, 127 papers remained for full-text screening. Of those papers, 43 were included in our data extraction displayed in Table 5.1. The remaining 84 articles were excluded for: not relating to the topic, not including a biomarker, not written as an article, not in English, inaccessible, and with insufficient data. This process is visualised in Figure 5.1, with a PRISMA flow chart diagram depicting the search process.

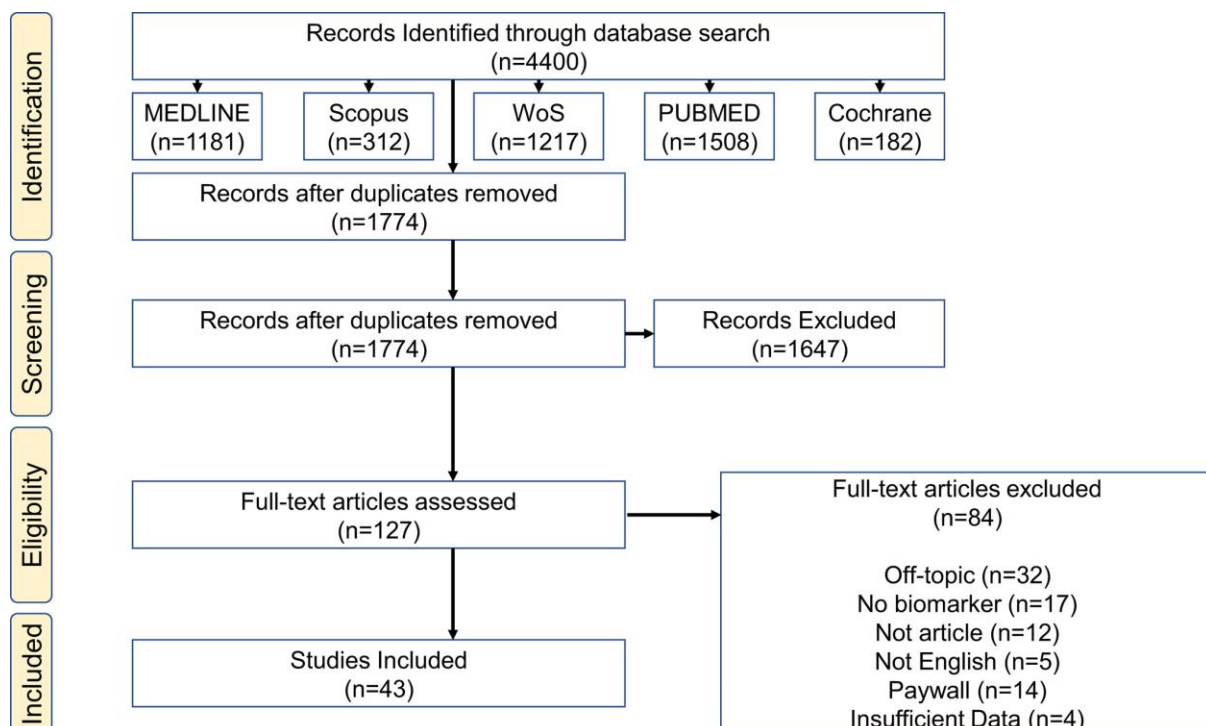


Figure 5.1 PRISMA flow diagram of search methodology

Table 5.1 Descriptive characteristics of included cardiac remodelling studies.

Year	Author	Country	Cohort Characteristics	Cases	Control	Mean Age	Biomarker	Biomarker Classification	Level of Evidence
2018	Lin et al.	Taiwan	CVD History	505	1416	57.1	NT-proBNP	2	C
2017	Lindholm et al.	International	CVD History	5141/542	8023/350	65/64.7	NT-proBNP (100 ng/l) hs-cTnT (14ng/l)	1	A
2013	Luchner et al.	Germany	General	19	858	48	NT-proBNP BNP	1	C
2013	Lupon et al.	Spain	HF Patient	314	562	70.3	NT-proBNP (1720 ng/l), hs-cTnT (16 ng/l), hs-ST2 (50 ng/l)	1	B
2014	McGrady et al.	Australia	High-risk HF	654	2896	70.4	NT-proBNP	1	A
2014	Motiwala et al.	USA	LVSD Outpatient	38/25	37/51	69.3/57.4	Galectin-3 (20 ng/mL)	2	B
2021	Myhre et al.	Norway	General	380	1678	63.9	cTnT, NT-proBNP, CRP, HbA1c	2	C
2019	Nwabuo et al.	USA	General	82	2570	66.9	Ceramides C16:0/C24:0	1	B
2016	Opincariu et al.	Romania	DM/MI Patient	45	43	61.3	hs-CRP, EAT	1	A
2017	Oliver et al.	USA	General	110	638	50	NT-proBNP, hs-cTnT, hs-CRP	3	B

2020	Parisi et al.	Italy	STEMI Patient	12	88	62.5	EAT	3	C
2020	Pecherina et al.	Russia	HF Patient	HFpEF : 11, HFrEF : 30	N/A	HFpEF : 57, HFrEF: 63	NT-proBNP, Galectin-3, sST2	1	B
2015	Peeters et al.	Europe	T1D Patient	493	N/A	39.5	TIMP-1, MMP-1, 2, 3, 9 , 10	2	B
2021	Pofi et al.	Italy	T2D Patient	51	20	60	miR122-5p	2	C
2018	Ruge et al.	Sweden	General	116/105	N/A	70.1/77.5	Endostatin, NT-proBNP	3	B
2009	Sato et al.	Japan	HF Patient	17	N/A	60.7	NT-proBNP, hs-cTnT	2	C
2016	Scirica et al.	Internatio nal	T2D Patient	12310	4182	65.1	NT-proBNP (450pg/mL), hs-cTnT (3pg/mL), hs-CRP (0.15 mg/L)	1	A
2017	Sharma et al.	Internatio nal	HF In-patient	922	1111	Diabetes : 70.3 Non-diabetes: 70	BNP (500pg/mL), NT-proBNP (2000pg/mL), sST2, Galectin-3, hs-CRP	1	B
2020	Sorensen et al.	Denmark	T2D Patient	246	N/A	Above median : 58 Below Median: 59	FGF-23 (median 74 ng/L)	2	C
2013	Spazzafumo et al.	Italy	General	533	1325	N/A	hs-CRP	1	B
2013	van der Velde et al.	CORONA : USA	HF Patient	CORONA: 333	N/A	CORONA: 71.6	Galectin-3 (17.8 ng/mL)	1	B

		COACH: USA		COACH: 95		COACH: 69.9			
2003	Vasan et al.	USA	General	Men: 41 Women: 42	N/A	Men: 87 Women: 78.6	hs-CRP, IL-6, TNF α	2	C
2010	Velagaleti et al.	USA	General	Men: 153 Women: 133	N/A	Men: 59 Women: 58	hs-CRP, BNP	2	C
2021	Verdonschot et al.	Europe	High Risk CVD	310	217	Diabetes : 71.9 Non-diabetes: 73.5	NT-proBNP (125- 1000 ng/L), Galectin-3, hs-cTnT	1	A
2008	Vorovich et al.	USA	HF Out-patient	117	N/A	56	BNP, MMP-9	1	C
2020	Wang et al.	USA	General	87	N/A	56	PIIINP	2	C
2007	Wang et al.	Taiwan	General	113	N/A	51.03	hs-CRP, NT-proBNP	1	B
2021	Watson et al.	Ireland	High Risk CVD	498	N/A	66.2	MMP-9	1	B
2008	Albertini et al.	France	T2D Patient	91	N/A	Men: 60 Women: 61	BNP	1	A
2006	Alla et al.	France	CHF Patient	64	92	Control: 56 T2D: 56	PIIINP, PICP, PINP, MMP-1, TIMP1	2	B
2005	Andersen et al.	Denmark	T2D Patient	60	30	Control:52 T2D: 55	NT-proBNP	1	A

2020	Bai et al.	China	CVD Patient	DM MACE: 89 DM MACE FREE: 113	748	DM MACE: 63.07 DM MACE FREE: 68.62	hs-ST2, NT-proBNP	1	B
2015	Bayes-Genis et al.	Spain	HF Patient	321	N/A	70.2	hs-ST2, NT-proBNP	1	B
2020	Bilovol et al.	Ukraine	T2D Patient	186	20	52.49	hs-CRP, Adiponectin, Omentin-1	2	B
2016	Borekci et al.	Turkey	STEMI Patient	71	207	55.3	NT-proBNP	2	B
2011	de Boer et al.	Netherlands	HF Patient	120	N/A	72	Galectin-3	1	B
2021	De Marco et al.	USA	HF Patient	116	132	DM: 69 Non-DM: 74.3	hs-CRP, hs-TnT, NT-proBNP, sST2, PICP, CITP, PIIINP, MMP-2,9, TIMP-1, Galectin-3	2	C
2011	Fousteris et al.	Greece	LVDD patients	(C) T2DM without LVDD: 48 (D) T2DM with LVDD: 50	(A) Healthy : 42 (B) Non -T2DM with LVDD: 18	A: 55.10 B: 60.33	sST2, BNP,	2	B

						C: 54.87 D: 56.98	hs-CRP		
2013	Ghanem et al.	Egypt	T2D Patient	EF<50%: 46 EF>50%: 54	50	EF<50%: 47.71 EF>50%: 44.89 Control: 45.05	IL-6, NT-proBNP	1	C
2013	Hao et al.	China	T2D Patient	110	N/A	EF<50%: 65.71 EF>50%: 66.29	Ang-II, NT-proBNP	2	C
	Jorgensen et al.	Denmark	T2D Patient	Microalbuminuria = 149, Macroalbuminuria = 563.	703	Control: 64 Microalbuminuria = 66 Macroalbuminuria = 67	Albumin	2	C
2013	Khalili et al.	Iran	STEMI Patient	DM normal {25 (OH)} = 12 DM deficient {25 (OH)} = 26	38	DM normal {25 (OH)} = 63.1 DM deficient {25 (OH)} = 59.6	25 (OH), MMP9	1	B
2012	Devaux et al.	England	MI Patient	Δ EDV \leq 0: 22 Δ EDV > 0: 24	42	63	VEGFB	2	B

The biomarker clinical application was classified as (1) potential biomarker (s) of remodelling; (2) inconclusive biomarker for remodelling, and (3) evidence not supportive as potential biomarker for remodelling (s). The level of evidence was classified in A (well-designed prognostic or diagnostic studies on relevant population), B (prognostic or diagnostic studies with minor limitations, overwhelmingly consistent evidence from observational studies), C (observational studies [case-control and cohort design]).

Abbreviations: 25 (OH), 25-hydroxy vitamin D; Ang II, angiotensin II; BNP, brain natriuretic peptide; CHF, chronic heart failure; C1P, carboxyl-terminal telopeptide type 1 collagen; CRP, C-reactive protein; cTnT, cardiac troponin T; CVD, cardiovascular disease; DM, diabetes mellitus; EAT, epicardial adipose thickness; FGF-23, fibroblast growth factor-23; HbA_{1c}, haemoglobin A_{1c}; HF, heart failure; hs-CRP, high-sensitivity C-reactive protein; hs-cTnT, high-sensitive cardiac troponin T; IL-6, interleukin 6; LVDD, left ventricular diastolic dysfunction; LVSD, left ventricular systolic dysfunction; MI, myocardial infarction; miR122-5p, MicroRNA-122-5p; MMP, matrix metalloproteinase; NT-proBNP, N-terminal pro b-type natriuretic peptide; PICP, procollagen type 1 carboxy-terminal propeptide; PIIINP, procollagen III N-terminal propeptide; PINP, procollagen type 1 N-terminal propeptide; sST2, soluble suppression of tumorigenesis-2; STEMI, ST-elevation myocardial infarction; T1D, type 1 diabetes mellitus; T2D, type 2 diabetes mellitus; TIMP-1, tissue inhibitor matrix metalloproteinase 1; TNF α , tumour necrosis factor alpha; VEGFB, vascular endothelial growth factor

5.4.2 Study Characteristics

Studies were extracted for descriptive data and displayed in Table 5.1, with a total of 43 studies that were included. The year of study ranged from 2003 to 2021. It was determined from our investigation that the origin country of study had a widespread reach, being conducted in over 24 separate countries (Figure 5.2). The most prevalent country was the USA ($n = 9$) where the most numerous studies were conducted.²¹⁻

²⁹ The countries following this were Denmark,^{30,32} and Italy^{33,35} ($n = 3$); China,^{36,37} Europe,^{38,39} France,^{40,41} Spain,^{42,43} and Taiwan^{44,45} ($n = 2$). Notably, three studies conducted multicentre studies across the world—categorised at International^{46,48} ($n = 3$).

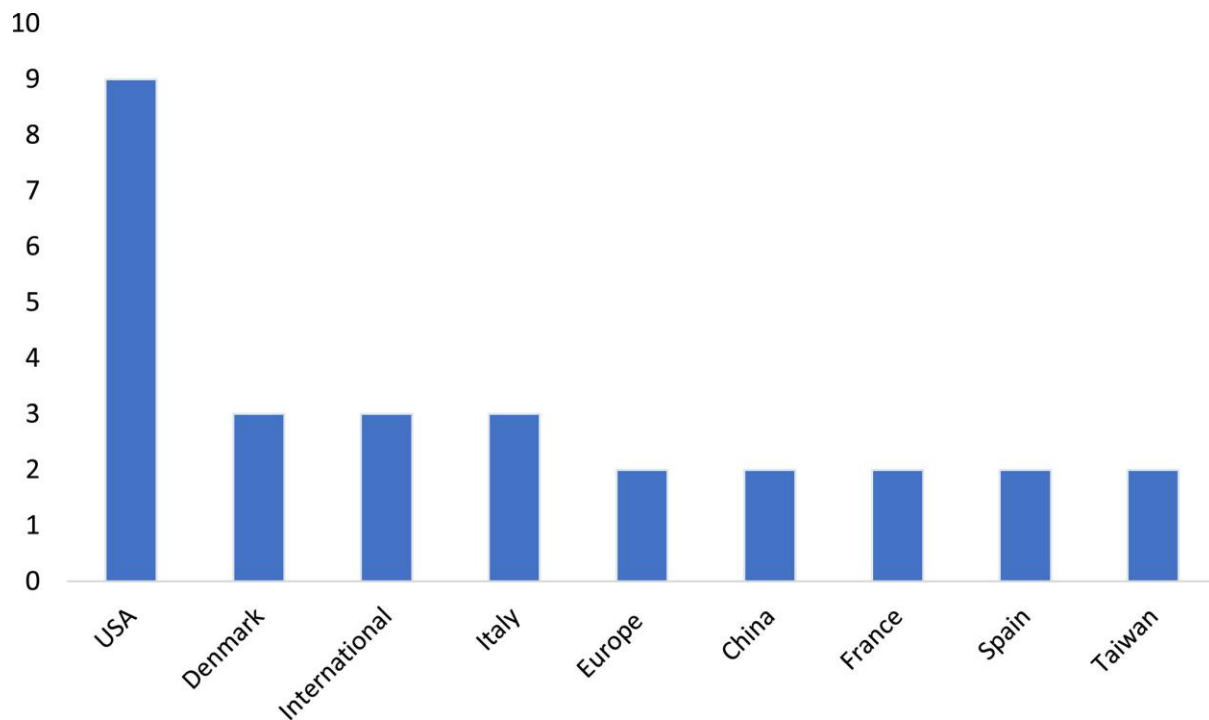


Figure 5.2 Distribution of adult participants according to country of study. United States of America ($n = 9$), Denmark ($n = 3$), International ($n = 3$), Italy ($n = 3$), China ($n = 2$), Europe ($n = 2$), France ($n = 2$), Spain ($n = 2$), Taiwan ($n = 2$). The following countries were not represented in the figure ($n = 1$): Australia, Egypt, England, Germany, Greece, Iran, Ireland, Japan, Netherlands, Norway, Romania, Russia, Sweden, Turkey, and Ukraine.

Our searches revealed a total of 15 unique biomarkers used in the detection of cardiac remodelling in DM, where potential biomarkers were described by at least two studies (Table 5.2). The most studied and represented biomarker was N-terminal (NT)-pro-brain natriuretic peptide (NT-proBNP, $n = 21$).^{23, 29, 31, 36, 37, 39, 42-56} Many studies had a multi-marker approach where NT-proBNP was included as one of the biomarkers; however, four studies used NT-proBNP as a sole biomarker in detecting signs of remodelling and CVD outcome. The next most studied biomarkers were high-sensitivity C-reactive protein (hs-CRP, $n = 12$)^{23, 25, 26, 29, 34, 46, 47, 51, 57-60} and high-sensitivity cardiac troponin T (hs-cTnT, $n = 8$),^{23, 29, 39, 43, 46, 48, 51, 54} Galectin-3 (Gal-

3, $n = 7$),^{21, 24, 29, 39, 47, 52, 61} and soluble suppression of tumorigenesis-2 (sST2) ($n = 7$).^{29, 36, 42, 43, 47, 52, 60} The vast majority of the studies included potential biomarkers collected from blood and plasma biomarkers with the exception of two papers, examining epicardial adipose thickness^{35, 57} as a potential biomarker.

Table 5.2 Potential Biomarkers Identified in adults studied

Biomarker	Number of studies
NT-proBNP	21
hs-CRP	12
MMP-1,2,3,9	10
hs-cTnT	8
Galectin-3	7
hs-ST2	7
BNP	6
PIIINP	3
TIMP-1	3
EAT	2
IL-6	2
PICP	2

Note: The following biomarkers were not presented in the table ($n = 1$): MMP10, 25 (OH), Adiponectin, Ang-II, Ceramide C16:0/C24:0, C1TP, Endostatin, FGF-23, HbA_{1c}, miR122-5p, Omentin-1, PINP, TNF α , and VEGFB.

5.4.3 Level of evidence and biomarker classification

The assessment of the included studies as per the level of evidence showed 7 studies were classified as 'A', having a well-designed study for the relevant population and sufficient level of evidence provided for the biomarker studied. Most studies were classified as 'B' ($n = 21$) where the diagnostic/prognostic study had minor limitations but consistent evidence. Lastly, 15 studies were classified as 'C', being an observational study with limited evidence provided (Table 5.1).

In terms of the biomarker classification, 22 studies were classified as (1), where the biomarker studies had the potential to be a reliable biomarker for detecting cardiac remodelling. Furthermore, 18 studies were classified as (2), being inconclusive as a biomarker for cardiac remodelling. Lastly, 3 studies were classified as (3), where insufficient evidence was provided for a biomarker of cardiac remodelling (Table 5.1).

5.5 Discussion

DM is a strong independent factor of CVD development associated with hyperglycaemia that affects heart function and contributes to worse CVD outcome.^{49, 50} This remains an important factor to account for when determining systemic biomarker concentrations in people with DM and CVD, which often differ from people without DM.⁶² Similarly, previous studies have shown that in the presence of DM, there is an up-regulation in inflammatory pathways, not present in people without DM.³⁹ Inflammation underpins potential mechanisms leading to adverse cardiac

remodelling and fibrotic processes in the presence of DM that still need to be fully elucidated.^{30, 47} The current diagnostic method for detecting cardiac fibrosis relies on invasive imaging methods such as cardiovascular magnetic resonance imaging that includes T1 mapping; however, it can vary in result depending on the practitioner and a patient in question.¹⁴ Often these methods need to be supported with additional assessments to confirm the diagnosis, which highlights the need for more reliable non-invasive methods that could be fulfilled by the emergence of new biomarkers that may be used in tandem with current methods. From the total of 15 biomarkers that were identified as promising within this scoping review, 7 studies were classified in the highest 1A category. This suggests that the quality of biomarkers from these studies is acceptable, and that these biomarkers have high potential of being reliable for cardiac remodelling.

5.5.1 NT-proBNP and BNP as a measure of cardiac remodelling

The natriuretic peptide (NP) system has shown to play an important role in the study of cardiac endocrinology with the regulation of circulating active BNP, and the inactive NT proBNP. These peptides are secreted primarily in response to atrial muscle stretch, but can also be influenced by hypoxia, inflammation, angiotensin II (Ang II), and endothelin stimuli.⁶³ Upon release, BNP binds to the particulate guanylyl cyclase A receptor, followed by the generation of 3'-5'-cyclic guanosine monophosphate. This interaction results in a series of cardioprotective responses such as reduced hypertrophy, fibrosis, and inhibition of the renin-angiotensin-aldosterone system.⁶⁴ Circulating levels of NPs typically remain at a low level, but upon stimulus are increased. Clinical data supports this, reporting higher levels of plasma BNP and

NT-proBNP in patients with HF, and hence these biomarkers have been the most widely used for the diagnosis and prognosis of HF.⁶⁵ In our current study, we found that out of the total 43 studies, 21 measured NT-proBNP concentration as a sole biomarker to determine remodelling or at least as a supplementary measure and six studies measured BNP as a biomarker.

The MESA study examined community patients for the presence of cardiac fibrosis measuring cardiovascular magnetic resonance T1 mapping and NT-proBNP levels. The findings of this study exhibit the relation of NPs and cardiac fibrosis, where a positive relation was found between plasma NT-proBNP levels and the presence of fibrotic changes within the heart. However, in the context of DM, the correlation between NPs and fibrosis displays an inverse relationship between plasma NP levels and insulin resistance across all body weights. The PARADIGM-HF trial measured a series of myocardial fibrosis plasma biomarkers in patients with HF, exhibiting a positive correlation of these biomarker levels to cardiovascular death and hospitalisation. The most notable changes in plasma biomarker concentrations recorded from this study were suppression of tumorigenesis-2 (ST2), tissue inhibitors of metalloproteinases (TIMP-1), and procollagen type III N-terminal peptide (PIIINP) at baseline; suggesting that TIMP-1 had the strongest prognostic value, exceeding BNP and NT-proBNP. It was also discovered that people with DM had a lower level of NT-proBNP, and significantly higher level of troponin T than people without DM. Out of all the studies included in this review, Lupon et al. 2013⁴³ provided similar insights and performed a multi-marker strategy, reporting a promising diagnostic potential of hs-cTnT and hs-ST2 biomarkers, which performed better together, whereas NT-

proBNP was not included in the risk stratification of HF and remodelling. Interestingly, Pecherina et al. 2020⁵² suggested that after multi-variate analysis, the prognostic value of NT-proBNP is more reliable for HF symptoms but not for cardiac remodelling.

From the findings of this study and previous studies, BNP's retain its diagnostic reliability as biomarkers for HF and show potential as biomarkers of cardiac remodelling in the presence of DM, albeit evidence is inconclusive so far based on extensive published research. However, as reported in previous studies, the non-specificity of BNP's may impede its potential as sole biomarkers, making them more beneficial when used in conjunction with other biomarkers of cardiac remodelling.

5.5.2 Inflammatory biomarkers of cardiac remodelling

Cardiac fibrosis is inextricably linked to dbCM and HF, where the underlying inflammatory process has shown an important role in its pathogenesis. DM exacerbates the inflammatory response, where a measure of inflammatory mediators at specific points in time can be indicative of the overall condition of the heart.⁶⁶

Gal-3 belongs to the B-galactoside-binding lectins, with an essential N-terminal domain proteolysed by matrix metalloproteinases (MMP) important for interaction with other intracellular proteins.⁶⁷ The ability to interact with other intracellular proteins allows Gal-3 to have a myriad of pleiotropic functions, notably within angiogenesis, inflammation, and fibrosis.^{67,68} Gal-3 promotes the chemoattraction of macrophages, fibroblast activity and ECM accumulation, displaying a close association with cardiac remodelling and HF pathophysiology.⁶⁸ Gal-3 typically is maintained at low plasma

concentration in healthy individuals, however in patients with HF its plasma concentration increases, where its initial anti-necrotic, and anti-apoptotic functions lead to adverse cardiac remodelling and fibrosis over time.⁶⁸ Thus Gal-3 has been implicated in the pathogenesis of cardiac remodelling and inflammatory processes and considered a novel biomarker.^{67,69} Serum Gal-3 and NT-proBNP concentrations have shown to be increased in HFpEF patients. In measuring ventricular remodelling in HFpEF patients using multivariate analysis, Gal-3 retains its association, whereas NT-proBNP does not and is rather attuned to HF symptoms.⁵² This apparent trend of increased Gal-3 levels corresponding with increased CVD risk and mortality was confirmed by Van der Velde et al., 2013.²⁴ By measuring percentage increase of Gal-3 over 3 months, the study found that an increase of >15% leads to a 50% higher risk of CVD adverse events compared to patients within 15% of their baseline Gal-3.²⁴ Conversely, De Boer et al., 2011⁶¹ reported that in hospitalised HF patients with DM, Gal-3 plasma concentration doubled, and showed high prognostic value for the primary endpoint of all-cause mortality and HF hospitalisation. Even when adjusted for covariates, including DM, Gal-3 retained promising prognostic value and even when measured at a later time point, it did not impair its prognostic value compared to other studies.⁶¹ Thus, Gal-3 may play an important prognostic role in detecting cardiac remodelling before severe damage or primary CVD mortality is reached, but its potential may be heightened in alliance with other biomarkers.

C-reactive protein (CRP) is a protein produced by hepatocytes within the liver, with serum concentration showing elevated trend under inflammatory conditions and age.⁷⁰ Hence, hs-CRP is widely used for its properties as an inflammatory marker,

where its sensitivity lies in its ability to accurately detect early, low-grade inflammation.^{70,71} In the presence of DM, systematic inflammation is present, which is often chronic and low-grade.⁷² Elevated serum CRP is associated with LV dysfunction, increased risk of DM, and it is overall a predictor of CVD risk and mortality.^{73,74} The role of CRP in the cardiac remodelling process has further been implicated with studies reporting increased CRP in conjunction with pro-fibrotic and pro-inflammatory properties in Ang II-induced cardiac remodelling through activation of the transforming growth factor- β (TGF- β) and nuclear factor- κ B (NF κ B) signalling pathways.⁷⁵ Hence hs-CRP may have the potential to detect early signs of cardiac remodelling in people with DM and provide tool for risk stratification due to its high sensitivity and possible mechanistic role in cardiac remodelling. Similarly, interleukin-6 (IL-6) is a versatile cytokine embedded within the inflammatory response and pathophysiology of T2D, activating the inflammatory pathways including Janus kinase (JAK) and signal transducers and activators of transcription (STAT).^{76,77} The pro-inflammatory properties of IL-6 coincide with the chronic inflammatory disease state of people with DM, further mediating the effects of endothelial dysfunction, a key process in the development of CVD.⁷⁸ IL-6 has been reported to be produced by cardiomyocytes upon myocardial infarction and hypoxia.⁷⁶ Though clear relationship between IL-6 in people with DM and related cardiac complications has been found, further studies are needed to understand the exact mechanisms involved.

ST2 is an interleukin receptor-1 (IL-1) family member that binds to the ligand IL-33, both of which play an integral role in the inflammatory and immune response, and

have emerged as promising markers of cardiovascular pathophysiology.⁷⁹ Both ST2 and IL-33 expression are regulated by the proinflammatory cytokines, IL-6 and tumour necrosis factor alpha (TNF), and impaired cardiac function.⁸⁰ Soluble ST2 (sST2) is an isoform of ST2 released by fibroblasts that freely circulate within the blood, and upon binding to IL-33 has cardioprotective and anti-inflammatory properties, preventing the actions of IL-33.⁷⁹ Hence sST2 is implicated in the cardiac remodelling process, indicative of fibrosis and hypertrophy.⁸¹ Clinically, sST2 has shown to be a prognostic marker of both acute and chronic HF, where elevated levels have been shown in patients with a higher New York Heart Association (NYHA) functional classification, poor LV function and higher incidence of DM.^{79,80} sST2 retains its promising biomarker potential as the influence of comorbidities of CVD, such as DM and hypertension, has shown a less of a confounding effect on sST2 than on NT-proBNP.⁴³ This presents the possibility of additional mechanisms in which sST2 may function and highlights the advantage of targeting patients with multiple comorbidities, where a combined biomarker strategy holds added potential.

5.5.3 *Cardiac-specific biomarkers*

Troponin is a contractile protein present within skeletal- and cardio-myocytes that facilitate beating of the heart.⁸² The most relevant of the isoforms is cardiac troponin in the context of CVD, where it is highly attuned to cardiomyocytes health and indicative of myocardial damage.⁸² Hence, the highly specific and sensitive cardiac troponin, hs-cTnT, has been clinically used in the risk stratification for CVD in patients.⁸³ Given the strong relationship between DM and CVD, studies have reported significantly increased systemic concentrations of hs-cTnT in patients with DM,

compared to those without DM.⁸³ Hs-cTnT measured in HFpEF patients with and without DM,²⁹ found no-significant differences initially observed between patient groups. However, after 12 months, hs-cTnT was one out of the two biomarkers significantly decreased when the groups were treated with a mineralocorticoid receptor inhibitor, spironolactone.²⁹ Meanwhile, people with DM and a CVD history with hs-cTnT systemic levels >14 ng/L experienced adverse cardiac outcomes.⁴⁸ The findings of this study and previous research indicate the influence of increasing hs-cTnT through coinciding developmental factors of both DM and CVD, such as microvascular disease, ventricular hypertrophy, inflammation, and endothelial dysfunction.⁸³ This presents the promising biomarker potential of hs-cTnT in elucidating the pathophysiological mechanisms between DM and CVD and detecting the early sign of cardiac remodelling.

Myocardium homeostasis involves the regulation of ECM proteins, namely collagen, for optimal function of the heart. In a disease state, ECM degradation is an integral process in cardiac remodelling aiming to preserve cardiac function through the breakdown of collagen.⁸⁴ These homeostatic disruptions result in CVD pathophysiology such as cardiac fibrosis, LV hypertrophy, atherosclerosis, and heart failure.⁸⁵ MMPs are a family of endopeptidases with the primary role of cleaving collagen, with 23 total family members.⁸⁶ MMP-1, 2, 8, 9, and 14 have been reported to have the ability to cleave collagen in CVD,⁸⁴ which align with our findings that identified studies reporting plasma MMP-1, 2, 3, and 9 concentrations to be reflective of early adverse cardiac remodelling. MMP-1 degrades fibrillar collagen, MMP-2 and

9 are involved in the angiogenic processes, and MMP-3 regulates ECM degradation. Hyperglycaemia is a key culprit of DM, where consistently high blood glucose contributes to oxidative stress and increased synthesis of MMP-9.⁸⁶

In relation to MMPs, tissue inhibitors of metalloproteinases (TIMP) play a critical role in the regulation of MMPs and the extent of ECM degradation and structural remodelling.⁸⁷ Studies have found that in patients with T2D and hypertension, there is a significant increase in TIMP-1 levels, TIMP-1: MMP-9 ratios, and increased TNF- α .⁸⁶

Given the mechanistic role of MMPs and TIMPs in the structural remodelling of the heart and CVD, they have become a prominent therapeutic target for the treatment of cardiac fibrosis, where their expression is increased in the early fibrosis, preceding scar tissue accumulation.⁸⁸ Thus, both MMPs and TIMP-1 exhibit a strong potential in the early detection of cardiac remodelling in patients with DM.

As described above, cardiac fibrosis is commonly present in many forms of CVDs, where the early stages of cardiac remodelling are influenced by ECM remodelling.^{14,84} MMPs have been established as critical regulators of these pathological changes in fibrosis,⁸⁶ notably involving excess collagen deposition through fibroblast activation. The major types of collagen present in cardiac muscle are collagen type I and III and account for 85% and 11%, respectively. The ratio of collagen type I to type III has been linked to cardiac fibrosis and underlying structural

remodelling, where they can be indicative of the underlying causes.¹⁴ Procollagen type 1 carboxy-terminal propeptide (PICP) and PIIINP are two collagen peptides extracted from our literature search, and both are associated with production of their respective collagen peptides.^{89,90} Previous studies have shown elevated PIIINP levels following myocardial infarction and LV⁹¹ dysfunction, with a poor prognosis.^{89,92} Similarly, increased PICP levels have been reported in patients with hypertrophic cardiomyopathy and hypertensive heart diseases but were more significantly elevated in cases of severe cardiac fibrosis.^{93,94} However, in T2D, PICP levels were reported to be elevated in the presence of LV diastolic dysfunction compared to the controls.⁹¹ Thus, plasma PIIINP and PICP concentrations have been associated with cardiac remodelling in attenuating the balance between collagen synthesis and degradation.⁹⁰ Both these collagen peptide precursors present promising biomarker potential reflective of the early adverse cardiac remodelling through collagen synthesis levels but require further research in people with DM.

5.5.4 Metabol(om)ic markers of T2D and CVD: Future perspectives

Although not identified as part of the inclusion criteria of this scoping review, as an emerging field, it is important to consider the potential of metabol(om)ic markers in CVD diagnosis and prognosis in the context of DM. The defining feature of DM is impaired glucose-insulin homeostasis accompanied by obesogenic systemic environment. Over the years, association between circulating amino acids and insulin has been established with some of the amino acids showing an insulinotropic effect. Previous studies have shown a correlation between significant increases in circulating

plasma concentrations of leucine, isoleucine, lysine, tryptophan, glutamine, and glycerol, which were identified as the strong metabolic predictors of impaired insulin sensitivity and the incidence of T2D.⁹⁵ In the longitudinal Framingham Heart Study, a metabolomic approach was used to measure plasma samples from 200 participants who proceeded to develop DM over a 12-year follow-up. Logistical regression models showed that increase in circulating concentrations of branched-chain amino acids (BCAAs) and aromatic amino acids were associated with future DM.⁹⁶ Phenylalanine, tyrosine, and isoleucine have also been reported to predict the onset of CVD.⁹⁷ However, the association of these amino acids with early adverse cardiac remodelling/fibrosis or dbCM have not been explored in-depth and this is an area of research that should be addressed in future.

Furthermore, an inverse association between the circulating aliphatic amino acid glycine concentration and risk of DM has been established.⁹⁸ Thus overall, the following amino acids have been identified as potential biomarkers of insulin resistance and DM: glutamate, glutamine, phenylalanine, tryptophan, tyrosine, glycine, isoleucine, leucine, and valine.^{95, 99} Comparable to BCAAs, the fatty acids (i.e. stearic, palmitic, oleic, linoleic, pentadecanoic, palmitoleic) and intact lipids (triacylglycerides) identified by metabolomics studies have shown potential use as early screening biomarkers for insulin resistance and subsequently DM.

Integration of the findings of GWAS with lipid data has highlighted genes such as *FADS1*, *FADS2*, *ELOVL2*, and *ELOVL6* to be associated with changes in

circulating lipid concentrations in patients.^{100,101} However, with the discovery of novel gene loci–lipid associations, links to insulin resistance endpoints including CVD will develop.

Further studies have implicated circulating metabolites and their potential role as a serum biomarker for dbCM in patients with DM and diastolic dysfunction. A high body mass index (BMI) and obesity have been correlated with the incidence of DM that is further linked to increases in fatty acid metabolism and impaired diastolic function.¹⁰² Shaver et al. (2016)¹⁰² reported the potential use of the metabolites as a biomarker in patients with diastolic dysfunction and DM compared to healthy controls. In the patient groups with the highest BMIs (DM, DM and diastolic dysfunction) leptin, triglyceride, TNF, and IL-6 concentrations were highest in these groups and inversely correlated with adiponectin levels. In line with these findings, high leptin and triglyceride levels have been associated with DM and fatty acid metabolism, where conversely, adiponectin presents antidiabetic and anti-inflammatory effects.¹⁰² With their present inflammatory role in DM, these biomarkers show a strong potential in detecting cardiac remodelling with supporting echocardiographic data. However, this remains an unexplored research field that is lacking information of how these metabolites can be used as biomarkers of early cardiac changes, including adverse cardiac remodelling especially given their close relationship to inflammatory mechanisms. This field of research should be investigated further given the importance of cardiac metabolism in the development of CVD.

The limitations of this research article may be attributed to the small number of studies including that specifically examining the narrow topic of cardiac remodelling in DM. From the hundreds of research articles screened in this study, only seven studies were found to be of high quality. Further assessment of these biomarkers in a diagnostic or prognostic scope may provide more insight to the quality of their biomarker or therapeutic target potential in cardiac remodelling. Further specification of patient groups, stage of CVD, and cardiac function would bolster the findings of this study, however, were not available in all studies. It is also possible that some biomarkers commonly associated with adverse cardiac remodelling were not found within our literature search because of the pre-set inclusion criteria, which narrows the range of research articles involving adverse cardiac remodelling. For example, growth differentiation factor 15 (GDF15) is a distant member of the TGF- β family with mechanistic roots in both CVD and DM.^{103,104} Despite showing strong prognostic potential as a biomarker for CVD, its role is not well understood currently, hence why GDF15, and other cardiac remodelling-implicated biomarkers were potentially not included. Future inference on this topic would include a systematic review for a more in-depth consideration at the biomarkers mentioned in this study to substantiate their potential as biomarkers of cardiac remodelling in the presence of DM.

5.6 Conclusion

Cardiac remodelling is inherently tied with cardiovascular outcomes, with DM being one of the main risk factors. The pathogenesis of cardiac remodelling in DM is yet to be elucidated and requires further investigation to understand the mechanisms involved. Through the data collected from this scoping review, it was revealed that NT-

proBNP was the most frequently measured biomarker in studies evaluating cardiac remodelling and related CVD outcomes in people with DM. However, the findings and multivariate analysis in the included studies of this scoping review suggest that NT-proBNP, although the standard diagnostic and prognostic biomarker in HF may not be the optimal biomarker in determining signs of cardiac remodelling in the presence of DM. Emerging biomarkers for cardiac remodelling including hs-CRP, hs-cTnT, and Gal-3 being rooted in inflammatory pathways, have shown promising results in the current studies as diagnostic and prognostic biomarkers of adverse cardiac remodelling in DM. Although outside of the scoping review inclusion criteria, with the strong evidence supporting the relationship of certain amino acids and impaired insulin sensitivity, and the emergence of advanced metabolomics technologies, the possibility for the amino acids to be developed as new biomarkers for the early detection of adverse cardiac remodelling and CVD in DM is highly likely. However, further research in larger studies must be conducted to confirm the effectiveness of these emerging biomarkers and understand the mechanisms of cardiac remodelling in DM.

5.7 Declarations

AUTHORS' CONTRIBUTIONS

Conceptualisation, LM and KM; methodology, data extraction, analysis, interpretation, and graphical abstract: MC, WL; contribution to data interpretation and manuscript content: MP and DA; writing—original draft preparation: MC. Manuscript editing: LM, MP, DA, KM. Supervision: LM and KM. All authors read and approved the final manuscript.

ACKNOWLEDGMENTS

Not applicable. Open access publishing facilitated by University of Technology Sydney, as part of the Wiley - University of Technology Sydney agreement via the Council of Australian University Librarians.

FUNDING INFORMATION

This research is supported by an Australian Government Research Training Program Scholarship (Michael Chhor).

CONFLICT OF INTEREST STATEMENT

The authors declare that they have no competing interests.

5.8 References

1. Key Statistics: Cardiovascular Disease. The Heart Foundation. <https://www.heartfoundation.org.au/activities-finding-or-opinion/key-stats-cardiovascular-disease>.
2. Cardiovascular diseases. https://www.who.int/health-topics/cardiovascular-diseases#tab=tab_1.
3. Roth GA, Mensah GA, Johnson CO, et al. Global burden of cardiovascular diseases and risk factors, 1990–2019: update from the GBD 2019 study. *J Am Coll Cardiol*. 2020;76:2982-3021.
4. Diabetes. https://www.who.int/health-topics/diabetes#tab=tab_1.
5. Henson SM, Aksentijevic D. Senescence and type 2 diabetic cardiomyopathy: how young can you die of old Age? *Front Pharmacol*. 2021;12:716517.
6. Dokken BB. The pathophysiology of cardiovascular disease and diabetes: beyond blood pressure and lipids. *Diabetes Spectrum*. 2008;21:160-165.

7. Leon BM, Maddox TM. Diabetes and cardiovascular disease: epidemiology, biological mechanisms, treatment recommendations and future research. *World J Diabetes*. 2015;6:1246.
8. Kannel WB, Hjortland M, Castelli WP. Role of diabetes in congestive heart failure: the Framingham study. *Am J Cardiol*. 1974;34:29- 34.
9. Kannel WB, McGee DL. Diabetes and cardiovascular disease: the Framingham study. *JAMA*. 1979;241:2035- 2038.
10. Kenny HC, Abel ED. Heart failure in type 2 diabetes mellitus: impact of glucose lowering agents, heart failure therapies and novel therapeutic strategies. *Circ Res*. 2019;124:121.
11. Tuleta I, Frangogiannis NG. Diabetic fibrosis. *Biochim Biophys Acta Mol Basis Dis*. 1867;2021:166044.
12. Liu T, Song D, Dong J, et al. Current understanding of the pathophysiology of myocardial fibrosis and its quantitative assessment in heart failure. *Front Physiol*. 2017;8:238.
13. Travers JG, Kamal FA, Robbins J, Yutzey KE, Blaxall BC. Cardiac fibrosis: the fibroblast awakens. *Circ Res*. 2016;118:1021.
14. Hinderer S, Schenke-Layland K. Cardiac fibrosis – A short re-view of causes and therapeutic strategies. *Adv Drug Deliv Rev*. 2019;146:77- 82.
15. Jia G, Hill MA, Sowers JR. Diabetic cardiomyopathy. *Circ Res*. 2018;122:624- 638.
16. Russo I, Frangogiannis NG. Diabetes-associated cardiac fibrosis: cellular effectors, molecular mechanisms and therapeutic opportunities. *J Mol Cell Cardiol*. 2016;90:84.
17. Yap J, Tay WT, Teng TK, et al. Association of Diabetes Mellitus on cardiac remodeling, quality of life, and clinical outcomes in heart failure with reduced and preserved ejection fraction. *J Am Heart Assoc*. 2019;8:e013114.
18. Ritchie RH, Dale Abel E. Basic mechanisms of diabetic heart disease. *Circ Res*. 2020;126:1501.

19. Tricco AC, Lillie E, Zarin W, et al. PRISMA extension for scoping reviews (PRISMA-ScR): checklist and explanation. *Ann Intern Med.* 2018;169:467- 473.
20. de Luca Canto G, Pachêco- Pereira C, Aydinoz S, Major PW, Flores- Mir C, Gozal D. Biomarkers associated with obstructive sleep apnea: a scoping review. *Sleep Med Rev.* 2015;23:28- 45. doi:10.1016/j.smrv.2014.11.004
21. Motiwala SR, Szymonifka J, Belcher A, et al. Serial measurement of galectin- 3 in patients with chronic heart failure: results from the ProBNP outpatient tailored chronic heart failure therapy (PROTECT) study. *Eur J Heart Fail.* 2013;15:1157- 1163.
22. Nwabuo CC, Duncan M, Xanthakis V, et al. Association of circulating ceramides with cardiac structure and function in the community: the Framingham heart study. *J Am Heart Assoc.* 2019;8:e013050.
23. Oliver W, Matthews G, Ayers CR, et al. Factors associated with left atrial remodeling in the general population. *Circ Cardiovasc Imaging.* 2017;10:e005047.
24. van der Velde AR, Gullestad L, Ueland T, et al. Prognostic value of changes in galectin- 3 levels over time in patients with heart failure: data from CORONA and COACH. *Circ Heart Fail.* 2013;6:219- 226.
25. Vasan RS, Sullivan LM, Roubenoff R, et al. Inflammatory markers and risk of heart failure in elderly subjects without prior myocardial infarction - the Framingham heart study. *Circulation.* 2003;107:1486- 1491.
26. Velagaleti RS, Gona P, Chuang ML, et al. Relations of insulin resistance and glycemic abnormalities to cardiovascular magnetic resonance measures of cardiac structure and function: the Framingham heart study. *Circ Cardiovasc Imaging.* 2010;3:257- 263.
27. Vorovich EE, Li M, Aversa J, et al. Comparison of matrix metalloproteinase 9 and brain natriuretic peptide as clinical biomarkers in chronic heart failure. *Am Heart J.* 2008;155:992- 997.
28. Wang K-T, Liu YY, Sung KT, et al. Circulating monocyte count as a surrogate marker for ventricular- arterial remodeling and incident heart failure with preserved ejection fraction. *Diagnostics.* 2020;10:287.

29. de Marco C, Claggett BL, de Denus S, et al. Impact of diabetes on serum biomarkers in heart failure with preserved ejection fraction: insights from the TOPCAT trial. *ESC Heart Fail.* 2021;8:1130- 1138. doi:10.1002/ehf2.13153
30. Sorensen MH, Bojer AS, Jørgensen NR, et al. Fibroblast growth factor- 23 is associated with imaging markers of diabetic cardiomyopathy and anti-diabetic therapeutics. *Cardiovasc Diabetol.* 2020;19:158.
31. Andersen NH, Poulsen SH, Knudsen ST, Heickendorff L, Mogensen CE. NT-proBNP in normoalbuminuric patients with type 2 diabetes mellitus. *Diabet Med.* 2005;22:188- 195.
32. Jørgensen PG, Biering-Sørensen T, Mogelvang R, et al. Presence of micro- and macroalbuminuria and the association with cardiac mechanics in patients with type 2 diabetes. *Eur Heart J Cardiovasc Imaging.* 2018;19:1034- 1041.
33. Pofi R, Galea N, Franccone M, et al. Diabetic Cardiomyopathy progression is triggered by miR122- 5p and involves extra-cellular matrix: a 5-year prospective study. *JACC Cardiovasc Imaging.* 2021;14:1130- 1142.
34. Spazzafumo L, Olivieri F, Abbatecola AM, et al. Remodelling of biological parameters during human ageing: evidence for complex regulation in longevity and in type 2 diabetes. *Age (Dordr).* 2013;35:419- 429.
35. Parisi V, Cabaro S, D'Esposito V, et al. Epicardial adipose tissue and IL- 13 response to myocardial injury drives left ventricular remodeling after ST elevation myocardial infarction. *Front Physiol.* 2020;11:575181.
36. Bai J, Han L, Liu H. Combined use of high-sensitivity ST2 and NT- proBNP for predicting major adverse cardiovascular events in coronary heart failure. *Ann Palliat Med.* 2020;9:1976- 1989.
37. Hao PP, Chen Y-G, Liu Y- P, et al. Association of Plasma Angiotensin- (1- 7) level and left ventricular function in patients with type 2 diabetes mellitus. *PLoS One.* 2013;8:e62788.
38. Peeters SA, Engelen L, Buijs J, et al. Associations between advanced glycation endproducts and matrix metalloproteinases and its inhibitor in individuals with type 1 diabetes. *J Diabetes Complications.* 2018;32:325- 329.

39. JAJ V, Ferreira JP, Pellicori P, et al. Proteomic mechanistic profile of patients with diabetes at risk of developing heart failure: insights from the HOMAGE trial. *Cardiovasc Diabetol*. 2021;20:163.
40. Albertini JP, Cohen R, Valensi P, Sachs RN, Charniot JC. B-type natriuretic peptide, a marker of asymptomatic left ventricular dysfunction in type 2 diabetic patients. *Diabetes Metab*. 2008;34:355- 362.
41. Alla F, Kearney-Schwartz A, Radauceanu A, das Dores S, Dousset B, Zannad F. Early changes in serum markers of cardiac extra-cellular matrix turnover in patients with uncomplicated hypertension and type II diabetes. *Eur J Heart Fail*. 2006;8:147-153.
42. Bayes-Genis A, Zhang Y, Ky B. ST2 and patient prognosis in chronic heart failure. *Am J Cardiol*. 2015;115:64B- 69B.
43. Lupón J, de Antonio M, Galán A, et al. Combined use of the novel biomarkers high-sensitivity troponin T and ST2 for heart failure risk stratification vs conventional assessment. *Mayo Clin Proc*. 2013;88:234- 243. 4
4. Lin J- L, Sung KT, Su CH, et al. Cardiac structural remodeling, longitudinal systolic strain, and torsional mechanics in lean and nonlean Dysglycemic Chinese adults. *Circ Cardiovasc Imaging*. 2018;11:e007047.
45. Wang TJ, Larson MG, Benjamin EJ, et al. Clinical and echo-cardiographic correlates of plasma procollagen type III amino-terminal peptide levels in the community. *Am Heart J*. 2007;154:291- 297.
46. Scirica BM, Bhatt DL, Braunwald E, et al. Prognostic implications of biomarker assessments in patients with type 2 diabetes at high cardiovascular risk: a secondary analysis of a randomized clinical trial. *JAMA Cardiol*. 2016;1:989- 998.
47. Sharma A, Demissei BG, Tromp J, et al. A network analysis to compare biomarker profiles in patients with and without diabetes mellitus in acute heart failure. *Eur J Heart Fail*. 2017;19:1310- 1320.
48. Lindholm D, Lindbäck J, Armstrong PW, et al. Biomarker-based risk model to predict cardiovascular mortality in patients with stable coronary disease. *J Am Coll Cardiol*. 2017;70:813- 826.

49. Luchner A, Behrens G, Stritzke J, et al. Long- term pattern of brain natriuretic peptide and N- terminal pro brain natriuretic peptide and its determinants in the general population: contribution of age, gender, and cardiac and extra-cardiac factors. *Eur J Heart Fail.* 2013;15:859- 867.
50. McGrady M, Reid CM, Shiel L, et al. N- terminal B- type natriuretic peptide and the association with left ventricular diastolic function in a population at high risk of incident heart failure: results of the SCReening Evaluation of the evolution of new- heart failure study (SCREEN- HF). *Eur J Heart Fail.* 2013;15:573- 580.
51. Myhre PL, Lyngbakken MN, Berge T, et al. Diagnostic thresholds for pre-diabetes mellitus and diabetes mellitus and sub-clinical cardiac disease in the general population: data from the ACE 1950 study. *J Am Heart Assoc.* 2021;10:e020447.
52. Pecherina T, Kutikhin A, Kashtalov V, et al. Serum and echocardiographic markers may synergistically predict adverse cardiac remodeling after ST-segment elevation myocardial infarction in patients with preserved ejection fraction. *Diagnostics.* 2020;10:301.
53. Ruge T, Carlsson AC, Ingelsson E, et al. Circulating endostatin and the incidence of heart failure. *Scand Cardiovasc J.* 2018;52:244- 249.
54. Sato Y, Nishi K, Taniguchi R, et al. In patients with heart failure and non- ischemic heart disease, cardiac troponin T is a reliable predictor of long- term echocardiographic changes and adverse cardiac events. *J Cardiol.* 2009;54:221- 230.
55. Börekçi A, Gür M, Türkoğlu C, et al. Neutrophil to lymphocyte ratio predicts left ventricular remodeling in patients with ST elevation myocardial infarction after primary percutaneous coronary intervention. *Korean Circ J.* 2016;46:15- 22.
56. Ghanem SE, Abdel-Samie M, Torkey MH, et al. Role of resistin, IL- 6 and NH2- terminal portion proBNP in the pathogenesis of cardiac disease in type 2 diabetes mellitus. *BMJ Open Diabetes Res Care.* 2020;8:e001206.
57. Opincariu D, Mester A, Dobra M, Rat N, Hodas R, Morariu M. Prognostic value of epicardial fat thickness as a biomarker of increased inflammatory status in patients with type 2 diabetes mellitus and acute myocardial infarction. *J Cardiovasc Emergen.* 2016;2:11- 18.

58. Wang TJ, Larson MG, Benjamin EJ, et al. Clinical and echo-cardiographic correlates of plasma procollagen type III amino-terminal peptide levels in the community. *Am Heart J.* 2007;154:291- 297.
59. Bilovol OM, Knyazkova II, Al-Travneh OV, Bogun MV, Berezin AE. Altered adipocytokine profile predicts early stage of left ventricular remodeling in hypertensive patients with type 2 diabetes mellitus. *Diabetes Metab Syndr.* 2020;14:109- 116.
60. Fousteris E, Melidonis A, Panoutsopoulos G, et al. Toll/inter-leukin- 1 receptor member ST2 exhibits higher soluble levels in type 2 diabetes, especially when accompanied with left ventricular diastolic dysfunction. *Cardiovasc Diabetol.* 2011;10:101.
61. de Boer RA, Lok DJ, Jaarsma T, et al. Predictive value of plasma galectin- 3 levels in heart failure with reduced and preserved ejection fraction. *Ann Med.* 2011;43:60- 68
62. Januszewski AS, Watson CJ, O'Neill V, et al. FKBPL is associated with metabolic parameters and is a novel determinant of cardiovascular disease. *Sci Rep.* 2020;10:21655.
63. Almeida AG. NT- proBNP and myocardial fibrosis the invisible link between health and disease*. *J Am Coll Cardiol.* 2017;70(25):3110- 3112.
64. Kuwahara K. The natriuretic peptide system in heart failure: diagnostic and therapeutic implications. *Pharmacol Ther.* 2021;227:107863.
65. Mckie PM, Burnett JC. NT- proBNP the gold standard biomarker in heart failure*. *J Am Coll Cardiol.* 2016;68(22):2437- 2439.
66. Lazar S, Rayner B, Lopez Campos G, McGrath K, McClements L. Mechanisms of heart failure with preserved ejection fraction in the presence of diabetes mellitus. *J Metab Syndr Res.* 2020;3:1- 5.
67. Dong R, Zhang M, Hu Q, et al. Galectin- 3 as a novel biomarker for disease diagnosis and a target for therapy (review). *Int J Mol Med.* 2018;41:599.
68. Blanda V, Bracale UM, di Taranto MD, Fortunato G. Galectin- 3 in cardiovascular diseases. *Int J Mol Sci.* 2020;21:1- 18.

69. Yakar Tülüce S, Tülüce K, Çil Z, Emren SV, Akyıldız Zİ, Ergene O. Galectin- 3 levels in patients with hypertrophic cardiomyop-athy and its relationship with left ventricular mass index and function. *Anatol J Cardiol*. 2016;16:344.
70. Li Y, Zhong X, Cheng G, et al. Hs-CRP and all-cause, car-diovascular, and cancer mortality risk: A meta- analysis. *Atherosclerosis*. 2017;259:75- 82.
71. Kamath DY, Xavier D, Sigamani A, Pais P. High sensitivity C- reactive protein (hsCRP) & cardiovascular disease: an Indian perspective. *Indian J Med Res*. 2015;142:261- 268. doi:10.4103/0971- 5916.166582
72. Walker AMN, Patel PA, Rajwani A, et al. Diabetes mellitus is as-sociated with adverse structural and functional cardiac remod-elling in chronic heart failure with reduced ejection fraction. *Diab Vasc Dis Res*. 2016;13:331- 340.
73. Pfützner A, Forst T. High-sensitivity C- reactive protein as car-diovascular risk marker in patients with diabetes mellitus. *Diabetes Technol Ther*. 2006;8:28- 36. <https://home.liebertpub.com/dia>
74. Nagai T, Anzai T, Kaneko H, et al. C- reactive protein overex-pression exacerbates pressure overload- induced cardiac remod-eling through enhanced inflammatory response. *Hypertension*. 2011;57:208- 215.
75. Zhang R, Zhang YY, Huang XR, et al. C- reactive protein promotes cardiac fibrosis and inflammation in angioten-sin II- induced hypertensive cardiac disease. *Hypertension*. 2010;55:953- 960.
76. Dawn B, Xuan YT, Guo Y, et al. IL- 6 plays an obligatory role in late preconditioning via JAK-STAT signaling and upregulation of iNOS and COX- 2. *Cardiovasc Res*. 2004;64:61- 71.
77. Akbari M, Hassan-Zadeh V. IL- 6 signalling pathways and the development of type 2 diabetes. *Inflammopharmacology*. 2018;26:685- 698.
78. Qu D, Liu J, Lau CW, Huang Y. IL- 6 in diabetes and cardiovas-cular complications. *Br J Pharmacol*. 2014;171:3595.
79. Dudek M, Dudek MA, Kałużna-Oleksy MB, Migaj JB, Straburzyńska- Migaj EA. Cite as the creative commons attribution 3.0 Unported (CC BY3.0) address for

correspondence Funding sources clinical value of soluble ST2 in cardiology. *Adv Clin Exp Med*. 2020;29:1205- 1210.

80. Lotierzo M, Dupuy AM, Kalmanovich E, Roubille F, Cristol JP. sST2 as a value-added biomarker in heart failure. *Clin Chim Acta*. 2020;501:120- 130.

81. Homsak E, Gruson D. Soluble ST2: A complex and diverse role in several diseases. *Clin Chim Acta*. 2020;507:75- 87.

82. Garg P, Morris P, Fazlanie AL, et al. Cardiac biomarkers of acute coronary syndrome: from history to high-sensitivity cardiac troponin. *Intern Emerg Med*. 2017;12:147.

83. Whelton SP, McEvoy J, Lazo M, Coresh J, Ballantyne CM, Selvin E. High-sensitivity cardiac troponin T (hs-cTnT) as a predictor of incident diabetes in the atherosclerosis risk in communities study. *Diabetes Care*. 2017;40:261- 269.

84. Yabluchanskiy A, Ma Y, Iyer RP, Hall ME, Lindsey ML. Matrix Metalloproteinase-9: many shades of function in cardiovascular disease. *Phys Ther*. 2013;28:391.

85. Nagase H, Visse R, Murphy G. Structure and function of matrix metalloproteinases and TIMPs. *Cardiovasc Res*. 2006;69:562- 573.

86. Cabral-Pacheco GA, Garza-Veloz I, Castruita-De la Rosa C, et al. The roles of matrix metalloproteinases and their inhibitors in human diseases. *Int J Mol Sci*. 2020;21:1- 53.

87. Wang X, Khalil RA. Matrix metalloproteinases, vascular remodeling, and vascular disease. *Adv Pharmacol*. 2018;81:241.

88. Chuang HM, Chen YS, Harn HJ. The versatile role of matrix metalloproteinase for the diverse results of fibrosis treatment. *Molecules*. 2019;24:4188.

89. Lee CH, Lee WC, Chang SH, Wen MS, Hung KC. The N-terminal propeptide of type III procollagen in patients with acute coronary syndrome: a link between left ventricular end-diastolic pressure and cardiovascular events. *PLoS One*. 2015;10:e114097.

90. Osokina A, Karetnikova V, Polikutina O, et al. Prognostic potential of cardiac structural and functional parameters and N-terminal propeptide of type III procollagen

in predicting cardiac fibrosis one year after myocardial infarction with pre-served left ventricular ejection fraction. *Aging (Albany NY)*. 2021;13:194.

91. Ihm SH, Youn HJ, Shin DI, et al. Serum carboxy- terminal pro-peptide of type I procollagen (PIP) is a marker of diastolic dysfunction in patients with early type 2 diabetes mellitus. *Int J Cardiol*. 2007;122:e36-e38.

92. Sugimoto M, Saiki H, Tamai A, et al. Ventricular fibrogenesis activity assessed by serum levels of procollagen type III N- terminal amino peptide during the staged Fontan procedure. *J Thorac Cardiovasc Surg*. 2016;151:1518- 1526.

93. Yang C, Qiao S, Song Y, et al. Procollagen type I carboxy- terminal propeptide (PICP) and MMP- 2 are potential bio-markers of myocardial fibrosis in patients with hypertrophic cardiomyopathy. *Cardiovasc Pathol*. 2019;43:107150.

94. Querejeta R, Varo N, López B, et al. Serum carboxy- terminal pro-peptide of procollagen type I is a marker of myocardial fibrosis in hypertensive heart disease. *Circulation*. 2000;101:1729- 1735.

95. Alqudah A, Wedyan M, Qnais E, Jawarneh H, McClements L. Plasma amino acids metabolomics' important in glucose management in type 2 diabetes. *Front Pharmacol*. 2021;12:695418.

96. Wang TJ, Larson MG, Vasan RS, et al. Metabolite profiles and the risk of developing diabetes. *Nat Med*. 2011;17:448.

97. Magnusson M, Lewis GD, Ericson U, et al. A diabetes- predictive amino acid score and future cardiovascular disease. *Eur Heart J*. 2013;34:1982.

98. Ferrannini E, Natali A, Camastra S, et al. Early metabolic markers of the development of dysglycemia and type 2 diabetes and their physiological significance. *Diabetes*. 2013;62:1730- 1737.

99. Roberts LD, Koulman A, Griffin JL. Towards metabolic bio-markers of insulin resistance and type 2 diabetes: progress from the metabolome. *Lancet Diabetes Endocrinol*. 2014;2:65- 75.

100. Tanaka T, Shen J, Abecasis GR, et al. Genome-wide association study of plasma polyunsaturated fatty acids in the InCHIANTI study. *PLoS Genet*. 2009;5:1000338.

101. Ameer A, Enroth S, Johansson A, et al. Genetic adaptation of fatty acid metabolism: a human-specific haplotype increasing the biosynthesis of long-chain Omega-3 and Omega-6 fatty acids. *Am J Hum Genet.* 2012;90:809.
102. Shaver A, Nichols A, Thompson E, et al. Role of serum bio-markers in early detection of diabetic cardiomyopathy in the west Virginian population. *Int J Med Sci.* 2016;13:161.
103. Eddy AC, Trask AJ. Growth differentiation factor-15 and its role in diabetes and cardiovascular disease. *Cytokine Growth Factor Rev.* 2021;57:11-18.
104. Wesseling M, de Poel JHC, de Jager SCA. Growth differentiation factor 15 in adverse cardiac remodelling: from biomarker to causal player. *ESC Heart Fail.* 2020;7:1488-1501.

Chapter 6

Discussion

6.1 General Discussion

Cardiovascular disease (CVD) is becoming concerningly prevalent within the current population, with many lifestyle choices shifting towards unhealthy and sedentary habits. Its societal burden has exponentially risen and holds a heavy socioeconomic burden. CVDs remain a difficult category of disease to manage due to the multifactorial nature of the pathogenesis. Frequently, the clinical manifestation of a CVD is not the result of a singular pathological condition, but rather a combination of coinciding factors. As a result, many CVDs have a poor prognosis and eventually result in heart failure (HF) and patient mortality.

Hence, in this thesis, we aimed to elucidate the emerging FKBPL mechanisms and their involvement in the pathophysiology of CVD, particularly heart disease. We specifically focused on early cardiovascular changes and the role FKBPL plays in the development of heart disease, due to risk factors including E-Cigarettes (E-Cigs), cardiac fibrosis and hypertrophic cardiomyopathy, that can lead to heart failure (HF). This work builds on previous findings that FKBPL is increased in human plasma from patients with CVD in the absence of diabetes mellitus (DM), and that it is positively correlated with a clinically utilized biomarker of HF, B-natriuretic peptide (BNP), and echocardiographic parameters of diastolic dysfunction⁹⁸. In addition, preliminary data from conferences proceedings also indicated that FKBPL is increased when cardiac fibroblasts were treated with well-established cardiac fibrosis stimuli, TGF- β , or hypoxia (2%). In the rat ischemia/perfusion model of cardiac ischemia, FKBPL was substantially downregulated, perhaps as a result of negative feedback mechanism to stimulate cardiac angiogenesis and regeneration¹⁰¹. These results suggest that

FKBPL could have a role in cardiac ischemia and fibrosis hence further work was conducted as part of my thesis to demonstrate this, particularly in the context of cardiac fibrosis and heart failure with preserved ejection fraction (HFpEF). HFpEF was pursued in this thesis due to poorly understood pathogenesis of this type of HF and the fact that aberrant angiogenesis, inflammation, and endothelial dysfunction are hallmark feature of HFpEF^{107–109}. Furthermore, HFpEF is lacking specific biomarkers and effective treatments even though it affects 50% of HF patients and it is associated with similar mortality as heart failure with reduced ejection fraction (HFrEF)¹¹⁰.

E-Cigs are emerging as a risk factor for CVD, however deeper understanding of the impact of E-Cigs on cardiovascular health is lacking. E-Cigs are a non-combustible and popular smoking cessation tool that has been dominating the market, concerningly in the demographics of adolescents and non-smokers. A number of recent studies with human participants have reported no association between exclusive E-Cig use and CVD or cardiovascular events^{111–113}. Nevertheless, the limitations of these studies include self-reporting, short follow-up and small samples size in the outcome group, hence larger studies with longer follow-up periods and adequate control groups are required to better understand a long-term impact of E-Cigs on cardiovascular health¹¹⁴. In the absence of more definitive evidence, we aimed to elucidate mechanisms involved in E-Cig-induced effects on endothelial cells and the heart. As part of the Chapter 2, we conducted various *in vitro* experiments using mono and co-culture of human coronary artery endothelial cells (HCAECs) and HCAECs in combination with human alveolar epithelial cells, respectively, to determine the contribution of the first pass metabolism of lung epithelial cells that are initially exposed to E-Cigs before reaching endothelial cells within blood vessels. In both models, we assessed cell viability, reactive oxygen species production, inflammation and FKBPL expression,

whereas using *in vivo* model of E-Cigs exposure, we elucidated the involvement of FKBPL and inflammatory (CD31, VCAM1 and ICAM1) mechanisms within the left ventricle of the heart. This work presents novel insights into the adverse effects of E-Cigs on cardiovascular health that could impact on the public perception of E-Cig use, and possible long-term effects associated with its use (Figure 6.1)¹¹⁵.

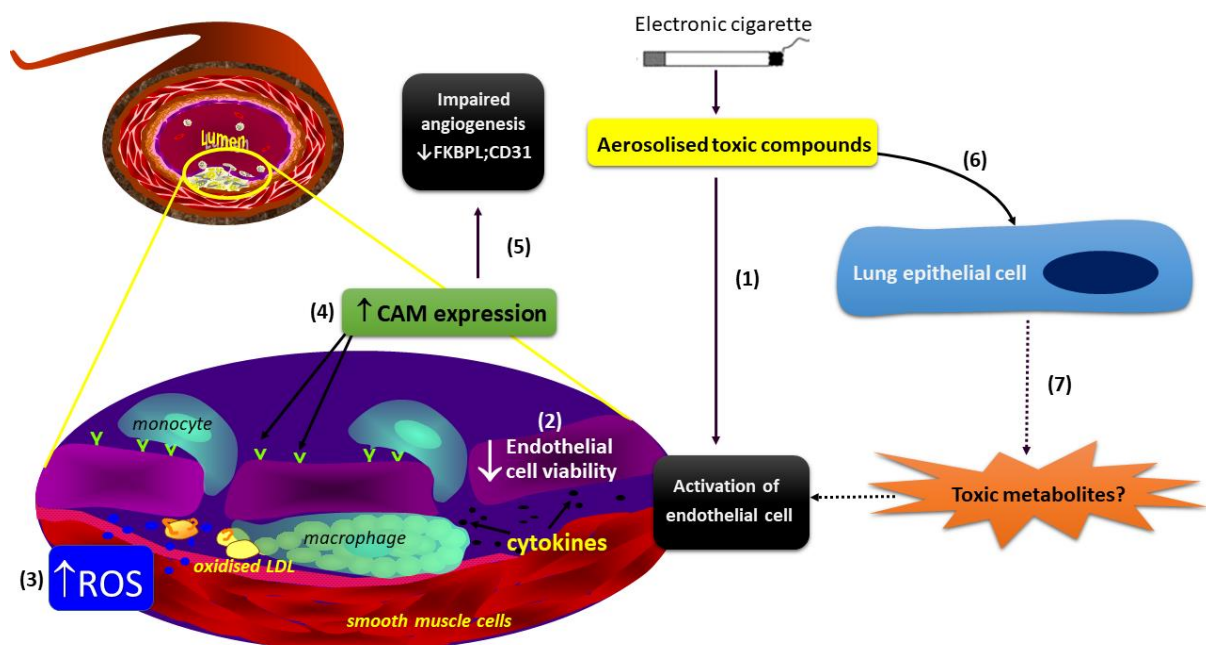


Figure 6.1 Schematic representation of the effect of E-cigarette aerosol directly on endothelial cell function or after first-pass metabolism by epithelial lung cells. Aerosolised toxic compounds from e-Cigs can incite endothelial cell activation. Resultant effects of decreased cell viability, increased ROS, increased CAM expression, and impaired angiogenesis follow. After first pass metabolism of epithelial cells, an enhanced effect may be pronounced.

In Chapter 3, 2D and 3D *in vitro* experiments were designed to better elucidate FKBPL-mediated mechanism in cardiac fibrosis and evaluate the therapeutic potential of FKBPL-based peptide mimetic, AD-01. The novelty of this chapter also lies within the methodology used to develop innovative 3D bioprinted model of cardiac fibrosis with specific cardiac peptides being added within the extracellular matrix (ECM) and the exposure to profibrotic stimuli including TGF- β and hypoxia-inducible factor- (HIF1- α). The impact of low FKBPL expression and/or AD-01 treatment was determined on cardiac pro-fibrotic genes expression, α -SMA regulation and monocyte adhesion in 2D models of cardiac fibrosis, recapitulating common features of cardiac fibrosis. In our new 3D bioprinted model of cardiac fibrosis, we determined cell proliferation, fibroblast cell survival and network formations as well as expression of FKBPL and vimentin. Vimentin was used to label all fibroblasts whereas FKBPL expression and regulation in profibrotic and hypoxic 3D environments shed new light on its importance in cardiac fibrosis processes. The findings of this work do not only introduce novel mechanism, centred around FKBPL, in cardiac fibrosis, condition with poorly understood pathogenesis, but also demonstrated the development of a robust 3D bioprinted model of cardiac fibrosis that can be used for high-throughput screening of future cardiac fibrosis therapies. Finally, we have also shown using the cardiac tissue from *fkbp1*^{+/-} transgenic mice, an increased collagen deposition and expression of *col1a1* gene responsible for synthesis of collagen, compared to wild-type mice.

In Chapter 4, we progressed to elucidate the importance of FKBPL in HFpEF and hypertrophic cardiomyopathy using clinical samples and *in vitro* model of cardiomyoblast hypertrophy. We investigated the effects of both angiotensin-II (Ang-II) and/or AD-01 treatments on cardiomyoblast nucleus and cell size, and FKBPL

expression. In collaboration with clinical cardiologists from various hospitals in Serbia and the Republic of Ireland, we determined FKBPL plasma concentration in three different types of HFpEF including chronic and acute HFpEF, and hypertrophic cardiomyopathy, compared to controls without CVD, as well as correlations with important echocardiography parameters. Here, we examined the role of FKBPL in the pathogenesis of cardiac hypertrophy as it is the subtype of HFpEF that is the most difficult to diagnose due to its heterogenous pathology⁷⁴. The findings of this work show, for the first time, that FKBPL mechanism could be important in the pathogenesis of HFpEF and that AD-01 could be a viable treatment for this condition¹¹⁶. As part of this chapter, we also carried our meta-analysis to evaluate current biomarkers for diagnosis of HFpEF. Our study is the first study to provide comprehensive and systematic review of current biomarkers used for diagnosis of HFpEF. The study reinforced that natriuretic peptides (BNP and NT-proBNP) are still the most reliable and widely used biomarkers despite their lack of specificity for this phenotype of HF. Our systematic review clearly outlines the need for more specific and improved biomarkers for HFpEF as well as inclusion of emerging biomarkers, galectin-3 (Gal-3) and suppression of tumorigenesis-2 (ST2), in larger studies¹¹⁷.

In the final chapter, given that cardiac remodelling is a common feature in people with DM and the underlying cause of CVD in this population¹¹⁸, we conducted a scoping review with the aim to assess the state of biomarkers currently used to detect signs of cardiac remodelling in people with DM. Cardiac remodelling can be one of the earliest signs of deteriorating cardiac health, however the mechanisms involved can differ in DM⁹⁸. In this paper, we aimed to elucidate the relationship between DM and CVD in the context of early cardiac remodelling. Through our assessment of the current

clinical biomarkers used to determine early cardiac remodelling in DM, we wanted to highlight the usefulness of these biomarkers in a clinical setting. Also, we discuss the diagnostic potential of other biomarkers through their relevance to the pathogenic mechanisms involved in DM-induced heart disease. Although we did not investigate the FKBPL mechanism in this context, it should be part of the future work especially in light of published research, which suggests that plasma FKBPL is increased in people with DM or CVD but not when the two are combined, suggesting a compensatory mechanism⁹⁸. Mechanisms of this compensation might involve certain miRNAs and should be investigated in future studies. Better understanding of the mechanisms involved in CVD including FKBPL, could lead to improved diagnosis, monitoring, treatment and prognosis in a clinical setting, improving patient quality of life and survival. FKBPL-based peptide, AD-01, could represent a new therapy for Ang-II-induced hypertrophic cardiomyopathy whereas lower expression of FKBPL could be beneficial in cardiac fibrosis. FKBPL could also be harnessed as a diagnostic and prognostic biomarker in the future, perhaps in combination with BNP/NT-proBNP or Gal-3, which could improve sensitivity of the diagnosis and prognosis of HFpEF as a heterogenous and multifactorial disease.

6.1.1 E-cigarettes as an emerging threat for CVDs

The prevalence of e-Cig use is rapidly rising amongst all age groups and is quickly becoming a public health concern¹¹⁹. The perceived harmlessness of e-Cigs are generally attributed to the lack of combustion within the devices, however, new studies are quickly refuting this mindset with more evidence revealing its negative cardiovascular effects¹¹⁹. In examining the effects of e-Cigs on endothelial cell health

in Chapter 2, we showed the cytotoxic effects of EAC across all treatment conditions through a significant decrease in cell viability and increase in ROS that remained consistent after first pass metabolism of epithelial lung cells. Additionally, inflammatory cellular adhesion molecules (CAMs) were significantly increased at the mRNA level, but not in protein expression. Measured membrane conductance, indicative of permeability, was also significantly increased in the presence of nicotine. Furthermore, in elucidating the role of FKBPL within e-Cig-mediated impact on the heart health, we revealed a trend of increasing FKBPL expression *in vivo* that is significant in the presence of nicotine.

Although the exact mechanisms of the e-Cig aerosol on endothelial cell health is yet to be determined, it is possible that it is caused by the aerosolised by-products of e-liquid. Particulates and by-products produced in the aerosol may possibly induce a proinflammatory response and disrupt endothelial homeostasis, leading to endothelial dysfunction¹²⁰. Studies have found that the constituents of e-liquid (PG, VG, nicotine) can undergo thermal decomposition and produce carbonyl compounds that are cytotoxic such as formaldehyde, acrolein, and acetylaldehyde, which are also present within tobacco cigarettes^{40,121,122}. There are many other factors including the e-Cig device and settings, e-liquid, and user habits that could contribute to the production of these toxic aerosol by-products^{123,124}. There also exists a possible nicotine-mediated mechanism on endothelial dysfunction as previous research indicates that nicotinic acetylcholine receptors (nAChRs), when binded to, can induce NO bioavailability and eNOS uncoupling, increasing angiogenesis, and possibly inflammatory mediators^{125,126}. This is supported by the findings in this study where significant

increases in CAM mRNA and CD31 and FKBPL protein expression was only seen within conditions with nicotine *ex vivo*. Similarly, in a study conducted by Janusewski et al. 2020⁹⁸, where FKBPL plasma concentration was correlated with smoking status, the highest FKBPL concentration was observed in patients who are current smokers, followed by ex-smokers, and non-smokers. However, signs of deteriorating endothelial cell health remained present even in conditions without nicotine that suggest other constituents of e-liquid can have similar cytotoxic effects apart from nicotine and should be explored further. Hence, from these findings it is possible that e-Cigs can cause inflammation and vascular damage, leading to the development of endothelial dysfunction and further CVDs. However, further research is required to understand this topic in more depth.

6.1.2 FKBPL-mediated mechanism in the development of cardiac hypertrophy and fibrosis

The development of cardiac fibrosis initially begins with pathogenic cardiac remodelling that is characterised by cardiac fibroblast differentiation into myofibroblasts, increased collagen synthesis and deposition, and the remodelling of the ECM. Key pathways that have been implicated in the cardiac remodelling process are the inflammatory NF- κ B and pro-fibrotic TGF- β pathways that recruit immune cells to the site of cardiac tissue damage, and direct fibroblast proliferation and differentiation into myofibroblasts respectively^{64,65}. Previous studies showed that FKBPL regulates a number of downstream pathways including the STAT3, HSP90, CD44, and NF- κ B pathways, although this was shown in the cancer settings, all of these pathways play an important role in the pathophysiology of HF, and similarly may

be implicated in cardiac remodelling^{127–129}. As described above, it has been shown that in cardiac fibroblasts, TGF- β leads to increased expression of FKBPL¹⁰¹. In our study, we showed that lower expression of FKBPL could be protective against cardiac fibrosis through downregulation of α -SMA that is highly expressed on pro-fibrotic myofibroblasts. On the other hand, treatment with AD-01, exacerbated, in the presence of TGF- β , the expression of *col1a1* gene, responsible for collagen synthesis, and metalloproteinase-2 (MMP2) responsible for degradation of type IV collagen within the ECM¹³⁰, showing aggravation of cardiac fibrosis features. Surprisingly, in the presence of hypoxic stimuli (i.e. DMOG), the effect of TGF- β ±AD-01 on *col1a1* was abrogated. In the 3D bioprinted model, both TGF- β , DMOG (hypoxic mimic) with or without AD-01 led to an increase in network formation by fibroblasts whilst downregulating FKBPL, perhaps as part of a compensatory mechanism. This was particularly prominent with DMOG reflective of hypoxic conditions. However, the specific role FKBPL has in cardiac remodelling needs to be further explored as well as the interplay between TGF- β , HIF-1 α and FKBPL or AD-01.

Furthermore, the findings of another study, presented within the Chapter 4, show FKBPL's hypertrophic effect on cardiomyoblast cells that is abrogated in the presence of Ang-II in an *in vitro* model. Both cell and nucleus size of cardiomyoblasts were significantly increased when treated with Ang-II or AD-01 individually, but when combined, AD-01 mitigated the hypertrophic effects. Interesting, whilst both AD-01 and Ang-II individually increased the expression of FKBPL, when used in combination FKBPL expression was reduced in association with a reduction in cardiomyoblasts hypertrophy. This suggests that similarly to cardiac fibrosis, lower FKBPL levels could be beneficial in hypertrophic cardiomyopathy and HFpEF. This was supported in the transgenic *fkbp1*^{+/-} mouse model, where collagen deposition and *col1a1* gene

expression were also reduced. Nevertheless, previous study has shown that whilst lower expression of FKBPL showed pro-angiogenic effect in *fkbp1*^{+/-} transgenic mice compared to wild type controls, the vascular and endothelial cell integrity was compromised⁹⁹. Therefore, this effect of low FKBPL levels on endothelial cells needs to be taken into the account in the context of cardiac fibrosis and HFpEF.

Importantly, Ang-II induces cardiac remodelling through the RAAS pathways and neuroendocrine signalling of the sympathetic nervous system increasing interstitial fibrosis and cardiac hypertrophy through the NF-κB and TGF-β pathways⁶⁴. Interestingly, in our study Ang-II whilst inducing cardiomyoblast hypertrophy, it also increased the expression of FKBPL, which was abrogated in the presence of AD-01. Additionally, in examining the regulation of the fibrotic gene (*post1*, *fsp-1*, *col1a1*, *ctgf* and *mmp2*) in fibroblast cells in the presence of hypoxic and fibrotic stimuli, low FKBPL did not seem to have an effect. However, in terms of *col1a1*, which is a master regulator of collagen production, the presence of AD-01 together with TGF-β, in low FKBPL settings, reduced the expression of this gene. In this context, where FKBPL expression is lowered, AD-01 seems to have a compensatory effect, abrogating profibrotic genes including MMP2. This was not observed with α-SMA protein levels where lower FKBPL expression in control settings (without TGF-β ± AD-01) led to a decrease in α-SMA protein expression. This implicates FKBPL within the mechanisms involved in ECM remodelling that can lead to cardiac fibrosis, where collagen deposition is a key process in the scar formation and reduction in contractility of the heart⁶⁴. Similarly, α-SMA expression is indicative of fibroblast transformation into myofibroblasts, which are essential to the remodelling process. These findings suggest a cardioprotective role of low FKBPL within cardiac fibrosis as a measure to mitigate structural changes and inhibit the onset of HF.

6.1.3 FKBPL's biomarker potential in C D and HF

HF incidence and burden is continually increasing in developed countries, where the early diagnosis of the disease is essential to improving patient prognosis and outcomes. The population of HF patients are evenly split amongst HFrEF and HFpEF patients, with both subtypes having a mortality rate of 50%, though the incidence of HFpEF is continually rising¹³¹. Due to the heterogeneity of HFpEF pathology, it is less understood in comparison to HFrEF, which has better outcomes^{74,132}. Currently, there exists only one category of biomarkers that is consistently used for the diagnosis of HF, natriuretic peptides, namely NT-proBNP and BNP. Natriuretic peptides are released by cardiomyocytes and cardiac fibroblasts upon mechanical stimulus of atrial or ventricular stretch, serving a reliable function for the early detection of HF and an early point of intervention^{133,134}. However, whilst natriuretic peptides are reliable in the diagnosis of HF, there remains some caveats in their diagnostic utility. Natriuretic peptides levels can be influenced by hypoxia, inflammation, and Ang-II¹³⁴ and can exhibit varying levels within different patient subgroups dependent on the age, sex, ethnicity, weight, and are also elevated in certain conditions including pulmonary embolism, renal failure, and T2DM^{133,135}. Hence there is the possibility of detecting false positives within patients when used as a sole diagnostic tool that urges for the identification of other potential biomarkers to be utilised in HF diagnosis, particularly HFpEF.

In assessing the current biomarkers for HFpEF, the results of our meta-analysis (Chapter 4) revealed that natriuretic peptides, namely NT-proBNP, retained the highest sensitivity and specificity in the diagnosis of chronic HFpEF patients. ST2 and Gal-3 were also identified as potential biomarkers from the screened studies, both of

which are inflammatory markers elevated in cases of CVD^{85,136}. However, ST2 revealed no significant diagnostic potential, whereas Gal-3 displayed promising potential. It should be noted that varying cut-off values and measurement in the chronic setting were observed where values are lower for these biomarkers, which could limit the application of these results in the acute settings. Conversely, the findings from the aforementioned scoping review (Chapter 5) that aimed to screen the diagnostic and prognostic biomarkers in cardiac remodelling in the context of DM, identified potentially new biomarkers that were implicated in the pathophysiology of DM-induced cardiomyopathy. From this study, we identified 15 unique biomarkers, with NT-proBNP being the most numerous. Despite being a reliable clinical biomarker, for the reasons listed above, NT-proBNP still has some limitations that may hinder its utility as a sole biomarker of cardiac remodelling. Notably, other emerging markers that were identified in addition to NT-proBNP were MMPs, hs (highly-sensitive)-CRP, hs-cTnT, Gal-3, and hs-ST2. In the niche patient population of these studies, we found that the diagnostic efficacy of a single biomarker, such as NT-proBNP, may be less effective than a combined measurement with other biomarkers. Similar to the identified markers from the meta-analysis in HFpEF, Gal-3 and ST2 were also identified in our scoping review that included only DM population. Although their diagnostic efficacy was not determined within this review due to the lack of studies reporting their role in cardiac remodelling in DM specifically, emphasis is placed on the inflammatory mechanisms within HF that may identify promising biomarkers for the diagnosis of HF and should be explored further in larger studies.

In examining the potential of biomarkers that are implicated in the mechanisms of HFpEF pathophysiology, FKBPL has shown promising potential in fulfilling this role. FKBPL's biomarker potential was examined through plasma concentration measurements in patients with different types of HFpEF, compared to non-CVD controls. Apart from FKBPL, NT-proBNP, an established clinical biomarker of HF, and Gal-3, a diverse marker with functionality within inflammation and fibrosis in myocardial remodelling¹³⁶, were also measured. Interestingly, there was no significant difference between plasma concentrations of these markers between different types of HFpEF including chronic and acute, HFpEF, and hypertrophic cardiomyopathy. No correlations between FKBPL and NT-proBNP or Gal-3 were observed, despite FKBPL being previously positively correlated with the natriuretic peptide, BNP, although in a more general CVD patient group without DM. In the same study, FKBPL and BNP exhibited similar AUC measurements reflective of their biomarker potential in CVD⁹⁸. Aligned to this study, FKBPL was positively correlated with intraventricular septal thickness in our study with HFpEF patients, likely reflective of its role in microvascular dysfunction, observed in the pathogenesis of HFpEF¹³⁷. These findings suggest a divergent mechanism of FKBPL within the microvascular and inflammatory complications of HFpEF, separate to NT-proBNP or Gal-3. As described above, *in vitro* studies supported these findings, demonstrating that FKBPL-based peptide mimetic, AD-01, abrogated hypertrophic effects of Ang-II induced remodelling in cardiomyoblasts in conjunction with increased expression of FKBPL. This suggests that FKBPL could be an early marker and therapeutic target of cardiac hypertrophy¹¹⁶. Ang-II signalling regulates natriuretic peptide secretion, that in addition to this proposed mechanism postures the potential biomarker combination of FKBPL and a natriuretic peptide for the early diagnosis of HF¹³⁴.

6.2 General conclusion

In conclusion, FKBPL mechanism is emerging as novel and important in the pathogenesis of heart disease leading to HF, by playing an important role in cardiac angiogenesis, fibrosis and hypertrophy. Given e-Cigs are becoming a new global health burden as part of the smoking cessation programs or recreational use, it is becoming evident that e-Cigs are harmful to both the respiratory and vascular health, perhaps even to a similar extent as traditional cigarettes. In this context, we report, for the first time, specific e-Cig toxicity on endothelial cells in a single and co-culture with lung epithelial cells, which are a first barrier of e-Cig entry. Also, nicotine seems to exacerbate the increase in the expression of FKBPL as an anti-angiogenic protein, and inflammatory CD31 and ICAM1 markers, suggesting that nicotine-containing e-Cigs might have worse impact on cardiovascular health and could, as other studies have shown, contribute to early atherogenesis¹³⁸.

Interestingly, based on our findings we suggest that low FKBPL expression in cardiac hypertrophy and fibrosis could be beneficial. Nevertheless, in the context of hypertrophic cardiomyopathy, FKBPL-based peptide mimetic, AD-01, potentially has a therapeutic role in reversing this process if induced by Ang-II. In lower FKBPL settings, in cardiac fibrosis models induced by TGF- β , AD-01 reduced pro-fibrotic *col1a1* gene expression. Whilst previous work has shown that AD-01 increases the expression of FKBPL in cancer cells⁸⁸, there seems to be a negative compensatory mechanism in fibroblasts and cardiomyoblasts on FKBPL expression, particularly in the presence of stress stimuli, with potential beneficial effects in cardiac hypertrophy and fibrosis.

In terms of the biomarker potential of FKBPL in HFpEF, given it likely has a role in the pathogenesis of this condition, it could be a helpful addition to current biomarkers, increasing sensitivity in HFpEF diagnosis in combination with NT-pro-BNP, BNP, Gal-3 and ST2. This is in light of its differential function to the current biomarkers, such as in cardiac angiogenesis and inflammatory responses.

These findings bring forth opportunities to elucidate the complex mechanisms underlying cardiac fibrosis and HF. The results of this thesis implicate FKBPL within the pathophysiology of cardiac ECM remodelling, where low FKBPL expression may contribute to a mitigative and cardioprotective role within cardiac fibrosis. Clinically, these finding presents the possibility of therapeutic intervention utilising FKBPL within the pathogenesis of cardiac fibrosis. In decreasing the burden of cardiac structural modelling, this may improve patient survival outcomes and the prognosis of HF. Similarly, in the evaluation of FKBPL as a potential biomarker for HFpEF, it presents a new perspective in the specific diagnosis of HF. As a supplementary biomarker to the clinical gold-standard natriuretic peptides, FKBPL's increased sensitivity in the diagnosis of HFpEF may improve the early detection and classification of HF, and the survival outcomes and prognosis of patients. Though, the findings in this thesis demonstrate the vast clinical utility and potential of FKBPL, further examination of FKBPL's mechanistic and biomarker role within the pathogenesis of HF is needed to establish its clinical relevance in the long term.

6.3 Future Perspectives

In light of the findings from the studies within this thesis, future perspectives pertaining to the specific mechanisms in which FKBPL and AD-01 may operate within cardiac fibrosis and HFpEF should be explored further to translate its use in a clinical context. The regulation of FKBPL by AD-01 in cardiac hypertrophy and fibrosis models, should include the use of FKBPL CRISPR-Cas9 gene delivery system that could stably knockdown or knockout FKBPL expression in both 2D and 3D bioprinted, models. It might be unachievable to induce a full knockout of FKBPL given its critical role in cell function and the fact that the full knockout is embryonically lethal in mice⁸⁸.

This work presents solid evidence towards moving to *in vivo*, to evaluate AD-01's potential in the murine or rat models of HFpEF or cardiac fibrosis, including in *fkbp1*^{+/-} mice and wild types. The models could include but are not limited to Ang-II infusion¹³⁹, transverse aortic constriction-induced pressure overload and/or high fat diet (HFD) together with eNOS inhibitor, L-NAME continuous administration¹⁴⁰. The dosing schedule of AD-01 should be carefully planned in these experiments and smaller doses might be required to prevent an unintentional upregulation of FKBPL. Another interesting revenue to explore would be inducing DM by using streptozotocin injection \pm HFD in *fkbp1*^{+/-} mice \pm AD-01 and evaluating the consequences on the cardiac function using echocardiography, blood pressure monitoring and *ex vivo* histology (picrosirius red) and protein/mRNA expression of cardiac remodelling, inflammatory and fibrosis markers. Single cell sequencing of the heart tissue would also be beneficial to determine cell-specific effects and mechanisms. In terms of FKBPL's biomarker potential in HFpEF diagnosis and prognosis, larger well-characterised

cohort studies are needed with follow-up patient information, that should compare well-known biomarkers of HFpEF to FKBPL. Together, these studies will further establish FKBPL's role within HF pathophysiology and open the discussion of its therapeutic applications and clinical utility.

References

1. Mattingly, Q. Cardiovascular diseases. *World Health Organisation* https://www.who.int/health-topics/cardiovascular-diseases/#tab=tab_1/ (2024)
2. Heart, stroke & vascular diseases Overview. *Australian Institute of Health and Welfare* <https://www.aihw.gov.au/reports-data/health-conditions-disability-deaths/heart-stroke-vascular-diseases/overview/> (2023).
3. Stewart, J., Manmathan, G. & Wilkinson, P. Primary prevention of cardiovascular disease: A review of contemporary guidance and literature. *JRSM Cardiovasc Dis* **6**, 204800401668721 (2017).
4. Lazar, S., Rayner, B., Lopez Campos, G., McGrath, K. & McClements, L. Mechanisms of heart failure with preserved ejection fraction in the presence of diabetes mellitus. *Translational Metabolic Syndrome Research* **3**, 1–5 (2020).
5. Gaziano, T., Reddy, K. S., Paccaud, F., Horton, S. & Chaturvedi, V. Cardiovascular Disease. *Disease Control Priorities in Developing Countries* (2006).
6. Lopez, E. O., Ballard, B. D. & Jan, A. Cardiovascular Disease. *Nursing (Brux)* (2022).
7. Australian Bureau of Statistics. Heart, stroke and vascular disease. *ABS*. <https://www.abs.gov.au/statistics/health/health-conditions-and-risks/heart-stroke-and-vascular-disease/latest-release/> (2022).
8. Biglu, M.-H., Ghavami, M. & Biglu, S. Cardiovascular diseases in the mirror of science. *J Cardiovasc Thorac Res* **8**, 158–163 (2016).
9. Mattingly, Q. Cardiovascular diseases. *World Health Organisation* https://www.who.int/health-topics/cardiovascular-diseases/#tab=tab_1/ (2024)
10. Jurgens, C. Y. *et al.* State of the Science: The Relevance of Symptoms in Cardiovascular Disease and Research: A Scientific Statement from the American Heart Association. *Circulation* **146**, E173–E184 (2022).
11. Barnes, V. A. & Orme-Johnson, D. W. Prevention and Treatment of Cardiovascular Disease in Adolescents and Adults through the Transcendental Meditation® Program: A Research Review Update. *Curr Hypertens Rev* **8**, 227 (2012).
12. Heart, stroke and vascular disease: Australian facts, Treatment and management - *Australian Institute of Health and Welfare*. <https://www.aihw.gov.au/reports/heart-stroke-vascular-diseases/hsvd-facts/contents/treatment-and-management/> (2023)
13. Gabb, G. M. *et al.* Guideline for the diagnosis and management of hypertension in adults — 2016. *Medical Journal of Australia* **205**, 85–89 (2016).
14. American Heart Association. Types of Heart Medications | *American Heart Association*. <https://www.heart.org/en/health-topics/heart-attack/treatment-of-a-heart-attack/cardiac-medications/> (2023)

15. Roth, G. A. *et al.* Global Burden of Cardiovascular Diseases and Risk Factors, 1990–2019: Update From the GBD 2019 Study. *J Am Coll Cardiol* **76**, 2982–3021 (2020).
16. Australian Bureau of Statistics. "Heart, stroke and vascular disease." *ABS* <https://www.abs.gov.au/statistics/health/health-conditions-and-risks/heart-stroke-and-vascular-disease/latest-release/> (2022)
17. Australian Institute of Health and Welfare. Heart, stroke and vascular disease: Australian facts, Expenditure on cardiovascular disease - *Australian Institute of Health and Welfare* <https://www.aihw.gov.au/reports/heart-stroke-vascular-disease/hsvd-facts/contents/impacts/expenditure-cvd/> (2023)
18. Ruan, Y. *et al.* Cardiovascular disease (CVD) and associated risk factors among older adults in six low-and middle-income countries: Results from SAGE Wave 1. *BMC Public Health* **18**, 1–13 (2018).
19. Marti, C. N. *et al.* Endothelial dysfunction, arterial stiffness, and heart failure. *Journal of the American College of Cardiology* **60**, 1455–1469 (2012).
20. Matsuzawa, Y., & Lerman, A. Endothelial dysfunction and coronary artery disease: assessment, prognosis, and treatment. *Coronary artery disease* **25**(8), 713–724 (2014).
21. Heusch, G., Libby, P., Gersh, B., Yellon, D., Böhm, M., Lopaschuk, G., & Opie, L. Cardiovascular remodelling in coronary artery disease and heart failure. *Lancet (London, England)* **383**(9932), 1933–1943 (2014).
22. Sun, H. J., Wu, Z. Y., Nie, X. W. & Bian, J. S. Role of endothelial dysfunction in cardiovascular diseases: The link between inflammation and hydrogen sulfide. *Front Pharmacol* **10**, 1568 (2020).
23. Rajendran, P. *et al.* The Vascular Endothelium and Human Diseases. *Int J Biol Sci* **9**, 1057 (2013).
24. Boulanger, C. M. Endothelium. *Arterioscler Thromb Vasc Biol* **36**, e26–e31 (2016).
25. Hirata, Y. *et al.* Diagnosis and Treatment of Endothelial Dysfunction in Cardiovascular Disease A Review. *Int Heart J* **51**, 1–6 (2010).
26. Endemann, D. H. & Schiffrin, E. L. Endothelial Dysfunction. *Journal of the American Society of Nephrology* **15**, 1983–1992 (2004).
27. Rajendran, P. *et al.* The Vascular Endothelium and Human Diseases. *Int. J. Biol. Sci* **9**, (2013).
28. Kota, S. *et al.* Aberrant angiogenesis: The gateway to diabetic complications. *Indian J Endocrinol Metab* **16**, 918 (2012).
29. Cai, H. & Harrison, D. G. Endothelial Dysfunction in Cardiovascular Diseases: The Role of Oxidant Stress. *Circ Res* **87**, 840–844 (2000).

30. Mudau, M., Genis, A., Lochner, A. & Strijdom, H. Endothelial dysfunction: the early predictor of atherosclerosis. *Cardiovasc J Afr* **23**, 222–231 (2012).
31. Davignon, J. & Ganz, P. Role of Endothelial Dysfunction in Atherosclerosis. *Circulation* **109**, III-27-III–32 (2004).
32. Liu, T., Zhang, L., Joo, D. & Sun, S. C. NF-κB signaling in inflammation. *Signal Transduction and Targeted Therapy* **2017 2:1 2**, 1–9 (2017).
33. Libby, P., Ridker, P. M. & Hansson, G. K. Progress and challenges in translating the biology of atherosclerosis. *Nature* **473**, 317–325 (2011).
34. Schiffrin, E. L. Role of Endothelin-1 in Hypertension. *Hypertension* **34**, 876–881 (1999).
35. Farsalinos, K. E. *et al.* Nicotine absorption from electronic cigarette use: Comparison between first and new-generation devices. *Sci Rep* **3**, (2014).
36. Tayyarah, R. & Long, G. A. Comparison of select analytes in aerosol from e-cigarettes with smoke from conventional cigarettes and with ambient air. *Regulatory Toxicology and Pharmacology* **70**, 704–710 (2014).
37. Tan, A. S. L. & Bigman, C. A. E-Cigarette Awareness and Perceived Harmfulness Prevalence and Associations with Smoking-Cessation Outcomes. *Am J Prev Med* **47**, 141–149 (2014).
38. Mantey, D. S., Cooper, M. R., Clendennen, S. L., Pasch, K. E. & Perry, C. L. E-Cigarette Marketing Exposure Is Associated With E-Cigarette Use Among US Youth. *Journal of Adolescent Health* **58**, 686–690 (2016).
39. Tegin, G., Mekala, H. M., Sarai, S. K. & Lippmann, S. E-cigarette toxicity? *Southern Medical Journal* **111**, 35–38 (2018).
40. Goniewicz, M. L. *et al.* Levels of selected carcinogens and toxicants in vapour from electronic cigarettes. *Tob Control* **23**, 133–139 (2014).
41. Osei, A. D. *et al.* Association Between E-Cigarette Use and Cardiovascular Disease Among Never and Current Combustible-Cigarette Smokers. *Am J Med* **132**, 949-954.e2 (2019).
42. Moheimani, R. S. *et al.* Increased Cardiac Sympathetic Activity and Oxidative Stress in Habitual Electronic Cigarette Users: Implications for Cardiovascular Risk. *JAMA Cardiol* **2**, 278 (2017).
43. Schweitzer, K. S. *et al.* Endothelial disruptive proinflammatory effects of nicotine and e-cigarette vapor exposures. *Am J Physiol Lung Cell Mol Physiol* **309**, 175–187 (2015).
44. Kuntic, M., Oelze, M., Steven, S., Kröller-Schön, S., Stamm, P., Kalinovic, S., Frenis, K., Vujacic-Mirski, K., Bayo Jimenez, M. T., Kvandova, M., Filippou, K., Al Zuabi, A., Brückl, V., Hahad, O., Daub, S., Varveri, F., Gori, T., Huesmann, R., Hoffmann, T., Schmidt, F. P., ... Münzel, T. Short-term e-cigarette vapour exposure causes vascular oxidative stress and dysfunction: evidence for a close

- connection to brain damage and a key role of the phagocytic NADPH oxidase (NOX-2). *European heart journal* **41**(26), 2472–2483 (2020).
45. Lerner, C. A. *et al.* Vapors produced by electronic cigarettes and E-juices with flavorings induce toxicity, oxidative stress, and inflammatory response in lung epithelial cells and in mouse lung. *PLoS One* **10**, e0116732 (2015).
 46. Tarran, R. *et al.* E-Cigarettes and Cardiopulmonary Health. *Function* **2**, 4 (2021).
 47. Navas-Acien, A. *et al.* Early Cardiovascular Risk in E-cigarette Users: the Potential Role of Metals. *Curr Environ Health Rep* **7**, 353–361 (2020).
 48. Putzhammer, R. *et al.* Vapours of US and EU Market Leader Electronic Cigarette Brands and Liquids Are Cytotoxic for Human Vascular Endothelial Cells. *PLoS One* **11**, e0157337 (2016).
 49. Carnevale, R. *et al.* Acute Impact of Tobacco vs Electronic Cigarette Smoking on Oxidative Stress and Vascular Function. *Chest* **150**, 606–612 (2016).
 50. Krishna Kolluru, G., Bir, S. C., Kevil, C. G. & Calvert, J. W. Endothelial Dysfunction and Diabetes: Effects on Angiogenesis, Vascular Remodeling, and Wound Healing. *Int J Vasc Med* **2012**, 30 (2012).
 51. WHO. Panos. Loke, A. Diabetes. *World Health Organisation* https://www.who.int/health-topics/diabetes#tab=tab_2/ (2023)
 52. Ramachandran, A. Know the signs and symptoms of diabetes. *Indian J Med Res* **140**, 579 (2014).
 53. Cheng, R., & Ma, J. X. Angiogenesis in diabetes and obesity. *Reviews in endocrine & metabolic disorders* **16**(1), 67–75 (2015).
 54. Regina, C. C., Mu'ti, A. & Fitriany, E. Diabetes Mellitus Type 2. *Verdure: Health Science Journal* **3**, 8–17 (2022).
 55. Petrie, J. R., Guzik, T. J. & Touyz, R. M. Diabetes, Hypertension, and Cardiovascular Disease: Clinical Insights and Vascular Mechanisms. *Can J Cardiol* **34**, 575 (2018).
 56. Tuleta, I. & Frangogiannis, N. G. Diabetic fibrosis. *Biochimica et Biophysica Acta (BBA) - Molecular Basis of Disease* **1867**, 166044 (2021).
 57. Strain, W. D. & Paldánus, P. M. Diabetes, cardiovascular disease and the microcirculation. *Cardiovascular Diabetology* **2018 17:1** **17**, 1–10 (2018).
 58. Jia, G., Hill, M. A. & Sowers, J. R. Diabetic Cardiomyopathy. *Circ Res* **122**, 624–638 (2018).
 59. Tan, Y., Zhang, Z., Zheng, C., Wintergerst, K. A., Keller, B. B., & Cai, L. Mechanisms of diabetic cardiomyopathy and potential therapeutic strategies: preclinical and clinical evidence. *Nature reviews. Cardiology* **17**(9), 585–607 (2020).

60. Rydén, L. *et al.* Guidelines on diabetes, pre-diabetes, and cardiovascular diseases: executive summary The Task Force on Diabetes and Cardiovascular Diseases of the European Society of Cardiology (ESC) and of the European Association for the Study of Diabetes (EASD). *Eur Heart J* **28**, 88–136 (2007).
61. Heusch, G. *et al.* Cardiovascular remodelling in coronary artery disease and heart failure. *The Lancet* **383**, 1933–1943 (2014).
62. Wu, Q. Q. *et al.* Mechanisms contributing to cardiac remodelling. *Clin Sci* **131**, 2319–2345 (2017).
63. Grieve, D. J., Byrne, J. A., Cave, A. C. & Shah, A. M. Role of Oxidative Stress in Cardiac Remodelling after Myocardial Infarction. *Heart Lung Circ* **13**, 132–138 (2004).
64. Frangogiannis, N. G. Cardiac fibrosis. *Cardiovasc Res* **117**, 1450–1488 (2021).
65. Travers, J. G., Kamal, F. A., Robbins, J., Yutzey, K. E. & Blaxall, B. C. Cardiac fibrosis: The fibroblast awakens. *Circ Res* **118**, 1021–1040 (2016).
66. Steyers, C. M. & Miller, F. J. Endothelial Dysfunction in Chronic Inflammatory Diseases. *Int. J. Mol. Sci* **15**, 11324–11349 (2014).
67. Baker, R. G., Hayden, M. S. & Ghosh, S. NF- κ B, inflammation, and metabolic disease. *Cell Metabolism* **13**, 11–22 (2011).
68. Ma, Z. G., Yuan, Y. P., Wu, H. M., Zhang, X. & Tang, Q. Z. Cardiac fibrosis: new insights into the pathogenesis. *Int J Biol Sci* **14**, 1645–1657 (2018).
69. Atherton, J. J., Audehm, R. & Connell, C. Heart Failure Guidelines. *Medicine Today* **20**, 14-24 (2019).
70. Bozkurt, B. *et al.* Universal definition and classification of heart failure: a report of the Heart Failure Society of America, Heart Failure Association of the European Society of Cardiology, Japanese Heart Failure Society and Writing Committee of the Universal Definition of Heart Failure. *Eur J Heart Fail* **23**, 352–380 (2021).
71. Baman, J. R. & Ahmad, F. S. Heart Failure. *JAMA* **324**, 1015 (2020).
72. Encyclopædia Britannica. (n.d.). Heart failure. *Britannica Academic* <https://academic-eb-com.ezproxy.lib.uts.edu.au/levels/collegiate/article/heart-failure/39721/> (2023)
73. Parsons, R. W. *et al.* The epidemiology of heart failure in the general Australian community - study of heart failure in the Australian primary care setting (SHAPE): methods. *BMC Public Health* **20**, (2020).
74. Schwinger, R. H. G. Pathophysiology of heart failure. *Cardiovasc Diagn Ther* **11**, 263 (2021).
75. McDonagh, T. A. *et al.* 2021 ESC Guidelines for the diagnosis and treatment of acute and chronic heart failure Developed by the Task Force for the diagnosis

- and treatment of acute and chronic heart failure of the European Society of Cardiology (ESC) With the special contribution of the Heart Failure Association (HFA) of the ESC. *Eur Heart J* **42**, 3599–3726 (2021).
76. Bursi, F. *et al.* Systolic and diastolic heart failure in the community. *J Am Med Assoc* **296**, 2209–2216 (2006).
 77. Kemp, C. D. & Conte, J. V. The pathophysiology of heart failure. *Cardiovascular Pathology* **21**, 365–371 (2012).
 78. Dekkerlegand, J. Congestive Heart Failure. Evidence-Based Examination, Evaluation, and Intervention. *Physical Rehabilitation* 669–688 (2007)
 79. Castiglione, V. *et al.* Biomarkers for the diagnosis and management of heart failure. *Heart Fail Rev* **27**, 625 (2022).
 80. Kuwahara, K. The natriuretic peptide system in heart failure: Diagnostic and therapeutic implications. *Pharmacol Ther* **227**, 107863 (2021).
 81. Nadar, S. K. & Shaikh, M. M. Biomarkers in Routine Heart Failure Clinical Care. *Card Fail Rev* **5**, 50 (2019).
 82. Atherton, J. J. *et al.* National Heart Foundation of Australia and Cardiac Society of Australia and New Zealand: Guidelines for the Prevention, Detection, and Management of Heart Failure in Australia 2018. *Heart Lung Circ* **27**, 1123–1208 (2018).
 83. Inamdar, A. & Inamdar, A. Heart Failure: Diagnosis, Management and Utilization. *J Clin Med* **5**, 62 (2016).
 84. Sinning, C., Kempf, T., Schwarzl, M., Lanfermann, S., Ojeda, F., Schnabel, R. B., Zengin, E., Wild, P. S., Lackner, K. J., Munzel, T., Blankenberg, S., Wollert, K. C., Zeller, T., & Westermann, D. Biomarkers for characterization of heart failure - Distinction of heart failure with preserved and reduced ejection fraction. *International journal of cardiology* **227**, 272–277 (2017).
 85. Ip, C. *et al.* Soluble suppression of tumorigenicity 2 (sST2) for predicting disease severity or mortality outcomes in cardiovascular diseases: A systematic review and meta-analysis. *Int J Cardiol Heart Vasc* **37**, 100887 (2021).
 86. Robson, T. & James, I. F. The therapeutic and diagnostic potential of FKBPL; a novel anticancer protein. *Drug Discov Today* **17**, 544–548 (2012).
 87. Valentine, A. *et al.* FKBPL and Peptide Derivatives: Novel Biological Agents That Inhibit Angiogenesis by a CD44-Dependent Mechanism. *Clinical Cancer Research* **17**, 1044–1056 (2011).
 88. Yakkundi, A. *et al.* The Anti-Migratory Effects of FKBPL and Its Peptide Derivative, AD-01: Regulation of CD44 and the Cytoskeletal Pathway. *PLoS One* **8**, e55075–e55075 (2013).

89. Kang, C. B., Hong, Y., Dhe-Paganon, S. & Yoon, H. S. FKBP family proteins: Immunophilins with versatile biological functions. *NeuroSignals* **16**, 318–325 (2008).
90. Yakkundi, A. *et al.* FKBPL is a critical antiangiogenic regulator of developmental and pathological angiogenesis. *Arterioscler Thromb Vasc Biol* **35**, 845–854 (2015).
91. McClements, L., Annett, S., Yakkundi, A., O'Rourke, M., Valentine, A., Moustafa, N., Alqudah, A., Simões, B. M., Furlong, F., Short, A., McIntosh, S. A., McCarthy, H. O., Clarke, R. B., & Robson, T. FKBPL and its peptide derivatives inhibit endocrine therapy resistant cancer stem cells and breast cancer metastasis by downregulating DLL4 and Notch4. *BMC cancer* **19**(1), 351 (2019).
92. Annett, S. *et al.* FKBPL-based peptide, ALM201, targets angiogenesis and cancer stem cells in ovarian cancer. *Br J Cancer* **122**, 361–371 (2020).
93. McClements, L. *et al.* Targeting treatment-resistant breast cancer stem cells with FKBPL and Its peptide derivative, AD-01, via the CD44 pathway. *Clinical Cancer Research* **19**, 3881–3893 (2013).
94. Helali, A. *et al.* 383PA phase I dose-escalation study of the novel peptide ALM201 in patients (pts) with advanced solid tumours. *Annals of Oncology* **28**, (2017).
95. Senbanjo, L. T. & Chellaiah, M. A. CD44: A multifunctional cell surface adhesion receptor is a regulator of progression and metastasis of cancer cells. *Frontiers in Cell and Developmental Biology* **5** (2017).
96. Tsuneki, M. & Madri, J. A. CD44 regulation of endothelial cell proliferation and apoptosis via modulation of CD31 and VE-cadherin expression. *Journal of Biological Chemistry* **289**, 5357–5370 (2014).
97. Granger, D. N. & Senchenkova. Angiogenesis. *Inflammation and the Microcirculation* (2010).
98. Januszewski, A. S. *et al.* FKBPL is associated with metabolic parameters and is a novel determinant of cardiovascular disease. *Scientific Reports* **2020 10:1** **10**, 1–7 (2020).
99. Yakkundi, A. *et al.* FKBPL is a critical antiangiogenic regulator of developmental and pathological angiogenesis. *Arterioscler Thromb Vasc Biol* **35**, 845–54 (2015).
100. Alqudah, A. *et al.* Downregulation of FKBPL influences vascular and metabolic function in experimental model of diabetes. *Diabetologia* **61**, S16–S16 (2018).
101. McClements, L., Rayner, B., Alqudah, A., Grieve, D. & Robson, T. FKBPL, a novel player in cardiac ischaemia and fibrosis. *J Mol Cell Cardiol* **140**, 5 (2020).

102. Libby, P. Inflammatory Mechanisms: the Molecular Basis of Inflammation and Disease. *Nutr Rev* **65**, S140–S146 (2007).
103. Jeong, J. H., Ojha, U. & Lee, Y. M. Pathological angiogenesis and inflammation in tissues. *Archives of Pharmacal Research* **44**, 1–15 (2020).
104. Gogiraju, R., Bochenek, M. L. & Schäfer, K. Angiogenic Endothelial Cell Signaling in Cardiac Hypertrophy and Heart Failure. *Front Cardiovasc Med* **6**, 442692 (2019).
105. Donley, C. *et al.* Identification of RBCK1 as a novel regulator of FKBPL: Implications for tumor growth and response to tamoxifen. *Br Dent J* **217**, 3441–3450 (2014).
106. Tian, Y. *et al.* RBCK1 negatively regulates tumor necrosis factor- and interleukin-1- triggered NF- κ B activation by targeting TAB2/3 for degradation. *Journal of Biological Chemistry* **282**, 16776–16782 (2007).
107. Chirinos, J. A. *et al.* Multiple Plasma Biomarkers for Risk Stratification in Patients With Heart Failure and Preserved Ejection Fraction. *J Am Coll Cardiol* **75**, 1281–1295 (2020).
108. Chen, H. *et al.* Systemic Biomarkers and Unique Pathways in Different Phenotypes of Heart Failure with Preserved Ejection Fraction. *Biomolecules* **12**, 1419 (2022).
109. Suvakov, S. *et al.* Overlapping pathogenic signalling pathways and biomarkers in preeclampsia and cardiovascular disease. *Pregnancy Hypertens* **20**, 131–136 (2020).
110. Lam, C. S. P. *et al.* Mortality associated with heart failure with preserved vs. reduced ejection fraction in a prospective international multi-ethnic cohort study. *Eur Heart J* **39**, 1770–1780 (2018).
111. Osei, A. D. *et al.* Association Between E-Cigarette Use and Cardiovascular Disease Among Never and Current Combustible-Cigarette Smokers. *Am J Med* **132**, 949-954.e2 (2019).
112. Farsalinos, K. E., Polosa, R., Cibella, F., & Niaura, R. Is e-cigarette use associated with coronary heart disease and myocardial infarction? Insights from the 2016 and 2017 National Health Interview Surveys. *Therapeutic advances in chronic disease*, **10**, 2040622319877741 (2019).
113. NAHDAP. Population Assessment of Tobacco and Health (PATH) Study [United States] Public-Use Files. *National Addiction & HIV Data Archive Program* <https://www.icpsr.umich.edu/web/NAHDAP/studies/36498/versions/V16/> (2021)
114. Berlowitz, J. B. *et al.* E-Cigarette Use and Risk of Cardiovascular Disease: A Longitudinal Analysis of the PATH Study (2013-2019). *Circulation* **145**, 1557–1559 (2022).

115. Chhor, M. *et al.* E-Cigarette Aerosol Condensate Leads to Impaired Coronary Endothelial Cell Health and Restricted Angiogenesis. *Int J Mol Sci* **24**, 6378 (2023).
116. Chhor, M. *et al.* FK506-Binding Protein like (FKBPL) Has an Important Role in Heart Failure with Preserved Ejection Fraction Pathogenesis with Potential Diagnostic Utility. *Biomolecules* **13**, (2023).
117. Chen, H., Chhor, M., Rayner, B. S., McGrath, K. & McClements, L. Evaluation of the diagnostic accuracy of current biomarkers in heart failure with preserved ejection fraction: A systematic review and meta-analysis. *Arch Cardiovasc Dis* **114**, 793–804 (2021).
118. Chhor, M. *et al.* Diagnostic and prognostic biomarkers reflective of cardiac remodelling in diabetes mellitus: A scoping review. *Diabet Med* **40**, (2023).
119. Jongenelis, M. I. E-cigarette product preferences of Australian adolescent and adult users: a 2022 study. *BMC Public Health* **23**, 1–8 (2023).
120. Barber, K. E., Ghebrehiwet, B., Yin, W. & Rubenstein, D. A. Endothelial Cell Inflammatory Reactions Are Altered in the Presence of E-Cigarette Extracts of Variable Nicotine. *Cell Mol Bioeng* **10**, 124–133 (2017).
121. Behar, R. Z., Wang, Y. & Talbot, P. Comparing the cytotoxicity of electronic cigarette fluids, aerosols and solvents. *Tob Control* **27**, 325 (2018).
122. Kosmider, L. *et al.* Carbonyl Compounds in Electronic Cigarette Vapors: Effects of Nicotine Solvent and Battery Output Voltage. *Nicotine & Tobacco Research* **16**, 1319 (2014).
123. Li, G. *et al.* Impact of maternal e-cigarette vapor exposure on renal health in the offspring. *Ann N Y Acad Sci* **1452**, 65–77 (2019).
124. Chen, H. *et al.* Maternal E-cigarette exposure in mice alters DNA methylation and lung cytokine expression in offspring. *Am J Respir Cell Mol Biol* **58**, 366–377 (2018).
125. Münzel, T., Sinning, C., Post, F., Warnholtz, A. & Schulz, E. Pathophysiology, diagnosis and prognostic implications of endothelial dysfunction. *Annals of Medicine* **40** 180–196 (2008).
126. Lee, J. & Cooke, J. P. Nicotine and Pathological Angiogenesis. *Life Sci* **91**, 1058 (2012).
127. Annett, S. *et al.* FKBPL-based peptide, ALM201, targets angiogenesis and cancer stem cells in ovarian cancer. *Br J Cancer* **122**, 361 (2020).
128. Yakkundi, A. *et al.* The Anti-Migratory Effects of FKBPL and Its Peptide Derivative, AD-01: Regulation of CD44 and the Cytoskeletal Pathway. *PLoS One* **8**, e55075 (2013).

129. Annett, S. L. *et al.* The Immunophilin Protein FKBPL and its Peptide Derivatives are Novel Regulators of Vascular Integrity and Inflammation via Nf-κB Signaling. *SSRN Electronic Journal* (2021) doi:10.2139/SSRN.3858052.
130. Monaco, S. *et al.* Enzymatic processing of collagen IV by MMP-2 (gelatinase A) affects neutrophil migration and it is modulated by extracatalytic domains. *Protein Sci* **15**, 2805 (2006).
131. Roger, V. L. Epidemiology of Heart Failure. *Circ Res* **128**, 1421–1434 (2021).
132. Gazewood, J. D. & Turner, P. L. Heart Failure with Preserved Ejection Fraction: Diagnosis and Management. *Am Fam Physician* **96**, 582–588 (2017).
133. Roxana, M. E., Georgică, T., Ionuț, D., Gianina, M. & Cristina, F. Atrial and Brain Natriuretic Peptides- Benefits and Limits of their use in Cardiovascular Diseases. *Curr Cardiol Rev* **15**, 283 (2019).
134. Almeida, A. G. *NT-proBNP and Myocardial Fibrosis The Invisible Link Between Health and Disease**.
135. Lewis, R. A., Durrington, C., Condliffe, R. & Kiely, D. G. BNP/NT-proBNP in pulmonary arterial hypertension: time for point-of-care testing? *European Respiratory Review* **29**, (2020).
136. Zhong, X., Qian, X., Chen, G. & Song, X. The role of galectin-3 in heart failure and cardiovascular disease. *Clin Exp Pharmacol Physiol* **46**, 197–203 (2019).
137. Kansal, S., Roitman, D. & Sheffield, L. T. Interventricular septal thickness and left ventricular hypertrophy. An echocardiographic study. *Circulation* **60**, 1058–1065 (1979).
138. George, J. *et al.* Cardiovascular Effects of Switching From Tobacco Cigarettes to Electronic Cigarettes. *J Am Coll Cardiol* **74**, 3112–3120 (2019).
139. Valero-Muñoz, M., Backman, W. & Sam, F. Murine Models of Heart Failure With Preserved Ejection Fraction: A “Fishing Expedition”. *JACC Basic Transl Sci* **2**, 770 (2017).
140. LaPenna, K. *et al.* A Novel Mouse Model of Cardiometabolic Heart Failure with Preserved Ejection Fraction. *The FASEB Journal* **35**, (2021).

Appendix



Article

E-Cigarette Aerosol Condensate Leads to Impaired Coronary Endothelial Cell Health and Restricted Angiogenesis

Michael Chhor¹, Esra Tulpar¹, Tara Nguyen¹, Charles G. Cranfield¹ , Catherine A. Gorrie¹, Yik Lung Chan¹, Hui Chen¹ , Brian G. Oliver¹ , Lana McClements^{1,2,*} and Kristine C. McGrath^{1,*}

¹ School of Life Sciences, Faculty of Science, University of Technology Sydney, Sydney, NSW 2007, Australia; michael.chhor@student.uts.edu.au (M.C.); esra.s.tulpar@student.uts.edu.au (E.T.); tara.nguyen@uts.edu.au (T.N.); charles.cranfield@uts.edu.au (C.G.C.); catherine.gorrie@uts.edu.au (C.A.G.); yik.chan@uts.edu.au (Y.L.C.); hui.chen-1@uts.edu.au (H.C.); brian.oliver@uts.edu.au (B.G.O.)

² Institute for Biomedical Materials and Devices, Faculty of Science, University of Technology Sydney, Sydney, NSW 2007, Australia

* Correspondence: lana.mcclements@uts.edu.au (L.M.); kristine.mcgrath@uts.edu.au (K.C.M.)

Abstract: Cardiovascular disease (CVD) is a leading cause of mortality worldwide, with cigarette smoking being a major preventable risk factor. Smoking cessation can be difficult due to the addictive nature of nicotine and the withdrawal symptoms following cessation. Electronic cigarettes (e-Cigs) have emerged as an alternative smoking cessation device, which has been increasingly used by non-smokers; however, the cardiovascular effects surrounding the use of e-Cigs remains unclear. This study aimed to investigate the effects of e-Cig aerosol condensate (EAC) (0 mg and 18 mg nicotine) in vitro on human coronary artery endothelial cells (HCAEC) and in vivo on the cardiovascular system using a mouse model of 'e-vaping'. In vitro results show a decrease in cell viability of HCAEC when exposed to EAC either directly or after exposure to conditioned lung cell media ($p < 0.05$ vs. control). Reactive oxygen species were increased in HCAEC when exposed to EAC directly or after exposure to conditioned lung cell media ($p < 0.0001$ vs. control). ICAM-1 protein expression levels were increased after exposure to conditioned lung cell media (18 mg vs. control, $p < 0.01$). Ex vivo results show an increase in the mRNA levels of anti-angiogenic marker, *FKBP1* ($p < 0.05$ vs. sham), and endothelial cell adhesion molecule involved in barrier function, *ICAM-1* ($p < 0.05$ vs. sham) in murine hearts following exposure to electronic cigarette aerosol treatment containing a higher amount of nicotine. Immunohistochemistry also revealed an upregulation of *FKBP1* and *ICAM-1* protein expression levels. This study showed that despite e-Cigs being widely used for tobacco smoking cessation, these can negatively impact endothelial cell health with a potential to lead to the development of cardiovascular disease.

Keywords: e-vaping; cardiovascular disease; smoking; nicotine; atherosclerosis



Citation: Chhor, M.; Tulpar, E.; Nguyen, T.; Cranfield, C.G.; Gorrie, C.A.; Chan, Y.L.; Chen, H.; Oliver, B.G.; McClements, L.; McGrath, K.C. E-Cigarette Aerosol Condensate Leads to Impaired Coronary Endothelial Cell Health and Restricted Angiogenesis. *Int. J. Mol. Sci.* **2023**, *24*, 6378. <https://doi.org/10.3390/ijms24076378>

Academic Editor: Lih Kuo

Received: 22 December 2022

Revised: 24 March 2023

Accepted: 25 March 2023

Published: 28 March 2023



Copyright: © 2023 by the authors. Licensee MDPI, Basel, Switzerland. This article is an open access article distributed under the terms and conditions of the Creative Commons Attribution (CC BY) license (<https://creativecommons.org/licenses/by/4.0/>).

1. Introduction

Cardiovascular diseases (CVD) and the resultant vascular complications are a major cause of mortality, accounting for 31% of all deaths worldwide [1,2]. The development of CVD is multifactorial and has been associated with risk factors including tobacco cigarette smoking, obesity, high cholesterol, and high blood pressure [2,3]. Notably, 10% of all CVD cases are attributable to smoking tobacco cigarettes [4]. Depending on an individual's frequency and habit, smoking can increase the risk by at least two-fold for developing conditions including heart failure and acute myocardial infarction (AMI) compared to the other risk factors [5]. Additionally, it is reported that smoking can act synergistically with other risk factors such as hypertension and diabetes mellitus in multiplying the level of risk for CVD development [6].

Electronic cigarettes (E-Cigs) have recently emerged as a supposedly less toxic and less carcinogenic alternative to traditional cigarettes without any combustion [7]. E-Cigs

are electronic devices that can differ in design between brands; however, they are generally composed of a rechargeable battery, an e-liquid tank (with thousands of potential flavouring) and an atomiser element that heats and aerosolises the e-liquid to create a vapour for smoking. The e-liquid is comprised of propylene glycol (PG), vegetable glycerin (VG), and, optionally, nicotine. There is also a large market for different flavouring [8–10]. E-Cigs use has been traditionally perceived as harmless, with recent trends showing an increase in usage amongst current smokers, but additionally, non-smokers and young adolescents [7,11]. Studies have reported the presence of carbonyl compounds in e-Cig aerosols, notably: formaldehyde, acetaldehyde, and acrolein, as well as long-chain and cyclic alkanes and alkenes [12]. Additionally, trace amounts of metals have been reported, such as aluminum, barium, chromium, and cadmium within the e-Cig aerosol [10,13]. These chemicals are known to be harmful and cytotoxic, causing pulmonary and cardiovascular stress [14]. Whilst these chemicals have been reported to be lower in concentration from their traditional tobacco cigarette counterparts, there remain many other residual chemicals generated during the heating process in addition to the role of nicotine that could contribute to early atherogenesis [15].

Endothelial cells play an important role in cardiovascular homeostasis, regulating the permeability of the arterial vessels, and are the first responders to inflammatory stimuli [16]. Endothelial dysfunction (ED) is an early critical event that leads to atherosclerosis and heart failure, affecting vascular integrity through reduced vasodilation, increased inflammation, and prothrombic activity [17,18]. Experimental studies have demonstrated that exposure to the harmful chemicals generated from tobacco smoke not only results in vascular dysfunction, but also leads to the activation of the vascular endothelium as a result of a shift to a pro-oxidative state and increased expression of adhesion molecules on the surface of endothelial cells—an early event in atherosclerosis [19,20].

FK506 binding protein-like (FKBPL), an anti-angiogenic protein and key determinant of CVD, was shown to be increased in human plasma as a result of smoking [21]. FKBPL is secreted by endothelium, and when knocked down in mice, it leads to endothelial dysfunction and impaired vascular integrity [22], suggesting that angiogenic balance is the key to maintaining healthy endothelium. CD31/PECAM1 is an endothelial cell adhesion and signalling molecule that mediates both homophilic and heterophilic adhesion in angiogenesis [23,24]. Increased levels of CD31 have also previously been associated with early COPD and cardiovascular complications as a result of smoking [25,26].

While e-Cigs have been considered a safe alternative to conventional cigarettes, their potential as a smoking cessation device remains controversial. Moreover, of concern is the rising usage of e-Cigs by adolescents and young adults who were never exposed to tobacco cigarettes. This is concerning given that the safety profile of e-Cigs is still unknown, including its impact on the cardiovascular system. Therefore, in this study, we aimed to determine the impact of e-Cigs aerosol condensate (EAC) on endothelial cell homeostasis through the assessment of its effects on the viability of human coronary artery endothelial cells (HCAECs). We further investigate EAC's contributions to endothelium inflammation, oxidative stress, and angiogenesis as part of the mechanisms implicated in this effect. Finally, the immediate impact of nicotine on cell membrane ion permeability was demonstrated using a tethered bilayer lipid membrane (tBLM) assay. The expression of key inflammatory endothelial cell (ICAM-1 and VCAM-1) and angiogenesis markers (FKBPL and CD31) were also assessed *ex vivo* in hearts from mice exposed to e-Cigs aerosol *in vivo*. It is hypothesized that EAC and e-cigarette aerosols will affect endothelial cell health, increasing the expression of inflammatory and anti-angiogenic markers related to endothelial dysfunction and the pathogenesis of cardiovascular disease.

2. Results

2.1. Exposure of HCAEC to EAC-Treated Lung Cell Conditioned Media Results in Cytotoxicity

HCAEC directly exposed to 4% and 8% EAC generated from PG/VG without flavouring or nicotine showed a significant reduction in cell viability to $34 \pm 8.9\%$ ($p < 0.001$)/ $47 \pm$

10.9% ($p < 0.05$) and $29 \pm 4.9\%$ ($p < 0.01$)/ $38 \pm 2.2\%$ ($p < 0.01$) compared to the control cells, respectively (Figure 1A). A decrease in cell viability to $46 \pm 6.2\%$ ($p < 0.05$ versus control cells) was shown for HCAEC exposed to tobacco flavour EAC generated from e-liquid without (0 mg/mL) nicotine at the more concentrated EAC of 8%.

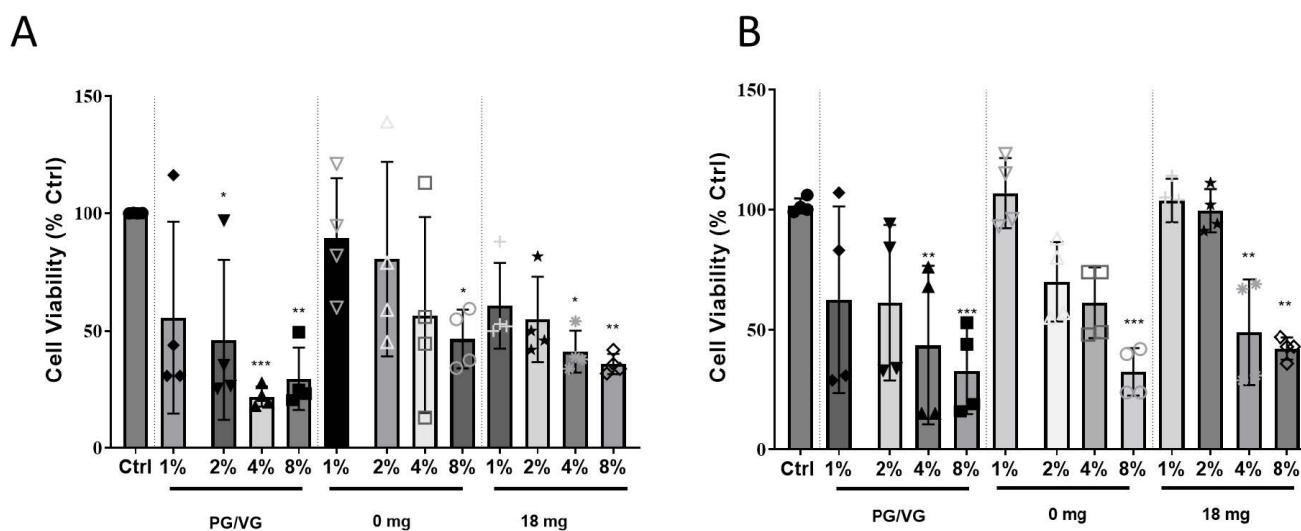


Figure 1. Cell viability in HCAEC exposed to (A) Direct effects of EAC. MTT Assay was performed on HCAEC after exposure to various concentration of EAC generated from: (i) a PG/VG solution (non-flavoured), (ii) 0 mg nicotine (tobacco flavoured), and (iii) 18 mg nicotine (tobacco flavoured) for 24 h. (B) Indirect effects of EAC. A549 epithelial lung cells were exposed to EAC under the same conditions. Media from the treated A549 cells were then used to treat HCAEC on a separate plate for 24 h before cell viability was assessed via MTT assay. Results are expressed as mean \pm SEM ($n = 4$ biological replicates). One-way ANOVA with Bonferroni post-tests was used for statistical analysis; * $p < 0.05$, ** $p < 0.01$, *** $p < 0.001$ versus Ctrl.

Using e-Cigs, the aerosol first comes into contact with the lung epithelial cells before influencing endothelial cells. Thus, to determine whether the response to the EAC from lung epithelial cells would affect the viability of HCAEC, A549 epithelial lung cells were exposed to EAC for 24 h before the conditioned media was used to treat HCAEC for another 24 h. Similar to the response of HCAEC directly exposure of EAC, exposure of conditioned lung epithelial cell media exposed to 4 and 8% EAC generated from PG/VG without flavouring or nicotine resulted in significantly reduced HCAEC viability (Figure 1B). Exposure of conditioned lung epithelial cell media exposed to EAC generated from tobacco flavoured e-liquid without nicotine (0 mg/mL) also resulted in a decrease in cell viability to $32 \pm 4.9\%$ ($p < 0.001$) compared to the control cells (Figure 1B).

Whilst the MTT assay is a widely used assay for detecting cellular toxicity, there are confounding variables that should be considered when performing the assay [27]. To assess if our EAC could reduce MTT, we performed an MTT assay to determine if there were any interference of the MTT dye with the EAC. The results show no difference in absorbance for the lower concentrations of EAC, except PG/VG at 2% where a significant increase in absorbance from 1.0 (ctrl) to 1.09 (** $p < 0.01$; Figure S1) was observed. A significant increase was also observed for 8% EAC 0 mg and 18 mg with absorbance of 1.2 and 1.1, respectively (** $p < 0.0001$ vs. Ctrl). This suggests a minor catalytic effect of EAC on MTT reduction that is mediated by EAC.

2.2. Direct Exposure to EAC or Indirectly to EAC-Lung Cell Conditioned Media Induces ROS Levels

ROS have been shown to play a crucial role in inducing endothelial dysfunction and oxidative stress in cells, a key mechanism behind atherogenesis and heart failure [28,29].

HCAEC exposed directly to 8% EAC generated from PG/VG or tobacco flavour e-liquid with (18 mg/mL) nicotine solution showed an increase in ROS levels by ~7.5-fold ($p < 0.01$) compared to control (Figure 2A).

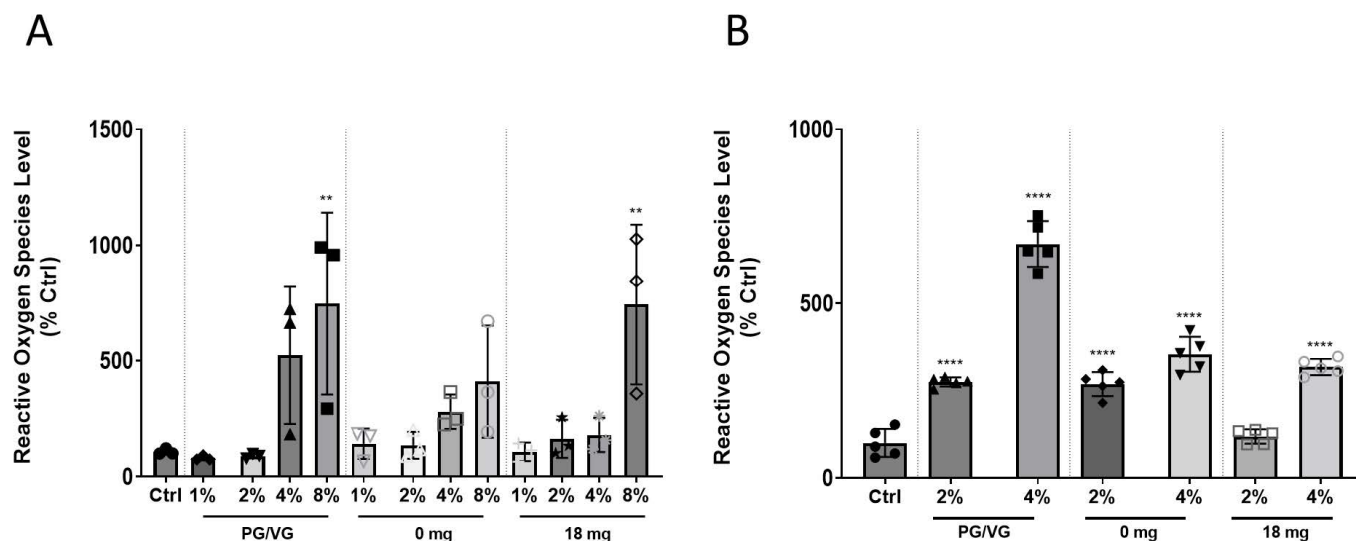


Figure 2. Reactive oxygen species levels in HCAEC after (A) Direct EAC exposure. ROS levels were measured in HCAEC after exposure to various concentration of EAC generated from: (i) a PG/VG standard (non-flavoured), (ii) 0 mg nicotine (tobacco flavoured), and (iii) 18 mg nicotine (tobacco flavoured) at for 24 h. Data shown is expressed as a mean \pm SEM ($n = 3$ biological replicates). (B) Indirect effects of EAC. A549 epithelial lung cells were exposed to EAC under the same conditions. Media from the treated A549 cells were then used to treat HCAEC on a separate plate for 24 h before a DCF assay was performed. Data shown is expressed as a mean \pm SEM ($n = 5$ biological replicates). One-way ANOVA with Bonferroni post-tests was used for statistical analysis, ** $p < 0.01$; **** $p < 0.0001$ versus Ctrl.

Given the results of the cell viability experiments (Figure 1A), we had selected 2% EAC, as this did not result in a significant reduction of cell viability following direct exposure for PG/VG and 4% EAC to assess for effects on the ROS levels produced by HCAEC in co-culture conditions. Similar to the results observed in monoculture, an increase in ROS levels were shown in the co-culture model for HCAEC exposed to lung epithelial cell conditioned media for 4% PG/VG EAC, 4% tobacco flavoured EAC with (18 mg), or without nicotine (0 mg) by 6.7-fold, 3.2-fold, and 3.5-fold compared to the control, respectively ($p < 0.0001$; Figure 2B). HCAEC exposed to lung cell conditioned media showed a significant increase in ROS levels for 2% PG/VG EAC and 2% tobacco flavoured EAC without nicotine (0 mg) by 2.7-fold and 2.6-fold compared to the control, respectively ($p < 0.0001$; Figure 2B). No significance was shown for 2% tobacco flavoured EAC with (18 mg).

2.3. Adhesion Molecule Expression Increases in HCAEC after EAC Exposure for ICAM-1, but Not VCAM-1

A critical early event in atherogenesis is the adhesion of monocytes to the endothelium. The adhesion of monocytes occurs when the endothelial cells become activated in response to several factors, including oxidative stress, which leads to the upregulation of cell adhesion molecules (CAMs), such as VCAM-1 and ICAM-1 [17]. VCAM-1 or ICAM-1 protein levels were not significantly changed in HCAEC monoculture regardless of EAC used (Figure 3A,B). Although no significance was shown, an increase in ICAM-1 protein expression level to $60 \pm 21.1\%$ ($p = 0.068$ compared to control) could also be observed for HCAEC directly exposed to 2% EAC generated from e-liquid containing 18 mg/mL (Figure 3B). Given the monoculture showed a strong trend to changes for ICAM-1 protein levels with nicotine at 2% EAC, next, we only assessed the ICAM-1 levels in the co-culture

model using 2% EAC. In contrast to the results of HCAEC directly exposed to EAC, exposure of HCAECs to conditioned media from lung epithelial cells treated with 2% EAC generated from e-liquid containing 18 mg/mL, an $83 \pm 8.9\%$ ($p < 0.01$ compared to control) increase in ICAM-1 protein levels was observed (Figure 3C).

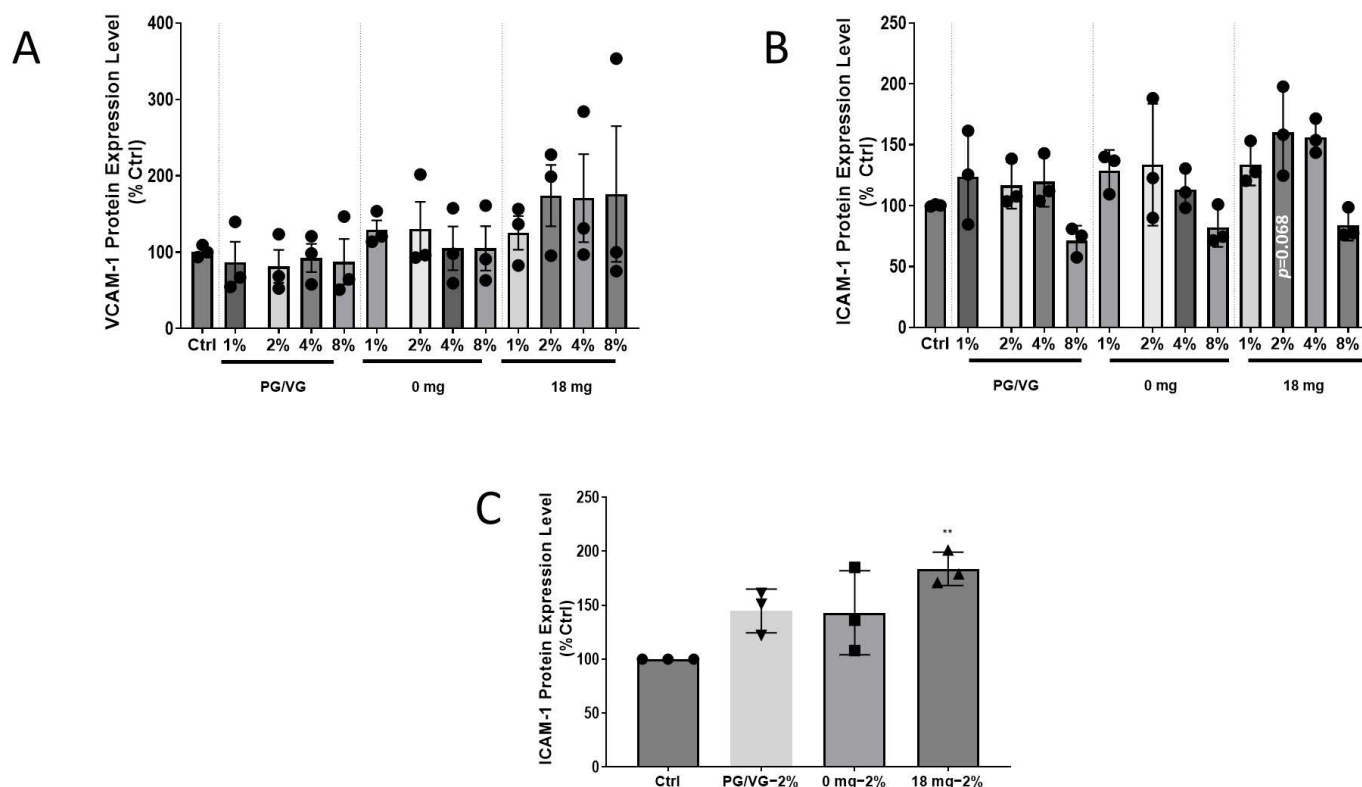


Figure 3. Expression of cellular adhesion molecules after exposure to EAC treatment. HCAEC were exposed to various concentrations of EAC generated from: (i) 0 mg nicotine (tobacco flavoured) and (ii) 18 mg nicotine (tobacco flavoured) for 24 h. (A) VCAM-1 protein expression. (B) ICAM-1 protein expression. (C) Indirect effects of EAC on ICAM-1 protein exposure. A549 epithelial lung cells were exposed to EAC under the same conditions. Media from the treated A549 cells were then used to treat HCAEC on a separate plate for 24 h before measuring ICAM-1 protein levels. Results are expressed as mean \pm SEM ($n = 3$ biological replicates). One-way ANOVA with Bonferroni post-tests was used for statistical analysis, ** $p < 0.01$ versus Ctrl.

2.4. EAC from Nicotine Containing e-Liquid Alters Membrane Permeability

Given nicotine is known to be membrane-permeable, we next assessed if EAC has an effect on membrane permeability using a tethered bilayer lipid membranes (tBLMs) assay [30]. These tBLMs are a model cell membrane anchored to a gold electrode that, when used in conjunction with electrical impedance spectroscopy techniques, enable a measure of how compounds and solutions can alter membrane structure and permeability to ions [31]. We tested 1% and 10% EAC generated from e-liquid with and without nicotine on tBLMs and measured the effects on membrane ion permeabilization using electrical impedance spectroscopy (Figure 4A). When the EAC is sourced from a fluid containing 18 mg/mL nicotine and applied to the tBLM, there is a marked increase in membrane conduction as measured using electrical impedance spectroscopy.

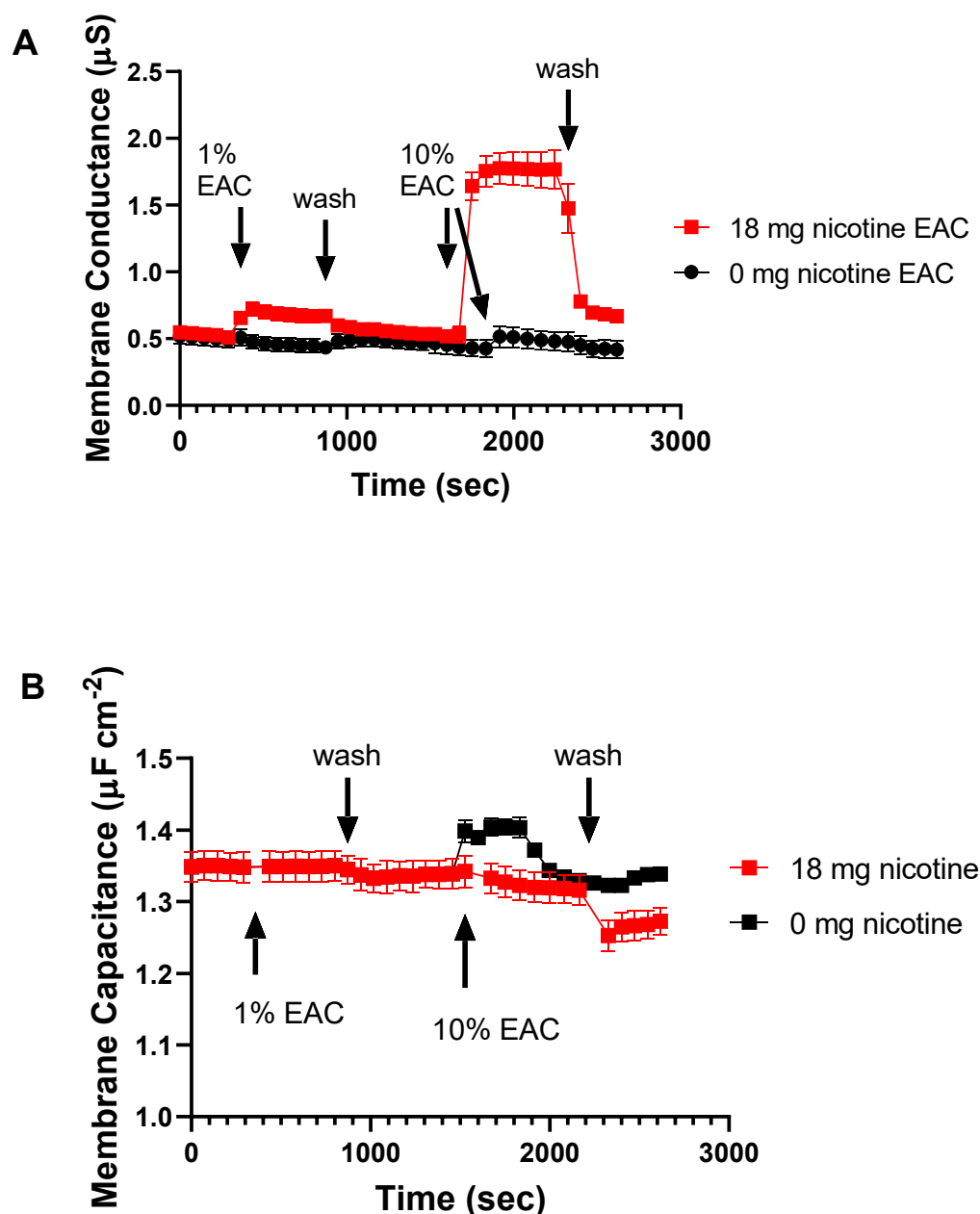


Figure 4. (A) Changes in membrane conductance of tethered bilayer lipid membranes (tBLM) in response to EAC (1% and 10%) in 100 mM NaCl 10 mM tris pH 7 buffer ($n = 3$). EAC solutions containing nicotine increase membrane conductance (membrane permeability). The effect of the nicotine-containing EAC rapidly falls away following a buffer wash. (B) In contrast, only minor changes of the membrane capacitances are observed in the same tBLMs, suggesting permeability changes aren't related to large membrane structural changes.

In contrast to the change in membrane conductance, the membrane capacitance does not show similar changes (Figure 4B). Membrane capacitance is a measure of membrane thickness and/or water content [31]. These data suggest that the EACs are not causing any significant membrane structural changes.

2.5. E-Cigarette Aerosol Increases ICAM-1 mRNA Expression in Murine Hearts

Adhesion molecules play a critical role in the pathogenesis of atherosclerosis, embedded with the inflammatory and immune response [32]. Systemic inflammation is a pivotal process of atherosclerosis and similarly contributes to the implication of endothelial cell

activation in the pathogenesis of developing heart failure [33]. We therefore assessed the expression of adhesion molecules in animals exposed to e-Cig aerosol with or without nicotine. A significant difference in the mRNA expression of *ICAM-1* and *FKBPL* levels were shown between the SHAM and 18 mg nicotine groups and SHAM and 0 mg nicotine groups, respectively (Figure 5B,C, $p < 0.05$). Contrastingly, the mRNA expression of *VCAM-1* and *CD31* exhibited no significant difference between groups (Figure 5A,D).

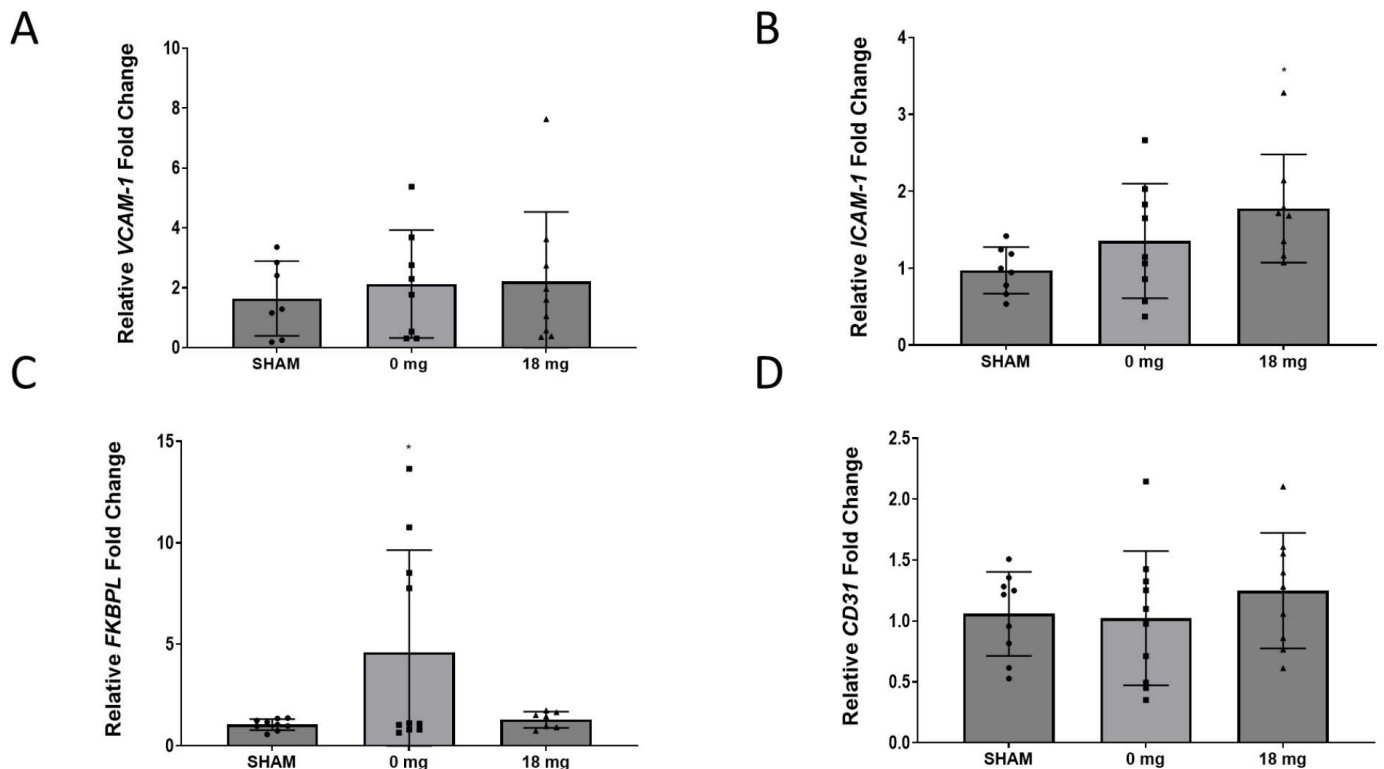


Figure 5. Cardiac VCAM1, ICAM1, and CD31 mRNA expression following treatment of mice with e-cigarettes with or without nicotine. RT-qPCR was performed on the left ventricle of mice exposed to ambient air (SHAM) or e-Cig aerosol (0 mg, 18 mg nicotine). (A) FKBPL. (B) CD31. (C) VCAM-1. (D) ICAM-1. All data expressed as mean fold change \pm SEM ($n = 5-9$). One-way ANOVA with Bonferroni post-test was used for statistical analysis, * $p < 0.05$ versus Sham.

2.6. Cardiac Angiogenesis Markers Are Dysregulated by E-Cig Aerosol Exposure

Angiogenic impaired regulation is an integral process in the development of cardiovascular diseases and therapeutic interventions. We therefore assessed FKBPL and CD31 protein expression in the LV of mice exposed to e-Cig aerosol with or without nicotine. Whilst no significant change in *FKBPL* or *CD31* mRNA expression was observed, immunohistochemistry showed a significant 10-fold increase in FKBPL protein in 18 mg nicotine treatment group ($p < 0.01$) (Figure 6B) compared to the SHAM group. CD31 level paralleled the trend of FKBPL protein expression, where a significant 1.7-fold increase was seen in the 18 mg nicotine treatment group ($p < 0.05$) (Figure 6C).

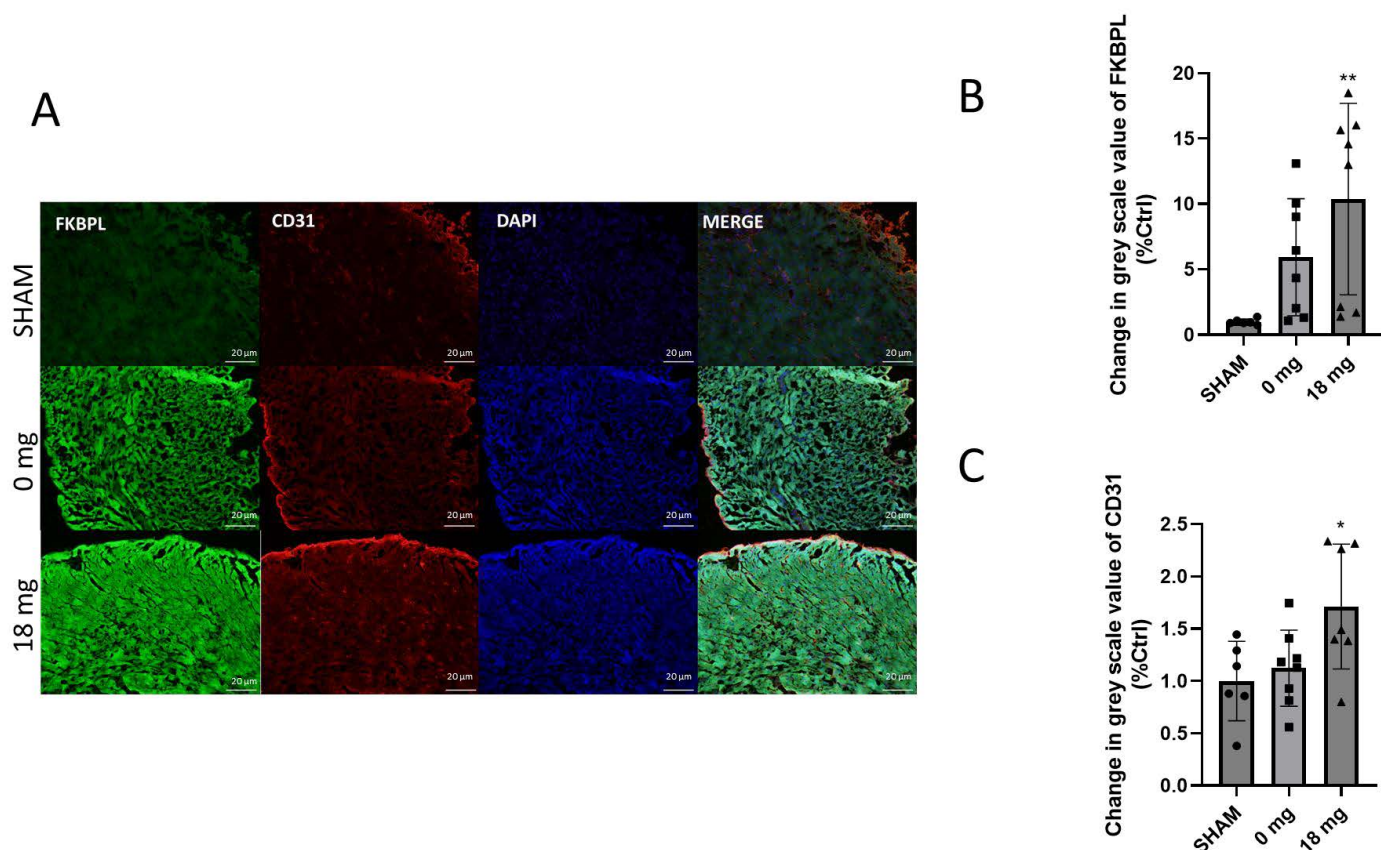


Figure 6. (A) Immunohistochemical on seven-week-old Balb/c female mice left ventricle sections (Scale bar = 20 μ m). Mice were treated in 3 groups: SHAM (ambient air), 0 mg (no nicotine), and 18 mg (nicotine) treatment groups. Sections were stained for FKBPL (green), CD31 (red), and DAPI (blue) and images were taken at 20 \times . (B) FKBPL staining intensity was quantified as the mean greyscale value in three images per sample, ** $p < 0.005$ (SHAM vs. 18 mg). (C) CD31 staining intensity was quantified as the mean greyscale value in three images per sample, * $p < 0.05$ (SHAM vs. 18 mg). Results are expressed as mean \pm SEM ($n = 5-9$) compared to SHAM. One-way ANOVA with Kruskal-Wallis post-tests was used for statistical analysis.

3. Discussion

The goal of the present study was to assess the effects of the use of e-Cigs on the health of endothelial cells. Our *in vitro* studies show endothelial cells exposed directly to EAC generated from the base e-liquid solution (PG/VG), e-liquid solution with or without nicotine induced a decrease cell viability, and an increase in ROS levels. Importantly, our study is the first to show that these adverse effects were exacerbated or remained even after exposure to lung cells using our indirect co-culture-like treatment model. *In vivo*, cardiac changes indicative of angiogenesis was observed in animals, albeit only in animals exposed to e-Cig aerosol containing nicotine. These findings suggest e-Cigs can modulate and induce adverse changes to endothelial cells and the heart.

We wanted to evaluate the effects of e-Cig vaping where the e-liquid is heated through a device to generate aerosol that is subsequently inhaled by the user. Current studies vary in the methodologies used to collect and use e-Cig aerosol [14]. In this study, we chose to collect the condensate from the e-Cig aerosol to evaluate their effects on the health of endothelial cells at varying concentrations. Many studies exhibit the effect of e-Cig aerosol in individual cultures of a single cell type in which they can examine, for example, the respiratory tract or the endothelial effect [34]. In this study, we used both A549 epithelial lung cells and HCAECs to emulate the process of contacting the epithelial layer of the lung first before the e-Cigs metabolites reach the endothelial cells in the blood vessel. The

exposure conditions used are based on previous studies within the same institute (UTS [35]). Tobacco flavouring was chosen due to its popularity amongst cigarette smokers [35] and relatively low ROS [36] content compared to its flavoured alternatives, and it is also the only flavour approved by the FDA [37]. Commercially available e-liquids can range from nicotine concentration of 0 mg/mL up to a concentration of 24 mg/mL, where 10 mg/mL appears to be the median amount for most users [38,39]. The chosen nicotine dose of 18 mg/mL is reflective of light smokers based on previously measured plasma cotinine levels [40,41]. Together, these treatment groups provide a reflective model of human e-Cig use, and importantly, our study shows that endothelial cells and markers of cardiac health are affected by e-Cig aerosol both *in vitro* and *in vivo*.

In this study, we demonstrated a significant reduction in cell viability of HCAECs following direct exposure to EAC generated from the e-liquid base constituents, PG and VG, alone. Noticeably, cell viability is shown to be decreased in all treatment groups, regardless of nicotine or flavouring, particularly using 8% EAC. This is consistent with the observations in the *in vivo* studies, where the effects on the lung, kidney, and liver seem to be nicotine-independent, suggesting the toxicity of heated base constituents and other mechanical factors, such as device settings, in the aerosolisation product [40–42]. The cytotoxic effect of PG/VG may be attributed to the thermal decomposition of the components, which produce toxic carbonyl compounds that are similarly present in cigarette smoke [43–45]. It was found that even the PG/VG treatment, absent of both flavouring and nicotine, is cytotoxic towards endothelial cells and possibly more so than the other treatment groups. Our results are in alignment with Anderson et al. (2016) [7] and Putzhammer et al. (2016) [46], who similarly showed significantly reduced cell viability in human umbilical vein endothelial cells (HUVEC) exposed to tobacco flavour and a variety of e-liquids. Of interest in our study, however, is that we showed significant cytotoxic effects in HCAECs exposed to conditioned media from lung cells exposed to EAC generated from the base/tobacco e-liquid (with or without nicotine), indicating the EAC likely initiate pro-inflammatory conditions in lung epithelial cells that subsequently induced a detrimental effect on the HCAECs.

Oxidative damage as a result of an imbalance in antioxidants and ROS levels has been shown to play an important role in atherogenesis and endothelial dysfunction during cigarette smoking [47–49]. In this study, we showed that HCAEC exposed directly to EAC at high concentrations with or without nicotine resulted in increased ROS levels in endothelial cells compared to the controls. Our results corroborate with previous studies, which showed e-Cig vapour extracts increased levels of ROS expression in varying types of endothelial cells and that the pre-treatment of antioxidants on cells abrogated this effect [7,46,50,51]. Nitric oxide (NO) generated by endothelial nitric oxide synthase (eNOS) plays a crucial role in maintaining vascular physiology. In an oxidative stress state, eNOS uncoupling occurs, which results in ROS rather than NO being produced, cascading into the production of peroxynitrite (ONOO⁻) that has oxidative and cytotoxic effects, exacerbating endothelial dysfunction [52]. Whilst we did not assess if EAC induced eNOS uncoupling in HCAECs, El-Mahdy et al. recently demonstrated *in situ* induction of Nox-dependent ROS production and uncoupling of endothelial NO synthase by e-Cig exposure [53]. Decreased cell viability was similarly observed with HCAECs exposed to conditioned media from lung cells, even at small doses of 2% EAC, demonstrating significantly increased ROS levels. Whether lung cells exposed to EAC result in an increase in the secretion of pro-inflammatory cytokines and therefore induce further adverse effects on the HCAECs requires further investigation.

The oxidative stress response is linked to the inflammatory pathway, both of which lead to a disruption in the endothelial equilibrium and subsequently endothelial dysfunction, pivotal in the early stages of atherosclerosis. The first step in endothelial dysfunction is the expression of molecules that aid in the adhesion of monocytes to the endothelium and subsequent migration into the subendothelial space [54]. Whilst no change in VCAM-1/ICAM-1 protein expression was observed following direct EAC treatment, indirect EAC treatment induced an increase in ICAM-1 in the HCAEC. In line with results from our study, a study by Makwana et al. (2021) [55] showed a significant increase in ICAM-1 expression

in human aortic endothelial cells (HAECs) within a cardiovascular microfluidic model was reported following treatment with traditional cigarette conditioned media, but not e-Cig conditioned media. Makwana et al., (2021) [55] also determined a significant e-Cig aerosol-induced (at the highest dose) increase in THP-1 monocyte adhesion to HAECs albeit only within 10 min of the adhesion period that diminished over time; the effect of tradition cigarette condition media was more pronounced at longer time points. Similarly, Muthumalage et al. (2017) [56] found significant dose-dependent increases in the pro-inflammatory cytokine, IL-8, following in vitro treatment of monocytic cells with flavoured e-liquid. IL-8 and ICAM-1 are, respectively, chemoattractant and adhesion molecules that are involved in monocyte adhesion [52]. However, it is noted that expression of these molecules can be dependent on the specific cell and stimuli type. It is noted that ROS generation reportedly increases *ICAM-1* transcription in endothelial cells, but not always in epithelial cells [57]. This presents a possible *ICAM-1* specific role in adhesion regulation after exposure to e-Cig condensate in endothelial cells. However, further investigation is required such as a monocyte adhesion assay that was performed by Makwana et al. (2021) [55] to determine the direct and indirect effect of EAC on THP-1 adhesion to HCAEC. Nevertheless, the assessment of murine hearts obtained from an in vivo model where mice were exposed to e-Cig aerosol with or without nicotine for 12 weeks showed an increase in cardiac *ICAM-1* protein levels in mice exposed to e-Cig aerosol containing nicotine, suggesting that in vivo *ICAM-1* could be initiating these early atherosclerosis changes. Nicotine has been demonstrated to have anti-inflammatory properties, suggesting that other factors, such as flavouring or the combination of both, are responsible for the increased inflammatory response [58].

In relation to angiogenesis, although changes were observed at the mRNA level only with 0 mg nicotine, FKBPL at the protein level was significantly increased following exposure to nicotine e-Cig aerosol (18 mg). Similarly, CD31 [21,59] was also increased following exposure to e-Cig aerosol with nicotine, perhaps as part of the compensatory mechanism. The changes at the mRNA and protein levels are not always aligned, and it is well-known that FKBPL undergoes post translational modification due to its co-chaperone role [22,23]. Both FKBPL and CD31 related phenotypical changes are due to the changes at the protein level rather than the mRNA level. Hence, these results are more relevant to the downstream effects than the mRNA levels. The determinant factor for these results appears to involve the presence of nicotine, which has been shown to have pro-angiogenic properties [13]. Nicotine exhibits dose-dependent impacts on endothelial cell homeostasis and exhibits angiogenic effects that may be responsible for the pathogenesis of diseases like atherosclerosis [5,15,43]. Nicotinic acetylcholine receptors (nAChRs) are ligand-gated cation channels abundant in endothelial cells and mediate functions, such as proliferation, migration, and angiogenesis in vivo [60]. The effects of nicotine binding to these receptors include endothelium vasodilation, reduced NO availability and eNOS uncoupling, and directly acting on the elements involved in plaque formation [52,61]. Increases in FKBPL as a key anti-angiogenic regulator [62,63] and CD31 in the presence of nicotine are indicative of restrictive angiogenesis and perhaps a compensatory increase in the number of endothelial cells [22], suggesting that the combination of e-Cigs with nicotine are damaging to the cardiac vasculature causing early endothelial cell damage. This was also demonstrated in vitro. Furthermore, using our tethered membrane conductance platform, it was determined that nicotine is capable of altering the permeability of lipid bilayers to ions, such as Na^+ , which would have implications for a cell's ability to maintain membrane potential homeostasis. The nicotine was also readily washed from the membrane, suggesting it has a rapid off-rate, as predicted by its membrane–water partition coefficient [64]. This is consistent with the rapid “hit” that smokers might feel upon initial nicotine exposure, which then rapidly falls away. Ultimately, nicotine plays a critical role in cell migration and vascular permeability, all of which can stimulate the development of atherosclerotic CVD [61].

Whilst we did not determine the exact mechanistic pathway of e-Cig aerosol that led to the adverse effects on endothelial health, we show that tobacco flavouring and nicotine can affect the extent of these adverse effects. However, this is the first study that implicates a critical anti-angiogenic protein, FKBPL, in the EAC-induced endothelial/heart damage. Unlike our *in vivo* results, our *in vitro* findings suggest that e-Cig aerosols affect endothelial homeostasis independent of nicotine. It has been shown that endothelial cell sensitivity of particulates, independent of nicotine, can elicit pro-inflammatory responses that disrupt endothelial cell homeostasis and progress CVD pathogenesis [16].

To the best of our knowledge, this is the first study to demonstrate the disruption of endothelial homeostasis following exposure to conditioned media from lung epithelial cells exposed to EAC, which seems to be more pronounced than direct EAC-exposure. This result is significant as it demonstrates that e-Cig use can potentially lead to the activation of endothelial cells, even after the EAC undergoes first-pass metabolism by lung epithelial cells. We are also reporting, for the first time, changes in a key anti-angiogenic mechanism mediated through FKBPL in murine hearts following exposure to E-cig aerosol with nicotine, suggesting that this combination can lead to cardiac damage and diastolic dysfunction, which we have previously shown in human studies where FKBPL was increased in the presence of diastolic dysfunction [21].

The limitations of this research article may be attributed to the wide and unregulated nature of the e-Cig market. We only used one flavour, one dose, and one e-Cig device in the animal modelling. There are thousands of e-Cig liquid flavours available in the market, and the by-products and constituents of the e-liquid differ between flavours. We only chose a relatively low dose exposure seen in light smokers, which cannot represent the situation of heavy smokers. Similarly, the e-Cig device market has grown exponentially in recent years, where different generations and styles of devices will contain varying atomiser strengths that can affect the aerosolisation process and chemical products of the e-liquids. We also used a different source of PG/VG mixture from that used in the commercial e-liquid and did not determine the exact amount of nicotine in our *in vitro* experiments. We used the conditioned media from A549 cells following exposure to EAC to assess if there are any metabolites from the A549 that could subsequently affect the HCAEC, the results may be an effect of unsuitable culture medium. Nevertheless, the control cells in the indirect co-culture like model were exposed similarly to conditioned media therefore any further effect from the EAC could still be observed. Future studies should examine the use of transwell membrane to confirm the results. We also note that the absorbance reading with incubation of the EAC with MTT reagent alone indicated interference of the EAC with the MTT assay. Therefore, future studies should ensure EAC-only controls are included when performing the MTT assay in addition to using complementary assays, such as the lactate dehydrogenase assay or live/dead staining to confirm the results. A further limitation of the study is that it remains largely descriptive of the effects of e-Cig extract, and more in-depth future studies addressing FKBPL-related molecular mechanism should be performed. We believe that these limitations must be taken into consideration in future studies. Additionally, there is no direct comparison of EAC to the effects of tobacco cigarettes, which needs to be compared in future studies. There was some variation in cardiac FKBPL and CD31 expression within the groups from our *in vivo* study, which could be due to a small number of murine hearts per group that were processed for analyses. Increasing the number of mice per group, or performing Western blot on homogenized tissue adjusted to a housekeeping protein may reduce variability.

4. Materials and Methods

4.1. Generation of EAC

E-Cigs utilise e-liquids that are heated to generate e-Cig vapour inhaled by users. To simulate a more physiological method of exposure, in preference of using e-liquid directly, we opted to heat the e-liquid as this will result in altered chemical composition to generate an aerosol [12]. For this study, EAC was generated using a KangerTech SUBOX mini

e-cigarette device (KangerTech, Shenzhen, China) and tobacco flavoured e-liquid (Vape Empire, Sydney, NSW, Australia), both with (18 mg/mL), and without (0 mg/mL) nicotine. As a vehicle control, EAC was also generated from a stock solution composed of 80% propylene glycol and 20% vegetable glycerine (PG/VG) without tobacco flavour—the base composition of the e-liquid used for this study. The e-cigarette device was set at 30 W, and the air pump was simultaneously switched on for 5 s bursts, with 20 s to rest in between bursts. This setup created a vacuum trap that drew e-cigarette smoke into a 25 cm² flask where the vaporised condensate was collected (Figure 7). The freshly generated condensate was rested upon dry ice for a minimum of 30 min before diluting to the final working concentrations and used immediately.

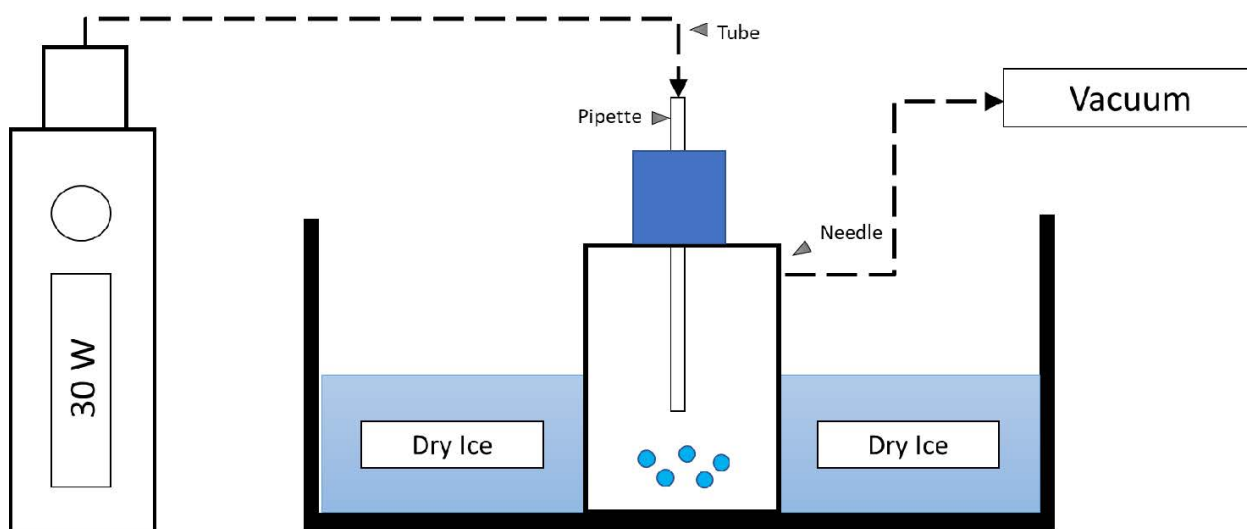


Figure 7. Experimental setup for e-cigarette aerosol condensate collection.

4.2. Cell Culture and Treatment Models

HCAECs (Cell Applications, San Diego, CA, USA) were cultured in Endothelial Cell Growth Medium (Cell Applications, San Diego, CA, USA) and used from passages 1–10 in this current study. To study the metabolic process of lung tissue, we used A549 cells to model alveolar Type II pulmonary epithelium. A549 cells, human alveolar basal epithelial cell line from adenocarcinoma (A549; ATCC, Manassas, Virginia, USA), were cultured in DMEM (Thermo Fisher Scientific, Gibco, Waltham, MA, USA) supplemented with 10% foetal bovine serum (FBS) at 37 °C in a humidified atmosphere containing 5% CO₂. A549 cells were used from passages 3–11 in this study.

A monoculture and indirect co-culture model using undiluted conditioned media (reviewed in Vis et al., 2020 [65]) treatment were utilized for this study. The monoculture involved direct treatment of the HCAECs with the EAC for 24 h. For the co-culture model, the A549 cells were seeded at 1×10^5 cells per well in a 12-well plate and exposed to the EAC for 24 h. HCAEC were then exposed to the conditioned media (100%) obtained from the EAC-exposed A549 cells for an additional 24 h.

4.3. Cytotoxicity Assay

HCAEC were seeded at a concentration of 1×10^4 cells per well in a 96-well plate and treated with EAC or conditioned media for 24 h. HCAEC not exposed to EAC or EAC-containing A549 conditioned media was used as the negative control. Following treatment, MTT reagent (10 µL of 5 mg/mL MTT; Sigma Aldrich, Castle Hill, NSW, Australia) was added to the media and cells were incubated for 3 h. Following incubation, the MTT/media mix was removed, cells were then washed with PBS before the addition of dimethyl sulfoxide (DMSO; 100 µL) to each well and absorbance at 565 nm was measured. Results were expressed as a percentage of negative control indicative of cell viability.

4.4. Intracellular Reactive Oxygen Species (ROS) Assay

HCAEC were seeded in a 96-well plate and treated with EAC or conditioned media for 24 h as described above. HCAEC not treated with EAC was used as the negative control, and cells treated with hydrogen peroxide (H₂O₂) were used as a positive control. Following treatment, the cells were incubated with 2',7'-dichlorodihydrofluorescein diacetate (H₂DCFDA) stain, and ROS level was determined as previously described [66]. Results were expressed as a percentage of negative control ROS activity.

4.5. Enzyme-Linked Immunosorbent Assay (ELISA)

HCAEC were seeded in a 96-well plate and treated for 24 h with EAC. HCAEC not treated with EAC was used as the negative control. After treatment, ELISA was performed on the cells as previously described to determine the expression of the markers, VCAM-1 and ICAM-1 [66]. Cotinine concentration was measured in plasma using an ELISA kit (Abnova, Taipei, Taiwan) as per the manufacturer's instructions.

4.6. Animal Exposure

Seven-week-old Balb/c female mice (n = 28) purchased from Animal Resource Centre (Perth, Western Australia, Australia) were housed in a 12 h light:12 h dark cycle with food and water available ad libitum. Following one week of acclimatisation, the mice in the same home cages were randomly assigned into three treatment groups (n = 9–10 per group) and exposed to ambient air (Sham): e-Cig aerosol generated from tobacco flavoured e-liquid with nicotine (18 mg/mL) or without nicotine (0 mg/mL). Each group was subjected to their respective treatment in a 9 L chamber filled with e-Cig aerosol in two fifteen-minute intervals with a five-minute aerosol free period in between, twice daily. Treatment conditions were based on previous maternal studies equating this exposure period to the smoke from two tobacco cigarettes. Tissue analysis on a subset of samples was performed in a double-blind manner, with group code only revealed during data analysis [67]. After 12 weeks of exposure, the mice were sacrificed, the left ventricle carefully excised, and snap-frozen in liquid nitrogen.

The human relevance of exposure to nicotine-containing e-Cig aerosol in this model has been characterised by the serum cotinine levels, a stable nicotine metabolite, measured 16 to 20 h post last exposure to sham/E-Cig aerosol [40]. Serum cotinine level were as follows sham: 3.31 ± 0.386 ng/mL; 18 mg: 17.41 ± 5.138 ng/mL; 0 mg: 5.97 ± 2.94 ng/mL. Additionally, previous studies have reported similar nicotine delivery volumes between e-Cigs and tobacco cigarettes (mean 1.3 mg e-Cig; 0.5–1.5 mg tobacco cigarette) [68]. These comparisons justify the comparison of cotinine levels between e-Cigs and cigarette users, in addition to the human relevance of mouse model illuminating the effects of e-Cig use. All animal experimental procedures were conducted in accordance with the guidelines described by the Australian National Health and Medical Research Council code of conduct for animals with approval from the University of Technology Sydney Animal Care and Ethics Committee (ETH15-0025).

4.7. Immunohistochemistry of the Heart Tissue

The frozen left ventricles (LV) were halved, embedded in OCT, and sectioned (10 µm) using a Cryostat NX70 (Thermo Fisher Scientific, Gibco, Waltham, MA, USA). Slides were adhered onto gelatin-coated slides by air drying for 20 min before they were fixed in 10% formalin at −20 °C in the freezer for 20 min. Slides were washed in PBST (phosphate buffer saline + 0.1 Tween-20), incubated in blocking buffer (3% Goat serum diluted in 1% BSA in PBST–PBS with 0.1% Triton-X) for 1 h at room temperature before incubation with rabbit anti-FKBPL polyclonal antibody (1:100, Proteintech, Manchester, UK) and mouse anti-CD31 monoclonal antibody (1:100, Proteintech, Manchester, UK) in a humidity chamber. The sections were then washed with PBST (3 times over 15 min), incubated with donkey anti-rabbit AlexaFlour 488 and goat anti-mouse Alexfluor 594 (Abcam, Cambridge, UK) at 1:500 dilution, and counterstained with DAPI (Thermo Fisher Scientific, Gibco, Waltham, MA,

USA; 1:20,000) at room temperature for 1 hr. Three images per section were captured at 20× magnification using an Olympus BX51 fluorescence microscope with an Olympus DP73 camera at varying exposure times (DAPI: 50 ms; FKBPL: 100 ms; CD31: 100 ms). ImageJ 1.53a was used to calculate the mean greyscale value of the fluorescent intensity of FKBPL and CD31 where values were normalised to the SHAM group as previously described [69,70]. To assess the validity of the immunohistochemistry staining, a negative control containing no primary antibody was used for each staining group.

4.8. Reverse Transcription-Polymerase Chain Reaction (RT-qPCR)

Total RNA was extracted from the other half of the LV by homogenisation in TRISURE (Bioline, Australia) using 1.4 mm zirconium oxide beads (Precellys, Bertin Technologies, Montigny-le-Bretonneux, France). Total RNA was then reverse transcribed using a Tetro cDNA synthesis kit (Bioline, Eveleigh, NSW, Australia) before qPCR was performed using SensiFAST SYBR No-ROX Kit (Bioline, Eveleigh, NSW, Australia) using the primers listed in Table 1. Total mRNA expression levels were calculated using the $2^{-\Delta\Delta CT}$ method using β -actin as the reference gene [69].

Table 1. qPCR primers and nucleotide sequence.

Primer Name	Primer Sequence (5'-3')
β -actin (sense)	GATGTATGAAGGCTTTGGTC
β -actin (anti-sense)	TGTGCACTTTTATGGTCTC
ICAM-1 (sense)	CAGTCTACAACCTTTTCAGCTC
ICAM-1 (anti-sense)	CACACTTCACAGTTACTTGG
VCAM-1 (sense)	ACTGATTATCCAAGTCTCTCC
VCAM-1 (anti-sense)	CCATCCACAGACTTTAATACC
CD31 (sense)	CATCGCCACCTTAATAGTTG
CD31 (anti-sense)	CCAGAAACATCATCATAACCG
FKBPL (sense)	TCTCTCAGGGATCAGGAG
FKBPL (anti-sense)	TATTTAAGATTTGCTGGGCG

4.9. Tethered Bilayer Lipid Membrane (tBLMs) Assay

Gold-coated microscope slides with a monolayer coating of 10% benzyl disulphide eleven-oxygen-ethylene-glycol reservoir linkers with a C20 phytanyl group as 'tethers' and 90% four-oxygen-ethylene-glycol reservoir linkers with a terminal OH group as 'spacers' were purchased from SDx Tethered Membranes Pty Ltd., Sydney, Australia. A lipid bilayer was then anchored to the slides using a solvent-exchange technique that employed 3 mM ethanolic solutions of 1,2-Dioleoyl-sn-glycero-3-phosphocholine (DOPC) (Avanti Polar Lipids Inc., Alabaster, AL, USA) [70]. The solvent used for the exchange was 100 mM NaCl 10 mM Tris buffer at pH 7. Dilutions of the EAC used this same buffer. Measurements of membrane conductance were done using swept frequency electrical impedance spectroscopy using an applied potential of 25 mV peak-to-peak, ranging from 0.1 Hz to 2000 Hz, delivered using a Tethapod™ electrical impedance spectrometer (SDx Tethered Membranes Pty Ltd., Sydney, Australia). The data from the impedance and phase profiles were fitted to an equivalent circuit consisting of a constant phase element, representing the imperfect capacitance of the tethering gold electrode and reservoir region, in series with a resistor/capacitor representing the lipid bilayer and a resistor, to represent the impedance of the surrounding electrolyte solution, as described previously [71]. A proprietary adaptation of a Levenberg–Marquardt fitting routine incorporated into the TethaQuick™ software v2.0.56 (SDx Tethered Membranes Pty Ltd., Sydney, Australia) was used to fit the data.

4.10. Statistical Analysis

All results are expressed as a mean \pm SEM. The data was checked for normal distribution before parametric (one-way ANOVA) or non-parametric tests (Kruskal-Wallis) with post-hoc multiple comparison tests were used. GraphPad Prism v8.00 (IBM, Boston, MA, USA) was used to analyse the results. Results with $p < 0.05$ were considered significant.

5. Conclusions

Whilst the long-term adverse effects of e-Cig use on cardiovascular health are yet unknown, this study demonstrated that e-Cig condensates are associated with an increase in endothelial cell oxidative stress, inflammation, and cytotoxicity. This can impair endothelial cell integrity, lead to the restricted angiogenesis in the heart, and result in atherosclerosis and subsequently CVD.

Supplementary Materials: The following supporting information can be downloaded at: <https://www.mdpi.com/article/10.3390/ijms24076378/s1>.

Author Contributions: All the experiments, analysis, and discussion of the results obtained in this study were completed by student M.C. except for the in vivo study. Conceptualisation: K.C.M. and L.M. Data acquisition, analysis and interpretation: E.T., T.N., Y.L.C., C.G.C., H.C., C.A.G., B.G.O., L.M. and K.C.M. Manuscript writing: M.C. Manuscript editing: K.C.M., L.M., C.G.C., H.C. and B.G.O. All authors have read and agreed to the published version of the manuscript.

Funding: This project funded was funded by the Australian Government RTP Fees Offset Scholarship as part of author Michael Chhor's doctoral degree. The animal study was supported by a project grant awarded to Hui Chen and Brian G Oliver by Australian National Health & Medical Research Council (APP1158186). Yik Lung Chan is supported by the Peter Doherty Fellowship, National Health & Medical Research Council of Australia.

Institutional Review Board Statement: The animal study protocol was approved by the Animal Care and Ethics Committee at the University of Technology Sydney (ETH15-0025).

Informed Consent Statement: Not applicable.

Data Availability Statement: All relevant data are contained within the article.

Conflicts of Interest: The authors have no relevant financial or non-financial interest to disclose.

References

1. Stewart, J.; Manmathan, G.; Wilkinson, P. Primary prevention of cardiovascular disease: A review of contemporary guidance and literature. *JRSM Cardiovasc. Dis.* **2017**, *6*, 204800401668721. [[CrossRef](#)]
2. Cardiovascular Diseases. Available online: https://www.who.int/health-topics/cardiovascular-diseases/#tab=tab_1 (accessed on 22 April 2020).
3. ABS. Heart, Stroke and Vascular Disease. Available online: <https://www.abs.gov.au/statistics/health/health-conditions-and-risks/heart-stroke-and-vascular-disease/latest-release>. (accessed on 22 April 2020).
4. WHO. *WHO Global Report: Mortality Attributable to Tobacco*; WHO: Geneva, Switzerland, 2014.
5. Banks, E.; Joshy, G.; Korda, R.; Stavreski, B.; Soga, K.; Egger, S.; Day, C.; Clarke, N.; Lewington, S.; Lopez, A. Tobacco smoking and risk of 36 cardiovascular disease subtypes: Fatal and non-fatal outcomes in a large prospective Australian study. *BMC Med.* **2019**, *17*, 128. [[CrossRef](#)]
6. Abbot, N.C.; Stead, L.F.; White, A.R.; Barnes, J. Hypnotherapy for smoking cessation. *Cochrane Database Syst. Rev.* **1998**, CD001008. [[CrossRef](#)]
7. Anderson, C.; Majeste, A.; Hanus, J.; Wang, S. E-Cigarette Aerosol Exposure Induces Reactive Oxygen Species, DNA Damage, and Cell Death in Vascular Endothelial Cells. *Toxicol. Sci.* **2016**, *154*, 332–340. [[CrossRef](#)]
8. Tayyarah, R.; Long, G.A. Comparison of select analytes in aerosol from e-cigarettes with smoke from conventional cigarettes and with ambient air. *Regul. Toxicol. Pharmacol.* **2014**, *70*, 704–710. [[CrossRef](#)] [[PubMed](#)]
9. Cobb, N.K.; Byron, M.J.; Abrams, D.B.; Shields, P.G. Novel nicotine delivery systems and public health: The rise of the 'E-Cigarette'. *Am. J. Public Health* **2010**, *100*, 2340–2342. [[CrossRef](#)] [[PubMed](#)]
10. Skotsimara, G.; Antonopoulos, A.; Oikonomou, E.; Siasos, G.; Ioakeimidis, N.; Tsalamandris, S.; Charalambous, G.; Galiatsatos, N.; Vlachopoulos, C.; Tousoulis, D. Cardiovascular effects of electronic cigarettes: A systematic review and meta-analysis. *Eur. J. Prev. Cardiol.* **2019**, *26*, 1219–1228. [[CrossRef](#)]

11. Tan, A.S.L.; Bigman, C.A. E-Cigarette Awareness and Perceived Harmfulness Prevalence and Associations with Smoking-Cessation Outcomes. *Am. J. Prev. Med.* **2014**, *47*, 141–149. [[CrossRef](#)] [[PubMed](#)]
12. Patel, D.; Taudte, R.; Nizio, K.; Herok, G.; Cranfield, C.; Shimmon, R. Headspace analysis of E-cigarette fluids using comprehensive two dimensional GC×GC-TOF-MS reveals the presence of volatile and toxic compounds. *J. Pharm. Biomed. Anal.* **2021**, *196*, 113930. [[CrossRef](#)]
13. Whitehead, A.K.; Erwin, A.P.; Yue, X. Nicotine and vascular dysfunction. *Acta Physiol.* **2021**, *231*, e13631. [[CrossRef](#)]
14. Cheng, T. Chemical evaluation of electronic cigarettes. *Tob. Control* **2014**, *23*, ii11. [[CrossRef](#)]
15. George, J.; Hussain, M.; Vadiveloo, T.; Ireland, S.; Hopkinson, P.; Struthers, A.; Donnan, P.; Khan, F.; Lang, C. Cardiovascular Effects of Switching from Tobacco Cigarettes to Electronic Cigarettes. *J. Am. Coll. Cardiol.* **2019**, *74*, 3112. [[CrossRef](#)]
16. Barber, K.E.; Ghebrehiwet, B.; Yin, W.; Rubenstein, D.A. Endothelial Cell Inflammatory Reactions Are Altered in the Presence of E-Cigarette Extracts of Variable Nicotine. *Cell. Mol. Bioeng.* **2017**, *10*, 124. [[CrossRef](#)] [[PubMed](#)]
17. Rajendran, P.; Rengarajan, T.; Thangavel, J.; Nishigaki, Y.; Sakthisekaran, D.; Sethi, G.; Nishigaki, I. The Vascular Endothelium and Human Diseases. *Int. J. Biol. Sci.* **2013**, *9*, 1057. [[CrossRef](#)]
18. Förstermann, U.; Xia, N.; Li, H. Roles of vascular oxidative stress and nitric oxide in the pathogenesis of atherosclerosis. *Circ. Res.* **2017**, *120*, 713–735. [[CrossRef](#)] [[PubMed](#)]
19. Celermajer, D.S.; Sorensen, K.; Gooch, V.; Miller, O.; Sullivan, I.; Lloyd, J.; Deanfield, J.; Spiehelhalter, D. Non-invasive detection of endothelial dysfunction in children and adults at risk of atherosclerosis. *Lancet* **1992**, *340*, 1111–1115. [[CrossRef](#)]
20. Bernhard, D.; Csordas, A.; Henderson, B.; Rossmann, A.; Kind, M.; Wick, G. Cigarette smoke metal-catalyzed protein oxidation leads to vascular endothelial cell contraction by depolymerization of microtubules. *FASEB J.* **2005**, *19*, 1096–1107. [[CrossRef](#)] [[PubMed](#)]
21. Januszewski, A.S.; Watson, C.; O’Niell, V.; McDonald, L.; Ledwidge, M.; Robson, T.; Jenkins, A.; Keech, A.; McClements, L. FKBPL is associated with metabolic parameters and is a novel determinant of cardiovascular disease. *Sci. Rep.* **2020**, *10*, 21655. [[CrossRef](#)] [[PubMed](#)]
22. Yakkundi, A.; Bennett, R.; Herenandez-Negrete, I.; Delalande, J.; Hanna, M.; Lyubomska, O.; Arthur, K.; Short, A.; McKeen, H.; Nelson, L.; et al. FKBPL is a critical antiangiogenic regulator of developmental and pathological angiogenesis. *Arterioscler. Thromb. Vasc. Biol.* **2015**, *35*, 845–854. [[CrossRef](#)]
23. DeLisser, H.M.; Christofidou-Solomidou, M.; Strieter, R.; Burdick, M.; Robinson, C.; Wexler, R.; Kerr, J.; Garlanda, C.; Merwin, J.; Madri, J.; et al. Involvement of endothelial PECAM-1/CD31 in angiogenesis. *Am. J. Pathol.* **1997**, *151*, 671.
24. Lertkiatmongkol, P.; Liao, D.; Mei, H.; Hu, Y.; Newman, P.J. Endothelial functions of PECAM-1 (CD31). *Curr. Opin. Hematol.* **2016**, *23*, 253. [[CrossRef](#)] [[PubMed](#)]
25. Gordon, C.; Gudi, K.; Krause, A.; Sackrowitz, R.; Harvey, B.; Strulovici-Barel, Y.; Mezey, J.; Crystal, R. Circulating Endothelial Microparticles as a Measure of Early Lung Destruction in Cigarette Smokers. *Am. J. Respir. Crit. Care Med.* **2012**, *184*, 224–232. [[CrossRef](#)]
26. Kato, R.; Mizuno, S.; Kadowaki, M.; Shiozaki, K.; Akai, M.; Nakagawa, K.; Oikawa, T.; Iguchi, M.; Osanai, K.; Ishizaki, T.; et al. Sirt1 expression is associated with CD31 expression in blood cells from patients with chronic obstructive pulmonary disease. *Respir. Res.* **2016**, *17*, 139. [[CrossRef](#)] [[PubMed](#)]
27. Ghasemi, M.; Turnbull, T.; Sebastian, S.; Kempson, I. The mtt assay: Utility, limitations, pitfalls, and interpretation in bulk and single-cell analysis. *Int. J. Mol. Sci.* **2021**, *22*, 12827. [[CrossRef](#)]
28. Van der Pol, A.; van Gilst, W.H.; Voors, A.A.; van der Meer, P. Treating oxidative stress in heart failure: Past, present and future. *Eur. J. Heart Fail.* **2019**, *21*, 425–435. [[CrossRef](#)] [[PubMed](#)]
29. Incalza, M.A.; D’Oria, R.; Natalicchio, A.; Perrini, S.; Laviola, L.; Giorgino, F. Oxidative stress and reactive oxygen species in endothelial dysfunction associated with cardiovascular and metabolic diseases. *Vascul. Pharmacol.* **2018**, *100*, 1–19. [[CrossRef](#)]
30. Squier, C.A. Penetration of nicotine and nitrosornicotine across porcine oral mucosa. *J. Appl. Toxicol.* **1986**, *6*, 123–128. [[CrossRef](#)]
31. Alghalayini, A.; Garcia, A.; Berry, T.; Cranfield, C.G. The Use of Tethered Bilayer Lipid Membranes to Identify the Mechanisms of Antimicrobial Peptide Interactions with Lipid Bilayers. *Antibiotics* **2019**, *8*, 12. [[CrossRef](#)]
32. Galkina, E.; Ley, K. Vascular adhesion molecules in atherosclerosis. *Arterioscler. Thromb. Vasc. Biol.* **2007**, *27*, 2292–2301. [[CrossRef](#)]
33. Patel, R.B.; Colangelo, L.; Bielinski, S.; Larson, N.; Ding, J.; Allen, N.; Michos, E.; Shah, S.; Lloyd-Jones, D. Circulating vascular cell adhesion molecule-1 and incident heart failure: The multi-ethnic study of atherosclerosis (MESA). *J. Am. Heart Assoc.* **2020**, *9*, e019390. [[CrossRef](#)]
34. Qasim, H.; Karim, Z.A.; Rivera, J.O.; Khasawneh, F.T.; Alshbool, F.Z. Impact of Electronic Cigarettes on the Cardiovascular System. *J. Am. Heart Assoc.* **2017**, *6*, e006353. [[CrossRef](#)]
35. Romijnnders, K.A.G.J.; Krusemann, E.; Boesveldt, S.; de Graaf, K.; de Vries, H.; Talhout, R. E-Liquid Flavor Preferences and Individual Factors Related to Vaping: A Survey among Dutch Never-Users, Smokers, Dual Users, and Exclusive Vapers. *Int. J. Environ. Res. Public Health* **2019**, *16*, 4661. [[CrossRef](#)] [[PubMed](#)]
36. Cao, Y.; Wu, D.; Ma, Y.; Ma, X.; Wang, S.; Li, F.; Li, M.; Zhang, T. Toxicity of electronic cigarettes: A general review of the origins, health hazards, and toxicity mechanisms. *Sci. Total Environ.* **2021**, *772*, 145475. [[CrossRef](#)] [[PubMed](#)]
37. FDA. Premarket Tobacco Product Marketing Granted Orders. Available online: <https://www.fda.gov/tobacco-products/premarket-tobacco-product-applications/premarket-tobacco-product-marketing-granted-orders> (accessed on 22 April 2020).




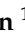
38. Fischman, J.S.; Sista, S.; Lee, D.K.; Cuadra, G.A.; Palazzolo, D.L. Flavorless vs. Flavored Electronic Cigarette-Generated Aerosol and E-Liquid on the Growth of Common Oral Commensal Streptococci. *Front. Physiol.* **2020**, *11*, 1513. [[CrossRef](#)] [[PubMed](#)]
39. Smets, J.; Baeyens, F.; Chaumont, M.; Adriaens, K.; van Gucht, D. When Less is More: Vaping Low-Nicotine vs. High-Nicotine E-Liquid is Compensated by Increased Wattage and Higher Liquid Consumption. *Int. J. Environ. Res. Public Health* **2019**, *16*, 723. [[CrossRef](#)]
40. Chen, H.; Li, G.; Chan, Y.; Chapman, D.; Sukjamnong, S.; Nguyen, T.; Annissa, T.; McGrath, K.; Sharma, P.; Oliver, B. Maternal E-cigarette exposure in mice alters DNA methylation and lung cytokine expression in offspring. *Am. J. Respir. Cell Mol. Biol.* **2018**, *58*, 366–377. [[CrossRef](#)]
41. Li, G.; Chan, Y.; Wang, B.; Saad, S.; George, J.; Oliver, B.; Chen, H. E-cigarettes damage the liver and alter nutrient metabolism in pregnant mice and their offspring. *Ann. N. Y. Acad. Sci.* **2020**, *1475*, 64–77. [[CrossRef](#)]
42. Li, G.; Chan, Y.; Nguyen, L.; Mak, C.; Zaky, A.; Answer, A.; Shi, Y.; Nguyen, T.; Pollock, C.; Oliver, B.; et al. Impact of maternal e-cigarette vapor exposure on renal health in the offspring. *Ann. N. Y. Acad. Sci.* **2019**, *1452*, 65–77. [[CrossRef](#)]
43. Behar, R.Z.; Wang, Y.; Talbot, P. Comparing the cytotoxicity of electronic cigarette fluids, aerosols and solvents. *Tob. Control* **2018**, *27*, 325. [[CrossRef](#)]
44. Kosmider, L.; Sobczak, A.; Fik, M.; Knysak, J.; Zaciera, M.; Kurek, J.; Goniewicz, M. Carbonyl Compounds in Electronic Cigarette Vapors: Effects of Nicotine Solvent and Battery Output Voltage. *Nicotine Tob. Res.* **2014**, *16*, 1319. [[CrossRef](#)]
45. Farsalinos, K.E.; Voudris, V.; Poulas, K. E-cigarettes generate high levels of aldehydes only in 'dry puff' conditions. *Addiction* **2015**, *110*, 1352–1356. [[CrossRef](#)] [[PubMed](#)]
46. Putzhammer, R.; Doppler, C.; Jakschitz, T.; Heinz, K.; Förste, J.; Danzl, K.; Messner, B.; Bernhard, D. Vapours of US and EU Market Leader Electronic Cigarette Brands and Liquids Are Cytotoxic for Human Vascular Endothelial Cells. *PLoS ONE* **2016**, *11*, e0157337.
47. Carnevale, R.; Sciarretta, S.; Violi, F.; Nocella, C.; Loffredo, L.; Perri, L.; Peruzzi, M.; Marullo, A.; De Falco, E.; Chimenti, I.; et al. Acute Impact of Tobacco vs. Electronic Cigarette Smoking on Oxidative Stress and Vascular Function. *Chest* **2016**, *150*, 606–612. [[CrossRef](#)] [[PubMed](#)]
48. Cai, H.; Harrison, D.G. Endothelial dysfunction in cardiovascular diseases: The role of oxidant stress. *Circ. Res.* **2000**, *87*, 840–844. [[CrossRef](#)] [[PubMed](#)]
49. Stocker, R.; Keaney, J.F. Role of Oxidative Modifications in Atherosclerosis. *Physiol. Rev.* **2004**, *84*, 1381–1478. [[CrossRef](#)]
50. Rao, P.S.S.; Ande, A.; Sinha, N.; Kumar, A.; Kumar, S. Effects of Cigarette Smoke Condensate on Oxidative Stress, Apoptotic Cell Death, and HIV Replication in Human Monocytic Cells. *PLoS ONE* **2016**, *11*, e0155791. [[CrossRef](#)]
51. Zhao, J.; Zhang, Y.; Sisler, J.D.; Shaffer, J.; Leonard, S.S.; Morris, A.M.; Qian, Y.; Bello, D.; Demokritou, P. Assessment of reactive oxygen species generated by electronic cigarettes using acellular and cellular approaches. *J. Hazard. Mater.* **2018**, *344*, 549–557. [[CrossRef](#)]
52. Münzel, T.; Hahad, O.; Kuntic, M.; Keaney, J.; Deanfield, J.; Daiber, A. Effects of tobacco cigarettes, e-cigarettes, and waterpipe smoking on endothelial function and clinical outcomes. *Eur. Heart J.* **2020**, *41*, 4057–4070. [[CrossRef](#)]
53. El-Mahdy, M.A.; Ewees, M.; Eid, M.; Mahgoub, E.; Khaleel, S.; Zweier, J. Electronic cigarette exposure causes vascular endothelial dysfunction due to NADPH oxidase activation and eNOS uncoupling. *Am. J. Physiol.-Heart Circ. Physiol.* **2022**, *322*, H549–H567. [[CrossRef](#)]
54. Steyers, C.M.; Miller, F.J. Endothelial Dysfunction in Chronic Inflammatory Diseases. *Int. J. Mol. Sci.* **2014**, *15*, 11324–11349. [[CrossRef](#)]
55. Makwana, O.; Smith, G.; Flockton, H.; Watters, G.; Lowe, F.; Breheny, D. Impact of cigarette versus electronic cigarette aerosol conditioned media on aortic endothelial cells in a microfluidic cardiovascular model. *Sci. Rep.* **2021**, *11*, 4747. [[CrossRef](#)]
56. Muthumalage, T.; Prinz, M.; Ansah, K.; Gerloff, J.; Sundar, I.; Rahman, I. Inflammatory and Oxidative Responses Induced by Exposure to Commonly Used e-Cigarette Flavoring Chemicals and Flavored e-Liquids without Nicotine. *Front. Physiol.* **2018**, *8*, 1130. [[CrossRef](#)] [[PubMed](#)]
57. Roebuck, K.A. Oxidant stress regulation of IL-8 and ICAM-1 gene expression: Differential activation and binding of the transcription factors AP-1 and NF-kappaB (Review). *Int. J. Mol. Med.* **1999**, *4*, 223–230. [[CrossRef](#)] [[PubMed](#)]
58. Gerloff, J.; Sundar, I.; Freter, R.; Sekera, E.; Friedman, A.; Robinson, R.; Pagano, T.; Rahman, I. Inflammatory Response and Barrier Dysfunction by Different e-Cigarette Flavoring Chemicals Identified by Gas Chromatography–Mass Spectrometry in e-Liquids and e-Vapors on Human Lung Epithelial Cells and Fibroblasts. *Appl. Vitro Toxicol.* **2017**, *3*, 28–40. [[CrossRef](#)]
59. Richards, C.; Sesperez, K.; Chhor, M.; Ghorpandour, S.; Rennie, C.; Chung Ming, C.; Evenhuis, C.; Nikolic, V.; Orlic, N.K.; Mikovic, Z.; et al. Characterisation of Cardiac Health in the Reduced Uterine Perfusion Pressure Model and a 3D Cardiac Spheroid Model, of Preeclampsia. *Biol. Sex Differ.* **2021**, *12*, 31. [[CrossRef](#)]
60. Cooke, J.P. Angiogenesis and the role of the endothelial nicotinic acetylcholine receptor. *Life Sci.* **2007**, *80*, 2347. [[CrossRef](#)] [[PubMed](#)]
61. Lee, J.; Cooke, J.P. Nicotine and Pathological Angiogenesis. *Life Sci.* **2012**, *91*, 1058. [[CrossRef](#)]
62. Alqudah, A.; Eastwood, K.; Jerotic, D.; Todd, N.; Hoch, D.; McNally, R.; Obradovic, D.; Dugalic, S.; Hunter, A.; Holmes, V.; et al. FKBP1 and SIRT-1 Are Downregulated by Diabetes in Pregnancy Impacting on Angiogenesis and Endothelial Function. *Front. Endocrinol.* **2021**, *12*, 459. [[CrossRef](#)] [[PubMed](#)]

63. Todd, N.; McNally, R.; Alqudah, A.; Jerotic, D.; Suvakov, S.; Obradovic, D.; Hoch, D.; Hombrebueno, J.; Campos, G.; Watson, C.; et al. Role of A Novel Angiogenesis FKBPL-CD44 Pathway in Preeclampsia Risk Stratification and Mesenchymal Stem Cell Treatment. *J. Clin Endocrinol. Metab.* **2021**, *106*, 26. [[CrossRef](#)]
64. Santi, P. Partition and transport of verapamil and nicotine through artificial membranes. *Int. J. Pharm.* **1991**, *68*, 43–49. [[CrossRef](#)]
65. Vis, M.A.M.; Ito, K.; Hofmann, S. Impact of Culture Medium on Cellular Interactions in in vitro Co-culture Systems. *Front. Bioeng. Biotechnol.* **2020**, *8*, 911. [[CrossRef](#)]
66. McGrath, K.C.Y.; Li, X.H.; McRobb, L.S.; Heather, A.K. Inhibitory Effect of a French Maritime Pine Bark Extract-Based Nutritional Supplement on TNF- α -Induced Inflammation and Oxidative Stress in Human Coronary Artery Endothelial Cells. *Evid.-Based Complement. Altern. Med.* **2015**, *2015*, 260530. [[CrossRef](#)] [[PubMed](#)]
67. Nguyen, T.; Li, G.E.; Chen, E.; Cranfield, C.G.; McGrath, K.C.; Gorrie, C.A. Maternal E-Cigarette Exposure Results in Cognitive and Epigenetic Alterations in Offspring in a Mouse Model. *Chem. Res. Toxicol.* **2018**, *31*, 601–611. [[CrossRef](#)]
68. StHelen, G.; Havel, C.; Dempsey, D.A.; Jacob, P.; Benowitz, N.L. Nicotine delivery, retention and pharmacokinetics from various electronic cigarettes. *Addiction* **2016**, *111*, 535–544. [[CrossRef](#)]
69. Bustin, S.A. Absolute quantification of mrna using real-time reverse transcription polymerase chain reaction assays. *J. Mol. Endocrinol.* **2000**, *25*, 169–193. [[CrossRef](#)] [[PubMed](#)]
70. Cranfield, C.; Carne, S.; Martinac, B.; Cornell, B. The assembly and use of tethered bilayer lipid membranes (tBLMs). *Methods Mol. Biol.* **2015**, *1232*, 45–53.
71. Berry, T.; Dutta, D.; Chen, R.; Leong, A.; Wang, H.; Donald, W.; Parviz, M.; Cornell, B.; Willcox, M.; Kumar, N.; et al. Lipid Membrane Interactions of the Cationic Antimicrobial Peptide Chimeras Melimine and Cys-Melimine. *Langmuir* **2018**, *34*, 11586–11592. [[CrossRef](#)] [[PubMed](#)]

Disclaimer/Publisher's Note: The statements, opinions and data contained in all publications are solely those of the individual author(s) and contributor(s) and not of MDPI and/or the editor(s). MDPI and/or the editor(s) disclaim responsibility for any injury to people or property resulting from any ideas, methods, instructions or products referred to in the content.

Article

FK506-Binding Protein like (FKBPL) Has an Important Role in Heart Failure with Preserved Ejection Fraction Pathogenesis with Potential Diagnostic Utility

Michael Chhor¹, Hao Chen¹, Djurdja Jerotić² , Milorad Tešić^{2,3} , Valentina N. Nikolić⁴, Milan Pavlović⁵, Rada M. Vučić^{6,7}, Benjamin Rayner⁸ , Chris J. Watson⁹, Mark Ledwidge^{10,11}, Kenneth McDonald^{10,11}, Tracy Robson¹², Kristine C. McGrath¹  and Lana McClements^{1,9,*}

¹ Faculty of Science, School of Life Sciences, University of Technology Sydney, Broadway, NSW 2007, Australia

² Faculty of Medicine, University of Belgrade, 11000 Belgrade, Serbia

³ Clinic for Cardiology, University Clinical Center of Serbia, 11000 Belgrade, Serbia

⁴ Department of Pharmacology and Toxicology, Faculty of Medicine, University of Nis, 18000 Nis, Serbia

⁵ Department of Internal Medicine—Cardiology, Faculty of Medicine, University of Nis, 18000 Nis, Serbia

⁶ Department of Internal Medicine, Faculty of Medical Sciences, University of Kragujevac, 34000 Kragujevac, Serbia

⁷ Department of Cardiology, Clinical Centre of Kragujevac, 34000 Kragujevac, Serbia

⁸ Inflammation Group, Heart Research Institute, University of Sydney, Sydney, NSW 2006, Australia

⁹ Wellcome-Wolfson Institute for Experimental Medicine, Queen's University Belfast, Belfast BT9 7BL, UK

¹⁰ STOP-HF Unit, St. Vincent's University Hospital, D04 T6F4 Dublin, Ireland

¹¹ School of Medicine, University College Dublin, D04 V1W8 Dublin, Ireland

¹² School of Pharmacy and Biomolecular Sciences, Royal College of Surgeons in Ireland, D02 YN77 Dublin, Ireland

* Correspondence: lana.mcclements@uts.edu.au



Citation: Chhor, M.; Chen, H.; Jerotić, D.; Tešić, M.; Nikolić, V.N.; Pavlović, M.; Vučić, R.M.; Rayner, B.; Watson, C.J.; Ledwidge, M.; et al. FK506-Binding Protein like (FKBPL) Has an Important Role in Heart Failure with Preserved Ejection Fraction Pathogenesis with Potential Diagnostic Utility. *Biomolecules* **2023**, *13*, 395. <https://doi.org/10.3390/biom13020395>

Academic Editors: Attila Tóth and Miklós Fagyas

Received: 23 December 2022

Revised: 9 February 2023

Accepted: 14 February 2023

Published: 18 February 2023



Copyright: © 2023 by the authors. Licensee MDPI, Basel, Switzerland. This article is an open access article distributed under the terms and conditions of the Creative Commons Attribution (CC BY) license (<https://creativecommons.org/licenses/by/4.0/>).

Abstract: Heart failure (HF) is the leading cause of hospitalisations worldwide, with only 35% of patients surviving the first 5 years after diagnosis. The pathogenesis of HF with preserved ejection fraction (HFpEF) is still unclear, impeding the implementation of effective treatments. FK506-binding protein like (FKBPL) and its therapeutic peptide mimetic, AD-01, are critical mediators of angiogenesis and inflammation. Thus, in this study, we investigated—for the first time—FKBPL's role in the pathogenesis and as a biomarker of HFpEF. In vitro models of cardiac hypertrophy following exposure to a hypertensive stimulus, angiotensin-II (Ang-II, 100 nM), and/or AD-01 (100 nM), for 24 and 48 h were employed as well as human plasma samples from people with different forms of HFpEF and controls. Whilst the FKBPL peptide mimetic, AD-01, induced cardiomyocyte hypertrophy in a similar manner to Ang-II ($p < 0.0001$), when AD-01 and Ang-II were combined together, this process was abrogated ($p < 0.01$ – 0.0001). This mechanism appears to involve a negative feedback loop related to FKBPL ($p < 0.05$). In human plasma samples, FKBPL concentration was increased in HFpEF compared to controls ($p < 0.01$); however, similar to NT-proBNP and Gal-3, it was unable to stratify between different forms of HFpEF: acute HFpEF, chronic HFpEF and hypertrophic cardiomyopathy (HCM). FKBPL may be explored for its biomarker and therapeutic target potential in HFpEF.

Keywords: heart failure; biomarkers; heart failure with preserved ejection fraction; HFpEF; HCM; hypertrophic cardiomyopathy; FKBPL; plasma; angiotensin; AD-01

1. Introduction

Heart failure (HF) is a complex cardiovascular disease (CVD) that is characterised by a failure to meet circulatory demands [1]. Apart from genetic causes, common modifiable risk factors include obesity, diabetes mellitus, high blood pressure and smoking. Clinical symptoms include fatigue, weight gain, shortness of breath, and difficulty performing daily tasks [2]. Worldwide, HF is estimated to affect 40 million people annually [2]. In Australia,

CVD is responsible for 25% of all mortalities, reaching an economic cost of 11.8 billion dollars per year [3].

HF diagnosis includes clinical symptoms, patient history and echocardiographic measurements [2]. Classification of HF into its phenotypes is based on the symptoms present and the left ventricular ejection fraction (EF). The European Society of Cardiology guidelines outline that an $EF \leq 40\%$ is defined as heart failure with a reduced ejection fraction (HFrEF), an $EF \geq 50\%$ as heart failure with a preserved ejection fraction (HFpEF) and an EF between 41–49% as heart failure with a mildly reduced ejection fraction (HFmrEF) [1,4]. Despite accounting for almost half the cases of HF, those with HFpEF have poorer management and prognosis compared to patients with HFrEF [5].

In conjunction with HF diagnosis, biomarker measurements provide crucial information surrounding the pathophysiology, severity and progression of HF [1]. Natriuretic peptides are the choice biomarkers to aid in such diagnosis—namely, brain natriuretic peptide (BNP) and N-terminal (NT)-pro hormone BNP (NT-proBNP), which are both reflective of myocardial stretch. Clinically, both BNP and NT-proBNP are reliable diagnostic and prognostic markers of HF. However, BNP levels have been shown to be elevated in cases of pulmonary and renal diseases, but are decreased in overweight patients [6]. NT-proBNP, in addition to having a longer half-life than BNP, has been shown to be less affected by parameters such as obesity—perhaps increasing its clinical utility [6]. Additionally, Galectin-3 is emerging as a promising biomarker of HFpEF [7]—the expression of which is positively correlated with adverse cardiac remodelling [8].

FK506-binding protein like (FKBPL) is a divergent member of the immunophilin family known for its role as a secreted anti-angiogenic protein that exhibits its action via CD44, establishing its critical role in angiogenesis [9,10]. Additionally, FKBPL has been shown to regulate steroid receptor and inflammatory signalling via CD44, HSP90 and STAT3, with an important regulatory function in vascular health [10–12]. AD-01 and ALM201 are FKBPL-based therapeutic peptides developed based on its anti-angiogenic domain, demonstrating effective anti-inflammatory and anti-angiogenic effects [13]. Even though full FKBPL knockout has been shown to be embryonically lethal, heterozygous knockdown of FKBPL in mice does not lead to any clinically detectable adverse phenotype; however, at the proteomic level, it shows early signs of endothelial dysfunction and impaired vascular integrity [10]. Recently, it was shown that FKBPL plasma concentrations are increased in the presence of CVD and the absence of diabetes mellitus compared to healthy controls, and FKBPL is positively correlated with the echocardiographic parameters of diastolic dysfunction [12]. However, its diagnostic or pathogenic role has not previously been demonstrated in HF. In light of these important functions associated with FKBPL, it is likely that it may have a role in the development of HF—particularly HFpEF—since inflammation and microvascular dysfunction are hallmark features of HFpEF [14]. Thus, this study evaluated the role of FKBPL in the development of cardiac hypertrophy and HFpEF using *in vitro* models of cardiomyoblasts exposed to a hypertensive stimulus, angiotensin-II (Ang-II), and/or the FKBPL mimetic AD-01, as well as human plasma samples from people with different forms of HFpEF and controls.

2. Methods and Materials

2.1. Cell Culture and Treatments

H9C2 rat cardiomyoblasts (Sigma Aldrich, Castle Hill, Australia) were cultured in Dulbecco's Modified Eagle's Medium (DMEM) (Thermofisher, Waltham, MA, USA), supplemented with 10% foetal bovine serum (FBS) (Thermofisher, Waltham, MA, USA). Cells were treated with Ang-II (100 nM)(Sigma Aldrich, Castle Hill, Australia), AD-01 (100 nM) (Sigma Aldrich, Castle Hill, Australia) or a combination of Ang-II and AD-01 for 48 h before measuring the cell/nucleus size and extracting RNA and protein.

2.2. Cell Size Analysis

The cell and nucleus size were determined using an Axio Imager A2 microscope (Carl Zeiss AG, Oberochen, Germany) and ZEISS Zen 2 imaging software (Carl Zeiss AG, Oberochen, German, v.1.0) at 20× magnification. ImageJ (National Institutes of Health, Bethesda, MD, USA) was used to measure and quantify cell/nucleus size.

2.3. Western Blot

Proteins were separated by molecular weight using sodium dodecyl sulfate polyacrylamide gel electrophoresis (SDS-PAGE). The loading buffer for the SDS-PAGE was Laemmli sample buffer (Bio-Rad Laboratories, Hercules, CA, USA) containing the reducing agent dithiothreitol (DTT), according to Laemmli (1970) [15]. The standard ladder used to estimate the molecular weight of the proteins was a Kaleidoscope protein ladder (Bio-Rad Laboratories, Hercules, CA, USA). FKBPL primary antibody (1:1000; in PBS; Proteintech, Rosemont, IL, USA) was used, alongside a β -actin primary antibody (1:10,000; in PBS; Abcam, Cambridge, UK) to normalise the relative FKBPL concentration. The membrane was scanned using the ChemiDoc imaging system (Bio-Rad Laboratories, Hercules, CA, USA). The scanned pictures with peptide bands were processed through ImageJ for relative quantification.

2.4. Reverse Transcription-Polymerase Chain Reaction (RT-qPCR)

Total RNA was extracted from the treated cells using the ISOLATE II RNA Mini Kit (Bioline, Eveleigh, Australia), following the manufacturer's guidelines. Reverse transcription was then performed using RT kit iScript Reverse transcription Supermix (Bio-Rad Laboratories, Hercules, CA, USA), before qPCR was performed using a SensiFAST SYBR No-ROX Kit (Bioline, Everleigh, Australia) and the primers listed for β -actin (FW: 5'-CGCGAGTACAACCTTCTTGC-3' and RW: 5'-CGTCATCCATGGCGAACTGG-3'), FKBPL (FW: 5'-TGGCCTCTCAGGTCTGAACTA-3' and RW: 5'-TGGGGACTGCTGCTTAATCG-3'), BNP (FW: 5'-TCCTTAATCTGTCCGCGCTG-3' and RW: 5'-TCCAGCAGCTTCTGCATCG-3') and ANP (FW: 5'-CTGGGACCCCTCCGATAGAT-3' and RW: 5'-TTCGGTACCGGAAGCTGTTG-3'). Total mRNA expression levels were calculated using the $2^{-\Delta\Delta CT}$ method, using β -actin as the reference gene.

2.5. Participants and Samples

A total of 33 patients diagnosed with HFpEF were enrolled in this study, according to the latest guidelines for HF [16]. Transthoracic echocardiography was performed and blood samples were collected from each participant at the time of the outpatient visit or hospital admission. Patients were excluded if there was a presence of significant valvular disease. Patients were divided into three sub-groups of HFpEF depending on their clinical symptoms: HCM ($n = 15$), acute HFpEF ($n = 9$) and chronic HFpEF ($n = 9$). A control group ($n = 40$) of participants who were high-risk for CVD, but without left ventricular diastolic dysfunction, were also included in this study (Table 1).

All participants provided written consent prior to inclusion and blood collection. This study was conducted in accordance with the Declaration of Helsinki and ethical approval was obtained from individual hospitals and institutions.

2.6. Plasma Marker Measurement

Blood samples collected from participants were centrifuged at 3000× g for 10 min to collect plasma. Plasma FKBPL concentrations were measured using an FKBPL ELISA assay (Cloud-Clone, Wuhan, China), following the manufacturer's guidelines. Plasma NT-proBNP and Gal-3 concentrations were also measured using an ELISA (NT-proBNP, Abcam, Cambridge, UK; Gal-3, Elabscience, Wuhan, China). Gal-3 and NT-proBNP concentrations were not measured within the control group—comparisons were only performed between different HFpEF groups.

Table 1. Patient groups and clinical characteristics.

Characteristics	Controls (n = 40)	Acute HFpEF (n = 9)	Chronic HFpEF (n = 9)	HCM (n = 15)
Age (years)	72.43 ± 6.4	73.4 ± 13.3	64.6 ± 10.6	50.7 ± 13.6
Female (no. [%])	13 (37.1)	4 (44.4)	3 (33.3)	3 (20)
BMI (kg/m ²)	27.6 ± 5.3	32 ± 4.4	28 ± 2.5	25.9 ± 4.1
EF (%)	n/a	57.6 ± 10.9	57.4 ± 8.0	64.5 ± 3.8
NYHA Class	n/a	I/II/III	I/II	I/II
Diabetes n (%)	20 (54)	5 (56)	2 (22)	0 (0)
NT-proBNP (ng/mL)	n/a	13.8 ± 20.9	2.3 ± 3.0	3.2 ± 3.0
FKBPL (ng/mL)	1.26 ± 0.3	1.8 ± 0.6	1.5 ± 0.9	1.6 ± 0.8
Gal-3 (ng/mL)	n/a	10.9 ± 6.6	8.5 ± 4.5	7.5 ± 4.6
Echocardiography measurement				
EDD (mm)	n/a	55.0 ± 11.6	52.8 ± 6.9	47.5 ± 5.5
ESD (mm)	n/a	37 ± 9.6	35.3 ± 8.2	28.9 ± 4.2
IVST (mm)	n/a	12.3 ± 2.9	12.4 ± 2.4	17.9 ± 2.3
PWT (mm)	n/a	11.7 ± 2.1	12.1 ± 1.5	9.3 ± 1.7
Medications				
Aspirin (no. [%])	n/a	7 (78)	4 (44)	1 (7)
Purinergic receptor antagonists (no. [%])	n/a	5 (56)	3 (33)	0
Statins (no. [%])	n/a	6 (67)	3 (33)	2 (13)
Isosorbide mononitrate (no. [%])	n/a	3 (33)	1 (11)	0
Beta-blockers (no. [%])	n/a	9 (100)	6 (67)	14 (93)
ACE-inhibitors (no. [%])	n/a	7 (78)	5 (56)	4 (27)
Diuretics (no. [%])	n/a	4 (44)	4 (44)	4 (27)
Calcium channel blockers (no. [%])	n/a	3 (33)	2 (22)	1 (7)
Warfarin (no. [%])	n/a	1 (11)	1 (11)	0
Amiodarone (no. [%])	n/a	0	0	1 (7)
PPIs (no. [%])	n/a	4 (44)	3 (33)	0
Trimetazidine (no. [%])	n/a	1 (11)	1 (11)	0
Molsidomine (no. [%])	n/a	1 (11)	1 (11)	0
Spirolactone (no. [%])	n/a	0	3 (33)	0
Allopurinol (no. [%])	n/a	0	1 (11)	0
Aminophylline (no. [%])	n/a	0	2 (22)	0

n/a—not applicable; BMI, body mass index; HF, heart failure; HFpEF, heart failure with preserved ejection fraction; EDD, end-diastolic dimension; EF, ejection fraction; ESD, end-systolic dimension; IVST, intraventricular septal thickness; PWT, posterior wall thickness; NT-proBNP, N-terminal pro-B-type natriuretic peptide; and NYHA, New York Heart Association Functional Classification; PPIs, proton pump inhibitors.

2.7. Statistical Analysis

All results are expressed as a mean ± SEM or SD. The data were checked for normal distribution before performing parametric tests (one-way ANOVA) with post-hoc multiple comparison testing. Correlations between two continuous variables were assessed based on the Pearson's correlation coefficient. Statistical significance was defined as $p < 0.05$ (two-sided). Statistical analyses were performed using SPSS software, version 24 (IBM Corp, Armonk, NY, USA) and GraphPad Prism v8.00 (Graphpad Software, Boston, MA, USA). Results with $p < 0.05$ were considered significant.

3. Results

3.1. FKBPL Peptide Mimetic, AD-01, and Angiotensin-II (Ang-II) Increase Cardiomyoblast Cell and Nucleus Size; However, AD-01 in the Presence of Ang-II Abrogates Ang-II-Induced Cardiac Hypertrophy

Given that cardiac hypertrophy often leads to HFpEF, we determined the effect of a hypertensive stimuli, Ang-II, on the nucleus and cell size of cultured H9C2 cardiomyoblasts [17,18]. Cardiomyoblast nucleus and cell size were significantly increased following both 24 h and 48 h treatment with Ang-II compared to the control (Figure 1A–D, $p < 0.0001$). The effect on the nucleus size was more pronounced after the 48 h treatment with Ang-II

(~70% increase) compared to the 24 h treatment (~13% increase). In the presence of AD-01 alone, nucleus size was also increased with both the 24 h (~60% increase) and 48 h treatment (~40% increase; Figure 1A,B, $p < 0.0001$). Interestingly, following the 24 h treatment with AD-01, cell size was modestly decreased (~7% decrease; Figure 1C, $p < 0.0001$), whereas the 48 h treatment with AD-01 led to an increase in cell size similar to that in the nucleus size (Figure 1D, $p < 0.0001$). When the AD-01 treatment was added to the Ang-II exposure, the increase in the nucleus size was abrogated both at 24 and 48 h ($p < 0.01$ and $p < 0.0001$, respectively; Figure 1A,B). The cardiomyoblast cell size was also abrogated when AD-01 was added to Ang-II both at 24 and 48 h ($p < 0.0001$); at both time points, AD-01 in the presence of Ang-II led to a ~30–40% reduction in cell size compared to Ang-II exposure alone (Figure 1C,D).

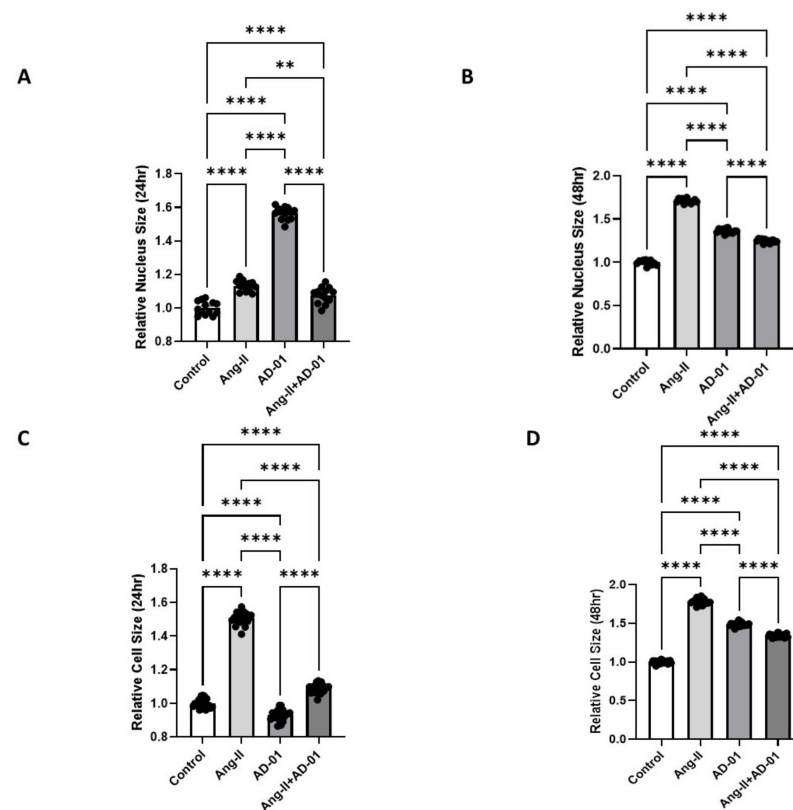


Figure 1. H9C2 cardiomyocyte cell size measurements following treatment with (i) Ang-II (100 nM), (ii) AD-01 (100 nM) and (iii) Ang-II (100 nM) + AD-01 (100 nM). (A) Relative nucleus size 24 h after treatments. (B) Relative nucleus size 48 h after treatments. (C) Relative cell size 24 h after treatments. (D) Relative cell size 48 h after treatments. Results expressed as Mean \pm SEM ($n = 6$); One-way ANOVA with Tukey's post-hoc; ** $p < 0.01$, **** $p < 0.0001$ against control; Ang-II—angiotensin II; AD-01—FKBPL-based therapeutic peptide.

3.2. AD-01 Abrogates Ang-II-Induced Increases in FKBPL Protein Expression

Next, we determined FKBPL, BNP and ANP mRNA expression following 24 h treatment with Ang-II and/or AD-01. Apart from with ANP following Ang-II exposure, no significant change was obtained in the mRNA expression of any of the three genes (Figure 2A–C). Following 48 h exposure of H9C2 cells to Ang-II, AD-01 or Ang-II + AD-01, the only statistically significant change was observed in FKBPL mRNA expression after AD-01 treatment ($p < 0.05$), and although BNP and ANP mRNA expression showed a trend towards an increase, this was not statistically significant at 48 h (Figure 2D–F). The increase in all three genes (FKBPL, BNP and ANP) was the largest following 48 h treatment with AD-01, compared to Ang-II or Ang-II plus AD-01. AD-01 in the presence of Ang-II showed a much lower induction in gene expression than AD-01 alone although this was not statistically significant (Figure 2D–F).

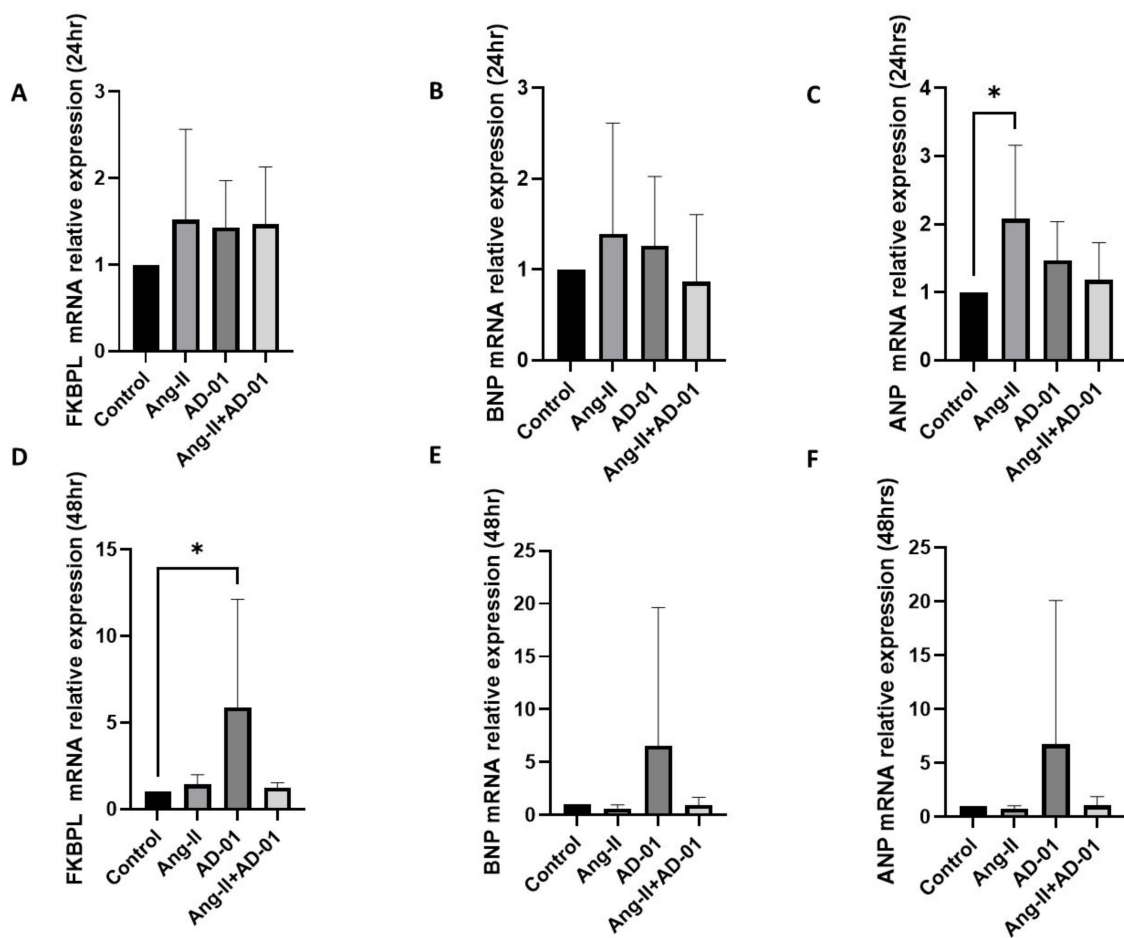


Figure 2. H9C2 cardiomyocyte mRNA expression of FKBPL, BNP and ANP following Ang-II and/or AD-01 treatment. H9C2 cells were exposed to treatment groups (i) Ang-II (100 nM), (ii) AD-01 (100 nM) and (iii) Ang-II (100 nM) + AD-01 (100 nM) for 24 or 48 h before RNA lysates were collected and qPCR performed. (A) FKBPL mRNA expression at 24 h; (B) BNP mRNA expression at 24 h; (C) ANP mRNA expression at 24 h; (D) FKBPL mRNA expression at 48 h; (E) BNP mRNA expression at 48 h; (F) ANP mRNA expression at 48 h. Results expressed as Mean \pm SEM ($n \geq 4$), One-way ANOVA with Tukey's post-hoc. * $p < 0.05$. Ang-II—angiotensin II; AD-01—FKBPL-based therapeutic peptide.

Interestingly, at the protein level, cardiomyoblasts exposed to Ang-II for 48 h showed a significant increase in FKBPL expression compared to the control (Figure 3, $p < 0.05$), and although not significant, a trend towards increased FKBPL protein expressed was observed following AD-01 treatment ($p = 0.07$). In combination with Ang-II, AD-01 was able to abrogate Ang-II-induced FKBPL overexpression (Figure 3, $p < 0.05$).

3.3. FKBPL Plasma Concentration Is Increased in Patients with HFpEF but Does Not Differ between Subgroups

The FKBPL plasma concentration was increased when all the HFpEF subgroups were combined together ($1.645 \text{ ng/mL} \pm 0.75 \text{ SD}$) and compared to the controls ($1.26 \text{ ng/mL} \pm 0.3 \text{ SD}$); Figure 4A, $p < 0.01$. However, when different HFpEF forms were separated into subgroups (acute, chronic and HCM), FKBPL plasma concentrations were only significantly increased in the acute HFpEF subgroup compared to the control (Figure 4B, $p < 0.05$), although there was a trend of increased FKBPL concentrations in HCM compared to controls ($p = 0.07$).

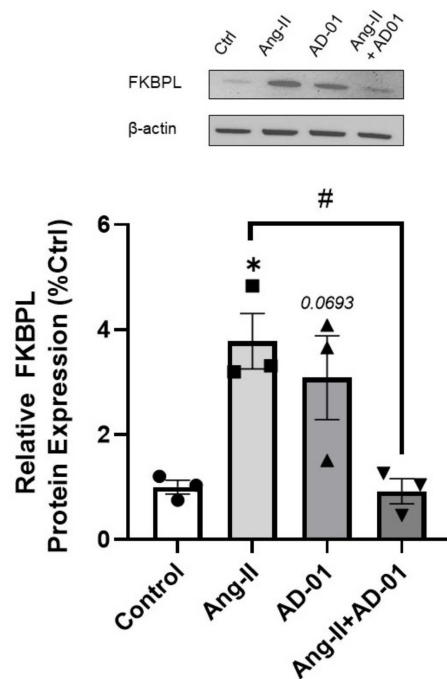


Figure 3. FKBPL protein expression in H9C2 cardiomyocytes following Ang-II and/or AD-01 treatment. H9C2 cells were exposed to treatment groups (i) Ang-II (100 nM), (ii) AD-01 (100 nM) and (iii) Ang-II (100 nM) + AD-01(100 nM) for 48 h. Relative FKBPL expression was measured. Results expressed as Mean \pm SEM ($n = 3$); One-way ANOVA with Tukey’s post-hoc; * $p < 0.05$ against control; # $p < 0.05$ against Ang-II group. Ang-II—angiotensin II; AD-01—FKBPL-based therapeutic peptide.

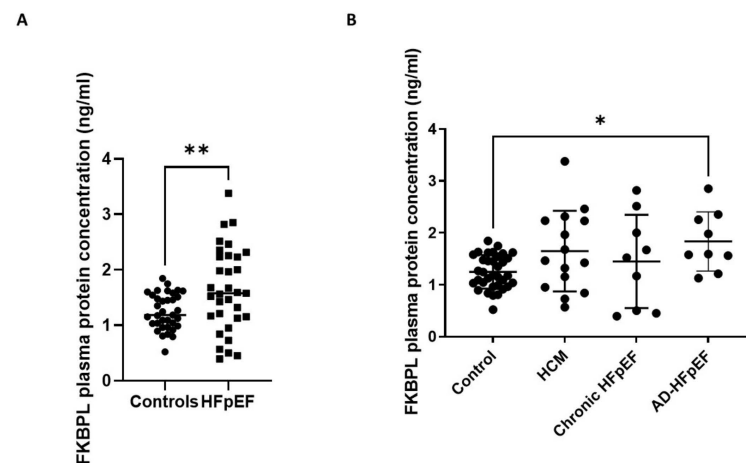


Figure 4. FKBPL plasma protein concentrations in patients with HFpEF. Patients were divided into subgroups based on HFpEF symptoms: HCM ($n = 15$), chronic HFpEF ($n = 9$) and acute decompensated HFpEF ($n = 9$). (A) FKBPL plasma concentration of combined HFpEF subgroups compared to controls ($n = 40$). (B) FKBPL plasma concentration within HFpEF subgroups, compared to controls. Results expressed as Mean \pm SD; One-way ANOVA with Tukey’s post-hoc; * $p < 0.05$, ** $p < 0.005$. HCM—hypertrophic cardiomyopathy; HFpEF—chronic heart failure with preserved ejection fraction; AD-HFpEF—acute decompensated HFpEF.

When FKBPL plasma concentrations were compared between different HFpEF forms, no significant differences were observed between HCM, acute and chronic HFpEF (Figure 5A). Interestingly, a well-established biomarker, NT-proBNP, and an emerging biomarker, Gal-3, also did not show significant differences between the three forms of HFpEF. Nevertheless, NT-proBNP showed a trend towards an increase in acute HFpEF compared to HCM ($p = 0.08$) or chronic HFpEF ($p = 0.1$).

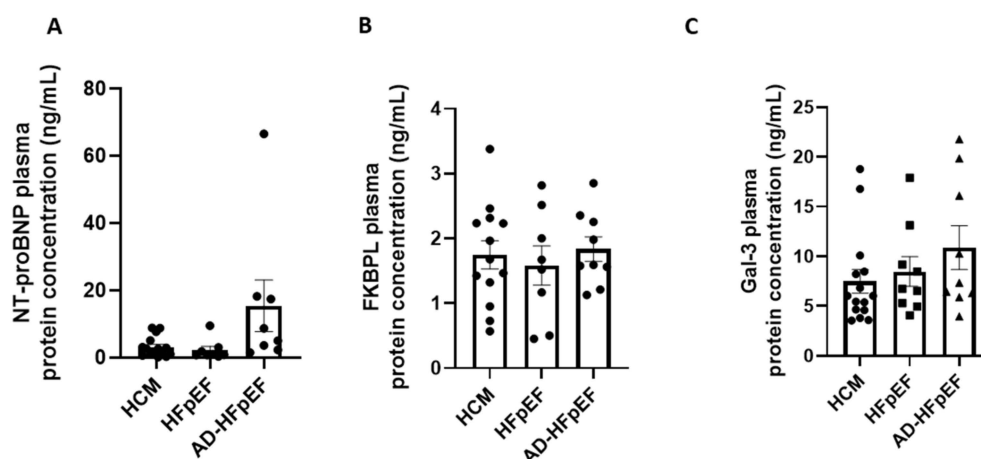


Figure 5. Biomarker plasma protein concentrations in subgroups of HFpEF. Patients were divided into subgroups based on HFpEF symptoms, HCM ($n = 15$), chronic HFpEF ($n = 9$) or acute decompensated HFpEF ($n = 9$). (A) NT-proBNP plasma concentration of HFpEF subgroups measured by ELISA. (B) FKBPL plasma concentration of HFpEF subgroups measured by ELISA. (C) Gal-3 plasma concentration of HFpEF subgroups measured by ELISA. Results expressed as Mean \pm SEM, One-way ANOVA with Tukey’s post-hoc. HCM—hypertrophic cardiomyopathy; HFpEF—chronic heart failure with preserved ejection fraction; AD-HFpEF—acute decompensated HFpEF.

3.4. FKBPL Is Positively Correlated with IVST, Indicative of Microvascular Dysfunction

Echocardiographic measurements are clinically used alongside symptomatic assessments of HF patients and biomarkers, providing key information on cardiac structure and function [4]. In this study we measured limited echocardiographic parameters including end-diastolic diameter (EDD), end-systolic diameter (ESD), posterior wall thickness (PWT) and intraventricular septal thickness (IVST); this is because we have previously shown correlations between FKBPL and echocardiographic parameters [12], whereas the aim of the study was to investigate FKBPL mechanisms in HFpEF patients specifically, in light of its significant role in vasculature function. Correlation analyses (Table 2) showed that FKBPL was positively correlated with IVST ($r_s = 0.621, p < 0.000$) and negatively correlated with ESD and PWT ($r_s = -0.361, p = 0.042$; $r_s = -0.401, p = 0.021$). There was no significant correlation between FKBPL and NT-proBNP or Gal-3 (Table 3). NT-proBNP and Gal-3 showed a positive correlation between each other ($r_s = 0.464, p < 0.007$).

Table 2. Correlations between FKBPL and echocardiography parameters.

	FKBPL	EDD	ESD	IVST	PWT	
FKBPL	Pearson Correlation	1	-0.281	-0.361 *	0.621 ***	-0.401 *
	Sig. (2-tailed)		0.119	0.042	0.000	0.021
	N	33	32	32	33	33

Two-tailed test, * $p < 0.05$, *** $p < 0.001$.

Table 3. Pearson’s correlations between FKBPL, NT-proBNP and Gal-3.

	FKBPL	NT-proBNP	Gal-3	
FKBPL	Pearson Correlation	1	0.063	-0.042
	Sig. (2-tailed)		0.731	0.815
	N	33	32	33

Table 3. Cont.

		FKBPL	NT-proBNP	Gal-3
NT-proBNP	Pearson Correlation	0.063	1	0.464 **
	Sig. (2-tailed)	0.731		0.007
	N	32	32	32
Gal-3	Pearson Correlation	−0.042	0.464 **	1
	Sig. (2-tailed)	0.815	0.007	
	N	33	32	33

Two-tailed test, ** $p < 0.01$.

4. Discussion

HF pathophysiology is complex and involves various mechanistic pathways as part of its development and progression. Changes in cardiomyocyte cell morphology and function play a key role in the progression of the key mechanisms and processes involved in HF pathogenesis [19]. The renin-angiotensin-aldosterone system (RAAS) is activated by hypovolemia and the sympathetic nervous system. The main product of the RAAS is Ang-II, which has compensatory systemic effects that, if they persist, can exacerbate HF. This is because, in HF, Ang-II is stimulated to maintain cardiac output through increased vasoconstriction, salt retention, contractility, and the activation of inflammatory mediators [1,20,21]. The neuroendocrine pathological mechanisms of HF are regulated by the sympathetic nervous system and are linked to the RAAS [21]. Ang-II has been implicated in adverse cardiac remodelling and leads to an increase in interstitial fibrosis, contributing to HF [1]. Adverse cardiac remodelling through hypertrophy, besides physical alterations, modulates gene expression and the viability of cardiomyocytes, which may contribute to cardiac dysfunction and HF [19]. Interestingly, a recent report demonstrated that the presence of adverse cardiac remodelling in HFpEF patients is associated with worse outcomes compared to those without adverse remodelling [22].

Our findings in this study reveal an interesting mechanism involving Ang-II and FKBPL-based peptide therapeutic, AD-01, when examining their effects on cell and nucleus size. Ang-II or AD-01 treatment led to a significant increase in both cell and nucleus size at 24 and 48 h, with Ang-II and AD-01 displaying similar trends—except in terms of cell size following 24 h treatment. Interestingly, when these two treatments were combined, Ang-II and AD-01 exhibited a significant decrease in cell and nucleus size compared to individual treatments, akin to the size of the control group. Consistent with these findings, 48 h treatment with Ang-II or AD-01 increased the protein expression of FKBPL, which was again abolished when combining these two treatments together. FKBPL plays a critical role in developmental and pathological angiogenesis and vascular function, which has been demonstrated in previous studies in which a murine homozygous knockout of FKBPL was embryonically lethal, whereas heterozygous knockdown resulted in impaired vascular integrity [10,11,23]. Furthermore, FKBPL has been shown to operate via the STAT3 [13], CD44 [24] and nuclear factor kappa B (NF- κ B) [9] inflammatory pathways that commonly underly HF pathophysiology [25]. Thus, vascular dysfunction due to aberrant endothelial cell homeostasis, pro-inflammatory signalling and restricted angiogenesis potentially implicate FKBPL in the development of HF. Our findings suggest that AD-01 may exacerbate hypertrophy within cardiomyocytes—likely via FKBPL. However, there exists a compensatory mechanism when Ang-II is present; AD-01 abrogates this effect via a negative feedback mechanism to reverse the hypertrophic effect. As an FKBPL mimetic, AD-01 has been shown previously and, in this study, to increase FKBPL mRNA and protein expression when used alone [24]; this mechanism is altered in the presence of Ang-II, whereby FKBPL expression is normalised. These findings present a complex and compensatory mechanism of AD-01 as a FKBPL mimetic, in producing an anti-hypertrophic effect in Ang-II-induced myopathy that needs to be further studied.

In evaluating the biomarker potential of FKBPL in HFpEF, NT-proBNP and Gal-3 plasma concentrations were also measured in this study. NT-proBNP has been well-established in the clinical diagnosis of HF [4], whereas Gal-3—although not clinically used—has been presented in recent literature as a promising biomarker candidate for the diagnosis of HFpEF [7,26]. Gal-3's diverse functionality in inflammation contributes to myocardial remodelling and fibrosis [8], where the inhibition of Gal-3 has been reported to ameliorate these conditions [27]. Previous reports have shown that FKBPL plasma concentrations are increased in the presence of CVD [12] and in the absence of diabetes mellitus, compared to healthy controls. FKBPL is also positively correlated with parameters of diastolic dysfunction including left atrium volume and size, IVST at the end of diastole and deceleration time [12]. In the same study, FKBPL was positively correlated with a clinically used marker of HFpEF, BNP, and it was one of the determinants of CVD in conjunction with age, gender, total-cholesterol, and systolic blood pressure (SBP) [12]. Here, we showed that the FKBPL plasma concentration was significantly increased between the control group and patients with HFpEF, implicating FKBPL's possible role as a biomarker for HFpEF. In further evaluating the biomarker potential of FKBPL in HFpEF, FKBPL plasma concentrations were found to be significantly increased when comparing the control group to acute HFpEF and only showed an increasing trend in HCM—suggesting a mechanistic role for FKBPL in the pathophysiology and progression of HFpEF. Previous studies have shown that in a murine model of HFpEF, deletion of STAT3 in cardiomyocytes resulted in the manifestation of the clinical characteristics of HFpEF [28]. Given that FKBPL is increased in HFpEF patients, and that it inhibits the inflammatory STAT3 pathway [13], this mechanism may contribute towards HFpEF pathophysiology.

When comparing different forms of HFpEF, our study found no significant differences in the plasma concentrations of FKBPL, NT-proBNP or Gal-3. Therefore, none of the examined biomarkers have shown to be able to stratify between specific forms of HFpEF in this study. FKBPL has previously been reported to be positively correlated with BNP [11]; however, we found no correlation with either NT-proBNP or Gal-3, whereas the latter two were positively correlated with each other. This is likely due to the diverse role of FKBPL in HFpEF, which is independent of NT-proBNP and Gal-3, and it might contribute to different pathogenic processes and mechanisms involved in microvascular dysfunction, inflammation and restricted angiogenesis. This could also be specific to our patient samples.

In patients with HCM, the presence of microvascular dysfunction has been recognized as a strong predictor of clinical deterioration and mortality [29,30]. In fact, myocardial wall thickness is the strongest predictor of reduced global hyperaemic myocardial blood flow in HCM [31]. Subsequently, there is a higher probability of the development of myocardial fibrosis in segments with reduced hyperaemic myocardial blood flow [32]. Our study demonstrated a clinically relevant positive correlation between FKBPL and IVST, likely implicating FKBPL in the microvascular dysfunction of the LV hypertrophy, which is related to the pathogenesis of HFpEF [33,34]. This was also confirmed in the *in vitro* part of the study where the FKBPL peptide mimetic, AD-01, induced cardiomyoblast hypertrophy whilst also increasing FKBPL expression.

The limitations of this study include the cross-sectional nature of the study in terms of the recruited controls and modest patient numbers. Nevertheless, we included well-known biomarkers of HFpEF—NT-proBNP and Gal-3—as a comparison and supported the findings with *in vitro* models of HFpEF that aligned with the clinical sample findings, showing that FKBPL is positively correlated with HFpEF and, potentially, its progression.

5. Conclusions

In this study, we demonstrated for the first time that FKBPL may be implicated in HFpEF. An FKBPL-based peptide therapeutic, AD-01, was able to abrogate Ang-II-induced FKBPL upregulation and cardiomyoblasts hypertrophy. Aligned to this, FKBPL human plasma levels were increased in HFpEF compared to controls; however, FKBPL was unable to distinguish between different forms of HFpEF, similar to NT-proBNP and Gal-3. Finally,

FKBPL was positively correlated with an echocardiography parameter reflective of cardiac microvascular dysfunction and hypertrophy, further strengthening the evidence for its role in the pathogenesis of HFpEF.

Author Contributions: M.C. performed the experiments, data analysis and interpretation and wrote the manuscript. H.C. performed and analysed experiments. D.J. analysed and interpreted data. M.T., V.N.N., M.P. and R.M.V., conceived the study; recruited the patients; performed echocardiography; retrieved the samples; recorded the clinical characteristics; stratified the patient cohorts; and edited the manuscript. B.R. supervised H.C. and contributed to the experimental design, data acquisition, analysis and interpretation. C.J.W., T.R., K.M. and M.L. contributed to the conception, experimental design or data interpretation. L.M. and K.C.M. supervised M.C. and K.C.M. contributed to data analysis and interpretation. L.M. conceived the study, the study design, performed experiments, data analysis and interpretation; and edited the manuscript. All authors have read and agreed to the published version of the manuscript.

Funding: The current study was funded by Research and Development Fund, Faculty of Science, University of Technology Sydney (Lana McClements). Michael Chhor was supported by an Australian Government Research Training Program (RTP) Stipend and RTP Fee-Offset Scholarship through the University of Technology Sydney.

Institutional Review Board Statement: The study was conducted in accordance with the Declaration of Helsinki and approved by the Human Ethics Committee of the University of Technology Sydney (ETH19-3461) on 13 August 2019. The use of the control samples and data was obtained from the STOP-HF study and was approved by the research ethics committee of St. Vincent's University Hospital, Dublin, which conformed to the principles of the Helsinki Declaration [35–37].

Informed Consent Statement: All participants provided written informed consent. The study was approved by all participating institutional human ethics boards.

Data Availability Statement: The data presented in this study are available on request from the corresponding author.

Acknowledgments: We thank the participants for taking part in this study and any healthcare staff for helping with the recruitment.

Conflicts of Interest: The authors declare no conflict of interest.

References

1. Malik, A.; Brito, D.; Vaqar, S.; Chhabra, L. *Congestive Heart Failure*; StatPearls: Tampa, FL, USA, 2022.
2. Baman, J.R.; Ahmad, F.S. Heart Failure. *JAMA* **2020**, *324*, 1015. [[CrossRef](#)] [[PubMed](#)]
3. Australian Institute of Health and Welfare. *Heart, Stroke and Vascular Disease: Australian Facts*; AIHW, Australian Government: Darlinghurst, Australia. Available online: <https://www.aihw.gov.au/reports/heart-stroke-vascular-diseases/hsvd-facts/contents/about> (accessed on 13 February 2023).
4. McDonagh, T.A.; Metra, M.; Adamo, M.; Gardner, R.S.; Baumbach, A.; Böhm, M.; Burri, H.; Butler, J.; Čelutkienė, J.; Chioncel, O.; et al. 2021 ESC Guidelines for the diagnosis and treatment of acute and chronic heart failure. Developed by the Task Force for the diagnosis and treatment of acute and chronic heart failure of the European Society of Cardiology (ESC) With the special contribution of the Heart Failure Association (HFA) of the ESC. *Eur. Heart J.* **2021**, *42*, 4901. [[CrossRef](#)] [[PubMed](#)]
5. Inamdar, A.A.; Inamdar, A.C. Heart Failure: Diagnosis, Management and Utilization. *J. Clin. Med.* **2016**, *5*, 62. [[CrossRef](#)] [[PubMed](#)]
6. Lewis, R.A.; Durrington, C.; Condliffe, R.; Kiely, D.G. BNP/NT-proBNP in pulmonary arterial hypertension: Time for point-of-care testing? *Eur. Respir. Rev.* **2020**, *29*, 200009. [[CrossRef](#)]
7. Chen, H.; Chhor, M.; Rayner, B.S.; McGrath, K.; McClements, L. Evaluation of the diagnostic accuracy of current biomarkers in heart failure with preserved ejection fraction: A systematic review and meta-analysis. *Arch. Cardiovasc. Dis.* **2021**, *114*, 793–804. [[CrossRef](#)]
8. Andrejic, O.M.; Vucic, R.M.; Pavlovic, M.; McClements, L.; Stokanovic, D.; Jevtovic-Stoimenov, T.; Nikolic, V.N. Association between Galectin-3 levels within central and peripheral venous blood, and adverse left ventricular remodelling after first acute myocardial infarction. *Sci. Rep.* **2019**, *9*, 13145. [[CrossRef](#)]
9. Annett, S.; Spence, S.; Garciarena, C.; Campbell, C.; Dennehy, M.; Drakeford, C.; Lai, J.; Dowling, J.; Moore, G.; Yakkundi, A.; et al. The immunophilin protein FKBPL and its peptide derivatives are novel regulators of vascular integrity and inflammation via NF- κ B signaling. *bioRxiv* **2021**. [[CrossRef](#)]

10. Yakkundi, A.; Bennett, R.; Hernández-Negrete, I.; Delalande, J.-M.; Hanna, M.; Lyubomska, O.; Arthur, K.; Short, A.; McKeen, H.; Nelson, L.; et al. FKBPL Is a Critical Antiangiogenic Regulator of Developmental and Pathological Angiogenesis. *Arter. Thromb. Vasc. Biol.* **2015**, *35*, 845–854. [[CrossRef](#)]
11. Alqudah, A.; Eastwood, K.-A.; Jerotic, D.; Todd, N.; Hoch, D.; McNally, R.; Obradovic, D.; Dugalic, S.; Hunter, A.J.; Holmes, V.A.; et al. FKBPL and SIRT-1 Are Downregulated by Diabetes in Pregnancy Impacting on Angiogenesis and Endothelial Function. *Front. Endocrinol.* **2021**, *12*, 459. [[CrossRef](#)]
12. Januszewski, A.S.; Watson, C.J.; O'Neill, V.; McDonald, K.; Ledwidge, M.; Robson, T.; Jenkins, A.J.; Keech, A.C.; McClements, L. FKBPL is associated with metabolic parameters and is a novel determinant of cardiovascular disease. *Sci. Rep.* **2020**, *10*, 1–7. [[CrossRef](#)]
13. Annett, S.; Moore, G.; Short, A.; Marshall, A.; McCrudden, C.; Yakkundi, A.; Das, S.; McCluggage, W.G.; Nelson, L.; Harley, I.; et al. FKBPL-based peptide, ALM201, targets angiogenesis and cancer stem cells in ovarian cancer. *Br. J. Cancer* **2019**, *122*, 361–371. [[CrossRef](#)]
14. Chen, H.; Tesic, M.; Nikolic, V.N.; Pavlovic, M.; Vucic, R.M.; Spasic, A.; Jovanovic, H.; Jovanovic, I.; Town, S.E.L.; Padula, M.P.; et al. Systemic Biomarkers and Unique Pathways in Different Phenotypes of Heart Failure with Preserved Ejection Fraction. *Biomolecules* **2022**, *12*, 1419. [[CrossRef](#)]
15. Laemmli, U.K. Cleavage of Structural Proteins during the Assembly of the Head of Bacteriophage T4. *Nature* **1970**, *227*, 680–685. [[CrossRef](#)]
16. Ponikowski, P.; Voors, A.; Anker, S.; Bueno, H.; Cleland, J.; Coats, A.; Falk, V.; González-Juanatey, J.R.; Harjola, V.-P.; Jankowska, E.; et al. 2016 ESC Guidelines for the diagnosis and treatment of acute and chronic heart failure: The Task Force for the diagnosis and treatment of acute and chronic heart failure of the European Society of Cardiology (ESC) Developed with the special contribution of the Heart Failure Association (HFA) of the ESC. *Eur. Heart J.* **2016**, *37*, 2129–2200.
17. Van Heerebeek, L.; Hamdani, N.; Handoko, M.L.; Falcao-Pires, I.; Musters, R.J.; Kupreishvili, K.; Ijsselmuiden, A.J.; Schalkwijk, C.G.; Bronzwaer, J.G.; Diamant, M.; et al. Diastolic stiffness of the failing diabetic heart: Importance of fibrosis, advanced glycation end products, and myocyte resting tension. *Circulation* **2008**, *117*, 43–51. [[CrossRef](#)]
18. Watkins, S.J.; Borthwick, G.M.; Arthur, H.M. The H9C2 cell line and primary neonatal cardiomyocyte cells show similar hypertrophic responses in vitro. *Vitr. Cell. Dev. Biol. Anim.* **2011**, *47*, 125–131. [[CrossRef](#)]
19. Peter, A.K.; Bjerke, M.A.; Leinwand, L.A. Biology of the cardiac myocyte in heart disease. *Mol. Biol. Cell* **2016**, *27*, 2149–2160. [[CrossRef](#)]
20. Nakano, S.; Muramatsu, T.; Nishimura, S.; Senbonmatsu, T. Cardiomyocyte and Heart Failure. In *Current Basic and Pathological Approaches to the Function of Muscle Cells and Tissues—From Molecules to Humans*; IntechOpen: London, UK, 2012. [[CrossRef](#)]
21. Orsborne, C.; Chaggar, P.S.; Shaw, S.M.; Williams, S.G. The renin-angiotensin-aldosterone system in heart failure for the non-specialist: The past, the present and the future. *Postgrad. Med. J.* **2016**, *93*, 29–37. [[CrossRef](#)]
22. Xu, L.; Pagano, J.; Chow, K.; Oudit, G.Y.; Haykowsky, M.J.; Mikami, Y.; Howarth, A.G.; White, J.A.; Howlett, J.G.; Dyck, J.R.; et al. Cardiac remodelling predicts outcome in patients with chronic heart failure. *ESC Heart Fail.* **2021**, *8*, 5352–5362. [[CrossRef](#)]
23. Todd, N.; McNally, R.; Qudhah, A.; Jerotic, D.; Suvakov, S.; Obradovic, D.; Hoch, D.; Hombrebueno, J.R.; Campos, G.L.; Watson, C.J.; et al. Role of A Novel Angiogenesis FKBPL-CD44 Pathway in Preeclampsia Risk Stratification and Mesenchymal Stem Cell Treatment. *J. Clin. Endocrinol. Metab.* **2020**, *106*, 26–41. [[CrossRef](#)]
24. Yakkundi, A.; McCallum, L.; O'Kane, A.; Dyer, H.; Worthington, J.; McKeen, H.D.; McClements, L.; Elliott, C.; McCarthy, H.; Hirst, D.G.; et al. The Anti-Migratory Effects of FKBPL and Its Peptide Derivative, AD-01: Regulation of CD44 and the Cytoskeletal Pathway. *PLoS ONE* **2013**, *8*, e55075. [[CrossRef](#)] [[PubMed](#)]
25. Zeng, H.; Chen, J.-X. Microvascular Rarefaction and Heart Failure With Preserved Ejection Fraction. *Front. Cardiovasc. Med.* **2019**, *6*, 15. [[CrossRef](#)] [[PubMed](#)]
26. De Boer, R.A.; Edelmann, F.; Cohen-Solal, A.; Mamas, M.A.; Maisel, A.; Pieske, B. Galectin-3 in heart failure with preserved ejection fraction. *Eur. J. Heart Fail.* **2013**, *15*, 1095–1101. [[CrossRef](#)] [[PubMed](#)]
27. Zhong, X.; Qian, X.; Chen, G.; Song, X. The role of galectin-3 in heart failure and cardiovascular disease. *Clin. Exp. Pharmacol. Physiol.* **2018**, *46*, 197–203. [[CrossRef](#)]
28. Zhao, W.; Chen, Y.; Yang, W.; Han, Y.; Wang, Z.; Huang, F.; Qiu, Z.; Yang, K.; Jin, W. Effects of Cardiomyocyte-Specific Deletion of STAT3—A Murine Model of Heart Failure With Preserved Ejection Fraction. *Front. Cardiovasc. Med.* **2020**, *7*, 613123. [[CrossRef](#)]
29. Cecchi, F.; Olivotto, I.; Gistri, R.; Lorenzoni, R.; Chiriatti, G.; Camici, P.G. Coronary Microvascular Dysfunction and Prognosis in Hypertrophic Cardiomyopathy. *N. Engl. J. Med.* **2003**, *349*, 1027–1035. [[CrossRef](#)]
30. Tesic, M.; Beleslin, B.; Giga, V.; Jovanovic, I.; Marinkovic, J.; Trifunovic, D.; Petrovic, O.; Dobric, M.; Aleksandric, S.; Juricic, S.; et al. Prognostic Value of Transthoracic Doppler Echocardiography Coronary Flow Velocity Reserve in Patients With Asymmetric Hypertrophic Cardiomyopathy. *J. Am. Heart Assoc.* **2021**, *10*, e021936. [[CrossRef](#)]
31. Bravo, P.E.; Pinheiro, A.; Higuchi, T.; Rischpler, C.; Merrill, J.; Santaularia-Tomas, M.; Abraham, M.R.; Wahl, R.L.; Abraham, T.P.; Bengel, F.M. PET/CT Assessment of Symptomatic Individuals with Obstructive and Nonobstructive Hypertrophic Cardiomyopathy. *J. Nucl. Med.* **2012**, *53*, 407–414. [[CrossRef](#)]
32. Ismail, T.F.; Hsu, L.-Y.; Greve, A.M.; Gonçalves, C.; Jabbour, A.; Gulati, A.; Hewins, B.; Mistry, N.; Wage, R.; Roughton, M.; et al. Coronary microvascular ischemia in hypertrophic cardiomyopathy—A pixel-wise quantitative cardiovascular magnetic resonance perfusion study. *J. Cardiovasc. Magn. Reson.* **2014**, *16*, 49. [[CrossRef](#)]

33. Yang, Y.; Li, Z.; Guo, X.; Zhou, Y.; Chang, Y.; Yang, H.; Yu, S.; Ouyang, N.; Chen, S.; Sun, G.; et al. Interventricular Septum Thickness for the Prediction of Coronary Heart Disease and Myocardial Infarction in Hypertension Population: A Prospective Study. *J. Clin. Med.* **2022**, *11*, 7152. [[CrossRef](#)]
34. Kansal, S.; Roitman, D.; Sheffield, L.T. Interventricular septal thickness and left ventricular hypertrophy. An echocardiographic study. *Circulation* **1979**, *60*, 1058–1065. [[CrossRef](#)]
35. Ledwidge, M.; Gallagher, J.; Conlon, C.; Tallon, E.; O’Connell, E.; Dawkins, I.; Watson, C.; O’Hanlon, R.; Bermingham, M.; Patle, A.; et al. Natriuretic peptide-based screening and collaborative care for heart failure: The STOP-HF randomized trial. *JAMA* **2013**, *310*, 66–74. [[CrossRef](#)]
36. Tonry, C.; McDonald, K.; Ledwidge, M.; Hernandez, B.; Glezeva, N.; Rooney, C.; Morrissey, B.; Pennington, S.R.; Baugh, J.A.; Watson, C.J. Multiplexed measurement of candidate blood protein biomarkers of heart failure. *ESC Heart Fail.* **2021**, *8*, 2248–2258. [[CrossRef](#)]
37. Watson, C.J.; Gallagher, J.; Wilkinson, M.; Russell-Hallinan, A.; Tea, I.; James, S.; O’Reilly, J.; O’Connell, E.; Zhou, S.; Ledwidge, M.; et al. Biomarker profiling for risk of future heart failure (HFpEF) development. *J. Transl. Med.* **2021**, *19*, 61. [[CrossRef](#)]

Disclaimer/Publisher’s Note: The statements, opinions and data contained in all publications are solely those of the individual author(s) and contributor(s) and not of MDPI and/or the editor(s). MDPI and/or the editor(s) disclaim responsibility for any injury to people or property resulting from any ideas, methods, instructions or products referred to in the content.



Available online at
ScienceDirect
www.sciencedirect.com

Elsevier Masson France
EM|consulte
www.em-consulte.com/en



CLINICAL RESEARCH

Evaluation of the diagnostic accuracy of current biomarkers in heart failure with preserved ejection fraction: A systematic review and meta-analysis

Évaluation de la précision diagnostique des biomarqueurs actuels dans l'insuffisance cardiaque avec fraction d'éjection préservée : étude systématique et méta-analyse

Hao Chen^{a,b}, Michael Chhor^a, Benjamin S. Rayner^b,
 Kristine McGrath^a, Lana McClements^{a,*}

^a School of Life Sciences, Faculty of Science, University of Technology Sydney, PO Box 123 Broadway, 2007 NSW, Australia

^b Inflammation Group, Heart Research Institute, University of Sydney, 2006 NSW, Australia

Received 16 March 2021; received in revised form 13 July 2021; accepted 21 October 2021
 Available online 19 November 2021

KEYWORDS

Heart failure with preserved ejection fraction;
 HFpEF;
 Biomarkers;
 Diagnosis;
 Meta-analysis

Summary

Background. – A number of circulating biomarkers are currently utilized for the diagnosis of chronic heart failure with preserved ejection fraction (HFpEF). However, due to HFpEF heterogeneity, the accuracy of these biomarkers remains unclear.

Aims. – This study aimed to systematically determine the diagnostic accuracy of currently available biomarkers for chronic HFpEF.

Abbreviations: AHA, American Heart Association; AUC, area under the curve; BNP, B-type natriuretic peptide; CI, confidence interval; ESC, European Society of Cardiology; FN, false negative; FP, false positive; Gal-3, galectin-3; HF, heart failure; HFpEF, heart failure with preserved ejection fraction; HFrEF, heart failure with reduced ejection fraction; HSROC, hierarchical summary of receiver operating characteristic; ln(DOR), natural logarithm-transformed diagnostic odds ratio; LVEF, left ventricular ejection fraction; NT-proBNP, N-terminal pro-B-type natriuretic peptide; PRISMA, Preferred Reporting Items for Systematic reviews and Meta-Analyses; QUADAS-2, Quality Assessment for Diagnostic Accuracy Studies-2; ST2, suppression of tumorigenesis-2; TN, true negative; TP, true positive.

* Corresponding author.

E-mail address: lane.mcclements@uts.edu.au (L. McClements).

<https://doi.org/10.1016/j.acvd.2021.10.007>

1875-2136/© 2021 Elsevier Masson SAS. All rights reserved.

Methods. – PubMed, Web of Science, MEDLINE and SCOPUS databases were searched systematically to identify studies assessing the diagnostic accuracy of biomarkers of chronic HFpEF with left ventricular ejection fraction (LVEF) $\geq 50\%$. All included studies were independently assessed for quality and relevant information was extracted. Random-effects models were used to estimate the pooled diagnostic accuracy of HFpEF biomarkers.

Results. – The search identified 6145 studies, of which 19 were included. Four biomarkers were available for meta-analysis. The pooled sensitivity of B-type natriuretic peptide (BNP) (0.787, 95% confidence interval [CI] 0.719–0.842) was higher than that of N-terminal pro-BNP (NT-proBNP) (0.696, 95% CI 0.599–0.779) in chronic HFpEF diagnosis. However, NT-proBNP showed improved specificity (0.882, 95% CI 0.778–0.941) compared to BNP (0.796, 95% CI 0.672–0.882). Galectin-3 (Gal-3) exhibited a reliable diagnostic adequacy for HFpEF (sensitivity 0.760, 95% CI 0.631–0.855; specificity 0.803, 95% CI 0.667–0.893). However, suppression of tumorigenesis-2 (ST2) displayed limited diagnostic performance for chronic HFpEF diagnosis (sensitivity 0.636, 95% CI 0.465–0.779; specificity 0.595, 95% CI 0.427–0.743).

Conclusion. – NT-proBNP and BNP appear to be the most reliable biomarkers in chronic HFpEF with NT-proBNP showing higher specificity and BNP showing higher sensitivity. Although Gal-3 appears more reliable than ST2 in HFpEF diagnosis, the conclusions are limited as only three studies were included in this meta-analysis.

© 2021 Elsevier Masson SAS. All rights reserved.

MOTS CLÉS

Insuffisance cardiaque avec fraction d'éjection préservée ;
HFpEF ;
Biomarqueurs ;
Diagnostic ;
Méta-analyse

Résumé

Contexte. – Un certain nombre de biomarqueurs circulants est actuellement utilisé pour le diagnostic de l'insuffisance cardiaque chronique avec fraction d'éjection préservée (HFpEF). Cependant, en raison de l'hétérogénéité de HFpEF, la précision de ces biomarqueurs demeure incertaine.

Objectifs. – Cette étude vise à déterminer de manière systématique la précision diagnostique des biomarqueurs actuellement disponibles pour HFpEF chronique.

Méthodes. – Les bases de données PubMed, Web of Science, MEDLINE et SCOPUS ont été utilisées pour identifier les études évaluant les potentiels de diagnostic des biomarqueurs de HFpEF chronique avec une fraction d'éjection ventriculaire gauche (FEVG) $\geq 50\%$. Toutes les études retenues ont chacune été évaluées pour la qualité et la pertinence des données obtenues. Des modèles à effets aléatoires ont été utilisés pour estimer l'exactitude diagnostique groupée des biomarqueurs de HFpEF.

Résultats. – Cette étude a permis d'identifier 6145 études. Les données de 19 d'entre elles ont été utilisées pour cette recherche. Quatre biomarqueurs ont été identifiés et évalués pour les méta-analyses. La sensibilité combinée du peptide natriurétique de type B (BNP) (0,787, intervalle de confiance [IC] à 95 % 0,719–0,842) était plus élevée que celle du peptide natriurétique de type pro-B N-terminal (NT-proBNP) (0,696, IC à 95 % 0,599–0,779) dans le diagnostic de HFpEF chronique. Cependant, le NT-proBNP a montré une meilleure spécificité (0,882, IC à 95 % 0,778–0,941) par rapport au BNP (0,796, IC à 95 % 0,672–0,882). Galectine-3 (Gal-3) a montré un potentiel diagnostique fiable pour HFpEF (sensibilité 0,760, IC à 95 % = 0,631–0,855; spécificité 0,803, IC à 95 % 0,667–, 0,893). Cependant, suppression de la tumorigenèse-2 (ST2) a montré des performances diagnostiques limitées pour HFpEF chronique (sensibilité 0,636, IC 95 % 0,465–0,779; spécificité 0,595, IC 95 % 0,427–0,743).

Conclusions. – La fiabilité diagnostique du NT-proBNP et du BNP semble être la plus prometteuse pour HFpEF chronique, avec une meilleure spécificité pour le NT-proBNP et une meilleure sensibilité pour le BNP. Bien que Gal-3 semble plus fiable que ST2 dans le diagnostic de HFpEF, les conclusions sont limitées car seules trois études ont été incluses dans cette méta-analyse.

© 2021 Elsevier Masson SAS. Tous droits réservés.

Background

Heart failure (HF) is an increasingly prominent disease in developed countries, placing a significant burden on patients and healthcare systems. It currently affects ~64 million people worldwide, with a rising prevalence [1]. HF is a complex syndrome characterized by abnormal cardiac structure and function of the heart, with impaired ability to fill and/or eject blood at normal pressure. In line with this definition, the latest clinical guidelines commonly classify HF into two subtypes based on the left ventricular ejection fraction (LVEF) [2,3]. An LVEF < 50 % is typically considered as HF with reduced LVEF (HFrEF), and LVEF ≥ 50 % is defined as HF with preserved LVEF (HFpEF). However, HF patients with LVEF ranging from 40 % to 50 % have recently been classified as HF with mid-range EF [2] or HFpEF borderline [3], an emerging grey area between HFrEF and HFpEF. HFpEF has increased in prevalence in recent years and is now associated with similar mortality rates as HFrEF [4]. However, this is controversial and HFrEF is still considered the more severe type of HF with the higher mortality rate [5,6]. Although HFpEF is often associated with less severe manifestations, currently available treatments remain limited for symptomatic control and ineffective for HFpEF management [7].

Circulating biomarkers are employed regularly in the diagnosis and prognosis of HFpEF. They have additional potential to provide a better understanding of the underlying pathogenesis, which could lead to the development of effective therapies. Natriuretic peptides, including B-type natriuretic peptide (BNP) and N-terminal pro-BNP (NT-proBNP), are recommended for the diagnosis of HFpEF [2,3]. In addition, galectin-3 (Gal-3) and suppression of tumorigenesis-2 (ST2) are emerging as clinical markers for risk stratification of HFpEF [3]. Nevertheless, their diagnostic reliability remains controversial due to the heterogeneity of data reported. Meta-analyses have been performed on the diagnostic accuracy of NT-proBNP and BNP for HFpEF with substantial heterogeneity observed [8], which may affect the application of the findings. Another relevant meta-analysis reported biomarkers in female patients with HFpEF and pre-eclampsia, whereas there were insufficient included studies for meta-analyses solely in HFpEF [9]. In this study, we systematically performed meta-analyses to comprehensively assess the diagnostic potential of all current biomarkers in the context of HFpEF only (defined as LVEF ≥ 50 %).

Methods

Search strategy and selection criteria

A systematic search was conducted to assess the diagnostic accuracy of biomarkers in HFpEF using the following databases: PubMed, Web of Science, MEDLINE and SCOPUS (1900 to February 2021). The literature search was performed using 'HFpEF AND biomarker' as well as other synonymous terms outlined in Text A.1. We included studies that defined HFpEF as per the latest clinical guidelines published by the American Heart Association (AHA) or European Society of Cardiology (ESC), including the presence of symptoms and signs of HF, and LVEF ≥ 50 % as confirmed by

echocardiography [2,3]. The history of congestive HF and the aetiology of HFpEF were not restricted in the definition of HFpEF.

To determine the biomarkers' suitability for HFpEF diagnosis, published data from observational studies that assessed the diagnostic accuracy of individual biomarkers to discriminate between cohorts or groups with and without chronic HFpEF were included. Studies were selected if diagnostic performance measures of individual biomarkers were reported. Studies were excluded if they were: non-English language publications, letters, editorials, conference abstracts, meta-analyses and reviews. Secondary or post-hoc studies in the excluded meta-analysis or review publications were only considered if the inclusion criteria were met.

Data extraction

Two independent investigators (H. C., M. C.) extracted data from included studies. Disagreements were resolved by consensus with a third investigator (L. M.). The recommendations of the Preferred Reporting Items for Systematic reviews and Meta-Analyses (PRISMA) guidelines [10] and a relevant guideline specialized for biomarker meta-analysis [11] were followed for data extraction. A conventional 2 × 2 table consisting of true positive (TP), true negative (TN), false positive (FP) and false negative (FN) was extracted from each included study. Only published data were extracted.

Quality assessment

The included studies were assessed for quality independently by three co-authors (M. C., B. S. R., K. M.) using the Quality Assessment for Diagnostic Accuracy Studies-2 (QUADAS-2) tool [12], which was composed of four domains:

- patient selection;
- index test;
- reference standard;
- patient flow and timing (for sub-questions, see Text A.2).

Low risk of bias in a domain referred to positive answers in all sub-questions. High risk of bias in a domain was defined as negative answers in 2/2 or 3/3 sub-questions. Unclear risk of bias was defined as 1/2, 1/3 or 2/3 negative answers. Results were compared between assessors and, in case of disagreement, individual studies were discussed to achieve a consensus.

Statistical analysis

The analyses of diagnostic accuracy test were performed in R (4.0.3) using 'mada' package, where a bivariate, random-effects meta-analysis model was applied. The analyses of diagnostic biomarkers were based on sensitivity and specificity discriminating between groups with and without HFpEF. The estimated sensitivity and specificity were calculated using the 2 × 2 tables extracted from the included studies. The sensitivity and specificity were pooled and analysed to generate random-effects model forest plots and random-effects model hierarchical summary of receiver operating characteristic (HSROC) curves. Natural

logarithm-transformed diagnostic odds ratio (ln-DOR) was reported along with heterogeneity of Higgins' I^2 and Cochran's Q . Publication bias was assessed through visual inspection of funnel plots of ln(DOR). Meta-analyses were only generated for diagnostic markers that were evaluated in three or more independent studies.

Results

Search results

The results for diagnostic markers of HFpEF yielded 6145 articles, of which 19 [13–31] met the inclusion criteria with sufficient evidence to conduct meta-analyses on individual biomarkers (Table 1; Fig. 1A). The overall quality of these studies was high (Fig. 1B and 1C). Approximately equal numbers of studies were prospective and retrospective ($n=10$ and $n=9$, respectively; Table 1). In total, 1452 patients with HFpEF and 1429 without HFpEF were included from all 19 studies. All patients were at the chronic stage of HFpEF and free from valvular diseases. Patients with HFpEF were generally older adults (mean age > 50 years old), with a control group appropriately matched for age and sex. Overall, selected studies yielded a total of four different diagnostic markers: NT-proBNP, BNP, Gal-3 and ST2. Natriuretic peptides were the most commonly reported diagnostic markers (17 studies), which is in line with their well-established role in current HFpEF management [2,3]. We were unable to complete meta-analyses on emerging biomarkers such as matrix metalloproteinases and growth differentiation factor 15 due to a small number of studies identified in relation to their diagnostic potential in HFpEF (< 3). However, these biomarkers, along with their supporting citations, are reported in Table A.1).

N-terminal pro-B-type natriuretic peptide

Studies that used NT-proBNP as a diagnostic marker of chronic HFpEF (12 studies [13–24]; 978 patients) reported optimal sensitivity and specificity at NT-proBNP cut-off concentrations ranging from 65 to 477 pg/mL, with the median of 227 pg/mL (Fig. 2A). Interestingly, the four studies that used an NT-proBNP cut-off around 227 pg/mL [19–22] had different values of sensitivity but consistent specificity. The pooled ln(DOR) was 2.97 (95 % confidence interval [CI] 2.19–3.76), and relatively low heterogeneity was observed (Higgins' $I^2=26.362$ %, Cochran's $Q=14.938$, $P=0.185$) (Fig. 2B). The random-effects HSROC curve revealed moderate sensitivity (0.696, 95 % CI 0.599–0.779) and reliable specificity (0.882, 95 % CI 0.778–0.941) in terms of the diagnostic performance of NT-proBNP in HFpEF, with an estimated area under the curve (AUC) of 0.836 (Fig. 2C). Fig. 2D shows the 95 % CI region for each study that used NT-proBNP as a diagnostic marker. Generally, the 95 % CI region of false positive rate appeared larger than that of sensitivity for most relevant studies. According to the funnel plot (Fig. A.1), there was some evidence of publication bias with NT-proBNP. However, the high statistical significance ($P<0.01$) of all 12 relevant studies suggests that the publication bias is not the underlying cause of this funnel asymmetry.

B-type natriuretic peptide

Seven studies [18,24–29] that investigated the diagnostic performance of BNP in HFpEF were analysed, with data extracted from 367 patients with HFpEF. The cut-off levels of BNP varied from 40 to 354 pg/mL (median 125 pg/mL) (Fig. 3A). In the random-effects forest plot (Fig. 3B), the pooled ln(DOR) was 2.70 (95 % CI 1.68–3.72), with no heterogeneity observed (Higgins' $I^2=0$ %, Cochran's $Q=4.422$, $P=0.620$). The pooled estimated sensitivity (0.787, 95 % CI 0.719–0.842) and specificity (0.796, 95 % CI 0.672–0.882) were well balanced when using BNP to diagnose HFpEF (Fig. 3C). The pooled AUC was 0.842. The number of participants was relatively small in three of the studies [25–27], resulting in the largest variance shown in Fig. 3D. Similarly to NT-proBNP, the funnel plot of BNP is asymmetrical (Fig. A.2). However, the high statistical significance ($P<0.01$) of all relevant studies suggests that publication bias is not the underlying cause of this funnel asymmetry.

Galectin-3

Analyses were performed on the diagnostic accuracy of Gal-3 using three studies [15,19,30]. The data were evaluated based on a total of 362 patients with HFpEF. Gal-3 cut-offs of 1.8 to 10.7 ng/mL (median 9.6 ng/mL) were reported (Fig. 4A). The pooled ln(DOR) was 2.94 (95 % CI 1.61–4.28), whereas substantial heterogeneity was observed (Higgins' $I^2=48.598$ %, Cochran's $Q=3.891$, $P=0.143$) (Fig. 4B). Sensitivity was relatively high (0.760, 95 % CI 0.631–0.855), as was specificity (0.803, 95 % CI 0.667–0.893) (Fig. 4C). The AUC was 0.851 for the diagnostic performance of Gal-3. Fig. 4D shows larger variance on false positive rate compared to sensitivity.

Suppression of tumorigenesis-2

Three studies [15,20,31] reported the diagnostic accuracy of ST2 in chronic HFpEF, with an adequate pooled number of patients with HFpEF ($n=290$), and the distribution of participants was well balanced across the studies. The cut-off levels of ST2 varied substantially across the three studies, ranging from 69 to 26470 pg/mL (Fig. 5A). The pooled ln(DOR) of ST2 as an individual diagnostic marker in HFpEF was 1.00 (95 % CI –0.07–2.07), with minimal heterogeneity (Higgins' $I^2=3.959$ %, Cochran's $Q=2.082$, $P=0.353$) (Fig. 5B). In line with the poor ln(DOR), sensitivity (0.636, 95 % CI 0.465–0.779) and specificity (0.595, 95 % CI 0.427–0.743) as well as AUC (0.647) were all unreliable (Fig. 5C). Although the number of participants was satisfactory in each study, the reported diagnostic accuracy varied highly, particularly in terms of false positive rate (Fig. 5D).

Discussion

HF can be categorized as acute or chronic, and it is possible and common for HF patients to experience acute episodes (e.g. acute exacerbation or decompensation) of HF with underlying chronic symptoms. Chronic underlying HFpEF accounts for a large proportion of its population and it must be noted that the biomarkers assessed in this study

Table 1 Characteristics of the included studies.

Study	Study design	Location	HFpEF				Control ^a			
			Mean LVEF (%)	<i>n</i>	Women (%)	Mean age (years)	Mean LVEF (%)	<i>n</i>	Women (%)	Mean age (years)
Liu et al., 2016 [17]	Retrospective	China	NA	50	46	64	NA	50	54	64
Cui et al., 2018 [15]	Retrospective	China	60	172	56	73	59	30	40	67
Tschope et al., 2005 [23]	Prospective	Germany	68	68	46	51	65	50	44	49
Santhanakrishnan et al., 2012 [20]	Prospective	Singapore	60	50	42	69	66	50	54	63
Stahrenberg et al., 2010 [22]	Retrospective	Germany	60	142	64	73	62	188	66	56
Kasner et al., 2011 [16]	Prospective	Germany	NA	107	40	53	NA	73	43	51
Dokainish et al., 2004 [26]	Prospective	USA	NA	19	NA	NA	NA	27	NA	NA
Liu et al., 2010 [27]	Prospective	China	65	39	50	52	67	20	46	46
Wei et al., 2005 [29]	Prospective	China	65	61	32	70	67	74	35	66
Lubien et al., 2002 [28]	Prospective	USA	NA	119	11	71	NA	175	9	60
Wang et al., 2013 [31]	Retrospective	China	68	68	54	68	68	39	33	60
Arques et al., 2007 [25]	Prospective	France	60	22	27	58	62	19	55	57
Mason et al., 2013 [18]	Retrospective	UK	NA	57	NA	NA	NA	308	NA	NA
Shuai et al., 2011 [21]	Prospective	China	66	45	52	67	67	53	50	62
Polat et al., 2016 [19]	Retrospective	Turkey	59	44	45	60	61	38	47	57
Celik et al., 2012 [14]	Retrospective	Turkey	72	71	63	57	68	50	38	56
Zapata et al., 2014 [24]	Prospective	Spain	60	50	51	68	59	36	19	57
Barutcuoglu et al., 2010 [13]	Retrospective	Turkey	NA	122	51	55	NA	119	55	53
Wu et al., 2015 [30]	Retrospective	China	68	146	62	70	NA	30	63	63

HF: heart failure; HFpEF: heart failure with preserved ejection fraction; LVEF: left ventricular ejection fraction; NA: not available.

^a Control is defined as participants without evidence of HF.

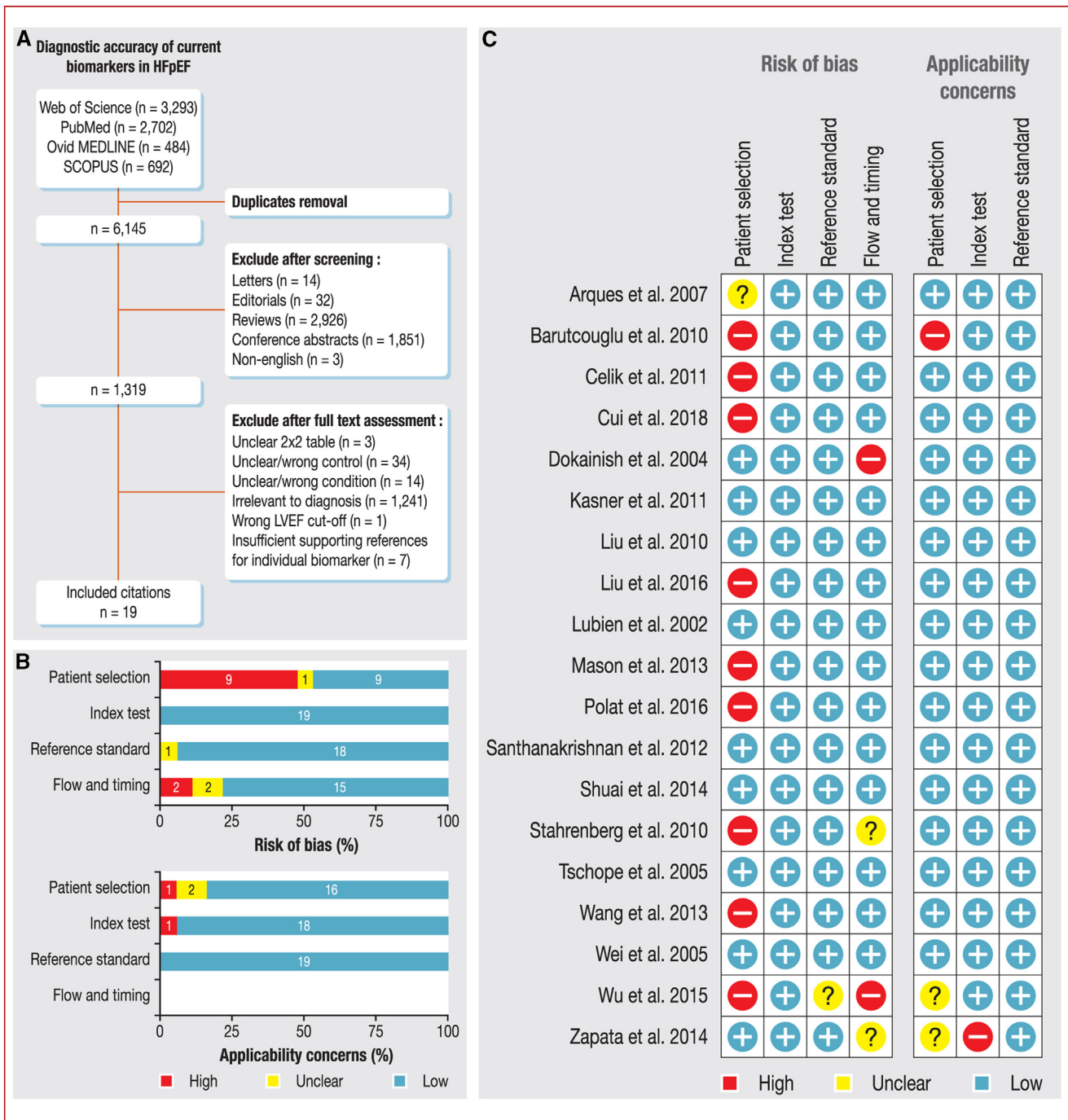


Figure 1. Summary of the study workflow and the number of included studies. A. Workflow of the systematic search according to PRISMA guidelines. B. Summary quality assessment of included studies independently evaluated using the QUADAS-2 tool. C. Outcomes of quality assessment of each included study. HFpEF: heart failure with preserved ejection fraction; LVEF: left ventricular ejection fraction; PRISMA: Preferred Reporting Items for Systematic reviews and Meta-Analyses; QUADAS-2: Quality Assessment for Diagnostic Accuracy Studies-2.

were performed in the context of patients with chronic HFpEF [32].

The diagnosis of chronic HFpEF is challenging as it is a multifactorial syndrome; it does not only include preserved LVEF, but additional symptoms of chronic HF are also considered in diagnosis [33]. However, the reliability of currently available biomarkers in the diagnosis of HFpEF remains partially unclear. Our study is the first to systematically and

comprehensively review the currently available circulating biomarkers (defined as proteins detected in blood-derived samples) in the diagnosis of chronic HFpEF. The main findings of this study are:

- NT-proBNP (ln(DOR) = 2.97) and BNP (ln(DOR) = 2.70) are the two most reliable individual diagnostic markers for HFpEF, albeit the diagnostic adequacy of both natriuretic peptides in chronic HFpEF remains moderate;

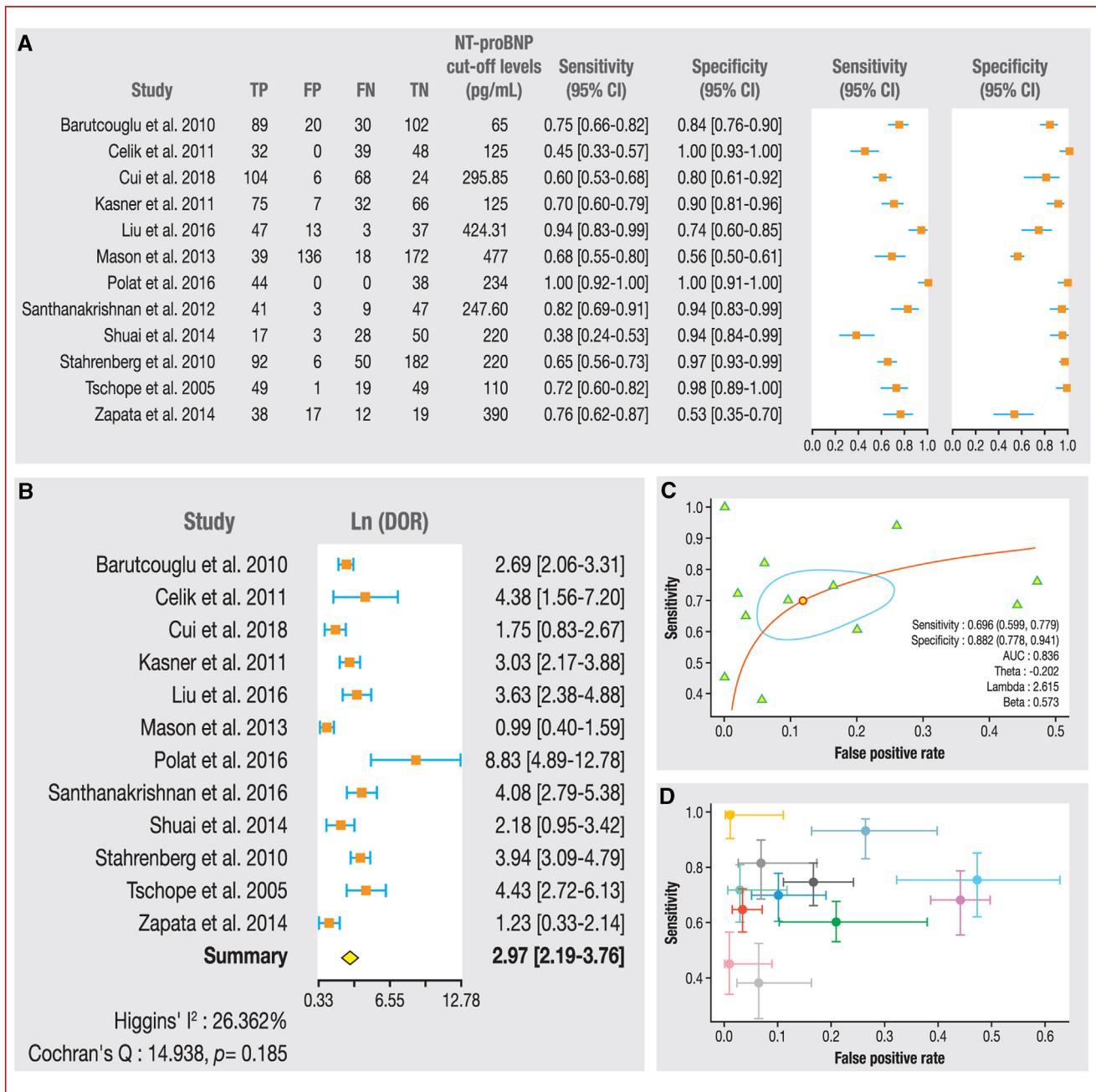


Figure 2. Diagnostic assessment of NT-proBNP in HFpEF using a bivariate, random-effects model. A. Forest plot of 12 studies that investigated the diagnostic performance of NT-proBNP in HFpEF, with sensitivity and specificity reported. B. Forest plot of $\ln(\text{DOR})$ related to the diagnostic accuracy of NT-proBNP in HFpEF. C. Plot of the HSROC curve showing the estimated pooled diagnostic accuracy. D. Plot of the HSROC curve showing the 95% CI of each study that evaluated the diagnostic accuracy of NT-proBNP in HFpEF. AUC: area under the curve; CI: confidence interval; FN: false negative; FP: false positive; HFpEF: heart failure with preserved ejection fraction; HSROC: hierarchical summary of receiver operating characteristic; $\ln(\text{DOR})$: natural logarithm-transformed diagnostic odds ratio; NT-proBNP: N-terminal pro-B-type natriuretic peptide; TN: true negative; TP: true positive.

- NT-proBNP shows higher specificity (0.882) than BNP (0.796) in the diagnosis of chronic HFpEF, whereas the sensitivity and specificity of BNP (0.787 and 0.796, respectively) are more balanced than for NT-proBNP (0.696 and 0.882, respectively);
 - Gal-3, an emerging biomarker for HFpEF management, displays promising diagnostic performance ($\ln(\text{DOR}) = 2.94$) for HFpEF;
 - ST2 shows no diagnostic potential ($\ln(\text{DOR}) = 1.00$) as an individual biomarker for the diagnosis of chronic HFpEF.
- Compared to a previous HFpEF biomarker meta-analysis [8], a lower degree of heterogeneity was detected in our study, as the heterogeneity statistics were only utilized for the estimation of $\ln(\text{DOR})$ rather than sensitivity and specificity. However, substantial heterogeneity was present related to the diagnostic accuracy of Gal-3, which could be

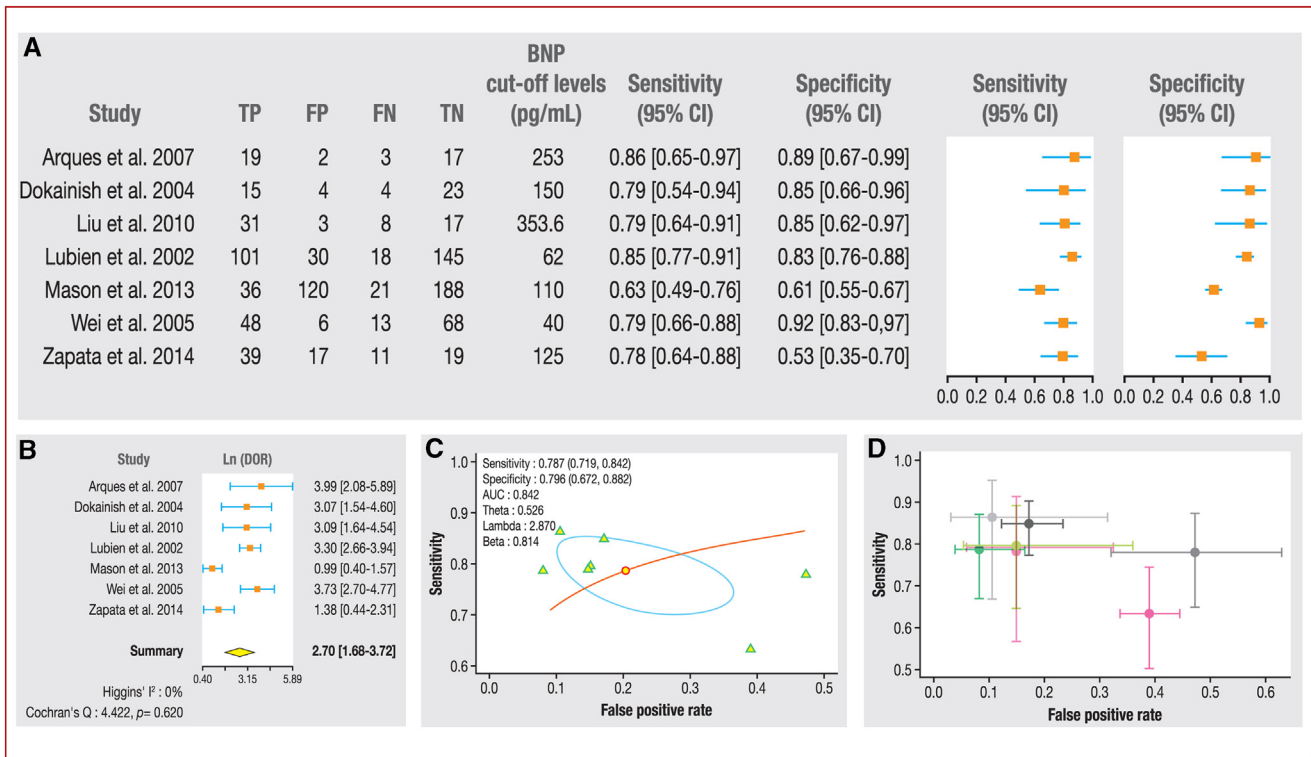


Figure 3. Diagnostic assessment of BNP in HFpEF using a bivariate, random-effects model. A. Forest plot of seven studies that investigated the diagnostic performance of BNP in HFpEF, with sensitivity and specificity reported. B. Forest plot of ln(DOR) related to the diagnostic accuracy of BNP in HFpEF. C. Plot of the HSROC curve showing the estimated pooled diagnostic accuracy. D. Plot of the HSROC curve showing the 95% CI of each study that evaluated the diagnostic accuracy of BNP in HFpEF. AUC: area under the curve; BNP: B-type natriuretic peptide; CI: confidence interval; FN: false negative; FP: false positive; HFpEF: heart failure with preserved ejection fraction; HSROC: hierarchical summary of receiver operating characteristic; ln(DOR): natural logarithm-transformed diagnostic odds ratio; TN: true negative; TP: true positive.

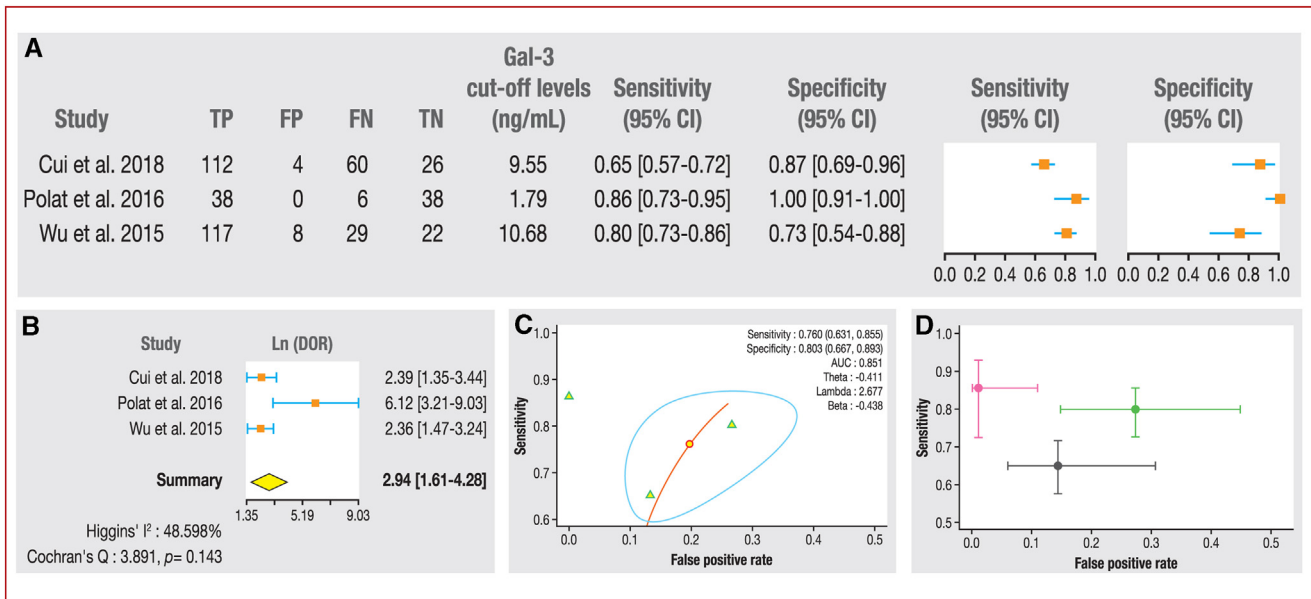


Figure 4. Diagnostic assessment of Gal-3 in HFpEF using a bivariate, random-effects model. A. Forest plot of three studies that investigated the diagnostic performance of Gal-3 in HFpEF, with sensitivity and specificity reported. B. Forest plot of ln(DOR) regarding the diagnostic accuracy of Gal-3 in HFpEF. C. Plot of the HSROC curve showing the estimated pooled diagnostic accuracy. D. Plot of the HSROC curve showing the 95% CI of each study that evaluated the diagnostic accuracy of Gal-3 in HFpEF. AUC: area under the curve; CI: confidence interval; FN: false negative; FP: false positive; Gal-3: galectin-3; HFpEF: heart failure with preserved ejection fraction; HSROC: hierarchical summary of receiver operating characteristic; ln(DOR): natural logarithm-transformed diagnostic odds ratio; TN: true negative; TP: true positive.

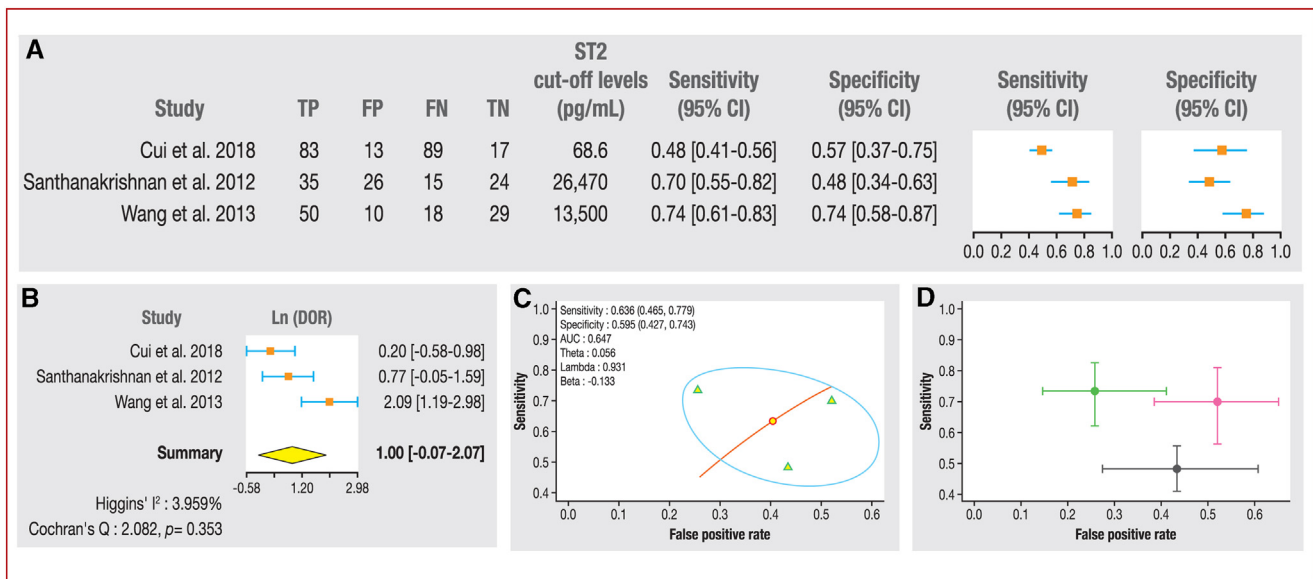


Figure 5. Diagnostic assessment of ST2 in HFpEF using a bivariate, random-effects model. A. Forest plot of three studies that investigated the diagnostic performance of ST2 in HFpEF, with sensitivity and specificity reported. B. Forest plot of ln(DOR) regarding the diagnostic accuracy of ST2 in HFpEF. C. Plot of the HSROC curve showing the estimated pooled diagnostic accuracy. D. Plot of the HSROC curve showing the 95% CI of each study that evaluated the diagnostic accuracy of ST2 in HFpEF. AUC: area under the curve; CI: confidence interval; FN: false negative; FP: false positive; HFpEF: heart failure with preserved ejection fraction; HSROC: hierarchical summary of receiver operating characteristic; ln(DOR): natural logarithm-transformed diagnostic odds ratio; ST2: suppression of tumorigenesis-2; TN: true negative; TP: true positive.

due to the retrospective design of all relevant selected studies [15,19,30]. In addition, specificity of 1.00 was introduced by one of the studies [19], which could be due to random chance. Another explanation for the heterogeneity could be caused by the wide difference of cut-off levels of Gal-3 (1.8, 9.6 and 10.7 ng/mL). The heterogeneous nature of HFpEF may also play a role in these differences between the studies included for Gal-3. All these underlying causes of heterogeneity could limit the applicability of the results of Gal-3. Therefore, it is important to note that the reliable diagnostic discriminative power of Gal-3 remains questionable.

A limited number of studies were included for the evaluation of the diagnostic accuracy of Gal-3 and ST2 in HFpEF, with only 362 and 290 patients with HFpEF, respectively. Trends of rising HF prevalence are shared amongst all countries, yet it is interesting that the studies included in the Gal-3 meta-analysis were largely conducted in Asia. With factors such as an ageing population and younger age range for HF patients, the generalizability of the findings in this study to patients of different ethnicities may be limited [32].

Natriuretic peptides are currently the most widely utilized biomarkers that support HFpEF diagnosis. Frequently, laboratories and clinical guidelines recommend the use of NT-proBNP over BNP in HFpEF diagnosis as the first-line option. This is likely due to the stability of NT-proBNP in blood samples for over 72 hours at room temperature without the need for additives. On the other hand, BNP is only stable in blood samples for 24 hours at room temperature, and the blood collection tubes are required to be coated with ethylenediaminetetraacetic acid [34].

NT-proBNP and BNP are strongly recommended for HFpEF diagnosis by current clinical guidelines [2,3], which is why there are a good number of high-quality observational

studies evaluating these biomarkers. As such, the diagnostic reliability of NT-proBNP and BNP is well-validated in our study. In this diagnostic accuracy meta-analysis, the pooled specificity of NT-proBNP for diagnosing HFpEF was higher than that of BNP, however the pooled sensitivity of BNP was better than NT-proBNP, consistent with another HFpEF biomarker meta-analysis [8]. Interestingly, both sensitivity and specificity of BNP were well balanced and reasonable. The AUC and ln(DOR) of NT-proBNP and BNP were satisfactory for diagnostic purposes. Therefore, the reliability of NT-proBNP and BNP are equal as diagnostic markers for chronic HFpEF, given that both natriuretic peptides are in the same biological pathway [35]. However, differential sensitivity and specificity were reported for NT-proBNP and BNP in HFpEF diagnosis, suggesting different utility in clinical settings. Due to the high specificity of NT-proBNP for HFpEF diagnosis, it is likely that NT-proBNP is more suitable for ruling out HFpEF. Higher sensitivity could be more applicable to secondary or tertiary care, whereas reliable specificity could be more important in primary care settings.

Overall, fairly consistent cut-off levels of NT-proBNP have been reported by relevant studies, with the best specificity being observed above 100-125 pg/mL [14,16,23], which is consistent with the cut-off (> 125 pg/mL) recommended by the 2016 ESC clinical guidelines for HF [2] and the new Heart Failure Association that include Pretest assessment, Echocardiographic and natriuretic peptide score, Functional testing in case of uncertainty, Final aetiology (HFA-PEFF) diagnostic algorithm [36]. Three studies utilized higher cut-off values of NT-proBNP (424 pg/mL [17] and 477 pg/mL [18], 390 pg/mL [24]), which led to the lowest specificity. This could further support utilizing the recommended cut-off values for NT-proBNP of approximately 100 pg/mL for

the diagnosis of HFpEF. Despite the recommended cut-off level of BNP being 35 pg/mL [2,36], the cut-off values for BNP reported by the studies we included varied widely. In addition, one study reported that the cut-off value of ~35 pg/mL provided an unreliable diagnostic accuracy (sensitivity: 0.67; specificity: 0.73) for chronic HFpEF [37]. However, considerably higher cut-off levels for BNP were reported in other relevant studies. Further population-based comparable investigations of the diagnostic performance of BNP at different cut-off concentrations for HFpEF diagnosis are therefore necessary.

ST2 is emerging as a new diagnostic marker for HFpEF and is recommended by the latest AHA guidelines [3]. Nevertheless, we observed a limited diagnostic accuracy of ST2 in chronic HFpEF diagnosis, supported by three studies reporting differential findings [15,20,31]. The limited diagnostic value of ST2 in HFpEF is likely caused by the lack of association of ST2 with left ventricular function and structure [38]. Despite the limited performance of ST2 in chronic HFpEF, ST2 is beneficial in the acute settings [39]. Although ST2 has been shown to be associated with HF diagnosis above the cut-off concentration of 35 ng/mL, as recommended by the Food and Drug Administration [40], the diagnostic adequacy in HF subtypes, including HFpEF and HFrEF, were modest in an older adult population [41]. Therefore, the optimal cut-off value of ST2 in HF subtypes should be re-evaluated in future observational studies that include specific HF phenotype.

Collectively, the specificity of NT-proBNP, BNP and Gal-3 are generally higher than their sensitivity, suggesting a more advanced ability of ruling out HFpEF, consistent with the proposals in current guidelines [2,42]. Generally, these biomarkers play a critical role in discriminating acute HF from non-cardiac dyspnoea in acute settings, as their concentrations are significantly elevated [39,43]. However, the opposite is true in chronic settings where the levels of biomarkers could be closer to normal ranges. Therefore, diagnosis of chronic HFpEF is still challenging, especially given the common comorbidities that further complicate the diagnosis. Overall, in line with the recommendations of the HFA-PEFF diagnostic algorithm [36], biomarkers should be used in addition to echocardiography for the early diagnosis of HFpEF. Future studies should therefore investigate the clinical utility of current biomarkers in combination with echocardiographic measurements.

Conclusions

HFpEF accounts for approximately half of all patients with HF, and it is associated with similar mortality to HFrEF, yet it is ineffectively managed with pharmacotherapies. Due to the poorly understood pathogenesis of HFpEF, there are often delays in its diagnosis and treatment, leading to worse outcomes for HFpEF patients. Accurate biomarkers are critical for the early diagnosis of HFpEF, emphasizing the urgent need for biomarker discovery and validation. Nevertheless, in this meta-analysis, it was demonstrated that NT-proBNP and BNP remain the most reliable biomarkers for HFpEF diagnosis. NT-proBNP is possibly more reliable for chronic HFpEF diagnosis given its more consistent and less varied cut-off diagnostic values and higher specificity than BNP. Gal-3 also displays a reliable diagnostic discriminative power, however

the high heterogeneity between the studies limits the applicability of Gal-3's for HFpEF diagnosis based on published studies included here. ST2 appears to have limited diagnostic potential for chronic HFpEF. Therefore, more robust and larger studies are warranted to evaluate these biomarkers and discover new biomarkers for HFpEF diagnosis and prognosis.

Funding

Hao Chen and Michael Chhor are supported by an Australian Government Research Training Program (RTP) Stipend and RTP Fee-Offset Scholarship through University of Technology Sydney.

Authors' contributions

H. C. (supervised by B. S. R., K. M. and L. M.) conducted the search, identified the studies, performed the statistical analyses and wrote the first draft of this manuscript. M. C. conducted the search, screened, assessed and identified the studies, extracted the data and contributed to the writing. B. S. R., M. C. and K. M. reviewed the quality of the studies. L. M. conceptualized the study and edited the manuscript. All authors reviewed and approved the manuscript.

Appendix A. Supplementary data

Supplementary data associated with this article can be found, in the online version, at <https://doi.org/10.1016/j.acvd.2021.10.007>.

Disclosure of interest

The authors declare that they have no competing interest.

References

- [1] Groenewegen A, Rutten FH, Mosterd A, Hoes AW. Epidemiology of heart failure. *Eur J Heart Fail* 2020;22:1342–56.
- [2] Ponikowski P, Voors AA, Anker SD, et al. 2016 ESC Guidelines for the diagnosis and treatment of acute and chronic heart failure: The Task Force for the diagnosis and treatment of acute and chronic heart failure of the European Society of Cardiology (ESC). Developed with the special contribution of the Heart Failure Association (HFA) of the ESC. *Eur Heart J* 2016;37:2129–200.
- [3] Yancy CW, Jessup M, Bozkurt B, et al. 2017 ACC/AHA/HFSA Focused Update of the 2013 ACCF/AHA Guideline for the Management of Heart Failure: A Report of the American College of Cardiology/American Heart Association Task Force on Clinical Practice Guidelines and the Heart Failure Society of America. *Circulation* 2017;136:e137–61.
- [4] Owan TE, Hodge DO, Herges RM, Jacobsen SJ, Roger VL, Redfield MM. Trends in prevalence and outcome of heart failure with preserved ejection fraction. *N Engl J Med* 2006;355:251–9.
- [5] Lam CSP, Gamble GD, Ling LH, et al. Mortality associated with heart failure with preserved vs. reduced ejection fraction in a

- prospective international multi-ethnic cohort study. *Eur Heart J* 2018;39:1770–80.
- [6] Meta-analysis Global Group in Chronic Heart Failure (MAG-GIC). The survival of patients with heart failure with preserved or reduced left ventricular ejection fraction: An individual patient data meta-analysis. *Eur Heart J* 2012;33:1750–7.
- [7] Zheng SL, Chan FT, Nabeebaccus AA, et al. Drug treatment effects on outcomes in heart failure with preserved ejection fraction: A systematic review and meta-analysis. *Heart* 2018;104:407–15.
- [8] Remmelzwaal S, van Ballegooijen AJ, Schoonmade LJ, et al. Natriuretic peptides for the detection of diastolic dysfunction and heart failure with preserved ejection fraction—a systematic review and meta-analysis. *BMC Med* 2020;18:290.
- [9] Alma LJ, Bokslag A, Maas A, Franx A, Paulus WJ, de Groot CJM. Shared biomarkers between female diastolic heart failure and pre-eclampsia: A systematic review and meta-analysis. *ESC Heart Fail* 2017;4:88–98.
- [10] Moher D, Liberati A, Tetzlaff J, Altman DG, Group PRISMA. Preferred reporting items for systematic reviews and meta-analyses: The PRISMA statement. *BMJ* 2009;339:b2535.
- [11] Liu Z, Yao Z, Li C, Liu X, Chen H, Gao C. A step-by-step guide to the systematic review and meta-analysis of diagnostic and prognostic test accuracy evaluations. *Br J Cancer* 2013;108:2299–303.
- [12] Whiting PF, Rutjes AW, Westwood ME, et al. QUADAS-2: A revised tool for the quality assessment of diagnostic accuracy studies. *Ann Intern Med* 2011;155:529–36.
- [13] Barutcuoglu B, Parildar Z, Basol G, Gurgun C, Tekin Y, Bayindir O. The detection of left ventricular diastolic dysfunction in hypertensive patients: Performance of N-terminal probrain natriuretic peptide. *Blood Press* 2010;19:212–7.
- [14] Celik A, Koc F, Kadi H, et al. Relationship between red cell distribution width and echocardiographic parameters in patients with diastolic heart failure. *Kaohsiung J Med Sci* 2012;28:165–72.
- [15] Cui Y, Qi X, Huang A, Li J, Hou W, Liu K. Differential and predictive value of galectin-3 and soluble suppression of tumorigenicity-2 (sST2) in heart failure with preserved ejection fraction. *Med Sci Monit* 2018;24:5139–46.
- [16] Kasner M, Gaub R, Westermann D, et al. Simultaneous estimation of NT-proBNP on top to mitral flow Doppler echocardiography as an accurate strategy to diagnose diastolic dysfunction in HFNEF. *Int J Cardiol* 2011;149:23–9.
- [17] Liu S, Iskandar R, Chen W, et al. Soluble glycoprotein 130 and heat shock protein 27 as novel candidate biomarkers of chronic heart failure with preserved ejection fraction. *Heart Lung Circ* 2016;25:1000–6.
- [18] Mason JM, Hancock HC, Close H, et al. Utility of biomarkers in the differential diagnosis of heart failure in older people: Findings from the heart failure in care homes (HFinCH) diagnostic accuracy study. *PLoS One* 2013;8:e53560.
- [19] Polat V, Bozcali E, Uygun T, Opan S, Karakaya O. Diagnostic significance of serum galectin-3 levels in heart failure with preserved ejection fraction. *Acta Cardiol* 2016;71:191–7.
- [20] Santhanakrishnan R, Chong JP, Ng TP, et al. Growth differentiation factor 15, ST2, high-sensitivity troponin T, and N-terminal pro brain natriuretic peptide in heart failure with preserved vs. reduced ejection fraction. *Eur J Heart Fail* 2012;14:1338–47.
- [21] Shuai XX, Chen YY, Lu YX, et al. Diagnosis of heart failure with preserved ejection fraction: Which parameters and diagnostic strategies are more valuable? *Eur J Heart Fail* 2011;13:737–45.
- [22] Stahrenberg R, Edelmann F, Mende M, et al. The novel biomarker growth differentiation factor 15 in heart failure with normal ejection fraction. *Eur J Heart Fail* 2010;12:1309–16.
- [23] Tschope C, Kasner M, Westermann D, Gaub R, Poller WC, Schultheiss HP. The role of NT-proBNP in the diagnostics of isolated diastolic dysfunction: Correlation with echocardiographic and invasive measurements. *Eur Heart J* 2005;26:2277–84.
- [24] Zapata L, Betbese AJ, Roglan A, Ordonez-Llanos J. Use of B-type natriuretic peptides to detect the existence and severity of diastolic dysfunction in non-cardiac critically ill patients: A pilot study. *Minerva Anestesiol* 2014;80:194–203.
- [25] Arques S, Roux E, Sbragia P, et al. Usefulness of bedside tissue Doppler echocardiography and B-type natriuretic peptide (BNP) in differentiating congestive heart failure from noncardiac cause of acute dyspnea in elderly patients with a normal left ventricular ejection fraction and permanent, nonvalvular atrial fibrillation: Insights from a prospective, monocenter study. *Echocardiography* 2007;24:499–507.
- [26] Dokainish H, Zoghbi WA, Lakkis NM, Quinones MA, Nagueh SF. Comparative accuracy of B-type natriuretic peptide and tissue Doppler echocardiography in the diagnosis of congestive heart failure. *Am J Cardiol* 2004;93:1130–5.
- [27] Liu H, Zhang YZ, Gao M, Liu BC. Elevation of B-type natriuretic peptide is a sensitive marker of left ventricular diastolic dysfunction in patients with maintenance haemodialysis. *Biomarkers* 2010;15:533–7.
- [28] Lubien E, DeMaria A, Krishnaswamy P, et al. Utility of B-natriuretic peptide in detecting diastolic dysfunction: Comparison with Doppler velocity recordings. *Circulation* 2002;105:595–601.
- [29] Wei T, Zeng C, Chen L, et al. Bedside tests of B-type natriuretic peptide in the diagnosis of left ventricular diastolic dysfunction in hypertensive patients. *Eur J Heart Fail* 2005;7:75–9.
- [30] Wu CK, Su MY, Lee JK, et al. Galectin-3 level and the severity of cardiac diastolic dysfunction using cellular and animal models and clinical indices. *Sci Rep* 2015;5:17007.
- [31] Wang YC, Yu CC, Chiu FC, et al. Soluble ST2 as a biomarker for detecting stable heart failure with a normal ejection fraction in hypertensive patients. *J Card Fail* 2013;19:163–8.
- [32] Chen YT, Wong LL, Liew OW, Richards AM. Heart failure with reduced ejection fraction (HFREF) and preserved ejection fraction (HFPEF): The diagnostic value of circulating microRNAs. *Cells* 2019;8:1651.
- [33] Gazewood JD, Turner PL. Heart failure with preserved ejection fraction: Diagnosis and management. *Am Fam Physician* 2017;96:582–8.
- [34] Weber M, Hamm C. Role of B-type natriuretic peptide (BNP) and NT-proBNP in clinical routine. *Heart* 2006;92:843–9.
- [35] de Lemos JA, McGuire DK, Drazner MH. B-type natriuretic peptide in cardiovascular disease. *Lancet* 2003;362:316–22.
- [36] Pieske B, Tschope C, de Boer RA, et al. How to diagnose heart failure with preserved ejection fraction: the HFA-PEFF diagnostic algorithm: A consensus recommendation from the Heart Failure Association (HFA) of the European Society of Cardiology (ESC). *Eur Heart J* 2019;40:3297–317.
- [37] Arques S, Jaubert MP, Bonello L, et al. Usefulness of basal B-type natriuretic peptide levels for the diagnosis of diastolic heart failure in young patients: An echocardiographic-catheterization study. *Int J Cardiol* 2010;145:51–2.
- [38] AbouEzzeddine OF, McKie PM, Dunlay SM, et al. Suppression of tumorigenicity 2 in heart failure with preserved ejection fraction. *J Am Heart Assoc* 2017;6:e004382.
- [39] Mueller T, Gegenhuber A, Leitner I, Poelz W, Haltmayer M, Dieplinger B. Diagnostic and prognostic accuracy of galectin-3 and soluble ST2 for acute heart failure. *Clin Chim Acta* 2016;463:158–64.
- [40] US Food and Drug Administration. Substantial equivalence determination decision summary assay only template. https://www.accessdata.fda.gov/cdrh_docs/reviews/k111452.pdf. [accessed 25 October 2021].

- [41] Parikh RH, Seliger SL, Christenson R, Gottdiener JS, Psaty BM, deFilippi CR. Soluble ST2 for prediction of heart failure and cardiovascular death in an elderly, community-dwelling population. *J Am Heart Assoc* 2016;5:e003188.
- [42] Paulus WJ, Tschope C, Sanderson JE, et al. How to diagnose diastolic heart failure: A consensus statement on the diagnosis of heart failure with normal left ventricular ejection fraction by the Heart Failure and Echocardiography Associations of the European Society of Cardiology. *Eur Heart J* 2007;28:2539–50.
- [43] Maisel AS, McCord J, Nowak RM, et al. Bedside B-Type natriuretic peptide in the emergency diagnosis of heart failure with reduced or preserved ejection fraction. Results from the Breathing Not Properly Multinational Study. *J Am Coll Cardiol* 2003;41:2010–7.

REVIEW ARTICLE

Diagnostic and prognostic biomarkers reflective of cardiac remodelling in diabetes mellitus: A scoping review

Michael Chhor¹ | William Law¹ | Milan Pavlovic² | Dunja Aksentijevic³ |
Kristine McGrath¹ | Lana McClements¹

¹School of Life Sciences, Faculty of Science, University of Technology Sydney, New South Wales, Sydney, Australia

²Department of Internal Medicine - Cardiology, Faculty of Medicine, University of Nis, Nis, Serbia

³Centre for Biochemical Pharmacology, William Harvey Research Institute, Barts and the London School of Medicine and Dentistry, Queen Mary University of London, London, UK

Correspondence

Lana McClements, School of Life Sciences, University of Technology Sydney, Sydney, NSW, Australia.
Email: [lana.mcclements@uts.edu.au](mailto: lana.mcclements@uts.edu.au)

Funding information

Australian Government Research Training Program Scholarship

Abstract

Aims: The aim of this scoping review is to evaluate the current biomarkers used in the assessment of adverse cardiac remodelling in people with diabetes mellitus (DM) and in the diagnosis and prognosis of subsequent cardiovascular disease. We aim to discuss the biomarkers' pathophysiological roles as a reflection of the cardiac remodelling mechanisms in the presence of DM.

Methods: We performed the literature search to include studies from 2003 to 2021 using the following databases: MEDLINE, Scopus, Web of Science, PubMed, and Cochrane library. Articles that met our inclusion criteria were screened and appraised before being included in this review. The PRISMA guidelines for Scoping Reviews were followed.

Results: Our literature search identified a total of 43 eligible articles, which were included in this scoping review. We identified 15 different biomarkers, each described by at least two studies, that were used to determine signs of cardiac remodelling in cardiovascular disease (CVD) and people with DM. NT-proBNP was identified as the most frequently employed biomarker in this context; however, we also identified emerging biomarkers including hs-CRP, hs-cTnT, and Galectin-3.

Conclusion: There is a complex relationship between DM and cardiovascular health, where more research is needed. Current biomarkers reflective of adverse cardiac remodelling in DM are often used to diagnose other CVDs, such as NT-proBNP for heart failure. Hence there is a need for identification of specific biomarkers that can detect early signs of cardiac remodelling in the presence of DM. Further research into these biomarkers and mechanisms can deepen our understanding of their role in DM-associated CVD and lead to better preventative therapies.

KEYWORDS

biomarker, cardiac fibrosis, cardiovascular disease, heart failure, metabolomics, scoping review

This is an open access article under the terms of the [Creative Commons Attribution-NonCommercial](https://creativecommons.org/licenses/by-nc/4.0/) License, which permits use, distribution and reproduction in any medium, provided the original work is properly cited and is not used for commercial purposes.

© 2023 The Authors. *Diabetic Medicine* published by John Wiley & Sons Ltd on behalf of Diabetes UK.

1 | INTRODUCTION

Cardiovascular disease (CVD) is an umbrella term encompassing any disorder affiliated with the heart and blood vessels, such as coronary artery disease (CAD) and heart failure (HF).¹ CVD is currently the highest cause of mortality worldwide, representing 32% of all deaths globally.² For perspective, prevalent cases of CVD have reportedly doubled between 1990 and 2019 from 271 million to 523 million people. CVD resultant deaths have similarly followed this trend and increased from 12.1 million to 18.6 million people between 1990 and 2019.³ Consequently, it is fast becoming a serious financial and medical burden to the entire population.

Meanwhile, diabetes mellitus (DM) is also a pervasive and deleterious disease. Worldwide, DM affects 422 million people and accounts for 1.6 million deaths a year.⁴ There are two key pathological processes that cause the development of DM: inadequate insulin production by beta islet cells of pancreas, and insulin resistance (IR), which results from impaired insulin response in peripheral tissues. DM is a heterogenous disease with multiple organs involved in the aetiology: liver, skeletal muscles, pancreas, kidneys, brain, small intestine, and adipose tissue.⁵ Hyperglycaemia associated with DM consequently triggers a surfeit of macro- and microvascular complications.⁶

The risk of CVD morbidity in DM is approximately two-three times more likely compared to those without DM.⁷ The Framingham Heart Study concluded that type-2 diabetes mellitus (T2D) independently increases the HF risk up to two-fold in men and five-fold in women compared to matched controls.^{8,9} Thus, accelerated HF is a common clinical manifestation of CVD in T2D.⁵ DM progression leads to specific changes to myocardial structure, function, and metabolism, collectively defined as diabetic cardiomyopathy (dbCM).^{5,10} Hyperglycaemia, insulin resistance as well as lipotoxicity drive numerous fibrogenic pathways, triggering generation of reactive oxygen species (ROS), enhancing neurohumoral responses, stimulating growth factor cascades (i.e., TGF- β /Smad3 and PDGFs), inducing pro-inflammatory cytokines and chemokines, generating advanced glycation end-products (AGEs), stimulating the AGE-receptor for AGE (RAGE) axis, and up-regulating fibrogenic matricellular proteins.¹¹ Despite DM-triggered fibrogenic signalling sharing common characteristics in multiple tissues, diabetic myocardium develops more pronounced and clinically significant fibrosis.¹¹

Myocardial fibrosis plays an essential role in cardiac remodelling and is linked to DM and many CVDs.¹² Its primary culprit is cardiac fibroblast (CF) to myofibroblast (MF) differentiation. CFs are one of the largest cardiac cell populations, responsible for extracellular matrix (ECM) homeostasis, however, once harmed they transform into

What's new?

Cardiovascular disease (CVD) is still the biggest killer with increasing incidence, and people with diabetes mellitus (DM) have a two-three-fold increased risk of CVD. Cardiac remodelling is an early sign of deteriorating cardiac health; however, the mechanisms are poorly understood and can differ in the presence of DM. In this scoping review, we assessed publicly available data on all biomarkers of adverse cardiac remodelling in people with DM. We identified fifteen reliable biomarkers that could also represent viable therapeutic targets for adverse cardiac remodelling in people with DM. Timely diagnosis of early cardiac changes could significantly improve the quality of life of people with DM with a potential to prevent or delay heart disease.

MFs.¹³ This considerably elevates ECM protein levels, which adversely augment ECM heart structure and promote formation of scar tissue.¹⁴ In DM, myocardial fibrosis and cardiac remodelling have become structural hallmarks of a diabetic heart. In fact, in absence of traditional cardiovascular risk factors, including hypertension, valvular disease and overt CAD, dbCM develops.¹⁵ Interestingly, myocardial fibrosis and adverse remodelling are the first signs of dbCM.^{15,16}

People with DM show signs of impaired left ventricular (LV) function, thickness, and remodelling, often resulting in LV diastolic dysfunction. Cardiac remodelling is a compensatory process exacerbated when the heart is under duress; however, exact mechanisms have yet to be elucidated. Insulin resistance and AGEs are key mechanisms in this compensation that may explain the development of hypertrophy of the heart in the presence of DM.¹⁷ Conversely, it should be noted that insulin sensitivity and signalling pathways play a significant role in dbCM both exacerbating its progression, but also having cardioprotective mechanisms. Particularly through the activation of the PI3Ka/Akt pathway, the suppression of cardiac ROS, and inflammation in dbCM, insulin signalling exhibit a mechanistic role in the diabetic heart. It should be noted that this evidence stems from animal studies and may not correspond to a human scenario.¹⁸ Thus, the effects of DM on cardiac remodelling evidently contain many complex mechanisms that need to be further studied.

Hence, this scoping review aims to provide an assessment of current biomarkers available that can be utilised in the detection of myocardial fibrosis/remodelling and,

diagnosis and prognosis of subsequent CVD or cardiovascular complications. Through assessing the viability of these biomarkers, efficient diagnostic, prognostic and therapeutic interventions could be developed to detect or stop the progression of myocardial fibrosis/remodelling in its early stages. This could aid early detection of myocardial fibrosis/cardiac remodelling to stop its permanent damage, and most importantly attenuate the development of lethal CVDs, such as HF, particularly in people with DM.

2 | METHODS

2.1 | Research question

The purpose of this scoping review is to appraise the current biomarkers used in the diagnosis of cardiac remodelling and prognosis of CVD, linking their pathophysiological roles as a reflection of the underlying mechanisms.

2.2 | Identification of studies

This scoping review was conducted following the PRISMA guideline for Scoping Reviews.¹⁹ The following search term sets were used:

Set (A): biomarker OR marker OR markers.

Set (B): cardiac remodelling OR remodelling OR cardiac remodeling OR remodeling.

Set (C): diabetes or diabetes mellitus.

The following databases: MEDLINE, Scopus, Web of Science, PubMed, and Cochrane library. All searches were conducted from June to September 2021 by investigators MC and WL.

2.3 | Study selection

2.3.1 | Inclusion criteria

Studies that were included had the main aim of assessing cardiac remodelling using a biomarker in people with DM. This includes studies that did not focus solely on DM but had a subpopulation of people with DM within the study. Studies that did not have a control group of people without DM were also selected. Only studies written in the English language were included.

2.3.2 | Exclusion criteria

Studies that were excluded did not examine people with DM or have a biomarker measure indicative of cardiac

remodelling. Further studies that were excluded were review articles, articles not in English, and case reports.

2.4 | Data extraction

Following full-text screening, papers that met the selection criteria were scanned for extraction. The following details were extracted: Year, Author, Country, Patient Characteristics, Patient numbers with DM or in the control group, Mean Age, Biomarker, Biomarker Classification, and Level of Evidence. No review protocol was available specific to the purposes of this scoping review, hence biomarker classification and the level of evidence were appropriated as per a scoping review conducted by De Luca Canto et al. 2015.²⁰ The biomarker clinical application was classified as: (1) potential biomarker(s) of cardiac remodelling; (2) inconclusive biomarker of cardiac remodelling, and (3) evidence not supportive as potential biomarker of cardiac remodelling. The level of evidence was classified as A (well-designed prognostic or diagnostic studies on relevant population), B (prognostic or diagnostic studies with minor limitations, overwhelmingly consistent evidence from observational studies) or C (observational studies [case-control and cohort design]).

3 | RESULTS

3.1 | Study selection

Two independent investigators, MC and WL, identified 4400 papers using the search terms set in the five databases outlined in the methodology. After removing any duplicate papers, a total of 1774 papers remained for Title and Abstract screening. Following the initial screening, 127 papers remained for full-text screening. Of those papers, 43 were included in our data extraction displayed in [Table 1](#). The remaining 84 articles were excluded for: not relating to the topic, not including a biomarker, not written as an article, not in English, inaccessible, and with insufficient data. This process is visualised in [Figure 1](#), with a PRISMA flow chart diagram depicting the search process.

3.2 | Study characteristics

Studies were extracted for descriptive data and displayed in [Table 1](#), with a total of 43 studies that were included. The year of study ranged from 2003 to 2021. It was determined from our investigation that the origin country of study had a widespread reach, being conducted in over 24

TABLE 1 Descriptive characteristics of included cardiac remodelling studies.

Country	Cohort characteristics	Cases	Control	Mean age	Biomarker	Biomarker classification	Level of evidence
Taiwan	CVD history	505	1416	57.1	NT-proBNP	2	C
International	CVD history	5141/542	8023/350	65/64.7	NT-proBNP (100 ng/L) hs-cTnT (14 ng/L)	1	A
Germany	General	19	858	48	NT-proBNP BNP	1	C
Spain	HF patient	314	562	70.3	NT-proBNP (1720 ng/L), hs-cTnT (16 ng/L), hs-ST2 (50 ng/L)	1	B
Australia	High-risk HF	654	2896	70.4	NT-proBNP	1	A
USA	LVSD outpatient	38/25	37/51	69.3/57.4	Galectin-3 (20 ng/mL)	2	B
Norway	General	380	1678	63.9	cTnT, NT-proBNP, CRP, HbA _{1c}	2	C
USA	General	82	2570	66.9	Ceramides C16:0/C24:0	1	B
Romania	DM/MI patient	45	43	61.3	hs-CRP, EAT	1	A
USA	General	110	638	50	NT-proBNP, hs-cTnT, hs-CRP	3	B
Italy	STEMI patient	12	88	62.5	EAT	3	C
Russia	HF patient	HFpEF: 11, HFrEF: 30	N/A	HFpEF: 57, HFrEF: 63	NT-proBNP, Galectin-3, sST2	1	B
Europe	T1D patient	493	N/A	39.5	TIMP-1, MMP-1, 2, 3, 9, 10	2	B
Italy	T2D patient	51	20	60	miR122-5p	2	C
Sweden	General	116/105	N/A	70.1/77.5	Endostatin, NT-proBNP	3	B

TABLE 1 (Continued)

Country	Cohort characteristics	Cases	Control	Mean age	Biomarker	Biomarker classification	Level of evidence
Japan	HF patient	17	N/A	60.7	NT-proBNP, hs-cTnT	2	C
International	T2D patient	12,310	4182	65.1	NT-proBNP (450 pg/mL), hs-cTnT (3 pg/mL), hs-CRP (0.15 mg/L)	1	A
International	HF in-patient	922	1111	Diabetes: 70.3 Non-diabetes: 70	BNP (500 pg/mL), NT-proBNP (2000 pg/mL), sST2, Galectin-3, hs-CRP	1	B
Denmark	T2D patient	246	N/A	Above median: 58 Below Median: 59	FGF-23 (median 74 ng/L)	2	C
Italy	General	533	1325	N/A	hs-CRP	1	B
CORONA: USA COACH: USA	HF patient	CORONA: 333 COACH: 95	N/A	CORONA: 71.6 COACH: 69.9	Galectin-3 (17.8 ng/mL)	1	B
USA	General	Men: 41 Women: 42	N/A	Men: 87 Women: 78.6	hs-CRP, IL-6, TNF α	2	C
USA	General	Men: 153 Women: 133	N/A	Men: 59 Women: 58	hs-CRP, BNP	2	C
Europe	High risk CVD	310	217	Diabetes: 71.9 Non-diabetes: 73.5	NT-proBNP (125-1000 ng/L), Galectin-3, hs-cTnT	1	A
USA	HF out-patient	117	N/A	56	BNP, MMP-9	1	C
USA	General	87	N/A	56	PIIINP	2	C
Taiwan	General	113	N/A	51.03	hs-CRP, NT-proBNP	1	B
Ireland	High risk CVD	498	N/A	66.2	MMP-9	1	B

(Continues)

TABLE 1 (Continued)

Country	Cohort characteristics	Cases	Control	Mean age	Biomarker	Biomarker classification	Level of evidence
France	T2D patient	91	N/A	Men: 60 Women: 61	BNP	1	A
France	CHF patient	64	92	Control: 56 T2D: 56	PIIINP, PICP, PINP, MMP-1, TIMP-1	2	B
Denmark	T2D patient	60	30	Control:52 T2D: 55	NT-proBNP	1	A
China	CVD patient	DM MACE: 89 DM MACE FREE: 113	748	DM MACE: 63.07 DM MACE FREE: 68.62	hs-ST2, NT-proBNP	1	B
Spain	HF patient	321	N/A	70.2	hs-ST2, NT-proBNP	1	B
Ukraine	T2D patient	186	20	52.49	hs-CRP, Adiponectin, Omentin-1	2	B
Turkey	STEMI patient	71	207	55.3	NT-proBNP	2	B
Netherlands	HF patient	120	N/A	72	Galectin-3	1	B
USA	HF patient	116	132	DM: 69 Non-DM: 74.3	hs-CRP, hs-TnT, NT-proBNP, sST2, PICP, CITP, PIIINP, MMP-2,9, TIMP-1, Galectin-3	2	C

TABLE 1 (Continued)

Country	Cohort characteristics	Cases	Control	Mean age	Biomarker	Biomarker classification	Level of evidence
Greece	LVDD patients	(C) T2DM without LVDD: 48 (D) T2DM with LVDD: 50	(A) Healthy: 42 (B) Non-T2DM with LVDD: 18	A: 55.10 B: 60.33 C: 54.87 D: 56.98	sST2, BNP, hs-CRP	2	B
Egypt	T2D patient	EF < 50%: 46 EF > 50%: 54	50	EF < 50%: 47.71 EF > 50%: 44.89 Control: 45.05	IL-6, NT-proBNP	1	C
China	T2D patient	110	N/A	EF < 50%: 65.71 EF > 50%: 66.29	Ang-II, NT-proBNP	2	C
Denmark	T2D patient	Microalbuminuria = 149, Macroalbuminuria = 563.	703	Control: 64 Microalbuminuria = 66 Macroalbuminuria = 67	Albumin	2	C
Iran	STEMI patient	DM normal {25 (OH)} = 12 DM deficient{25 (OH)} = 26	38	DM normal {25 (OH)} = 63.1 DM deficient{25 (OH)} = 59.6	25 (OH), MMP9	1	B
England	MI patient	Δ EDV \leq 0: 22 Δ EDV >0: 24	42	63	VEGFB	2	B

Note: The biomarker clinical application was classified as (1) potential biomarker (s) of remodelling; (2) inconclusive biomarker for remodelling, and (3) evidence not supportive as potential biomarker for remodelling (s). The level of evidence was classified in A (well-designed prognostic or diagnostic studies on relevant population), B (prognostic or diagnostic studies with minor limitations, overwhelmingly consistent evidence from observational studies), C (observational studies [case-control and cohort design]).

Abbreviations: 25 (OH), 25-hydroxy vitamin D; Ang II, angiotensin II; BNP, brain natriuretic peptide; CHF, chronic heart failure; C1TP, carboxyl-terminal telopeptide type 1 collagen; CRP, C-reactive protein; cTnT, cardiac troponin T; CVD, cardiovascular disease; DM, diabetes mellitus; EAT, epicardial adipose thickness; FGF-23, fibroblast growth factor-23; HbA_{1c}, haemoglobin A_{1c}; HF, heart failure; hs-CRP, high-sensitivity C-reactive protein; hs-cTnT, high-sensitive cardiac troponin T; IL-6, interleukin 6; LVDD, left ventricular diastolic dysfunction; LVSD, left ventricular systolic dysfunction; MI, myocardial infarction; miR122-5p, MicroRNA-122-5p; MMP, matrix metalloproteinase; NT-proBNP, N-terminal pro b-type natriuretic peptide; PICP, procollagen type 1 carboxy-terminal propeptide; PIIINP, procollagen III N-terminal propeptide; PINP, procollagen type 1 N-terminal propeptide; sST2, soluble suppression of tumorigenesis-2; STEMI, ST-elevation myocardial infarction; T1D, type 1 diabetes mellitus; T2D, type 2 diabetes mellitus; TIMP-1, tissue inhibitor matrix metalloproteinase 1; TNF α , tumour necrosis factor alpha; VEGFB, vascular endothelial growth factor B.

separate countries (Figure 2). The most prevalent country was the USA ($n = 9$) where the most numerous studies were conducted.^{21–29} The countries following this were Denmark,^{30–32} and Italy^{33–35} ($n = 3$); China,^{36,37} Europe,^{38,39} France,^{40,41} Spain,^{42,43} and Taiwan^{44,45} ($n = 2$). Notably, three studies conducted multicentre studies across the world—categorised at International^{46–48} ($n = 3$).

Our searches revealed a total of 15 unique biomarkers used in the detection of cardiac remodelling in DM, where potential biomarkers were described by at least two studies (Table 2). The most studied and represented biomarker was N-terminal (NT)-pro-brain natriuretic peptide (NT-proBNP, $n = 21$).^{23,29,31,36,37,39,42–56} Many studies had a multi-marker approach where NT-proBNP was included as one of the biomarkers; however, four studies used NT-proBNP as a sole biomarker in detecting signs of remodelling and CVD outcome. The next most studied biomarkers were high-sensitivity C-reactive protein (hs-CRP, $n = 12$)^{23,25,26,29,34,46,47,51,57–60} and high-sensitivity cardiac

troponin T (hs-cTnT, $n = 8$),^{23,29,39,43,46,48,51,54} Galectin-3 (Gal-3, $n = 7$),^{21,24,29,39,47,52,61} and soluble suppression of tumorigenesis-2 (sST2) ($n = 7$).^{29,36,42,43,47,52,60} The vast majority of the studies included potential biomarkers collected from blood and plasma biomarkers with the exception of two papers, examining epicardial adipose thickness^{35,57} as a potential biomarker.

3.3 | Level of evidence and biomarker classification

The assessment of the included studies as per the level of evidence showed 7 studies were classified as ‘A’, having a well-designed study for the relevant population and sufficient level of evidence provided for the biomarker studied. Most studies were classified as ‘B’ ($n = 21$) where the diagnostic/prognostic study had minor limitations but consistent evidence. Lastly, 15 studies were classified as

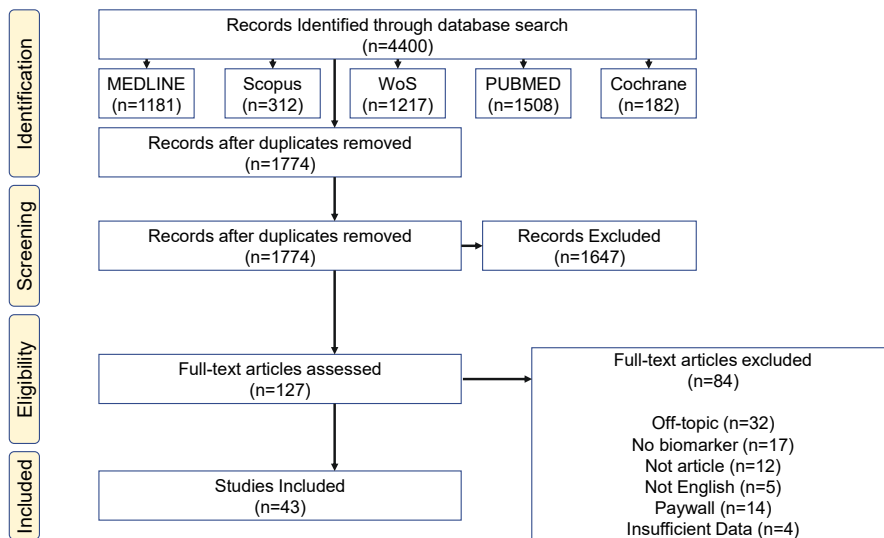


FIGURE 1 PRISMA flow diagram of search process.

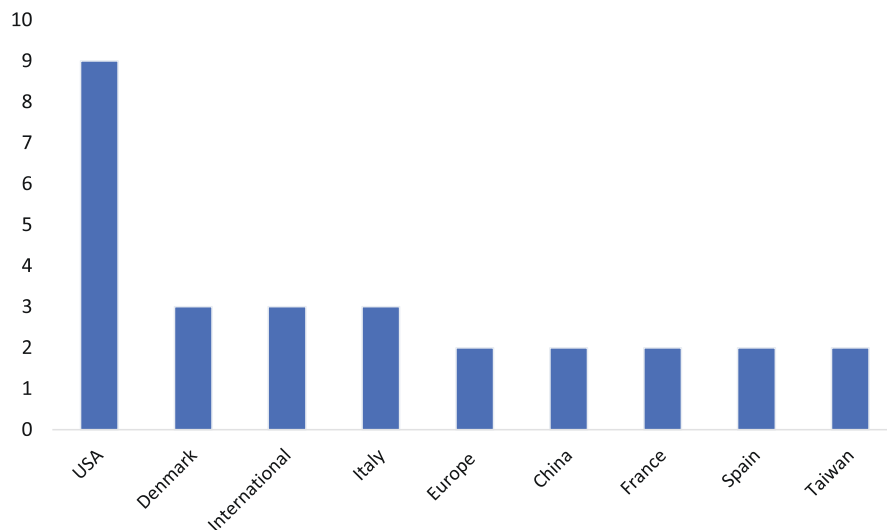


FIGURE 2 Distribution of adult participants according to country of study. United States of America ($n = 9$), Denmark ($n = 3$), International ($n = 3$), Italy ($n = 3$), China ($n = 2$), Europe ($n = 2$), France ($n = 2$), Spain ($n = 2$), Taiwan ($n = 2$). The following countries were not represented in the figure ($n = 1$): Australia, Egypt, England, Germany, Greece, Iran, Ireland, Japan, Netherlands, Norway, Romania, Russia, Sweden, Turkey, and Ukraine.

TABLE 2 Potential biomarkers identified in adults studied.

Biomarker	Number of studies
NT-proBNP	21
hs-CRP	12
MMP-1,2,3,9	10
hs-cTnT	8
Galectin-3	7
hs-ST2	7
BNP	6
PIIINP	3
TIMP-1	3
EAT	2
IL-6	2
PICP	2

Note: The following biomarkers were not presented in the table ($n = 1$): MMP10, 25 (OH), Adiponectin, Ang-II, Ceramide C16:0/C24:0, C1TP, Endostatin, FGF-23, HbA_{1c}, miR122-5p, Omentin-1, PINP, TNF α , and VEGFB.

'C', being an observational study with limited evidence provided (Table 1).

In terms of the biomarker classification, 22 studies were classified as (1), where the biomarker studies had the potential to be a reliable biomarker for detecting cardiac remodelling. Furthermore, 18 studies were classified as (2), being inconclusive as a biomarker for cardiac remodelling. Lastly, 3 studies were classified as (3), where insufficient evidence was provided for a biomarker of cardiac remodelling (Table 1).

4 | DISCUSSION

DM is a strong independent factor of CVD development associated with hyperglycaemia that affects heart function and contributes to worse CVD outcome.^{49,50} This remains an important factor to account for when determining systemic biomarker concentrations in people with DM and CVD, which often differ from people without DM.⁶² Similarly, previous studies have shown that in the presence of DM, there is an up-regulation in inflammatory pathways, not present in people without DM.³⁹ Inflammation underpins potential mechanisms leading to adverse cardiac remodelling and fibrotic processes in the presence of DM that still need to be fully elucidated.^{30,47} The current diagnostic method for detecting cardiac fibrosis relies on invasive imaging methods such as cardiovascular magnetic resonance imaging that includes T1 mapping; however, it can vary in result depending on the practitioner

and a patient in question.¹⁴ Often these methods need to be supported with additional assessments to confirm the diagnosis, which highlights the need for more reliable non-invasive methods that could be fulfilled by the emergence of new biomarkers that may be used in tandem with current methods. From the total of 15 biomarkers that were identified as promising within this scoping review, 7 studies were classified in the highest 1A category. This suggests that the quality of biomarkers from these studies is acceptable, and that these biomarkers have high potential of being reliable for cardiac remodelling.

4.1 | NT-proBNP and BNP as a measure of cardiac remodelling

The natriuretic peptide (NP) system has shown to play an important role in the study of cardiac endocrinology with the regulation of circulating active BNP, and the inactive NT proBNP. These peptides are secreted primarily in response to atrial muscle stretch, but can also be influenced by hypoxia, inflammation, angiotensin II (Ang II), and endothelin stimuli.⁶³ Upon release, BNP binds to the particulate guanylyl cyclase A receptor, followed by the generation of 3'-5'-cyclic guanosine monophosphate. This interaction results in a series of cardioprotective responses such as reduced hypertrophy, fibrosis, and inhibition of the renin-angiotensin-aldosterone system.⁶⁴ Circulating levels of NPs typically remain at a low level, but upon stimulus are increased. Clinical data supports this, reporting higher levels of plasma BNP and NT-proBNP in patients with HF, and hence these biomarkers have been the most widely used for the diagnosis and prognosis of HF.⁶⁵ In our current study, we found that out of the total 43 studies, 21 measured NT-proBNP concentration as a sole biomarker to determine remodelling or at least as a supplementary measure and six studies measured BNP as a biomarker.

The MESA study examined community patients for the presence of cardiac fibrosis measuring cardiovascular magnetic resonance T1 mapping and NT-proBNP levels. The findings of this study exhibit the relation of NPs and cardiac fibrosis, where a positive relation was found between plasma NT-proBNP levels and the presence of fibrotic changes within the heart. However, in the context of DM, the correlation between NPs and fibrosis displays an inverse relationship between plasma NP levels and insulin resistance across all body weights. The PARADIGM-HF trial measured a series of myocardial fibrosis plasma biomarkers in patients with HF, exhibiting a positive correlation of these biomarker levels to cardiovascular death and hospitalisation. The most notable changes in plasma biomarker concentrations recorded from this study were

suppression of tumorigenesis-2 (ST2), tissue inhibitors of metalloproteinases (TIMP-1), and procollagen type III N-terminal peptide (PIINP) at baseline; suggesting that TIMP-1 had the strongest prognostic value, exceeding BNP and NT-proBNP. It was also discovered that people with DM had a lower level of NT-proBNP, and significantly higher level of troponin T than people without DM. Out of all the studies included in this review, Lupon et al. 2013⁴³ provided similar insights and performed a multi-marker strategy, reporting a promising diagnostic potential of hs-cTnT and hs-ST2 biomarkers, which performed better together, whereas NT-proBNP was not included in the risk stratification of HF and remodelling. Interestingly, Pecherina et al. 2020⁵² suggested that after multi-variate analysis, the prognostic value of NT-proBNP is more reliable for HF symptoms but not for cardiac remodelling.

From the findings of this study and previous studies, BNP retains its diagnostic reliability as biomarkers for HF and show potential as biomarkers of cardiac remodelling in the presence of DM, albeit evidence is inconclusive so far based on extensive published research. However, as reported in previous studies, the non-specificity of BNP may impede its potential as sole biomarkers, making them more beneficial when used in conjunction with other biomarkers of cardiac remodelling.

4.2 | Inflammatory biomarkers of cardiac remodelling

Cardiac fibrosis is inextricably linked to dbCM and HF, where the underlying inflammatory process has shown an important role in its pathogenesis. DM exacerbates the inflammatory response, where a measure of inflammatory mediators at specific points in time can be indicative of the overall condition of the heart.⁶⁶

Gal-3 belongs to the B-galactoside-binding lectins, with an essential N-terminal domain proteolysed by matrix metalloproteinases (MMP) important for interaction with other intracellular proteins.⁶⁷ The ability to interact with other intracellular proteins allows Gal-3 to have a myriad of pleiotropic functions, notably within angiogenesis, inflammation, and fibrosis.^{67,68} Gal-3 promotes the chemoattraction of macrophages, fibroblast activity and ECM accumulation, displaying a close association with cardiac remodelling and HF pathophysiology.⁶⁸ Gal-3 typically is maintained at low plasma concentration in healthy individuals, however in patients with HF its plasma concentration increases, where its initial anti-necrotic, and anti-apoptotic functions lead to adverse cardiac remodelling and fibrosis over time.⁶⁸ Thus Gal-3 has been implicated in the pathogenesis of cardiac remodelling and inflammatory processes and considered a novel

biomarker.^{67,69} Serum Gal-3 and NT-proBNP concentrations have shown to be increased in HFpEF patients. In measuring ventricular remodelling in HFpEF patients using multivariate analysis, Gal-3 retains its association, whereas NT-proBNP does not and is rather attuned to HF symptoms.⁵² This apparent trend of increased Gal-3 levels corresponding with increased CVD risk and mortality was confirmed by Van der Velde et al., 2013.²⁴ By measuring percentage increase of Gal-3 over 3 months, the study found that an increase of >15% leads to a 50% higher risk of CVD adverse events compared to patients within 15% of their baseline Gal-3.²⁴ Conversely, De Boer et al., 2011⁶¹ reported that in hospitalised HF patients with DM, Gal-3 plasma concentration doubled, and showed high prognostic value for the primary endpoint of all-cause mortality and HF hospitalisation. Even when adjusted for covariates, including DM, Gal-3 retained promising prognostic value and even when measured at a later time point, it did not impair its prognostic value compared to other studies.⁶¹ Thus, Gal-3 may play an important prognostic role in detecting cardiac remodelling before severe damage or primary CVD mortality is reached, but its potential may be heightened in alliance with other biomarkers.

C-reactive protein (CRP) is a protein produced by hepatocytes within the liver, with serum concentration showing elevated trend under inflammatory conditions and age.⁷⁰ Hence, hs-CRP is widely used for its properties as an inflammatory marker, where its sensitivity lies in its ability to accurately detect early, low-grade inflammation.^{70,71} In the presence of DM, systematic inflammation is present, which is often chronic and low-grade.⁷² Elevated serum CRP is associated with LV dysfunction, increased risk of DM, and it is overall a predictor of CVD risk and mortality.^{73,74} The role of CRP in the cardiac remodelling process has further been implicated with studies reporting increased CRP in conjunction with pro-fibrotic and pro-inflammatory properties in Ang II-induced cardiac remodelling through activation of the transforming growth factor- β (TGF- β) and nuclear factor- κ B (NF κ B) signalling pathways.⁷⁵ Hence hs-CRP may have the potential to detect early signs of cardiac remodelling in people with DM and provide tool for risk stratification due to its high sensitivity and possible mechanistic role in cardiac remodelling. Similarly, interleukin-6 (IL-6) is a versatile cytokine embedded within the inflammatory response and pathophysiology of T2D, activating the inflammatory pathways including Janus kinase (JAK) and signal transducers and activators of transcription (STAT).^{76,77} The pro-inflammatory properties of IL-6 coincide with the chronic inflammatory disease state of people with DM, further mediating the effects of endothelial dysfunction, a key process in the development of CVD.⁷⁸ IL-6 has been reported to be produced by cardiomyocytes

upon myocardial infarction and hypoxia.⁷⁶ Though clear relationship between IL-6 in people with DM and related cardiac complications has been found, further studies are needed to understand the exact mechanisms involved.

ST2 is an interleukin receptor-1 (IL-1) family member that binds to the ligand IL-33, both of which play an integral role in the inflammatory and immune response, and have emerged as promising markers of cardiovascular pathophysiology.⁷⁹ Both ST2 and IL-33 expression are regulated by the proinflammatory cytokines, IL-6 and tumour necrosis factor alpha (TNF), and impaired cardiac function.⁸⁰ Soluble ST2 (sST2) is an isoform of ST2 released by fibroblasts that freely circulate within the blood, and upon binding to IL-33 has cardioprotective and anti-inflammatory properties, preventing the actions of IL-33.⁷⁹ Hence sST2 is implicated in the cardiac remodelling process, indicative of fibrosis and hypertrophy.⁸¹ Clinically, sST2 has shown to be a prognostic marker of both acute and chronic HF, where elevated levels have been shown in patients with a higher New York Heart Association (NYHA) functional classification, poor LV function and higher incidence of DM.^{79,80} sST2 retains its promising biomarker potential as the influence of comorbidities of CVD, such as DM and hypertension, has shown a less of a confounding effect on sST2 than on NT-proBNP.⁴³ This presents the possibility of additional mechanisms in which sST2 may function and highlights the advantage of targeting patients with multiple comorbidities, where a combined biomarker strategy holds added potential.

4.3 | Cardiac-specific biomarkers

Troponin is a contractile protein present within skeletal and cardio-myocytes that facilitate beating of the heart.⁸² The most relevant of the isoforms is cardiac troponin in the context of CVD, where it is highly attuned to cardio-myocytes health and indicative of myocardial damage.⁸² Hence, the highly specific and sensitive cardiac troponin, hs-cTnT, has been clinically used in the risk stratification for CVD in patients.⁸³ Given the strong relationship between DM and CVD, studies have reported significantly increased systemic concentrations of hs-cTnT in patients with DM, compared to those without DM.⁸³ Hs-cTnT measured in HFpEF patients with and without DM,²⁹ found no-significant differences initially observed between patient groups. However, after 12 months, hs-cTnT was one out of the two biomarkers significantly decreased when the groups were treated with a mineralocorticoid receptor inhibitor, spironolactone.²⁹ Meanwhile, people with DM and a CVD history with hs-cTnT systemic levels >14 ng/L experienced adverse cardiac outcomes.⁴⁸ The findings of this study and previous research indicate the

influence of increasing hs-cTnT through coinciding developmental factors of both DM and CVD, such as microvascular disease, ventricular hypertrophy, inflammation, and endothelial dysfunction.⁸³ This presents the promising biomarker potential of hs-cTnT in elucidating the pathophysiological mechanisms between DM and CVD and detecting the early sign of cardiac remodelling.

Myocardium homeostasis involves the regulation of ECM proteins, namely collagen, for optimal function of the heart. In a disease state, ECM degradation is an integral process in cardiac remodelling aiming to preserve cardiac function through the breakdown of collagen.⁸⁴ These homeostatic disruptions result in CVD pathophysiology such as cardiac fibrosis, LV hypertrophy, atherosclerosis, and heart failure.⁸⁵ MMPs are a family of endopeptidases with the primary role of cleaving collagen, with 23 total family members.⁸⁶ MMP-1, 2, 8, 9, and 14 have been reported to have the ability to cleave collagen in CVD,⁸⁴ which align with our findings that identified studies reporting plasma MMP-1, 2, 3, and 9 concentrations to be reflective of early adverse cardiac remodelling. MMP-1 degrades fibrillar collagen, MMP-2 and 9 are involved in the angiogenic processes, and MMP-3 regulates ECM degradation. Hyperglycaemia is a key culprit of DM, where consistently high blood glucose contributes to oxidative stress and increased synthesis of MMP-9.⁸⁶

In relation to MMPs, tissue inhibitors of metalloproteinases (TIMP) play a critical role in the regulation of MMPs and the extent of ECM degradation and structural remodelling.⁸⁷ Studies have found that in patients with T2D and hypertension, there is a significant increase in TIMP-1 levels, TIMP-1: MMP-9 ratios, and increased TNF- α .⁸⁶

Given the mechanistic role of MMPs and TIMPs in the structural remodelling of the heart and CVD, they have become a prominent therapeutic target for the treatment of cardiac fibrosis, where their expression is increased in the early fibrosis, preceding scar tissue accumulation.⁸⁸

Thus, both MMPs and TIMP-1 exhibit a strong potential in the early detection of cardiac remodelling in patients with DM.

As described above, cardiac fibrosis is commonly present in many forms of CVDs, where the early stages of cardiac remodelling are influenced by ECM remodelling.^{14,84} MMPs have been established as critical regulators of these pathological changes in fibrosis,⁸⁶ notably involving excess collagen deposition through fibroblast activation. The major types of collagen present in cardiac muscle are collagen type I and III and account for 85% and 11%, respectively. The ratio of collagen type I to type III has been linked to cardiac fibrosis and underlying structural remodelling, where they can be indicative of the underlying causes.¹⁴ Procollagen type 1 carboxy-terminal propeptide (PICP)

and PIIINP are two collagen peptides extracted from our literature search, and both are associated with production of their respective collagen peptides.^{89,90} Previous studies have shown elevated PIIINP levels following myocardial infarction and LV⁹¹ dysfunction, with a poor prognosis.^{89,92} Similarly, increased PICP levels have been reported in patients with hypertrophic cardiomyopathy and hypertensive heart diseases but were more significantly elevated in cases of severe cardiac fibrosis.^{93,94} However, in T2D, PICP levels were reported to be elevated in the presence of LV diastolic dysfunction compared to the controls.⁹¹ Thus, plasma PIIINP and PICP concentrations have been associated with cardiac remodelling in attenuating the balance between collagen synthesis and degradation.⁹⁰ Both these collagen peptide precursors present promising biomarker potential reflective of the early adverse cardiac remodelling through collagen synthesis levels but require further research in people with DM.

4.4 | Metabol(om)ic markers of T2D and CVD: Future perspectives

Although not identified as part of the inclusion criteria of this scoping review, as an emerging field, it is important to consider the potential of metabol(om)ic markers in CVD diagnosis and prognosis in the context of DM. The defining feature of DM is impaired glucose-insulin homeostasis accompanied by obesogenic systemic environment. Over the years, association between circulating amino acids and insulin has been established with some of the amino acids showing an insulinotropic effect. Previous studies have shown a correlation between significant increases in circulating plasma concentrations of leucine, isoleucine, lysine, tryptophan, glutamine, and glycerol, which were identified as the strong metabolic predictors of impaired insulin sensitivity and the incidence of T2D.⁹⁵ In the longitudinal Framingham Heart Study, a metabolomic approach was used to measure plasma samples from 200 participants who proceeded to develop DM over a 12-year follow-up. Logistical regression models showed that increase in circulating concentrations of branched-chain amino acids (BCAAs) and aromatic amino acids were associated with future DM.⁹⁶ Phenylalanine, tyrosine, and isoleucine have also been reported to predict the onset of CVD.⁹⁷ However, the association of these amino acids with early adverse cardiac remodelling/fibrosis or dbCM have not been explored in-depth and this is an area of research that should be addressed in future.

Furthermore, an inverse association between the circulating aliphatic amino acid glycine concentration and risk of DM has been established.⁹⁸ Thus overall, the following amino acids have been identified as potential biomarkers

of insulin resistance and DM: glutamate, glutamine, phenylalanine, tryptophan, tyrosine, glycine, isoleucine, leucine, and valine.^{95,99} Comparable to BCAAs, the fatty acids (i.e. stearic, palmitic, oleic, linoleic, pentadecanoic, palmitoleic) and intact lipids (triacylglycerides) identified by metabolomics studies have shown potential use as early screening biomarkers for insulin resistance and subsequently DM.

Integration of the findings of GWAS with lipid data has highlighted genes such as *FADS1*, *FADS2*, *ELOVL2*, and *ELOVL6* to be associated with changes in circulating lipid concentrations in patients.^{100,101} However, with the discovery of novel gene loci-lipid associations, links to insulin resistance endpoints including CVD will develop.

Further studies have implicated circulating metabolites and their potential role as a serum biomarker for dbCM in patients with DM and diastolic dysfunction. A high body mass index (BMI) and obesity have been correlated with the incidence of DM that is further linked to increases in fatty acid metabolism and impaired diastolic function.¹⁰² Shaver et al. (2016)¹⁰² reported the potential use of the metabolites as a biomarker in patients with diastolic dysfunction and DM compared to healthy controls. In the patient groups with the highest BMIs (DM, DM and diastolic dysfunction) leptin, triglyceride, TNF, and IL-6 concentrations were highest in these groups and inversely correlated with adiponectin levels. In line with these findings, high leptin and triglyceride levels have been associated with DM and fatty acid metabolism, where conversely, adiponectin presents antidiabetic and anti-inflammatory effects.¹⁰² With their present inflammatory role in DM, these biomarkers show a strong potential in detecting cardiac remodelling with supporting echocardiographic data. However, this remains an unexplored research field that is lacking information of how these metabolites can be used as biomarkers of early cardiac changes, including adverse cardiac remodelling especially given their close relationship to inflammatory mechanisms. This field of research should be investigated further given the importance of cardiac metabolism in the development of CVD.

The limitations of this research article may be attributed to the small number of studies including that specifically examining the narrow topic of cardiac remodelling in DM. From the hundreds of research articles screened in this study, only seven studies were found to be of high quality. Further assessment of these biomarkers in a diagnostic or prognostic scope may provide more insight to the quality of their biomarker or therapeutic target potential in cardiac remodelling. Further specification of patient groups, stage of CVD, and cardiac function would bolster the findings of this study, however, were not available in all studies. It is also possible that some biomarkers commonly associated with adverse cardiac remodelling

were not found within our literature search because of the pre-set inclusion criteria, which narrows the range of research articles involving adverse cardiac remodelling. For example, growth differentiation factor 15 (GDF15) is a distant member of the TGF- β family with mechanistic roots in both CVD and DM.^{103,104} Despite showing strong prognostic potential as a biomarker for CVD, its role is not well understood currently, hence why GDF15, and other cardiac remodelling-implicated biomarkers were potentially not included. Future inference on this topic would include a systematic review for a more in-depth consideration at the biomarkers mentioned in this study to substantiate their potential as biomarkers of cardiac remodelling in the presence of DM.

5 | CONCLUSION

Cardiac remodelling is inherently tied with cardiovascular outcomes, with DM being one of the main risk factors. The pathogenesis of cardiac remodelling in DM is yet to be elucidated and requires further investigation to understand the mechanisms involved. Through the data collected from this scoping review, it was revealed that NT-proBNP was the most frequently measured biomarker in studies evaluating cardiac remodelling and related CVD outcomes in people with DM. However, the findings and multivariate analysis in the included studies of this scoping review suggest that NT-proBNP, although the standard diagnostic and prognostic biomarker in HF may not be the optimal biomarker in determining signs of cardiac remodelling in the presence of DM. Emerging biomarkers for cardiac remodelling including hs-CRP, hs-cTnT, and Gal-3 being rooted in inflammatory pathways, have shown promising results in the current studies as diagnostic and prognostic biomarkers of adverse cardiac remodelling in DM. Although outside of the scoping review inclusion criteria, with the strong evidence supporting the relationship of certain amino acids and impaired insulin sensitivity, and the emergence of advanced metabolomics technologies, the possibility for the amino acids to be developed as new biomarkers for the early detection of adverse cardiac remodelling and CVD in DM is highly likely. However, further research in larger studies must be conducted to confirm the effectiveness of these emerging biomarkers and understand the mechanisms of cardiac remodelling in DM.

AUTHORS' CONTRIBUTIONS

Conceptualisation, LM and KM; methodology, data extraction, analysis, interpretation, and graphical abstract: MC, WL; contribution to data interpretation and

manuscript content: MP and DA; writing—original draft preparation: MC. Manuscript editing: LM, MP, DA, KM. Supervision: LM and KM. All authors read and approved the final manuscript.

ACKNOWLEDGMENTS

Not applicable. Open access publishing facilitated by University of Technology Sydney, as part of the Wiley - University of Technology Sydney agreement via the Council of Australian University Librarians.

FUNDING INFORMATION

This research is supported by an Australian Government Research Training Program Scholarship (Michael Chhor).

CONFLICT OF INTEREST STATEMENT

The authors declare that they have no competing interests.

DATA AVAILABILITY STATEMENT

I confirm that my Data Availability Statement (pasted below) complies with the Expects Data Policy. The data that support the findings of this study are available from the corresponding author upon reasonable request.

REFERENCES

1. Key Statistics: Cardiovascular Disease. The Heart Foundation. <https://www.heartfoundation.org.au/activities-finding-or-opinion/key-stats-cardiovascular-disease>.
2. Cardiovascular diseases. https://www.who.int/health-topics/cardiovascular-diseases#tab=tab_1.
3. Roth GA, Mensah GA, Johnson CO, et al. Global burden of cardiovascular diseases and risk factors, 1990–2019: update from the GBD 2019 study. *J Am Coll Cardiol*. 2020;76:2982–3021.
4. Diabetes. https://www.who.int/health-topics/diabetes#tab=tab_1.
5. Henson SM, Aksentijevic D. Senescence and type 2 diabetic cardiomyopathy: how young can you die of old Age? *Front Pharmacol*. 2021;12:716517.
6. Dokken BB. The pathophysiology of cardiovascular disease and diabetes: beyond blood pressure and lipids. *Diabetes Spectrum*. 2008;21:160–165.
7. Leon BM, Maddox TM. Diabetes and cardiovascular disease: epidemiology, biological mechanisms, treatment recommendations and future research. *World J Diabetes*. 2015;6:1246.
8. Kannel WB, Hjortland M, Castelli WP. Role of diabetes in congestive heart failure: the Framingham study. *Am J Cardiol*. 1974;34:29–34.
9. Kannel WB, McGee DL. Diabetes and cardiovascular disease: the Framingham study. *JAMA*. 1979;241:2035–2038.
10. Kenny HC, Abel ED. Heart failure in type 2 diabetes mellitus: impact of glucose lowering agents, heart failure therapies and novel therapeutic strategies. *Circ Res*. 2019;124:121.
11. Tuleta I, Frangiannis NG. Diabetic fibrosis. *Biochim Biophys Acta Mol Basis Dis*. 1867;2021:166044.
12. Liu T, Song D, Dong J, et al. Current understanding of the pathophysiology of myocardial fibrosis and its quantitative assessment in heart failure. *Front Physiol*. 2017;8:238.

13. Travers JG, Kamal FA, Robbins J, Yutzy KE, Blaxall BC. Cardiac fibrosis: the fibroblast awakens. *Circ Res*. 2016;118:1021.
14. Hinderer S, Schenke-Layland K. Cardiac fibrosis – A short review of causes and therapeutic strategies. *Adv Drug Deliv Rev*. 2019;146:77-82.
15. Jia G, Hill MA, Sowers JR. Diabetic cardiomyopathy. *Circ Res*. 2018;122:624-638.
16. Russo I, Frangogiannis NG. Diabetes-associated cardiac fibrosis: cellular effectors, molecular mechanisms and therapeutic opportunities. *J Mol Cell Cardiol*. 2016;90:84.
17. Yap J, Tay WT, Teng TK, et al. Association of Diabetes Mellitus on cardiac remodeling, quality of life, and clinical outcomes in heart failure with reduced and preserved ejection fraction. *J Am Heart Assoc*. 2019;8:e013114.
18. Ritchie RH, Dale Abel E. Basic mechanisms of diabetic heart disease. *Circ Res*. 2020;126:1501.
19. Tricco AC, Lillie E, Zarin W, et al. PRISMA extension for scoping reviews (PRISMA-ScR): checklist and explanation. *Ann Intern Med*. 2018;169:467-473.
20. de Luca Canto G, Pachêco-Pereira C, Aydinov S, Major PW, Flores-Mir C, Gozal D. Biomarkers associated with obstructive sleep apnea: a scoping review. *Sleep Med Rev*. 2015;23:28-45. doi:10.1016/j.smrv.2014.11.004
21. Motiwala SR, Szymonifka J, Belcher A, et al. Serial measurement of galectin-3 in patients with chronic heart failure: results from the ProBNP outpatient tailored chronic heart failure therapy (PROTECT) study. *Eur J Heart Fail*. 2013;15:1157-1163.
22. Nwabuo CC, Duncan M, Xanthakis V, et al. Association of circulating ceramides with cardiac structure and function in the community: the Framingham heart study. *J Am Heart Assoc*. 2019;8:e013050.
23. Oliver W, Matthews G, Ayers CR, et al. Factors associated with left atrial remodeling in the general population. *Circ Cardiovasc Imaging*. 2017;10:e005047.
24. van der Velde AR, Gullestad L, Ueland T, et al. Prognostic value of changes in galectin-3 levels over time in patients with heart failure: data from CORONA and COACH. *Circ Heart Fail*. 2013;6:219-226.
25. Vasan RS, Sullivan LM, Roubenoff R, et al. Inflammatory markers and risk of heart failure in elderly subjects without prior myocardial infarction - the Framingham heart study. *Circulation*. 2003;107:1486-1491.
26. Velagaleti RS, Gona P, Chuang ML, et al. Relations of insulin resistance and glycemic abnormalities to cardiovascular magnetic resonance measures of cardiac structure and function: the Framingham heart study. *Circ Cardiovasc Imaging*. 2010;3:257-263.
27. Vorovich EE, Li M, Aversa J, et al. Comparison of matrix metalloproteinase 9 and brain natriuretic peptide as clinical biomarkers in chronic heart failure. *Am Heart J*. 2008;155:992-997.
28. Wang K-T, Liu YY, Sung KT, et al. Circulating monocyte count as a surrogate marker for ventricular-arterial remodeling and incident heart failure with preserved ejection fraction. *Diagnostics*. 2020;10:287.
29. de Marco C, Claggett BL, de Denus S, et al. Impact of diabetes on serum biomarkers in heart failure with preserved ejection fraction: insights from the TOPCAT trial. *ESC Heart Fail*. 2021;8:1130-1138. doi:10.1002/ehf2.13153
30. Sorensen MH, Bojer AS, Jørgensen NR, et al. Fibroblast growth factor-23 is associated with imaging markers of diabetic cardiomyopathy and anti-diabetic therapeutics. *Cardiovasc Diabetol*. 2020;19:158.
31. Andersen NH, Poulsen SH, Knudsen ST, Heickendorff L, Mogensen CE. NT-proBNP in normoalbuminuric patients with type 2 diabetes mellitus. *Diabet Med*. 2005;22:188-195.
32. Jørgensen PG, Biering-Sørensen T, Mogelvang R, et al. Presence of micro- and macroalbuminuria and the association with cardiac mechanics in patients with type 2 diabetes. *Eur Heart J Cardiovasc Imaging*. 2018;19:1034-1041.
33. Pofi R, Galea N, Francone M, et al. Diabetic Cardiomyopathy progression is triggered by miR122-5p and involves extracellular matrix: a 5-year prospective study. *JACC Cardiovasc Imaging*. 2021;14:1130-1142.
34. Spazzafumo L, Olivieri F, Abbatecola AM, et al. Remodelling of biological parameters during human ageing: evidence for complex regulation in longevity and in type 2 diabetes. *Age (Dordr)*. 2013;35:419-429.
35. Parisi V, Cabaro S, D'Esposito V, et al. Epicardial adipose tissue and IL-13 response to myocardial injury drives left ventricular remodeling after ST elevation myocardial infarction. *Front Physiol*. 2020;11:575181.
36. Bai J, Han L, Liu H. Combined use of high-sensitivity ST2 and NT-proBNP for predicting major adverse cardiovascular events in coronary heart failure. *Ann Palliat Med*. 2020;9:1976-1989.
37. Hao PP, Chen Y-G, Liu Y-P, et al. Association of Plasma Angiotensin-(1-7) level and left ventricular function in patients with type 2 diabetes mellitus. *PLoS One*. 2013;8:e62788.
38. Peeters SA, Engelen L, Buijs J, et al. Associations between advanced glycation endproducts and matrix metalloproteinases and its inhibitor in individuals with type 1 diabetes. *J Diabetes Complications*. 2018;32:325-329.
39. JAJ V, Ferreira JP, Pellicori P, et al. Proteomic mechanistic profile of patients with diabetes at risk of developing heart failure: insights from the HOMAGE trial. *Cardiovasc Diabetol*. 2021;20:163.
40. Albertini JP, Cohen R, Valensi P, Sachs RN, Charniot JC. B-type natriuretic peptide, a marker of asymptomatic left ventricular dysfunction in type 2 diabetic patients. *Diabetes Metab*. 2008;34:355-362.
41. Alla F, Kearney-Schwartz A, Radauceanu A, das Dores S, Dousset B, Zannad F. Early changes in serum markers of cardiac extra-cellular matrix turnover in patients with uncomplicated hypertension and type II diabetes. *Eur J Heart Fail*. 2006;8:147-153.
42. Bayes-Genis A, Zhang Y, Ky B. ST2 and patient prognosis in chronic heart failure. *Am J Cardiol*. 2015;115:64B-69B.
43. Lupón J, de Antonio M, Galán A, et al. Combined use of the novel biomarkers high-sensitivity troponin T and ST2 for heart failure risk stratification vs conventional assessment. *Mayo Clin Proc*. 2013;88:234-243.
44. Lin J-L, Sung KT, Su CH, et al. Cardiac structural remodeling, longitudinal systolic strain, and torsional mechanics in lean and nonlean Dysglycemic Chinese adults. *Circ Cardiovasc Imaging*. 2018;11:e007047.
45. Wang TJ, Larson MG, Benjamin EJ, et al. Clinical and echocardiographic correlates of plasma procollagen type III amino-terminal peptide levels in the community. *Am Heart J*. 2007;154:291-297.
46. Scirica BM, Bhatt DL, Braunwald E, et al. Prognostic implications of biomarker assessments in patients with type 2 diabetes

- at high cardiovascular risk: a secondary analysis of a randomized clinical trial. *JAMA Cardiol.* 2016;1:989-998.
47. Sharma A, Demissei BG, Tromp J, et al. A network analysis to compare biomarker profiles in patients with and without diabetes mellitus in acute heart failure. *Eur J Heart Fail.* 2017;19:1310-1320.
 48. Lindholm D, Lindbäck J, Armstrong PW, et al. Biomarker-based risk model to predict cardiovascular mortality in patients with stable coronary disease. *J Am Coll Cardiol.* 2017;70:813-826.
 49. Luchner A, Behrens G, Stritzke J, et al. Long-term pattern of brain natriuretic peptide and N-terminal pro brain natriuretic peptide and its determinants in the general population: contribution of age, gender, and cardiac and extra-cardiac factors. *Eur J Heart Fail.* 2013;15:859-867.
 50. McGrady M, Reid CM, Shiel L, et al. N-terminal B-type natriuretic peptide and the association with left ventricular diastolic function in a population at high risk of incident heart failure: results of the SCReening Evaluation of the evolution of new-heart failure study (SCREEN-HF). *Eur J Heart Fail.* 2013;15:573-580.
 51. Myhre PL, Lyngbakken MN, Berge T, et al. Diagnostic thresholds for pre-diabetes mellitus and diabetes mellitus and sub-clinical cardiac disease in the general population: data from the ACE 1950 study. *J Am Heart Assoc.* 2021;10:e020447.
 52. Pecherina T, Kutikhin A, Kashtalov V, et al. Serum and echocardiographic markers may synergistically predict adverse cardiac remodeling after ST-segment elevation myocardial infarction in patients with preserved ejection fraction. *Diagnostics.* 2020;10:301.
 53. Ruge T, Carlsson AC, Ingelsson E, et al. Circulating endostatin and the incidence of heart failure. *Scand Cardiovasc J.* 2018;52:244-249.
 54. Sato Y, Nishi K, Taniguchi R, et al. In patients with heart failure and non-ischemic heart disease, cardiac troponin T is a reliable predictor of long-term echocardiographic changes and adverse cardiac events. *J Cardiol.* 2009;54:221-230.
 55. Börekçi A, Gür M, Türkoğlu C, et al. Neutrophil to lymphocyte ratio predicts left ventricular remodeling in patients with ST elevation myocardial infarction after primary percutaneous coronary intervention. *Korean Circ J.* 2016;46:15-22.
 56. Ghanem SE, Abdel-Samie M, Torky MH, et al. Role of resistin, IL-6 and NH2-terminal portion proBNP in the pathogenesis of cardiac disease in type 2 diabetes mellitus. *BMJ Open Diabetes Res Care.* 2020;8:e001206.
 57. Opincariu D, Mester A, Dobra M, Rat N, Hodas R, Morariu M. Prognostic value of Epicardial fat thickness as a biomarker of increased inflammatory status in patients with type 2 diabetes mellitus and acute myocardial infarction. *J Cardiovasc Emergen.* 2016;2:11-18.
 58. Wang TJ, Larson MG, Benjamin EJ, et al. Clinical and echocardiographic correlates of plasma procollagen type III amino-terminal peptide levels in the community. *Am Heart J.* 2007;154:291-297.
 59. Bilovol OM, Knyazkova II, Al-Travneh OV, Bogun MV, Berezin AE. Altered adipocytokine profile predicts early stage of left ventricular remodeling in hypertensive patients with type 2 diabetes mellitus. *Diabetes Metab Syndr.* 2020;14:109-116.
 60. Fousteris E, Melidonis A, Panoutsopoulos G, et al. Toll/interleukin-1 receptor member ST2 exhibits higher soluble levels in type 2 diabetes, especially when accompanied with left ventricular diastolic dysfunction. *Cardiovasc Diabetol.* 2011;10:101.
 61. de Boer RA, Lok DJ, Jaarsma T, et al. Predictive value of plasma galectin-3 levels in heart failure with reduced and preserved ejection fraction. *Ann Med.* 2011;43:60-68.
 62. Januszewski AS, Watson CJ, O'Neill V, et al. FKBPL is associated with metabolic parameters and is a novel determinant of cardiovascular disease. *Sci Rep.* 2020;10:21655.
 63. Almeida AG. NT-proBNP and myocardial fibrosis the invisible link between health and disease*. *J Am Coll Cardiol.* 2017;70(25):3110-3112.
 64. Kuwahara K. The natriuretic peptide system in heart failure: diagnostic and therapeutic implications. *Pharmacol Ther.* 2021;227:107863.
 65. Mckie PM, Burnett JC. NT-proBNP the gold standard biomarker in heart failure*. *J Am Coll Cardiol.* 2016;68(22):2437-2439.
 66. Lazar S, Rayner B, Lopez Campos G, McGrath K, McClements L. Mechanisms of heart failure with preserved ejection fraction in the presence of diabetes mellitus. *J Metab Syndr Res.* 2020;3:1-5.
 67. Dong R, Zhang M, Hu Q, et al. Galectin-3 as a novel biomarker for disease diagnosis and a target for therapy (review). *Int J Mol Med.* 2018;41:599.
 68. Blanda V, Bracale UM, di Taranto MD, Fortunato G. Galectin-3 in cardiovascular diseases. *Int J Mol Sci.* 2020;21:1-18.
 69. Yakar Tülüce S, Tülüce K, Çil Z, Emren SV, Akyıldız Zİ, Ergene O. Galectin-3 levels in patients with hypertrophic cardiomyopathy and its relationship with left ventricular mass index and function. *Anatol J Cardiol.* 2016;16:344.
 70. Li Y, Zhong X, Cheng G, et al. Hs-CRP and all-cause, cardiovascular, and cancer mortality risk: A meta-analysis. *Atherosclerosis.* 2017;259:75-82.
 71. Kamath DY, Xavier D, Sigamani A, Pais P. High sensitivity C-reactive protein (hsCRP) & cardiovascular disease: an Indian perspective. *Indian J Med Res.* 2015;142:261-268. doi:10.4103/0971-5916.166582
 72. Walker AMN, Patel PA, Rajwani A, et al. Diabetes mellitus is associated with adverse structural and functional cardiac remodeling in chronic heart failure with reduced ejection fraction. *Diab Vasc Dis Res.* 2016;13:331-340.
 73. Pfützner A, Forst T. High-sensitivity C-reactive protein as cardiovascular risk marker in patients with diabetes mellitus. *Diabetes Technol Ther.* 2006;8:28-36. <https://home.liebertpub.com/dia>
 74. Nagai T, Anzai T, Kaneko H, et al. C-reactive protein overexpression exacerbates pressure overload-induced cardiac remodeling through enhanced inflammatory response. *Hypertension.* 2011;57:208-215.
 75. Zhang R, Zhang YY, Huang XR, et al. C-reactive protein promotes cardiac fibrosis and inflammation in angiotensin II-induced hypertensive cardiac disease. *Hypertension.* 2010;55:953-960.
 76. Dawn B, Xuan YT, Guo Y, et al. IL-6 plays an obligatory role in late preconditioning via JAK-STAT signaling and upregulation of iNOS and COX-2. *Cardiovasc Res.* 2004;64:61-71.
 77. Akbari M, Hassan-Zadeh V. IL-6 signalling pathways and the development of type 2 diabetes. *Inflammopharmacology.* 2018;26:685-698.
 78. Qu D, Liu J, Lau CW, Huang Y. IL-6 in diabetes and cardiovascular complications. *Br J Pharmacol.* 2014;171:3595.
 79. Dudek M, Dudek MA, Kałużna-Oleksy MB, Migaj JB, Straburzyńska-Migaj EA. Cite as the creative commons

- attribution 3.0 Unported (CC BY 3.0) address for correspondence Funding sources clinical value of soluble ST2 in cardiology. *Adv Clin Exp Med*. 2020;29:1205-1210.
80. Lotierzo M, Dupuy AM, Kalmanovich E, Roubille F, Cristol JP. sST2 as a value-added biomarker in heart failure. *Clin Chim Acta*. 2020;501:120-130.
 81. Homsak E, Gruson D. Soluble ST2: A complex and diverse role in several diseases. *Clin Chim Acta*. 2020;507:75-87.
 82. Garg P, Morris P, Fazlanie AL, et al. Cardiac biomarkers of acute coronary syndrome: from history to high-sensitivity cardiac troponin. *Intern Emerg Med*. 2017;12:147.
 83. Whelton SP, McEvoy J, Lazo M, Coresh J, Ballantyne CM, Selvin E. High-sensitivity cardiac troponin T (hs-cTnT) as a predictor of incident diabetes in the atherosclerosis risk in communities study. *Diabetes Care*. 2017;40:261-269.
 84. Yabluchanskiy A, Ma Y, Iyer RP, Hall ME, Lindsey ML. Matrix Metalloproteinase-9: many shades of function in cardiovascular disease. *Phys Ther*. 2013;28:391.
 85. Nagase H, Visse R, Murphy G. Structure and function of matrix metalloproteinases and TIMPs. *Cardiovasc Res*. 2006;69:562-573.
 86. Cabral-Pacheco GA, Garza-Veloz I, Castruita-De la Rosa C, et al. The roles of matrix metalloproteinases and their inhibitors in human diseases. *Int J Mol Sci*. 2020;21:1-53.
 87. Wang X, Khalil RA. Matrix metalloproteinases, vascular remodeling, and vascular disease. *Adv Pharmacol*. 2018;81:241.
 88. Chuang HM, Chen YS, Harn HJ. The versatile role of matrix metalloproteinase for the diverse results of fibrosis treatment. *Molecules*. 2019;24:4188.
 89. Lee CH, Lee WC, Chang SH, Wen MS, Hung KC. The N-terminal propeptide of type III procollagen in patients with acute coronary syndrome: a link between left ventricular end-diastolic pressure and cardiovascular events. *PLoS One*. 2015;10:e114097.
 90. Osokina A, Karetnikova V, Polikutina O, et al. Prognostic potential of cardiac structural and functional parameters and N-terminal propeptide of type III procollagen in predicting cardiac fibrosis one year after myocardial infarction with preserved left ventricular ejection fraction. *Aging (Albany NY)*. 2021;13:194.
 91. Ihm SH, Youn HJ, Shin DI, et al. Serum carboxy-terminal propeptide of type I procollagen (PIP) is a marker of diastolic dysfunction in patients with early type 2 diabetes mellitus. *Int J Cardiol*. 2007;122:e36-e38.
 92. Sugimoto M, Saiki H, Tamai A, et al. Ventricular fibrogenesis activity assessed by serum levels of procollagen type III N-terminal amino peptide during the staged Fontan procedure. *J Thorac Cardiovasc Surg*. 2016;151:1518-1526.
 93. Yang C, Qiao S, Song Y, et al. Procollagen type I carboxy-terminal propeptide (PICP) and MMP-2 are potential biomarkers of myocardial fibrosis in patients with hypertrophic cardiomyopathy. *Cardiovasc Pathol*. 2019;43:107150.
 94. Querejeta R, Varo N, López B, et al. Serum carboxy-terminal propeptide of procollagen type I is a marker of myocardial fibrosis in hypertensive heart disease. *Circulation*. 2000;101:1729-1735.
 95. Alqudah A, Wedyan M, Qnais E, Jawarneh H, McClements L. Plasma amino acids metabolomics' important in glucose management in type 2 diabetes. *Front Pharmacol*. 2021;12:695418.
 96. Wang TJ, Larson MG, Vasan RS, et al. Metabolite profiles and the risk of developing diabetes. *Nat Med*. 2011;17:448.
 97. Magnusson M, Lewis GD, Ericson U, et al. A diabetes-predictive amino acid score and future cardiovascular disease. *Eur Heart J*. 2013;34:1982.
 98. Ferrannini E, Natali A, Camastra S, et al. Early metabolic markers of the development of dysglycemia and type 2 diabetes and their physiological significance. *Diabetes*. 2013;62:1730-1737.
 99. Roberts LD, Koulman A, Griffin JL. Towards metabolic biomarkers of insulin resistance and type 2 diabetes: progress from the metabolome. *Lancet Diabetes Endocrinol*. 2014;2:65-75.
 100. Tanaka T, Shen J, Abecasis GR, et al. Genome-wide association study of plasma polyunsaturated fatty acids in the InCHIANTI study. *PLoS Genet*. 2009;5:1000338.
 101. Ameur A, Enroth S, Johansson A, et al. Genetic adaptation of fatty-acid metabolism: a human-specific haplotype increasing the biosynthesis of long-chain Omega-3 and Omega-6 fatty acids. *Am J Hum Genet*. 2012;90:809.
 102. Shaver A, Nichols A, Thompson E, et al. Role of serum biomarkers in early detection of diabetic cardiomyopathy in the west Virginian population. *Int J Med Sci*. 2016;13:161.
 103. Eddy AC, Trask AJ. Growth differentiation factor-15 and its role in diabetes and cardiovascular disease. *Cytokine Growth Factor Rev*. 2021;57:11-18.
 104. Wesseling M, de Poel JHC, de Jager SCA. Growth differentiation factor 15 in adverse cardiac remodelling: from biomarker to causal player. *ESC Heart Fail*. 2020;7:1488-1501.

How to cite this article: Chhor M, Law W, Pavlovic M, Aksentijevic D, McGrath K, McClements L. Diagnostic and prognostic biomarkers reflective of cardiac remodelling in diabetes mellitus: A scoping review. *Diabet Med*. 2023;40:e15064. doi:[10.1111/dme.15064](https://doi.org/10.1111/dme.15064)